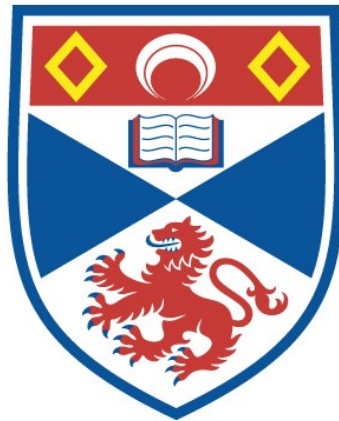


LITHIUM AND TANTALUM MINERALIZATION IN
RARE-ELEMENT PEGMATITES FROM SOUTHERN
AFRICA

Joy Rosina Baldwin

A Thesis Submitted for the Degree of PhD
at the
University of St Andrews



1994

Full metadata for this item is available in
St Andrews Research Repository
at:
<http://research-repository.st-andrews.ac.uk/>

Please use this identifier to cite or link to this item:
<http://hdl.handle.net/10023/15468>

This item is protected by original copyright

**LITHIUM AND TANTALUM MINERALIZATION IN
RARE-ELEMENT PEGMATITES FROM SOUTHERN AFRICA**

by

Joy Rosina Baldwin

Thesis submitted for the degree of
Doctor of Philosophy

June 1993

St Andrews



ProQuest Number: 10170811

All rights reserved

INFORMATION TO ALL USERS

The quality of this reproduction is dependent upon the quality of the copy submitted.

In the unlikely event that the author did not send a complete manuscript and there are missing pages, these will be noted. Also, if material had to be removed, a note will indicate the deletion.



ProQuest 10170811

Published by ProQuest LLC (2017). Copyright of the Dissertation is held by the Author.

All rights reserved.

This work is protected against unauthorized copying under Title 17, United States Code
Microform Edition © ProQuest LLC.

ProQuest LLC.
789 East Eisenhower Parkway
P.O. Box 1346
Ann Arbor, MI 48106 – 1346

Th B 434

iii.

ABSTRACT

Lithium and tantalum mineralization in rare-element pegmatites has been studied in 4 field areas. Three field areas are within a pegmatite belt which stretches for 450 km from Steinkopf, Namaqualand in the west, to Kenhardt in the east along the Orange river in South Africa, incorporating Tantalite Valley, Namibia in the central area. This Belt is considered to be of 1200 my age. The 4th field area is in central Namibia in the Karibib-Usakos region of 500 my age.

Lithium mineralization involves primary minerals, petalite and spodumene (crystallizing < 650°C) and amblygonite which crystallize from a magma ± an aqueous fluid, and lithian mica which along with cleavelandite is one of the last mineral assemblages to form, probably these last two assemblages are replacement in origin. Petalite is dominant in the Karibib area and spodumene in Steinkopf, Namaqualand and Tantalite Valley. The Kenhardt area is poor in lithium in comparison with the western and central portions of the Pegmatite Belt. Amblygonite-montebrazite is present in Karibib and Tantalite Valley usually in association with cleavelandite and lithian mica.

Hydrothermal low temperature replacements, < 400°C occur in spodumene in the Steinkopf and Tantalite Valley pegmatites, being pseudomorphed by albite and mica ± sericite. Amblygonite-montebrazite in Karibib displays replacements of natromontebrazite (the first occurrence in Karibib, Namibia), crandallite, brazilianite and possibly cookeite. Apatite is always prominent at the contact. An unusual occurrence of Mn-tantalite lamellae, primarily parallel, lying in microlite, is intergrown with montebrazite at the Rubicon pegmatite, Karibib, suggesting simultaneous crystallization of these three minerals, i.e. Ta-dominated tantalite and microlite and $\text{LiAl}(\text{F}/\text{PO}_4)$ involving late fluids rich in F, P and Ta.

Mn-tantalite and Ta-rich microlite are the dominant Ta-minerals in the rare-element Li-rich pegmatites of Namaqualand, Tantalite Valley and Karibib. In contrast, columbite (Nb-rich) is prevalent in the Li-poor, less differentiated pegmatites in the eastern Pegmatite Belt near Kenhardt. Microlite replaces Mn-tantalite in Li-rich rare-element pegmatites in all three field areas. A uranmicrolite from Karibib, Namibia contains 14.35% UO_2 , 1.03% PbO, 56.12% Ta_2O_5 , 13.18% Nb_2O_5 , 0.58% Fe_2O_3 , 6.87% CaO, 0.54% SrO, 0.59% MnO, 0.86% Na_2O and 0.47% F. U-plumbomicrolite or Pb-uranmicrolite is intergrown with manganotantalite from the same pegmatite. Throughout one aggregate of microlite PbO varied from 21.98 to 1.57% and UO_2 from 12.89 to 16.20%. Pb appears to be concentrated around the periphery of the crystal. Backscattered electron images reveal metamict textures in radioactive microlites and distinctive subspheroidal features. A uranoan microlite from Tantalite Valley, Namibia, revealed two essentially different compositions; a more hydrated rim area of 200 μm radius containing 7% higher Ta_2O_5 , 10% lower CaO and 1.3% lower F than a main central area of slightly variable composition. Crystals of uranoan microlite from Steinkopf, Namaqualand contain remnants of a bismuth phase. Bismuth intergrowths with quartz reveal the presence of two rare-minerals, pyromorphite $[\text{Pb}_5(\text{PO}_4)_3\text{Cl}]$ and mottramite $[\text{PbCu}(\text{VO}_4)\text{OH}]$, new data is given for these minerals. Ferrotantalite occurs at Rubicon mine.

A schematic diagram is produced for the paragenetic sequence of mineral assemblage in each of the pegmatite areas in Karibib, Tantalite Valley, and Steinkopf, Namaqualand in relation to T and P of formation, and the magma and fluids effecting the crystallization sequence.

Finally different fractionation trends of Ta-Nb, Mn-Fe, Rb-K and Cs-K in columbite-tantalites and lithian mica have highlighted variable paths of differentiation in contrasting rare-element pegmatites which may reflect different sources of original parental magma.

ACKNOWLEDGEMENTS

I am indebted to Dr. von Knorring of Leeds University and the Geological Survey of Namibia, for guiding me around each of the pegmatite areas and for invaluable discussion. Thanks also to the University of Witwatersrand, Johannesburg for transporting the geological specimens to Scotland and for microprobe and photographic facilities and polished thin sections. I am also indebted to Dr. Peter Hill at the Edinburgh microprobe unit for his invaluable help and guidance and especially for his expertise in the standardization of the rare-minerals. Thank you also to the computing laboratory in St. Andrews, where I seem to have spent a great deal of time, for their excellent facilities. In "Geology "in St. Andrews, many thanks go to the XRF laboratory, Donald Hird for BSE images, Jim Allan for photography, Richard Batchelor for Rb and Cs analyses and Andie Mackie in the section room. Finally thank you to all my colleagues, friends and family in particular Dr. Luigi Nocera, Professor Tom Clifford, Professor E.K.Walton, Dr. E. Stephens and Professor D. Hogarth for help and support through the period of the thesis and especially to Dr. G. J. H. Oliver who had the courage to finally see the thesis to its conclusion.

This thesis is dedicated to my father, the late:

ALFRED GEORGE BALDWIN

and to my mother

HILDA PITT EDWARDS BALDWIN

CONTENTS

ABSTRACT

ACKNOWLEDGEMENTS

PART I

INTRODUCTION

Page

CHAPTER 1. AIM AND INTRODUCTION

1..... 1.1. AIM

3..... 1.2. INTRODUCTION

CHAPTER 2. THE MINERALIZED PEGMATITES AND THE GEOLOGICAL OCCURRENCE OF LITHIUM AND TANTALUM

6.... 2.1. INTRODUCTION

2.2. THE MINERALIZED PEGMATITES

11..... 2.2.1. Introduction

18..... 2.2.2. The Kenhardt area, Northern Cape, South Africa

19..... 2.2.3. The Steinkopf area, Namaqualand, South Africa

24..... 2.2.4. Tantalite Valley, Warmbad, Namibia

30..... 2.2.5. The Karibib-Usakos area, Namibia

2.3. THE OCCURRENCE AND GEOCHEMISTRY OF LITHIUM AND TANTALUM

38.... 2.3.1 Lithium

40.... 2.3.2 Tantalum

PART II

LITHIUM MINERALIZATION

Page CHAPTER 3.

3.1 INTRODUCTION

42..... 3.1.1 Lithium minerals and the aim of this lithium study

44..... 3.1.2 The distribution of lithium, rubidium and caesium

3.2 SPODUMENE

- 48..... 3.2.1 Introduction
- 49..... 3.2.2 General distribution and geochemistry
- 53..... 3.2.3 Replacement of spodumene, Norrabees, Namaqualand
- 59..... 3.2.4 Pseudomorphic replacement or seritization of spodumene, Noumas, Namaqualand
- 64..... 3.2.5 Spodumene from SW. Witkop pegmatite, Tantalite Valley, Namibia
- 68.... 3.2.6 Discussion

3.3 PETALITE - MONTMORILLONITE

- 71..... 3.3.1 Introduction
- 73..... 3.3.2 Petalite replacement by albite
- 74..... 3.3.3 Petalite in association with yellow-black tourmaline

3.4. REPLACEMENT PHENOMENA IN AMBLYGONITE-MONTEBRASITE

- 80.... 3.4.1 Introduction: amblygonite-montebbrasite
- 84.... 3.4.2 Primary and secondary montebbrasite, and apatite: replacement by mica
- 94.... 3.4.3 Montebbrasite-natromontebbrasite inclusions
- 97.... 3.4.4 Montebbrasite, crandallite, topaz and cleavelandite
- 102.. 3.4.5 Brazilianite, montebbrasite and apatite
- 108.. 3.4.6 Montebbrasite, apatite, and tantalite
- 110.. 3.4.7 Montebbrasite, indicolite, lithian mica and Mn-apatite
- 114.. 3.4.8 Summary - amblygonite-montebbrasite alteration
- 116.. 3.4.9 Discussion- montebbrasite alteration

3.5. LITHIOPHILITE-TRIPHYLITE AND ASSOCIATED MINERALS

- 117... 3.5.1 Occurrence and geochemistry
- 121... 3.5.2 Conclusions - composition of postmagmatic fluids effecting the metasomatic alteration of primary lithium minerals

3.6. LITHIAN MICA

- 123.... 3.6.1 Introduction
- 125.... 3.6.2 Occurrence and geochemistry
- 130... 3.6.3 Replacement characteristics of Li-mica

PART III

TANTALUM MINERALIZATION

CHAPTER 4. COLUMBITE-TANTALITE, WODGINITE AND TAPIOLITE

Page

136.... 4.1. INTRODUCTION - TANTALUM MINERALS

4.2. COLUMBITE-TANTALITE: GEOCHEMISTRY AND DISTRIBUTION

138... 4.2.1 Introduction

138.... 4.2.2 Columbite from the Northern Cape pegmatites, South Africa

141.... 4.2.3 Columbite-tantalite from Karibib-Usakos pegmatites, Namibia

145.... 4.2.4 Manganotantalite from Tantalite Valley, Namibia and Steinkopf, Namaqualand

4.3. REPLACEMENT PHENOMENA IN MANGANOTANTALITE

147.... 4.3.1 Replacement of manganotantalite by ferrotantalite, Rubicon, Karibib

150.... 4.3.2 Manganotantalite lamellae in microlite, Rubicon, Karibib

167.... 4.3.3 Manganotantalite, M1 pegmatite, Okatjimukuju, Karibib

4.4. WODGINITE

174.... 4.4.1 Introduction

176... 4.4.2 Wodginite associated with manganotantalite, M3 pegmatite, Okatjimukuju, Karibib

186.... 4.4.3 Discussion - geochemical considerations

189.... 4.5. TAPIOLITE

194... 4.6. DISCUSSION : COLUMBITE-TANTALITE, WODGINITE AND TAPIOLITE

CHAPTER 5. MICROLITE

Page

- 199.... **5.1. INTRODUCTION**
- 201.... **5.2. PRIMARY MICROLITE**
- 205.... **5.3. SECONDARY MICROLITE**
- 211.... **5.4. URANOAN MICROLITE AND URANMICROLITE**
- 223.... **5.5. DISCUSSION**
- 226.... **5.6. URANIUM PLUMBOMICROLITE**
- 232.... **5.7. GENERAL DISCUSSION**

CHAPTER 6. EXTREME FRACTIONATION OF Rb, Cs , Ba, Ta AND Mn

- 237.... **6.1. INTRODUCTION: THE K/Rb AND K/Cs RATIOS**
- 6.2. RUBIDIUM AND CAESIUM IN LITHIAN MICAS**
- 240.... **6.2.1 Rb, Cs and Li data from the Karibib/Usakos rare-element
pegmatites, Namibia**
- 244.... **6.2.2 Rb, Cs and Li data from rare-element pegmatites in Tantalite
Valley, Namibia and the Steinkopf area, Namaqualand**
- 250.... **6.3. RUBIDIUM AND CAESIUM IN K-FELDSPAR**
- 257.... **6.4. BARIUM AND THE Ba/Rb RATIO**
- 260.... **6.5. Fe/Mn VERSUS Nb/Ta FRACTIONATION TRENDS**
- 266.... **6.6. THE K/Rb VERSUS Nb/Ta RATIOS IN TANTALITE
MINERALS AND K-FELDSPAR**

PART IV

DISCUSSION AND CONCLUSIONS

CHAPTER 7. PETROGENESIS OF LITHIUM PEGMATITES

268.... 7.1. CLASSIFICATION OF RARE-ELEMENT PEGMATITES

271... 7.2. GENERAL PETROGENESIS OF LITHIUM PEGMATITES

7.2.1. Pegmatite zonation - a framework.
Introduction : lithium minerals

273.... 7.2.2 Crystallization of primary lithium minerals and lepidolite

277.... 7.2.3. The melt and supercritical fluid and the process of accumulation
of volatiles: Jahns and Burnham model

280..... 7.2.4. Late stage fluid phases (hydrothermal stage of pegmatite
formation)

283.... 7.2.5. The pegmatite P-T regime

284.... 7.2.6 Evidence of hydrothermal activity: the effect of postmagmatic
fluids

7.3. PARAGENETIC SEQUENCE OF THE RARE-ELEMENT PEGMATITES

287.... 7.3.1. Pegmatites in the Karibib-Usakos area, Karibib, Namibia

289.... 7.3.2. Paragenetic sequence of mineral assemblages in the Tantalite Valley,
Namibia and the Steinkopf area pegmatites, Namaqualand

294.... 7.3.3. Thermogravitational diffusion

297.... 7.3.4. Derivation of the rare-element pegmatites

297.... 7.3.5. " Disequilibrium versus equilibrium fractional crystallization"

300.... 7.3.6. Derivation of fertile granites

CHAPTER 8. CONCLUSIONS

303.... REFERENCES

PART V

APPENDICES

APPENDIX 1 THE MINERALIZED PEGMATITES	Page
A1.1. KENHARDT AREA, NORTHERN CAPE, SOUTH AFRICA	A1
A1.2. STEINKOPF AREA, NAMAQUALAND, SOUTH AFRICA	A4
A1.3. TANTALITE VALLEY, WARMBAD, NAMIBIA	A7
A1.4. KARIBIB-USAKOS-CAPE CROSS, NAMIBIA	A11
APPENDIX 2 ANALYSES AND METHODS	
A2.1. ANALYSES	A12
A2.2. ANALYTICAL METHODS	A20
APPENDIX 3 SAMPLE NUMBERS	A24

Index to Plates

Frontispiece and 2.1	
Plate 2.2,2.3	25
2.4,2.5	26
2.6a,2.6b	27
2.7,2.8	28
CHAPTER 3	
3.1a,3.1b	56
3.2	57
3.3a,3.3b	58
3.4a,3.4b	63
3.5,3.6	70
3.7	77
3.8,3.9	78
3.10	79
3.11,3.12	90
3.13,3.14	91
3.15,3.16	92
3.17,3.18	93
3.19	100
3.20	101
3.21a,3.21b.....	105
3.22,3.23	106
3.24a,b,c	107
3.25,3.26	113
3.27	133
3.28,3.29	134
3.30	135
CHAPTER 4	
Plate 4.1,4.2	149
4.3	153
4.4	156
4.5	162
4.6a,4.6b	165
4.7	169
4.8a,4.8b	170
4.9	171
4.10,4.11	172
4.12,4.13a,b	177
4.14	193
CHAPTER 5	
5.1	206
5.2,5.3	207
5.4,5.5	208
5.6,5.7	209
5.8	212
5.9,5.10	217
5.11,5.12	221
5.13,5.14	222
5.15,5.16	228a
5.17	228b
5.18	228c

Index to Figures

Figure 2.1..	10
2.2	13
2.3	14
2.4	15
2.5	16
2.6	17
2.7	21
2.8	23
2.9	31
2.10	32
CHAPTER 3		
3.1a	44
3.1b	47
3.2	60
3.3	65
3.4	67
3.6	112
3.7	115
3.8	120
3.9	128
CHAPTER 4		
Figure 4.1	139
4.1a,4.1b	144
4.2	151
4.3	152
4.4	155
4.5	166
4.6	173
4.7	180
4.8	181
4.9a,4.9b	184
4.10a,4.10b	192
4.11a,4.11b	196
4.12a,4.12b.....	197
4.13	198
CHAPTER 5		
Figure 5.1a	202
5.1b,5.1c	203
5.2	213
5.3	219
5.4	220
5.5	229
CHAPTER 6		
Figure 6.1	240
6.2	241
6.3	242
6.4,6.5	243
6.6	245
6.7,6.8	246
6.9	251
6.10	252
6.11	254
6.12,6.13	258
6.14	259
6.15a,6.15b	262
6.16a,6.16b	263
6.17	264
6.18	267
CHAPTER 7		
Figure 7.1,7.2,7.3	291-293

PART I

INTRODUCTION

Chapters 1 and 2

PANORAMA FROM TANTALITE VALLEY, WARMBAD, NAMIBIA



FRONTISPIECE. The Orange River which marks the border between South Africa and Namibia, as seen from Signalberg, Tantalite Valley, Namibia, 10 km to the north.

**LITHIUM AND TANTALUM MINERALIZATION IN
RARE-ELEMENT PEGMATITES FROM SOUTHERN AFRICA**

PART I

INTRODUCTION

CHAPTER 1. AIM AND INTRODUCTION

1.1. AIM

The aim of this thesis is to discuss the petrogenesis of some lithium and tantalum rare-metal pegmatites from South Africa and Namibia involving:

- 1) Crystallization of primary Li-minerals, petalite, spodumene and amblygonite
- 2) Crystallization of cleavelandite-albite and lepidolite (lithian mica) units
- 3) Primary crystallization of Ta-minerals in cleavelandite and lepidolite zones
- 4) Rb-K, Cs-K, Ta-Nb and Mn-Fe fractionation and element enrichment involving differentiation
- 5) Li-mineral and Ta-mineral replacements at low T

in relation to the magmatic and fluid stages of pegmatitic evolution.

The thesis is set out in the following way: -

CHAPTER 2 describes the four field areas being studied and classifies the pegmatites in relation to a general introduction to pegmatites and in particular to pegmatites containing rare-metals. Their zonal structure is described in relation to the general crystallization sequence.

The four areas being studied are as follows:

- Area 1. The eastern Kenhardt-Gordonia pegmatites, Northern Cape, South Africa
- Area 2. The Steinkopf pegmatites, Namaqualand, Northern Cape, South Africa
- Area 3. The Tantalite Valley, pegmatites, south of Warmbad, Namibia
- Area 4. The Karibib-Usakos-Cape Cross pegmatites, central and eastern, Namibia

CHAPTER 3 describes the lithium minerals, from the point of view of i) geochemistry and occurrence and ii) initial formation in relation to the pegmatite internal zonation and the paragenetic sequence of mineral assemblage and iii) mineral intergrowths and replacements and pseudomorphic replacements of the primary lithium minerals.

CHAPTERS 4 and 5 describe and document the geochemistry and occurrence of tantalum minerals, as both primary occurrences and replacement phenomena. The minerals are placed in a paragenetic sequence according to Ta-content.

CHAPTER 6 describes the fractionation trends of Ta-Nb, Mn-Fe in certain tantalum minerals and Rb-K, Cs-K in lithium-rich mica through the pegmatite evolution.

CHAPTER 7 discusses the petrogenesis and relates the lithium and tantalum minerals to the magma and fluids throughout the evolution of the pegmatites.

The term primary is generally applied to a mineral or an assemblage that appears to have crystallized from a melt \pm the participation of an aqueous fluid phase from the interpretation of Jahns and Burnham (1969). Minerals generally are regarded as secondary or replacement only if recognizable evidence of replacement, for example, pseudomorphism, crystallographic continuous relicts of a host phase or embayment at crystal edges, is apparent.

1.2. INTRODUCTION

Most pegmatite fields are genetically related to large granite intrusions or high-grade metamorphism. They are an important source of rare-elements such as lithium, caesium, rubidium, beryllium, tantalum, niobium and sometimes bismuth, yttrium and Rare Earth Elements. In this study, lithium and tantalum mineralization has been specifically investigated. However, it is impossible to isolate these mineralizations from rubidium and caesium in the case of lithium, and niobium is part of an isomorphous series with tantalum. Also bismuth mineralization is compatible with tantalum minerals, it has therefore been included in a crystallization sequence where it is closely associated with tantalite.

It has been observed that tantalum and lithium are enriched in granite pegmatites of the rare-element class. Tantalum is enriched in lithium-bearing pegmatites (von Knorring 1970, 1985b, von Knorring and Fadipe, 1981). Niobium may be enriched in pegmatites which do not contain lithium minerals and particularly in typical beryl-bearing pegmatites.

In this thesis tantalum mineralization and fractionation has been studied throughout the mineral zones of the pegmatites. Commonly, the last zones to crystallize, zones proximal to the core and the replacement zones, are richer in tantalum and poorer in niobium (von Knorring et al. 1984). Tantalum enrichment has been studied in rare-

element pegmatite areas: firstly in those with 1100 my ages ; secondly, those with 550 my ages. Thus the similarities and dissimilarities of source and therefore derivation from parental granites can be considered. For comparison, tantalum-niobium has been studied in a fourth group of pegmatites, which generally may be considered to be Li-poor and Be-rich, from the same Pegmatite Belt of 1100 my age.

The enrichment and fractionation of Ta may be considered as a ratio of Ta:Nb: - the ratios of pairs of chemically coherent elements such as Ta:Nb, Rb:K and Cs:K are found to increase in pegmatite minerals in contrast to the behaviour in common magmatic rocks (Ahrens, 1966 ; Cerny and Ercit, 1985). Extreme differentiation of melt is required to achieve changes of these ratios (Moller, 1989) because of the nearly identical chemical behaviour of the related element pairs i.e. similarity in ionic radii and valence (Ahrens, 1966).

Therefore the patterns of Ta enrichment and fractionation in terms of both the Ta:Nb and Mn:Fe ratios in tantalum minerals, specifically tantalite, manganotantalite and ferrotantalite or tapiolite, columbite, manganocolumbite, ferrocolumbite, wodginite and microlite, will be studied within pegmatites of 3 separate groups in a Pegmatite Belt lying along the Orange River on the South African, Namibian border and a 4th group of pegmatites of different genesis in central Namibia.

As tantalum enrichment is prevalent in Li-pegmatites, lithium minerals, specifically petalite, spodumene, amblygonite and lithian mica (lepidolite) have been studied. The occurrence of lithium minerals is late in the pegmatite sequence (von Knorring, 1970, 1985, 1987). The chemistry of these minerals has been investigated by many authors by various analytical techniques, however, the electron microprobe has revealed alteration phenomena which will be related to late metasomatic fluids. In addition, as the enrichment of Li in pegmatites is a late phenomenon, how and why is this achieved in terms of magmatic differentiation and do lithium minerals

crystallize from a magma or a hydrous fluid? Rb and Cs are enriched in K-minerals, specifically lithian-mica (lepidolite) and K-feldspar. The chemically coherent pairs Rb:K, Cs:K and Rb:Cs are studied in lithian mica and the enrichment and fractionation of Rb and Cs in the pegmatite co-genetic groups will be studied to establish similar and diverse patterns in comparison with Ta enrichment. K-feldspar is normally common throughout the pegmatite zones from early to late crystallizates. It is therefore a useful mineral from which to study Rb and Cs fractionation and to verify the data from the lithian mica.

Finally Li and Ta petrogenesis will be discussed in terms of magma-fluid medium with metasomatic alteration by aqueous fluids. The ultimate aim is to consider a common or diverse source for the pegmatite formations by studying the mineralization patterns of Ta and Li (+Rb, Cs) in each group and to establish a paragenetic sequence for Ta and Li minerals in terms of a magma or fluid. The geochemical signatures of rare-element pegmatites are significant because they represent the extremes of fractionation trends encountered in the final stages of granitic differentiation in high-silicon, metaluminous to peraluminous granites. The study of tantalum and lithium mineralization with selected examples such as the Ta-Nb, Mn-Fe, Rb-K, Cs-K ratios may best document the extreme character of rare-element magmatic stages of granitic crystallization during the transition into supercritical and subcritical regimes (London, 1984a, b, 1987, 1992).

CHAPTER 2.

THE MINERALIZED PEGMATITES AND THE GEOLOGICAL OCCURRENCE OF LITHIUM AND TANTALUM

2.1 INTRODUCTION

The aim of this chapter is to describe features of pegmatites in the four areas under study, as observed in the field, especially from the point of view of lithium and tantalum mineralization. More detailed descriptions are given in Appendix 1.

Cerny (1982) pointed out that Ginsburg et al. (1979) provided the most general classification of granitic pegmatites based on essentially geological - petrogenetic criteria refined from several earlier versions. They distinguished four pegmatite formation types characterized by different depths of consolidation, mineralization and relations to igneous processes and metamorphic environment.

1. Pegmatites of shallow depth (1.5-3.5 km) located in upper parts of epizonal granites, intrusive into rocks of lowest metamorphic grade (generating quality beryl).
2. Pegmatite formation of intermediate depths (3.5-7 kms): rare-element pegmatites with Li, Rb, Cs, Be, Ta, (Sn, Nb), mineralization, generated by fractionation of differentiated granites.

3. Pegmatite formation of great depth (7-8 to 10-11 km), hosted by metamorphic rocks of almandine - amphibolite facies (Winkler, 1967) and carrying minimal rare-element mineralization.

4. Pegmatite formation of maximal depths (above 11 km), usually with no obvious granitic parents.

Pegmatites may be either homogeneous or internally zoned. Magmatic differentiation adequately explains the sequence of zones in zoned pegmatites including the abrupt appearance of Li-minerals in quantity. The sequence of 11 mineral assemblages in zoned pegmatites reported by Cameron et al. (1949) on their work with the pegmatites of South Dakota is listed in Table 2.1. Not all assemblages occur in all the pegmatites or in all the pegmatite districts. Crystallization proceeded from the country rock contact inward because no outer assemblage cuts an inner assemblage, but inner assemblages do cut outer assemblages.

TABLE 2.1. Sequence of zones in pegmatite (after Cameron et al. 1949)

1	Plagioclase + quartz + muscovite	OUTER ZONES
2.	Plagioclase + quartz	
3.	Quartz + plagioclase + K-feldspar + muscovite + biotite	
4.	K-feldspar + quartz	
5.	K-feldspar + quartz + plagioclase + amblygonite + spodumene	
6.	Plagioclase + quartz + spodumene	
7.	Quartz + spodumene	
8.	Lepidolite + plagioclase + quartz	
9.	Quartz + K-feldspar	
10.	K-feldspar + plagioclase + Li-mica + quartz	INNER ZONES
11.	Quartz	

Zones 1-11, in order of crystallization

The first four assemblages are feldspar-rich and differ from granite only in the ratio of one feldspar to another and in the abundance of muscovite. Where muscovite is abundant, potassic feldspar (perthite) is ordinarily absent or sparse. The limited data show that these assemblages may be richer in Al_2O_3 than many granites and may have in some circumstances reacted with the country rock or lost alkalies to it (Stewart, 1978). Lithium minerals do not become a major component until assemblage 5, but persist through assemblages 5 to 8. The content of quartz increases in these assemblages and quartz becomes dominant in assemblage 7. The core commonly is almost entirely quartz. A brief examination of some 60 pegmatites in the Karibib and Warmbad areas of Namibia by Cameron (1955) indicated that many of these pegmatites have internal structures comparable to those described from South Dakota; however, petalite is common in Karibib whereas spodumene is prevalent in South Dakota.

Replacement zones are not well defined in the scheme in Table 2.1. Ginsburg (1955, 1960) developed a simple geochemical classification scheme; a sequence in the development of primary zones: -

Na,Ca (plagioclase) - K (K-feldspar) - Li (spodumene, amblygonite)

and a sequence of secondary metasomatic units: -

Na (albite) - K (muscovite, late K-feldspar) - Li (Cs) (lepidolite, pollucite).

Petalite must be included in the primary zones with spodumene and amblygonite. However, the term "secondary metasomatic units" may not encompass correctly huge replacement units of coarse-grained cleavelandite albite which may have been formed under subsolidus conditions and which cross-cut earlier primary zones. Evidence of replacement is not always clear, however, the author would prefer to consider cleavelandite for example to be a primary mineral occurring in a replacement zone, and would prefer to use the term "secondary metasomatic" for fine-grained pseudomorphic replacements.

Lithium, a typical trace element in light residual rocks such as granite, is relatively concentrated in the residual solutions of granite pegmatites and very concentrated in large unique granite pegmatites where it occurs in the minerals spodumene, petalite, amblygonite and lepidolite to such an extent to make exploration viable; granite pegmatites of this type are termed "Lithium pegmatites" (von Knorring, 1985, 1987). Normally, within an extensive pegmatite field only a few distinct Li-pegmatites are found but in some pegmatitic terrains, especially in parts of Central and Southern Africa, Madagascar, Central Asia (including Afghanistan), U.S.A. and Canada distinct geochemical provinces can be established where Li-pegmatites predominate. The lithium pegmatites in the Karibib-Usakos-Cape Cross region of Namibia, an area 200 km long and 100 km wide is comparable to the most extensive Li-pegmatite fields in other parts of the world (von Knorring, 1985a). Figure 2.1. shows an example of a complex zoned lithium pegmatite in the Karibib region of Namibia.

Whilst Li-pegmatites have Be phases, not all beryllium pegmatites have Li phases in sufficient quantities to be termed Li-pegmatites. Ta enrichment is prominent in Li-pegmatites, however Nb-Ta phases may be the more common mineralization in beryl pegmatites (see Hugo, 1969; Baldwin, 1979; von Knorring, 1985).

The lithium aluminosilicates, spodumene, petalite and lepidolite are the most abundant and frequently encountered lithium minerals in pegmatites, they are extremely sensitive to changes in their physical and chemical environments and are therefore excellent indicators of subsolidus conditions in pegmatites. The stability relations amongst these minerals are fundamental to lithium pegmatite petrogenesis and their phase relations in natural and experimental conditions have been documented by Burt et al. (1977), Stewart (1978), Burt and London (1982) and London (1984a, 1986a, 1990).

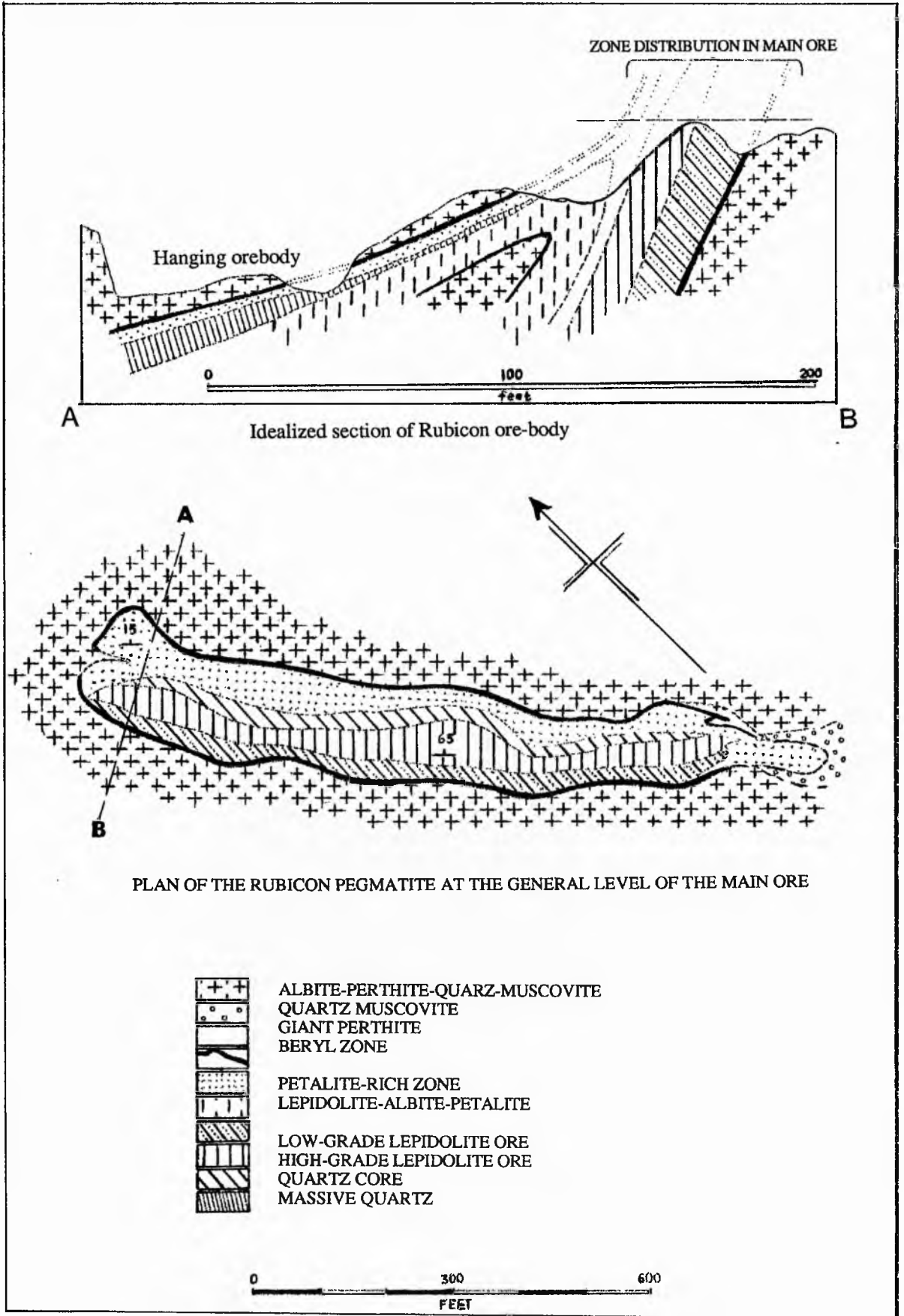


Fig. 2.1. Sections through the Rubicon lithium pegmatite showing complex zonation (after Roering and Gevers, 1962), Okongava Ost, Karibib, Namibia

2.2. THE MINERALIZED PEGMATITES

2.2.1 Introduction

Lithium and beryllium pegmatites have been examined from four separate areas. (1) the Kenhardt area, North Western Cape, South Africa, (2) the Steinkopf area Namaqualand, (3) Tantalite Valley, south of Karasburg, Namibia and (4) the Karibib-Usakos district of Namibia.

The pegmatites discussed here are largely from two structural provinces, namely the orogenic zones of (i) the Kibaran Belt (1100 ± 200 m.y.) and (ii) the Pan-African Belt (550 ± 100 m.y. Clifford, 1966). Some aspects of field occurrence are summarized below together with certain mineralogical data, while detailed descriptions are given in Appendix 1 both from the literature and with additional information from the present examination. In terms of the granite pegmatite classification of Ginsburg et al. (1979), the majority of pegmatites discussed are mineralogically similar to Type 2, rare-element pegmatites of intermediate depth (3.5 - 7 km) with Li, Rb, Cs, Be, Ta, (Sn, Nb) mineralization.

Areas 1-3 which lie in the 1100 ± 200 m.y. Kibaran Structural Belt occur essentially in a well defined pegmatite province known as the Namaqualand, Kenhardt, Gordonia Pegmatite Belt some 30-60 km wide and 450 km long which extends from Putsonderwater in the east to Steinkopf in the west, in the Northern Cape of South Africa and includes an area north of the Orange River in Namibia in the central part of the Belt known as Tantalite Valley (see Figs. 2.2, 2.3). Only the major lithium bearing pegmatites in this belt have been examined and in common with other large pegmatite regions of the world, the Li-pegmatites are found sporadically or locally concentrated.

The pegmatites are connected with Precambrian granites and granite gneisses and are intrusive into the Archaean rocks of the Kheis system (Gevers et al., 1937; Hugo, 1969; von Backström and de Villiers, 1972; von Backstrom, 1976; Moore, 1975). Although most of the pegmatites are rather small and poorly mineralized, many are of a considerable size (see Appendix 1.2) and have been mined over the past fifty years for beryl, lithium, tantalum and other rare-metal minerals. In this particular region, smaller lithium deposits are found in the easternmost part of the pegmatite belt north and southeast of Kenhardt (see Fig. 2.2). Another important area of lithium mineralization is located at Tantalite Valley, approximately 60 km west of Onseepkans. By far the most extensive concentration of lithium pegmatites occurs in the eastern part of the belt, in the desert region north to northeast of Steinkopf in Namaqualand and extends as far as Goodhouse on the Orange River (see Fig. 2.3). Although the known lithium deposits form a minor part of the pegmatites, they are in many respects the more productive, containing larger varieties and concentrations of economic minerals.

Area 4, lies in the 550 ± 100 m.y. Pan African Belt. The major lithium pegmatites of Namibia are confined to the central part of the country in the Karibib and Swakopmund districts (see Fig. 2.4). In the Karibib-Usakos-Cape Cross areas, numerous mineralized pegmatites have been known for many years as important sources of Li, Cs, Be, Nb, Ta and Bi minerals. This pegmatite field is some 200 km long and up to 100 km wide. The pegmatites are connected with late kinematic granites of the Salem Suite that have intruded a variety of sediments of the Damara Sequence (Roering and Gevers 1962; Smith, 1965).

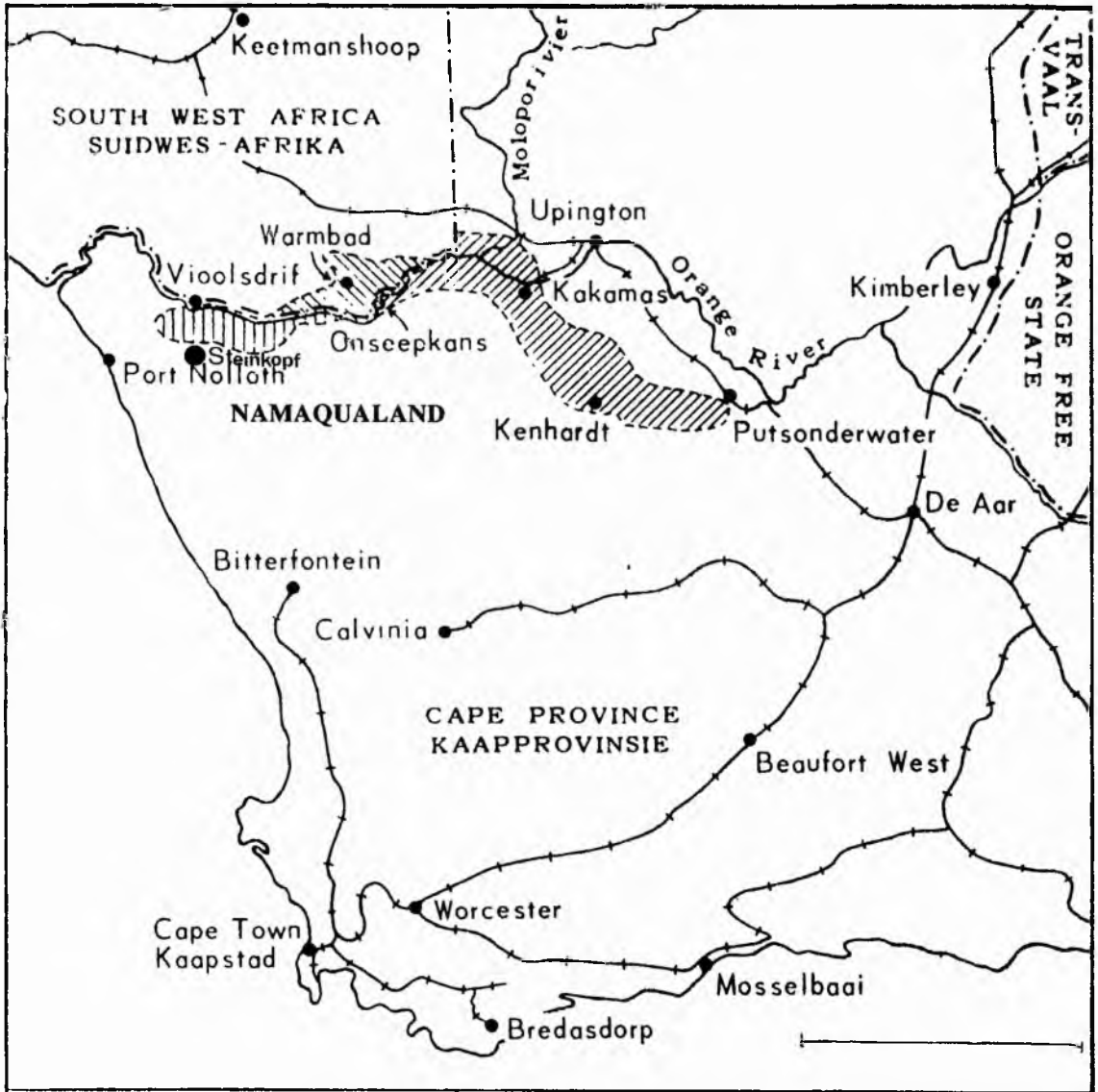


Fig. 2.2. The Cape Province of South Africa, showing the extent of the Pegmatite Belt lying along the Orange River between Putsonderwater and Steinkopf (after Hugo 1969). ▨ represents the Kenhardt-Gordonia Field; ▩ the Tantalite Valley Pegmatite Field and ▮ the Namaqualand Pegmatite Field. Scale bar : 200 km.

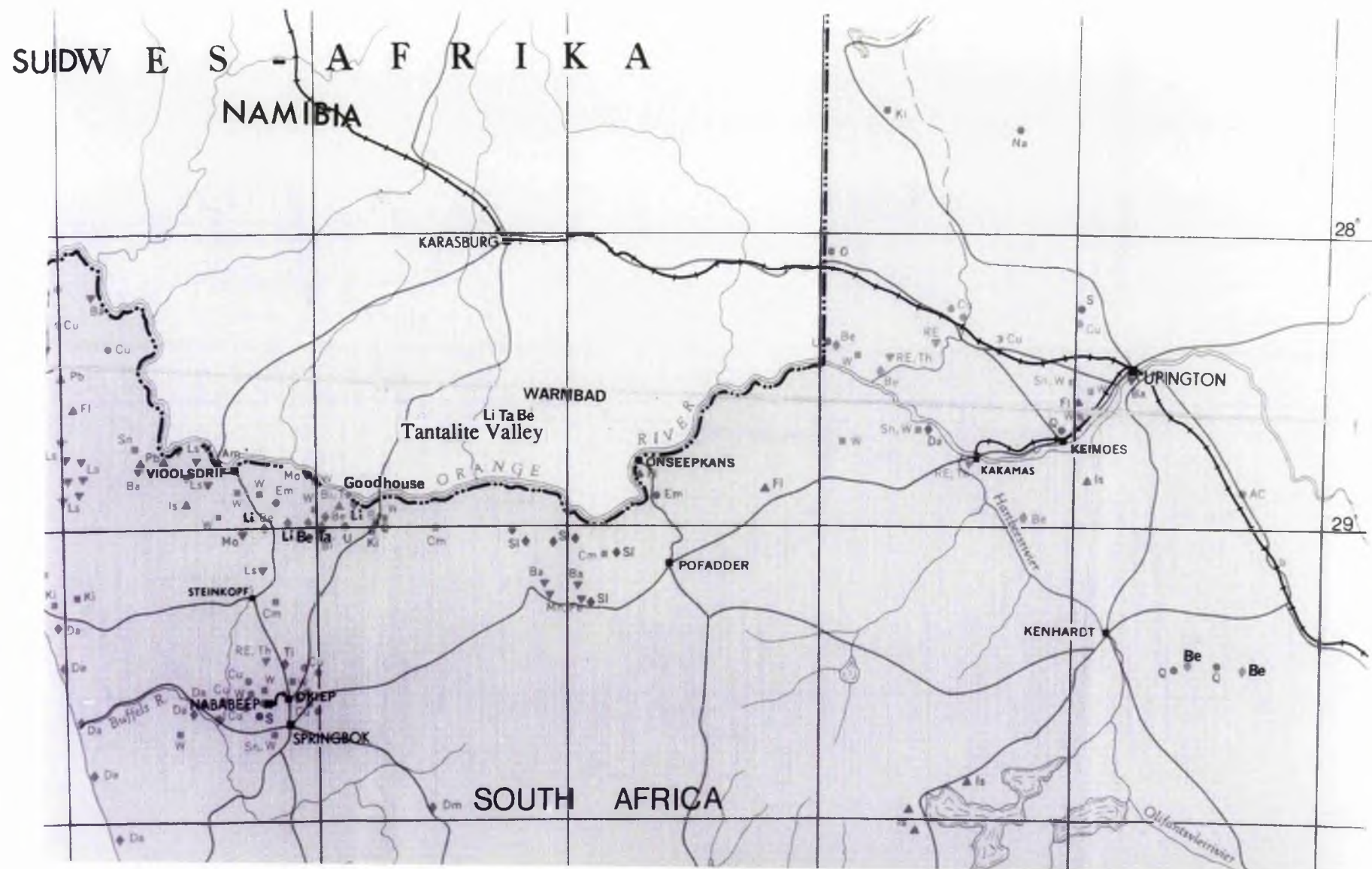


Fig. 2.3. The Orange River section of the Namaqualand Pegmatite Belt from Putsonderwater to Steinkopf showing the three mineralized localities described in the text 1) east of Kenhardt, 2) Tantalite Valley and 3) north and east of Steinkopf. Scale 25miles=1". (after "The Mineral Resources of the Union of South Africa" 1959)

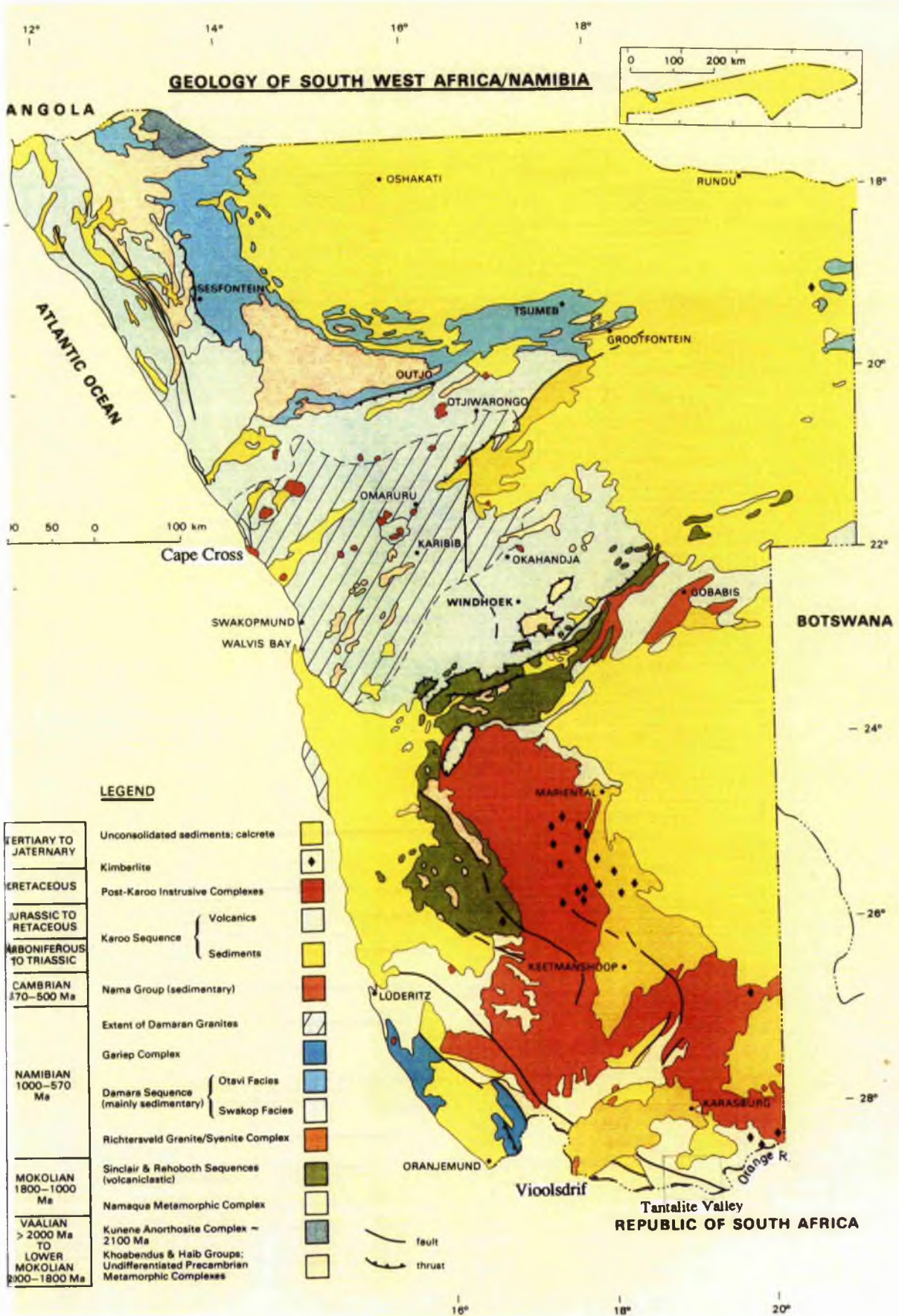


Fig. 2.4. Geological map of Namibia (from Geological Survey Map, 1980) showing the location of two of the pegmatite areas described in the text; the Karibib-Cape Cross area; and the area in the inset box along the Orange River, south of Karasburg which represents the Tantalite Valley Complex (Moore, 1975).

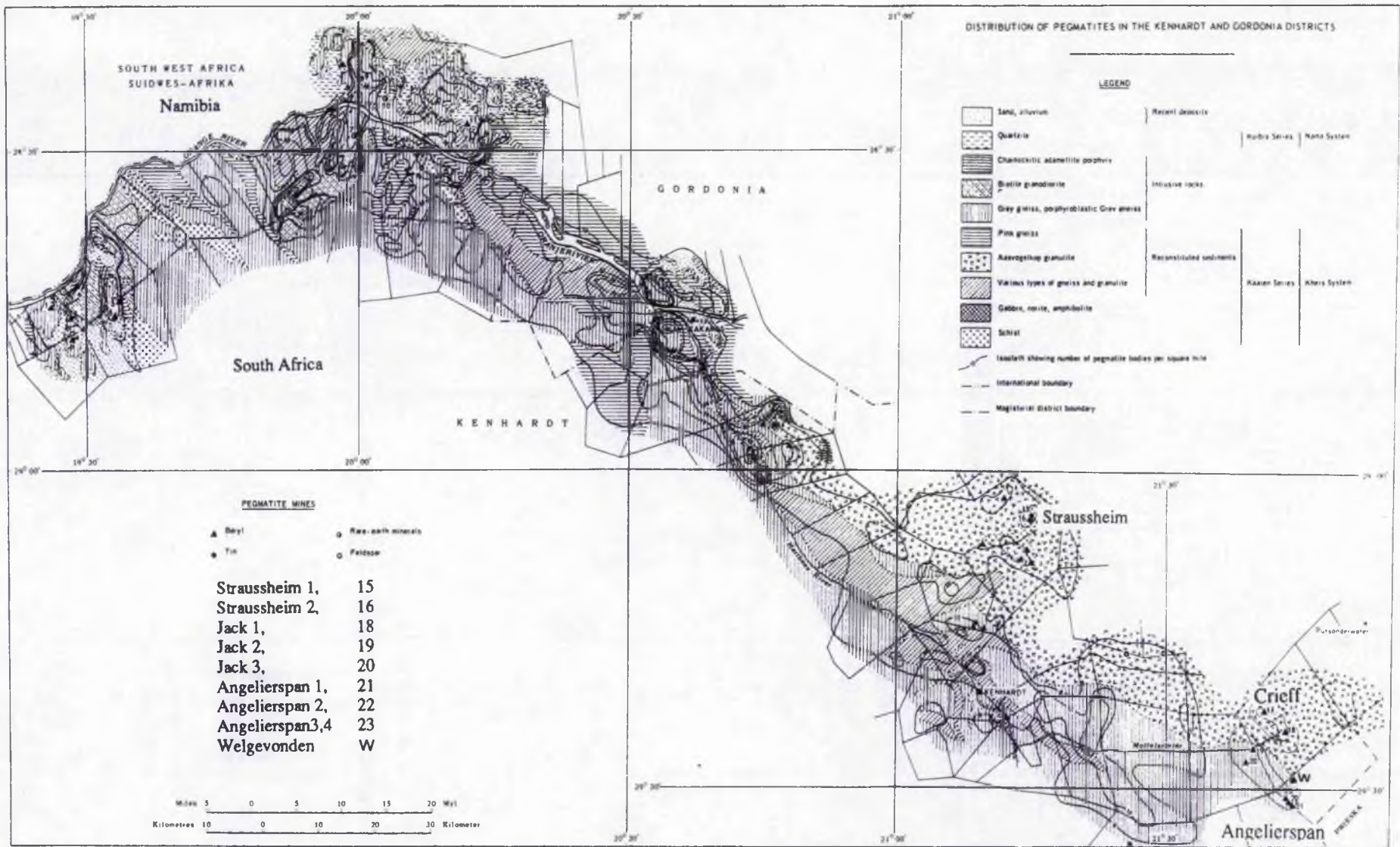


Fig. 2.5. Location of the Angelierspan, Welgevonden, Jack, Crieff and Straussheim pegmatites, Kenhardt District (Area 1 described in the text), Northern Cape, South Africa (after Hugo 1969).

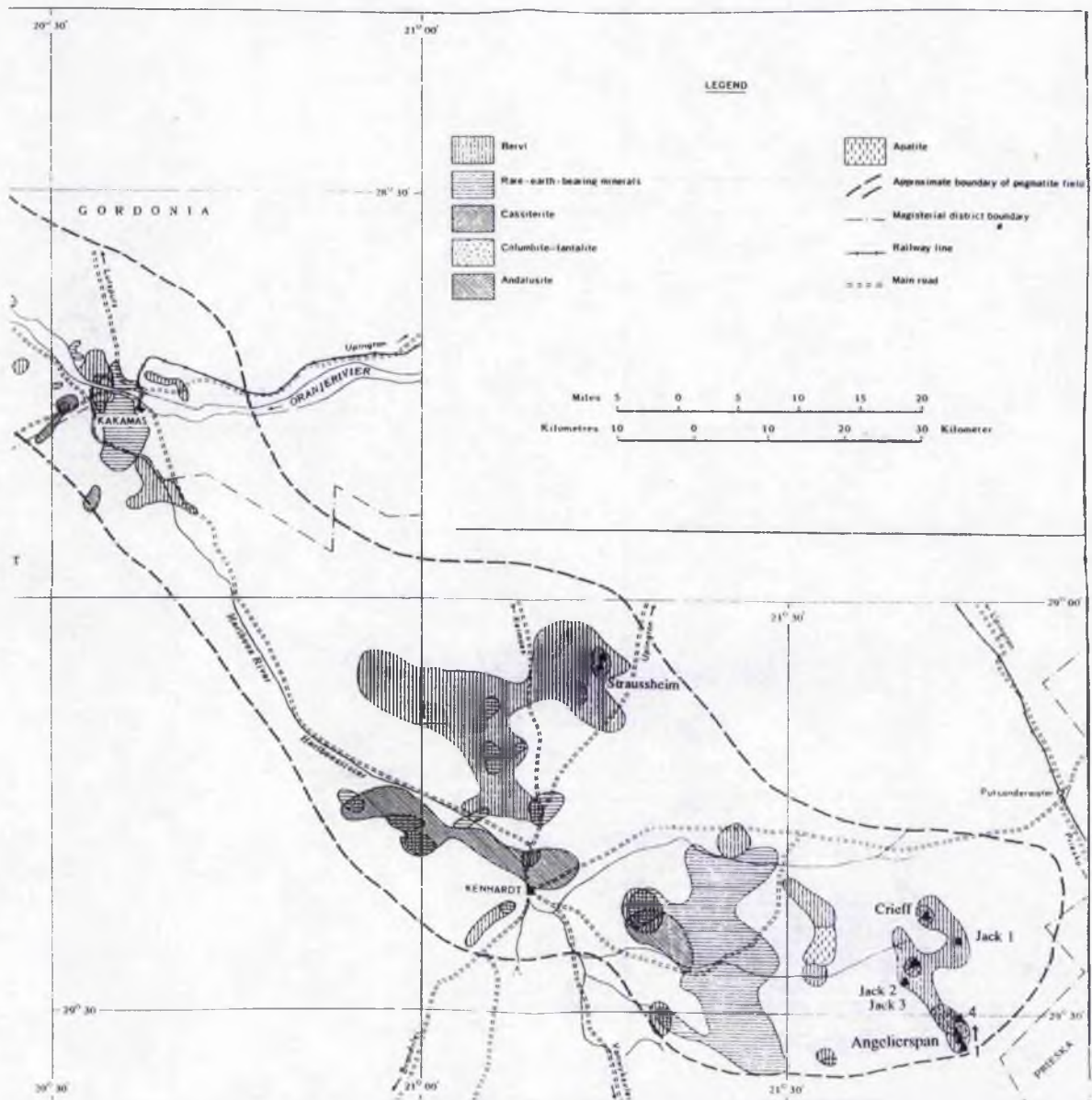


Fig. 2.6. The mineralized pegmatites described in the text in Area 1, the eastern section of the Kenhardt Gordonia field, Northern Cape, South Africa (after Hugo, 1969).

2.2.2 The Kenhardt Area, Northern Cape, South Africa

In the eastern section of the Pegmatite Belt in the Kenhardt District, Northwestern Cape, only two pegmatites Angelienspan No.3 and Jack No.1 show mineralization in the form of Li-mica. Five pegmatites were examined at Angelienspan, Nos. 1-4 and the Welgevonden pegmatite and in addition two pegmatites Jack 3 and Jack 1, situated 8-10 km northeast and north of Angelienspan (see Figs. 2.5, 2.6).

Most of the deposits in this area do not contain Li but contain beryl and columbite-tantalite (Fig. 2.5). The pegmatites lie 88 km south-east of Kenhardt and approximately 9.5 km due south of the homestead of Crieff. One of the major lithium pegmatites, the Crieff Pegmatite, lies about 13 km southwest of Crieff farm. The pegmatite contains in addition to lithium mica, beryl and columbite-tantalite. The pegmatites are essentially well-zoned, bodies which have been excavated along strike for 70-80 m. Thirty five km north of Kenhardt on the farm N'Rougas Noord there are a great number of pegmatites of which two, Strausheim Nos. 1 and 2, are Li and Be-bearing (see Figs. 2.5, 2.6). Strausheim 1 has been extensively excavated for mica, beryl and cassiterite, it contains lithiophilite and related phosphates and spodumene, but the spodumene content is too low for exploitation. The Li content in general in this whole area is minimal in comparison with areas 2-4.

The Angelienspan, Welgevonden, and Jack 3 pegmatites occur in grey gneiss and the Strausheim, Jack 1 and Crieff pegmatites in granulite (Fig. 2.5).

2.2.3. The Steinkopf area, Namaqualand, South Africa

In the Steinkopf region of the Namaqualand Belt lithium minerals are widely distributed, with spodumene of major significance; tantalite is also of major importance. North of Steinkopf (see Figs. 2.2, 2.7) numerous homogeneous and heterogeneous pegmatites (von Backstrom and de Villiers, 1972) occur within a well-defined zone about 8 km wide and 80 km long trending westwards from the Farms Ramansdrift and Hom, east of Goodhouse via Henkries, Norrabees and Kokerboomrand (K, see Fig. 2.7) to east and southeast of Noumas.

The pegmatites form either steeply dipping dykes or massive lenticular bodies with low inclination, ranging in size from mere veinlets to dykes of more than 2 km in length. They contain a variety of minerals including spodumene, lithian mica, beryl, columbite-tantalite, microlite, rare-earth-bismuth and tungsten-minerals, in addition to large amounts of feldspar, quartz and mica. Of these, the lithium minerals are widely distributed, but only spodumene is found in mineable quantities. A systematic search for tantalum minerals in recent times has exposed many new occurrences in the mountainous desert area, covered by sand and surface limestone. Mining, at present is centred on ceramic feldspar, muscovite and tantalum minerals.

The following pegmatites in the area have been investigated and sampled: Noumas, Swartzberg, Kokerboomrand, Uranoop and Norrabees (see Fig. 2.7). Of these, the Noumas lithium pegmatite, the largest mined deposit in the area is about 1000 m long and 10 - 45 m wide and is exposed on the western slope of Blesberg mountain and is emplaced in granodiorite. A parallel, smaller pegmatite, Noumas 2 lies immediately north of the main deposit. The pegmatite zonal sequence is well developed with the intermediate zone carrying the main lithium mineralization in the form of spodumene

which is often intergrown with quartz and replaced by cleavelandite and muscovite, in addition to beryl and tantalite. This zone is best developed on the footwall side of the pegmatite. Spodumene occurs in large concentrations in this zone and in the quartz core margin where laths are frequently seen up to 70 cm in length. A large portion of spodumene is however decomposed by weathering or hydrothermally altered to various clay minerals, the latter phenomenon is often accompanied by a marginal replacement of spodumene by lithian mica. The quartz core unit carries nodules of lithiophilite and the replacement zones are composed mainly of albite with occasional lithian mica, in addition to tantalite, microlite and alkali beryl.

A swarm of lithium pegmatites occurring in the Norrabees area, some 25 km east of Noumas (see Fig. 2.7), represent the greatest concentration of lithium minerals in South Africa (Gevers et al. 1937), and most of these pegmatites have been mined extensively for beryl and spodumene. The most important Norrabees pegmatite, No 1. is exposed for more than 100m on a steep mountainous slope (see Plate 2.2). In the quarry at Norrabees 1, the zoning is well-exposed and of the zones the intermediate one is best developed and consists of a rather uniform mixture of blocky microcline in a finer matrix of cleavelandite, spodumene, lithian mica, lithian tourmaline, quartz and muscovite. Spodumene is mostly fresh, of a pinkish colour, occasionally forming giant-size crystals close to the quartz core. Replacement units composed of lithian mica with cleavelandite carry multicoloured tourmaline, pink beryl and pollucite. The lithian mica is invariably microlite bearing. Spodumene is the major economic mineral in the Norrabees area in addition to beryl, tantalite, pollucite and bismuth minerals.

The other pegmatites which were examined in detail contain much smaller amounts of lithium minerals with tantalite and beryl. The Kokerboomrand, Uranoop and Spodumene Kop pegmatites contain considerable spodumene, a large portion of which is kaolinized and the Uranoop pegmatite has considerable deposits of lithian mica.

UNION OF SOUTH AFRICA, DEPARTMENT OF MINES, GEOLOGICAL SURVEY.

THE PEGMATITE AREA, NAMAQUALAND.

Between STEINKOPF and GOODHOUSE.

Geologically surveyed in 1934 by T. W. Gevers, M.A., Ph.D., D.Sc.

S. H. Houghton, D.Sc.,—Director.

— REFERENCE. —

<p>Alluvium (silt and gravel).</p> <p>Spring Deposits in Hekker's Valley.</p> <p>Limestone Terraces in Hekker's Valley.</p> <p>Surface limestone and lime-concreted gravel.</p> <p>Unconsolidated rock-debris and sand, mostly wind-blown.</p> <p>Quartz and breccia along Steinkopf fault.</p> <p>Dwika Series : Trilites, sandstones and shales.</p> <p>Malmsbury Series : Limestones, shales, flagstones and quartzites.</p> <p>Nieuwvlei Series : Conglomeratic arkoses, grits and quartzites.</p>	<p>INTRUSIVES OF UNCERTAIN AGE (Pans-Pegmatite-Pre-Nama ?). Dykes of Soudanite (S), Spinel-schists (S₂), Microsyenite (MS), altered Comphogryne (C).</p> <p>PRE-NAMA POST-PEGMATITE INTRUSIVES. Dykes of diabase and gabbro (altered).</p> <p>Quartz in general.</p> <p>Pegmatites (P) and Pegmatitic Quartz (PQ).</p> <p>Reddish pegmatitic granites.</p> <p>Quartz porphyry, granite porphyry, etc.</p> <p>Red fucrocratic granite, reddish-yellow spilitic, quartz-fuquar granitite, muscovite gneiss, etc.</p> <p>Granite and gneiss of Namaqualand massif.</p> <p>Porphyritic biotite gneiss.</p> <p>Biotite-sillimanite gneiss and corduroy-sillimanite gneiss.</p>	<p>Muchly Microgranulite, microgranodiorite, etc., grading into granite porphyry, granodiorite porphyry, etc.</p> <p>Basins and biotite-hornblende granite, grading into granodiorite, quartzodiorite, etc.; in part gneissitic.</p> <p>Mixed Rocks : Predominantly diorite (metamocratic), quartz-diorite and granodiorite. Also increasing hornblende granite, biotite granite and microcrystalline varieties.</p> <p>Dark Rocks : Mafic hornblende diorite, hornblende and quartz hornblende, gabbro, olivine norite, pyroxenite, peridotite and dioritic amphibolite and epidiorite.</p> <p>Massive amygdaloidal diabasic lavas.</p> <p>Shaped lavas : epidiorite, greenstones, biotite lapilli, etc. and subordinate acid lavas (fluodolite, etc.).</p> <p>Amphibolites, amphibole schist, biotite granite, etc.</p> <p>Highly recrystallized quartzite (Kaason Series ?).</p> <p>Quartz-sericite, sericite-sillimanite and biotite schists; calc silicate rock on Kotsabees.</p>	<p>ANCIENT INTRUSIVES OLDER GROUP</p> <p>ANCIENT INTRUSIVES YOUNGER GROUP.</p> <p>KARROO SYSTEM.</p> <p>NAMA SYSTEM.</p>
--	--	--	--



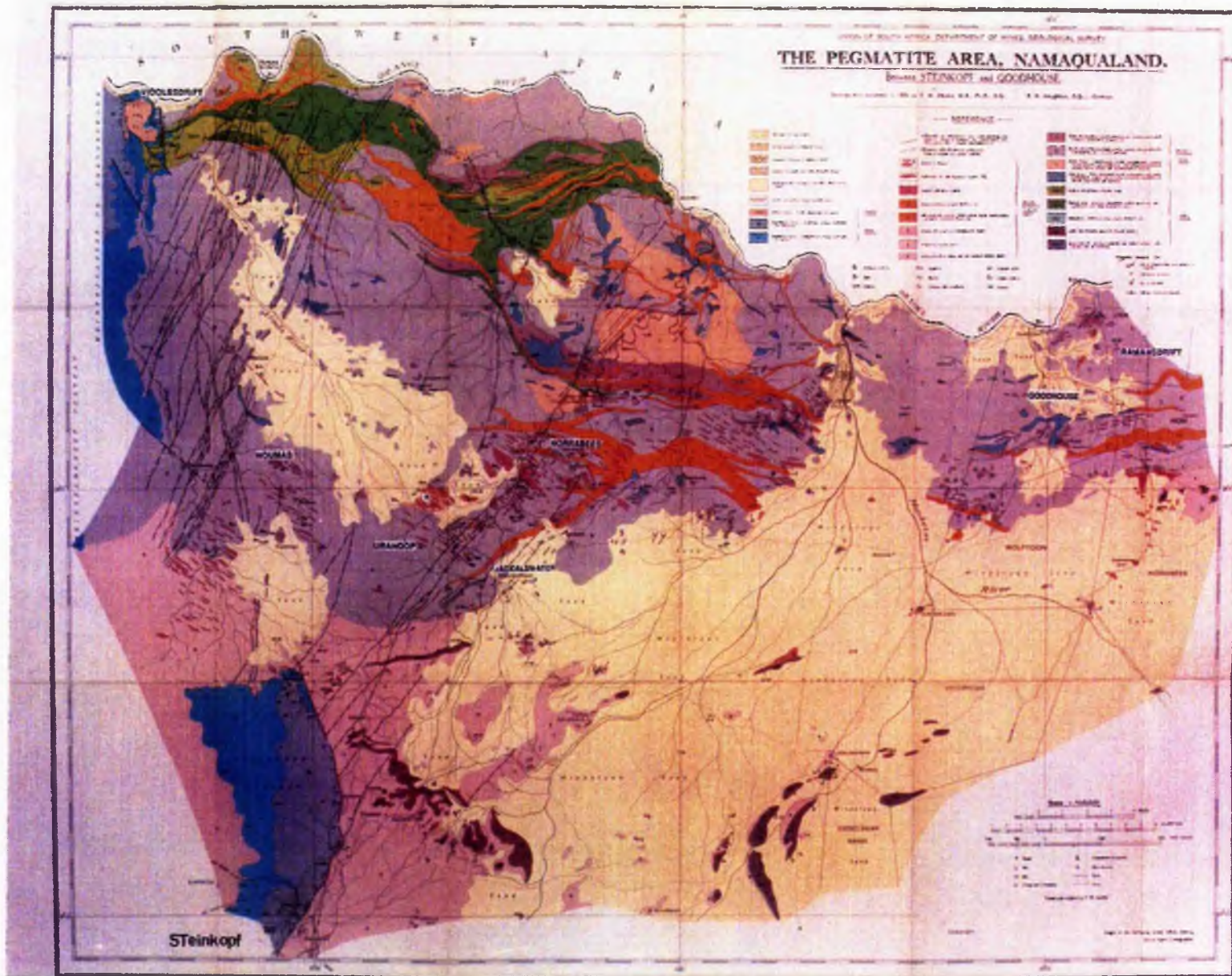


Fig. 2.7. The pegmatite area, Namaqualand; the Nourmas, Norrabees, Uranoop and Kokerboomrand pegmatites described in the text (Area 2). (Geological Survey Map, Gevers, 1934). Key opposite.

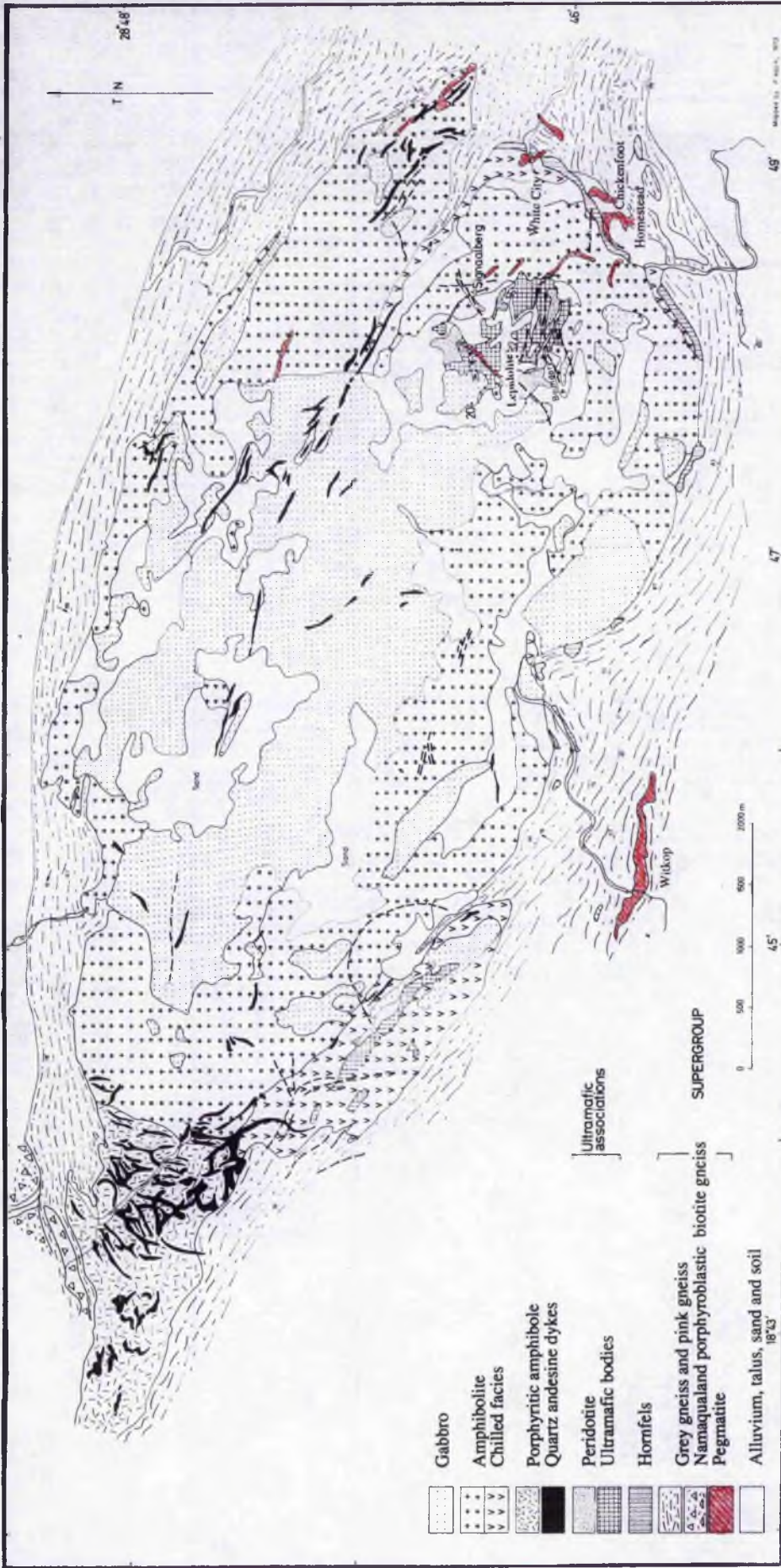


Fig. 2.8. The Tantalite Valley Complex, Warmbad, Namibia showing pegmatites on the Eastern flank described in the text (Area 3) (after von Backstrom, 1976).

2.2.4. Tantalite Valley, Karasburg, Namibia

Tantalite Valley is located at the central area of the Namaqualand pegmatite Belt, in the Karasburg district of Namibia (Figs.2.2, 2.4). It is a mountainous area 50 km square, situated some 40 km south of Warmbad and 10 km north of the Orange River (see Plate 2.1, frontispiece and Plate 2.3). The distribution of economic mineralized pegmatites is related to several periods of deformation and the "Tantalite Valley Complex" which is a poorly mineralized peridotite-gabbroic intrusion, approximately concentric in form (Moore,1975, see Fig. 2.8). The pegmatites which crop out along the steep sides of high mountains (see Plate 2.3) are typically zoned, up to 1,000 m along strike, transgressive and most commonly have shallow angles of dip. The four largest, prominently mineralized pegmatites in the Valley, Witkop, Homestead, White City and Lepidolite and three smaller pegmatites, "Chickenfoot", "T", and Signaalberg (Fig 2.8) have been examined in addition to the SW. Witkop pegmatite on the northeastern flank of the Complex.

The pegmatites emplaced on the eastern flank of the Complex (Fig.2.8) of which Homestead is the largest, have a typical zonal pattern; - i) a contact zone 2-5 cm thick consisting of fine-grained muscovite and quartz with muscovite flakes lying parallel to the contact (see Plate 2.4), ii) a wall zone consisting of albite and muscovite plates iii) an intermediate zone consisting of blocky microcline, cleavelandite and quartz (see Plates 2.5, 2.6) and a quartz core of varying thickness. The smaller pegmatites are named "Chickenfoot" on account of a characteristic wall zone composed of microcline and biotite mica in the shape of a chicken's claw (see Plate 2.7). The "T" pegmatite also contains a "Chickenfoot" wall zone. The Witkop pegmatite on the southern side of the Tantalite Valley Complex is emplaced in grey and pink gneiss (in contrast to the Homestead, White City and Chickenfoot pegmatites which occur partly in amphibolite,



Plate 2.2. The Norrabees pegmatite, the Steinkopf area, Namaqualand



Plate 2.3. The eastern section of the Tantalite Valley Complex, Warmbad, Namibia. The excavations in the background are the Homestead and Chickenfoot pegmatites,

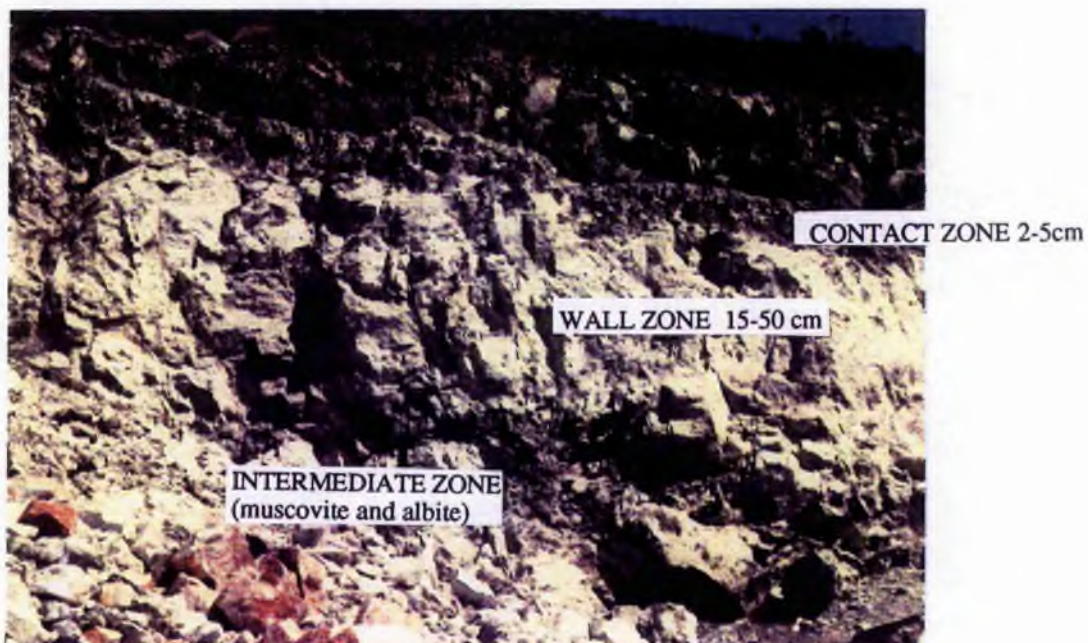


Plate 2.4. The contact (quartz and mica), wall zone (albite and mica) and intermediate zone (muscovite and albite) of the White City pegmatite, Tantalite Valley, Warmbad, Namibia (Main quarry). Height: 7 m.

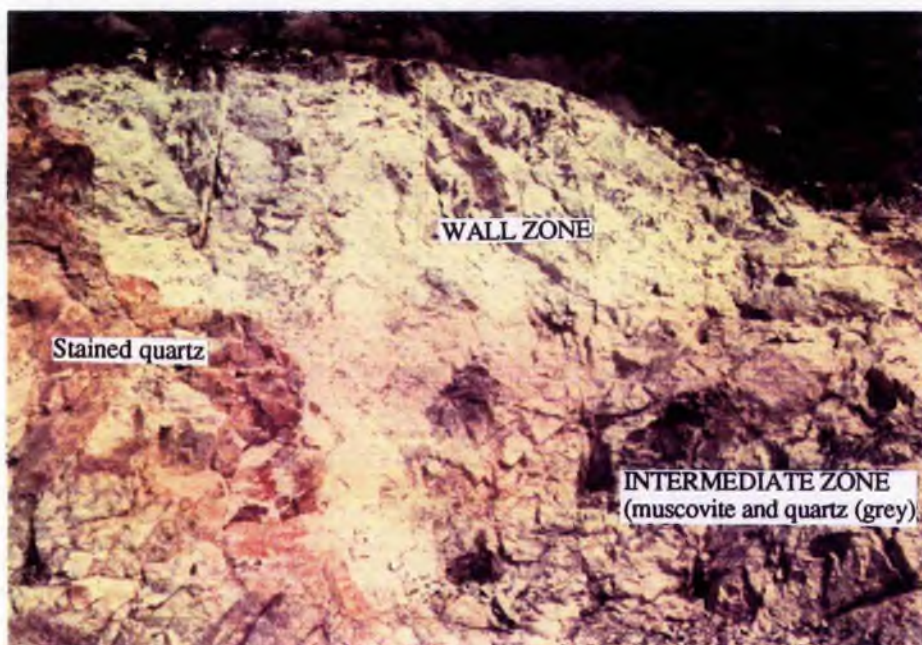


Plate 2.5. Contact, wall and intermediate zone (cleavelandite, blocky microcline) White City pegmatite, Tantalite Valley, Warmbad, Namibia. height of exposure 7m. (Small quarry to north). Mazimum width=15m across

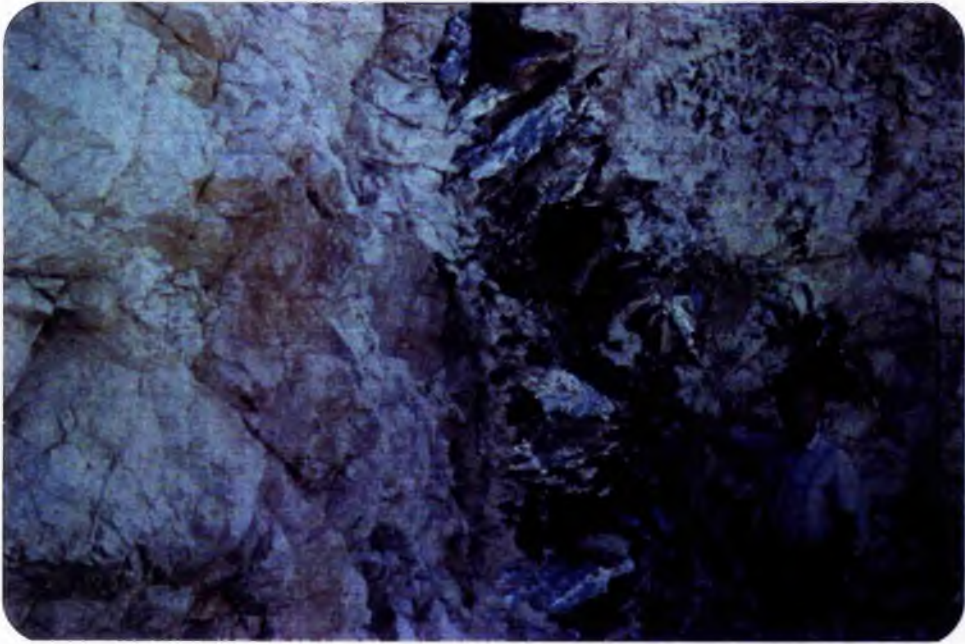


Plate 2.6a. The Witkop pegmatite, Tantalite Valley, Namibia, showing a 50 cm zone of herringbone mica with a "Chickenfoot" wall zone to the right and albite and quartz (stained) to the left.



Plate 2.6b. An extension of Plate 2.6a to the left, showing a cutting through the quartz core (stained) with albite and muscovite and minor blocky microcline.

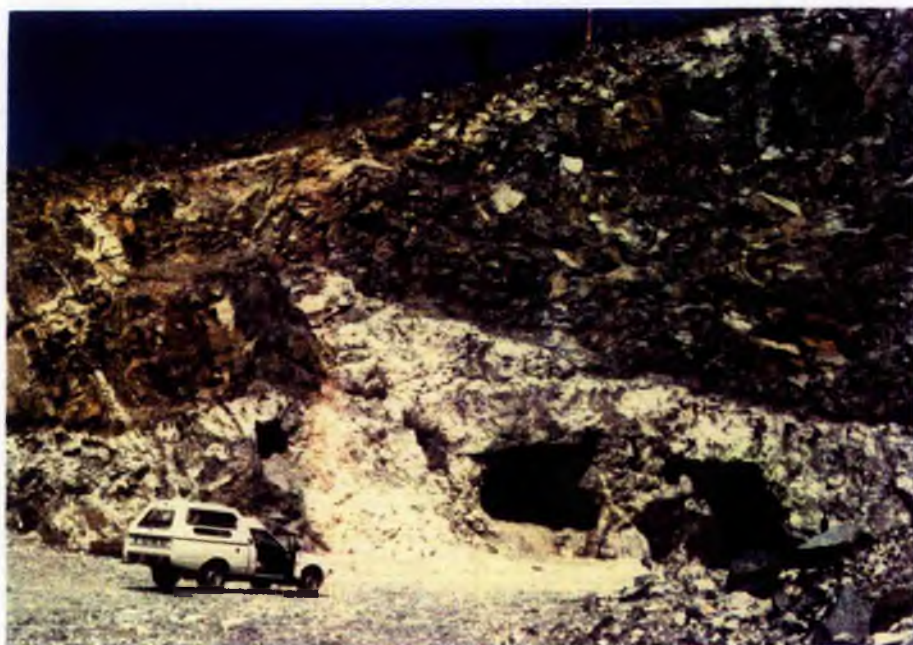


Plate 2.7. The Homestead pegmatite, emplaced in amphibolite, Tantalite Valley, Namibia. The adits indicate the intermediate zone which has been mined for tantalite, beryl and spodumene.

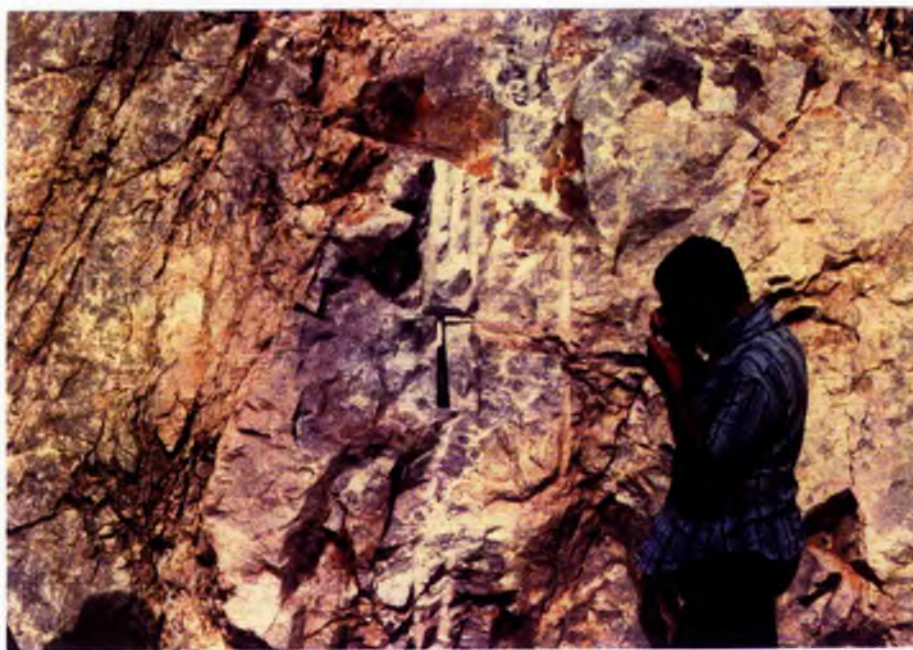


Plate 2.8. The lepidolite-albite zone of the Lepidolite pegmatite, Tantalite Valley, Namibia.

gabbro and hornfels rock, see Plate 2.7) and the contact-wall zone consists of a quartz and feldspar graphic intergrowth and in places of coarse-grained feldspathic intergrowths. The Witkop pegmatite also contains a striking rose quartz core. The Lepidolite pegmatite, intrusive into ultramafic rocks contains an intermediate zone of lepidolite (see Plate 2.8).

The pegmatites in the Valley have been mined for beryl, spodumene amblygonite, bismutite, native bismuth, microlite and tantalite and von Backstrom (1976) has located monazite, gadolinite and uraninite. The Homestead, White City and Lepidolite pegmatites contain prominent Li-mineralization, high grade tantalite, microlite and pink beryl (morganite). These accessory economic minerals occur in the intermediate zones close to the quartz core.

The Chickenfoot pegmatite below Homestead and the Witkop pegmatite have been sampled throughout the pegmatite zones especially for blocky microcline, specifically to examine the Rb contents throughout the pegmatites. Initially the Witkop pegmatite was chosen as it is emplaced in gneiss, in addition to the Chickenfoot pegmatite which is partly emplaced in gneiss. Partial melting of the gneiss was considered by Moore (1975) to be the origin of the Tantalite Valley pegmatites. All the pegmatites in Tantalite Valley were sampled for tantalite, beryllium and Li-minerals specifically in the replacement inner zones. Von Backström (1976) noted that the Li-mica units are cross-cutting and probably are replacement zones.

2.2.5. The Karibib-Usakos Area, Namibia

The Precambrian Damara Sequence (See Table 2.2) is well known for its numerous granite pegmatites (Gevers and Frommurse, 1929; Cameron 1955; Roering, 1961; Roering and Gevers, 1962; Smith, 1965; Von Knorring, 1970, 1985, 1985b; Keller and von Knorring, 1989; Diehl and Schneider 1990 and Keller, 1991.

In 1980 the author visited economically viable pegmatites in the Karibib-Usakos-Cape Cross area (Figs. 2.4, 2.9, 2.10), specifically looking for tantalum and lithium mineralization. Of the pegmatites visited on this occasion in the Karibib-Usakos area, only Rubicon and Helicon, on Okongava Ost 72 Farm and a mica pegmatite on Okatjimukuju were in production. Other pegmatites such as Mon Repos on Mon Repos Farm and Viljoen's on Okongava Ost were comparatively very small excavations as was Dernburg on Karibib 54; while the Daheim pegmatites on Daheim 106, Jooste's pegmatite on farm Okongava Ost 72 and pegmatites on Okatjimukuju were larger excavations due to mining in the past. Although minerals containing lithium, columbite-tantalite and microlite were collected from every possible zone, the smaller pegmatites were not sampled systematically because of the lack of exposure. A few specimens have been studied in this work from the E tiro pegmatite, on E tiro 50 and the Sandamap pegmatite, Sandamap 64, Damaraland in the Southern tin belt by courtesy of O. von Knorring, but the writer did not visit these pegmatites personally. In the Northern tin belt the Strathmore pegmatite which was being mined for cassiterite was visited. Most of the specimens from the Karibib area were collected in 1980 and work was commenced on these by the author at the University of Witwatersrand, Johannesburg. Kohero and Okatjimukuju were visited in 1984.

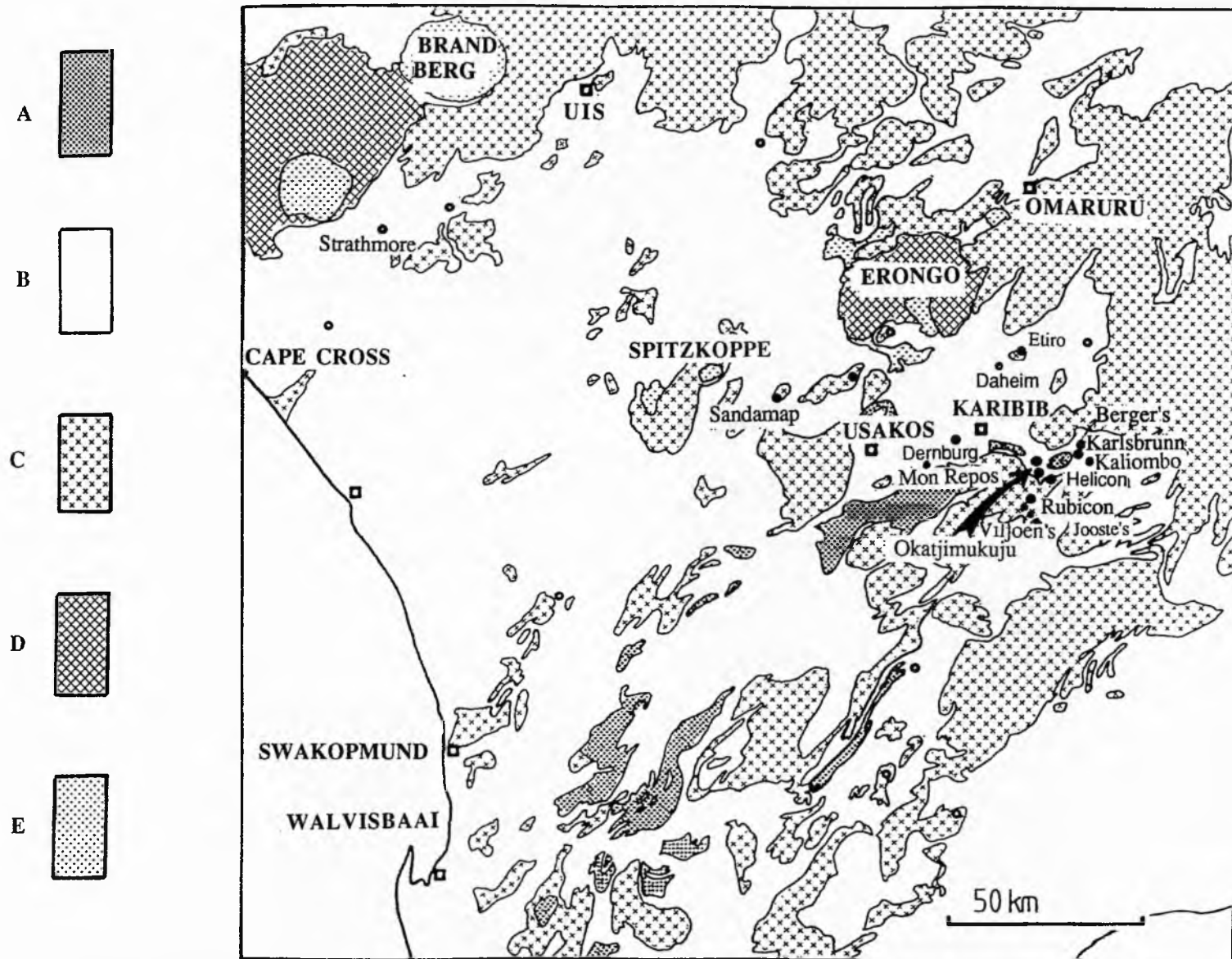
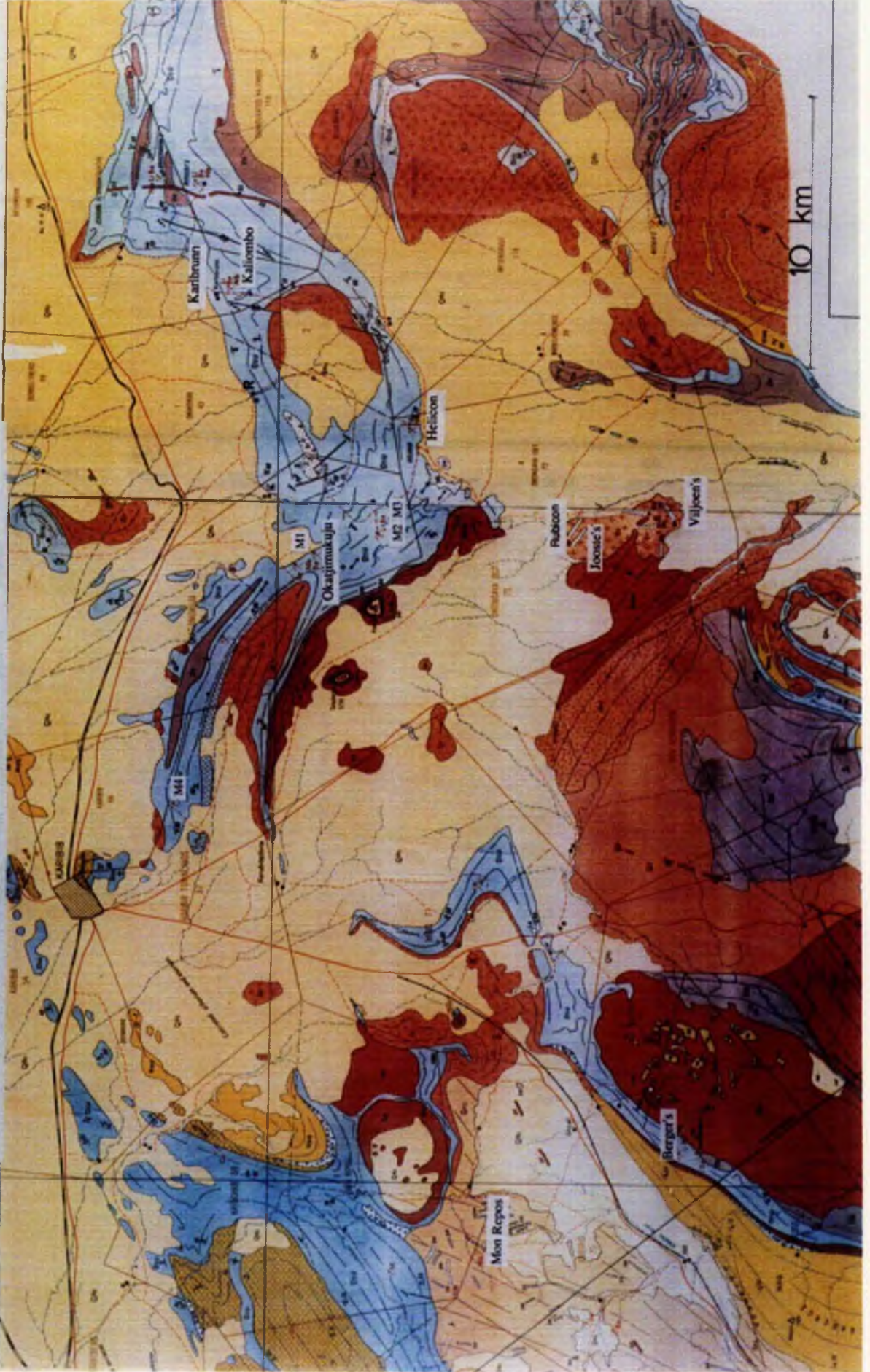


Fig. 2.9. Pegmatites of the Karibib-Usakos- Cape Cross area, Namibia (Area 4 described in the text). A:Basement; (Abbabis Formation); B: micaschists, marbles and quartzites (Damara sequence); C:granites (Damara sequence); D Basalts rhyodacites (Karoo sequence); E: granites (anorogenic) (after Keller and von Knorring, 1989).

Fig. 2.10. The location of pegmatites described in the text in Area 4, Karibib, Namibia (see Smith, 1966 for Key to geology).



The Karibib-Usakos area consists of a metamorphic basement containing the Abbabis Formation, mostly covered by high-grade, regionally metamorphosed sediments of the Upper Precambrian Damara Sequence, trending NE-SW. During the Damaran Orogeny, different syn-to post-tectonic granites were intruded into the Damaran metasediments to which the pegmatites in the area are related (Roering, 1961, 1966; Smith, 1965). The majority of the pegmatites are without any economic minerals and are emplaced in various magmatic and metamorphic rocks with which they are commonly concordant.

The economic highly differentiated pegmatites have intruded tightly folded micaschists, dolomitic marbles and quartzites. The pegmatites are predominantly concordant with the host rocks, they are unmetamorphosed and post-tectonic. The lithium-bearing pegmatites may also be situated within larger bodies of pegmatite granite (Roering, 1961).

The major lithium pegmatites of Namibia, in the Karibib-Usakos-Cape Cross area (see Fig. 2.9) vary to some extent in their internal structure and mineral composition, but most have a common geochemical pattern where Li, Na, K phases are well developed (von Knorring 1985a). Among the major mineral constituents, lepidolite, petalite and amblygonite, various Li-Mn-Fe phosphates, microcline, albite, muscovite, beryl and tourmaline are of common occurrence. The majority of the deposits may be considered as Li-Be pegmatites. Spodumene has been noted (von Knorring pers. comm) in some isolated areas north of Spitzkop (see Fig. 2.9). Associated with the lithium pegmatites are coloured varieties of beryl and tourmaline and various tantalum and bismuth minerals.

The Rubicon, Helicon, Karlsbrunn, Becker's on Otjua and the Dernberg pegmatites (see Fig. 2.10), all within a 20 mile radius from Karibib were mapped in detail by Roering and Gevers (1962). The Etiro pegmatite north of Karibib (Fig. 2.9) was mapped by

Miller (1968,1969) and Diehl and Schneider (1990) have remapped the Rubicon pegmatite. An overall zonal pattern from the margin to the core has been recognized by Roering and Gevers (1962) as follows :-

1. Granitic zone of albite-perthite-quartz-muscovite
2. Cleavelandite-quartz-muscovite with accessory beryl, frondellite and columbite-tantalite
3. Lithium-bearing ore zones
4. Cleavelandite-beryl-columbite-tantalite-cassiterite
5. Quartz core, either pure or mixed with adjacent minerals

In the Karibib - Usakos area the Rubicon pegmatite situated about 14 miles southeast of Karibib on Okongava Ost 72 Farm (see Fig. 2.10) has been one of the main exploration lithium ore deposits in southern Africa for 60 years. In this general area the main rock type consists of a pegmatitic granite containing smaller lenticular segregation pegmatites which are commonly mineralized; the larger dyke-like pegmatite bodies including the lithium bearing ones appear to have formed from this widespread pegmatitic granite. The main Rubicon ore body (see Fig. 2.1) which forms a prominent ridge is well-zoned and is approximately 300 m long and 15-40 m wide. The main ore occurs at the base of a larger mass of late-tectonic coarse-grained pegmatitic granite while along its footwall the basal granite is intrusive into quartz-diorite (Roering and Gevers, 1962). The intermediate zone incorporates the lithium-ore-body: petalite in the hanging wall and in the footwall the lithian mica-albite unit. Of these, the petalite unit is rather narrow, on average 1-2 m wide, but broadens to 6 m or more in places. The petalite varies in colour from pure white to grey and pink, locally large patches have altered to a pinkish montmorillonitic clay mineral, a common feature observed in petalite pegmatites elsewhere.

The lithian mica at Rubicon forms an uninterrupted zone of lithian and beryllium mineralization stretching for a total length of over 1,000 m (see Fig. 2.1); the average thickness is from 30-50 m. It is intergrown with albite and quartz except near the quartz core margin. Amblygonite is scattered throughout the lepidolite zone in aggregates and

nodules and occurs also in distinct purplish-blue crystals up to 6 cm, in the hanging wall with petalite. Petalite is also commonly found in the footwall of the lepidolite zone.

Beryl forms a distinct unit along the contact between the lithian ore zones and the enclosing albite-microcline-muscovite-quartz rock. It is best developed along the southern footwall margin of the lepidolite zone; it is of a glassy vitreous type, colourless, pink, orange or bluish-green in colour.

The quartz core unit is often discontinuous and forms smaller and larger independent lenses. In places rich bismuth mineralization has been noted; the quartz often a glassy vitreous variety being intergrown with grey, yellow or greenish bismutite associated with smaller amounts of malachite and other bismuth minerals.

The Rubicon pegmatite extends towards the northwest for some 600 m where smaller excavations are found with some lithium and beryllium mineralization: a large amount of lithiophilite and other lithium phosphates were noted from one excavation. South of the main Rubicon quarry, an extensive parallel pegmatite, the Jooste's pegmatite, with similar mineralization to Rubicon was examined. In addition to good quality petalite and lepidolite this pegmatite carries beryl, pollucite, a great variety of bismuth minerals and, in contrast to Rubicon, a large amount of the tantalum mineral microlite disseminated in lepidolite and albite.

Some 6 km north of Rubicon mine two important lithium pegmatites, Helicon 1 and 2, also located on Okongava Ost 72, have been mined intermittently for more than 30 years. Helicon 1 is located approximately 13 miles E.S.E. of Karibib on the north eastern corner of the Farm Okongava Ost. The pegmatite consists of an elongated body which strikes east-west and can be followed for a distance of some 400 m. In contrast to Rubicon, this pegmatite is devoid of petalite and was mined mainly for lepidolite and amblygonite.

The pegmatite is well zoned although the individual zones are rather irregular in their development. The intermediate unit again carries the majority of the lithium ores. The major lithium unit is up to 25 m wide and consists of lepidolite intergrown with albite and quartz in various proportions; high grade ore is often found in the form of separate lenses. Within the lepidolite unit there are smaller quartz segregations carrying beryl, amblygonite and tantalite. Towards the quartz core margin the intermediate zone becomes more albitic with some development of beryl and pollucite.

Helicon 2 pegmatite has developed into a large mine; it is rather narrow, 10-20 m wide but stretches for a distance of some 800 m, the quartz core forming a prominent undulating ridge. Petalite is a major mineral mined and it occurs with some lepidolite in a zone 1-3 m in width. Amblygonite and beryl are scattered along the outer margins and pollucite is found in the quartz core. Smaller nodules of pollucite were noticed and some columbite-tantalite is recovered as a by-product.

Rubicon and Helicon are by far the most important pegmatite occurrences in Namibia and account for the bulk of lithium, caesium, beryllium and bismuth minerals produced in the past 50 years. With regard to lithium mineralization, amblygonite, lepidolite and petalite are the principal minerals and, of these, lepidolite constituted in the past about 90%. Within a radius of 25 km from Karibib, there are many important lithium pegmatites which have been mined in the past. Some of them are of large dimensions and contain potential reserves of lithium and beryllium.

Okatjimukuju 55 Farm (Fig. 2.10) 5 km east of Karibib and north of the Rubicon and Helicon pegmatites revealed many occurrences of lithian mica, amblygonite, petalite, accessory beryl, niobium and tantalum minerals including wodginite and cassiterite. Four major excavations on the farm, termed (M1), (M2) (M3) and (M4) were visited. M1 contains a mica separation plant as there are vast quantities of muscovite, in addition

to grey and pink Li-mica proximal to the quartz core. Tantalite occurs as euhedral crystals up to half a cm in length in a matrix of cleavelandite, microcline, grey mica and quartz. M3 is a partly altered pegmatite, wodginite associated with tantalite occurs in altered cleavelandite and mica. Blue manganoapatite associated with quartz and black tourmaline occurs at the cleavelandite contact. M4 contains pink beryl, grey topaz, cassiterite and montebrazite with which is associated the rare mineral brazilianite, all occurring in the cleavelandite-lepidolite zone which is 30 m long, 4 m wide and 4 m deep.

Daheim 50, a farm situated on the east side of the Erongo mountains (see Fig. 2.9) some 20 km north-west from Karibib contains several smaller pegmatites with excellent petalite, tantalite and cassiterite. Of the three major pegmatites: Daheim 1, Daheim P, and Daheim 3, Daheim 1 the largest pegmatite on the farm, contains Li-mica, pink tourmaline and tantalite associated with cleavelandite, and dark-blue tourmaline. Daheim P contains grey petalite and Li-mica and Daheim 3, a pink variety of petalite.

Smaller excavations visited include the Mon Repos pegmatite (Figs. 2.9, 2.10) a series of small excavations containing manganotantalite, tapiolite, large dark-blue tourmalines in quartz and pinkish and white amblygonite also associated with quartz. The Viljoen's pegmatite (Fig. 2.9) on Okongava Ost Farm contains pink feldspar with green mica, a green crystalline apatite, globular grey mica and beryl and the Dernberg pegmatite (Figs. 2.9, 2.10) which had been excavated on the surface but not mined in 1980, contains tantalite and apatite.

Etiro, the largest mining enterprise in the area after Rubicon and Helicon is situated about 20 km north of Karibib on the Khan river. The major Etiro pegmatite is some 800 m long and contains high grade lepidolite, amblygonite and a glassy pink beryl

(morganite) which occurs often in large pods. Accessory minerals include tantalite and a great variety of bismuth minerals (von Knorring 1972).

2.3. THE OCCURRENCE AND GEOCHEMISTRY OF LITHIUM AND TANTALUM

2.3.1. Lithium

The geochemical distribution of the lightest alkali metal, lithium, is of unusual interest because this element tends to follow a well-defined path of its own. In fact the distribution of lithium is almost entirely distinct from the other alkali metals. These characteristics arise from the fact that not only is Li^+ distinctly smaller (radius = 0.68 Å) than the other alkali metal cations ($\text{Na}^{2+} = 0.97\text{Å}$, $\text{K}^+ = 1.33\text{Å}$, $\text{Rb}^+ = 1.45\text{Å}$, $\text{Cs}^+ = 1.67\text{Å}$) but it is the smallest of all singly charged cations and unlike the larger cations which occur in eightfold (or higher) co-ordination in silicate minerals, co-ordination about Li^+ is invariably sixfold (Ahrens, 1966).

With regard to Li^+ in the sequence of magmatic crystallization; lithium has only a single charge, it cannot therefore be expected to enter early crystallizates in other than very subordinate amounts. When cations of differing charge compete for a given structure site in a silicate mineral that is growing from a cooling silicate melt, ions with the higher charge tend to be accepted preferentially because the magnitude of the positive forces associated with these ions will be greater than those associated with the less strongly charged ions. Therefore, the singly charged ion Li^+ tends to concentrate in the rocks which crystallize late in the magmatic sequence and the lithium distribution in igneous rocks tends to be inversely related to that of magnesium and iron. Lithium is a scarce element in the upper lithosphere. It is more likely to replace divalent ions and less likely to replace trivalent and quadrivalent ions in natural minerals. The following ions have a sufficient similarity in radius: $\text{Mg}^{2+} = 0.78\text{Å}$, $\text{Fe}^{2+} = 0.82\text{Å}$, $\text{Al}^{3+} = 0.57\text{Å}$ and $\text{Ti}^{4+} =$

0.64Å. Lithium is not associated with the other alkali metals, the next alkali metal sodium has an ionic radius of 0.97Å, a difference so great that only limited substitution may be expected. The radii of the two singly charged alkali metals K^+ and Rb^+ are even greater, namely 1.33 and 1.45 Å respectively.

Lithium is a typical trace element in light residual rocks, such as granite and is relatively concentrated in the residual solutions of granite pegmatites and very concentrated in large unique granite pegmatites. In rare-element pegmatites some lithium becomes incorporated in early crystallizing phases for example plagioclase, black tourmaline and green beryl before its accumulation reaches the level, sufficient to establish the crystallization of anhydrous lithium aluminosilicates, lithium phosphate and Li-F-enriched micas. Lithium minerals are associated with cleavelandite, K-feldspar, quartz and less commonly, topaz. Lithium occurring along with residual solutions rich in fluorine leads to the unique group of complex aluminium fluoride minerals. The concentration of lithium is often paralleled by a concentration of rubidium, and caesium in the mineral pollucite

With regard to the principal carriers of lithium in granite pegmatites, although some 30 lithium bearing minerals are known, only four spodumene, petalite, amblygonite and lepidolite are found in sufficient quantities to be regarded as lithium ores. Less prominent Li-minerals include: eucryptite and Li-Mn-Fe phosphates (lithiophilite-triptylite). Minerals which may admit Li into their structure include amazonite, muscovite, biotite, tourmaline and transparent varieties of beryl.

In the four field areas being studied lithium minerals are of major importance in the Karibib-Usakos area, Namibia with petalite, lepidolite and amblygonite being of major significance. The pegmatites in the Karibib area are essentially lithium-bearing on a far greater scale than the pegmatites of the Orange River Namaqualand Pegmatite Belt. In the

Steinkopf region, the western section of the Pegmatite Belt, however, lithium minerals are of significance, especially spodumene, but in the eastern section in the Kenhardt area, a few pegmatites contain small deposits of lithium in the form of lepidolite and spodumene (see Figs. 2.2,2.3). In Tantalite Valley in the northern section of the Belt, three of the four main pegmatites contain lithium in the form of lepidolite, spodumene and amblygonite. In the adjoining Tantalite Valley, (SW Witkop) rare high quality spodumene is of major importance.

2.3.2. Tantalum

The tantalite-columbite group comprises minerals of the isomorphous series FeTa_2O_6 - MnTa_2O_6 - FeNb_2O_6 - MnNb_2O_6 . In the series there is unlimited isomorphism between Nb and Ta and also between Mn and Fe and gradual transitions are observed from columbite (the more predominant) to tantalite and from their iron to their manganese varieties. Tantalum varieties generally contain a lower proportion of Mn+Fe than their columbite counterparts. Tantalum and niobium are concentrated in late crystallizates during magmatic differentiation. The concentration is very pronounced in granites and tantalum shows a maximum in granite pegmatites. Niobium though concentrated in granites, has greater concentrations in syenites and nepheline syenites.

The discovery of niobium was announced by Hatchett(1802) in England, in 1801, who gave it the name 'Columbian' after America, the source of the specimen he studied. A new acidic metallic oxide was isolated by Ekeberg (1802) from several Swedish and Finnish minerals. He gave the oxide the name 'Tantalum' because of its tantalizing behaviour in attempts to dissolve the product in acid. A sample of columbite from Bodenmais, Bavaria, was examined by Rose (1844) from which he isolated two new acidic elements. One of these appeared to be similar to Ekeberg's tantalum. He named the other 'Niobium' after Niobe, the mythological daughter of Tantalus, in Greek

mythology. Many notable chemists of the time studied these elements and came to the conclusion that Hatchett's columbian and Rose's niobium were the same element.

Cerny (1975) and Foord (1982) have provided a summary of research into the Fe-Mn-Nb-Ta oxides; in so much as it concerns the minerals in this study, (ixiolite is not included) it may be summarized as shown below:-

1. The essentially two-element compounds, approaching FeNb_2O_6 , MnNb_2O_6 and MnTa_2O_6 show mostly the ordered columbite-tantalite structure.
2. Minerals with compositions close to FeTa_2O_6 crystallize as tetragonal tapiolite.
3. Wodginite is known to contain Fe_2O_3 . In most well-ordered columbite-tantalite specimens the Fe_2O_3 content is low or negligible.
4. Both columbite-tantalite and pseudo-ixiolite produce wodginite upon prolonged heating in air, evidently in response to oxidation of ferrous iron. Wodginites originate under f_{O_2} conditions distinctly higher than those characteristic for the stability of columbite-tantalite.

Crystal structures have been done for manganotantalite (Grice et al., 1976), manganocolumbite (Foord, 1976), wodginite (Ferguson et al., 1976) and columbites (Weitzel, 1976). Zelt (1975) has pointed out that there is no correlation between individual parameters and chemical composition but the unit cell volume seems to be a reflection of the Mn/Fe ratio. Minerals in this group may be metamict or partly metamict (Heinrich, 1962; Cerny and Turnock, 1971). Crystallinity may be restored by heating in a reducing environment so as to prevent oxidation of Fe^{2+} to Fe^{3+} .

The mineralogy of Ta in granitic rare-element pegmatites is complex (von Knorring and Fadipe (1981). Cerny et al. (1985a) pointed out that the distribution of individual Ta-minerals with regard to different pegmatite types is partly governed by the ranges in the Nb/Ta ratio. In the rare-element complex, highly fractionated pegmatites of Karibib-Usakos pegmatite field, Namibia, Ta-dominant minerals prevail, i.e. manganotantalite, ferrotantalite, wodginite and microlite. In the less complex pegmatites manganocolumbite and ferrocolumbite are more common and in the more primitive less mineralized pegmatites, columbite is dominant. In the complex spodumene pegmatites of Steinkopf, Namaqualand, and Tantalite Valley, Namibia manganotantalite and microlite with a very low Nb/Ta ratio prevail. While in the eastern section of the "Pegmatite Belt" in the Kenhardt area, the pegmatites are less mineralized and the columbite-tantalite group of minerals are represented by columbite, ferrocolumbite and manganocolumbite with an Nb/Ta ratio > 1 . The columbite-tantalite group of minerals commonly occur late in the pegmatite crystallization sequence in association with cleavelandite, quartz and lepidolite.

PART II

LITHIUM

Chapter 3

PART II

LITHIUM MINERALIZATION

CHAPTER 3.

3.1 INTRODUCTION

3.1.1 Lithium minerals and aim of this lithium study

The aim of this study on lithium is i) to investigate lithium mineralization in the Karibib, Tantalite Valley and Namaqualand areas, ii) to examine pseudomorphic replacements of these minerals, and iii) to investigate the associated rare accessory secondary mineralization with backscattered electron imaging techniques coupled with quantitative electron microprobe analysis.

Although some 30 lithium bearing minerals are known, in pegmatites only four, the four main lithium-bearing minerals, spodumene, petalite, amblygonite and lepidolite are found in sufficient quantities to be regarded as lithium ores.

Main Li-bearing ores:

$\text{LiAl}(\text{Si}_2\text{O}_6)$	SPODUMENE	($\text{Li}_2\text{O} = 4-8\%$)
$\text{Li}(\text{AlSi}_4\text{O}_{10})$	PETALITE	($\text{Li}_2\text{O} = 2-4\%$)
$\text{LiAl}(\text{F}/\text{PO}_4)$	AMBLYGONITE	($\text{Li}_2\text{O} = 8-10\%$)
$\text{K}_2(\text{LiAl})_6(\text{SiAl})_8\text{O}_{20}(\text{FOH})_4$	LEPIDOLITE *	($\text{Li}_2\text{O} = 2-4\%$)**

* The term 'Lepidolite' in the Table above includes all lithium-bearing micas. Lithian-muscovite is the same $2M_1$ (dioctahedral) structural type as muscovite and a different structural type from lepidolite which could be any of $1M$, $2M_2$, $3T$, $2M_1$ (trioctahedral) types. Lepidolite, mixed types and Li-muscovite may be distinguished by their Li_2O content as well as by their structural polytype (London and Burt, 1982b). Normally the term Li-mica i.e. lithian mica will be used in this text, to describe and denote these minerals, except where lepidolite has specifically been used in the literature. These Li-Al micas will be discussed in more detail in the Li-mica section.

** Li-mica contents reach 6.2% in this study from the Karibib area, so that this figure taken of 2-4% from the Geological Survey of Namibia is an average value for this area.

Minor Li-bearing minerals include:

Lithiophilite-triophylite:	$\text{Li}(\text{MnFe})\text{PO}_4$
Eucryptite:	LiAlSiO_4 (rare)
Li-bearing tourmaline:	$\text{Na}(\text{LiAl}_3)\text{Al}_6(\text{BO}_3)_3\text{Si}_6\text{O}_{18}(\text{OH})_4$

The lithium aluminosilicates, spodumene, petalite and lepidolite are the most abundant and most frequently encountered lithium minerals in pegmatites, they are extremely sensitive to changes in their physical and chemical environment and are therefore excellent indicators of subsolidus conditions in pegmatites. The stability relations amongst these minerals are fundamental to lithium pegmatite petrogenesis and their phase relations in natural and experimental conditions have been documented by Burt et al. (1977), Stewart (1978), London and Burt (1982a), London (1984a, 1990) (see Fig. 3.1a). Burt and London (1982) have provided a schematic diagram for the system $\text{LiAlO}_2\text{-SiO}_2\text{-PbO}_2\text{-NaLi}$. In the presence of Na- P- F-rich fluids the lithium aluminosilicates become unstable relative to amblygonite+albite (see Fig. 3.1b) and albite-amblygonite-quartz assemblages form outside the lithium aluminosilicate stability region.

Eucryptite has been identified in the Karibib area by von Knorring (1985), however, it is an extremely rare-mineral and has not been included in this study. The rarity of this mineral is due to its instability with quartz at moderate to high P and T and its relative instability in P- and F- rich acidic fluids in which the stable assemblage is spodumene + amblygonite and to K+H metasomatism by which eucryptite is converted to muscovite (Burt and London, 1982).

Petalite and spodumene may occur as primary and secondary phases. Petalite and spodumene forming as secondary and isochemical replacements have been documented from several localities (Baldwin, 1979 and Burt and London, 1982). However, metasomatic replacement of petalite, spodumene and eucryptite is far more common and

the lithium aluminosilicates frequently exhibit pseudomorphic replacement by albite and / or micas (muscovite and lepidolite) (Burt and London, 1982).

$P(H_2O)$, kbar

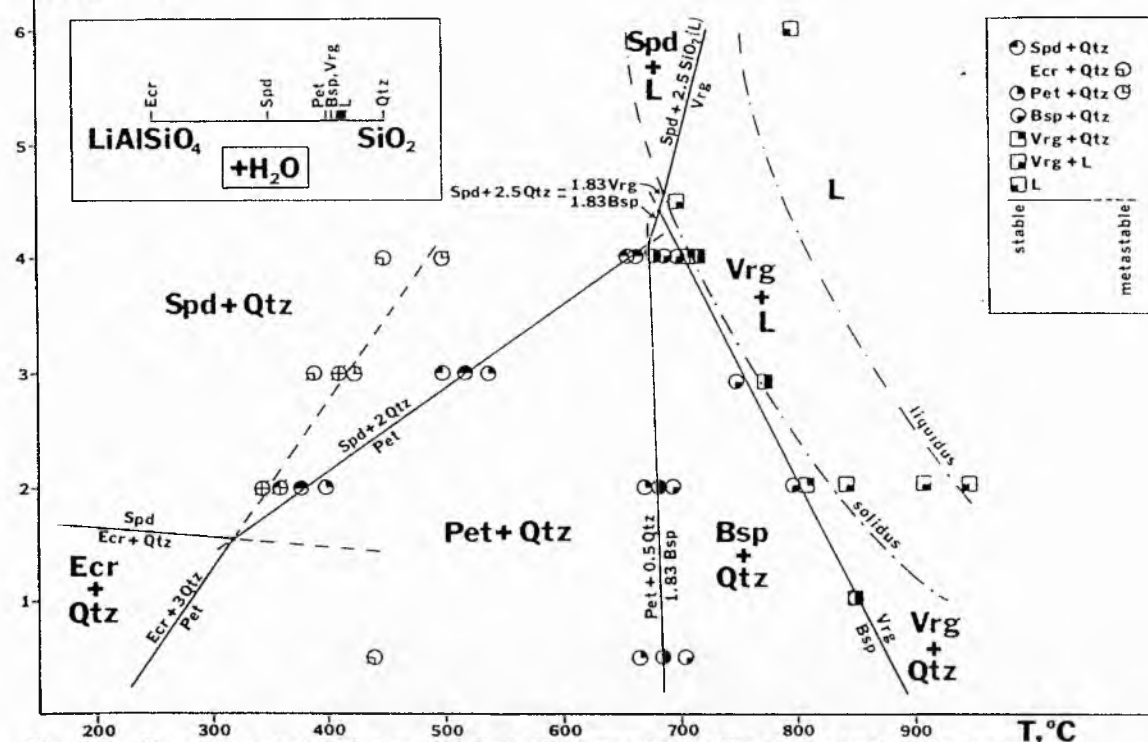


Fig. 3.1a. Experimental P-T diagram for the bulk composition 20Ecr80Qtz (mol %) in the system $LiAlSiO_4-SiO_2-H_2O$ (taken from London, 1990). Symbols show the locations of bracketing or delimiting runs (see London, 1984a for further information). Solid lines: stable portions of univariant reactions; dashed lines: metastable extensions; dashed lines represent solidus and liquidus for the bulk composition $LiAlSi_5O_{12}$. Compositions of phases are shown in the upper left corner. Pet: petalite; Spd: spodumene, Ecr: eucryptite, Bsp: beta-spodumene, Vrg= virgilite; Qtz: quartz; L: melt.

3.1.2 The distribution of lithium, rubidium and caesium

Of the common lithium minerals, petalite, spodumene, amblygonite-montebbrasite and lithiophilite-triophyllite appear to be primary in origin, having crystallized from magmas or fluids and typically form extremely large crystals, up to several meters in dimension. These minerals are commonly associated with microcline, albite-cleavelandite and muscovite in quartz-rich zones. In contrast, eucryptite and much lepidolite and lithian mica replace other minerals and are secondary in origin. Eucryptite frequently occurs with albite or quartz in pseudomorphs of spodumene and petalite (London and Burt, 1982b and c). Microcline as well as lepidolite and lithian mica replace spodumene in numerous localities (Norton et al., 1962; Jahns and Ewing, 1976; Crouse et al., 1979).

Lithium is one of the characteristic elements in differentiated granite pegmatites, where it is concentrated to varying degrees. Li-pegmatites of the Karibib area, Namibia are unique in that the major Li-mineral in most of them is petalite and not spodumene which is the more common Li mineral in other provinces of the world. Since the 1930's, the lithium minerals amblygonite, petalite and lepidolite have been recovered from the Helicon and Rubicon pegmatites on Okongava Ost 72 (see Figs. 2.9, 2.10). Large reserves of these minerals are believed to be present in these huge pegmatites. Significant quantities of these minerals occur in beryl, tin and tantalite bearing pegmatites in the Karibib area.

In Tantalite Valley, Namibia small deposits of amblygonite, lepidolite and spodumene occur and lithiophilite is also present; petalite does not occur. In Namaqualand, spodumene is the main Li-mineral, lithian mica and lithiophilite and related phosphates are extensive, especially in the Noumas pegmatite. In the Kenhardt area, N.W.Cape, Li-mica and lithiophilite are present, spodumene is rare and petalite and amblygonite are not recorded.

The lithian micas, in particular, may have substantial concentrations of Rb and Cs. The bulk of the rare alkali elements is generally camouflaged in the lithian micas and in microcline (Rinaldy et al., 1972). Of these rubidium, a heavy alkali metal, is a rare element; it is approximately 1/250 as abundant as potassium. The radii of these two singly charged cations are very similar, being 1.33 Å and 1.45 Å respectively and consequently minerals are able to substitute Rb for K freely, to such an extent that rubidium never forms a mineral of its own, a situation which may be contrasted with that of caesium. The ratio of potassium to rubidium remains the same (250 to 1) throughout magmatic crystallization until the final residual crystallization where there is a distinct enrichment of Rb in lithian mica in rare-element pegmatites. Rb is also more easily accommodated in the 'roomier' biotite structure than in the feldspar structure (Ahrens, 1966).

The relationship between caesium, the heaviest alkali metal, and potassium is similar, in a general way to that of rubidium and potassium. The radii of caesium (1.67 Å) and K (1.33 Å) are similar though by no means as close as Rb and K. This difference probably accounts for the fact that compared with the K/Rb relationship, the relationship between K and Cs is not so well developed and shows a much greater variation in granites and related rocks in comparison with the K/Rb relationship. There is also a much greater enrichment of caesium relative to rubidium in "residual crystallization." Thus for example, whereas the ratio K/Rb remains fairly steady in granite and related rocks, K/Cs shows a much greater variation in the same rocks (Ahrens, 1966); this will be demonstrated in the pegmatite Li-micas. Enrichment occasionally is so marked that despite its rarity, caesium may sometimes form a distinct mineral, of its own, namely pollucite. Pollucite ($\text{CsAlSi}_2\text{O}_6$) is restricted to complex rare-element Li-rich pegmatites which have reached the highest level of differentiation either as late member of primary crystallization or as a product of late replacement and albitization.

With regard to the analytical technique involved in the lithium minerals studied, textural features, due to variations in composition, are well displayed by backscattered electron imagery. It is shown by this technique that compositional zonation patterns occur in cassiterite, tantalite, wodginite and microlite and in the case of the lithium minerals the technique also highlights very rare accessory minerals associated, in particular, with amblygonite. Variations in composition are normally displayed as different grey-levels, the brighter areas having high values of atomic number. It must be pointed out however, that as the contrast levels may be enhanced artificially, grey-levels of the same mineral may not be compared from one backscatter image to another, especially where different minerals are concerned.

Geochemical data on rare minerals such as natromontebbrasite, crandallite and brazilianite, (natromontebbrasite noted for the first time from the Karibib area) will be

provided and their association with amblygonite - montebrasite will set limits on their P and T of formation.

Experimental data available on spodumene and petalite (Fig. 3.1a) are used to determine P-T conditions of formation of the magmatic and fluid stage in pegmatites in Karibib, Tantalite Valley and Namaqualand coupled with P-T data derived from fluid inclusion studies (see London, 1990).

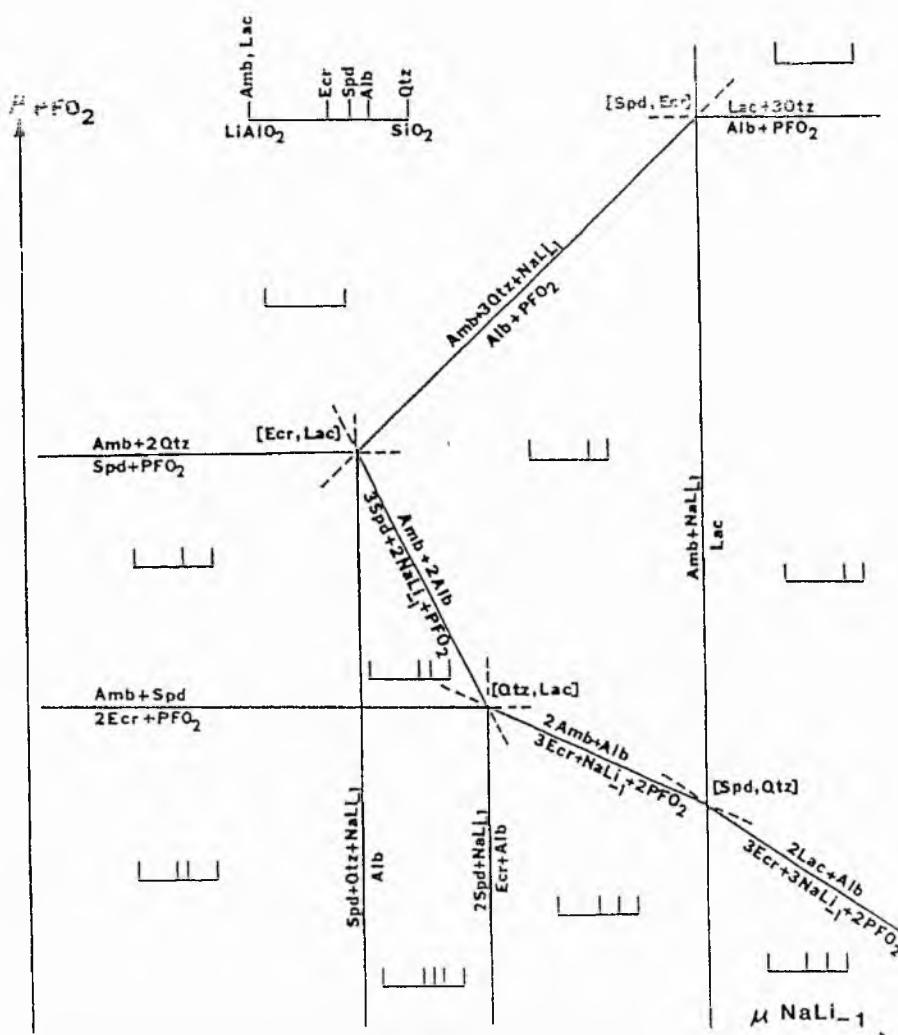


Fig. 3.1b. Schematic isobaric-isothermal diagram for the system $\text{LiAlO}_2\text{-SiO}_2\text{-PFO}_2\text{-NaLi}_{-1}$ at temperatures too low for the stability of petalite (from Burt and London, 1982). The X and Y-axes represent increasing activity of NaLi and PFO_2 fluids respectively.

3.2 SPODUMENE

3.2.1 Introduction

Spodumene is one of the principal sources of lithium in granite pegmatites where it is usually confined to the inner zones. It is a member of the pyroxene family and may contain between 4-8% Li_2O . The mineral usually occurs as euhedral to subhedral prismatic or tabular crystals which may reach several metres in size, for example a crystal 2 m thick and 13 m long was located at Etta, South Dakota (Swartz and Leonard, 1926). Fresh spodumene is transparent, vitreous or silky, and may be white, grey, green, pink or lilac; the altered variety is opaque and kaolinized. Spodumene (Plate 3.1a) is easily distinguished from the other ores of lithium by its prismatic cleavage.

The structure of spodumene is similar to that of diopside. However, the SiO_4 tetrahedra chains are more closely packed together in spodumene with the result that the number of minor-element ions tolerated in the structure is small. Most natural spodumenes approach the ideal composition, but they may contain up to 2 wt % impurities (Na, K and Fe). Some Na may be due to Li substitution but probably most of it is in solution in the abundant fluid inclusions which are characteristic of spodumenes (Sheshulin, 1961; Gordiyenko and Kalenchuk, 1966). Essentially pure spodumenes contain both Fe^{2+} and Fe^{3+} with green spodumenes characterized by high Fe^{3+} contents, up to 40 times higher than white spodumenes (Heinrich, 1975).

There are two types of gem spodumene, hiddenite the Cr-rich transparent emerald-green variety and kunzite, lilac rose to amethyst-pink. Gem varieties are quite rare and although of exceptional beauty, the prismatic cleavage makes them difficult to polish. In pegmatites spodumene occurs principally in three different settings: (1) in unzoned or poorly zoned pegmatites where they occur quite extensively; (2) as primary giant lath-shaped

crystals in the inner units or core of zoned pegmatites, commonly set in massive quartz or in assemblages containing quartz, microcline, albite, mica and amblygonite - montebrasite or (3) as secondary fine-grained fibrous intergrowths with quartz in pseudomorphs of primary petalite (Quensel, 1946; Cerny and Ferguson, 1972).

Spodumene plays an important role in the crystallization processes associated with the formation of complex lithium-rich pegmatites. The object of this section is to present paragenetic details and data concerning the spodumene occurrences in three pegmatite bodies, Norrabees and Noumas from Namaqualand and the SW. Witkop pegmatite from Tantalite Valley, and to describe the primary versus metasomatic nature of these occurrences.

3.2.2 General distribution and geochemistry

Spodumene was not recognized in the Kenhardt district of the Namaqualand Pegmatite Belt. However, in Namaqualand, spodumene is of major significance and samples were collected from the Norrabees and the Noumas pegmatite and in Namibia, from Tantalite Valley where spodumene occurs in the Homestead and SW. Witkop (see Fig. 2.8) pegmatites. In the Karibib area spodumene is not the common lithium mineral, however, it does occur at the desert pegmatites, south of Brandberg (Fig.2.9)(pers. com. O.von Knorring).

Spodumene occurs as giant lath-shaped crystals at two localities in Tantalite Valley, in the outer core and inner intermediate zones. At the SW. Witkop pegmatite on the eastern flank of the complex pale lilac vitreous giant lath shaped crystals (1-24 cm long) are essentially fresh primary spodumene. Lithium was determined by flame photometric techniques as 7.71% Li_2O . A polished thin section could not be made of this spodumene owing to the difficulty in attaching this spodumene to the glass section. The spodumene from Homestead is also lath shaped (4-20 cm long), it is however milky greyish-white in colour, and contains 7.56% Li_2O .

A green spodumene milky lath from the Noumas pegmatite, Steinkopf area, was analysed by gravimetric techniques, it contains 63.87% SiO₂, 27.87% Al₂O₃ and 7.64% Li₂O (see Table 3.1 anal. 1); an EDS analysis of purple spodumene gave similar results (see anal. 2). The analyses from Noumas compare favourably with spodumene from the Tanco pegmatite, Manitoba (Cerny and Ferguson, 1972) and from the Haapalvöma pegmatite, Finland (Haapala, 1966)(see Table 3.1). The pinky spodumene laths from the Norrabees pegmatite, Steinkopf, Namaqualand contain only 4.90% Li₂O (see Table 3.1 anal. 5). If compared with analyses 1-4, the Li₂O content is low for spodumene, probably the spodumene may be partly altered and Li may have been leached out; H₂O+ has not been determined. There is however evidence of other replacement in the Norrabees pegmatite, for example pollucite has been completely replaced by albite in certain areas. Spodumene from the SW. Witkop and Homestead pegmatites, Tantalite Valley and pegmatite south of Brandberg, Namibia contain 7.71, 7.56 and 7.57% Li₂O respectively .

The analysed spodumenes quoted in Table 3.4 from Noumas, Steinkopf, Namaqualand are characteristic of Type (2) - large lath-shaped crystals associated with inner and core unit minerals. They have some impurities - pink spodumene from SW.Witkop, Tantalite Valley has many fluid inclusions which is probably reflected in the 0.45% Na₂O content. The spodumenes from the Homestead pegmatite, Tantalite Valley and from pegmatite south of Brandberg, containing 0.45 and 0.84% Na₂O respectively also have fluid inclusions. Analysis 4 (Haapala, 1966) with 0.45% Fe₂O₃ is type (2) pegmatite. Analysis (3) (Cerny and Ferguson, 1972) has been included as an example of a replacement type (3) spodumene after petalite, and has few impurities.

TABLE 3.1. Composition of spodumenes, and albite
(see Plate 3.2 for point analyses, 5,9,10)

Sample 6N	1.	2.	3.	4.	5.	9.	10.
SiO ₂	63.87	64.60	63.45	63.30	66.53	68.93	66.89
TiO ₂	-	0.00	-	0.00	0.01	0.03	0.00
Al ₂ O ₃	27.87	27.34	27.40	27.19	28.50	19.92	28.62
Fe ₂ O ₃	tr	0.29	0.05	0.45	0.00	0.00	0.01
FeO	-	-	0.10	-	0.38	-	-
MnO	-	0.20	0.00	0.19	0.07	0.00	0.10
MgO	-	-	0.01	0.20	0.01	0.01	0.02
CaO	-	-	0.16	0.00	0.00	0.03	0.02
K ₂ O	*0.42	0.40	0.04	0.10	0.01	0.08	0.00
Na ₂ O	*0.77	0.60	0.11	0.13	0.11	12.02	0.13
Li ₂ O*	*7.64	*7.07	7.87	7.76	4.90	-	4.90
H ₂ O ⁺			0.30	0.64			
H ₂ O ⁻			0.11	0.04			
	100.57	100.50	99.50	99.81	100.16	101.02	100.69

No. of ions O=12(spodumene) O=32(albite)

	1.	2.	3.	4.	5.	9.	T.
Si	3.905	4.012	3.974	3.968	4.127	11.924	11.9
Al	0.095	0.0	0.026	0.032	-	-	12
Al	1.910	2.00	1.996	1.976	2.083	4.062	4
Fe ³⁺	-	0.0	0.002	0.022	-	-	-
Fe ²⁺	-	-	-	0.006	-	-	-
Mn	-	0.010	-	0.010	-	-	-
Mg	-	-	0.002	0.018	-	-	-
Ca	-	-	0.010	0.004	-	0.005	-
K	0.308	0.032	0.004	0.008	0.001	0.017	-
Na	0.091	0.072	0.014	0.016	0.013	4.03	4
Li	1.878	1.765	1.982	1.956	1.222	-	4

1. Green spodumene, Noumas 1, Namaqualand. Analyst: J.R.Baldwin (Gravimetric).
2. Altered purple spodumene, Noumas 1, Namaqualand. Analyst P.Hill (EDS).
3. Spodumene, Tanco pegmatite, Bernic Lake, Manitoba (Cerny and Ferguson, 1972).
4. Fresh-reddish-white spodumene, Haapalvoma pegmatite, Peraseinajoki, Finland (Haapala, 1966).
- 5,10. Whitish-grey spodumene, Norrabees pegmatite, Namaqualand. Analyst: J.R.Baldwin (electron-probe).
9. Cleavelandite (electron probe).
- 6-10. Norrabees pegmatite, Namaqualand. Analyst: J.R. Baldwin.
- * Analysis by flame emission; H₂O, not determined.
- T. Theoretical ions-albite.

TABLE 3.2. Composition of Li-mica and partial analyses of tourmalines, Norrabees pegmatite, Namaqualand (see Plates 3.2 & 3.3 for point locations)

	6.	7.	8.	11.	12.	13.	15.	16.	17.
SiO ₂	51.02	52.57	50.35	38.21	38.21	38.20	38.33	37.58	36.78
TiO ₂	0.02	0.00	0.00	0.08	0.11	0.12	-	-	-
Al ₂ O ₃	29.23	22.61	25.71	39.71	39.74	39.78	39.78	42.65	40.70
B ₂ O ₃				nd	nd	nd	nd	11.22	10.95
Fe ₂ O ₃	-	0.12	0.12	-	-	-	-	0.06	0.14
FeO	0.38	-	-	3.19	3.06	3.08	2.45	0.00	2.10
MnO	0.47	1.11	1.07	1.45	1.43	1.67	1.64	0.26	0.44
MgO	0.13	-	-	0.12	0.12	0.11	-	0.00	0.18
CaO	-	0.02	0.01	-	0.25	0.20	0.22	0.58	0.65
Na ₂ O	0.08	0.18	0.19	1.93	1.95	2.18	1.84	1.87	2.05
K ₂ O	9.33	9.97	10.13	-	0.02	0.02	-	0.03	0.03
Li ₂ O	nd	3.56*	3.56*	nd	nd	nd	nd	1.24	1.85
Rb ₂ O	nd	1.52	1.52	-	-	-	-	-	-
Cs ₂ O	nd	0.47	0.47	-	-	-	-	-	-
F	0.99	5.80	4.85	0.77	0.82	0.67	0.72	0.84	1.08
H ₂ O ⁺	not determined ----->>>							3.85	3.35
H ₂ O-								0.08	0.05
Total	91.65	97.93	97.98	85.26	85.68	85.93	87.55	100.27	100.46
-O=F	0.41	2.44	2.04	0.32	0.34	0.28	0.30	0.35	0.45
Total	91.27	95.51	95.94	84.94	85.34	85.65	87.25	99.92	100.01

No. of ions on the basis of O=22(mica)

	6.	7.	8.
Si	6.83	8	7.57
Al	1.17		0.43
Al	3.44		3.41
Fe	-	3.9	0.01
Mn	0.05		0.14
Mg	0.49		0.01
Li			
Ca	-		-
K	1.60	1.6	1.83
Na	-		0.05
Rb			
Cs			
F	0.42	2.64	2.19

6. Fine-grained muscovite replacing spodumene lath at the base of Plate 4 (electron probe)

7,8. Li-mica (electron probe, lithium by flame photometer, Rb by XRF, Cs by AA)

11-15. Tourmaline (electron-probe)

16,17. Pink elbaite, green elbaite (London and Burt, 1982b)

3.2.3 Replacement of spodumene, Norrabees, Namaqualand

In the Steinkopf area of Namaqualand, spodumene is of major significance. At the Norrabees pegmatite purple spodumene is associated with pollucite, pink and green tourmaline (Plate 3.1b), quartz, cleavelandite, Li-mica and in some areas with blocky microcline. Pale pink tourmaline crystals with dark green rims occur in both quartz and pollucite; some tourmalines contain inclusions of pollucite. In Plate 3.2 elongated cleavelandite laths radiate out in the shape of a fan at right angles to the spodumene plate at the base of the photomicrograph. Pollucite has been identified (indicated as 'p' in Plate 3.2), it is isometric and is directly associated with the tourmaline (T), cleavelandite and mica, and at the right hand margin, with altered spodumene.

Spodumene occurring in both primary and replacement forms was investigated with the electron microprobe. The spodumene lath at the base of Plate 3.2 is composed essentially of primary spodumene (Table 3.1. anal. 5,10 indicated in Plate 3.2) with the exception of the top right hand corner of the lath, indicated by point analysis 6, which is composed of fine-grained muscovite (Table 3.2), clearly a replacement phase.

To investigate replaced spodumene in detail, the backscattered electron image, of the area in the inset box shown in Plate 3.2, is magnified and presented in Plates 3.3; (inverted from top to bottom). The white area in the centre is composed of pollucite (this appears black in the photomicrograph in Plate 3.2). The altered spodumene directly to the right of the pollucite is composed of mica (dark grey), remnant spodumene (light grey) and pollucite (white). Plate 3.3b shows a magnification of this area.

With regard to the relationship between spodumene, Li-mica and pollucite: - in the petrographic microscope, mica is replacing spodumene but only in one area is pollucite

visible as an area of isotropic material within the mica. Also in one area of the unaltered pollucite, a serrated edge shows mica replacing pollucite. Therefore the order of crystallization could be (1) spodumene followed by (2) Li-mica replacement. Pollucite is also before Li-mica, but the relationship between spodumene and pollucite is not clear. There is a distinct margin around the pollucite except for the one edge in contact with the replacing mica. Plate 3.3 however, may suggest that pollucite is after spodumene and it may be suggested that spodumene has been replaced by pollucite and then both of these minerals have been replaced by Li-mica.

With regard to the minerals associated with spodumene; the main minerals are cleavelandite feldspar indicated by point 9 in Plate 3.2 (see Table 3.1. anal.9) and quartz. Purple Li-mica is also prominent in the pegmatite in association with spodumene and this is indicated in the photomicrograph in Plate 3.2 as points 7 and 8. Li-mica often occurs as a pinkish coating on spodumene at Norrabees.

Pink and green tourmaline is associated with pollucite, pink Li-mica, microcline, quartz and spodumene (Plate 3.2.). The elbaite tourmaline with a green rim and pink centre was investigated with the electron probe (Table 3.2. anal. 12-15). There is a small difference in the Na_2O and MnO contents of the pink and green varieties. There is a slightly higher Fe content in the green elbaite at the edge, than in the pink elbaite in the centre which is compatible with green and pink tourmaline from the literature. The large tourmaline in Plate 3.2 also follows this pattern. Only partial analyses have been completed on the tourmaline, owing to the analytical time consuming difficulties of determining boron and to a certain extent lithium. Elbaite tourmalines have been included from the literature with B and Li for comparative purposes. The amounts of Li in elbaite and indicolite tourmalines usually does not reach above 2%.

Tourmaline as the black variety (schorl) is ubiquitous in zoned pegmatites, usually in the outer zones. Green, pink and blue tourmalines generally occur in the inner zones. The cation boron is obviously available in a highly differentiated magma phase which is contemporaneously able to crystallize tourmaline in the presence of (1) cleavelandite, (2) petalite, (3) Li-mica or, (4) primary amblygonite, but as it is practically confined to the mineral tourmaline this suggests that either, (a) it is limited in availability and not able to participate in later postmagmatic fluids in which F and P participate or, (b) it is unstable in an environment rich in P and F fluids at lower temperatures. In fact London (1992) stated that boron is preferentially incorporated into Fe-Mg minerals, which are formed by wall rock reactions with the original pegmatitic magma upon emplacement. This therefore accounts for the ubiquitous nature of black tourmaline in the contact zones of pegmatites. Boron is mostly depleted before inner zone crystallization and is only rarely available to form blue, pink and green tourmaline, with albite and quartz in the inner intermediate zones.

Tourmaline occurrences in Karibib and Namaqualand

Pegmatite Locality	Type	Associated Minerals
Mon Repos, Karibib	blue(indicolite)	amblygonite, quartz, microcline, albite
Daheim 3, Karibib	yellow	petalite, microcline
Okatjimukuju, Karibib	blue(indicolite)	albite, amblygonite?
Norrabees, Namaqualand	elbaite(pink, green)	pollucite, cleavelandite, quartz, Li-mica
Daheim 1, Karibib	rubellite(pink)	microcline cleavelandite

Elbaite tourmaline, a product of inner pegmatite zones is invariably associated with cleavelandite and quartz (Plate 3.2). As cleavelandite is considered by many authors (see London and Burt 1982c) to be a replacement mineral the P-T conditions of tourmaline crystallization may also apply to cleavelandite when considering the genesis of this mineral.

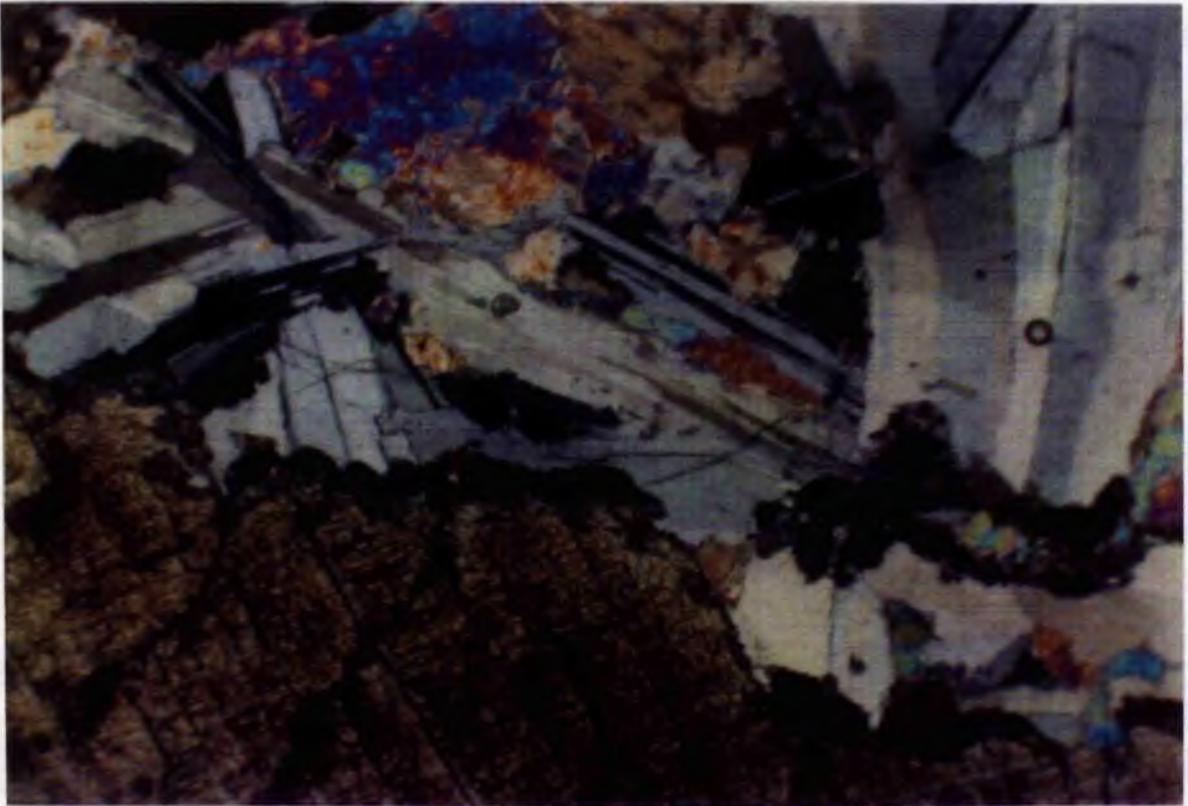


Plate 3.1a. Photomicrograph of primary spodumene showing two cleavages cleavelandite laths (grey), muscovite and aggregates of a late phase of spodumene forming in cracks and along grain boundaries, Norrabees pegmatite, Namaqualand. Crossed polarized light. Scale bar: 5 mm

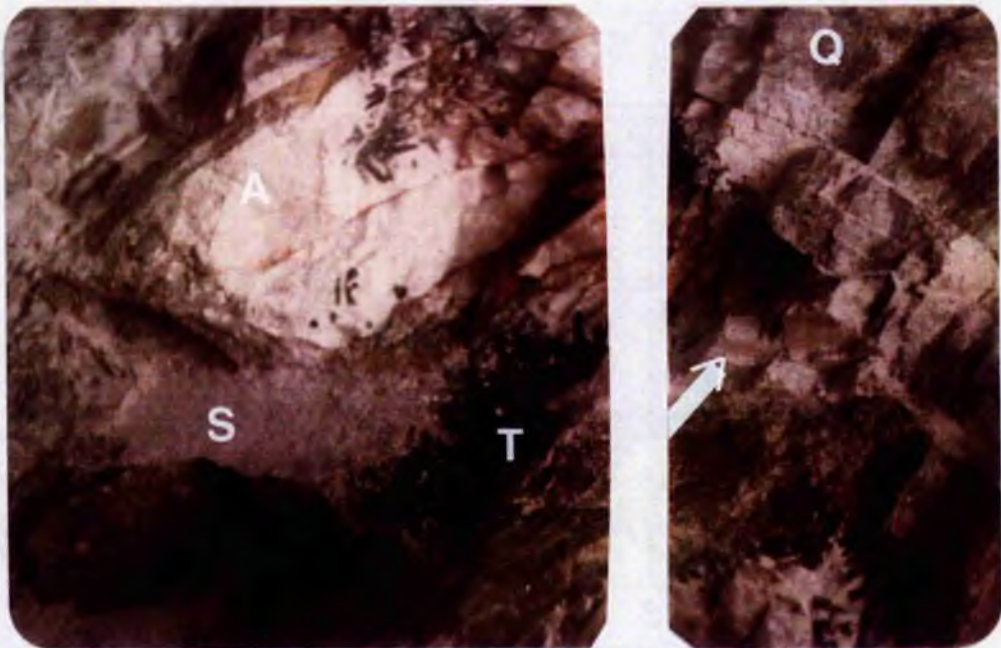


Plate 3.1b. A photograph of quartz (Q), pink spodumene (S) edged with Li-mica with a prolific intergrowth of green tourmaline (T), blocky microcline (arrowed), and albitic replacement of pollucite (A) with intergrown tourmaline, taken in situ at the Norrabees pegmatite, Namaqualand. Scale bar: _____ 20mm.

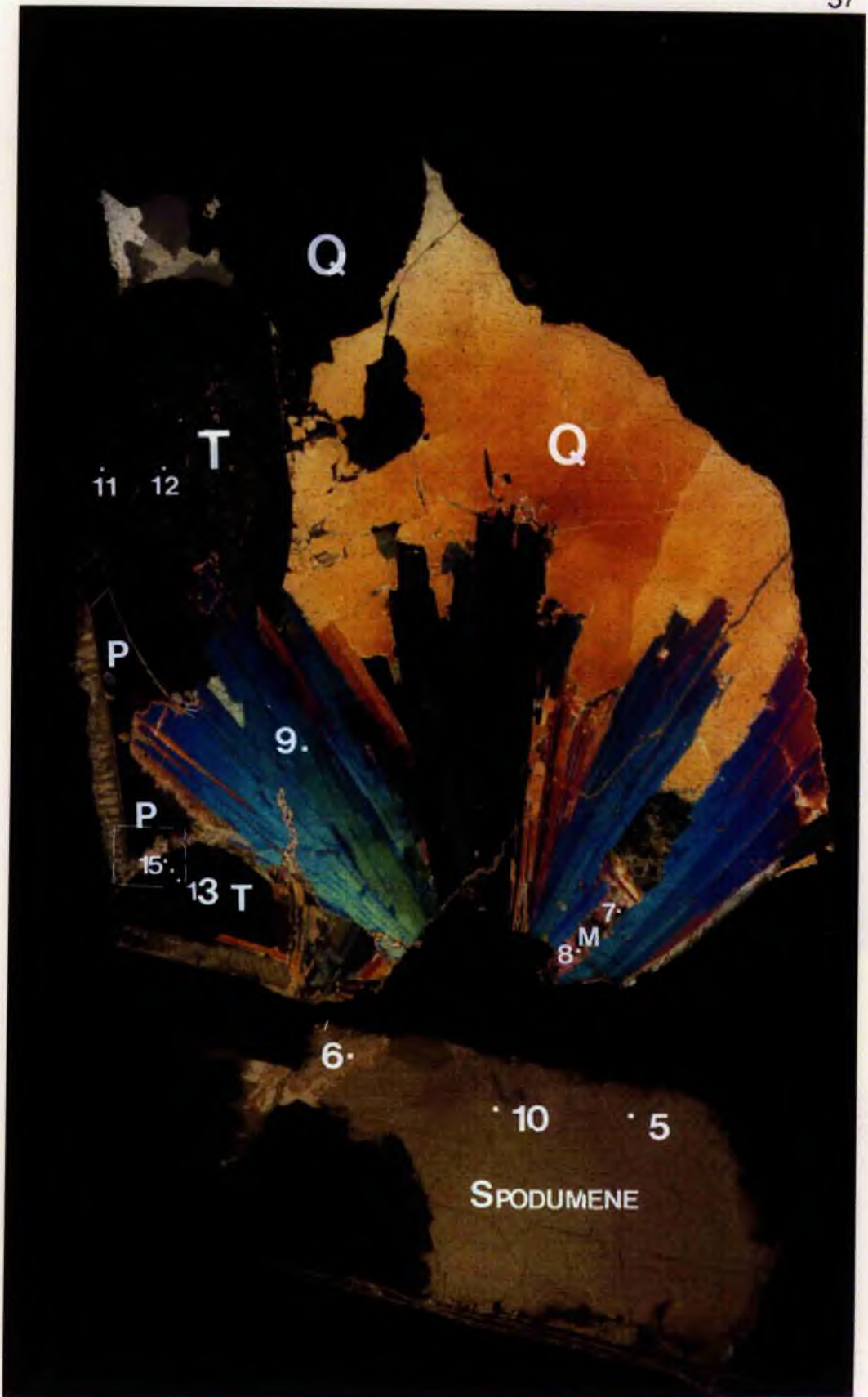


Plate 3.2. Photomicrograph of spodumene, spodumene pseudomorph, pollucite (p); tourmaline (T); Li-mica (m); quartz (Q) and cleavelandite (fan shaped laths). The numbers mark point analyses given in Tables 3.1, 3.2; the area marked in the box is shown in backscattered images in Plates 3.3, Norraabees pegmatite, Namaqualand. Section 3.2 cm long.

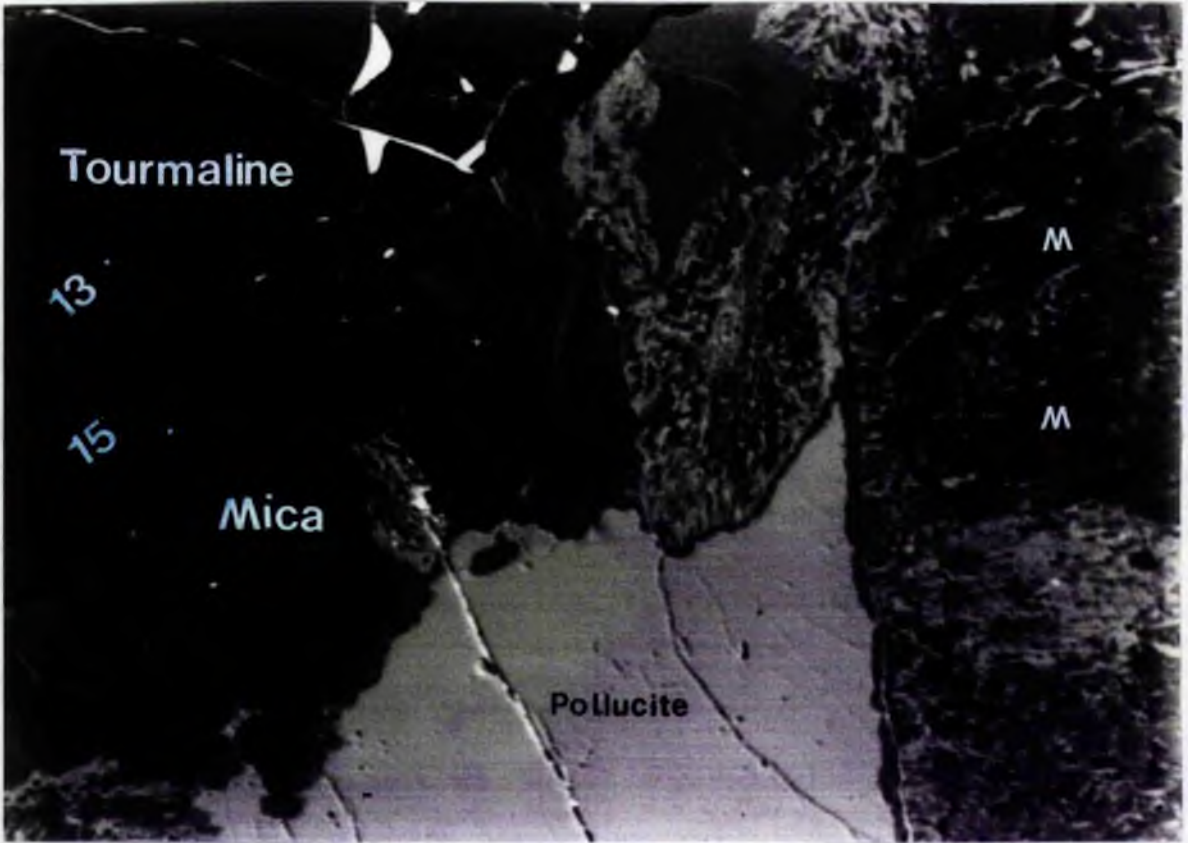


Plate 3.3a. Backscattered electron image of lower pollucite area in Plate 3.2 (inverted top to bottom). To the right of the pollucite, spodumene (s) is pseudomorphed by mica (m) and pollucite (white). Plate 3.3b below shows this latter area. Scale bar: 100 microns.



Plate 3.3b. Backscattered image of spodumene (s) (light grey) replaced by pollucite (white) and mica (m) (dark-grey). Scale bar: 100 microns.

3.2.4 Pseudomorphic replacement, or sericitization of spodumene, Noumas pegmatite, Namaqualand

A grey specimen of replaced spodumene associated with albite, muscovite and quartz, in layers, has been analysed with the electron microprobe. In this particular hand specimen (see Plate 3.4a), replaced "spodumene plates" occur next to a layer of feldspar and mica, on average 0.5 cm thick, which in turn is associated with muscovite sheets 2 cm in thickness intergrown with massive quartz. In spite of the authentic spodumene lath- or plate-shape in handspecimen, the lath proved to be composed of very fine-grained mica flakes and sericite, as the spodumene is retaining its original form it has therefore been pseudomorphed by mica and sericitized.

An analytical traverse was taken across the section starting at point S (Plate 3.4b). The analyses are given in Appendix (2) Table 3.3. and representative analyses with ionic proportions are given in Table 3.4a in the text. The traverse is shown graphically in Figure 3.2 by a plot of SiO₂ against distance in microns from the start (S). The fine-grained mica and sericite replacing spodumene (a distance of 13 mm., starting at 100 microns from the edge) are represented by analyses 20-23 of sericite, which compare with sericite from Amelia, Virginia (Table 3.4b. anal. DHZ9) and analyses 24-26, 29, 30 of mica, (Appendix (2) Table A3.3) with an average of 48.74 % SiO₂, 31.07% Al₂O₃, 10.91% K₂O, 0.44% F and 0.6% FeO. The mica (a clear area through the microprobe optics, anals. 24-26) gave an average analysis of 46.42% SiO₂, and 37.00% Al₂O₃, 10.69% K₂O, 0.4% FeO and no fluorine (anal. 24, 25. Appendix (2) Table A 3.3). It compares favourably with muscovite from Sweden (Table 3.4b, DHZ3) which contains > 4% H₂O. These analyses from the literature are used for comparison when it is impossible to determine H₂O and Li₂O in such minute alterations. The next layer is composed mainly of albite (see Appendix Table A3.3, anals. 27-28, 31-32, 34-37 interspersed with mica (anals. 29,30,33). The next layer composed of large micas, contain slightly less SiO₂ and

more FeO than the fine-grained sericite and mica layers; this area is represented by analyses 38-46 (Appendix (2) Table A 3.3). An analytical comparison of the sericite and mica, replacing spodumene, and the large mica sheets, indicate that the former contain little Fe in comparison with the large micas which contain 4.5 % total iron as FeO (Table A3.3, anal.38,46). The absence of Fe in the replaced spodumene will reflect the negligible Fe content of the original spodumenes (Table 3.3.anal.38-46). The mica plates contain 1.06% Li₂O (see Table 3.4b).

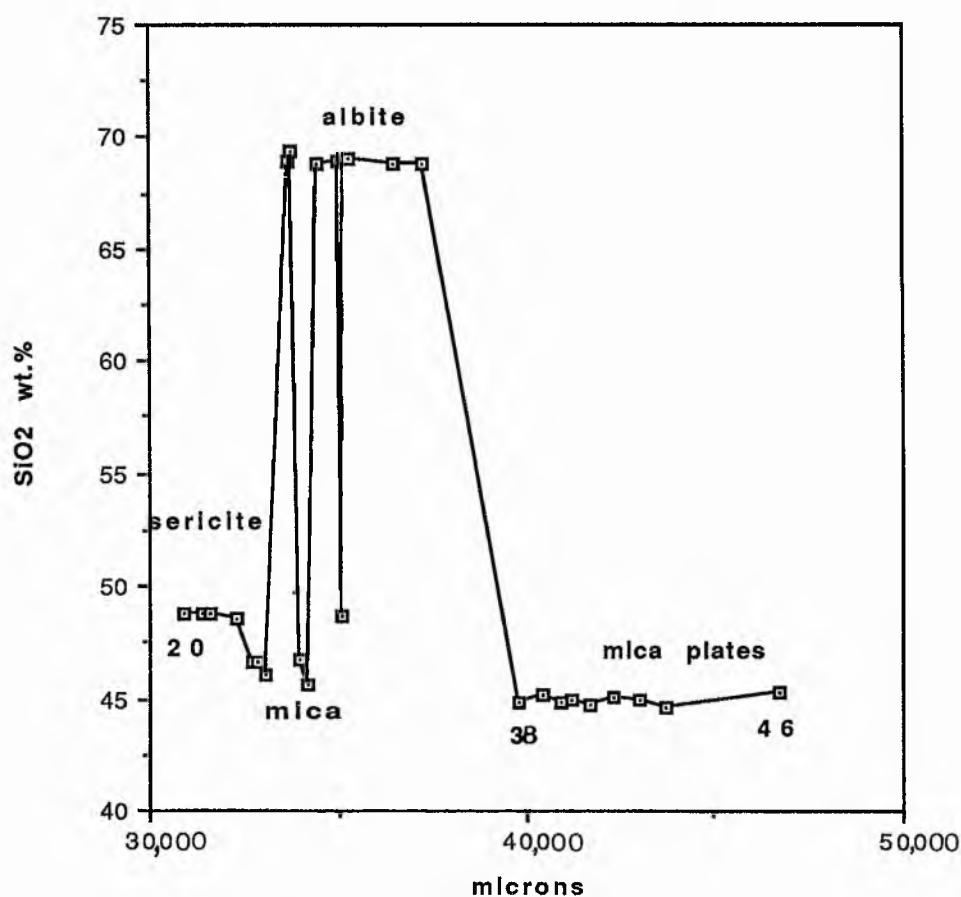


Fig.3.2. An analytical traverse across the Noumas polished section shown in Plate 3.4. Point 20 (sericite) marks the beginning of the traverse, onwards through mica and albite and finally to large mica plates (37-46). Analyses given in Appendix (2) Table 3.3).

TABLE 3.4a. Point analyses across traverse on Plate 3.4b,

Noumas pegmatite, Steinkopf, Namaqualand

Sample Bl	20.	21.	25.	29.	31.	32
SiO ₂	48.73	48.83	46.64	46.73	68.84	68.94
TiO ₂	0.01	0.03	0.02	0.03	0.02	0.01
Al ₂ O ₃	31.10	31.23	37.14	38.45	20.00	20.06
FeO	0.61	0.63	0.41	0.31	0.00	0.00
MnO	0.18	0.16	0.22	0.29	0.00	0.02
CaO	0.01	0.00	0.01	0.01	0.14	0.17
MgO	2.94	3.09	0.46	0.04	0.02	0.02
Na ₂ O	0.17	0.17	0.25	0.38	12.00	11.89
K ₂ O	10.93	10.92	10.61	10.35	0.07	0.08
F	0.39	0.51	0.07	0.01	0.01	0.00
H ₂ O ⁺	nd	nd	nd	nd		
Total	95.07	95.57	96.46	96.6	101.10	101.17
-O=F	0.16	0.21	0.03			
Total	94.91	95.36	96.43	96.60	101.10	101.17

No of ions on the basis 0=22 (mica) 0=8 (albite)

	20.	21.	25.	29.	31.	32.
Si	6.511] 8	6.499] 8	6.137] 8	6.081] 8	2.978] 3	2.979] 3
Al	1.489]	1.501]	1.863]	1.919]		
Ti	0.001]	0.003]	0.002]	0.003]	0.001]	0.000]
Al	3.408]	3.397]	3.896]	3.979]	1.020]	1.022]
Fe ²⁺	0.069] 4.1	0.070] 4.3	0.045] 4.1	0.039] 4.1	0.000] 1	0.000] 1
Mn	0.020]	0.018]	0.024]	0.031]	0.000]	0.001]
Mg	0.584]	0.613]	0.091]	0.008]	0.001]	0.001]
Na	0.002]	0.001]	0.001] 1.8	0.095] 1.8	1.006]	0.996]
K	1.863] 1.9	1.853] 1.9	1.178]	1.718]	0.004] 1	0.004] 1
F	0.164	0.214		0.003	0.002	0.000

20,21. sericite.

25,29. muscovite after spodumene.

31,32. albite. nd = not determined.

TABLE 3.4b. Point analyses of muscovite (Plate 3.4b)

Noumas pegmatite, Steinkopf, Namaqualand

	38.	46.	DHZ9.	DHZ3.
SiO ₂	44.83	45.31	49.16	46.01
TiO ₂	0.56	0.56	-	0.00
Al ₂ O ₃	30.83	29.18	30.81	35.64
FeO	4.49	4.92	1.43	0.00
Fe ₂ O ₃	-	-	-	0.13
MnO	0.32	0.38	-	0.09
MgO	1.47	1.49	2.21	0.04
CaO	0.00	0.00	0.00	1.12
Na ₂ O	0.45	0.35	0.48	1.88
K ₂ O	10.22	10.08	10.90	8.19
Rb ₂ O	0.46	0.46	-	1.20
Cs ₂ O	0.48	0.48	-	0.20
Li ₂ O	1.06	1.06	-	0.69
H ₂ O ⁺	4.00*	4.00*	4.23	4.65
H ₂ O ⁻			0.15	0.08
F	0.86	1.48	-	0.54
Total	100.03	99.75	100.07	100.23
-O=F	0.36	0.62		0.23
Total	99.66	99.13	100.07	100.00

No. of ions on the basis of O=22 (38,46) O=24 (DHZ)

	38.		46.		DHZ9.		DHZ3.	
Si	5.628	8	5.711	8	6.536	8	6.090	8
Al	2.372		2.289		1.464		1.910	
Ti	0.053		0.053		-		-	
Al	2.188		2.289		3.365		3.646	
Fe ³⁺	-	3.6	-	3.7	-	4	0.013	4.
Fe ²⁺	0.471		0.519		0.159		-	
Mn	0.034		0.041		-		0.010	
Mg	0.275		0.280		0.440		0.008	
Li	0.535		0.537		-		0.366	
Ca	-		-		-		0.159	
Na	0.110		0.086		0.124		0.476	
K	1.636	1.8	1.620	1.8	1.850	2	1.384	2.1
Rb	0.037		0.037		-		0.102	
Cs	0.026		0.026		-		0.012	
OH	3.351*	3.7	3.365*	4.0	4.196	4.2	4.106	4.2
F	0.341		0.590		-		0.113	

38,46. Muscovite plates on traverse across Plate 3.4b, Noumas pegmatite, Steinkopf, Namaqualand. (Sample 94J).
 DHZ9. Yellow sericite, Amelia, Virginia (Schaller, 1950) (+0.19 other components).
 DHZ3. Rose muscovite, Varutrask, Sweden (Berggren, 1940). nd = not determined. * estimated value.

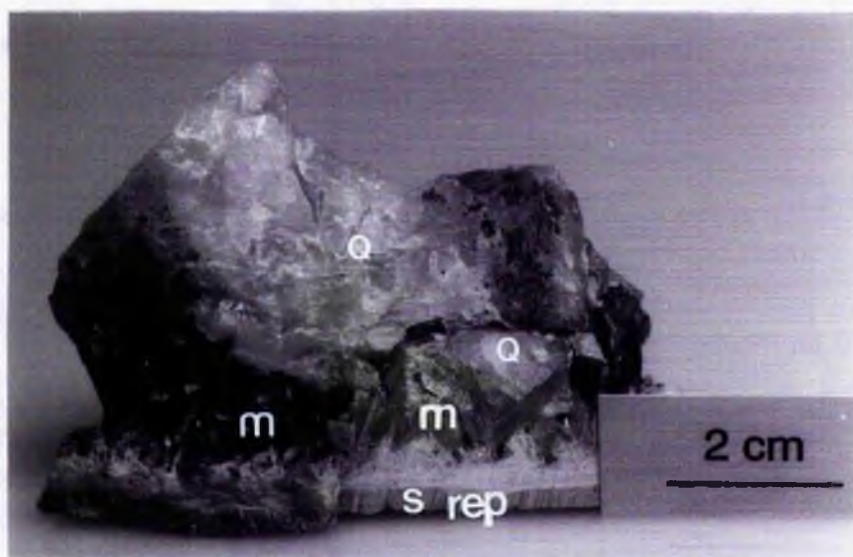


Plate 3.4 a. Alternating layers of replaced spodumene, albite and mica, large mica plates and quartz, shown below in the photomicrograph, Noumas pegmatite, Namaqualand.

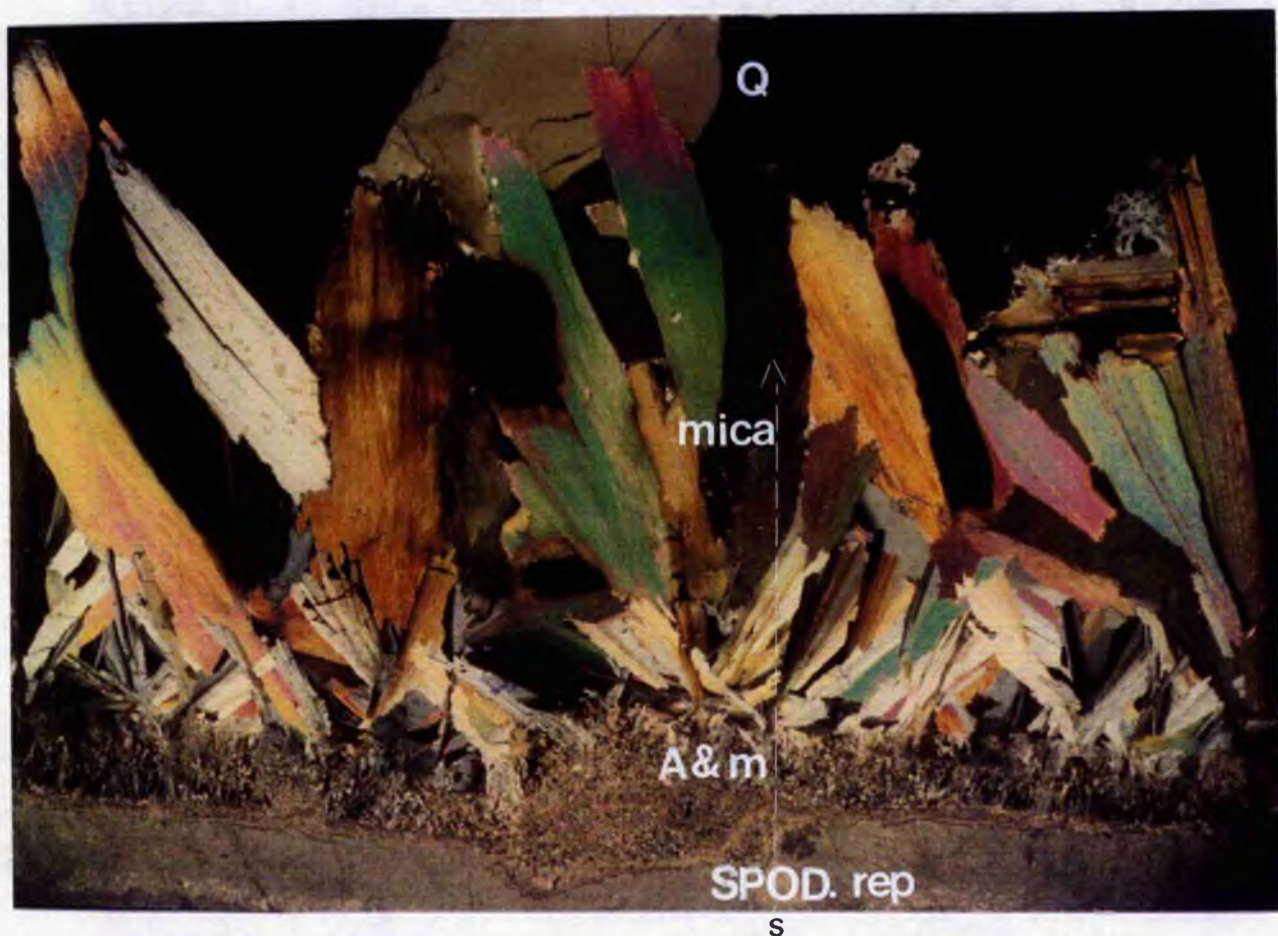


Plate 3.4b. Photomicrograph of layers of replaced spodumene (spod. rep) by mica and sericite; fine-grained albite and mica (A+m); mica plates and quartz (Q). S marks the start of an analytical traverse across the section (marked by a dotted line) Noumas pegmatite, Namaqualand. Width of section along traverse: 2.3 cm. Crossed polarized light.

3.2.5. Spodumene from the SW. Witkop pegmatite, Tantalite Valley, Namibia

On the northeastern side of the Tantalite Valley Complex, Warmbad (Fig. 2.8) in a parallel valley, unaltered pink spodumene laths, up to 20 cm in length, occur with cleavelandite and quartz at the SW. Witkop pegmatite. Spodumene also occurs as fibrous needles or rosettes in a concentric arrangement within large cleavelandite crystals as a later phase. The "rosettes" appear to be invading the feldspar along cleavages and cracks (Plate 3.5).

Whitish-grey spodumene associated with cleavelandite was analysed on the electron microprobe. The spodumene contained 65.23-66.75% SiO₂ (see Appendix (2) Table A3.5) which is a high silica total due to using a rastered beam over an area of 10 microns on the microprobe. Spodumene is highly unstable under the beam. The spodumene is partly replaced by mica and albite and an analytical traverse was completed across the specimen commencing at the point (S) indicated in Plate 3.6. The traverse is represented graphically in Figure 3.3 which shows the variations in content of the minerals across the traverse in terms of the SiO₂ content with analytical numbers from 49 -68. Point analyses were taken at approximately 500 micron intervals.

Fig 3.3. shows the SiO₂ content across the spodumene into mica + albite (fine-grained) and finally into cleavelandite (course-grained), such that numbers 49 - 54 represent the SiO₂ content of the spodumene approximately 66%; 55 represents mica with 47% SiO₂; 56 represents spodumene with 66% SiO₂; 58-59 represents albite(68% SiO₂); 60 represents mica (44% SiO₂) in albite; 61 represents spodumene in albite; (62 represents K-feldspar in albite, 64% SiO₂) and 63 represents mica (44% SiO₂) in the albitic matrix. Points 64-68 represents the area of large cleavelandite laths and points 69-71 spodumene "rosettes" which are lying along the elongation of the

crystal boundaries of the cleavelandite laths. The horizontal axis represents the distance across the traverse from the starting position marked S in Plate 3.8 approximately 20 mm. Analyses 54-62 shown in Table 3.5 represent

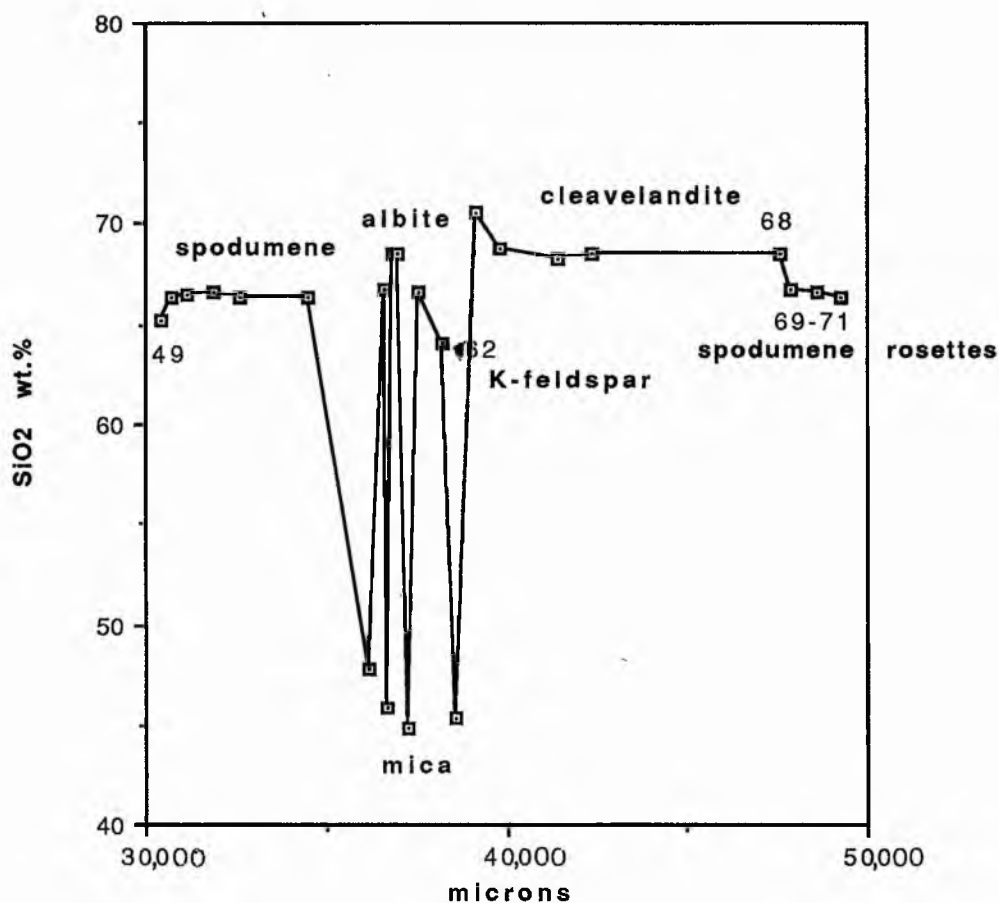


Fig. 3.3. Traverse across spodumene, mica+ spodumene, and cleavelandite SW. Witkop, Tantalite Valley, Namibia starting at point 49 which represents analysis 49 in Table 3.5. The different SiO₂ contents signify each mineral type across the traverse; the traverse is indicated in Plate 3.6. Analyses 49-54,56,61 represent spodumene occurring across the traverse; 55,57,60,63....mica; 58,59,64-68.....cleavelandite; 62....K-feldspar; 69-71....spodumene rosettes.

the part of the traverse showing the spodumene replacement by albite and by mica (see Fig. 3.3); a remnant of K-feldspar also occurs. As the spodumene and albite analyses are of constant composition only a representative section of the analyses are given in Table 3.5, the remainder are shown in Appendix 2, Table A.3.5 Cleavelandite and albite analyses are high due to the rastered beam.

The evidence from the backscattered image of the probe section (which is not included) shows the spodumene being replaced spacially by albite with isolated areas of mica developing, a remnant of K-feldspar is also present or possibly late K-feldspar may be developing. This order of replacement is consistent with the phase relation schematic diagram after Burt and London (1982) (see Fig. 3.4). At point B with decreasing SiO_2 activity, spodumene is converted to albite and at point C with still lowering SiO_2 activity and increasing albitization (NaLi activity), albite may be replaced by Li-mica.

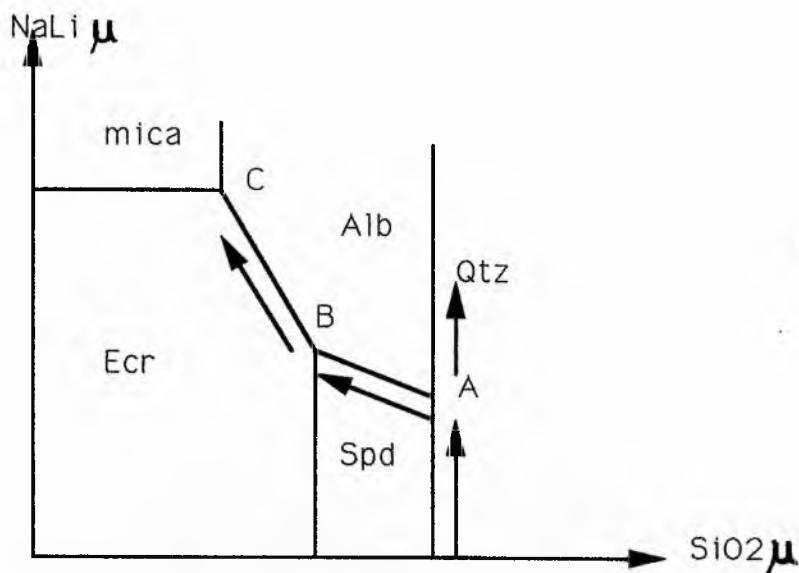


Fig. 3.4. A schematic diagram in the system $\text{LiAlSiO}_2\text{-SiO}_2\text{-NaLi}$ at T too low for the stability of petalite (after Burt and London, 1982). The arrows along the X-axis represent increasing SiO_2 activity and along the Y-axis increasing albitization - activity of Na and Li in late fluids reacting with primary minerals. The other arrows indicate likely phase changes as a result of changes in NaLi and Si activity. At point B spodumene is converted to albite, with lowering SiO_2 activity and increasing albitization

3.2.6 Discussion

The object of this section is to present paragenetic details and data concerning the spodumene occurrences in three pegmatite bodies and to describe the primary versus metasomatic nature of these occurrences.

Spodumene crystallization ranges from early to late with regard to the main stages of feldspar crystallization. There appears to be no change in spodumene composition (from early to late) i.e. regardless of paragenesis in the sequence of crystallization. The secondary rosettes have the same composition as the primary spodumene laths at SW. Witkop.

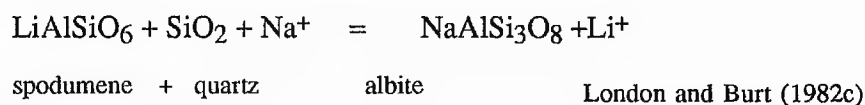
Unaltered spodumene is virtually constant in composition and close to the theoretical formula regardless of its paragenetic placement in the crystal sequence and the P.T. conditions. Crystallization during post consolidation events also is evident, i.e. fine-grained spodumene rosettes in fractures and along grain boundaries is due to metasomatic late stage aqueous fluids and implies that Li-Al saturated fluids percolated through largely consolidated spodumene and cleavelandite-bearing bodies. Where there are Li-Al silicates instead of Li-mica, fluorine activity was low throughout consolidation and stabilized Li-Al silicate phases instead of lepidolite. This is pertinent to the S.W. Witkop pegmatite on the eastern flank of the Tantalite Valley Complex. Where F has a little more significant role, the association of Li-mica, cleavelandite (also boron) and tourmaline-rich assemblages are apparent for example at the Norrabees pegmatite where these three minerals are in close association. Aqueous fluids are also apparent at Noumas when spodumene in association with fresh pink K-feldspar has been converted to kaolinite.

The alteration sequence for spodumene from pegmatites in the Steinkopf area, Namaqualand and from Tantalite Valley implies that initial replacement involved sodium -

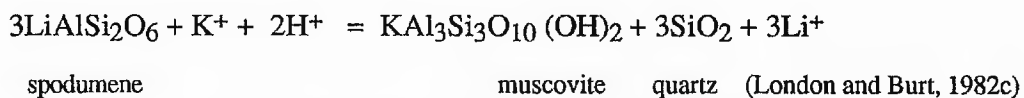
for-lithium ion exchange, as evidenced by the formation of albite, followed by K + H metasomatism resulting in the conversion of spodumene and albite to mica.

Spodumene forms coarse (1-24 cm long) euhedral lath-shaped crystals, milky white to pale purple in SW. Witkop pegmatite, Tantalite Valley. Abundant elongate laths of spodumene (locally forming inward radiating clusters) occur together with large crystals of cleavelandite feldspar., both are distributed with a well-exposed alignment normal to the fine-grained margins, which is indicative of conditions of rapid growth from a metastably supersaturated melt (Charoy et al. 1992).

The position of spodumene in the sequence of crystallization remain ambiguous- several generations of spodumene are obvious. The early phase precedes the first appearance of albite. However, albitization of spodumene at SW. Witkop may be described by the following reaction:



and the formation of pseudomorphic mica in spodumene suggests the local lowering of silica activity. The direct conversion of spodumene to muscovite liberates silica:



Quartz is not present in muscovite pseudomorphs in the Steinkopf pegmatites, Namaqualand or in Tantalite Valley and it is suggested by London and Burt (1982c) that where spodumene is embedded in pure cleavelandite zones (this is applicable to the Steinkopf area examples) the replacement of quartz-spodumene pegmatite by large masses of cleavelandite, may facilitate the above conversion of spodumene to muscovite by the absorption of the excess silica into the cleavelandite.



Plate 3.5. Photomicrograph of cleavelandite (Cl) and secondary spodumene forming rosettes along the cleavelandite grain boundaries. Width of rosettes: 30 microns. Crossed polarized light.

Plate 3.6. Photomicrograph (polished thin section) of albite and mica (A+M) replacing spodumene (spodumene pseudomorph) fine-grained albite (a) and cleavelandite laths, SW. Witkop pegmatite, Tantalite Valley, Namibia. S marks the start of an analytical traverse across the section which represents 20 mm. Analyses given in Table A3.3. Crossed polarized light. spodumene "rosettes"



3.3. PETALITE - MONTMORILLONITE

3.3.1 Introduction

Lithium was first discovered in petalites, $\text{Li}(\text{AlSi}_4\text{O}_{10})$, by Alfredson in 1817. The mineral occurs in inner zones of pegmatites with spodumene, tourmaline, lepidolite, topaz, microcline, amblygonite, apatite, pollucite and columbite. Petalite has been investigated by Quensel (1957), Cerny and Ferguson (1972) Heinrich (1975), von Knorring (1970, 1985) and experimentally by Sebastian and Lagache (1991).

Petalite is the third most abundant lithium mineral and occurs principally as giant crystals in the inner parts of zoned pegmatites (see Plate 3.7). Heinrich (1975) concluded from petalite-spodumene investigations that petalite occurs in two ways: (1) as primary, generally large crystals in intermediate zones of complex pegmatites; and (2) less commonly, as minor fine-grained replacement, mainly of spodumene, i.e. isochemical replacements of petalite by spodumene + quartz.

Petalite is a ubiquitous mineral in the Karibib pegmatites. In the hanging wall of the core zone of the Rubicon pegmatite (see Fig. 2.1) petalite is the main lithium mineral along with subordinate amblygonite. The petalite unit at Rubicon is rather narrow, on average 1-2 m wide, broadening to 6 m or more in places. Plate 3.8 shows crystals of petalite of 1-2 metres in length occurring in cleavelandite at Rubicon. Clear glassy petalite from Rubicon varying in colour from pure white to grey and pink, has previously been analysed by von Knorring (1970) by gravimetric techniques, (see Table 3.6) it may be observed that the petalite contains SiO_2 from 77-78%, with 4.40-4.56% Li_2O . The analyses show only slight deviations from the ideal formula. Minor constituents such as Na, K, Fe and Mn are usually present in trace amounts. Minor amounts probably occur in saline fluid inclusions. The theoretical value of petalite is 78.48% SiO_2 , 16.64% Al_2O_3 and 4.88% Li_2O .

TABLE 3.6. Compositions of petalite-montmorillonite

	Vas.	Nel.	OvkI	OvkII	III	OvkIV	V	X99	X100
SiO ₂	78.00	77.18	78.36	77.30	73.83	52.65	56.35	73.86	67.14
TiO ₂									0.03
Al ₂ O ₃	17.03	16.04	17.06	17.68	18.28	22.30	19.29	17.00	19.61
Fe ₂ O ₃	0.01	0.64	0.04	0.02	tr	0.02		0.14	0.14
FeO	0.03	-	-	0.03	0.04	0.38	0.17	0.01	0.03
MnO	-	-	-	0.03	0.04	0.38	0.17	0.01	0.03
MgO	-	0.26	-	-	0.54	2.76	3.03	0.31	-
CaO	-	0.22	-	-	0.61	2.19	2.06	0.38	0.28
Na ₂ O	0.07	1.14	0.07	0.09	0.12	0.25	0.33	0.31	10.42
K ₂ O	0.05	-	0.06	0.18	0.10	0.12	0.24	0.91	0.30
Li ₂ O	4.74	4.36	4.56	4.40	2.91	tr	tr	2.71	-
H ₂ O+	0.04	0.40	0.05	0.34	1.42	9.80	9.00	*4.40	1.0*
H ₂ O-	0.00	0.02	0.05	0.26	2.12	9.72	9.59		
	99.97	100.26	100.25	100.30	99.97	100.19	100.06	100.04	99.33

No. of ions on the basis of O=20

	Vas	Nel	vk1
Si	7.968	8	8
Al	0.032	0.042	0.028
Al	2.018	2.02	2.017
Fe ³⁺	0.001	0.050	0.003
Mg	-	0.04	-
Fe ²⁺	0.002	-	-
Li	1.948	1.97	1.864
Na	0.014	0.227	0.073
Ca	-	0.024	-
K	0.006	-	-
OH			

- Vas. Petalite, Finland (Vesalio, 1959)
 Nel. Petalite, Karibib, South West Africa (Nel, 1948)
 vkI White clear petalite, Rubicon, Karibib, Namibia (von Knorring, 1970)
 vk2II Pink clear petalite, Rubicon, Karibib, Namibia (von Knorring, 1970)
 III Altered petalite, Karibib, Namibia, analyst, Erna Padget unpublished analysis
 vkIV Pink montmorillonite, after petalite, Rubicon, Karibib, Namibia (von Knorring, 1985)
 V Grey montmorillonite, after petalite, Rubicon, Karibib, analyst, Erna Padget (von Knorring 1985).
 X99 Chalky altered petalite associated with blue cleavelandite, Helicon 2, Karibib, Namibia (X.R.F)
 X100 Blue cleavelandite associated with petalite, Helicon 2, Karibib, Namibia (X.R.F)
 * Fusion loss

Petalite commonly alters to montmorillonite which may occur as a fibrous pale to deep pink coating on the petalite. At Rubicon locally large patches have altered to bright pinkish-grey montmorillonite. Analysis III (Table 3.6) shows values for altered petalite to contain 1.42% total water, less SiO₂ 73.83%, more Al₂O₃ 18.28%, less Li₂O 2.91% than the unaltered petalite. Montmorillonite after petalite is hydrated (18-20% H₂O) contains less SiO₂, higher Al₂O₃, lithium having been leached out. From the analyses given in Table 3.9., it is clear that glassy pale pink petalite and clear white petalite contain almost identical amounts of lithium, 4.40 and 4.56% Li₂O respectively, however the pink variety contains 0.03% MnO. Altered petalite, and montmorillonite after petalite, are hydrated, contain less or no lithium, and in the case of montmorillonite, less Si (52-56%), more Al (19-22%) with minor amounts of CaO and MgO (Table 3.6).

3.3.2 Petalite replacement by albite

Clear petalite has not been reanalysed from the Rubicon or Helicon pegmatites, as the fresh glassy varieties have already been very adequately hand picked and analysed by O.von Knorring (see Table 3.6). The major consideration in the thesis is to analyse petalite which is associated directly with other minerals to determine their sequence in the crystallization process.

Petalite is a major mineral at Helicon 2 where it occurs with lepidolite and cleavelandite in a zone 1-3 m in width. A distinctive association of fine-grained chalky, which signifies alteration, rather than glassy petalite occurs with blue cleavelandite (see Table 3.6. anal. x100) in alternate striations 2 cm wide (see Plate 3.7). In thin section the petalite appears altered which is compatible with the analysis (see Table 3.6, anal. x99). Albite is enclosed within petalite, suggesting albitic replacement of petalite. Minor amblygonite is intergrown with petalite (see Plate 3.9). The amblygonite crystal, identified by petrographic techniques, is very broken up and in optical continuity; it is partly replaced

by albite. It appears to be in a more advanced stage of replacement than the petalite. The relationship between the petalite and amblygonite is not shown so clearly as albite is replacing both of the minerals along their junction, however, there is more evidence to suggest that the amblygonite is after the petalite than vice versa. The relationship in general in the Helicon 2 pegmatite between amblygonite and petalite suggests that amblygonite is after petalite as it occurs on the outer margins of the main lithium zone which consists mainly of petalite.

3.3.3. Petalite in association with yellow-black tourmaline

Grey petalite is common at Daheim 3 pegmatite, where yellow tourmaline is intergrown with primary petalite. Petalite is a very prominent Li-mineral in this pegmatite. The pegmatite, however, was not examined in any great detail and had not been excavated to any great depth. Tourmaline has been found to contain 0.5% ZnO and 0.70% TiO₂ (see Table 3.7). Tourmaline is interesting as it occurs in various units throughout the pegmatites, normally black tourmaline (Fe-rich and Li-deficient) occurs in the outer zones and blue, pink, red and green in the inner zones which, in contrast to schorl contains Mn and Li (see Baldwin, 1979). In particular its association with cleavelandite which is the host mineral for tantalite and the fact that it contains boron may contribute to the paragenetic sequence in the pegmatites and the behaviour of volatiles.

Petalite at Daheim is intergrown with microcline and tourmaline, it has been examined by microprobe in 3 different areas, in particular, in close proximity to the yellow tourmaline. One large tourmaline 100,000 microns across occurs at the top of Plate 3.11 and analyses 80/1, 80/2 (Table 3.7) of petalite are taken in close proximity to this tourmaline. Petalite was analysed close to a smaller tourmaline of 5,000 microns width (see anals 80/3 and 80/4) and finally near a comparatively small tourmaline of 1,000 microns width(1 mm)

(anal. 80/5). The smaller tourmalines are situated in petalite-microcline intergrowths. The analyses of the primary petalite are shown in Table 2.3.2 - the theoretical value of Li_2O is 4.88% (Table 3.10 anal. T). There is little variation in the composition of the petalite apart from anal. 80/3, the SiO_2 varies from 79.25 -> 79.74 and the Al_2O_3 from 16.41- 16.63%.

It is suggested that as a result of subsolidus cation exchange with residual pegmatitic liquid, petalite has been partially altered, in an alkaline environment, to albite in the Helicon 2 pegmatite. Petalite may be converted to albite in quartz-saturated, Na-rich environments (London and Burt, 1982a).

The primary lithium aluminosilicates in pegmatites, spodumene and petalite frequently exhibit partial to complete alteration to a variety of fine-grained mineral assemblages and replacement of petalite by albite has been reported from numerous localities (London and Burt, 1982a). The phase diagram constructed by London and Burt (1984) in the system $\text{LiAlSi}_2\text{O}_4\text{-SiO}_2$, from available experimental data shows that spodumene is stable at high P, spodumene + petalite is stable at moderate P and T and petalite is stable at moderate T and low P. The lithium aluminosilicate phase diagram accounts for their observed replacement of petalite by spodumene + quartz at relatively high P and decreasing T. However, this type of replacement has not been observed in the Karibib pegmatites studied, where petalite commonly alters to montmorillonite.

Table 3.7. Composition of petalite in close proximity to tourmaline and microcline, Daheim 3 pegmatite, Karibib, Namibia

Specimen	80/1	80/2	80/3	80/4	80/5	T	80/M	80/T	80/T1
SiO ₂	79.49	79.74	78.52	79.25	79.70	78.48	62.24	37.01	36.73
TiO ₂	-	0.02	0.03	-	0.01	-	0.03	0.70	0.64
Al ₂ O ₃	16.44	16.63	16.21	16.41	16.62	16.64	18.50	39.04	39.11
Fe ₂ O ₃	0.03	0.01	0.00	0.02	0.00	-	0.01	-	-
FeO	-	-	-	-	-	-	-	7.68	3.11
ZnO	-	-	-	-	-	-	-	0.34	-
MnO	0.00	0.02	0.03	0.00	0.00	-	-	0.28	0.22
CaO	0.01	0.01	-	-	-	-	-	0.08	0.12
MgO	0.00	0.02	0.02	0.01	0.00	-	0.01	0.10	0.11
Na ₂ O	0.02	0.02	0.03	0.02	0.00	-	0.91	2.46	2.61
K ₂ O	-	-	-	0.01	0.01	-	13.57	0.04	0.03
P ₂ O ₅	-	-	-	-	-	-	0.64	-	-
Li ₂ O	4.88	-	4.88	-	-	4.88	nd	-	-
Rb ₂ O	-	-	-	-	-	-	1.60	-	-
Cs ₂ O	-	-	-	-	-	-	0.28	-	-
F	-	0.54	-	-	0.12	-	0.33	1.34	1.07
Total	96.26	97.01	99.72	95.72	96.46	100.00	98.02	87.73	82.78.
-O=F	-	0.23	-	-	0.05	-	0.14	0.56	0.34
Total	96.26	96.78	99.72	95.72	98.41	100.00	97.7	87.17	82.44

No of ions on the basis 0=20 (petalite) and 0=16 (microcline)

	80/1	80/3	T	80/M
Si	8.03	8.03	8	4.145
Al	0.00	0.00		
Ti				0.002
Al	1.96	1.95	2	1.452
Fe ³⁺	0.03	-		
Fe ²⁺	-	-		
Mn	-	0.003		
Mg	-	-	2	
Ca	0.001	-		
Li	1.980	2.006		
Na	0.004	0.006		
K	-	-		10.858
Rb				0.069
Cs				0.008

80/1,80/2 Proximal to large tourmaline

80/3,80/4 Proximal to medium size tourmaline

80/5 Proximal to small tourmaline

T Theoretical value of Li(AlSi₄O₁₀) petalite.

80/M Microcline associated with petalite(anal.80/3,80/4)

80/T,80/T1 Pale yellow tourmaline associated with petalite.



Plate 3.7. Giant crystals of pink petalite (+montmorillonite (1m) occurring in cleavelandite, Rubicon pegmatite, Karibib.

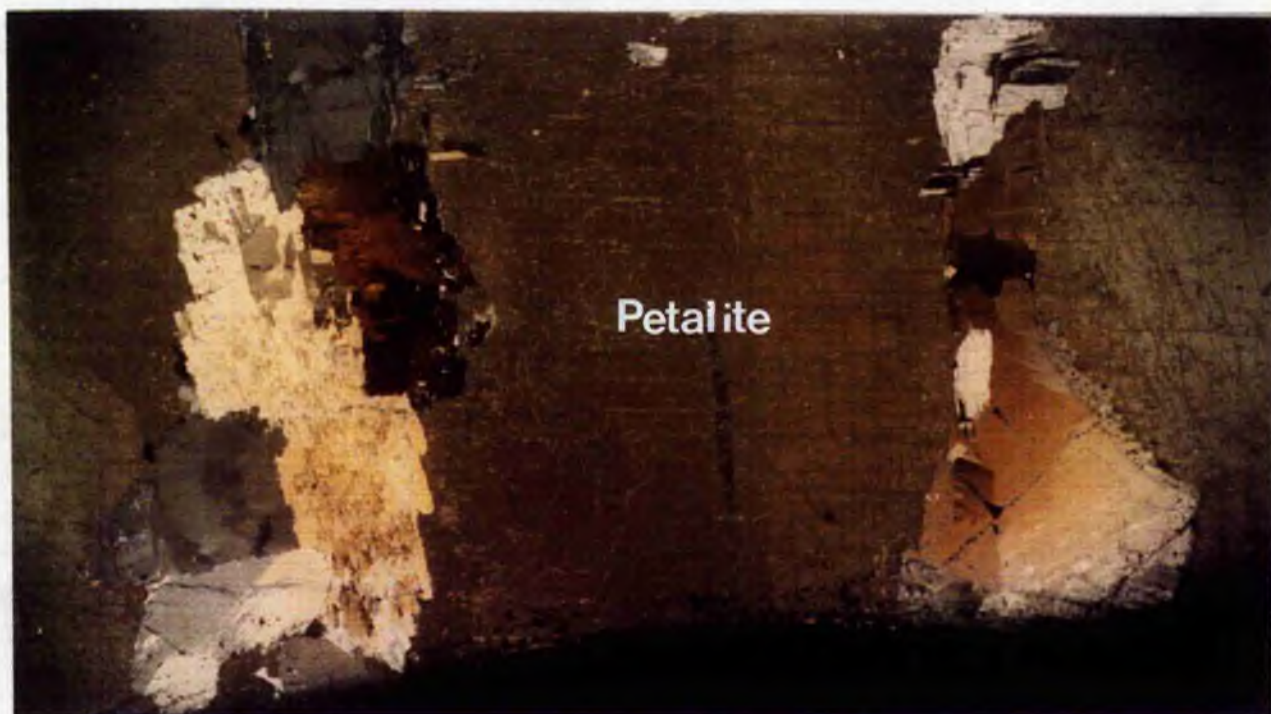


Plate 3.8. Photomicrograph of intergrown petalite (tan-dark brown with 2 cleavages) and albite, Helicon 2 pegmatite, Karibib, Namibia. The lower part of the section with the tan -coloured petalite is magnified in Plate 3.9. Section : 2 cm.

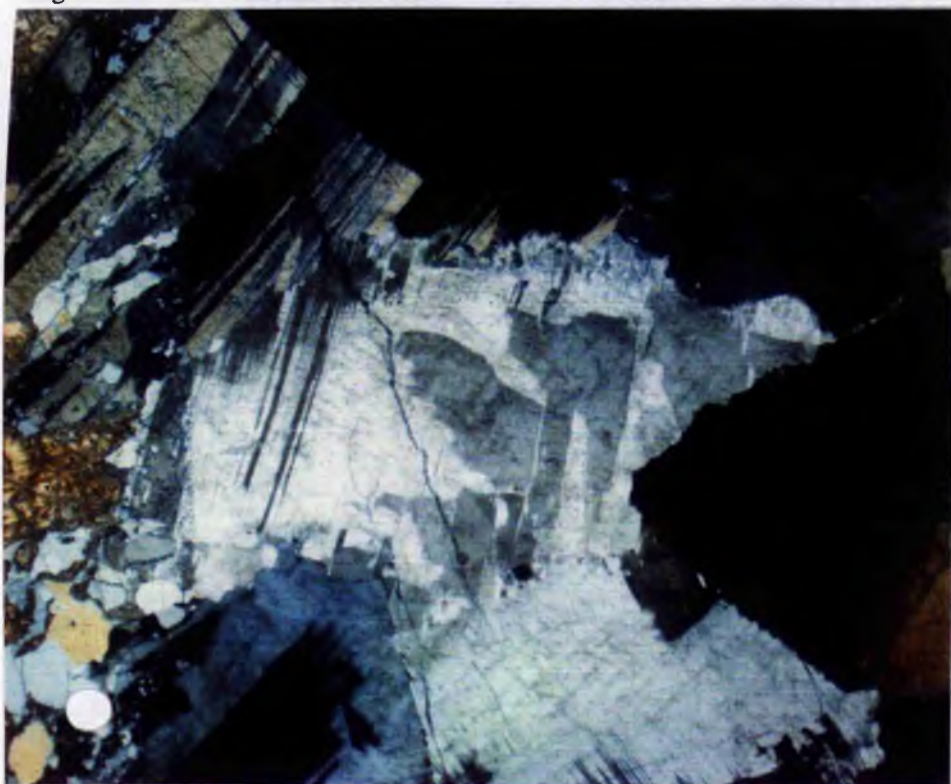


Plate 3.9. Photomicrograph of petalite (yellow-tan) being replaced by albite (grey), Helicon 2 pegmatite Karibib, Namibia. Scale bar: 1 mm _____ Crossed polarized light.

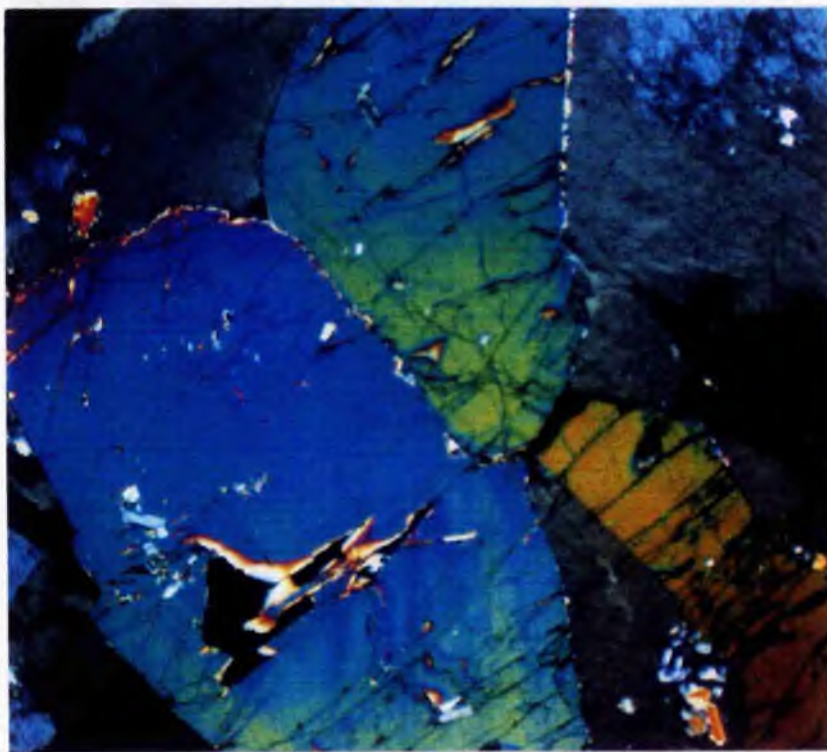


Plate 3.10. Photomicrograph of yellow Zn-Ti-tourmaline (blue-green) occurring in petalite (grey), Daheim 3 pegmatite, Karibib, Namibia. Crossed polarized light.
Scale bar: _____ 1.5 mm.

3.4.

REPLACEMENT

PHENOMENA IN AMBLYGONITE-MONTEBRASITE

3.4.1. Introduction: amblygonite-montebbrasite

Amblygonite $(\text{Li,Na})\text{AlPO}_4(\text{F,OH})$ with $\text{Li} > \text{Na}$ and $\text{F} > \text{OH}$ forms a series with montebbrasite $(\text{Li,Na})\text{AlPO}_4(\text{OH,F})$ where $\text{F} < \text{OH}$ and fluorine is less than 7% (Dubois et al., 1973). Of the common Li-bearing minerals, it is the richest, containing usually between 8-10% Li_2O . The name amblygonite generally has been used to refer to any member of the series, but the majority of analysed specimens are montebbrasite. Dana (1963) gives the following specifications : -

$\text{F} > \text{OH}$	$\text{Li} > \text{Na}$	$\text{Na} > \text{Li}$
$\text{OH} > \text{F}$	Amblygonite	Not known
	Montebbrasite	Natromontebbrasite

Primary montebbrasite typically contains 4-7 wt.% F (see Table 3.8. anal.1, 4-11) it may be extensively replaced by secondary montebbrasite containing 1-4 wt % F (see Table 3.8 anal. 2,3) (Cerna et al., 1972, Kallio, 1978).

Members of the amblygonite-montebbrasite series occur as large subhedral crystals in rounded nodules. They are common constituents of the inner zones and quartz-rich cores of zoned lithium pegmatites. Amblygonite is extremely rare; however, von Knorring has analysed an amblygonite from Maridge Mine, Mozambique with 10% F (Table 3.8, anal. 9); montebbrasite is the most commonly occurring form. Associated minerals include microcline, cleavelandite albite, lepidolite, tourmaline and columbite-tantalite.

The amblygonite-montebbrasite series are rather common minerals in most of the Li-pegmatites in the Karibib area and are in many instances the only lithium minerals to form in pegmatites. Their position within the pegmatite body is commonly within the quartz

core and along the quartz core margin, however they may also occur in the intermediate zone. The mineral generally forms rounded nodules of varying size and occasionally

TABLE 3.8. Analyses of amblygonite - montebrasite

	A1	A2	A3	A4	A5	A6	A7	A8	A9	A10	A11
P ₂ O ₅	48.85	49.21	49.38								
Al ₂ O ₃	34.26	35.53	35.26								
Fe ₂ O ₃	0.00	0.11	0.00			0.01	0.03	0.23	0.04		0.02
CaO	0.08	0.17	0.00		0.11	0.43	0.36		0.03	0.02	
Na ₂ O	0.17	0.03	0.08	1.24	0.90	0.88	0.44	1.47	0.52	0.40	3.03
Li ₂ O	9.30	9.86	9.47	9.28	9.00	9.26	9.49	8.77	9.86	9.15	8.09
H ₂ O ⁺	3.29	4.09	5.98								
H ₂ O ⁻	0.23	0.04	0.10								
F	7.07	3.65	0.30	5.08	5.34	7.77	5.94	6.80	10.00	6.22	5.83
Total	103.25	102.69	100.57								
-O=F	2.96	1.53	0.13								
	100.29	101.16	100.44								

Partial analyses

No. of ions on the basis of O=10

	A1	A2	A3
P	2.016] 2	2.016] 2	2.025] 2
Al	1.970] 2	2.028] 2	2.015] 2
Fe	0.000] -	0.004] -	-
Ca	0.004] -	0.009] -	-
Na	0.016] 1.8	0.003] 1.9	0.008] 1.8
Li	1.824] -	1.921] -	1.846] -
OH	1.071] 2.1	1.323] 1.9	1.935] 2
F	1.091] -	0.559] -	0.046] -

- A1. Montebrasite, (London and Burt 1982b).
 A2,3. Secondary montebrasite (London and Burt, 1982b).
 A4. Montebrasite crystals, De Bruin pegmatite, Karibib, Namibia (von Knorring, 1985)
 A5. White montebrasite, associated with turquoise, Dernburg 2 pegmatite, Karibib, Namibia (von Knorring, 1985)
 A6. Purplish white amblygonite, Etiro 50, Karibib, Namibia (von Knorring, 1985))
 A7. Montebrasite, Becker's pegmatite, Namibia (von Knorring, 1985)
 A8. Montebrasite, Riksburg pegmatite, Okakoara, Namibia. (von Knorring, 1985)
 A9. Amblygonite, Maridge Mine, Alto Ligonha, Mozambique. Analyst: O von Knorring
 A10. Glassy purple montebrasite, Rubicon, Karibib. Analyst: J.R. Baldwin
 A11. White montebrasite, Lepidolite, Tantalite Valley, Namibia. Analyst: J.R. Baldwin

larger aggregates up to a few tons may be found. At the Rubicon pegmatite, Okongava Ost 72, amblygonite occurs with petalite on each side of the quartz core,

Von Knorring (1985) has published partial analyses of montebrasite from pegmatites in the Karibib area, Namibia (see Table 3.8). Montebrasite associated with turquoise, from the Dernburg pegmatite, Karibib and from the De Bruin pegmatite contains 9.00 and 9.28% Li_2O with 5.34 and 5.08 % F respectively (anals. 4,5). Amblygonite from Etiro, which is the largest mining enterprise after Rubicon and Helicon in the Karibib area, contains 9.26% Li_2O and a very high F content 7.77% (see anal.6).

The analyses presented in Table 3.8 from Karibib are primary montebrasite with high F contents from 5.08 to 6.80% with the exception of amblygonite from Etiro Mine with 7.77% F. The Li_2O contents are also high ranging from 8.77 - 9.49%. It may be observed from Table 3.8 that the Li_2O content of amblygonite does not alter due to any metasomatic change from amblygonite to primary montebrasite, to secondary montebrasite. The Li content remains constant as the F content changes from 0.3 to 10% with a corresponding increase in the H_2O^+ content with lithium. In the probe analyses in this section on montebrasite therefore Li_2O will be estimated at 9% and H_2O^+ will be estimated according to the contents in Table 3.8 in order to complete the microprobe analyses.

Purple glassy primary montebrasite from Rubicon Mine has been analysed by flame photometric techniques; it contains high F and high Li_2O : 6.22% and 9.15% respectively. It has been observed (von Knorring, 1985), that a bluish-purplish coloration of this mineral indicates a higher fluorine content; the specimens from Rubicon, and from the Etiro pegmatite (Table 3.8 anals. 6,10) emphasize this assumption.

The Lepidolite pegmatite in Tantalite Valley, also contains amblygonite-montebbrasite. White montebbrasite from the Lepidolite pegmatite has been analysed by flame photometric techniques; this is also primary montebbrasite with 5.83% F and 8.09% Li_2O (anal.11).

Amblygonite has not been recovered from Steinkopf, Namaqualand (Area 2) and the Kenhardt area (Area 3), of the Gordonia-Kenhardt Field, Northern Cape, South Africa. However, amblygonite-montebbrasite has been found in the in the westernmost part of the Namaqualand pegmatite belt, north west of Steinkopf (Fig. 2.3). This area was not visited due to the mountainous nature of the terrain, therefore apart from a small amount of amblygonite recovered from the Lepidolite pegmatite in Tantalite Valley the Pegmatite Belt from Steinkopf to Goodhouse is rather deficient in the amblygonite-montebbrasite series of minerals.

Amblygonite-montebbrasite is frequently replaced by other phosphate minerals. The mineral may be partially replaced by apatite, crandallite, eosphorite, wavellite, triplite, lazulite, scorzalite and brazilianite. Apart from marginal alteration to various clay minerals, von Knorring (1985) has observed a number of replacements in the Karibib area : brazilianite at Okajimukuju 55, and brazilianite, morinite and eosphorite at E tiro 50. Particular replacements which have been investigated in the Karibib area in this study are reported in sections 3.4.2 - 3.4.7 involving apatite, both fluor- and hydroxyl, Li-mica, cookeite, natromontebbrasite, crandallite, blue tourmaline (indicolite), brazilianite and an interesting intergrowth with tantalite and microlite. These occurrences are all from the Karibib area, Namibia.

The object of this section is to present data concerning the replacement characteristics of amblygonite-montebbrasite and to establish a paragenetic sequence with intergrown minerals and the process which is affecting the metasomatic alteration.

3.4.2. Primary montebrasite, secondary montebrasite and apatite: replacement by mica

Daheim 1 pegmatite, Karibib exhibits rectangular blocks of amblygonite-montebrasite, 5cm by 3 cm lying in alternating areas of muscovite and quartz (Plate 3.11). Specimen D4 was analysed with the electron microprobe and replacement of the montebrasite by mica and quartz (Plate 3.12) were studied on the boundaries of the intergrowth (Plates 3.13-3.16).

The analyses in this section range from number 72 to 98 in Tables 3.9-3.11. The montebrasite, associated directly with mica is low in fluorine with 2.36% (Table 3.9. anal. 80-83) and is therefore secondary montebrasite on account of the low F content and the instability of the mineral under the electron beam. However, the analyses vary throughout the section and away from the contact contain 7-8% F, are less unstable and are considered to be amblygonite or primary montebrasite (Table 3.9 anal. 87-93, see Plate 3.13). Apatite (Table 3.10 anal. 78, 79 and 86) is situated at the junction of the mica, which is zoned (see Plate 3.14), and the amblygonite, and extends down cracks into the amblygonite - montebrasite; the white area on the back-scattered image represents the mineral apatite which is a later phase than the montebrasite (Plates 3.15 and 3.16). Primary montebrasite has been replaced at the "mica contact" by secondary montebrasite and apatite. Points 92 and 93 (Plate 3.13) represent the locations of analyses of a twinned crystal of primary montebrasite (Table 3.9); 94 and 95 (Table 3.10) represent analyses of apatite lamellae in the twinned crystal.

The amblygonite-montebrasite analyses in Table 3.9 have a high P_2O_5 content (52%) in comparison with montebrasite in Table 3.8. For the purpose of calculating cation proportions Li_2O and H_2O^+ were estimated according to Table 3.8 which confirms this assumption. The ionic proportions were calculated on selected characteristic analyses.

With regard to the mica, Rb, Cs and H₂O have not been determined, however, Cs has been noted as present by the microprobe. The backscattered image of an area at the junction of the montebrasite and mica shows the mica as light grey, against the darker grey secondary montebrasite, and the white apatite (see Plates 3.15,3.16). The mica appears zoned, and especially at the edges shows a difference in contrast with the centre of the crystal; point analyses were taken in dark mica (72,73,85, see Table 3.11) and in the light mica (anals. 74 and 75) at the edge near the crystal boundaries with montebrasite. The main mica (anals 72,73, 85) has the composition of muscovite; lepidolite with a comparatively high F and Si content and a lower Al content involving Li substitution of Al occurs at the edges (anals. 74, 75) i.e. the lighter area in the backscattered images in Plates 3.14 and 3.15. This non-planar compositional zoning of mica, for example lepidolite replacement of muscovite at the crystal edges, is quite common in lithium pegmatites (pers. comm. O.von Knorring).

An aluminium silicate mineral with fluorine, containing apatite lamellae, is situated in the mica and is intergrown with Mn-apatite . On the backscattered image this mineral , an alteration phase of mica is shown as a black image in Plates 3.15 and 3.16. The mineral (Table 3.11. anals. 76,77,84 and 96) is similar to cookeite $\text{LiAl}_4(\text{Si}_3\text{Al})_{10}(\text{OH})_8$ (Fleisher,1987). However, analyses reported in the literature are not always close to the ideal formula (anal. C, Table 3.11a) with the exception of analysis C₁ (Sahama, von Knorring and Lehtinen, 1968). Enrichment in Al commonly occurs with alteration of mica, however, cookeite has not been confirmed by X-ray diffraction and it must be pointed out that the F-content is high and does not conform to the ideal formula.

The apatite analyses are given in Table 3.10. This is an Mn-Sr- apatite. If compared with the analysis by Quensel (1937) there is a deficiency in Ca ions in some analyses, which may be explained by the presence of Sr to several percent. The analyses are low and it must be pointed out that H₂O has also not been determined.

TABLE 3.9. Amblygonite- montebrasite, Daheim 1 pegmatite, Karibib

	D4/80	D4/81	D4/82	D4/83	D4/87	D4/88	D4/89	D4/90	D4/91	D4/92**	D4/93**
SiO ₂	0.01	0.02	0.01	0.01	0.03	0.02	0.02	0.04	0.02	0.01	0.02
TiO ₂	0.06	0.07	0.08	0.08	0.07	0.09	0.09	0.08	0.09	0.06	0.00
Al ₂ O ₃	36.13	35.94	35.96	35.16	36.26	37.55	35.71	36.01	35.26	36.04	35.77
Fe ₂ O ₃	-	-	0.02	0.02	-	-	-	-	-	-	0.00
MnO	0.02	-	0.02	0.02	-	0.01	-	0.01	-	0.04	-
CaO	0.09	0.03	0.03	0.01	0.01	-	0.02	0.02	0.01	0.01	0.28
MgO	0.02	-	0.01	0.01	0.01	-	0.02	0.03	0.01	-	-
Na ₂ O	-	-	0.01	-	-	0.04	0.65	-	0.05	-	0.17
*Li ₂ O	*9.0	*9.0	*9.0	*9.0	*9.0	*9.0	*9.0	*9.0	*9.0	*9.0	*9.0
*H ₂ O	4.0	*4.0	*4.0	*4.0	*1.5	-	*3.5	*1.5	*1.5	*1.5	*1.5
P ₂ O ₅	51.60	50.93	51.97	51.47	52.07	52.71	50.97	49.97	49.97	51.05	51.46
F	2.23	2.20	1.60	2.36	7.79	8.00	4.90	7.00	6.45	6.52	6.71
	103.16	102.19	102.71	103.14	106.74	107.42	104.88	104.57	102.36	104.23	104.91
-O=F	0.93	0.92	0.67	0.99	3.27	3.36	2.06	2.94	2.71	2.74	2.82
Total	102.23	101.27	102.04	102.15	103.47	104.07	102.82	101.63	99.65	101.49	102.59

No of ions on the basis of O=10 (calculated with estimated Li and OH)

	D4/80		D4/87		D4/93	
Al	2.044		2.037		1.995	
Ti	0.002	2	0.003	2	-	2
Si	0.001		0.001		0.001	
P	2.09	2.1	2.099	2.1	2.060	2.1
Li	1.737		1.725		1.713	
Ca	0.005	1.7	0.001	1.7	0.014	1.7
Na	0.007		0.006		0.016	
OH	1.282	1.6	1.174	1.6	0.948	2
F	0.339		0.477		1.004	

80-83 Secondary montebrasite (point analyses in Plate 3.14)

87-88 Amblygonite (point analyses in Plate 3.12)

89-91 Primary montebrasite (point analyses in Plate 3.12)

**92,93 Twinned crystals of primary montebrasite above the main area and the intergrown mica.

* Estimated (see Table 3.8)

TABLE 3.10. Mn-apatite, Daheim 1 pegmatite, Karibib

SampleD4/	78	D4/79	D4/86	D4/94	D4/95	Q
P ₂ O ₅	37.60	37.22	36.92	40.77	43.02	41.50
FeO	-	-	-	-	0.39	0.26
MnO	1.95	1.80	1.77	0.31	0.70	5.32
MgO	-	-	-	-	-	0.04
CaO	46.78	46.78	47.03	53.88	51.46	50.31
Na ₂ O	0.03	0.04	-	0.27	0.21	0.00
F	2.96	4.45	3.64	4.44	4.11	3.41
H ₂ O ⁺	nd	nd	nd	nd	nd	0.25
H ₂ O ⁻						0.03
	89.32	90.29	89.36	99.67	99.59	101.47
- O=F	1.24	1.87	1.52	1.86	1.76	1.44
Total	87.08	88.42	87.84	97.81	97.74	100.12

No. of ions on the basis of O=25

P	6.050] 6:	6.034] 6:	6.002] 6:	5.932] 6:	6.050] 6:	5.980] 6:
Fe ²⁺	0.00]	0.00]	0.000]	0.000]	0.05]	0.037]
Mn	0.314] 9.9:	0.291] 9.9:	0.288] 10:	0.045] 10:	0.099] 9.4:	0.767] 10:
Na	0.012]	0.015]	0.000]	0.090]	0.07]	-]
Ca	9.526]	9.601]	9.677]	9.920]	9.159]	9.175]
Sr	present----->					
F	1.78	2.694	2.21	2.411	2.161	1.835] 2.1:
OH	nd	nd	nd	nd	nd	0.284]

78,79,86. Daheim 1 pegmatite, Karibib, Namibia (point analyses, Plate 3.14)
 94,95. Manganoapatite lamellae in a twinned crystal of montebrasite (92,93 see Plate 3.12)
 Q Bluish green manganoapatite, pegmatite, Varutrask, Sweden (Quensel, 1937)O=26
 nd not determined

TABLE 3.11a

Zoned mica (Li-muscovite) and altered mica (cookeite) analyses taken at points marked in Plates 3.13-3.16 (sample D4)

Sample D4	74(l)	75(l)	76.	77.	84.	96.	C.	C ₁
SiO ₂	56.69	56.83	38.05	42.08	40.23	41.91	35.25	34.15
TiO ₂	0.05	0.03	0.02	0.02	0.07	0.01	-	-
Al ₂ O ₃	15.59	16.52	42.25	38.24	39.50	38.09	42.58	46.35
Fe ₂ O ₃	0.00	-	-	-	-	-	0.25	0.02
B ₂ O ₃	-	-	-	-	-	-	-	0.38
FeO	0.16	0.14	0.05	0.05	0.05	0.04	0.70	-
MnO	0.61	0.40	0.06	0.06	0.04	0.03	0.06	-
CaO	0.02	0.02	0.03	0.02	0.02	0.03	0.51	0.16
BeO	-	-	-	-	-	-	-	1.06
MgO	0.00	0.03	0.01	0.00	0.00	0.00	0.59	-
Na ₂ O	0.02	0.14	0.01	0.03	0.02	0.00	0.00	0.10
K ₂ O	8.87	8.21	0.02	0.05	0.03	0.03	1.48	-
Li ₂ O*	5.0*	5.0*	3.18*	3.18*	3.18*	3.18*	0.60	3.18
Rb ₂ O*	2.0*	2.0*	-	-	-	-	-	-
Cs ₂ O*	0.5*	0.5*	-	-	-	-	-	-
H ₂ O ⁺ *	3.0*	3.0*	13.*	13.*	13.*	13*	13.84	14.06
H ₂ O ⁻ *	-	-	-	-	-	-	3.59	-
F	6.89	7.52	2.31	3.68	3.22	3.91	0.34	0.35
-O=F	99.41	100.34	99.00	100.40	99.25	100.23	100.00	99.81
	2.89	3.16	0.97	1.54	1.35	1.64	0.14	0.15
Total	96.52	97.16	98.03	98.86	97.90	98.59	98.86	99.66

No. of ions on the basis of O=22(mica) and O=36 (cookeite)

	74.	76.	84.	C.	C ₁	T.					
Si	6.965	8	6.704	6.7	7.05	7	6.489	6.5	5.915	5.9	6
Al	1.035										
Al	1.222		8.772	8.8	8.161	8.2	9.237	9.3	9.459	9.6	10
Ti	0.005		0.003		0.009		-		-		
Fe ³⁺	-		-		-		0.035		0.003		
B	-		-		-		-		0.114		
Fe ²⁺	0.016	3.8	0.007		0.007		0.108		-		
Mn	0.064		0.009		0.006		0.009		-		
Mg	-		-		-		-		-		
Li	2.469		2.252		2.241		0.444		2.214		
Ca	0.003	1.6	0.006	2.3	0.004	2.3	0.004	0.8	0.030	2.6	2
Be	-		-		-		-		0.441		
Na	0.034		0.003		0.007		0.007		0.034		
K	1.390		0.004		-		0.348		-		
Rb	0.158		-		-		-		-		
Cs	0.026		-		-		-		-		
OH	2.460	5.1	15.285	16.5	15.21	17	17.002	17.2	16.251	16.4	16
F	2.676		1.287		1.785		0.198		0.192		

74,75(l) Light area in mica : Li-muscovite, * estimated values. nd=not determined
 76,77,84, 96. Altered mica, (cookeite), Daheim 1 pegmatite, Karibib, Namibia.
 C. Cookeite (London and Burt, 1982)
 C₁ Cookeite (Sahama et al. 1968) Analyst: O. von Knorring. T=theoretical value.

TABLE 3.11b

Zoned mica (Li-mica), point analyses shown on Plates 3.13-3.16.

D4/	72(d)	73(d)	85(d)	97	98	DHZ8
SiO ₂	46.07	47.42	48.40	46.86	48.09	46.30
TiO ₂	0.03	0.02	0.03	0.05	0.02	0.00
Al ₂ O ₃	34.42	31.20	29.40	31.78	29.41	33.08
FeO	0.13	0.13	0.19	0.26	0.36	1.20
MnO	0.24	0.32	0.44	0.39	0.62	0.28
CaO	0.01	-	-	0.00	0.00	-
MgO	0.01	0.03	0.03	0.01	0.01	0.14
Na ₂ O	0.78	0.60	0.60	0.57	0.43	0.63
K ₂ O	9.38	9.24	9.37	9.54	9.68	10.09
Rb ₂ O	nd	nd	nd	nd	nd	1.37
Cs ₂ O	pres.	----->	----->	pres.	----->	0.41
Li ₂ O	nd	nd	nd	nd	nd	1.80
P ₂ O ₅	0.08	0.05	0.01	0.03	0.04	
F	1.87	3.44	3.88	3.23	4.93	2.06
H ₂ O ⁺	nd	nd	nd	nd	nd	3.06
H ₂ O ⁻						0.34
	93.02	92.45	93.06	92.72	93.59	100.76
-O = F	0.79	1.41	1.63	1.36	2.07	0.87
Total	92.23	91.04	91.43	91.36	91.52	99.89

No of ions on the basis of O=22

D4	72.	73.	85.	97.	98.	DHZ8.
Si	6.32] 8	6.64] 8	6.32]	6.56] 8	6.79] 8	6.270] 8
Al	1.68]	1.36]	1.68]	1.44]	1.21]	1.730]
Al	3.89	3.79	3.22	3.80	3.69	3.552]
Fe ²⁺						0.136]
Mn						0.032] 4.73
Mg						0.028]
Li						0.980]
Na	0.193]	1.52]	1.73]	2.08]	2.21]	0.166]
K	1.64]					1.742] 2.05
Rb	-]	-]	-]	-]	-]	0.118]
Cs						0.024]
F	0.81	1.52	1.73	2.08	2.21	0.882] 3.65
OH	-	-	-	-	-	2.766]

72-75, 85,97,98 Zoned mica, Daheim 1 pegmatite, Karibib, Namibia
(d) = dark area (see Plates 3.14 and 3.15)

DHZ8. Grey "lepidolite", Varutrask, Sweden (Berggren,1940).

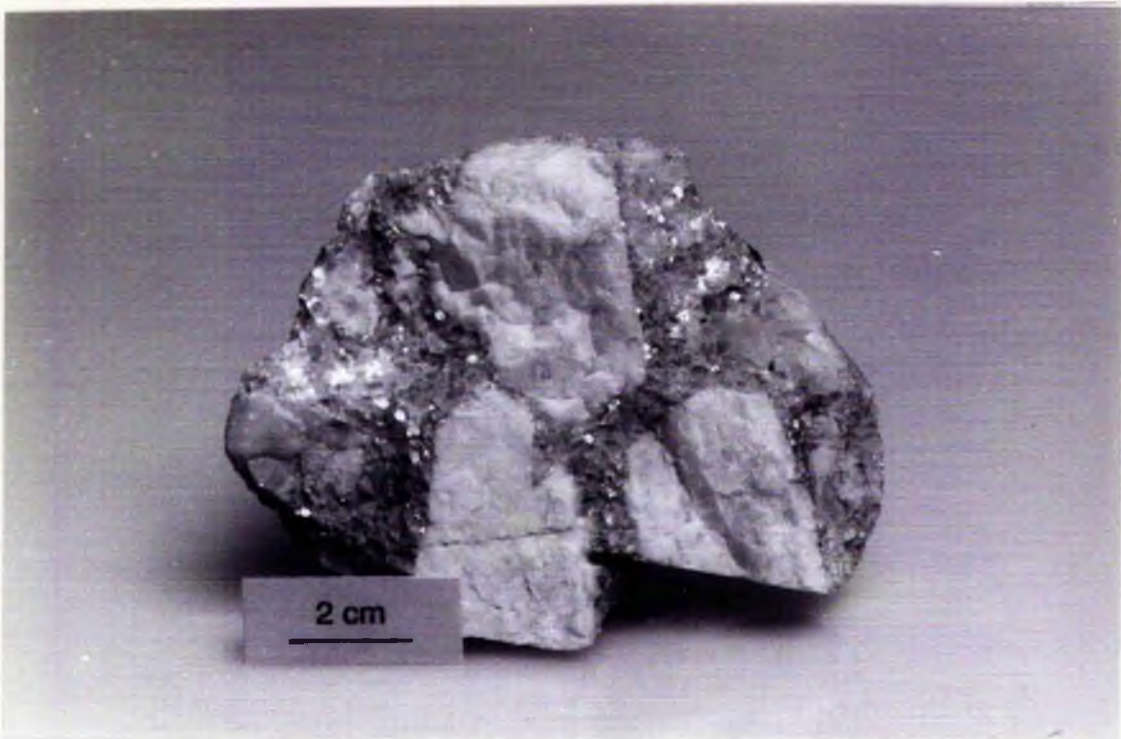
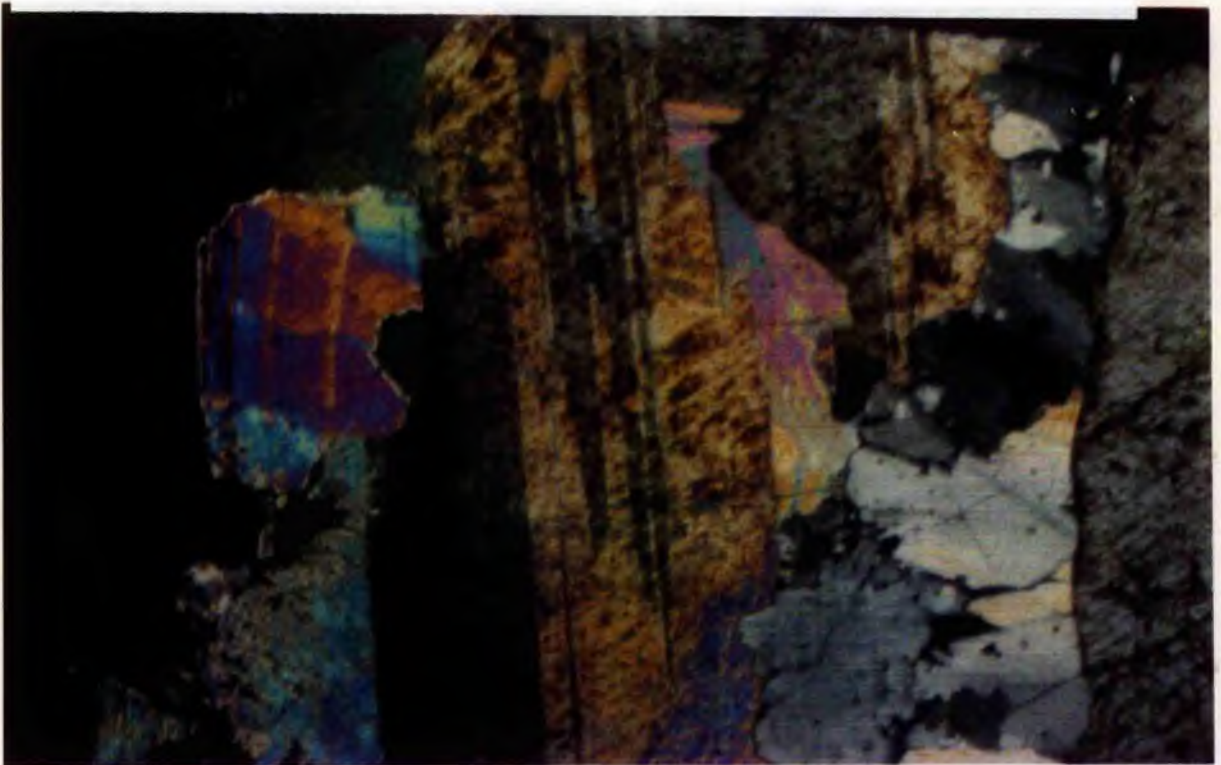


Plate 3.11. Montebasite and mica, Daheim 1 pegmatite, Karibib, Namibia. Sample D4.
Plate 3.12. Photomicrograph of replacement of twinned crystals of montebrasite by mica and quartz, Daheim 1 pegmatite, Karibib, Namibia. Crossed polarized light. Scale bar: 2mm



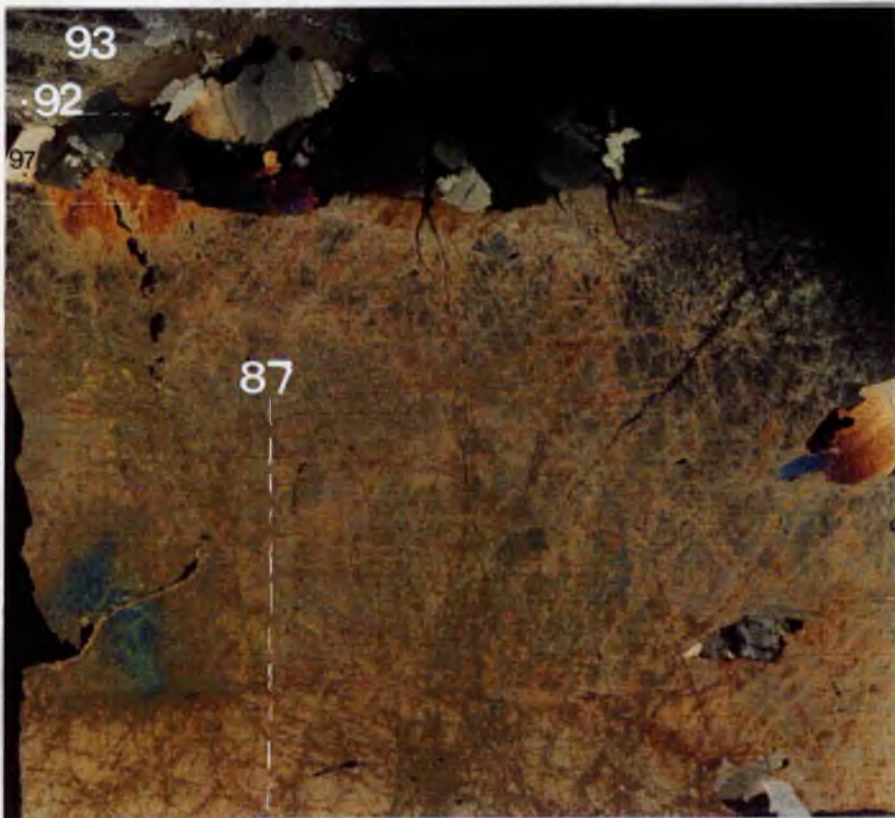


Plate 3.13. Photomicrograph of replacement of primary montebrasite by quartz and mica. Daheim 1 pegmatite, Karibib, Namibia. (Polished thin section D4; length of section : 3.5 cm) . 87-93 represent point analyses given in Table 3.9. The area within the dotted inset represents the BSE images shown in Plates 3.14-3.16.

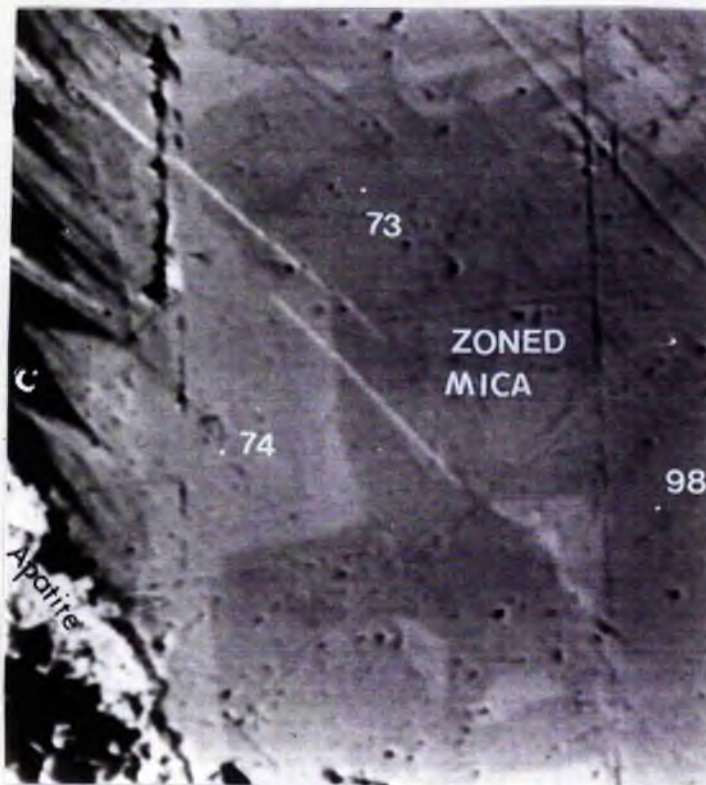
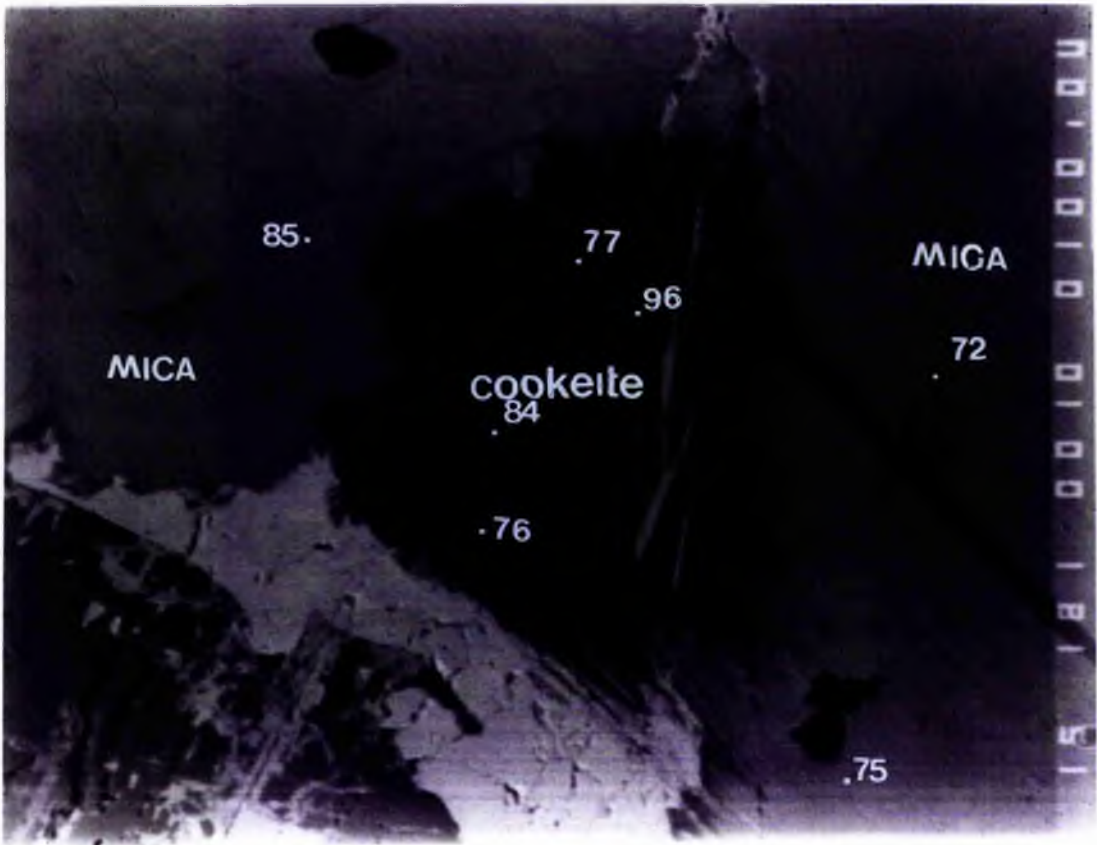
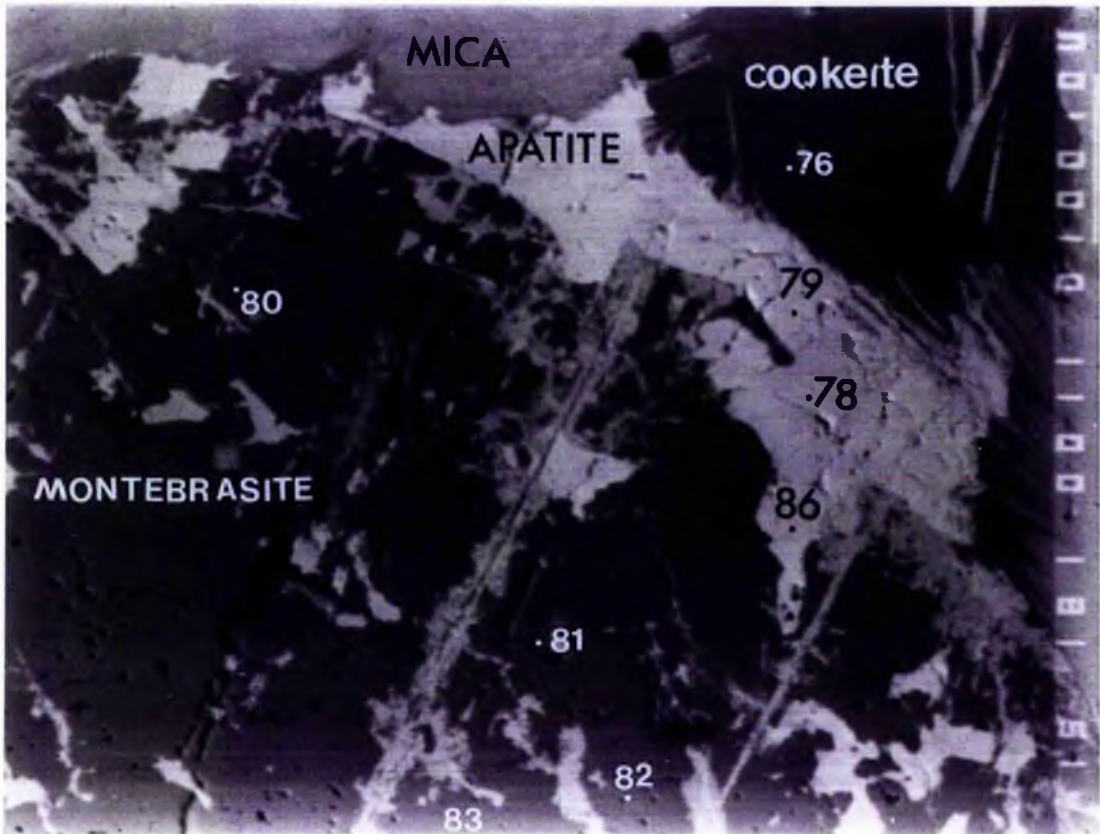


Plate 3.14. Backscattered electron image continued from Plate 3.16 showing apatite lamellae(white) and cookeite (c)(black) penetrating zoned Li-mica. 73, 74, 98 represent point analyses given in Tables 3.10, 3.11. Scale bar: 100 microns.



Plates 3.15 above and 3.16 below. Backscattered electron image of the area shown in the inset box in Plate 3.13 showing cookeite (black) with point analyses 76, 77, 84, 96; montebrasite (dark-grey) 80 - 83; mica (light grey) 72, 75, 85 and apatite (white) 78, 79, 86, Daheim 1 pegmatite, Karibib, Namibia. Analyses are given in Tables 3.9-3.11. Scale bar: 100 microns



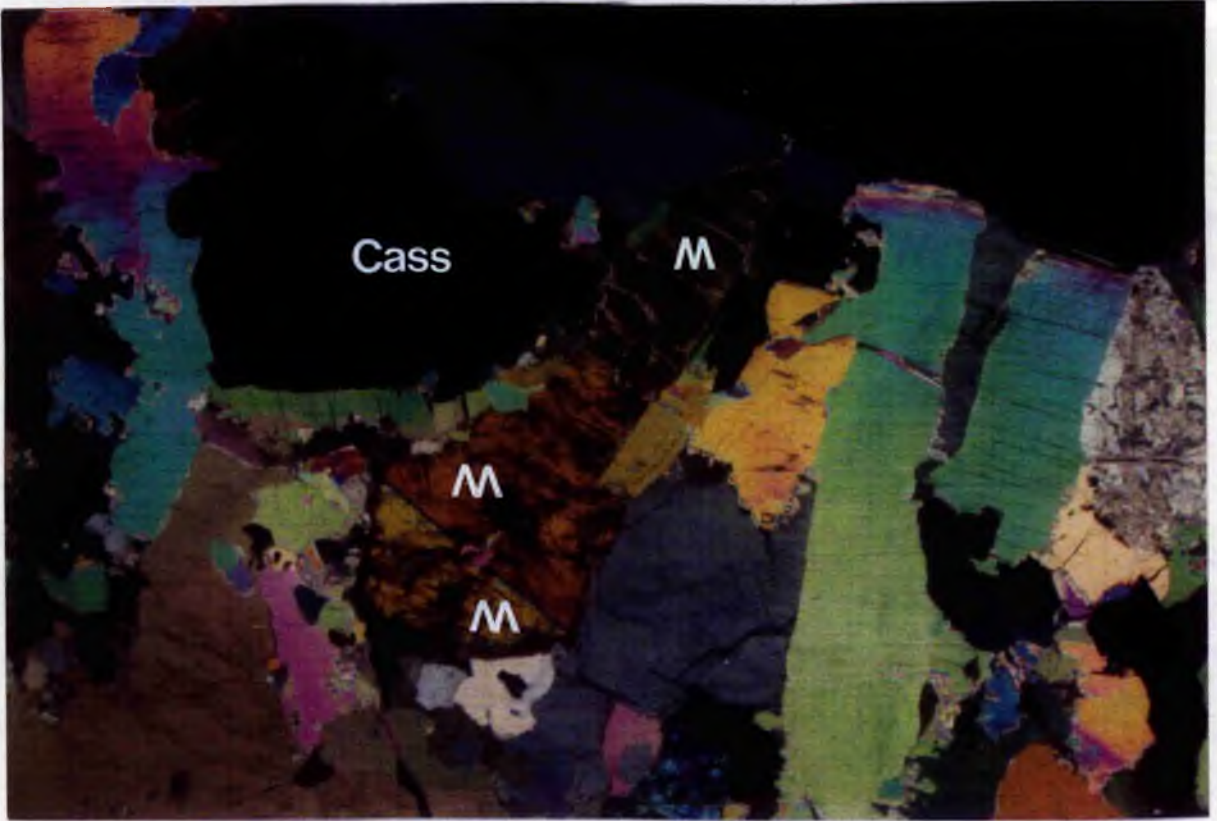


Plate 3.17. Photomicrograph of 'racquet' shaped crystal of montebrasite-natromontebrasite (3 sections are marked 'm') occurring with cassiterite (Cass), mica and quartz, Daheim 3 pegmatite, Karibib, Namibia. Length of montebrasite crystal: 2mm.



Plate 3.18. Backscattered electron image of the central area of the 'racquet' shaped crystal showing montebrasite (m) (dark grey) and natromontebrasite (N) (light grey) with crosscutting apatite veins (white), Daheim 3 pegmatite, Karibib. Scale bar : ----- 10 microns.

3.4.3 Montebrasite - natromontebrasite inclusions

Montebrasite occurs at Daheim 3 pegmatite, Karibib associated with cassiterite, mica and quartz. A "racquet" shaped crystal of montebrasite of length 1mm (Plate 3.17) appears to have three separate sections, a dark handle and a tan and yellow racquet head; each separate section marked with the letter M in Plate 3.17. A backscattered image was taken with the electron-probe. The lower section of the "head" contains homogeneous amblygonite-montebrasite while the central area which appears as patchy zones is composed of montebrasite in the dark areas (Plate 3.18 and Table 3.12 anal. 99 - 100) and an Na-Al-phosphate mineral containing fluorine, in the light areas (anal. 101 and 102).

The Na phosphate mineral is situated along cracks and is replacing the amblygonite. The Na-mineral has the composition of natramblygonite-natromontebrasite which forms an isomorphous series with amblygonite-montebrasite. This is the first reported occurrence of natramblygonite-natromontebrasite in the Karibib area.

Appreciable amounts of Na may substitute for lithium in the amblygonite-montebrasite series forming an isomorphous series with natramblygonite-natromontebrasite. With regard to an Na-rich variety of montebrasite, there are two known minerals of this composition: according to London and Burt (1982b), hebronite is extremely rare, and natromontebrasite has only four known localities (Schaller, 1912, Mrose, 1971 and Dubois et al., 1973). In Fremont County, Colorado, natromontebrasite occurs as rare crystals with albite, lepidolite and polychrome tourmaline (Schaller, 1911). Mrose (1971) reports an occurrence of natromontebrasite with lacroixite, augelite, brazillionite and apatite at Strickland pegmatite, Connecticut. Natromontebrasite is also reported with lacroixite at Kongswort and Jeclov, Czechoslovakia (Mrose, 1971). Dubois (1973) does not document a new occurrence of natromontebrasite which he reports as being extremely rare

along with amblygonite; he supplied new X-ray data and thermodynamic peaks of the series of minerals.

Schaller (1912) published an analysis of natramblygonite (fremontite) from pegmatite, near Canon City, Fremont County, Colorado, containing 44.35% P_2O_5 , 33.59% Al_2O_3 and 11.23% Na_2O (Table 3.12 anal.103) with a 1 : 1 : 1 cation ratio. This ratio is compatible with the ratio for fremontite in this study (Table 3.12. anal. 101), though the phosphate is a little high. However, the natromontebbrasite from Karibib in this study contains a higher content of Na_2O , 17.04% (anal. 101) with 44.53% P_2O_5 , 31.37% Al_2O_3 , and 5.34% F with the possibility of a similar content of H_2O . This conforms almost to the $NaAl(PO_4)(OH)$ end-member, published by Dana (1963) which contains 19.14% Na_2O , 31.47% Al_2O_3 and 43.83% P_2O_5 with 5.56% H_2O and no F (i.e H_2O greater than F, see anal. 104)). Therefore secondary montebrasite with 1.61-2.75% F is being replaced by natromontrebrasite with 5.34-5.50% F (Table 3.12) by circulating Na-F-rich fluids.

It is necessary to distinguish between the usage of natramblygonite and natromontebbrasite. Schaller (1912) and Dana (1963) referred to natramblygonite, however, Dubois et al. (1973) have since verified that Schaller's data represents natromontebbrasite though they do not give an analysis of the mineral.

Apatite (white) is visible in the cracks on the backscattered image (Plate 18) crossing both the montebrasite and the natromontebbrasite, therefore the order of crystallization was montebrasite, followed by natromontebbrasite which cuts across montebrasite, followed by apatite. With regard to the schematic diagram (Burt and London, 1982); a muscovite inclusion in the montebrasite containing apatite (see Table 3.12 anal. 105) may indicate muscovite replacement of montebrasite, natromontebbrasite and apatite. However there does not appear to be any further evidence of muscovite replacement of these phosphate minerals.

TABLE 3.12 Montebbrasite, natromontebbrasite and apatite, Daheim 3 pegmatite, Karibib

Sample 78	78/99.	78/100.	78/101.	78/102.	78/103.	theor.	78/105.
SiO ₂	0.01	0.02	0.02	-	-	-	0.03
TiO ₂	0.04	0.04	0.02	0.02	-	-	0.03
Al ₂ O ₃	34.07	35.30	31.37	31.20	33.59	31.47	0.08
Fe ₂ O ₃	0.01	0.02	0.02	0.02	-	-	0.38
MnO	0.01	0.02	0.01	-	-	-	9.51
CaO	0.07	0.01	0.02	0.04	-	-	45.18
MgO	0.01	0.01	0.01	0.02	-	-	0.01
Na ₂ O	0.02	0.01	17.04	16.98	11.23	19.14	0.45
K ₂ O	0.02	0.01	0.00	0.01	0.14	-	0.01
Li ₂ O	*9.5	*9.5	*1.0	*1.0	3.21	-	nd
P ₂ O ₅	49.12	49.92	44.53	43.71	44.35	43.83	41.79
H ₂ O ⁺	*5.5	**4.5	**3.0	**3.0	4.78	5.56	nd
F	1.61	2.75	5.34	5.50	5.63	-	2.35
Total	100.18	102.10	102.38	101.50	102.9	100.00	99.86
O=F	0.68	1.16	2.24	2.31	2.37		0.99
Total	99.50	100.94	100.14	99.19	100.53		98.87

Li₂O* Li₂O and H₂O estimated (according to Table 3.8).

H₂O**

99,100. Secondary montebbrasite, Daheim 3 (78) associated with cassiterite, Karibib, Namibia

101,102. Natromontebbrasite (NaLi)Al(PO₄)OH.F

103. Natromontebbrasite (fremontite), Fremont County, Colorado (Schaller,1912)

104. NaAlPO₄.OH, natromontebbrasite (theoretical Na end member, Dana,1963).

105. Manganoapatite, Daheim 3 pegmatite, Karibib, Namibia.

theor : Theoretical value.

No of ions on the basis of O =10 (montebbrasite); O=25(apatite)

	100.		101.		103.		theor.	78/105
Si	0.001]		-]		-]			0.005]
Ti	0.001]	2	-]	2	-]	2	2	0.004]
Al	2.014]		1.980]		2.026]			0.016]
Mn	-]		-]		-]			1.379]
Ca	0.001]		-]		-]			8.292]
Na	0.001]		1.769]	2	1.109]	1.8	2	0.151]
Li	1.849]	1.9	0.215]		0.658]			
K	0.001]		-]		0.086]			
P	2.044]	2	2.017]	2.	1.919]	1.9	2	6.060] 6.1
F	0.421]	1.9	0.904]	2	0.908]	2.5		1.273]
OH	1.454]		1.072]		1.62]		2	

Analysis 78/101 and therefore 78/102 with 1% Li₂O and 3% H₂O (estimated due to lack of material) is near the

theoretical 2. nd=not determined.

3.4.4 Montebbrasite, crandallite, topaz and cleavelandite

M4 pegmatite, Okatjimukuju, carries amblygonite - montebbrasite in association with cassiterite, topaz, cleavelandite (see Plate 3.19) and Li-mica. The amblygonite-montebbrasite area, from this pegmatite, on the back scatter image (Plate 3.20) is patchily zoned with three distinct areas; the primary montebbrasite with 6.43 and 4.94% F (Table 3.13 anal. 106,107) appears in the dark areas; apatite in the light areas and the intermediate areas which are extremely unstable under the electron beam are Ca Al phosphates.

Analysis 110 (Table 3.13) taken in the intermediate area could represent the mineral crandallite, $\text{CaAl}_3\{(\text{PO}_4)_2(\text{OH})_5\text{H}_2\text{O}\}$ with a ratio of P: Al : Ca of 4 : 6 : 2 (see Table 3.13.). Dana (1963) points out that all the crandallite analyses have high H_2O and low P_2O_5 , indicating substitution of hydroxyl for (PO_4) : CaO varies from 7-17%; P_2O_5 from 25-34% and Al_2O_3 from 28-38% and H_2O^+ from 15-20% (Dana, 1963). Analysis 110 from Okatjimukuju does not correspond exactly to analyses quoted in Dana for crandallite, it does, however, correspond very closely with the theoretical analysis given in Dana (1963) (see Table 3.13, T-108) and is possibly the first analysis of crandallite reported from Karibib. It must, however, be pointed out that these are areas of a few hundred microns of crandallite (Plate 3.20) and it is impossible to determine the H_2O^+ content of the mineral.

Topaz $\text{Al}_2\text{SiO}_4(\text{F},\text{OH})_2$ shows little variation in composition, SiO_2 varying from 31.98 to 32.19%, Al_2O_3 ; the analyses are low but water has not been determined.. The only major substitution in topaz is F for OH exchange. Small amounts of transition metals (measured in ppm) may enter the structure and give rise to the pale colour of topaz (Hawthorne and Cerny, 1982) from 56.81 to 56.93%; the fluorine is high in this mineral with 13.05 -

TABLE 3.13.

Montebrasite and crandallite, Myer's Farm (M4) pegmatite, Karibib

Sample 78	78/106.	78/107.	T-108.	78/110.
SiO ₂	0.02	0.03		0.86
TiO ₂	0.53	0.07		0.07
Al ₂ O ₃	36.47	36.43	36.93	35.76
Fe ₂ O ₃	0.01	0.02		0.13
MnO	0.02	0.02		0.15
CaO	0.03	0.13	13.55	13.26
MgO	-	0.01		0.05
Na ₂ O	0.03	0.03		1.18
K ₂ O	-			0.01
P ₂ O ₅	51.32	51.51	34.29	34.64
H ₂ O ⁺	nd	nd	15.23	nd
F	6.43	4.94		3.52
	94.86	93.20	100.00	89.63
-O=F	2.70	2.07		1.48
	92.16	91.13		88.15

No of ions on the basis of O=10 for montebrasite and O=28 for crandallite

	O=10		O=28	
	MONTEBRASITE		CRANDALLITE	
	78/106.		78/110.	
P	2.51]	1	4.18]	4.2
Si	2.48]	1	6.0]	6.0
Ti				
Al				
Fe ³⁺				
Mn			2.03]	2.3
Ca				
Mg				
Na				
K				
F	0.59]		1.59]	
OH	nd]		nd]	

Back scattered image 20 : Dark(montebrasite) -> Intermediate

78/106,107. Primary montebrasite, (dark area). nd=not determined

78/110. Crandallite (intermediate area)

T-108. Theoretical value CaAl₃(PO₄)₂(OH)₅H₂O

78/106, ions compiled by Edinburgh microprobe

13.79% (Table 3.13). It is intergrown with cleavelandite laths in one area and may be penetrating amblygonite. The montebrasite area contains one relatively large crystal of cleavelandite (see Plate 3.19); the topaz may contain montebrasite; the major mineral in this area of the pegmatite is cleavelandite, this may suggest that cleavelandite is in equilibrium with topaz and montebrasite + apatite + crandallite (apatite being prominent at the topaz-cleavelandite-montebrasite contact). There is no evidence to suggest that the cleavelandite is being replaced by topaz directly, possibly from the texture it may be suggested that there may be simultaneous crystallization of topaz and montebrasite, both of these minerals containing high F. Topaz theoretically should form in place of mica when there is a deficiency of K (Burt and London, 1982).

TABLE 3.14 Topaz, M4 pegmatite, Myer's Farm Karibib

Sample 78	78/111.	78/112.	78/113.	78/114.	78/115.
SiO ₂	32.05	32.10	31.98	32.00	32.19
Al ₂ O ₃	56.81	56.93	56.80	56.88	56.83
FeO	0.03	-	-	-	0.02
MnO	0.03	0.02	0.01	-	0.03
CaO	-	0.01	0.02	0.01	0.01
MgO	0.01	0.01	0.02	0.01	0.02
Na ₂ O	0.02	0.01	0.02	0.02	0.01
K ₂ O	-	-	0.01	0.01	0.01
P ₂ O ₅	0.02	0.01	0.02	0.03	0.01
F	13.67	13.05	13.79	13.31	13.55
H ₂ O+	nd	nd	nd	nd	*3.3
Total	102.64	102.14	102.67	102.27	106.01
-O=F	5.74	5.48	5.79	5.59	5.69
Total	96.90	96.66	96.88	96.68	100.29

* estimated; nd: not determined.

No of ions on the basis of O=5 (111-114) and O=12(115)

78/	78/111.	78/112.	78/113.	78/114.	78/115.
Si	0.973 1	0.973 1	0.972 1	0.971 1	1.96 1
Al	2.033 2	2.034 2	2.035 2	2.035 2	4.07 2
F	1.284	1.252	1.325	1.278	2.61 3
OH	nd	nd	nd	nd	1.34

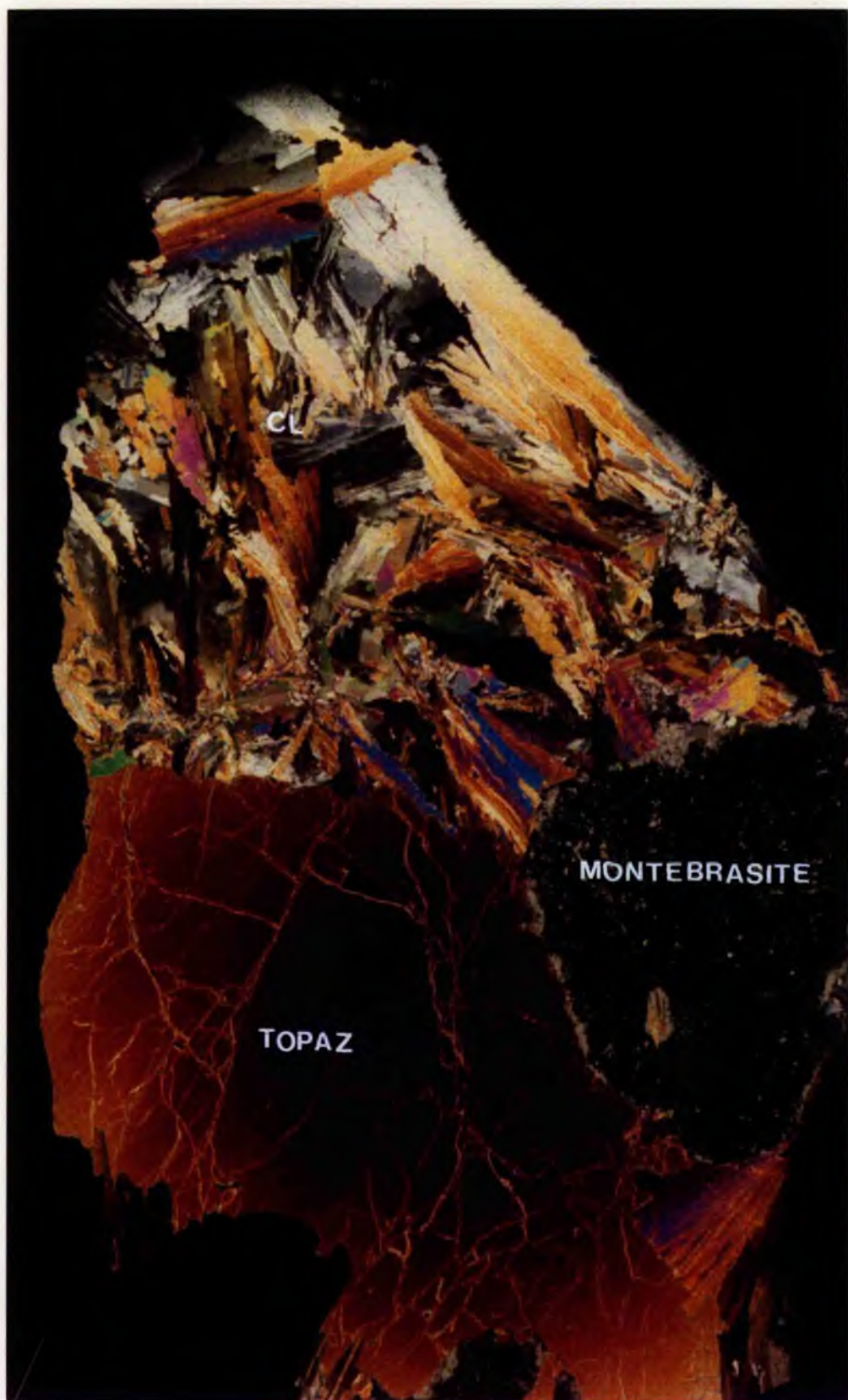


Plate 3.19. Photomicrograph of topaz, cleavelandite (Cl) and montebrasite (M) (+ apatite + crandallite), M4 pegmatite, Okatjimukuju, Karibib, Namibia. Length of section: 3.7 cm

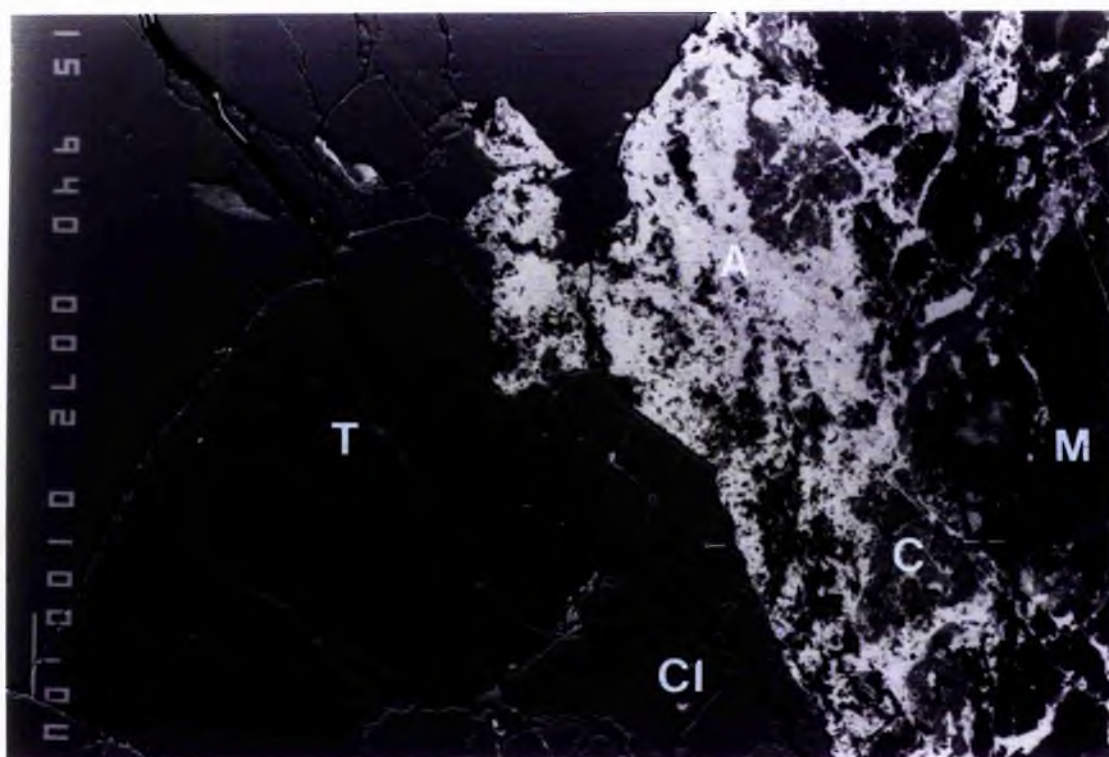


Plate 3.20. Backscattered electron image of junction of topaz (T), cleavelandite (Cl) and montebrasite, seen in Plate 3.19. The montebrasite area includes apatite (white) and crandallite (c)(grey) and montebrasite (m)(black). The cleavelandite and topaz are reversed top to bottom when compared with Plate 3.19. The topaz-cleavelandite contact is marked by a white dash. Scale bar: 100 microns.

3.4.5 Brazilianite, montebrasite and apatite

Brazilianite $\text{NaAl}_3[(\text{OH})_4(\text{PO}_4)_2]$ occurs with apatite in pegmatite on Okatjimukuju Farm, Karibib, Namibia. The brazilianite which has been identified in the pegmatite by von Knorring (1985), in hand specimen appears greyish-white in comparison with white montebrasite; brazilianite appears to be replacing montebrasite (pers.comm. O.von Knorring). In thin section the brazilianite is associated with apatite in a very fine-grained intergrowth, to such an extent that it is hardly possible to analyse apatite without brazilianite interference (see Plates 3.21). Brazilianite appears to be the major phase and is replacing apatite in certain areas. In addition to apatite, a third mineral is present, in the form of euhedral grains, a qualitative analysis revealed a very unstable magnesium aluminium phosphate (unidentified) (see Plate 3.21).

The brazilianite was analysed by electron microprobe. Initially only Na, Al and P were analysed, as F by the formula was not expected; these four elements are difficult to analyse accurately at the same time on the Camebax microprobe, taking into account that brazilianite is very unstable under the electron beam, even though a rastered beam is used over a 10-15 micron area. To analyse F on the same crystal spectrometer would necessitate a longer period of time and introduce greater inaccuracies. Therefore brazilianites 121-124 (Table 3.15) were analysed without F. Brazilianites 119 and 120 (Table 3.15) were analysed including F and other elements, in an area intergrown with apatite. Fluorine is significant in the brazilianite as Ca, P and Al are not dissimilar to analyses 121-124.

Plates 3.21 show backscattered electron images of brazilianite and apatite. The white area in Plate 3.21a shows apatite at the contact with quartz (grey lower area) and the very intergrown apatite and brazilianite above the apatite. Plate 3.21b shows apatite

disseminated in brazilianite and a magnification of the brazilianite-apatite intergrowth with the unstable magnesium aluminium phosphate crystals which may be lazulite (pers. comm. O.von Knorring).

Table 3.15. Analyses of brazilianite and apatite, Okatjimakuju, Karibib, Namibia

sample B	B/118.	B/119.	B/120.	NH.	MG.	B/121.	B/123.	B/124.	B/122.
SiO ₂	0.11	0.00	0.42						
TiO ₂	0.04	0.04	0.00	0.05					
Al ₂ O ₃	0.29	41.57	41.55	42.85	43.82	41.02	41.29	41.42	37.30
Fe ₂ O ₃	0.0	0.02	2.38	0.03					
CaO	51.27	0.03	0.06						
MnO	0.11	0.00	0.02	tr					
MgO	0.07	0.00	0.03						
Na ₂ O	0.26	8.16	8.43	8.29	8.42	8.42	8.29	8.40	7.36
K ₂ O	0.02	0.01	0.01	0.20	0.37				
P ₂ O ₅	38.04	40.15	39.53	38.79	37.97	39.92	40.24	40.36	36.79
H ₂ O ⁺		8.5*		9.91	9.65				
F	3.95	1.60	2.14	0.00	0.00	nd	nd	nd	
total	94.16	100.08	94.57	100.16	100.23	89.36	89.82	90.18	81.45
-O=F	1.66	0.67	0.89						
Total	92.50	99.41	93.68						

Cations based on 24 oxygens (119, MG) and O=20(B/121,B/122)

	B/121.	B/122.	T(hydrous, hydrated)	B/119.	MG.
Na		2.	2:	2:	1.923]
K		1.9			0.002]
					1.9
					1.974]
					0.057]
Al		5.9	6:	6:	5.959]
Fe ³⁺		5.8			0.002]
					6
					6.248]
					6.2
P		4.1	4:	4:	4.130]
		4.1			4.1
					3.885]
					3.9
OH			8	12	6.900]
F					0.615]
					7.5
					7.792]
					7.8

118.

119-121,123,124.

122.

NH.

MG.

Fluorapatite, white area above quartz in Plate 3.21a.

Brazilianite, below apatite in Plates 3.21. * estimated value

Hydrated brazilianite.

Brazilianite, Palermo mine, New Hampshire (Dana, 1963).

Brazilianite, Minas Geraes, Brazil (Dana, 1963).

The brazilianite appears in both hydrous and hydrated forms: the hydrous form $\text{NaAl}_3[(\text{OH})_2(\text{PO}_4)_2]$ with 41.29-41.57% Al_2O_3 , 8.16-8.42% Na_2O , 39.53-40.36% P_2O_5 and the hydrated form $\text{NaAl}_3(\text{PO}_4)_2(\text{OH})_4 \cdot 2\text{H}_2\text{O}$ with 37.30% Al_2O_3 , 7.36% Na_2O and 36.79% P_2O_5 (Hey, 1956) (see Table 3.15, anal. B/122). The apatite intergrown with brazilianite (Plate 3.21a) did not contain F, it is probably hydroxyapatite. Fluorapatite is present in the contact area below quartz in Plate 3.21a (Table 3.15. anal. 118).

Brazilianite analyses have been reported by Dana (1963) (see Table 3.15). The occurrence from Conselheira Pena, Minas Geraes, Brazil, occurring with muscovite, albite, apatite and tourmaline in cavities in pegmatite has been described by Pecora and Fahey (1949). The brazilianite described in this study from Okatjimukuju is near the theoretical formula; however, the mineral from this locality evidently contains F. H_2O has not been determined on account of the intergrown nature with other secondary phosphate minerals.

From the backscattered images the sequence of mineralization of brazilianite and apatite is not clear; also montebrasite was not identified on the microprobe. However brazilianite appears to be the major phase and is very closely intergrown with (hydroxy)apatite. London and Burt (1982c) have found brazilianite cross cutting apatite veins in the pegmatites of the White Picacho District, Arizona and propose that it forms late in the alteration history of montebrasite.

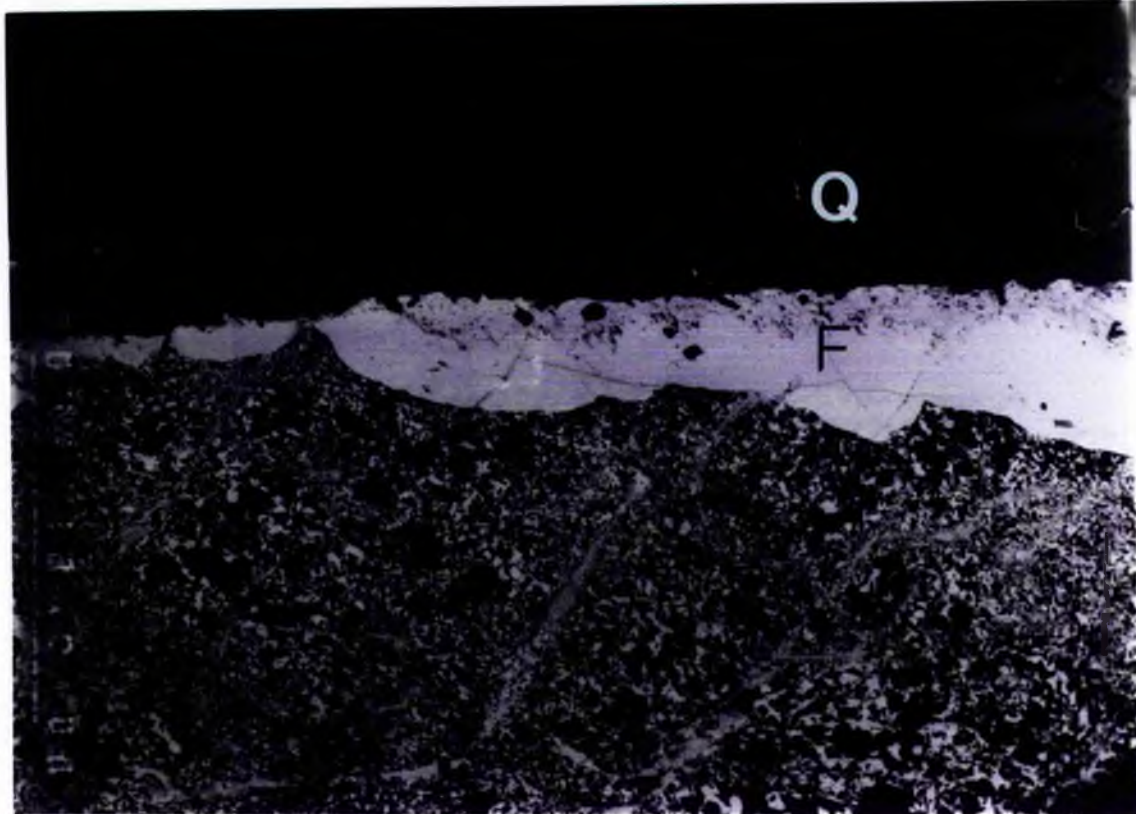
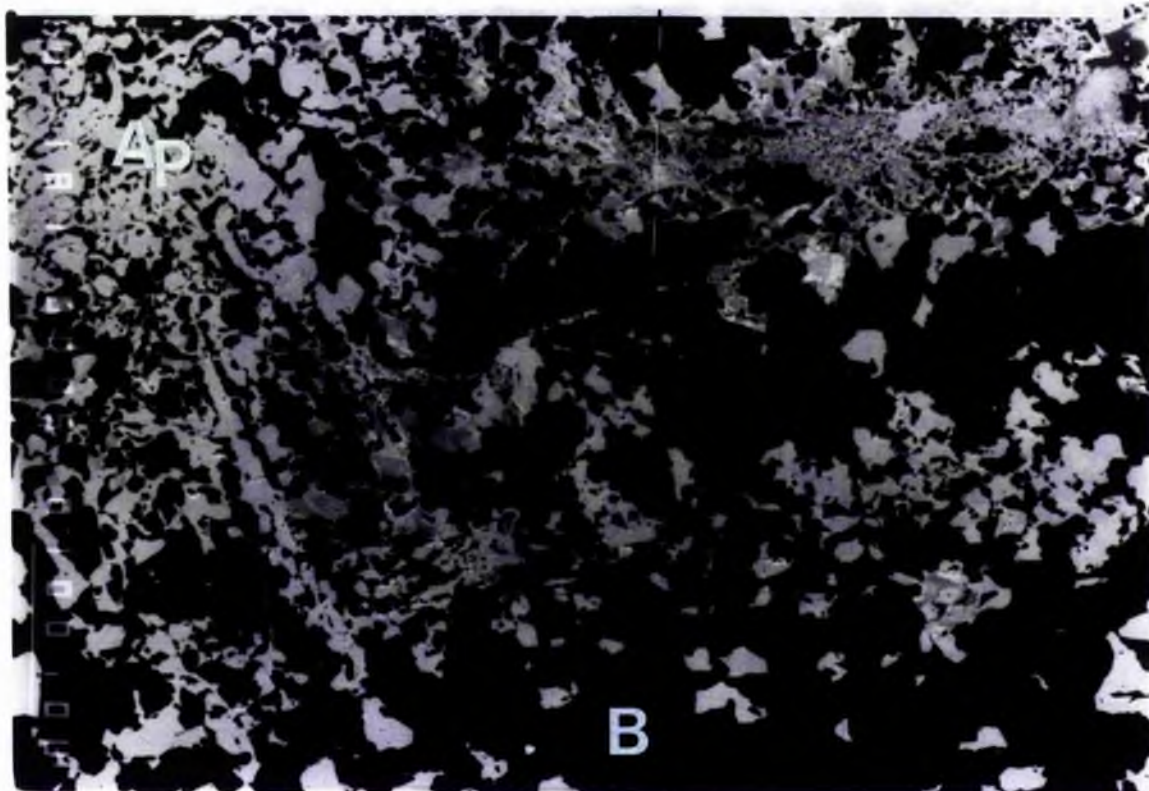


Plate 3.21a. Backscattered electron image of quartz (grey), fluorapatite (white) and brazilianite (black) intergrown with apatite (white), M4 pegmatite, Okatjimukuju, Karibib. Scale bar: 1000 microns.

Plate 3.21b. A magnification of part of Plate 3.21a showing the brazilianite (black) apatite (white) intergrowth and including a magnesium aluminium phosphate mineral (unidentified). Scale bar: 100 microns.



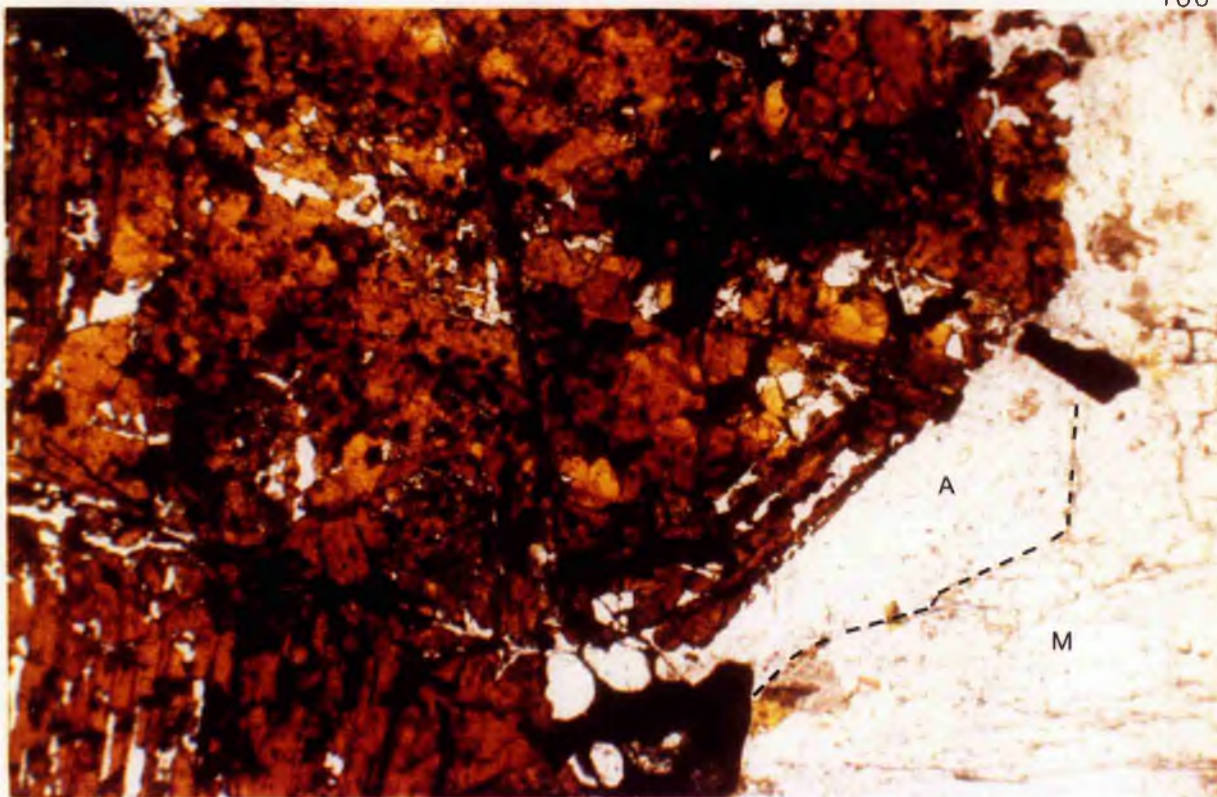
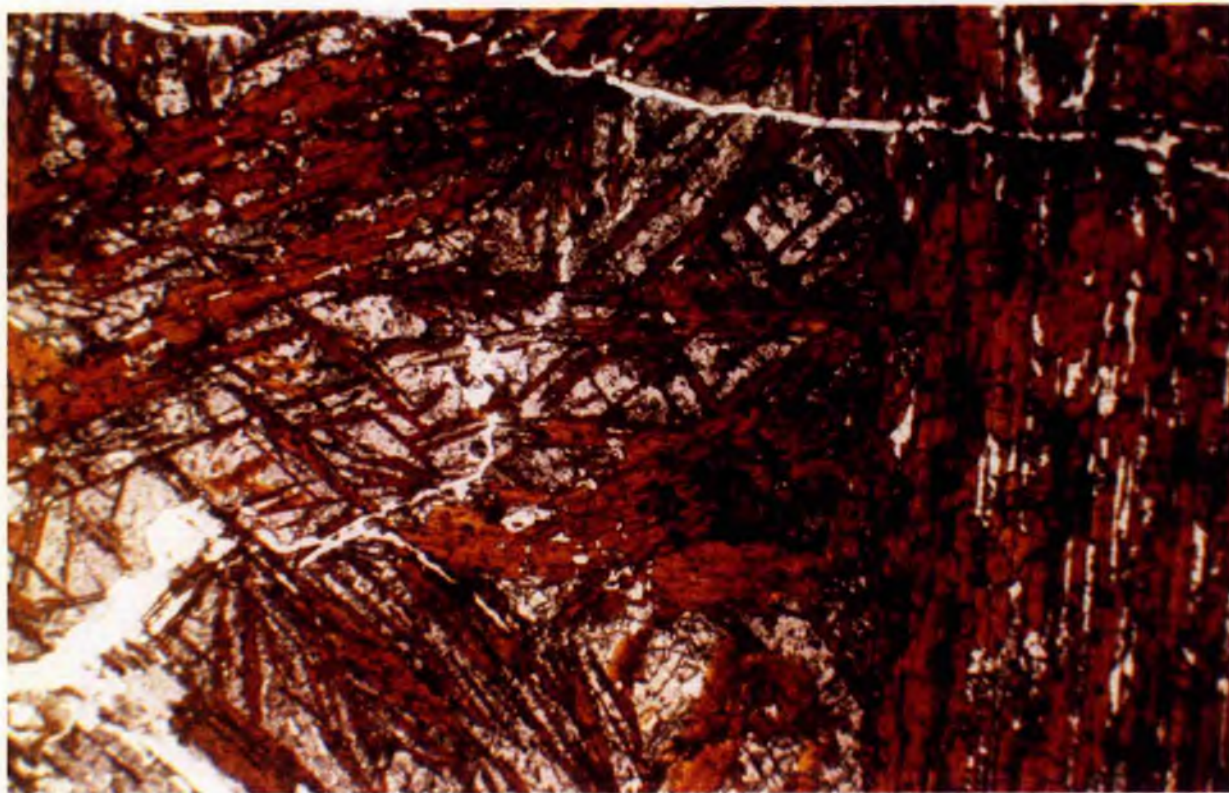


Plate 3.22. Photomicrograph of the junction between montebrasite (M) and tantalite (orange brown). Apatite (A) occurs at the contact—the division between apatite and montebrasite is marked by a dashed line, Rubicon pegmatite, Karibib, Namibia. Plane polarized light. Scale bar. 1 mm

Plate 3.23 Photomicrograph of apatite veins (white) cutting across tantalite (orange-brown) in a microlite matrix (grey), Rubicon pegmatite, Karibib, Namibia. Plane polarized light. Scale bar: 1 mm.



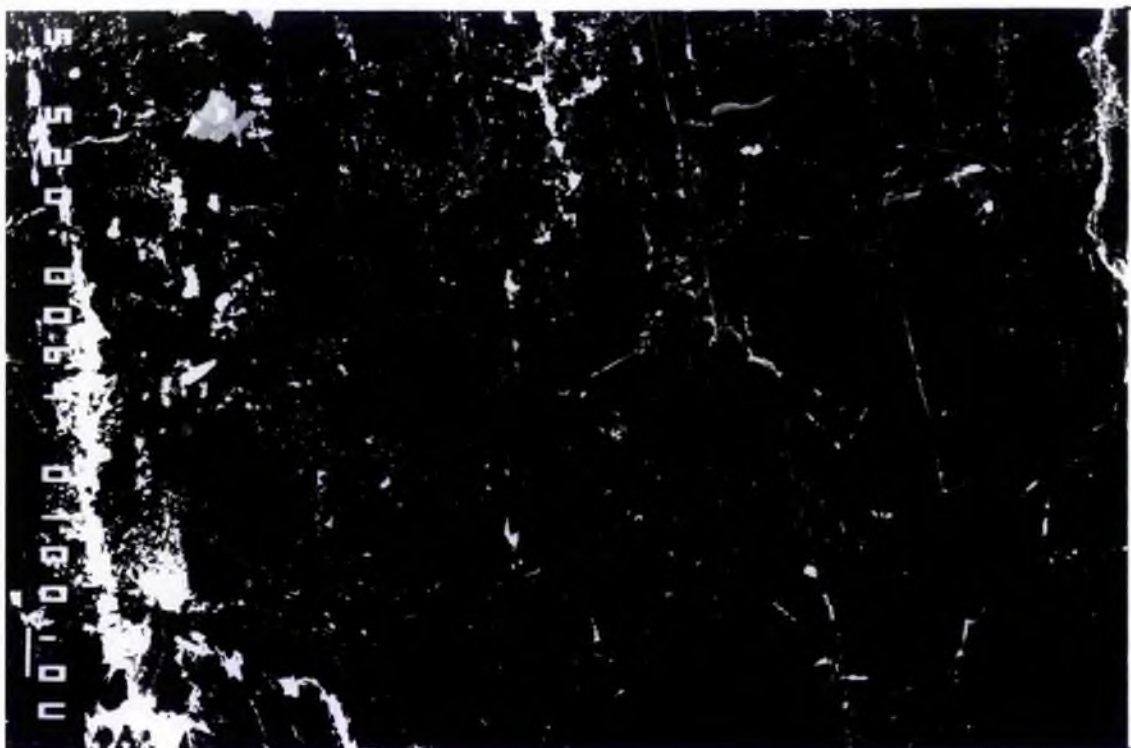
a



b



Plates 3.24. Backscattered electron image at the contact of Mn-tantalite and montebrasite, Rubicon Mine, Karibib a) a complex association of minerals (unidentified), b) tantalite (white), apatite (grey) and montebrasite (black) and c) patchy alteration primary and secondary montebrasite (shades of grey). Scale bar: 100 microns



c

3.4.6. Montebbrasite, apatite and tantalite

Secondary milky-white montebbrasite containing 3.14- 3.79% F (Table 3.16) is associated with an unusual occurrence of Mn-tantalite laths and microlite (Plate 3.22) at the Rubicon mine, Karibib. The montebbrasite, in thin section does not appear altered, except at the contact with the laths, where it is in association with apatite. In some areas, apatite appears to be filling in the spaces between the Ta laths and would appear to have therefore crystallized after the Ta-laths, and this may be confirmed by apatite veins which cut across the Ta-laths and the enclosing microlite (Plate 3.23). Scattered crystals of mica also occur at the montebbrasite contact in association with the Mn-tantalite.

The secondary montebbrasite was analysed with the electron-probe. It contains 49.36 - 50.16% P_2O_5 and 34.40-36.22% Al_2O_3 and 1.14-3.79% F giving a total of 87.98% thus allowing for approximately 9% Li_2O and 3% H_2O^+ (Table 3.16a).

The montebbrasite was analysed along the contact between the apatite and the Mn-tantalite laths. The first 4 analyses in Table 3.16a are at the contact and the next three analyses are moving in towards the apatite. There is little difference in the composition along and around the contact. The next 3 analyses are further from the contact which shows the F content increasing away from the contact. There is also a variation in the F-content of the apatite along the contact (Table 3.16b).

Backscattered images taken along the contact (Plates 3.24) show a complex association of phases (unidentified) in one area of the contact in Plate 3.24a and tantalite (white) with apatite(grey) replacement of montebbrasite (black) in Plate 3.24b. Plate 3.24c at a different intensity of image showed zoning in montebbrasite; an interpretation of the order of crystallization may be, primary and secondary montebbrasite cut by later apatite veins.

Table 3.16a Partial analyses of montebrasite, Rubicon, Okongava Ost, Karibib.

Sample MOR/125.	126.	127.	128.	129.	130.	131.	132.	133.	
Al ₂ O ₃	34.57	34.43	36.22	35.88	34.50	34.40	34.48	36.08	34.53
P ₂ O ₅	49.11	50.17	49.92	49.38	49.36	49.51	49.92	49.87	50.09
F	3.62	3.65	3.46	3.40	2.67	2.63	3.08	3.46	3.79
-O=F	87.3	88.25	89.6	86.93	86.53	86.54	87.48	89.41	88.41
	1.52	1.53	1.45	1.43	1.12	1.10	1.29	1.45	1.59
Total	85.78	86.72	88.15	85.50	85.41	85.44	86.19	87.96	86.82

Distance away from contact analyses (125-128): -100 -200 +700 +600 +500 microns

MOR125-128. Moving along the contact between apatite and montebrasite.

MOR129-130 Moving inwards apatite.

MOR131-133. Moving out from the contact towards montebrasite.

Table 3.16b Analyses of apatite in association with montebrasite, Rubicon, Okongava Ost, Karibib

Sample MOR/134.	135.	136.	137.	138.	139.	140.	141.	142.	143.	
P ₂ O ₅	41.98	41.79	42.39	42.01	42.15	42.14	41.83	41.88	41.99	42.32
MnO	3.40	3.41	3.55	3.15	3.31	3.44	3.67	1.27	2.45	3.66
CaO	52.27	52.29	52.30	52.64	52.90	52.36	51.93	54.54	53.06	52.42
F	5.01	5.04	5.10	4.74	5.09	5.95	4.22	4.77	4.70	4.62
total	102.66	102.22	103.34	102.5	103.45	103.89	101.65	102.39	102.2	103.02
-O= F	2.10	2.12	2.14	1.99	2.14	2.50	1.77	2.00	1.97	1.94
Total	100.56	100.10	101.20	100.51	101.31	101.49	99.88	100.39	100.23	101.08

Moving along the contact

The montebrasite analytically should be classified as secondary i.e. F less than 4 %, however, it is questionable that these analyses are totally representative of the montebrasite composition as the backscattered image shows areas of different composition as contrasting grey areas (Plate 3.24c). A variable F-content implies primary and secondary compositions of montebrasite and it is suggestive of alteration and replacement particularly at the contact. Both primary and secondary compositions have been analysed from the Rubicon pegmatite where an essentially chalky variety occurs with petalite and lepidolite, on either side of the quartz core. However, a fresh primary

glassy purple variety containing 6.22% F occurs in the hanging wall of the lepidolite unit (Fig. 2.1).

3.4.7. Montebbrasite, indicolite, lithian mica and Mn-apatite

Montebbrasite has been recovered from the Mon Repos pegmatite, Karibib from the quartz core, in association with indicolite (blue tourmaline) (Plate 3.25). An apatite rim occurs around the contact of the tourmaline and montebbrasite; the apatite is Mn-rich (Table 3.17 anal.144). A traverse was taken across part of the montebbrasite in proximity with the indicolite and the results are presented in Table 3.17a. The montebbrasite mostly is secondary, as indicated by an F content below 4%; there is, however, a variation in the F content (see Fig. 3.6) indicating remnants of primary montebbrasite, i.e. F, 4-5% (anals. 151,153,154). The diverse patterns in the F-content indicate perhaps a irregular development of secondary montebbrasite, after primary montebbrasite, not associated with the indicolite, leading to patchy zoning and possible further nodular development.

TABLE 3.17a. Montebbrasite along traverse

sample M	148.	149.	150.	151.		152.	153.	154.	155.
Al ₂ O ₃	35.22	35.06	34.27	32.74	T	34.58	34.46	33.61	32.27
P ₂ O ₅	48.21	49.23	48.38	46.39	T	48.53	48.53	49.81	50.53
Li ₂ O*	9.5	9.5	9.5	9.5	T	9.5	9.5	9.5	9.5
H ₂ O**	4.0	5.0	5.0	4.0	T	5.0	4.0	4.0	5.5
F	3.98	2.33	2.82	5.57	T	2.18	4.58	4.76	1.60
	100.91	101.12	99.97	98.2		99.79	101.07	101.68	99.40
-O=F	1.67	0.98	1.18	2.33		0.92	1.92	2.00	0.67
	99.24	100.14	98.79	95.87		98.87	99.15	99.68	98.73

T denotes the position of the tourmaline

** H₂O+ and * Li₂O estimated (see Table 3.8)

148-150,152,155. Secondary montebbrasite

151,153,154. Primary montebbrasite

Fibrous Li-mica with apatite is associated with the secondary montebbrasite (Plate 3.26), suggesting Li-mica and apatite replacement of montebbrasite (Table 3.17b) .

Table 3.17b.

Montebbrasite, Mn-apatite, and Li-mica, Mon Repos pegmatite , Karibib

Sample M	M/144.	M/145.	M/146.	M/147.
SiO ₂	0.01	0.04	57.54	54.06
Al ₂ O ₃	0.00	34.91	21.25	28.79
FeO	0.51	0.06	1.99	0.31
MnO	2.32	0.00	0.18	0.07
CaO	53.34	0.02	0.00	0.00
Li ₂ O		9.0*	3.0	3.0
K ₂ O	-		8.96	9.57
Rb ₂ O			1.07	1.02
P ₂ O ₅	43.10	51.59	0.00	0.00
F	1.21	2.01	9.75	6.63
H ₂ O ⁺	nd	4.0*	nd	nd
	100.49	101.63	103.74	103.45
-O=F	0.51	0.84	4.10	2.78
Total	99.98	100.79	99.64	100.67

No of Cations O=25 (apatite), O=20(montebbrasite), O=22 (Li-mica)

	144.	145.	146.	147.	T(mica)
Si			6.957	8 6.525	8 8
Al			1.043	1.475	
Al		4.81	1.984	2.111	
Fe ²⁺	0.07	9.9	0.201	3.7 0.031	3.6 4
Mn	0.33		0.018	0.007	
Li			1.458	1.456	
Ca	9.46				
K			1.382	1.5 1.473	1.6 2
Rb			0.083	0.079	
P	6.04	6	5.11	1:	
F		0.74	3.726	3.7 2.82	2.8 4
OH				nd	

144. Apatite associated with fibrous Li-mica (ions calculated by Edinburgh microprobe)

145. Secondary montebbrasite (ions calculated by Edinburgh microprobe)* estimated (see Table 3.8)

146,147. Li-mica; T=theoretical

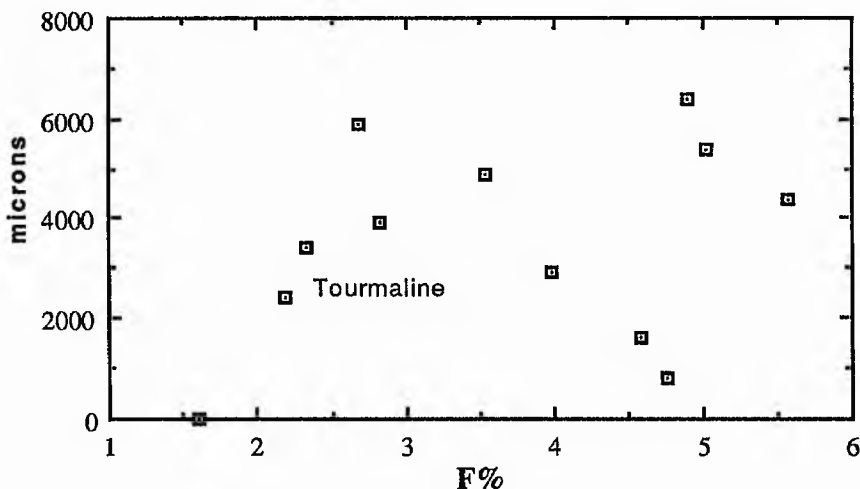


Fig. 3.6 Variation in F% content of montebrasite moving along traverse in relation to a crystal of tourmaline (sample M).

Blue tourmaline, indicolite, occurs at the Mon Repos pegmatite in the quartz core with creamy microcline and albite and also with amblygonite - montebrasite (Plates 3.25, 3.26). The tourmaline associated with montebrasite is not zoned, and chemically it contains 8.30% FeO, 1.30% ZnO, 0.10% CaO and 2.50% Na₂O (Li was not determined). A core and rim analysis revealed no change in composition. The euhedral tourmaline is surrounded by apatite at the contact with secondary montebrasite which is consistent with other mineral contact zones where primary montebrasite has been replaced by late-stage (hydrothermal) fluids containing Ca or by cation exchange and the occurrence of apatite.

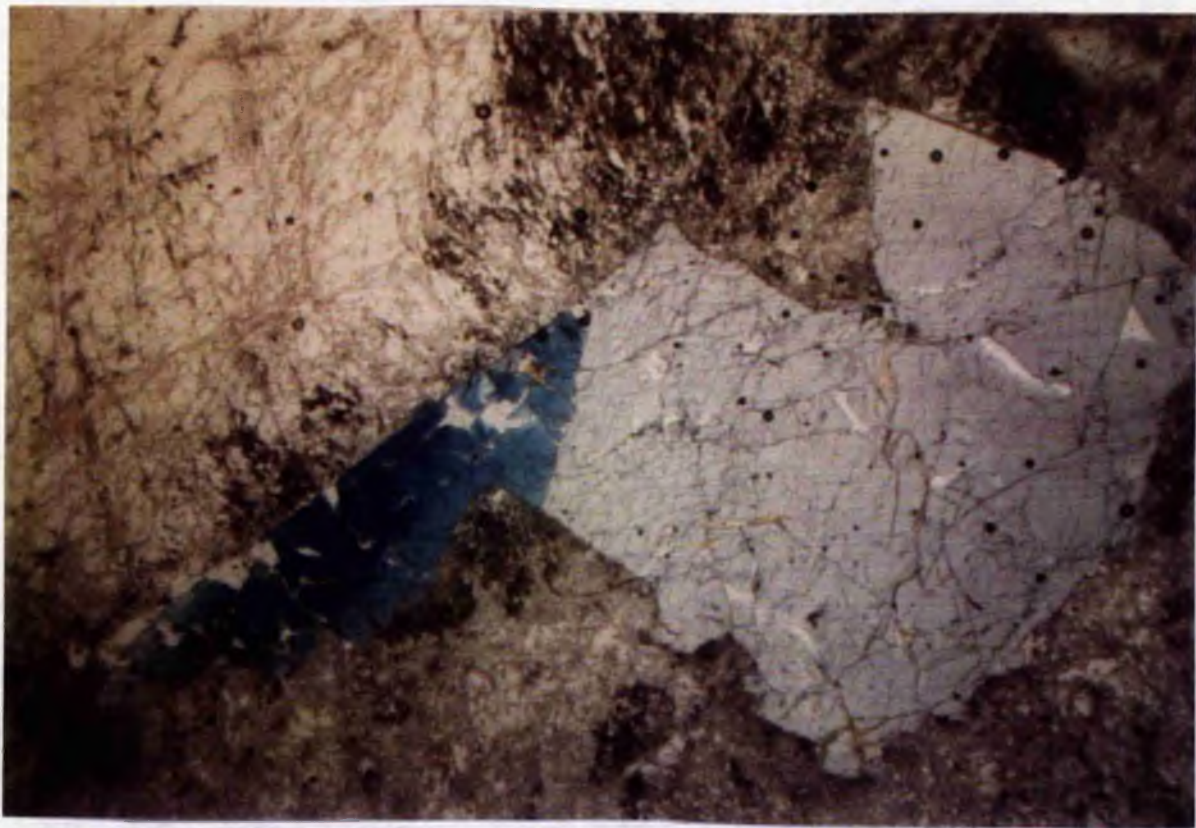
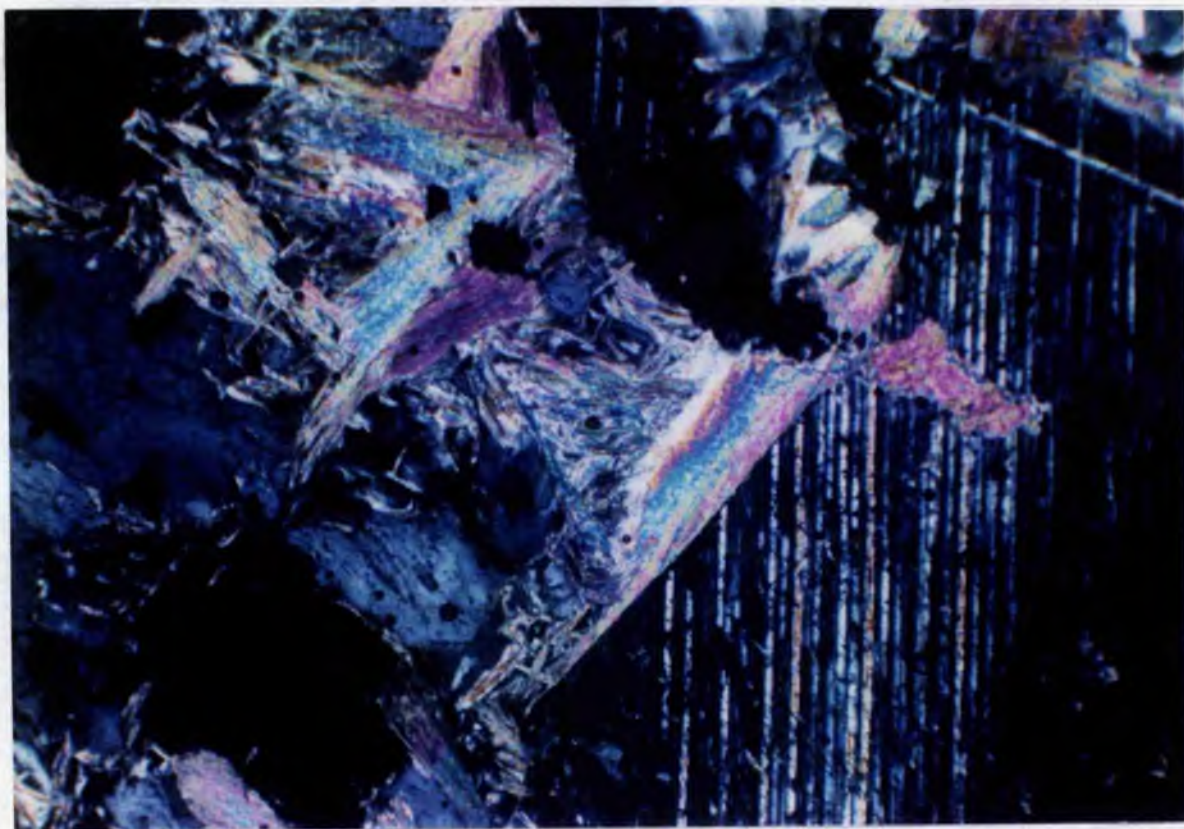


Plate 3.25. Photomicrograph of indicolite tourmaline occurring in amblygonite, Mon Repos pegmatite, Karibib, Namibia. Width of photomicrograph 1.2 cm. Plane-polarized light.

Plate 3.26. Photomicrograph of fibrous Li-mica, apatite (dark-blue) and twinned amblygonite, Mon Repos pegmatite, Karibib. Scale bar: ———1 mm



3.4.8. Summary - amblygonite-montebbrasite alteration

At the Daheim 1 and 3 , Mon Repos, Okatjimukuju Farm and Rubicon pegmatites, montebbrasite has been replaced by a number of secondary phases, in the general sequence illustrated in Fig. 3.7. Incipient alteration of primary montebbrasite and in some cases amblygonite, involved hydroxyl exchange for fluorine, producing low-fluorine secondary montebbrasite along cleavages and montebbrasite boundaries and junctions with other phases. The secondary montebbrasite contains between 1.60 - 3.46% F (Table 3.18); these secondary phases are indistinguishable in hand specimen but are quite common in the Karibib pegmatites. Subsequent alteration of primary and secondary montebbrasite produced fine-grained crandallite, natromontebbrasite, hydroxyapatite, muscovite and brazilianite. The calcium aluminium phosphate analysis corresponds to the mineral crandallite but positive identification has not been possible with X-ray powder patterns. Although crandallite and apatite appear together at the grain boundaries of the montebbrasite probably crandallite was the first to crystallize as apatite often crosscuts the other secondary phases.

TABLE 3.18.

Summary of minerals in association with montebbrasite, Karibib Area Namibia

Prim.monte F%	Sec.monte F%	Alteration	Locality	Mineral Assoc.	Spec.No
4.9->8	1.6->2.36	apatite,Cs mica altered mica	Daheim 1	cleavelandite	D4
-	1.6->2.75	natromontebbrasite	Daheim 3	albite,mica,quartz cassiterite	78
4.94->6.43	-	apatite crandallite	M4 (Okatjimukuju)	topaz,cleavelandite	M4
-	-	brazilianite	M4 (Okatjimukuju)	amblygonite nodules	B
lost data	3.46	apatite	Rubicon	tantalite, microlite	R6

This phenomenon is apparent also with the intergrowth of secondary montebrasite, the very rare-mineral natromontebrasite, and apatite, where the apatite cuts across the two other phases. Brazilianite, the secondary sodium aluminium phosphate forms comparatively large crystals of more than 1 cm., it replaces amblygonite (pers. comm. O. von Knorring) and is very intergrown with hydroxyapatite at Okatjimukuju.

Alteration sequence of amblygonite-montebrasite in the Karibib
Area

SEQUENCE

**Amblygonite/
montebrasite-->low F Montebrasite->Crandallite--> Hydroxyapatite ->Muscovite**

+

Natromonte-
brasite

+

Muscovite

+

Brazilianite

Process

OH-F Exchange ----->

Li-leaching (cation exchange for Ca & Na)

Ca-metasomatism ----->

Na-metasomatism ----->

K+H metasomatism ----->

Fig. 3.7. A diagram to show the processes operating through the alteration sequence of amblygonite to muscovite, so that OH-F exchange operates for the process from amblygonite to low F montebrasite and Li-Ca cation exchange in the process from secondary montebrasite to crandallite and natromontebrasite etc.

3.4.9. Discussion-montebbrasite alteration

The formation of secondary montebbrasite by OH-for F exchange in the primary phase presumably reflects an increase in the ratio $a_{\text{H}_2\text{O}} / a_{\text{HF}}$ in the residual fluid. Increase in this activity ratio implies a depletion in fluorine (perhaps due to crystallization of apatite or of micas, or of the montebbrasite or it implies a relative increase in aqueous activity with decreasing temperature (Korzhinskii, 1957; Munoz and Eugster, 1969).

The initial cation metasomatism of primary and secondary montebbrasite involved Ca-for-Li exchange, producing hydroxyl-apatite and minor crandallite. Subsequent conversion of montebbrasite to muscovite was far more extensive and reflects high mobility of Li, K, Si, P but not Al and in the case of the Cs-rich micas Cs and probably Rb.

In spite of their rarity in these pegmatites the occurrences of brazilianite offers additional insight into the chemistry of the postmagmatic fluids. Brazilianite is normally the most abundant rare-accessory secondary phosphate. According to London and Burt (1982) its occurrence late in the montebbrasite alteration sequence suggests that its stability is analogous to that of iacoxite which is unstable with lithium aluminosilicates in the presence of quartz as the Na/Li activity ratio is too low to enable the formation of the lithium minerals. They suggest that as montebbrasite occurs near or with, spodumene + quartz the alteration of montebbrasite to brazilianite probably took place only after spodumene had been totally converted to albite and / or muscovite.

The inclusions of natromontebbrasite with secondary montebbrasite from Daheim 1 pegmatite are very small, approximately 2 mm and it is suggested, as it is F-rich and due to the very small amounts that are being formed, and also it is cross cut by apatite, that the natromontebbrasite formed early in the Na metasomatic sequence and before brazilianite. Apatite cuts across the zoned patchy formation of montebbrasite-natromontebbrasite.

3.5. LITHIOPHILITE - TRIPHYLITE AND ASSOCIATED MINERALS

3.5.1 Occurrence and geochemistry

Lithiophilite-triphyllite occurrences are minor in the four areas studied, in comparison with the four major lithium minerals, and only partial analyses of the series have been analysed in order to relate the Mn/ (Mn+Fe) ratio of lithiophilite generally to other Mn-minerals in each specific area. The series and their alteration products from the Karibib area have been extensively studied by and Keller and von Knorring (1989) and Keller (1991). The Li-Mn-Fe phosphates described in this study, have been discussed before lithian mica, and after amblygonite in the lithium sequence, owing to their similarity with amblygonite, both in composition, and in the crystallization sequence with regard to late fluids.

Members of the lithiophilite-triphyllite series $\text{Li}(\text{MnFe})\text{PO}_4$, are commonly observed in lithium pegmatites generally as minor concentrations. They are usually confined to the quartz core forming coarse-grained nodules (rounded and irregular aggregates) up to 1 metre in size where they occur in the Okatjimukuju pegmatites, Karibib. More details of the Okatjimukuju occurrence are given in Keller and von Knorring (1989) and Keller (1991).

Lithiophilite nodules occur in quartz with alteration phosphates at the White City pegmatite, Tantalite Valley, Namibia. In Tantalite Valley, lithiophilite and Mn-Fe phosphates are only present to any degree in the White City pegmatite, with minor amounts occurring in the Homestead pegmatite. At the White City pegmatite lithiophilite contains 8.24% Li_2O with 0.40% Na_2O and MnO 38% with 6.76% FeO, the same mineral from Homestead has 8.03% Li_2O and 0.71% Na_2O . The Homestead lithiophilite contains a high percentage of MnO and with only 0.36% FeO and 0.23% Fe_2O_3 (Table 3.19, anal.158) it represents the lithiophilite end-member.

Lithiophilite at the Homestead pegmatite occurs in a matrix of dark purple lithium mica with cleavelandite, the lithiophilite end-member is very rare and with an Mn/Mn+Fe ratio approaching 1, it represents an Fe-poor, Mn-rich, i.e. an extremely fractionated environment (von Knorring, 1976). Other phosphate minerals analysed from Tantalite Valley include triplite [(Mn,Fe,Mg,Ca)₂PO₄(F,OH)] (Table 3.19 anal. 159) from the White City which is manganese-rich with 47.82 % MnO and 11.79% FeO. The alteration products of lithiophilite have, however, not been examined in detail from this pegmatite area.

Lithiophilite is subject to late metasomatic alteration to a large number of secondary rare and complex phases. Lithiophilite from Noumas 1, Namaqualand (Table 3.19. anal. 160) occurs with triploidite, (Mn,Fe²⁺)₂(PO₄)(OH), strengite, phosphosiderite [Fe³⁺PO₄.2H₂O], and stewartite [MnFe₂³⁺(OH.PO₄)₂.H₂O as secondary replacement or alteration products, and with apatite, all of which occur in the quartz core (Baldwin, 1979).

TABLE 3.19

Partial analyses of lithiophilite and triplite from pegmatite

	156.	157.	158.	159.	160.
P ₂ O ₅	44.82	43.02	43.91	31.65	
Fe ₂ O ₃			0.23		
FeO	13.44	6.76	.36	11.79	
MnO	31.55	38.00	44.60	47.82	31.84
CaO	0.02	0.03	-	1.73	
MgO		0.03	-	0.56	
Li ₂ O		8.24	8.03		
Na ₂ O		0.40	0.71		
K ₂ O		0.16	0.06	0.00	
F		0.04	0.06	8.00	
H ₂ O+			1.12		
H ₂ O-			0.16		
Total		96.68	99.24	101.55	
-O=F		0.02	0.03	3.36	
		96.66	99.21	98.19	
Mn/(Mn+Fe)	0.70	0.85		0.80	

156. Lithiophilite, Rubicon, Karibib, Namibia. (156,157,159, analysts: R.Davies and J.R.Baldwin)
 157. Lithiophilite, White City, Tantalite Valley, Namibia
 158. Lithiophilite, Homestead, Tantalite Valley, Namibia (von Knorring, 1976)
 159. Triplite (WC4), White City, Tantalite Valley, Namibia
 160. Lithiophilite, Noumas 1, Namaqualand, South Africa (Baldwin, 1979)

From the Kenhardt-Marydale district, lithiophilite and alteration products metastrengite ($\text{Fe}^{3+}\text{PO}_4 \cdot 2\text{H}_2\text{O}$) and heterosite ($\text{Fe}^{3+}\text{PO}_4$) have been identified from the Strausheim 1 pegmatite (von Knorring, 1985).

In the Karibib area, lithiophilite containing 31.55% MnO and 13.44% FeO occurs at the Rubicon pegmatite. Lithiophilite from Noumas, Namaqualand with 31.84% MnO is very similar in Mn content to the Rubicon lithiophilite and consequently the Mn/Mn+Fe ratio in lithiophilite is lower in both the former pegmatites with 0.70 at Rubicon in comparison with the Tantalite Valley pegmatites where the Mn/Mn+Fe ratio in lithiophilite is 0.85 at White City, and practically 1 at Homestead, Tantalite Valley (Table 3.19). It will be shown that the Mn/(Mn+Fe) ratios for lithiophilite are compatible with the same ratios for tantalite (for each field area).

Lithiophilite may also occur in cleavelandite assemblages and London and Burt (1982c) suggest that the mineral displays two different replacement sequences depending on whether the lithiophilite is embedded in quartz or albite. The least alteration occurs in quartz. At the Rubicon mine, Okongava Ost 72, Karibib, von Knorring (1985) has observed the following secondary minerals: heterosite, sicklerite, hureaulite $\text{Mn}_5(\text{PO}_4)_2(\text{PO}_3(\text{OH}))_2 \cdot 4\text{H}_2\text{O}$, tavorite, barbosalite, frondelite, strengite, phosphosiderite, bermanite and stewartite. For further details, the reader is referred to Keller and von Knorring (1989). In the pegmatites on Okatjimukuju 55, Karibib, numerous phosphates mostly of secondary origin have also been reported by von Knorring (1985a). The secondary minerals so far identified in the Rubicon pegmatite do not contain Ca or Na, but Ca is represented in mitridatite $[\text{Ca}_3\text{Fe}_4^{3+}(\text{PO}_4)_4(\text{OH})_6 \cdot 3\text{H}_2\text{O}]$, collinsite $[\text{Ca}_2(\text{Mg},\text{Fe})(\text{PO}_4)_2 \cdot 2\text{H}_2\text{O}]$ and apatite, and Na in eosphorite $[\text{NaLiAl}_2(\text{Al}_2\text{Si}_2)\text{O}_{10}(\text{OH})_2]$ in the pegmatites on Okatjimukuju 55.

In the Karibib area replacement of lithiophilite to form hureaulite and triploidite involved hydration and removal of lithium. Replacement phosphates containing Ca is supportive evidence for postmagmatic fluids rich in Ca involving Ca-for-Mn cation exchange comparable with montebbrasite alteration to crandallite, and similarly eosphorite containing Na is supportive evidence for Na metasomatism, which has already been reported from the Karibib area. Ca metasomatism is evident in Tantalite Valley in the formation of triplite. In Namaqualand, at Noumas, replacement of lithiophilite by triploidite, and stewartite involved hydration and removal of lithium, replacement by strengite and phosphosiderite involved hydration and the removal of Li and Mn; replacement by apatite, if it is secondary, involved Ca metasomatism (see Fig. 3.8). However, London and Burt (1982) report that stewartite, and strengite may be the result of weathering rather than metasomatism in the White Picacho District pegmatites, Arizona, as these secondary phases are not present on any freshly mined samples.

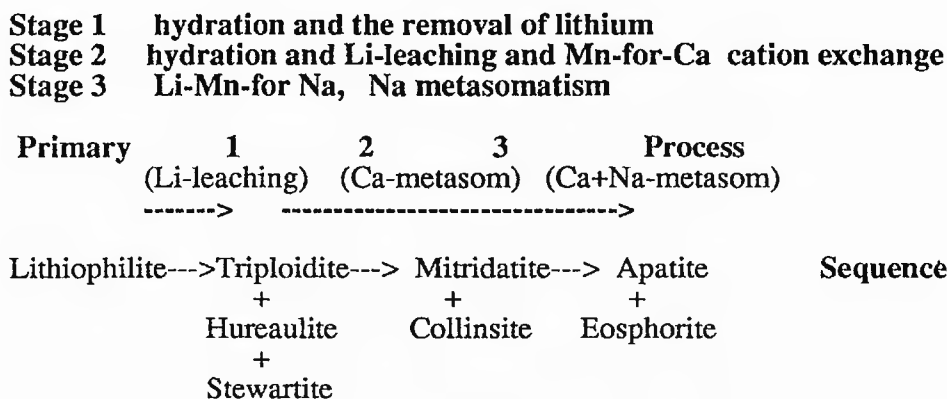


Fig. 3.8. Generalized alteration sequence of lithiophilite in the Karibib area and inferred chemical processes involved.

Lithiophilite typically occurs in quartz cores and apparently is probably, along with amblygonite-montebbrasite the last primary lithium mineral to crystallize in pegmatites. Lithiophilite, triphylite, triplite, amblygonite-montebbrasite and Mn-

apatite appear to be the only primary phosphate minerals that crystallize directly from either a residual silicate melt (magmatic) or a liquid or vapour phase. As they reflect the final conditions during pegmatite crystallization when most of the silicates have already formed, concentration of F and P suggests a post magmatic fluid stage (vapour or liquid) rather than a residual magmatic (silicate melt) stage. In terms of the Jahns and Burnham' model (1969,1982) crystallization from a " supercritical fluid" enriched in volatiles when all the silicate melt had crystallized forming at temperatures in the region of 450-400° C. The secondary minerals could be related to a lower temperature hydrothermal stage with temperatures below 400° C.

2.5.2 Conclusions - Composition of postmagmatic fluids effecting metasomatic alteration of primary lithium minerals

Initial subsolidus metasomatism in the Karibib area, Namibia, of the primary lithium minerals, petalite and amblygonite, took place in an alkaline environment, as evidenced by the albitization of petalite and montebrasite and the Ca metasomatism of lithiophilite. The formation of replacement zones of fine-grained micas reflects a change from alkaline to relatively acidic postmagmatic fluids as (K+H) metasomatism produced greisen-like Li-mica. The pegmatites are F-rich as evidenced by the high F content in lithian mica and lepidolite and primary and secondary montebrasite and the presence of topaz.

In Tantalite Valley, Namibia, initial subsolidus metasomatism of the primary Li minerals, spodumene, amblygonite and lithiophilite took place in an alkaline environment as evidenced by the albitization of spodumene and the Ca-metasomatism of lithiophilite. The formation of secondary micas in spodumene reflects a change from alkaline to relatively acidic postmagmatic fluids as (K+H) metasomatism

produced greisen-like or sericitic alteration. These pegmatites were both F-rich as evidenced by the high F content in micas, and montebrasite, and in the formation of the triplite and fluorite, and relatively P-rich which is shown by the formation of montebrasite and lithiophilite.

In Namaqualand, in the pegmatites in the Steinkopf Area, there is no conclusive evidence of replacement minerals of lithiophilite, but spodumene presents supportive evidence for an initial alkaline environment with Na-metasomatism of spodumene, followed by relatively acid postmagmatic fluids and the formation of micas in spodumene. However, these pegmatites were not particularly F or P-rich, which is reflected in the rarity of Li-mica and the absence of amblygonite-montebrasite respectively, in contrast to the pegmatites in the north-western section of the Namaqualand Pegmatite Belt at Tantalite Valley, and in contrast to the rich F and P bearing pegmatites of the Karibib area, Namibia.

The abundance of minerals containing Li, Be, Mn, Nb, Ta and Bi indicate that pegmatites studied in the three main Li-rich areas originated from a highly differentiated granitic source.

There is a distinct difference in the composition of pegmatite minerals in the Kenhardt-Marydale district of the Northern Cape, South Africa. The Mn/Mn+Fe ratio is much lower in minerals containing these elements than the previous areas and a predominance of Nb over Ta, the type of Be-minerals present, and the rarity of Li, indicate a less differentiated source for the pegmatites, in the Kenhardt area of the Namaqualand Pegmatite Belt. This observation leads to the suggestion that "Namaqualand Pegmatites Belt", from Steinkopf in the west to Kenhardt in the east, is composed of several generations of injected differentiated magma each with its own differentiated postmagmatic fluids.

3.6 LITHIAN - MICA

3.6.1 Introduction

The lithian micas which are pink to purple and occasionally grey in colour are a group of striking minerals typically associated with Li-pegmatites. In terms of morphology the lithian micas range from dense masses of microscopic flakes to giant flat or curved tabular crystals. They usually form late in the crystallization sequence and in some cases replace pre-existing minerals such as spodumene, albite etc. as discussed earlier in this chapter. Replacement of muscovite by lepidolite is widespread. The lithian micas commonly form separate units near the core of the pegmatites or replacement units and are intergrown with variable amounts of cleavelandite albite. At the Harding pegmatite, South Dakota, primary microcline and spodumene are replaced by assemblages consisting principally of cleavelandite and lithian muscovite-lepidolite, leaving abundant rounded relics of spodumene and microcline (Jahns and Ewing, 1976; Chakoumakos, 1978). However, sometimes a replacement origin is not apparent, as contacts between lepidolite units and other zones may be clearly defined implying a primary phase.

Munoz (1971) demonstrated complex relationships in lepidolite compositions and liquidus to subsolidus stabilities dependent on Si-saturation, f_{H_2O} and f_{HF} . His results confirm the observation that natural Li-Al micas can be either secondary metasomatic products generated by the action of late F-bearing aqueous fluids on early lithium aluminosilicates and K-feldspar, or primary melt phases which do not replace pre-existing minerals.

The lithian mica occurrences are not only important for their Li, Rb and Cs contents, but being formed late in the crystallization sequence, they may contain a variety of rare-element minerals, such as caesium beryl, cassiterite, hafnian zircon (von Knorring, 1970) and a variety of niobium-tantalum minerals, such as manganotantalite, wodginite and microlite.

The bulk of the rare-alkali elements Rb and Cs occur in the lithian micas and in microcline in addition to the rare Cs-mineral, pollucite.

Hawthorne and Cerny (1982) have reviewed the three groups in the Li-Al mica family. Structural polytype and Li_2O content are adequate for distinguishing the three groups 1) lithian muscovite 2) the intermediate variety, muscovite-lepidolite, and 3) true lepidolite. Lithian muscovite is characterized by the 2M1 polytype with Li_2O approximately less than 3.5%. Muscovite-lepidolite i.e. the transitional structures of Levinson (1953), mixed forms of Foster (1960), mixed types of Rinaldi et al. (1972) consist of the 2M1 muscovite component and one or other of the polytypes characteristic of lepidolite, commonly 2M2 or 1M; their Li_2O contents vary between about 3.5 to approximately 4.5 wt.%. True lepidolites may have the 1M, 2M2, 2M1, 3T or 3M2 structure and Li_2O contents higher than about 4.0 wt.%. Among the lepidolites, numerous authors have unsuccessfully attempted to correlate Li_2O percentages with polytypism, due to the substitution mechanisms operating in natural Li-Al micas. However, Chaudry and Howie (1973), Sartori (1976) and Swanson and Bailey (1981) concluded that certain significant factors other than composition, such as T-P, volatiles, degree of cooling and saturation are more important in determining the occurrence of lepidolite polytypes. In this study the term lithian-mica (Li-mica) will be used because structural polytype has not been determined and the Li_2O content in micas in the Karibib area varies from 1.71 to 6.20 wt.%. (see Table 3.21).

In the late stages of evolution of complex pegmatites, muscovite may be produced by hydrolysis of K-feldspars, the hydrolytic breakdown often resulting in the formation of greisen-like muscovite + quartz assemblages which may carry cassiterite and Nb-Ta-bearing minerals. However, the majority of these Nb-Ta-bearing minerals occur in coarse-grained cleavelandite. Sericite, not to be confused with late muscovite, is generated by late rare-element-bearing fluids (Hawthorne and Cerny, 1982).

Munoz (1971) showed by experiment that lepidolite is stable at low temperatures in pegmatite mineral assemblages and that it can form by subsolidus reaction of spodumene and K-feldspar by F-rich aqueous fluids. Textural and structural relations of certain lepidolite alterations from spodumene and microcline (London and Burt, 1982c) indicate that lepidolite does form in sequence at lower temperatures <450-400 during the main stage of crystallization from residual magmas (as opposed to the "hydrothermal stage" which follows in the crystallization sequence) and after the crystallization of the main lithium minerals (Norton 1973). Some lepidolite assemblages have a disordered texture and very coarse-grained features, however, they also form fine-grained units of great magnitude in other pegmatites, analogous to the formation in the Rubicon pegmatite, Karibib. On the whole, they lack evidence of any pre-existing minerals and are the host rock of manganotantalite and U-Pb-rich microlite in the Rubicon pegmatite (see Plate 3.27 and Plate 5.16). However, lepidolite greisen is considered to be of replacement origin, for example at the Noumas pegmatite, Steinkopf (pers.comm. O.von Knorring).

3.6.2 Occurrence and geochemistry

Li-mica is very prominent in the Karibib area of Namibia. In the two main pegmatites of the area, Rubicon and Helicon, Okongava Ost 72, it is the main Li-mineral and forms huge zones which appear to correlate with petalite and beryllium and cleavelandite zones (see Fig 2.1) in the inner areas of the pegmatite near the quartz core. In the Rubicon pegmatite, the lepidolite unit is intergrown with albite and quartz and petalite except near the quartz core margin. Amblygonite occurs as scattered nodules within the lepidolite zone. Nodules of amblygonite also occur within the petalite. In the Helicon 1 pegmatite, lepidolite is intergrown with albite in the intermediate unit, in places 25 metres wide; a comparatively narrow cleavelandite-beryl unit separates it from the quartz core. Amblygonite occurs as nodules within the lepidolite. The individual zones in this pegmatite are rather irregular in their development, and in the lepidolite zone high grade ore is found in the form of separate lenses.

pegmatite are rather irregular in their development, and in the lepidolite zone high grade ore is found in the form of separate lenses.

TABLE 3.20. Compositions of lithian mica and muscovite

Sample No.	68j	33j.	Mon	Nor	M1	Strath	R48j
SiO ₂	44.75	45.27	54.10	49.77	47.08	44.69	49.59
TiO ₂	0.05	0.14	0.02	0.03	0.00	0.10	0.01
Al ₂ O ₃	34.44	34.06	22.02	25.95	25.57	37.25	28.68
Fe ₂ O ₃	3.20	3.80	0.05	0.01	3.87	0.50	0.01
MnO	0.74	0.07	0.14	0.45	0.52	0.02	0.12
MgO	0.20	0.69	-	-	-	-	0.31
CaO	0.06	0.06	-	-	-	-	0.07
Na ₂ O	0.31	0.55	0.10	0.29	0.18	0.63	0.31
K ₂ O	10.37	10.52	9.60	10.08	9.57	10.25	10.68
Li ₂ O	0.48	-	pr	4.09	nd	nd	3.96
Rb ₂ O	1.35	0.17	0.83	1.65	0.45	1.66	1.81
Cs ₂ O	0.11	nd	nd	nd	nd	nd	0.15
F	0.36	0.25	9.19	9.26	6.02	0.12	5.25
H ₂ O+	4.75	4.25	nd	nd	nd	nd	nd
Total	101.17	99.94	96.05	102.28	97.23	94.01	100.95
-O=F	0.15	0.10	3.86	3.89	2.53	0.05	2.20
Total	101.02	99.84	96.05	98.39	94.70	93.96	98.75

No. of ions on the basis of O=22 and O=24(68j,33j)

	68j		33j		Mon		Strath		48j
Si	5.973]	8	6.095]	8	7.070]	8
Al	2.027]		1.905]		0.930]	
Al	3.390]		3.499]		2.460]	
Ti	0.005]		0.014]		0.002]	
Fe ³⁺	0.321]	4.1	0.385]	4.0	0.005]	3.5
Mn	0.077]		0.008]		0.016]	
Mg	0.040]		0.138]		-]	
Li	0.258]		0.000]		-]	
Ca	0.009]		0.009]		-]	
Na	0.080]		0.144]		0.029]	
K	1.765]	2.0	1.806]	2.1	1.600]	1.7
Rb	0.116]		0.015]		0.070]	
Cs	0.006]		-]		-]	
F	0.152]	4.4	0.098]	3.9	3.80]	
OH	4.230]		3.819]		-]	
]]		0.049]	2.092

- 68j. Green muscovite plates (+albite+tantalite), White City pegmatite, Tantalite Valley (XRF + wet chemical)
 33j. Muscovite plates, Witkop pegmatite, Tantalite Valley, Namibia (XRF +wet chemical))
 Mon. Lithian muscovite, Mon Repos pegmatite, Karibib, Namibia (Probe analysis, J.R. Baldwin)
 Nor. Purple Li-mica, Norrabees pegmatite, Steinkopf, Namaqualand (Probe analysis, J.R. Baldwin)
 M1. Li-mica Okatjimukuju, Karibib, Namibia (XRF + wet chemical)
 Strath. Muscovite, Strathmore, Cape Cross, Namibia (Probe analysis, J.R. Baldwin)
 48j. Purple lithian muscovite, Rubicon pegmatite

Although there are numerous compositional and structural varieties of Li-micas, chemically they are essentially similar to muscovite, but due to lithium substitution their Al content is lower and that of silicon higher (Table 3.20). In addition, they are much richer in F and poorer in Fe than the pegmatite muscovites and there is an apparent correlation between Li and F (see Fig. 3.9).

From Table 3.21 it may be observed that the F content of Li-mica is very high, reaching 8.07 and 8.12% (anal. 166, 167) at the Etiro pegmatite. Von Knorring (1985) has pointed out that F correlates with Li and this may be observed at Etiro where the corresponding Li_2O values are 6.04 and 6.20% respectively; where the F content decreases to 6.86% in Li-mica at Etiro, the Li_2O content is similarly lower at 4.41% (Table 3.21, anal. 165). This correlation may also be observed in Li-mica at the Rubicon pegmatite (Table 3.21, anal. 161, 162 and Table 3.20, anal. 48J); there is a slight variation but the general trend is the same throughout the Li-micas in the Karibib region.

The same general trend may be observed in Tantalite Valley, though the level of F and Li in Li-micas is lower than the compositions of Li-mica in the Karibib pegmatites (Table 3.22) and approximately similar to the compositions in the Steinkopf area, Namaqualand (Table 3.23). In the Kenhardt district, Northern Cape, South Africa, where lithium minerals occur sporadically, Li-mica at the Jack 1 pegmatite contains 5.03% F and 4.05% Li_2O . The analyses from Tantalite Valley are arranged in order of decreasing Li_2O content - the F-content also decreases in the same order (Table 3.22, anal. 170-173).

With regard to the mineral paragenesis of Li-micas, in the Karibib area a high F content is apparent where Li-mica is associated with topaz, at the Etiro, M4 and Jooste's pegmatite, Karibib (Table 3.21 anal. 164, 167, 169) signifying very F-rich post-magmatic fluids in these three pegmatites.

TABLE 3.21

Partial analyses of Li-mica in the Karibib area

	161.	162.	163.	164.	165.	166.	167.	168.	169.
Fe ₂ O ₃	6.97	0.01	0.07	0.11	4.83	0.15	0.03	0.02	0.04
MnO	1.16	-	0.30	0.57	2.10	1.62	1.57	0.24	1.18
Na ₂ O	0.54	0.32	0.37	0.46	0.35	0.35	0.42	0.60	0.43
K ₂ O	10.38	11.37	11.23	11.09	10.66	10.91	11.09	10.87	10.61
Li ₂ O	1.71	4.13	4.13	5.34	4.41	6.04	6.20	4.75	5.57
Rb ₂ O	1.32	-	1.93	1.94	1.04	1.31	1.41	3.02	1.98
Cs ₂ O	0.04	0.21	0.17	0.40	0.13	0.18	0.19	0.74	0.22
F	3.29	5.11	5.59	7.55	6.86	8.07	8.12	6.35	7.17

161. Li-mica - fine-grained, Rubicon (39j)
 162. Globular Li-mica plates-grey, Rubicon (23o)
 163. Grey Li-mica, Koopman's M1, Okatjimukuju 55 (1o)
 164. Li-mica, M4 Okatjimukuju Farm, Okatjimukuju 55(+ topaz+ cassiterite)(40)
 165. Li-mica - grey plates, E tiro 50
 166. Li-mica - satellite crystals, E tiro 50 (56o)
 167. Li-mica plates (+ topaz), E tiro 50 (24o)
 168. Li-mica (+albite + rubellite), Daheim 1, Daheim 106
 169. Globular Li-mica (columbite+cleavelandite), Jooste's, Okongava Ost 72

Sample numbers given in brackets see Appendix 2. Analysts: J.R. Baldwin and D. Richardson
 (-) = not determined.

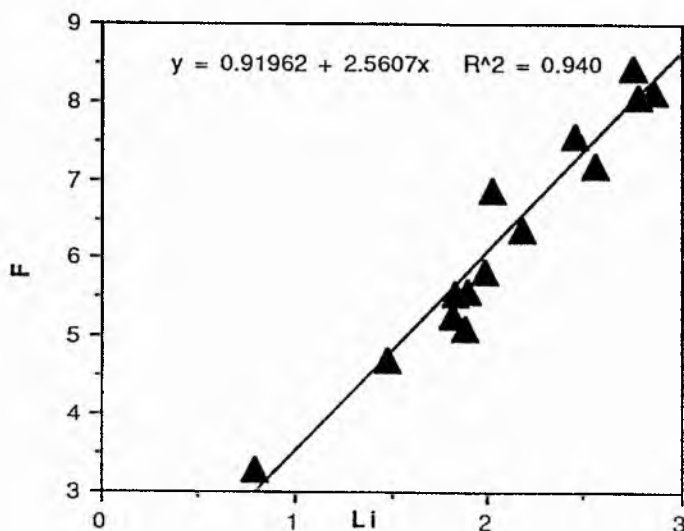


Fig. 3.9. Plot of F versus Li, (wt.%)for the lithian micas from Karibib, Namibia showing a positive linear correlation of 0.94.

TABLE 3.22.

Partial analyses of Li-mica in Tantalite Valley, Warmbad, Namibia

	170.	171.	172.	173.
Fe ₂ O ₃	0.03	2.42	0.19	4.96
MnO	0.23	1.72	1.42	0.77
Na ₂ O	0.50	0.48	0.46	0.31
K ₂ O	10.62	10.77	10.99	11.08
Li ₂ O	3.58	2.58	2.15	0.48
Rb ₂ O	1.46	1.50	1.36	1.34
Cs ₂ O	0.19	0.11	0.14	0.10
F	4.54	4.08	3.20	1.05

170. Purple Li-mica associated with amblygonite, Lepidolite pegmatite
 171. Purple Li-mica (compact) associated with lithiophilite, Homestead pegmatite
 172. Globular grey mica, Lepidolite pegmatite
 173. Green mica plates, White City pegmatite

TABLE 3.23

Partial analyses of muscovites from South African pegmatites

	174.	175.	176.	177.	178.	179.	180.	181.	182.
Fe ₂ O ₃	0.65	1.84	7.01	0.08	0.07	0.32	0.08	4.93	0.06
MnO	0.18	0.18	0.45	1.14	0.86	1.59	0.47	0.39	0.98
Na ₂ O	0.83	0.64	0.44	0.39	0.25	0.48	0.64	0.24	0.59
K ₂ O	10.51	10.44	10.58	10.85	11.09	11.20	10.64	10.55	10.61
Li ₂ O	0.00	0.06	1.32	3.56	3.27	3.05	0.35	0.19	4.05
Rb ₂ O	-	-	-	1.66	1.56	1.50	-	-	-
Cs ₂ O	-	-	-	0.50	0.53	0.55	-	-	-
F	0.32	0.26	2.67	4.78	3.85	3.92	6.38	0.34	5.03

174. Pink mica associated with albite, Noumas, Steinkopf, Namaqualand
 175. Mica associated with U-Zr minerals and albite, Noumas, Steinkopf, Namaqualand
 176. Globular muscovite associated with beryl and albite, Noumas, Steinkopf, Namaqualand
 177. Li-mica greisen (pure) associated with muscovite, Uranoop, Steinkopf, Namaqualand
 178. Li-mica greisen associated with albite and quartz, Norrabees, Steinkopf, Namaqualand
 179. Purple Li-mica associated with muscovite and bismuth, Norrabees, Namaqualand
 180. Purple Li-mica fish tail, Norrabees, Namaqualand
 181. Stellate green mica associated with columbite, Angelienspan, Marydale, Northern Cape
 182. Li-mica associated with Mn-apatite and quartz, Jack1, Marydale, Northern Cape

Analysts: Tables 3.21-3.23: wet chemical, D.Richardson, (Rb and Cs, J.R.Baldwin, flame immission and XRF) (-) = not determined.

2.6.3 Replacement characteristics of Li-mica

Small pegmatite occurrences in the Karibib area have not been examined in detail specifically with regard to zonation. In many cases the pegmatites have not been well excavated. Evidence of cross cutting relationships of the cleavelandite albite zones in the pegmatites has not been ascertained. There is, however, evidence of replacement of albite by mica (discussed in general in this chapter) at certain localities in the Karibib pegmatite field. At the Jooste's pegmatite, a richly mineralized pegmatite parallel to the Rubicon mine on Okongava Ost 72, fine-grained purple lithium mica (Table 3.21, anal. 171) is intergrown with spherically oriented laths of cleavelandite albite, quartz and microlite. Plate 3.28 shows the fine-grained mica and quartz replacing the cleavelandite. Replacement of albite is also visible at the E tiro pegmatite, where fine-grained mica and quartz are seen replacing cleavelandite laths (Plate 3.29). This has also been observed at the M4 pegmatite Okatjimukuju and at the M3 pegmatite where Li-mica replaces cleavelandite (Plate 3.30).

At the Mon Repos pegmatite, Karibib, fibrous mica with minor apatite occurs within amblygonite (Plate 3.26). The mica, both from the texture and the chemistry (Table 3.20, anal. Mon) is a late phase, and although lithium could not be determined on the microprobe, the Rb content of 1%, indicates a Li-rich mica (Baldwin, 1985). In fact Li-mica has not been located in this small excavation. The isolated fibrous mica within the amblygonite covers an area of 1 square cm in Plate 3.26.

At Rubicon mine purple fine-grained Li-mica is replacing amblygonite. The Li_2O content is 4.09% (H_2O by difference, 4-5%). At the junction of Li-mica and amblygonite small aggregates of topaz (50-100 microns in size) are apparent in the microprobe optics. Topaz is generally a late-stage replacement mineral in pegmatites. At Rubicon, topaz is forming from F-rich postmagmatic fluids.

In the Karibib area, after the crystallization of the primary lithium aluminosilicate petalite, amblygonite-montebbrasite apparently succeeded as the primary lithium mineral in these pegmatites. This sequence implies that the activities of the acidic volatiles P and F increased as crystallization proceeded and that petalite became unstable with respect to montebbrasite and quartz. F activities continued in the final stages of postmagmatic subsolidus conditions, where acidic fluids (K+H) with a high capacity to hydrolyse, converted the Li Al silicates to Li-mica where there was sufficient K, and topaz where there was a deficiency of K (London and Burt, 1982).

It is suggested by Stewart (1963,1978) and Norton (1983) that lepidolite in large zones may have crystallized directly from a siliceous "gas" if accompanied by quartz. This terminology may be consistent with the "supercritical fluid" described by Jahns and Burnham (1969,1982). Alternately lepidolite may be formed by subsolidus reaction of whatever residual mobile fluid remains at the temperatures below the stability of spodumene, perhaps trapped in the central areas of the pegmatite (Norton 1983).

Purple fine-grained lepidolite is intergrown in the form of abundant veining of cleavelandite at the Jooste's pegmatite, Karibib where it also contains microlite (see Plate 3.28) and the Homestead pegmatite in Tantalite Valley, Namibia where it contains spessartine garnet with a high Mn content. Where lepidolite occurs with cleavelandite, its origin from a "gaseous medium" or directly from a silicate melt (magma) at higher temperatures which crystallize the primary feldspar becomes implausible (Norton, 1973).

London (1990) points out that evidence suggests that rare-element pegmatites may not become vapour saturated until they approach solidus conditions at about 450°C, (a concept that disagrees with the Jahn's and Burnham's genetic model, 1982, which supports the hypothesis of a separate immiscible 'supercritical fluid' reacting alongside the silicate melt, initially at high temperatures) at which stage internal retrograde

recrystallization and wall rock alteration occur. According to London (1990) aqueous vapour has only a nominal effect on primary crystallization and fabric development within pegmatites.

The origin of cleavelandite albite and lepidolite zones has been discussed by London (1990) as follows. Evidence from fluid inclusions indicates that late stage silicate melts are alkaline and sodic in bulk composition. Crystallization of such hydrous silicate fluids yields bodies of albite \pm mica + quartz, and the exsolved aqueous vapour, which contains the excess alkaline components not taken up by crystallization of primary silicates, promotes the metasomatic alteration of enclosed or adjacent lithium minerals by cation exchange with the alkaline fluid. Hence this provides a mechanism for a replacement origin for large bodies of cleavelandite albite, as relicts of partially replaced microcline and spodumene (Harding mine, New Mexico and the Tanco pegmatite, Manitoba) and the fluid inclusions provide evidence of a primary origin for cleavelandite zones.

Late stage albite bodies form from residual Na-rich hydrous silicate melts (possibly + Na-rich aqueous vapour on the solidus). Excess Na-rich aqueous vapour may then sequentially be the source of fluids which form replacement lepidolite complexes. After initial reaction with lithium minerals and formation of lepidolite units these fluids become sufficiently acidic in character, by cation exchange to convert microcline and spodumene to mica elsewhere in the pegmatite, i.e., later residual fluids become K-rich after the initial formation of albite cleavelandite bodies and the reactive residual fluids on spodumene complexes, thereby creating an excess of K by ion exchange, and the formation of lithian mica or lepidolite.

Late-stage mica bodies that contain appreciable albite, quartz and sometimes tourmaline are compositionally similar to late-stage hydrous silicate melts such as those found in fluid inclusions in spodumene and these bodies may be primary in origin (London, 1990). This

type of association of cleavelandite and albite is typical of pegmatites in the Karibib area Namibia, i.e. the Rubicon and Jooste's pegmatite which might suggest that these units were primary rather than secondary in origin. Therefore from the evidence produced by London (1990), large-scale cleavelandite-lepidolite bodies may be either primary or replacement in origin which is compatible with conclusions drawn by previous authors for the formation of these two units in pegmatites.

Manganotantalite (+intergrown Pb-U-microlite)

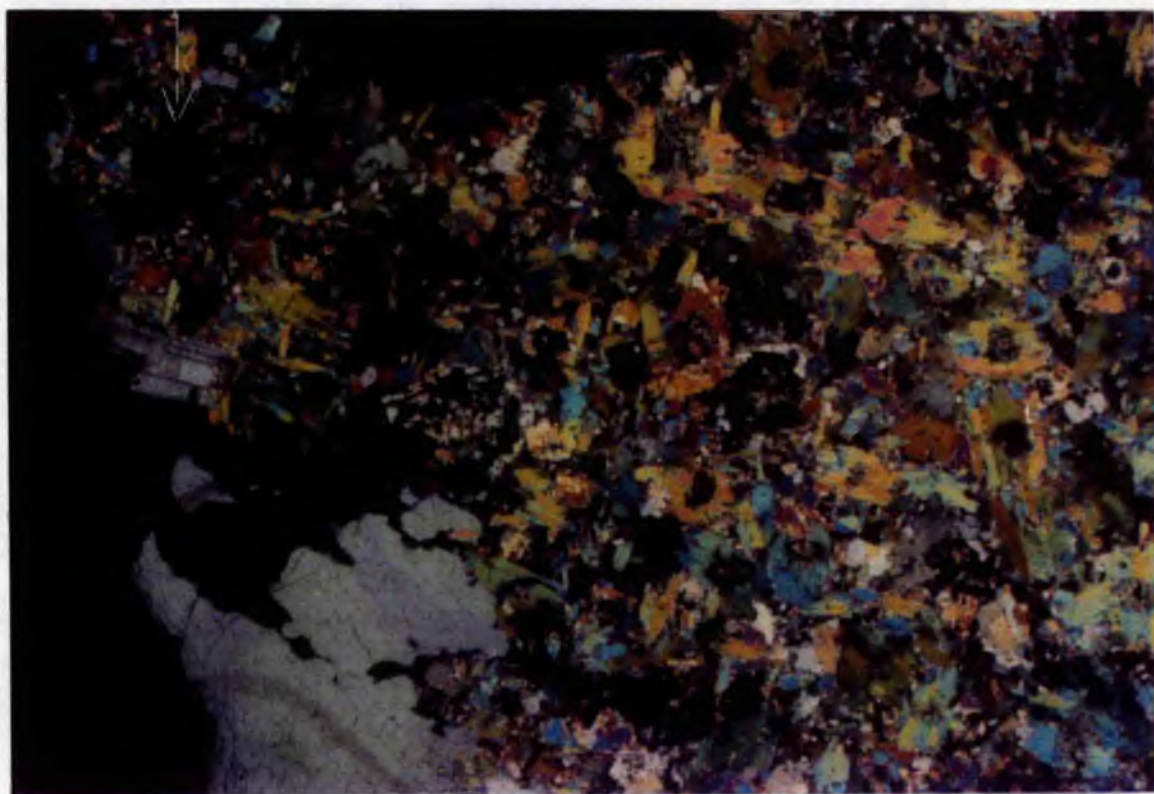


Plate 3.27. Photomicrograph of manganotantalite and intergrown Pb-U-microlite occurring in lithian mica and quartz the Rubicon pegmatite, Karibib, Namibia. Crossed polarized light. Scale bar: ----- 1.5 mm



Plate 3.28. Photomicrograph of fine-grained Li-mica replacing circular oriented cleavelandite laths and microlite crystals (black), Jooste's pegmatite, Okongava, Karibib, Namibia. Crossed polarized light. Scale bar: 0.5 mm

Plate 3.29. Photomicrograph of fine-grained mica and quartz intergrown with albite, Eitiro pegmatite, Karibib, Namibia. Crossed polarized light. Scale bar: 0.5 mm

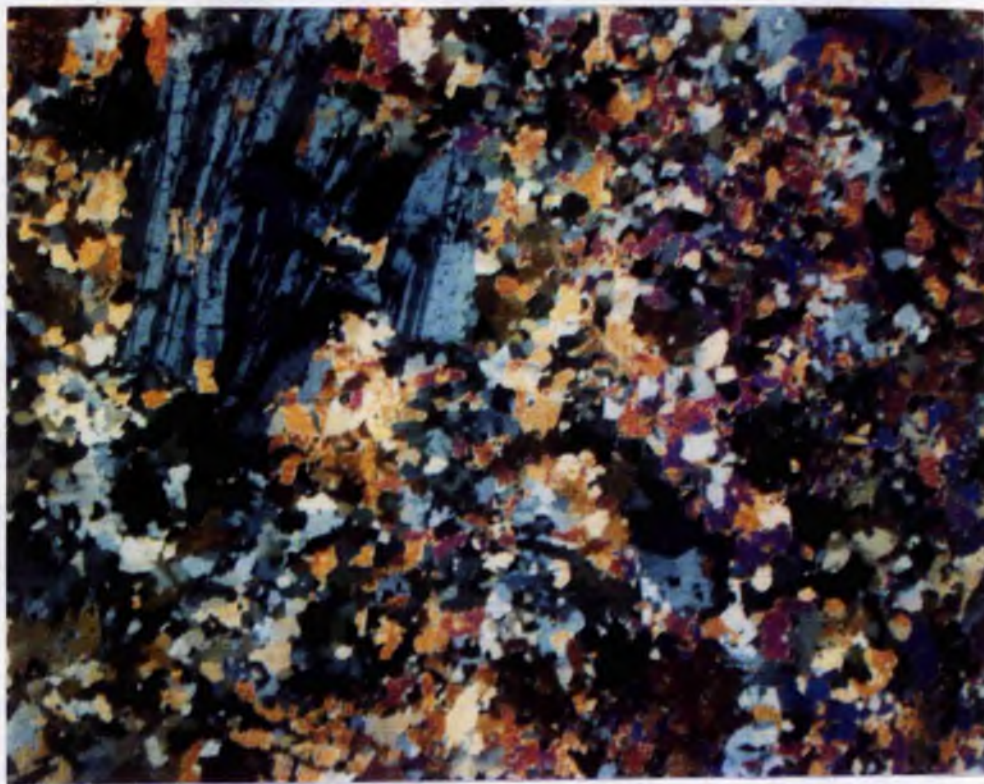




Plate 3.30. Photomicrograph of Li-mica intergrown with cleavelandite, M3 pegmatite, Okatjimukuju, Karibib, Namibia, Crossed polarized light. Scale bar: 0.5 mm _____

PART III

TANTALUM

Chapters 4 , 5, 6

PART III

TANTALUM MINERALIZATION

CHAPTER 4

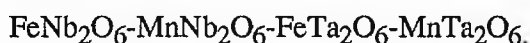
COLUMBITE-TANTALITE, WODGINITE AND TAPIOLITE

4.1. INTRODUCTION - TANTALUM MINERALS

The aim of this tantalum section is to investigate the geochemistry, the compositional zoning, replacement phenomena and paragenesis of tantalum minerals in order to reveal information on the composition of the late magmas and postmagmatic fluids from which these minerals crystallized.

In the course of analytical work at Leeds University, five years was spent analysing the niobium-tantalum group of minerals in connection with O. von Knorring's pegmatite investigations into minerals of the rare-elements. These analyses are reported in the annual reports of the Research Institute of African Geology in Leeds (von Knorring, 1964,1965,1966,1967,1968,1971). Wet chemical gravimetric methods using cupferron to separate niobium, tantalum, titanium, and tungsten were applied. Because of minute impurities, in the form of alteration products and other mineral inclusions, the minerals were crushed, washed, sieved and the grains carefully hand-picked under a stereobinocular microscope and ground to a fine powder in an agate mortar. However, these minerals as revealed in the electron microscope are often complexly compositionally zoned and replacement phenomena may be examined in detail in co-ordination with backscatter imaging. This compositional zoning, replacement phenomena and geochemistry reveal much information on the composition of the late magmas and postmagmatic fluids from which these rare minerals crystallized. Analytical details are given in Appendix 2.

The columbite-tantalite group comprises minerals of an isomorphous series:



In the series there is unlimited isomorphism between Nb and Ta and also between their Mn and Fe varieties. The majority of minerals in the columbite -tantalite series however are niobium-rich columbites and tantalum-rich members are rather rare. When tantalum is present in excess there is a tendency for other Ta minerals to be formed, i.e. ixiolite, wodginite, tapiolite, microlite.

Microlite is the tantalum end-member of the pyrochlore-microlite-betafite series. It is a comparatively rare accessory mineral of lithium pegmatites and is frequently associated with other tantalum minerals often replacing them. Quite commonly small amounts of microlite are seen associated with, or replacing other Ta-minerals and only rarely are larger concentrations of the mineral found in specific zones of Li-pegmatites. Microlite is mostly disseminated in cleavelandite albite - lithium mica units (see Plate 3.27), or in more complex albite - spodumene - lithian mica units. As microlite is a F, OH - bearing mineral, it is one of the last minerals to crystallize in the pegmatite sequence and is prominent in the latest micaceous replacing units in the pegmatite which are frequently replacing, or are associated with, the inner zones and quartz core zones in the pegmatite (von Knorring et al. 1981; Baldwin, 1989).

Geochemically microlite is invaluable, as it can accommodate a large number of elements such as U, Bi, Pb, Sn, W in its structure indicating the composition of a late highly differentiated source magma. The Ta content of microlite is usually high reaching 84% Ta₂O₅. Uranmicrolite and plumbomicrolite have Ta contents much lower.

The following tantalum minerals have been considered in this study :-

COLUMBITE-TANTALITE (orthorhombic)

TAPIOLITE Fe(Ta,Nb)₂O₆(tetragonal)

MICROLITE (Ca,Na,U)₂(Ta,Nb,Ti)₂(O,OH,F)₇ (cubic)

WODGINITE (Ta,Nb,Sn,Mn,Fe)₁₆O₃₂ (monoclinic)

4.2. COLUMBITE - TANTALITE : GEOCHEMISTRY AND DISTRIBUTION

4.2.1. Introduction

Von Knorring (1981) has grouped the orthorhombic columbite-tantalite group on the basis of chemical composition as follows:-

- a) Columbite $(\text{Fe, Mn})(\text{Nb, Ta})_2\text{O}_6$ ($\text{Fe}=\text{Mn}$, $\text{Nb} > \text{Ta}$)
- b) Manganocolumbite $(\text{Mn, Fe})(\text{Nb, Ta})_2\text{O}_6$ ($\text{Mn} > \text{Fe}$, $\text{Nb} > \text{Ta}$)
- c) Ferrocolumbite $(\text{Fe, Mn})(\text{Nb, Ta})_2\text{O}_6$ ($\text{Fe} > \text{Mn}$, $\text{Nb} > \text{Ta}$)
- d) Tantalite $(\text{Fe, Mn})(\text{Ta, Nb})_2\text{O}_6$ ($\text{Mn}=\text{Fe}$, $\text{Ta} > \text{Nb}$)
- e) Manganotantalite $(\text{Mn, Fe})(\text{Ta, Nb})_2\text{O}_6$ ($\text{Mn} > \text{Fe}$, $\text{Ta} > \text{Nb}$)

The compositions are plotted in Figure 4.1a (Page 144).

Columbite-tantalite minerals from Africa have been described by von Knorring (1970) and von Knorring et al. (1981) and from the Karibib-Usakos-Cape Cross area, Namibia by von Knorring (1985b). Some of these data from Karibib have been included from these publications mostly for comparative purposes, for example the majority of pegmatites in the region are niobium-rich, while the rare-element Li-pegmatites are in the minority, they also are Ta and Mn-rich and these are the subject of this present study. Figure 4.1 shows Mn-columbite, Fe-columbite, tantalite, Mn-tantalite and tapiolite $\text{Fe}(\text{Ta, Nb})_2\text{O}_6$ plotted on a quaternary diagram (data this study), as an example of the spread from the Nb end-member to the Ta end-member.

4.2.2. Columbite from the Northern Cape pegmatites, South Africa

Columbite $(\text{Fe, Mn})(\text{Nb, Ta})_2\text{O}_6$ is the commonest member of the Nb-Ta minerals in pegmatites. It frequently occurs in tabular, prismatic crystals, with well developed crystal faces, a submetallic lustre and has a dark-brown to almost black streak in some

varieties. The varieties with high Nb are not concentrated in Li-pegmatites but occur in this area of the Namaqualand pegmatite belt.

The columbite-tantalites, from the pegmatites in the Northern Cape Province of South Africa, show that this section of the Namaqualand Pegmatite is not rich in tantalum and that niobium is prominent in this area. This is in contrast to the western section of the pegmatite belt in Tantalite Valley, in Namibia for example, where tantalite is the dominant member of the series.

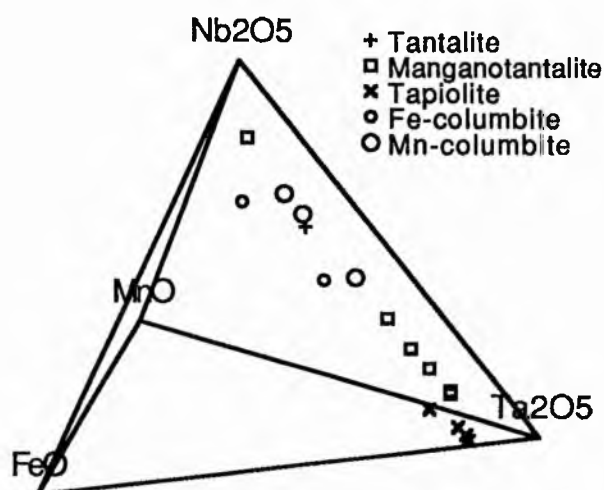


Fig. 4.1. Examples of Mn-columbite, Fe-columbite, Mn-tantalite, tantalite and tapiolite plotted on a quaternary diagram to show the range from Ta end-member to Nb end-member. Data this study (Tables 4.1, 4.2, 4.3, tapiolite from Section 4.5).

TABLE 4.1. Columbite compositions from the Northern Cape Pegmatites, South Africa

sample	S5/1.	J2/a.	J2/b.	A7/a.	A7/b.
Nb ₂ O ₅	38.19	44.13	46.92	53.17	54.75
Ta ₂ O ₅	42.83	36.18	32.11	25.73	26.63
TiO ₂	0.17	1.10	1.09	1.10	0.14
SnO ₂	0.06	0.05	0.05	0.02	0.00
WO ₃	0.19	0.19	0.34	0.34	0.40
FeO	6.67	12.31	12.30	9.35	9.72
MnO	11.36	5.78	5.77	9.50	9.12
UO ₂	0.06	0.04	0.04	0.00	0.00
Total	99.53	99.78	98.65	99.21	100.76

No of ions on the basis of 6 oxygens

Nb	1.179	1.309	1.384	1.513	1.542
Ta	0.795	0.646	0.570	0.441	0.451
Ti	0.009	0.054	0.054	0.052	0.007
Sn	0.002	0.001	0.001	0.001	0.000
W	0.003	0.003	0.006	0.006	0.007
Fe	0.381	0.675	0.672	0.492	0.507
Mn	0.657	0.321	0.319	0.507	0.481
U	0.001	0.001	0.001	0.000	0.000
Total	3.027	3.010	3.007	3.012	2.995

S5/1. Manganocolumbite, Straussheim, Kenhardt, South Africa (S5)
 J2/a,J2/b. Ferrocolumbite, Jack 2, Marydale, Northern Cape, South Africa (J2)
 A7a,A7b. Columbite, Angelierspan, Marydale, Northern Cape, South Africa (A7)
 Johannesburg microprobe. Analysts: R.Davies and J.R.Baldwin.

In the Northern Cape, the Straussheim 1 pegmatite on Farm N'Rougas Noord, about 35 kms north of Kenhardt (see Fig. 2.5) contains the most tantalite, with Ta₂O₅ reaching 43% in manganocolumbite (Table 4.1). The Angelierspan pegmatites lie about 88 km southeast of Kenhardt (Fig. 2.6); the columbite is Ta-poor with 25-27% Ta₂O₅. Jack 1 pegmatite in the same general area (Fig. 2.6) contains a ferrocolumbite with Ta₂O₅ varying from 32-36% ; Nb₂O₅ varies from 47-44% (see Table 4.1).

4.2.3. Columbite-tantalite from the Karibib-Usakos pegmatites, Namibia

Manganocolumbite $[(\text{Mn,Fe})(\text{Nb,Ta})_2\text{O}_6]$ is a type mineral of the Karibib Li-rich pegmatites and is found as tabular, striated crystals, with a vitreous to submetallic lustre and yellowish-green to dark-brown streak (von Knorring 1985b). Manganocolumbite is distinctly black in colour, in contrast to manganotantalite which is often red to brown. The Mn content is exceptionally high 17.91 - 19.04%, (Table 4.2) a typical feature of this late stage mineral, in the highly fractionated Li-pegmatites of the region.

The tantalite $[(\text{Fe,Mn})(\text{Ta,Nb})_2\text{O}_6]$ group includes rare-members of the columbite-tantalite series with Ta predominating over Nb (Table 4.2) while Fe and Mn are of intermediate concentration. Tantalite may be observed in both Li-poor and Li-rich pegmatites. The colour of tantalite is generally black but when the Ta content is high the colour is red-brown and in appearance this tantalite is identical to manganotantalite. Tantalite with 53.77% Ta_2O_5 has been observed in disseminated grains in late, Fe-rich muscovite replacement units at Viljoen's claim, Okongava Ost 72, and in pockets intergrown with microlite and manganoapatite in a Li-pegmatite at Ricksburg (Ta_2O_5 76.11%, Table 4.2).

Manganotantalite $[(\text{Mn,Fe})(\text{Ta,Nb})_2\text{O}_5]$ with Ta and Mn in excess of Nb and Fe are more widespread than tantalites and may be regarded as type minerals of tantalum mineralization in the highly fractionated Li pegmatites of the Karibib area. In contrast to the columbites which are generally opaque, the manganotantalites are commonly translucent with a characteristic golden-brown to red-brown colour. However, the colour and transparency are variable, dependent on the concentrations of Nb and Fe present.

TABLE 4.2. Columbite, manganocolumbite, ferrocolumbite and tantalite in pegmatite, Karibib-Usakos-Cape Cross, Namibia

Sample	Sand	H	Ru	K(A)	Da	Okat	Okon	KSp	Sw	(78)Da	D2	V8	Rk
Nb ₂ O ₅	42.21	57.67	53.59	50.35	35.29	36.67	69.11	62.41	53.16	41.42	24.66	29.35	9.59
Ta ₂ O ₅	38.96	20.89	27.76	29.57	44.10	47.36	4.67	13.13	24.05	38.63	55.94	53.77	76.11
TiO ₂	0.52	0.28	0.14	0.16	0.00	0.28	1.8	1.07	1.75	0.00	1.42	0.09	0.12
WO ₃	-	0.68	-	0.14	-	-	2.83	2.00	0.43	0.66	0.26	0.26	-
SnO ₂	0.44	0.18	0.24	0.18	0.00	0.25	0.11	0.03	-	1.12	0.00	0.00	0.08
ZrO ₂	0.12	-	0.19	-	-	0.21	0.39	0.21	0.46	-	-	0.19	-
FeO	9.76	1.14	0.25	0.30	0.07	0.66	13.63	15.19	14.87	13.29	6.88	6.97	7.62
MnO	8.05	17.91	18.34	19.04	18.54	16.44	6.53	4.76	3.95	3.76	9.21	9.45	7.17
UO ₂	-	tr	tr	-	-	-	-	-	-	-	-	-	-
	100.06	98.75	100.51	99.74	98.0	99.87	99.32	99.07	99.55	98.22	99.11	100.08	100.69

	No of ions on the basis of 0=6												
Nb	1.27	1.62	1.52	1.46	1.12	1.09	1.81	1.70	1.50	1.27	0.81	0.95	0.35
Ta	0.70	0.35	0.47	0.51	0.84	0.89	0.07	0.21	0.41	0.71	1.10	1.04	1.65
Ti	0.03	0.01	0.007	0.008	-	0.01	0.08	0.05	0.08	-	0.08	0.01	0.01
W	-	0.01	-	0.002	-	-	0.04	0.03	0.01	0.01	0.01	0.01	-
Sn	0.01	0.005	0.006	0.005	-	0.01	0.003	0.01	0.02	0.03	-	-	-
Zr	0.004	-	0.01	-	-	0.01	0.01	0.03	0.01	-	0.02	0.01	-
Fe	0.54	0.06	0.01	0.002	0.004	0.04	0.66	0.76	0.78	0.75	0.42	0.42	0.51
Mn	0.45	0.94	0.97	1.03	1.10	0.96	0.32	0.24	0.21	0.22	0.57	0.57	0.48
U	3.004	2.995	2.993	3.035	3.064	3.01	2.996	3.01	3.02	3.99	3.013	3.01	3.00

Sand.	Columbite, Sandamap (von Knorring, 1985)
H.	Manganocolumbite, Helicon 2, Okongava Ost (von Knorring, 1985)
Ru.	Manganocolumbite, Rubicon, Okongava Ost (von Knorring, 1985)
(K)A.	Manganocolumbite, Albrechtshöhe, Karlsbrunn, Kaliombo (von Knorring, 1985)
Da.	Manganocolumbite, Daheim 106 (gravimetric) Analyst: J.R.Baldwin (von Knorring, 1970)
Okat.	Manganocolumbite, Okatjimukuju (von Knorring, 1985)
Okon.	Ferrocolumbite, Okongava Ost (von Knorring, 1985)
KSp.	Ferrocolumbite, Klein Spitskop (von Knorring, 1985)
Sw.	Ferrocolumbite, Swakopmund, Strathmore, Cape Cross area (von Knorring, 1985)
78/Da.	Ferrocolumbite, Daheim 106. Analyst: J.R.Baldwin
D2.	Tantalite, Dernburg, Karibib 54. Analyst: J.R.Baldwin and R. Davies
V8.	Tantalite, Viljoen's, Analyst: J.R. Baldwin & R. Davies
Rk.	Tantalite, Ricksburg. (von Knorring, 1985)

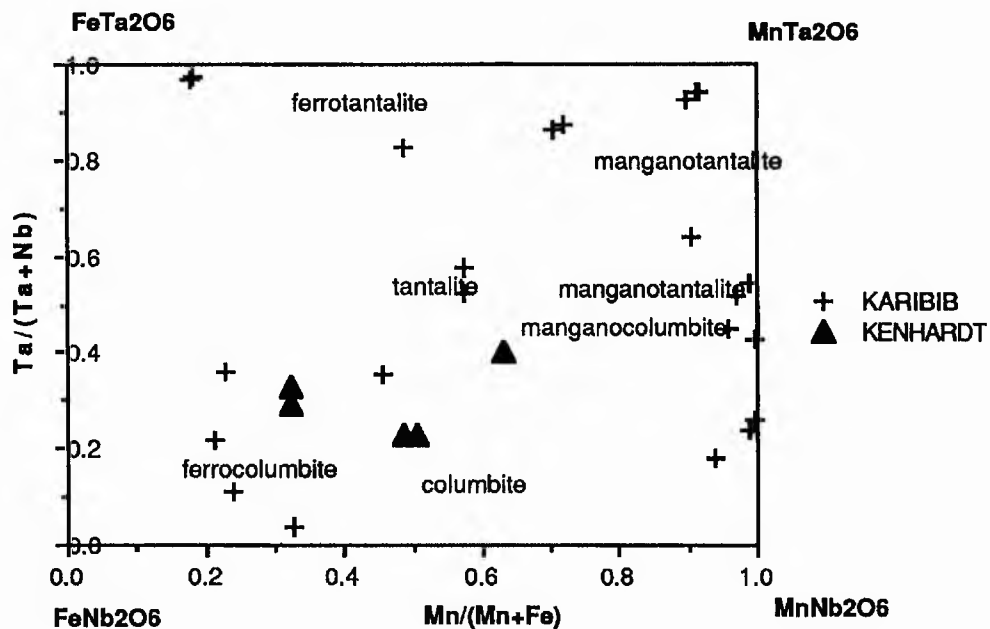
Manganotantalites from the Karibib area have been subject to a detailed geochemical investigation with the microprobe because this type mineral is so intimately associated with other tantalum minerals, for example microlite which often replaces it. Detailed descriptions will be given separately in association with the replaced and closely associated minerals. Examples given in Table 4.3 are not included in the detailed descriptions.

TABLE 4.3. Manganotantalite from pegmatite, Karibib, Namibia

Sample	Der.	MonR.	R.10	R.11
Ta ₂ O ₅	62.22	81.44	53.95	52.44
Nb ₂ O ₅	21.00	3.81	27.30	29.59
TiO ₂	0.37	0.07	0.00	0.00
SnO ₂	0.12	0.00	0.10	0.08
FeO	1.43	1.45	0.21	0.53
MnO	13.50	12.61	15.95	16.01
PbO	-	-	0.06	0.00
UO ₂	-	-	0.32	0.14
	98.64	99.38	97.89	93.79
No of ions based on 6 oxygens				
Ta	1.282]	1.856]	1.082]	1.029]
Nb	0.719] 2	0.144] 2	0.910] 2	0.965] 2
Ti	0.021]	0.004]	0.000]	0.000]
Sn	0.007]	-]	0.003]	0.002]
Fe	0.091]	0.102]	0.013]	0.032]
Mn	0.866] 1	0.895] 1	0.996] 1	0.978] 1
Pb	-]	-]	0.001]	-]
U	-]	-]	0.005]	0.002]
	2.986	3.001	3.010	3.008

Der. Dernburg, Karibib 54 (gravimetric). Analyst: J.R.Baldwin (von Knorring, 1970)
 MonR. Mon Repos, Okongava Ost (gravimetric). Analyst: J.R.Baldwin (von Knorring, 1970)
 R10, R11. Mn-tantalite enclosing Pb-U microlite, Rubicon, Okongava Ost (R)
 Analyst: J.R.Baldwin (electron-probe, Edinburgh)

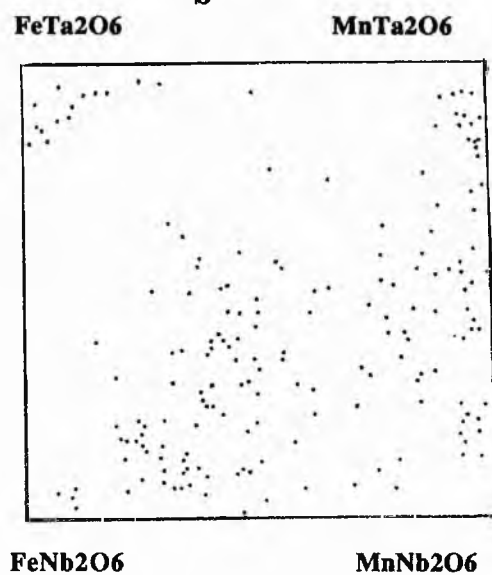
The columbite-tantalite compositions from Karibib and from the Kenhardt area, Northern Cape are plotted on a Ta/(Ta+Nb) versus Mn/(Mn+Fe) quaternary diagram (data from Tables 4.1-4.3, 4.5 and compared with compositions from pegmatites generally in Africa (von Knorring and Condliffe, 1981) (see Figs. 4.1a and 4.1b).



a

Fig. 4.1.a). Compositions of columbite-tantalite minerals plotted on a Ta/(Ta+Nb) versus Mn/(Mn+Fe) diagram (the columbite quadrilateral) from Karibib, Namibia and the Kenhardt area, Northern Cape, South Africa, data this study (from Tables 4.1-4.3, 4.5) in comparison with, b) compositions of columbite-tantalite from African pegmatites in general (from von Knorring and Condliffe, 1981).

b



4.2.4. Manganotantalite, from Tantalite Valley, Namibia and Steinkopf, Namaqualand

In Tantalite Valley manganotantalite, which is the prevalent Nb-Ta mineral in this area, occurs in two differentiated pegmatites, White City and Homestead. In the Homestead pegmatite, dark orange-brown manganotantalite is being replaced by pink microlite (this will be described in Chapter 5: Microlite. The manganotantalite and microlite occur in the quartz core margin, where they were observed in irregular pods of lithian mica which is veined with albite. A microprobe traverse was completed across the

TABLE 4.4. Compositions of Mn-tantalite and columbite from Steinkopf, Namaqualand and Tantalite Valley, Namibia

Sample	Rep1	Rep2	Rep3	Rep4	Rep5	6.	7.	WC3	Ho2/1
Ta ₂ O ₅	71.82	71.84	72.29	73.63	72.14	68.00	12.05	85.51	83.14
Nb ₂ O ₅	12.68	12.88	11.98	11.48	12.83	15.5	65.24	0.25	1.40
TiO ₂	0.48	0.65	0.84	0.81	0.58	0.90	1.37	0.00	0.10
ZrO ₂	0.00	0.00	0.00	0.00	0.00	0.00	0.15	0.00	0.40
SnO ₂	-	-	-	-	-	-	0.55	-	-
WO ₃	0.70	0.63	0.57	0.63	0.78	-	1.10	-	0.13
Bi ₂ O ₃	0.04	0.05	0.07	0.04	-	-	-	-	-
FeO	0.51	0.51	0.64	0.49	0.64	1.6	10.00	0.21	0.15
MnO	13.95	14.09	13.46	13.93	14.05	13.26	9.47	13.82	13.83
Na ₂ O	-	0.15	-	-	-	-	-	-	-
UO ₂	0.03	0.39	0.47	0.34	-	-	-	-	-
Total	100.21	101.15	100.32	101.35	101.02	99.26	99.93	99.79	99.15

No. of ions on the basis of 6 (O)

Ta	1.53	1.50	1.54	1.56	1.52	1.43	0.19	1.98	1.92
Nb	0.45	0.45	0.42	0.40	0.45	0.54	1.74	0.01	0.05
Ti	0.03	0.04	0.05	0.05	0.03	0.05	0.06	0.00	0.006
Zr	-	-	-	-	-	-	0.004	-	0.02
Sn	-	-	-	-	-	-	0.013	-	-
W	0.01	0.03	0.02	0.01	0.02	-	0.02	-	0.003
Bi	0.001	0.001	0.001	0.001	0.00	-	-	-	-
Fe ²⁺	0.03	0.07	0.04	0.03	0.04	10.10	0.49	0.01	0.01
Mn	0.92	0.92	0.89	0.92	0.92	0.87	0.47	1.00	1.00
Na	-	0.02	-	-	-	-	-	-	-
U	0.00	0.01	0.01	0.01	-	-	-	-	-
Total	2.971	3.041	2.971	2.981	2.96	2.99	2.987	3.01	3.009

Rep1-5 Mn-tantalite associated with microlite, Noumas pegmatite, Steinkopf, Namaqualand. Analyst: J.R. Baldwin

6. Mn-tantalite associated with spessartine garnet, Noumas pegmatite (Baldwin, 1979)

7. Columbite, Noumas pegmatite, Namaqualand (von Knorring, 1985)

WC3. White City pegmatite, Tantalite Valley, Namibia. Analyst: J.R. Baldwin

Ho2/1 Mn-tantalite, Homestead pegmatite, Tantalite Valley. Analyst: J.R. Baldwin

manganotantalite and an average analysis contained 83.14% Ta_2O_3 , over the range 82.17 - 84.13% in 13 analyses, 13.83% MnO over the range 13.56-14.07%, 1.4% Nb_2O_5 and FeO 0.15% (Table 4.4, anal. HO2/1). At the White City pegmatite, Tantalite Valley, Mn-tantalite which occurs in and cleavelandite and quartz is high in tantalum with 85.51% Ta_2O_5 and MnO 13.82% (Table 4.4 anal. WC3).

In the Steinkopf area of Namaqualand few columbite-tantalites have been collected. Manganotantalite occurs in the Noumas differentiated pegmatite; it has been located in two separate occurrences i) intergrown with garnet and quartz on the edge of the quartz core and ii) being replaced by microlite. Columbite has previously been analysed from this pegmatite (von Knorring, 1985b).

ii) Variation in manganotantalite associated with microlite is shown in Table 4.4. A microprobe traverse across the manganotantalite, which is opaque in transmitted light, showed Ta_2O_5 to have a composition over the range 71.84 - 73.63%, Nb_2O_5 11.48 - 14.80%, MnO 13.46 - 14.14% and FeO 0.5 - 1.11%. The previously described occurrences contain less Ta, with Ta_2O_5 68% and Nb_2O_5 15.5% in manganotantalite (Baldwin 1979; Table 4.4. anal.6) and Ta_2O_5 12.05% in columbite with 65.24% Nb_2O_5 (von Knorring 1985b; Table 4.4. anal. 7). The composition of columbite-tantalites in this pegmatite is therefore extremely variable.

The occurrences of Mn-tantalite replacement by microlite will be discussed in the microlite investigation: - Chapter 5.

4.3.1. Replacement of manganotantalite by ferrotantalite , Rubicon, Karibib

Manganotantalite occurs with cleavelandite in the intermediate zone of the Rubicon pegmatite, Karibib. A single zoned crystal of manganotantalite, approximately 2 cm by 1cm (see Plate 4.1) was investigated with the electron probe. The crystal shows three distinct areas, a main area and a marginal area consisting of two zones (Plates 4.1,4.2). A traverse across the crystal (Plate 4.1) from left to right revealed the main area to be manganotantalite (Table 4.5 anal.s. S4/1-4, 6) with a Ta₂O₅ content between 83.86 and 84.95% and a MnO content between 12.33 and 12.49%.

The upper margin of the crystal (Plate 4.2) contrasts sharply with the main area (Plate 4.1). At the extreme margin the Ta₂O₅ content lies between 85.13 and 85.86%; however, in contrast to the main area, where the MnO ranges from 12.33 to 12.49%, the MnO value is only 2.44% with a FeO content of 11.25% (Table 4.5. anal.s. S4/8, 9,10). This chemical composition corresponds to an iron-rich tantalite, and also to the mineral tapiolite, Fe(Ta,Nb)₂O₆; however the X-ray diffraction data so far indicated that only the orthorhombic tantalite phase is present (von Knorring pers. comm.).

It is interesting to note that in the intermediate rim area, represented by the tan colour in Plate 4.2. the Ta : Nb ratio has changed, indicating enrichment of Nb relative to Ta (Table 4.5, anal.s. S4/5,7); at the extreme rim however, the situation is reversed, and the Ta : Nb ratio is similar to the interior of the crystal. The Mn : Fe ratio has also changed, but in this case indicating a progressive enrichment of Fe in the upper margin .

Von Knorring and Condliffe (1984) have pointed out that manganotantalites sometimes display a simple macrozoning visible to the naked eye: a light coloured Ta-rich marginal zone representing Ta enrichment during the last stages of pegmatitic crystallization. In the

Rubicon crystal, although there is a slight Ta enrichment in the marginal upper zone (see Table 4.5 anal. 8-10), the area is on the contrary darker, which in this case is controlled by Fe enrichment relative to Mn, rather than Ta enrichment relative to Nb (anals. S4/ 5, 7-10).

The compositional pattern at the margin of the Rubicon crystal could be due to growth zoning; the zones are quite sharply defined. However, contrary to the findings of von Knorring and Condliffe (1984) not only is there Nb enrichment in the margin, but Plate 4.2. strongly suggests that the areas of different composition are rather a feature of replacement than of growth zoning, replacement taking effect along cleavages, initially at one margin.

TABLE 4.5. Traverse across a composite crystal of manganotantalite and ferrotantalite, Rubicon, Namibia

Sample S4	S4/1.	S4/2.	S4/3.	S4/4.	S4/5.	S4/6.	S4/7.	S4/8.	S4/9.	S4/10.
Ta ₂ O ₅	84.11	83.86	84.95	83.88	78.72	83.71	79.42	85.30	85.13	85.86
Nb ₂ O ₅	3.06	3.03	3.02	3.15	7.68	3.14	7.02	1.70	1.78	1.38
TiO ₂	0.01	0.02	0.03	0.02	0.01	0.02	0.01	0.04	0.04	0.01
WO ₃	0.41	0.41	0.45	0.44	0.29	0.37	0.33	0.39	0.43	0.63
MnO	12.38	12.33	12.49	12.35	9.91	12.37	10.00	2.41	2.43	2.46
FeO	1.19	1.17	1.16	1.20	4.23	1.19	3.98	11.37	11.24	11.18
UO ₂	0.07	0.10	0.04	0.13	0.12	0.07	0.07	0.04	0.10	0.07
Total	101.23	100.92	102.14	101.17	100.99	100.87	100.83	101.25	101.15	101.59
No. of ions on the basis of O=6										
	S4/1.	S4/2.	S4/3.	S4/4.	S4/5.	S4/5.	S4/7.	S4/8.	S4/9.	S4/10.
Ta	1.894	1.894	1.896	1.889	1.726	1.890	1.751	1.938	1.936	1.949
Nb	0.115	0.114	0.112	0.118	0.279	0.118	0.257	0.064	0.067	0.052
Ti	0.001	0.001	0.002	0.001	0.001	0.001	0.001	0.003	0.003	0.001
W	0.009	0.009	0.010	0.009	0.006	0.083	0.007	0.008	0.009	0.014
Mn	0.868	0.867	0.868	0.866	0.677	0.870	0.687	0.171	0.172	0.174
Fe	0.082	0.081	0.080	0.083	0.285	0.083	0.270	0.794	0.786	0.780
U	0.001	0.002	0.001	0.002	0.002	0.001	0.001	0.001	0.002	0.001
Total	2.969	2.969	2.968	2.969	2.977	3.046	2.973	2.978	2.974	2.971
S4/1-4,6.	Manganotantalite (light area) see Plate 4.1.									
S4/5,7	Area of intermediate composition (dark tan area)									
S4/8-10.	Ferrotantalite (black areas)									

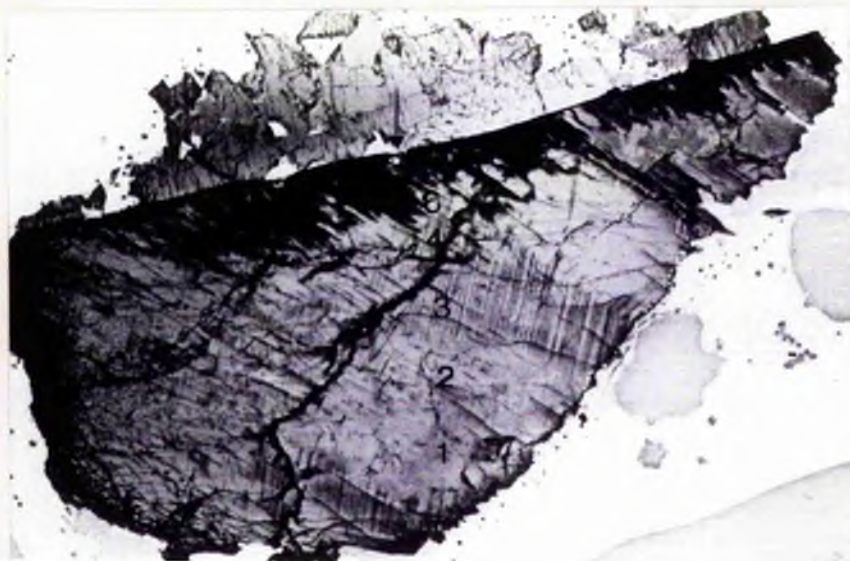


Plate 4.1. A composite crystal of manganotantalite with ferrotantalite replacement at the top edge, Rubicon pegmatite, Karibib, Namibia. Crystal 3cm by 1cm. The arrow marks the position of Plate 4.2.

Plate 4.2. A photomicrograph of the ferrotantalite replacement (black, Fe-Ta) of manganotantalite (yellow, 6, Mn-Ta) with an intermediate composition (tan, 5, 7) associated with cleavelandite, Rubicon pegmatite, Karibib, Namibia. Data of point analyses shown in Table 4.5. Scale bar: 1000 microns. Section: S4.



4.3.2. Manganotantalite laths in microlite, Rubicon, Karibib

An unusual occurrence of reddish tantalite lamellae, in a matrix of microlite occurs within or in association with, amblygonite nodules at the Rubicon rare-metal pegmatite, Namibia. Interspersed between and across the laths, aggregates of ferrotantalite and manganotantalite occur and in addition, apatite, native bismuth and numerous secondary minerals have been observed.

Plate 4.3 illustrates the mangano-tantalite laths (red) in a grey matrix of microlite. The light tan aggregates are manganotantalite rich in Ta and the dark red aggregates are ferrotantalite. A bismuth phase is represented by black cross-cutting veins and aggregates, and apatite by the white areas. Initially a traverse 5.5 mm long was run across the section and 110 analyses were made with the electron microprobe at 50 μm intervals to investigate; 1) the composition and variety of the Ta minerals; and 2) to establish the association of the Ta and Bi minerals. The line of the traverse is indicated on the section. The traverse indicated that, the matrix mineral is microlite (Table 4.6, Appendix 2.1) of almost constant composition - in 42 analyses Ta_2O_5 varied from 78.12 - 80.11% (see Fig. 4.2); and there are varying compositions in manganotantalite, ferrotantalite or tapiolite. Bismuth metal is present and the traverse also indicated the presence of Sn. The bismuth phase in addition to bismuth metal has been identified as a bismuth carbonate BiCO_3 a slightly unstable carbonate, probably bismutite, but without CO_2 analyses this cannot be verified.

The Ta-laths were found to be of variable composition, from manganotantalite containing 62.45% Ta_2O_5 , to a type richer in Ta, with 76.87% Ta_2O_5 (Table 4.7). Ferrotantalite contains 82.86 - 84.62% Ta_2O_5 in 4 analyses with 9.86 - 11.16% FeO. The manganotantalite, on the otherhand, contains a maximum of 82.58% Ta_2O_5 and 11.29% MnO. There is a great variation in the Ta_2O_5 content from 63.91 - 82.58% and Nb_2O_5 varies from 20.02 - 1.57% (see Table 4.7, Appendix 2.1).

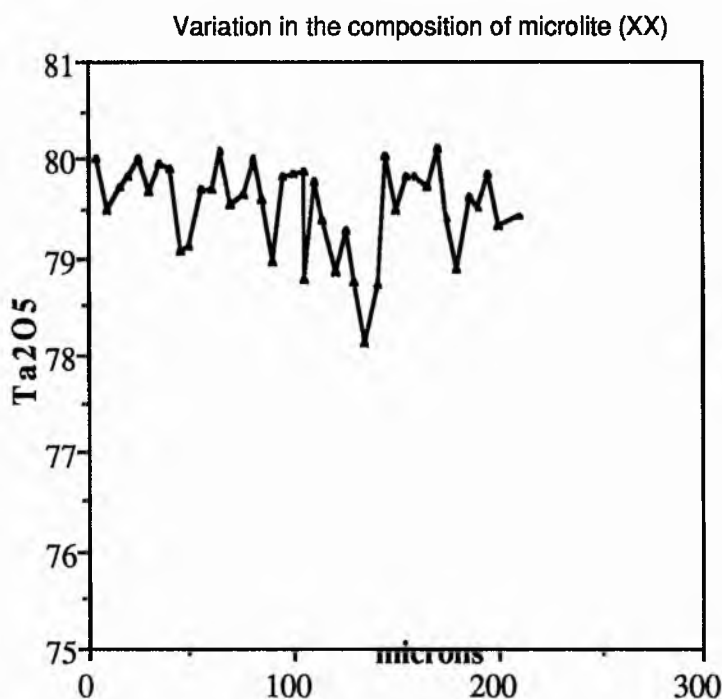


Fig. 4.2. Variation in the composition of Ta_2O_5 in microlite which occurs between Ta-laths along a traverse indicated in Plate 4.3. Data from Table 4.6. Sample XX, Rubicon, Karibib, Namibia.

Selected areas were analysed in detail in conjunction with the backscattered electron images shown in Plates 4.4 and 4.5. Firstly point analyses were selected in the microlite, in areas of tantalite in between the tantalite lamellae, and finally in the lamellae. Apatite is cross cutting and appears to be later than the microlite. The analyses are given in Table 4.8. a,b (Appendix 2.1). The point analyses in Appendix Table 4.8 indicate a lower content of Ta_2O_5 in microlite from 79-75% with a corresponding increase in Nb_2O_5 from 0.8-4.5%, in comparison with the analytical traverse data shown in Table 4.6

(Appendix 2.1) and Figure 4.2. The compositions of point analyses given in Tables 4.8 to 4.11 are shown in Figure 4.3 from sample XX.

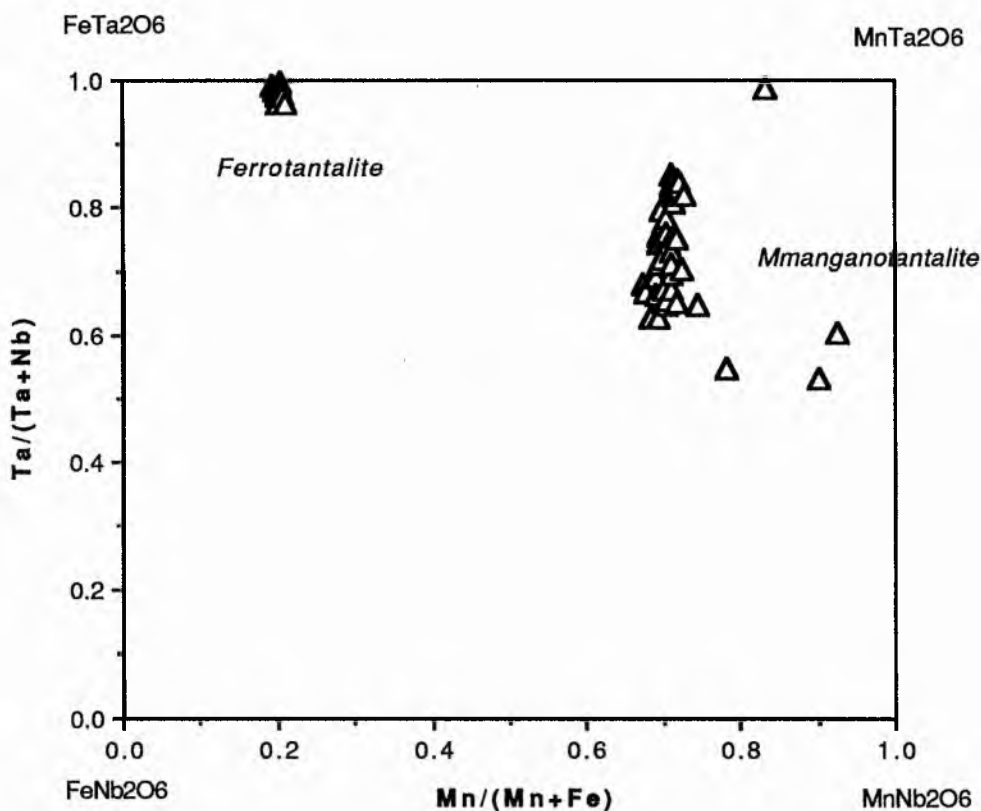


Fig.4.3. Compositions of tantalites plotted on the columbite quadrilateral from sample XX, Rubicon, Karibib. Data from Tables 4.8 to 4.11.

Detailed analyses have been completed across manganotantalite lamellae in Plate 4.4 in order to determine their chemistry. T1, T2 and T3 represent traverses across manganotantalite laths, in the directions indicated, to investigate the change in composition across the laths and to correlate the compositional changes with the differences in intensity in the back scatter images.

Analyses 1-6 (Table 4.9) represent traverse 1 (T1) shown in Plate 4.4 across a manganotantalite lath. The light area at the top of the crystal corresponds to the



Plate 4.3. Manganotantalite lamellae (red-brown) occurring in a microlite matrix (grey) with bismuth (black), apatite (white) and tantalite (tan), lower right . The darker red areas are ferrotantalite. Plane polarized light. Length of section 2.5 cm. The arrow marks the line of the traverse across the section $\times\times$.

tantalum-rich areas 75 - 76 % Ta_2O_5 . If the tantalum content is followed across the lath it may be noted that the darker areas (see Plate 4.4) correspond to Ta-poor, Nb-rich compositions (Table 4.9). The isomorphism between Ta and Nb and the change in composition across the lath is illustrated in Figure 4.4 which shows that the centre of the lath is Nb-rich and the edges of the lath - the last areas to crystallize are Ta-rich.

Traverse 2 (T2 in Plate 4.4) is represented by analyses 7-17 (Table 4.9). The observations accorded to traverse 1, apply to traverse 2. This part of the lath is interesting as the lath is comparatively broader in width with a lighter coloured area in the centre. The Ta_2O_5 value is highest again at the top edge - a very light area, (anals. 7 & 8) then decreases towards the centre (anals. 9 - 12), increases in a lighter area (anals. 13 & 14), decreases again (anal. 15) to increase again towards the edge (anals. 16 & 17, see also Fig.4.4, T2). Traverse 3, represented by analyses 18 - 22 (Table 4.9) represents on the whole, varying lighter areas, with correspondingly high amounts of Ta_2O_5 from 76 to 69%.

Analyses 23 and 24 are light areas on the edge of the same lath; they both contain 74% Ta_2O_5 . Analyses 25 and 26 represent an edge and centre of a lath with 75.7 and 68.2% Ta_2O_5 respectively; similarly analyses 31 and 32, and 35 and 34 with 74.5% (edge), 65.5% (centre), 70.8% (edge), and 65.9% (centre) Ta_2O_5 respectively and analysis 36 in a central area with 67.8% Ta_2O_5 follow the same general pattern.

The wide oblique lath on the left of Plate 4.4. contains 76 and 74% Ta_2O_5 in the edge (anals. 27 and 28) and 70 and 72% in the centre (anals. 29 and 30). Analyses 37 and 38 contain very high amounts of Ta_2O_5 : - 83.94 and 84.77% respectively, representing tantalite, a Ta-rich end member of the columbite-tantalite series and probably one of the last tantalite areas to form on the basis that Ta-rich tantalite forms last and Nb-rich columbite form

first, in the generalized sequence of the series (von Knorring and Condliffe, 1984 and Baldwin, 1989).

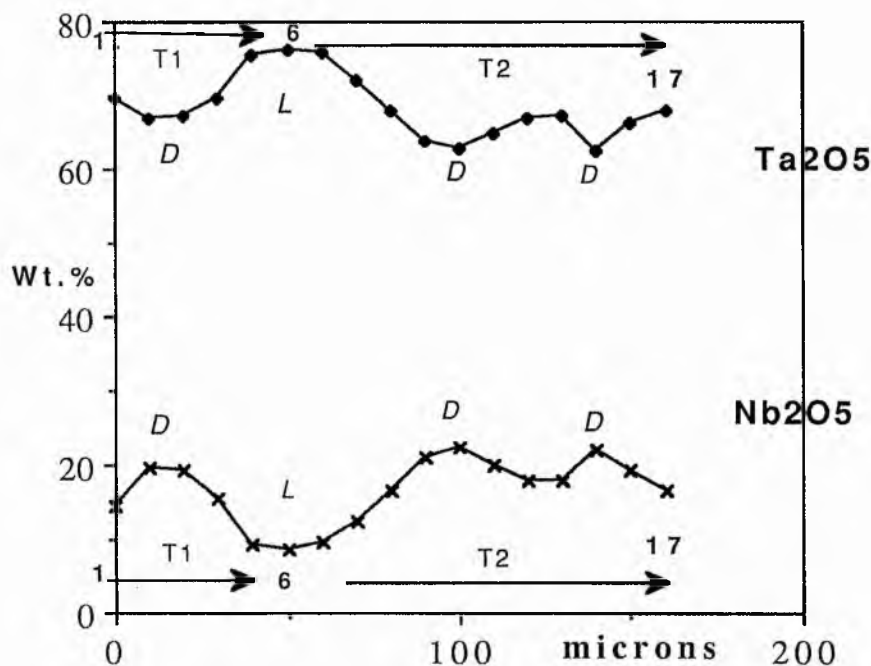


Fig. 4.4. Ta₂O₅ and Nb₂O₅ along traverse 1 (anal. 1-6) and traverse 2 (anal. 7-17) across a tantalite lath, Rubicon pegmatite, Karibib. D=dark area, L= light area on back-scattered image, Plate 4.4. Data from Table 4.9.

The conclusions reached from these observations are as follows: (i) the lighter areas in the Ta-laths contain higher amounts of tantalum, and correspondingly lower amounts of Nb. The darker areas contain lower amounts of tantalum and correspondingly higher amounts of Nb; (ii) Ta increases towards the edge of lath. The centre of the laths, the first to crystallize has the lowest Ta content; the edge of the laths, the last to crystallize has the highest Ta content.

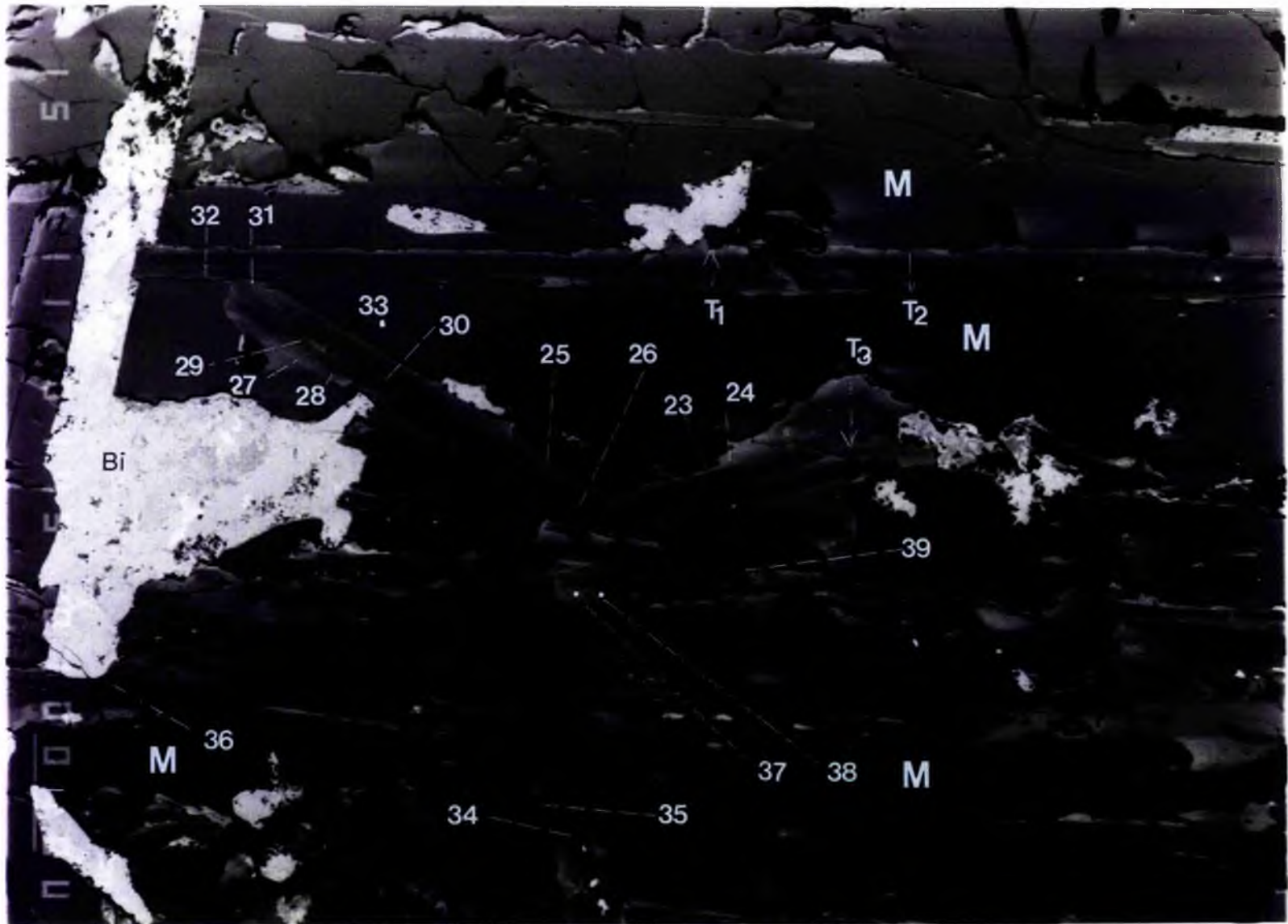


Plate 4.4. Backscattered electron image of exsolved manganotantalite lamellae in a matrix of microlite (M) with crosscutting veins of a bismuth phase, Rubicon pegmatite, Karibib, Namibia (section XX). The numbers correspond to data given in Tables 4.9, 4.10; T1, T2 and T3 correspond to point analyses along a traverse across tantalite. Scale bar: 100 microns.

TABLE 4.9 (i) Compositions of Mn-tantalite laths, Rubicon, Karibib. Sample XX
(points of analysis indicated in Plate 4.4)

Sample XX	xx/1.	xx/2.	xx/3.	xx/4.	xx/5.	xx/6.	xx/7.	xx/8.	xx/9.	xx/10.	xx/11.	xx/12.	xx/13.	xx/14.
Ta ₂ O ₅	69.783	66.740	67.377	69.784	75.348	78.073	75.796	72.088	68.021	63.898	62.653	64.748	66.874	67.189
Nb ₂ O ₅	14.548	19.771	19.163	15.474	9.151	8.517	9.540	12.398	16.628	20.887	22.373	19.874	17.859	17.917
TiO ₂	0.053	0.055	0.045	0.017	0.025	0.048	0.042	0.043	0.037	0.038	0.042	0.045	0.028	0.042
SnO ₂	0.0	0.0	0.032	0.011	0.0	0.01	0.029	0.0	0.039	0.058	0.042	0.043	0.0	0.0
FeO	4.561	4.348	4.465	4.270	4.136	4.096	4.182	4.427	4.603	4.377	4.612	4.588	4.644	4.661
MnO	10.287	8.935	9.089	10.407	12.522	10.301	10.181	10.252	10.274	10.290	10.281	10.184	10.148	10.073
CaO	0.029	0.020	0.025	0.022	0.011	0.022	0.074	0.029	0.014	0.034	0.018	0.013	0.049	0.035
Na ₂ O	0.0	0.09	0.113	0.057	0.0373	0.071	0.084	0.065	0.121	0.111	0.096	0.067	0.125	0.053
Total	99.261	99.959	100.310	100.042	99.266	99.141	99.929	99.303	99.738	99.693	100.116	99.562	99.727	99.969
no. of ions on the basis of O=6														
Ta	1.488	1.376	1.389	1.470	1.660	1.685	1.656	1.556	1.426	1.309	1.267	1.335	1.393	1.396
Nb	0.516	0.678	0.657	0.542	0.335	0.314	0.346	0.445	0.580	0.711	0.752	0.681	0.618	0.619
Ti	0.003	0.003	0.003	0.001	0.002	0.003	0.003	0.003	0.002	0.002	0.002	0.003	0.002	0.002
Sn	0.000	0.000	0.001	0.000	0.000	0.000	0.001	0.000	0.001	0.002	0.001	0.001	0.000	0.000
Fe	0.299	0.276	0.283	0.277	0.280	0.279	0.281	0.294	0.297	0.276	0.287	0.291	0.297	0.298
Mn	0.683	0.574	0.584	0.683	0.722	0.711	0.693	0.689	0.671	0.656	0.648	0.654	0.658	0.652
Ca	0.002	0.002	0.002	0.002	0.001	0.002	0.006	0.002	0.001	0.003	0.001	0.001	0.004	0.003
Na	0.000	0.013	0.017	0.009	0.011	0.011	0.013	0.010	0.018	0.016	0.014	0.010	0.019	0.008
	2.991	2.922	2.935	2.984	3.011	3.004	2.999	3.000	2.996	2.974	2.973	2.976	2.991	2.978

TABLE 4.9 (ii) . Compositions of Mn-tantalite laths, Rubicon , Karibib. Sample XX
(points of analysis indicated in Plate 4.4)

Sample XX	15.	16.	17.	18.	19.	20.	21.	22.	23.	24.	25.	26.	27.	28.
Ta ₂ O ₅	62.454	66.182	68.083	76.498	75.218	71.376	70.317	69.921	74.828	74.808	75.697	68.211	76.136	74.920
Nb ₂ O ₅	22.103	19.328	16.464	8.510	9.9175	13.629	14.637	14.424	9.823	9.722	9.071	17.853	8.669	10.006
TiO ₂	0.028	0.048	0.047	0.052	0.055	0.057	0.060	0.050	0.063	0.048	0.045	0.035	0.048	0.042
SnO ₂	0.022	0.062	0.039	0.009	0.0	0.083	0.0	0.0	0.011	0.009	0.052	0.061	0.0	0.018
FeO	4.781	4.049	4.287	4.112	4.175	4.169	4.288	4.428	3.998	4.160	4.180	3.997	4.056	4.144
MnO	10.278	9.780	10.451	10.217	10.309	9.865	10.074	10.518	10.582	10.424	10.188	9.697	10.441	10.508
CaO	0.036	0.039	0.027	0.046	0.021	0.035	0.020	0.041	0.039	0.060	0.039	0.028	0.029	0.052
Na ₂ O	0.055	0.062	0.061	0.069	0.085	0.057	0.078	0.096	0.046	0.084	0.078	0.101	0.077	0.059
Total	99.757	99.560	99.458	99.513	99.038	99.270	99.452	99.477	99.391	99.316	99.350	99.983	99.456	99.748
No. of ions on the basis O=6														
Ta	1.269	1.371	1.433	1.688	1.660	1.532	1.497	1.488	1.639	1.641	1.667	1.421	1.679	1.634
Nb	0.747	0.666	0.576	0.312	0.337	0.486	0.518	0.510	0.358	0.355	0.332	0.618	0.318	0.363
Ti	0.002	0.003	0.003	0.003	0.003	0.003	0.004	0.003	0.004	0.003	0.003	0.002	0.003	0.003
Sn	0.001	0.002	0.001	0.000	0.000	0.003	0.000	0.000	0.000	0.000	0.002	0.002	0.000	0.001
Fe	0.299	0.258	0.277	0.279	0.283	0.275	0.279	0.290	0.269	0.281	0.283	0.256	0.275	0.278
Mn	0.650	0.632	0.685	0.702	0.709	0.659	0.668	0.697	0.722	0.712	0.699	0.629	0.717	0.714
Ca	0.003	0.003	0.002	0.004	0.002	0.003	0.002	0.003	0.003	0.005	0.003	0.002	0.003	0.004
Na	0.008	0.009	0.009	0.011	0.013	0.009	0.012	0.015	0.007	0.0130.012		0.015	0.012	0.015
	2.978	2.944	2.987	3.000	3.008	2.971	2.979	3.006	3.003	3.010	3.002	2.945	3.007	3.006

Analys 1-6 across lath. Traverse 1 (T1) in Plate 4.4.

Analys 7-17 across lath. Traverse 2 (T2) in Plate 4.4.

Analys 18-22. Traverse 3 (T3) in Plate 4.4.

23,24, lath edge. 25,26, lath edge and centre. 27,28, lath edge.

TABLE 4.10. Compositions of Mn-tantalite laths and microlite, Rubicon pegmatite, Karibib, Namibia
Sample XX (points of analysis indicated in Plate 4.4)

Sample XX	29.	30.	31.	32.	33.	34.	35.	36.	37.	38.	39.
Ta ₂ O ₅	70.714	72.479	74.459	65.499	80.389	65.924	70.767	67.784	83.936	84.771	76.871
Nb ₂ O ₅	14.152	11.971	10.685	19.373	0.664	15.461	13.693	17.148	0.649	0.631	8.130
TiO ₂	0.048	0.058	0.033	0.043	0.050	0.025	0.047	0.045	0.053	0.073	0.073
SnO ₂	0.018	0.006	0.024	0.000	0.000	0.034	0.029	0.039	0.545	0.004	0.028
FeO	4.097	4.415	4.202	4.504	0.000	4.245	4.527	4.227	2.251	2.307	4.159
MnO	10.316	10.304	10.353	10.402	0.025	9.594	10.188	10.953	11.139	11.305	10.115
CaO	0.049	0.034	0.034	0.020	10.974	0.011	0.045	0.041	0.299	0.225	0.043
Na ₂ O	0.073	0.071	0.077	0.132	4.056	0.055	0.036	0.057	0.294	0.199	0.051
F	0.000	0.000	0.000	0.000	3.472	0.106	0.000	0.000	0.000	0.000	0.000
Total	99.467	99.338	99.866	99.974	99.629	95.456	99.332	100.294	99.167	99.515	99.471
-O=F					1.46	0.044					
Total	99.467	99.338	99.866	99.974	98.169	95.412	99.332	100.294	99.167	99.515	99.471
							No. of ions on the basis O=6				
Ta	1.509	1.568	1.616	1.349		1.452	1.516	1.409	1.950	1.965	1.701
Nb	0.502	0.430	0.386	0.663		0.566	0.488	0.593	0.025	0.024	0.299
Ti	0.003	0.003	0.002	0.002		0.002	0.003	0.003	0.003	0.005	0.004
Sn	0.001	0.000	0.001	0.000		0.001	0.001	0.001	0.019	0.000	0.001
Fe	0.269	0.294	0.280	0.285		0.287	0.298	0.270	0.161	0.164	0.283
Mn	0.686	0.694	0.700	0.667		0.658	0.680	0.709	0.806	0.816	0.697
Ca	0.004	0.003	0.003	0.002		0.001	0.004	0.003	0.027	0.021	0.004
Na	0.011	0.011	0.012	0.019		0.009	0.006	0.008	0.049	0.033	0.008
F						0.027					
Total	2.985	3.004	3.000	2.988		3.002	2.994	2.997	3.040	3.028	2.998
29,30,31.	Lath centre, centre and edge in Plate 4.4.(27,28, see Table 4.3.4. lath edge)										
32.	Lath centre										
33.	Microlite (ions in Chapter 5)										
34,35.	Centre and edge of lath										
36.	Lath centre										
37,38,39.	Indeterminate light areas between laths										

Microlite occupies the areas between the laths (see anal. 33); metallic bismuth or bismuth phases in general occupy the very white, highly reflective areas in Plate 4.4. Apatite forms occasionally between the laths and in association with bismuth.

The following interpretation of the order of crystallization may be suggested: (i) and (ii) microlite $\{(Ca,Na,Mn,Fe)_2(Ta,Nb)_2FO_7\}$ the matrix mineral intergrown with the tantalite laths, leaving Ca available to form (iii) apatite in the presence of P- and F-rich solutions and finally (iv) bismuth minerals are a last phase, they cut across the tantalite laths via fractures. In some circumstances apatite and bismuth minerals appear to form contemporaneously (see Plates 4.3, 4.4).

It is suggested that the apatite phase intergrown with montebrasite - at the contact with microlite and Mn-tantalite (see Plate 3.22) may be later than the laths. However, perhaps primary montebrasite may have formed contemporaneously with primary microlite.

In order to determine the relationship between aggregates of Mn-tantalite, ferrotantalite, the matrix mineral microlite, and the Mn-tantalite laths, the backscattered image of another area was examined in detail. Analytically tapiolite corresponds to ferrotantalite; however, as tapiolite is the established mineral with this composition, normally this mineral in sample XX would be referred to as tapiolite, however, as tapiolite has not been identified at Rubicon this Fe-tantalite is referred to as ferrotantalite (see section 4.3.1).

An aggregate of Mn-tantalite, a dark oblong crystal about 200/100 microns situated between a bismuth phase {Plate 4.5, white area (Bi)} is zoned. The fringe zoning, a disequilibrium growth (Table 4.11 anal. 55) contained low Ta, with 54% Ta_2O_5 , the central areas are richer, with 60.64% Ta_2O_5 (anal. 53 and Plate 4.5). This crystal is generally low in Ta in comparison with associated tantalum (see Plate 4.5 for contrasts in the backscattered images). However, the core is Ta-rich, in comparison to the pattern of

crystallization of the lamellae so the composition of the fringe zoning at the periphery indicates a change in melt composition contrary to the pattern of crystallization in the tantalite lamellae.

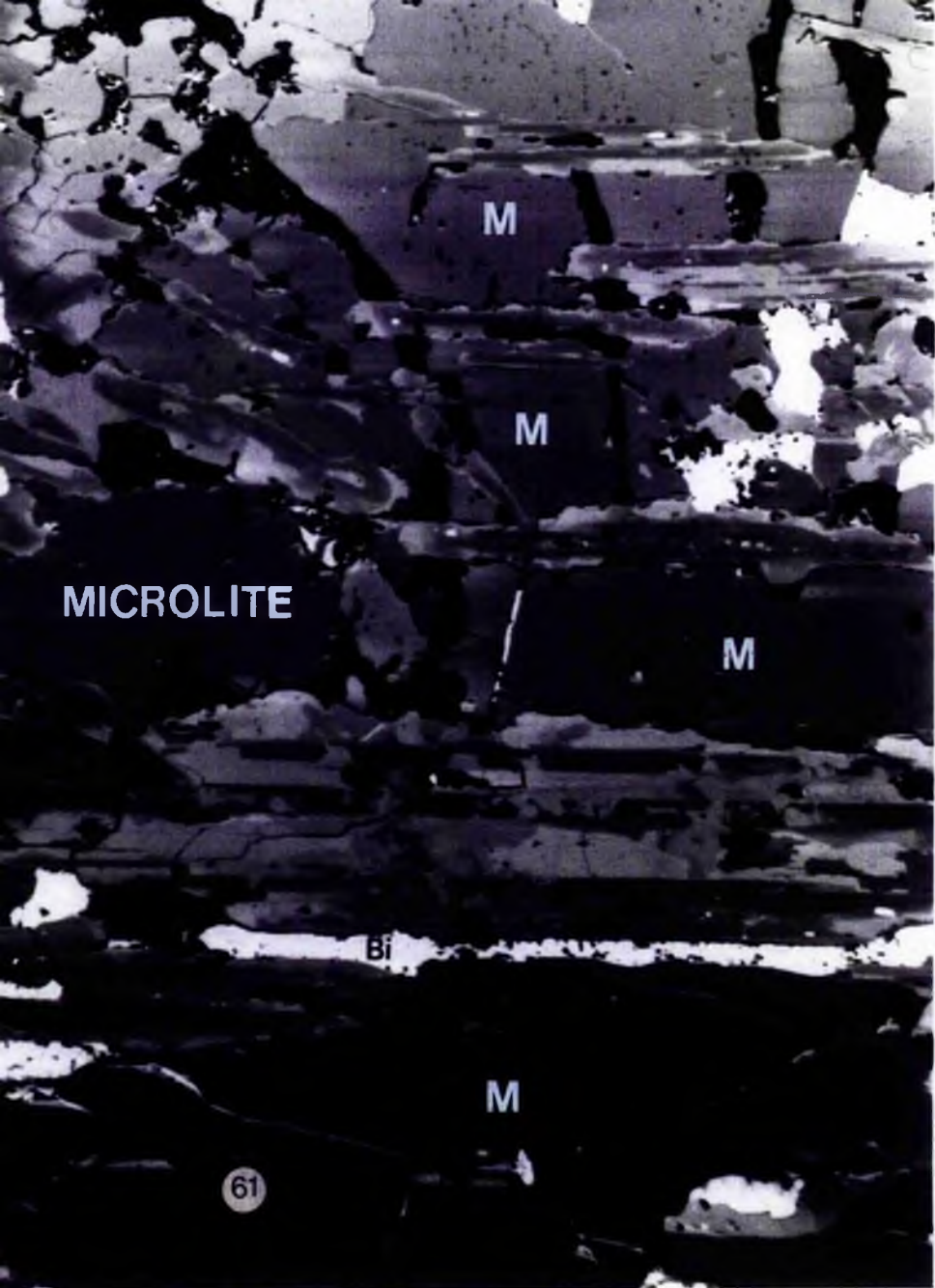
Associated aggregates of Mn-tantalite are comparatively Ta-rich with 63 and 74% Ta_2O_5 , which corresponds to dark and light areas respectively in Plate 4.5 (56 and 57). The composition of the lamellae (Table 4.11. anal. 58) correspond to previous analyses (see Plate 4.4 and Table 4.9).

A suggested order of crystallization for the minerals in section XX as determined by Plates 4.4 and 4.5 is given in Table 4.12. Ferrotantalite appears to be earlier than the manganotantalite laths because the laths cross cut the ferrotantalite. Bismuth is the last phase because it cuts across, microlite, ferrotantalite, tantalite aggregates both Ta-rich and Ta-poor, and also the Ta-laths. In thin section in plane polarized light (Plate 4.3) microlite is the matrix mineral and the tantalite laths are intergrown with the microlite. The Ta-rich tantalite corresponds to the light tan phase and the ferrotantalite to the more intense coloured phase due to high Fe rather than Mn. The exact relationship of these two phases has not been established in plane polarized light, but ferrotantalite could be contemporaneous with microlite and also the larger aggregates of tantalite. Apatite may have formed after the Ta-laths and before the bismuth phase.

Commonly microlite replaces tantalite with the addition of F-rich fluids. It is suggested that the microlite has replaced both varieties of tantalite and in a state of disequilibrium excessive Ta, Fe and Mn cations, coupled with a final lack of activity of F bearing solutions containing Ca caused the crystallization of Mn-tantalite, (along certain crystallographic axes, a majority in one specific direction) simultaneously with microlite.

Plate 4.5. Backscattered electron image of intergrown manganotantalite lamellae in microlite (M), and ferrotantalite (Fe-Ta), manganotantalite (Mn-Ta) and a crosscutting bismuth phase (Bi), Rubicon pegmatite, Karibib, Namibia (section XX). Data corresponding to point analyses given in Table 4.11. Scale bar : 100 microns.





MICROLITE

M

M

M

Bi

M

61

TABLE 4.11. Compositions of Mn-tantalite laths, ferrotantalite and microlite, Rubicon pegmatite, Karibib, Namibia (points of analysis indicated in Plate 4.5)

XX/4.5	XX53	XX54	XX55	XX56	XX57	XX58	XX59	XX60
	MnTa	MnTa	MnTa	MnTa	MnTa	Lath	FeTa	FeTa
Ta ₂ O ₅	60.637	55.798	54.336	63.942	74.072	63.784	83.098	84.486
Nb ₂ O ₅	23.765	27.749	28.586	20.363	11.460	20.175	1.874	1.326
TiO ₂	0.022	0.040	0.038	0.068	0.045	0.038	0.023	0.065
SnO ₂	0.025	0.028	0.042	0.022	0.00	0.056	0.072	0.048
FeO	1.186	3.561	1.617	4.339	4.431	4.530	11.091	11.239
MnO	14.528	12.657	14.462	10.942	10.090	10.677	2.936	2.845
CaO	0.021	0.032	0.049	0.046	0.004	0.038	0.042	0.039
Na ₂ O	0.043	0.097	0.089	0.078	0.10	0.071	0.097	0.075
Total	100.227	99.962	99.219	99.801	100.201	99.368	99.234	100.124

No. of ions on the basis O=6

Ta	1.214	1.094	1.067	1.310	1.596	1.314	1.920	1.942
Nb	0.791	0.905	0.933	0.694	0.410	0.691	0.072	0.051
Ti	0.001	0.002	0.002	0.004	0.003	0.002	0.001	0.004
Sn	0.001	0.001	0.001	0.001	0.000	0.002	0.002	0.002
Fe ²⁺	0.073	0.215	0.098	0.273	0.294	0.287	0.788	0.794
Mn	0.906	0.773	0.885	0.698	0.677	0.685	0.211	0.204
Ca	0.002	0.002	0.004	0.004	0.000	0.003	0.004	0.004
Na	0.006	0.014	0.012	0.011	0.015	0.010	0.016	0.012
Total	2.993	3.005	3.002	2.995	2.995	2.994	3.015	3.012

XX/4.5	XX61	XX62	XX63	XX64	XX65	XX66
	Mic	FeTa	FeTa	FeTa	FeTa	Mic
Ta ₂ O ₅	80.378	84.574	84.411	84.273	85.020	79.276
Nb ₂ O ₅	0.913	0.346	1.227	1.320	0.607	0.794
TiO ₂	0.038	0.032	0.048	0.032	0.030	0.037
SnO ₂	0.047	0.095	0.072	0.069	0.0	0.0
FeO	0.013	11.308	11.255	11.237	11.214	0.017
MnO	0.015	2.679	2.763	2.817	2.806	0.025
CaO	10.986	0.111	0.057	0.032	0.057	10.954
Na ₂ O	4.033	0.139	0.108	0.127	0.057	4.106
F	2.222	0.0	0.0	0.0	0.0	3.282
Total	98.645	99.284	99.943	99.907	99.791	98.490
-O=F	0.933					3.37
	97.712	99.284	99.943	99.907	99.791	95.120

No. of ions on the basis O=6 (tantalite) A₂B₂X₇(microlite)

Ta	1.958	1.971	1.945	1.941	1.970	1.946	
Nb	0.037	0.013	0.047	0.051	0.023	0.033	
Ti	2 0.003	0.003	0.002	0.002	0.000	0.002	2
Sn	0.002	0.003	0.002	0.002	0.000	0.000	
Fe ²⁺	0.001	0.811	0.797	0.796	0.799	0.001*	
Mn	0.001	0.195	0.198	0.202	0.203	0.002	
Ca	1.755 1.054	0.010	0.005	0.003	0.005	1.069	1.796
Na	0.700	0.023	0.018	0.021	0.009	1.725	
F	0.656					0.958	
Total		3.029	3.016	3.018	3.012		

Lath= Mn-tantalite; ; MnTa= manganotantalite; FeTa=ferrotantalite. Analyst: J.R.Baldwin.

TABLE 4.11a, Description of Plate 4.5
(analyses shown in Table 4.11)

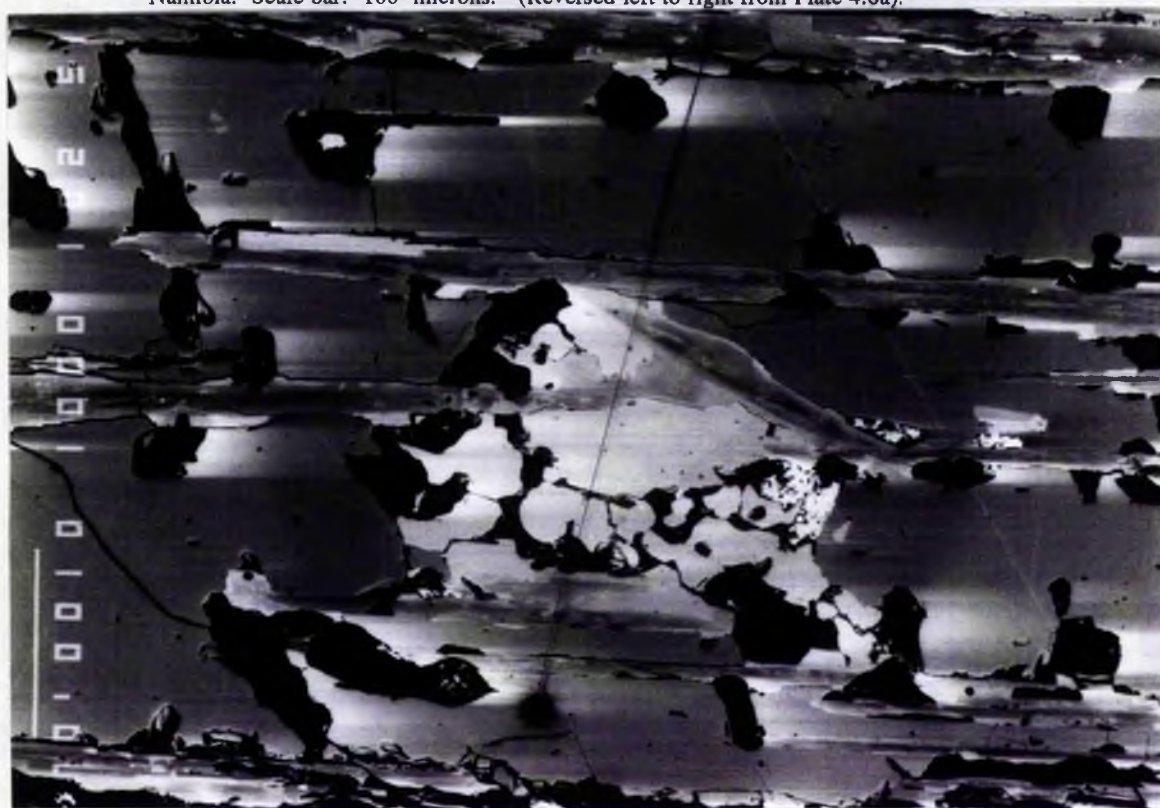
Mineral	Analysis No.	Description in Plate 4.5	Crystallization order
Zoned Mn-tantalite (Ta-poor)	53,54,55	dark bean shaped crystal with fringe zoning	1
Ferrotantalite	59,60,62-65	matrix mineral between laths (left hand side) (Fe-Ta & Ta)	2
Zoned Mn-tantalite (Ta-rich)	56,57	light area (zoned) top left hand corner	3
Microlite	61,66	matrix mineral between laths (M) (right hand side)	4a
Mn-tantalite laths	58		4b
Apatite	-	black areas associated with Bi	6
Bismuth	-	White area (Bi)	7

Finally an analytical traverse was completed across tantalite lamellae, microlite and a crystal of ferrotantalite (see Plates 4.6a, 4.6b) for the photomicrograph and backscattered image respectively. The result of the traverse (see Tables 4.12 for data -Appendix 2) is illustrated in Figure 4.5 which shows the Ta_2O_5 content across all the minerals. The traverse commenced in microlite, crosses a lamella, continues through microlite, crosses a parallel lamella into an oblique lamella encountering microlite in the apex of the two lamellae. The traverse then encounters the aggregate of ferrotantalite, which is transgressed by another parallel lath, and into the main ferrotantalite area (see Fig. 4.5 and Plate 4.6b). The traverse then crosses another parallel lath, marginal microlite, a parallel lath and finally ends in microlite. The analytical data agrees with the backscattered image and clearly verifies that the lamellae cut across ferrotantalite and are therefore a later phase than the ferrotantalite.



Plate 4.6a. Photomicrograph of manganotantalite laths in a microlite matrix; xx marks the line of an analytical traverse, shown in Plate 4.6b through a crystal of ferrotantalite, Rubicon pegmatite, Karibib, Namibia. Plane polarized light. Scale bar: 100 microns Sample XX. 

Plate 4.6b. Backscattered electron image showing the line of the analytical traverse in Plate 4.6a through tantalite lamellae, microlite and ferrotantalite (white), Rubicon pegmatite Karibib, Namibia. Scale bar: 100 microns. (Reversed left to right from Plate 4.6a).



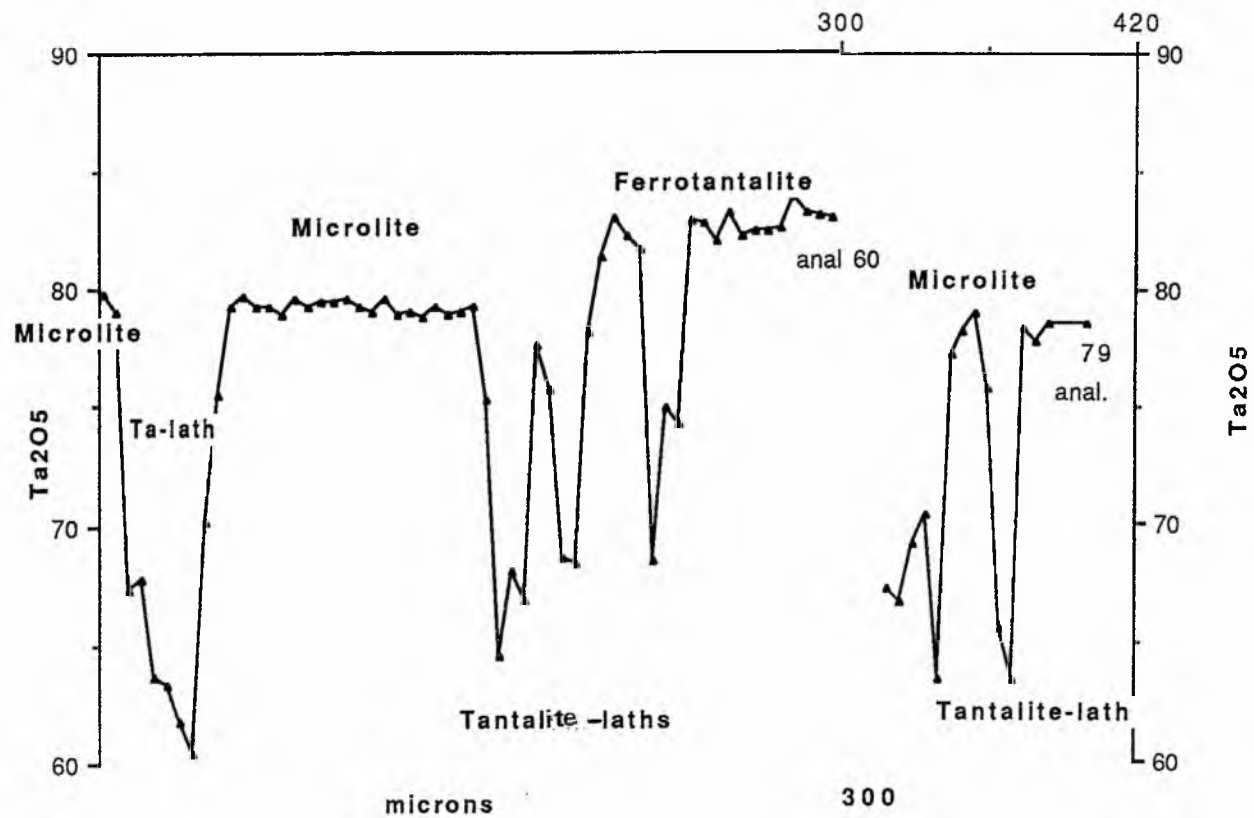


Fig 4.5. The Ta₂O₅ content of microlite minerals along an analytical traverse across microlite, manganotantalite laths (Ta-laths) and ferrotantalite (Fe-tant). The line of the traverse is shown in Plates 4.6a and 4.6b.

4.3.3. Manganotantalite, M1 pegmatite, Okatjimukuju, Karibib

Manganotantalite is intergrown with microcline and grey Li-mica, in the inner intermediate zone at the M1 pegmatite, Okatjimukuju, Karibib (see location map Fig. 2.10). There are four main sets of tantalite crystals marked in Plate 4.7 which are indicated by the letters A, B, C1 and C2, ('A' and 'B' being the 2 larger crystals and crystals 'C' the smaller concentrations). The opaque crystals of tantalite seen in Plate 4.7 in normal light optics do not appear to be zoned, crystal "B" in particular is very dark.

An analytical traverse was taken directly across crystal "A" from right to left in Plate 4.7 and the analyses 77/A1-77/A5 are shown in Table 4.13.; analyses A1 and A5 represent the rim, and analyses 77/A2-A4 the interior of crystal "A". Analyses were completed on crystal "B", core and rim (Table 4.13. anal.77/B1,B2). Similarly a core and rim analysis were taken on small crystal "C1" (anal.77/ C1,C2). The largest manganotantalite crystal "A", a zoned crystal of manganocolumbite in the core and manganotantalite in the rim, is richer in Ta than crystals "B" and "C1". This is compatible with previous results, i.e. in simultaneously crystallizing columbite and tantalite, tantalite is the last to crystallize (see this study, section 4.3.2, von Knorring and Condliffe, 1984; Cerny et al. 1985; Baldwin, 1989). Crystal "A", showed an irregular pattern of composition across the crystal (see Table 4.13) with Ta₂O₅ varying from 44.66 to 52.19% and Nb₂O₅ from 37.32 to 30.11% respectively.

From the backscattered images shown in Plates 4.8a, 4.8b and 4.9 it is apparent that crystal "A" and crystal "C1" are zoned. The zoning is not visible in normal light optics. Apart from fringe zoning (Plate 4.8a) the zoning in the crystals is symmetrical about the exterior of the crystal i.e. crystal face parallel zoning. The zoning in crystal "A" is however interrupted, on the one long edge of the crystal the zoning is non-planar which may account for the different Ta₂O₅ contents in each rim and the Ta-content varying irregularly across

the crystal (Table 4.13. anal. 77/A1-A5). It has been established previously that the light coloured zones are Ta-rich (high atomic number) and the dark zones conversely are Nb-rich (low atomic number) with isomorphic replacement between Ta and Nb in manganotantalite. This is expressed in the result of the traverse across crystal "A" (Table 4.13). It is impossible to pinpoint the light and dark zones in the limited light optics on the Camebax electron microprobe, it is possible however to take a controlled analytical traverse at set intervals across the crystal and perhaps locate the zoning from a definite fixed point composition after the analyses have been completed.

The manganotantalite is directly associated with both Li-mica and microcline and Li-mica is intergrown with tantalite and replacing K-feldspar (Plates 4.10, 4.11); the grain boundaries of both tantalite and feldspar crystals are edged with mica (Plate 4.10) and tantalite crystal "C2" has irregular grain boundaries where it is intergrown with mica (Plate 4.11).

TABLE 4.13. Mn-tantalite and Mn-columbite, Okatjimukuju M1 pegmatite, Karibib

Sample 77	77/A1	77/A2	77/A3	77/A4	77/A5	77/B1	77/B2	77/C1	77/C2
	Rim	core			Rim	core	Rim	core	Rim
Ta ₂ O ₅	44.66	52.19	44.95	50.08	52.08	39.78	43.24	41.77	42.91
Nb ₂ O ₅	37.32	30.11	37.17	32.60	30.67	41.82	38.77	40.42	38.74
TiO ₂	0.12	0.14	0.13	0.11	0.13	0.24	0.15	0.07	0.10
SnO ₂	0.10	0.11	0.13	0.05	0.11	0.10	0.09	0.03	0.06
MnO	14.17	13.54	13.51	13.50	13.57	13.89	13.61	13.74	13.73
FeO	3.03	2.96	3.65	3.01	2.96	3.59	3.73	3.69	3.79
Total	99.40	99.05	99.54	99.35	99.52	99.42	99.59	99.72	99.33
No. of ions based on O=6									
Ta	0.834	1.016	0.839	0.961	1.007	0.725	0.800	0.766	0.796
Nb	1.158	0.974	1.153	1.039	0.986	1.266	1.193	1.233	1.194
Ti	0.006	0.008	0.007	0.006	0.007	0.012	0.008	0.004	0.005
Sn	0.003	0.003	0.004	0.001	0.003	0.003	0.002	0.001	0.002
Mn	0.824	0.821	0.785	0.806	0.817	0.788	0.784	0.785	0.793
Fe ²⁺	0.174	0.177	0.210	0.178	0.176	0.201	0.212	0.208	0.210
Total	2.996	2.999	2.998	2.991	2.996	2.995	2.999	2.997	3.000

77/A1,A3,A4, B1,B2,C1,C2. Manganocolumbite

77/A2,A5. Manganotantalite. Analysts: P.J. Hill and J.R. Baldwin



Plate 4.7. Zoned mangantalite-manganocolumbite crystals (A, B, C1, C2) in K-feldspar and mica, M1 pegmatite, Okatjimukuju, Karibib, Namibia. Plane polarized light; length of section 3 cm.



Plate 4.8a. Backscattered image of lower half of zoned manganotantalite-manganocolumbite crystal 'A' shown in Plate 4.7. The line of the analytical traverse from right to left, is represented by analyses 77/1-5 (Table 4.13) M1 pegmatite, Okatjimukuju, Karibib, Namibia. Scale bar: 100 microns.

Plate 4.8b. Backscattered image of zoned crystals 'C2', shown in Plate 4.7. Scale bar: 100 microns.





Plate 4.9. Backscatter image of manganocolumbite crystal 'C1' shown in Plate 4.7 showing crystal face parallel zoning, M1 pegmatite, Karibib, Namibia. Scale bar: 100 microns. Sample 77.

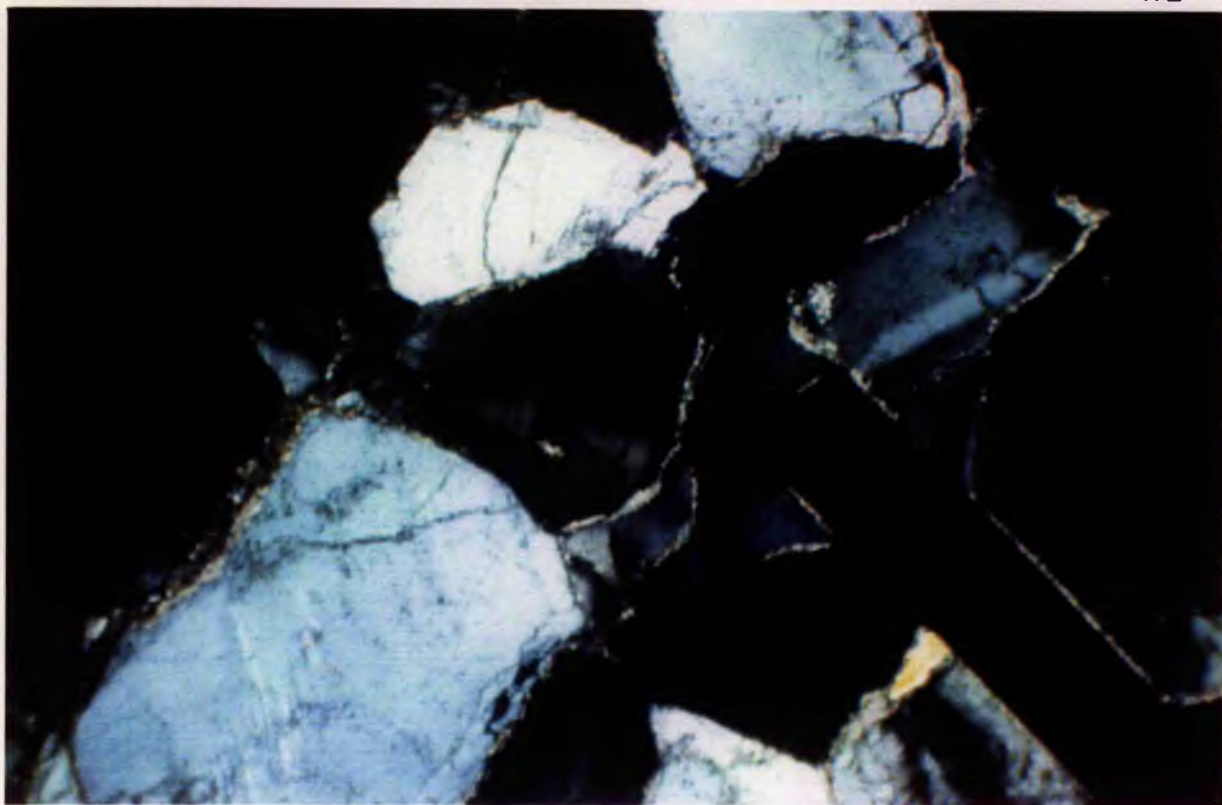
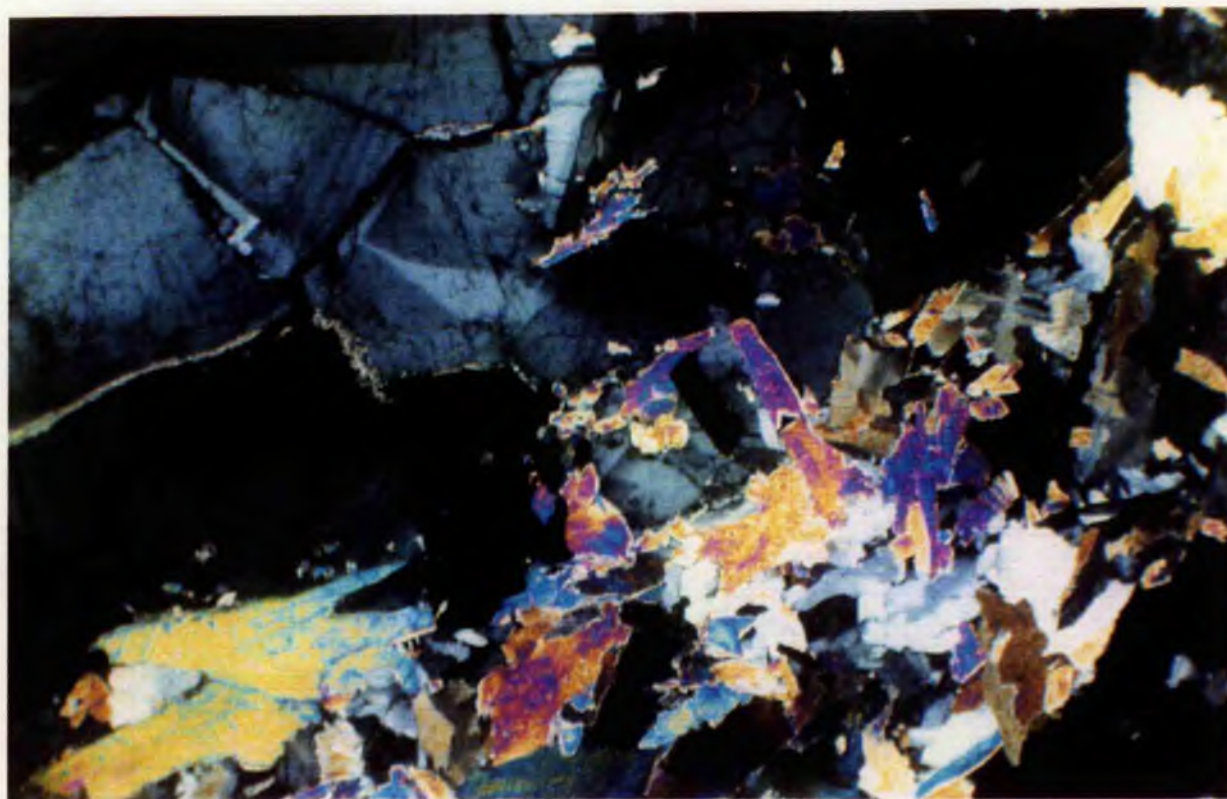


Plate 4.10. Photomicrograph of opaque euhedral manganocolumbite crystal 'B' with mica lying along the grain boundary and subhedral K-feldspar crystals rimmed with mica, M1 pegmatite, Okatjimukuju, Karibib, Namibia (sample 77). Length of crystal 'B': 3mm.

Plate 4.11. Photomicrograph of crystal 'C2' showing tantalite intergrown with mica, M1 pegmatite, Karibib, Namibia. Length of crystal: 1000 microns.



The manganocolumbite and manganotantalite from the M1 pegmatite are plotted in Figure 4.6 which shows the division between the two fields.

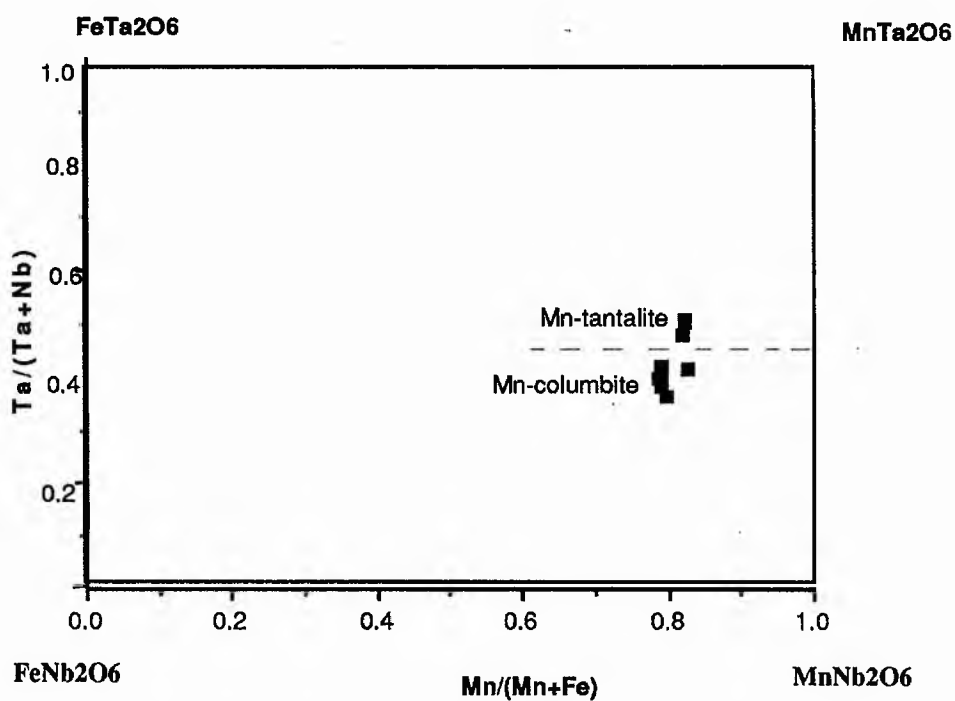


Fig. 4.6. The $Ta/(Ta+Nb)$ versus $Mn/(Mn+Fe)$ plot for manganotantalite and manganocolumbite, M1 pegmatite, Okatjimukuju pegmatite, Karibib, Namibia. (Data from Table 4.13).

4.4. WODGINITE

4.4.1. Introduction

This section documents the occurrence and chemistry of wodginite, a rare-Sn-Ta mineral from Okatjimukuju, Karibib and discusses the paragenesis of this mineral.

Structurally wodginite differs from orthorhombic columbite-tantalite and ixiolite groups by being monoclinic. The mineral was first established as an independent species by Nickel et al. (1963) on mineral species from Wodgina, Australia and Bernic Lake, Canada and was given the formula $(\text{Ta,Nb,Sn,Mn,Fe})_{16}\text{O}_{32}$, and later was investigated by von Knorring (1967) who encountered one of the first known ferroan wodginites. Ideal wodginite corresponds to the formula, $\text{MnSnTa}_2\text{O}_8$, however, von Knorring (1970), and von Knorring and Fadipe (1981) and Ercit et al. (1992) showed that wodginite can also contain major amounts of Fe^{2+} , Fe^{3+} , Ti, Nb and Li and minor to trace amounts of Sn^{2+} , Zr, Sc, W, Ca with vacancies occurring at the A (Mn) site and seem likely for the B (Sn) site.

Wodginites reported by von Knorring and Fadipe (1981) from African pegmatites have a large excess of tantalum over niobium and apart from one "ferroan" wodginite they are manganese dominant (see Table 4.14.). Molecular proportions of these wodginites from the literature have been calculated and these are given in Table 4.14. The tin content is variable but is generally high and titanium may be substantial. Minor amounts of Zr, Sc, W, Ca and trace amounts of U and Y are recorded, though Li has not been determined and in analysis 1 (Table 4.14, gravimetric) these elements have not been determined. The mineral is difficult to distinguish from the more common tantalites and especially manganotantalites. Ercit, Cerny and Hawthorne (1992) have defined new members, which are known to the wodginite group which consist of the following four solid solution hyperthetical end members i) wodginite, ideally $\text{MnSnTa}_2\text{O}_8$, ii) ferrowodginite

$\text{Fe}^{2+}\text{SnTa}_2\text{O}_8$, (iii) titanowodginite $\text{MnTiTa}_2\text{O}_5$ and iv) lithiowodginite, ideally $\text{LiTiTa}_2\text{O}_8$. The criteria for this new classification requires ferrowodginite to contain greater than 50% Fe^{2+} in the A-site (the A-site consisting of Mn^{2+} , Fe^{2+} , Li^+). Ercit et al. (1992) consider ferroan wodginite from Ankole, Uganda (von Knorring, 1969) to be only a variety of wodginite. The analysis (5) from Nyanga (see Table 4.14) has Fe reported as FeO, and does not specify an amount of Fe_2O_3 , however the A-site is oversubscribed and Mn appears to occupy more than 50% of the A site.

TABLE 4.14. Published analyses of Wodginite from Africa

	1.	2.	3.	4.	5.	6.	7.	8.	
Ta_2O_5	74.00	70.69	69.31	68.00	68.00	72.37	71.28	65.12	
Nb_2O_5	3.00	6.92	4.25	12.7	7.7	4.30	2.83	7.56	
TiO_2	tr	1.28	0.34	0.00	2.30	0.52	0.80	1.78	
SnO_2	13.00	8.25	11.89	7.1	8.6	11.09	11.25	8.24	
ZrO_2	-	-	0.29	-	-	-	-	0.27	
Sc_2O_3	-	-	0.14	-	-	-	-	0.18	
WO_3	-	0.05	-	0.3	-	-	0.41	0.92	
FeO	tr	1.71	2.53	2.8	6.7	2.68	2.44	3.56	
MnO	10.00	11.95	9.09	8.4	6.00	10.39	10.73	10.58	
CaO	-	-	0.37	-	-	-	-	0.22	
Total	100.0	100.85	98.23	99.6	99.3	101.35	99.74	98.43	
No of ions on the basis O=32									
Ta	8.880	8.100	8.311	7.795	7.795	8.430	8.467	7.513	T.
Nb	0.598	1.318	0.847	2.420	1.467	0.832	0.559	1.450	8
Ti	-	0.405	0.113	-	0.729	0.168	0.263	0.568	
Sn	2.287	1.386	2.090	1.193	1.445	1.894	1.959	1.394	
Zr	-	-	0.062	-	-	-	-	0.056	4
Sc	-	-	0.054	-	-	-	-	0.066	
W	-	0.006	-	0.033	-	-	0.046	0.101	
Fe^{2+}	-	0.602	0.938	0.987	2.362	0.960	0.891	1.263	
Mn	3.73	4.264	3.394	2.999	2.142	3.769	3.969	3.801	4
Ca	-	-	0.175	-	-	-	-	0.100	
Total	15.502	16.08	15.978	15.426	15.94	16.052	16.154	16.311	16

1. M3, Okatjimukuju, Karibib, Namibia (von Knorring et al. 1969)
2. Bikita, Zimbabwe (von Knorring and Fadipe, 1981)
3. Mtoko, Zimbabwe, U_3O_8 0.03%, Y_2O_3 0.02 (von Knorring and Fadipe, 1981)
4. Kivu, Zaire (von Knorring and Fadipe, 1981)
5. Ferroan wodginite, Nyanga, Uganda (von Knorring and Fadipe, 1981)
6. Bikita, Zimbabwe (von Knorring and Fadipe, 1981)
7. Makaha, Zimbabwe (von Knorring and Fadipe, 1981)
8. Bikita, Zimbabwe, (Y_2O_3 0.05%, U_3O_8 0.05%) (von Knorring and Fadipe, 1981)
- T. Theoretical value of wodginite.

This rather rare Ta mineral (identified by X-ray, von Knorring, 1967), is found abundantly at Okatjimukuju (M3) pegmatite in the cleavelandite - muscovite zone (see Plate 4.12) next to the quartz core, forming yellowish, brown to black, dark rimmed spheroidal crystals and aggregates up to 10 mm in size. An analysis of the yellowish clear portions (von Knorring et al. 1969) showed the mineral to contain 13.00 % SnO₂ and 10% MnO and being almost devoid of Fe (see Table 4.14. anal.1) the mineral was given the composition Mn₄(Sn,Nb)₄ Ta₈O₃₂, a tin-bearing end-member of the wodginite series.

4.4.2 Wodginite associated with manganotantalite, Okatjimukuju M3 pegmatite, Karibib

In this investigation of the wodginite from Okatjimukuju, M3 pegmatite, two separate specimens of wodginite in a matrix of cleavelandite and mica were investigated: - samples 79 (i) and 79 (ii) . Initially 3 crystals of Mn-tantalite and wodginite which occur in mica and altered cleavelandite in specimen 79 (i) were investigated with the microprobe.

TABLE 4.15. Mn-Tantalite associated with wodginite, Okatjimukuju M3; sample 79(i)

Sample 79 (i)	A/1	A/2	A/3	A/4	A/5	A/6	A/7	A/8	A/9
Ta ₂ O ₅	68.39	70.29	71.52	72.18	72.13	71.81	64.38	71.19	66.49
Nb ₂ O ₅	15.25	14.13	12.07	11.14	11.38	11.30	18.01	12.01	16.22
TiO ₂	0.21	0.12	0.10	0.17	0.16	0.13	0.43	0.13	0.20
SnO ₂	0.10	0.11	0.13	0.25	0.48	0.50	0.16	0.14	0.05
FeO	1.92	1.62	1.52	1.48	1.48	1.28	4.66	1.48	2.14
MnO	13.04	13.36	13.32	13.30	13.32	13.01	10.74	13.19	12.87
Total	98.91	99.63	98.66	98.52	98.95	98.03	98.38	98.14	97.97
No. of ions on the basis of O=6									
Ta	1.453	1.495	1.550	1.578	1.576	1.577	1.349	1.555	1.417
Nb	0.539	0.500	0.436	0.405	0.408	0.413	0.627	0.436	0.574
Ti	0.012	0.007	0.006	0.010	0.009	0.008	0.025	0.008	0.012
Sn	0.003	0.003	0.004	0.008	0.015	0.016	0.005	0.004	0.002
Fe	0.125	0.106	0.102	0.100	0.098	0.086	0.300	0.099	0.140
Mn	0.863	0.885	0.902	0.906	0.894	0.890	0.701	0.897	0.854
Total	2.995	2.996	3.000	3.007	3.000	2.890	3.007	2.999	2.999



Plate 4.12. Photomicrograph of wodginite (W) occurring in cleave landite and mica, M3 pegmatite, Okatjimukuju, Karibib, Namibia. Length of wodginite crystal : 5 mm. Sample 79(ii).

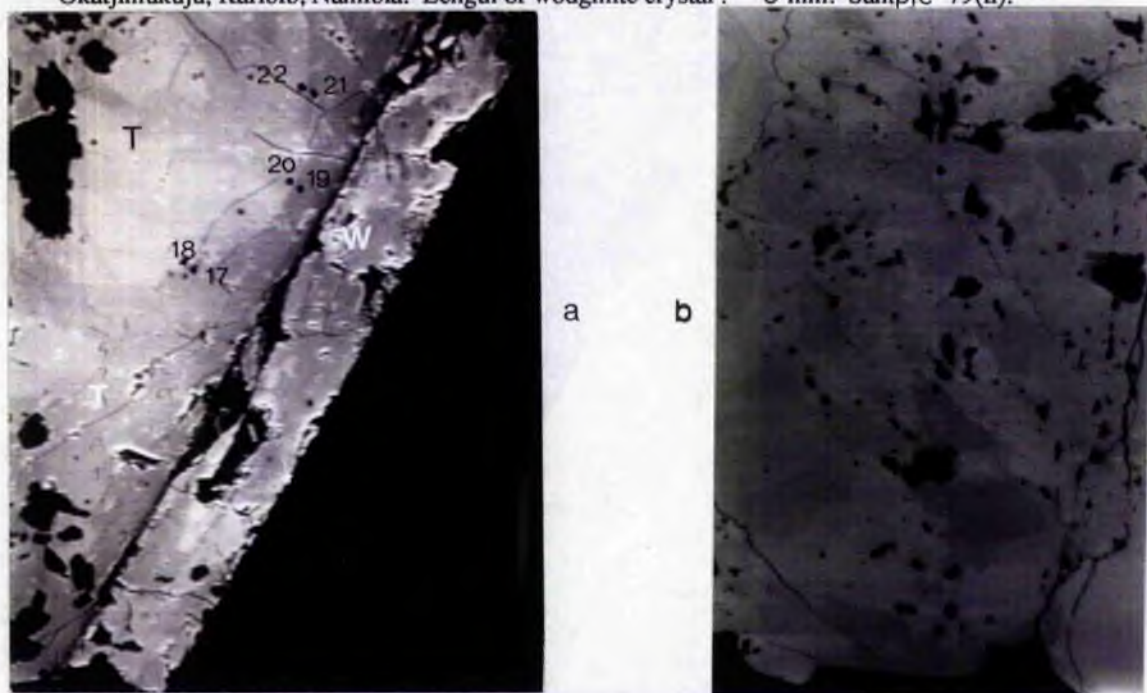


Plate 4.13a,b. Backscattered electron image of a) zoned tantalite (T) with wodginite (W) in the margin of the crystal, and b) wodginite showing patchy zoning, Okatjimukuju M3 pegmatite, Karibib, Namibia. Scale bar: 100 microns (the numbers correspond to analyses given in Table 4.17b).

Point analyses were taken on an analytical traverse across the base of fragmented crystal A which is composed of manganotantalite with a variable composition of Ta and Nb (see Table 4.15), Figure 4.7 shows a good correlation between Ta-Nb oxides in the manganotantalite. Random points were then selected which revealed the presence of zoned wodginite in this fragmented crystal (Table 4.16).

TABLE 4.16. Wodginite, Okatjimukuju M3 pegmatite, sample 79(i)

	79/1	79/2	79/3	79/4	79/5	79/6	79/7	
Ta ₂ O ₅	62.37	63.96	63.28	63.05	62.97	63.12	61.93	
Nb ₂ O ₅	6.10	5.92	6.45	7.71	7.38	6.23	7.76	
SnO ₂	16.61	16.31	16.02	13.78	13.64	16.20	13.98	
Fe ₂ O ₃	5.12	4.88	4.95	6.75	6.56	5.22	6.54	
MnO	7.60	7.72	8.00	6.54	6.65	7.76	6.41	
Total	97.8	98.79	98.70	97.83	97.20	98.53	96.62	
No. of ions on the basis of O=32								
Ta	6.82]	6.86]	6.76]	6.53]	6.58]	6.80]	6.50]	8
Nb	1.18]	1.14]	1.24]	1.47]	1.42]	1.20]	1.50]	
Ta	0.44]	0.54]	0.54]	0.72]	0.72]	0.49]	0.70]	
Sn	2.84] 4.9	2.77] 4.9	2.71] 4.8	2.32] 4.2	2.32] 5.1	2.74] 4.9	2.38]	5.2
Fe ³⁺	1.65]	1.56]	1.58]	1.15]	2.10]	1.67]	2.10]	
Mn	2.76	2.78	2.87	2.34	2.40	2.79	2.32	2.32
	15.69	15.65	15.70	14.53	15.54	15.69	15.50	

79/1-2. Crystal A (random point analysis)
 79/3-6. Crystal C (plate 4.13a, random point analysis)
 79/7. Edge, rim area (Plate 4.13a)

Crystal C was investigated in some detail. The composition of wodginite varied from 13-16% SnO₂ with corresponding values of Fe₂O₃ from 6.5-4.5% (Table 4.16): Ta₂O₅ remained almost constant at 63%, but there appeared to be an interchange of values between Nb, Sn and Ta (see Table 4.16). The wodginite in Crystal A contained 16% SnO₂. Plate 4.13a shows a backscattered image of one edge of crystal C. Wodginite is situated in the outer margin of the crystal shown and manganotantalite at the inner margin. Both wodginite and manganotantalite show compositional zoning, the lighter zone in Plate

4.13a, towards the centre of the crystal, contains a slightly higher Ta content (and lower Nb) than the darker zone, proximal to the edge, which is compatible with the high atomic number of Ta, proportional to Nb with a lower atomic number. This is illustrated in Plate 4.13a where three alternating "light" and "dark" zones have been examined: the "light" zone (Table 4.17b, anal. 79/18, 79/20, 79/22) contain approximately 1% more Ta₂O₅ than the "dark" zone (anal. 79/17, 79/19, 79/21). Similarly wodginite with a higher content of Ta₂O₅, corresponds to the lighter areas.

TABLE 4.17a Compositions of manganotantalite, M3 pegmatite, Okatjimukuju

Crystal C, sample 79(i)				
	79/8	79/9	79/10	79/11
Ta ₂ O ₅	69.43	68.40	69.38	69.42
Nb ₂ O ₅	13.97	14.65	13.56	13.18
TiO ₂	0.23	0.27	0.25	0.26
SnO ₂	0.17	0.20	0.15	0.16
FeO	1.63	1.73	1.65	1.69
MnO	13.42	13.37	13.26	13.23
Total	98.85	98.62	98.25	97.94
No. of ions on the basis of O=6				
Ta	1.487	1.461	1.497	1.506
Nb	0.497	0.520	0.486	0.475
Ti	0.014	0.016	0.015	0.016
Sn	0.005	0.006	0.005	0.005
Fe	0.107	0.114	0.110	0.113
Mn	0.895	0.889	0.891	0.894
	3.005	3.006	3.004	3.009

Analyst: P.J.Hill

Plate 4.13b. shows the backscattered image of zoned wodginite in sample 79 (ii). The zoning would account for the variable composition in wodginite. The second sample of wodginite 79(ii) is not altered; the crystals of wodginite approximately 12-30 mm in size

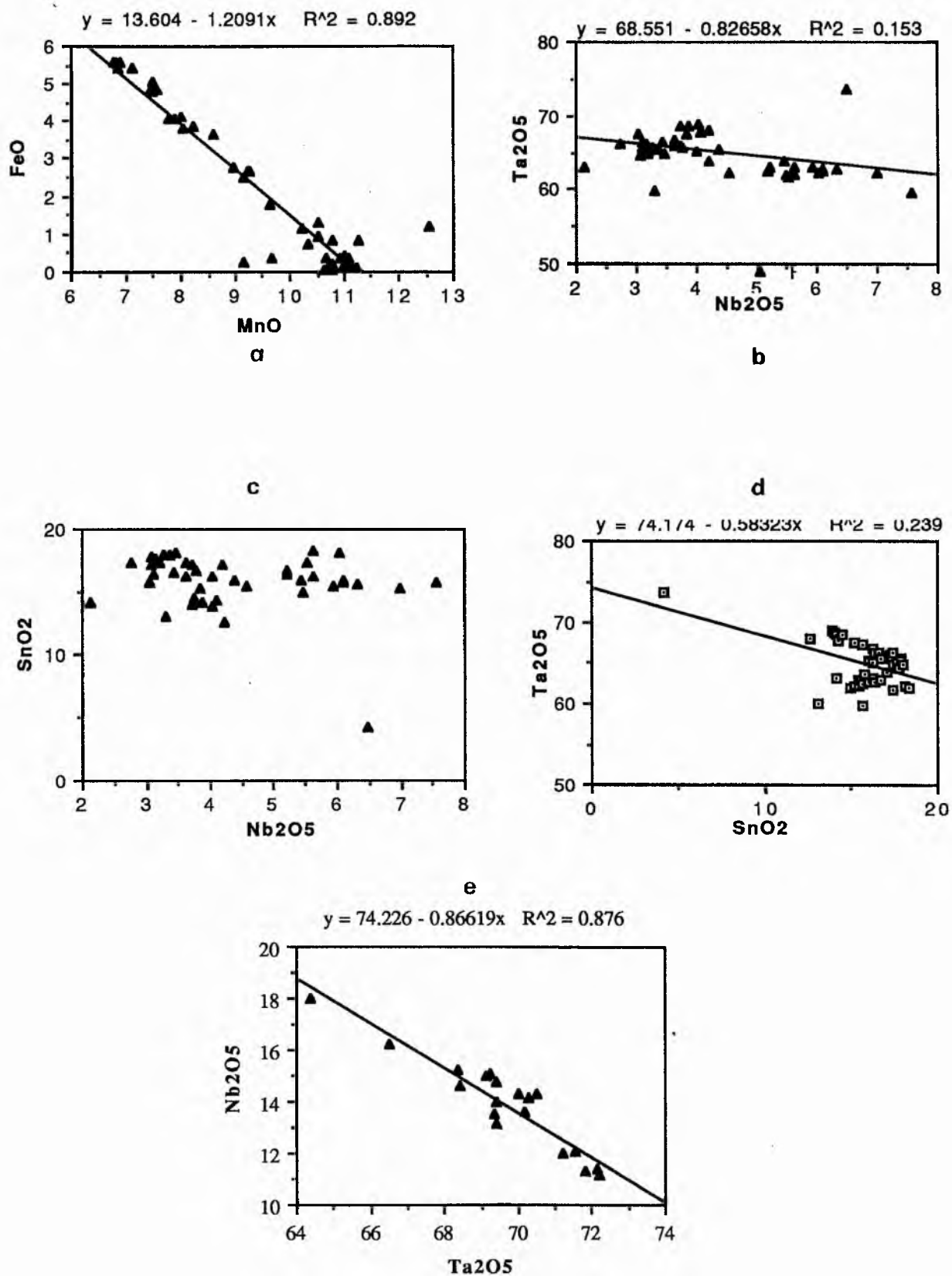


Fig.4.7. Correlations between oxides of a)Fe-Mn b)Ta-Nb c)Sn-Nb and d)Sn-Ta in wodginite and e)Nb-Ta in manganotantalite from M3 pegmatite, Okatjimukuju, Karibib.

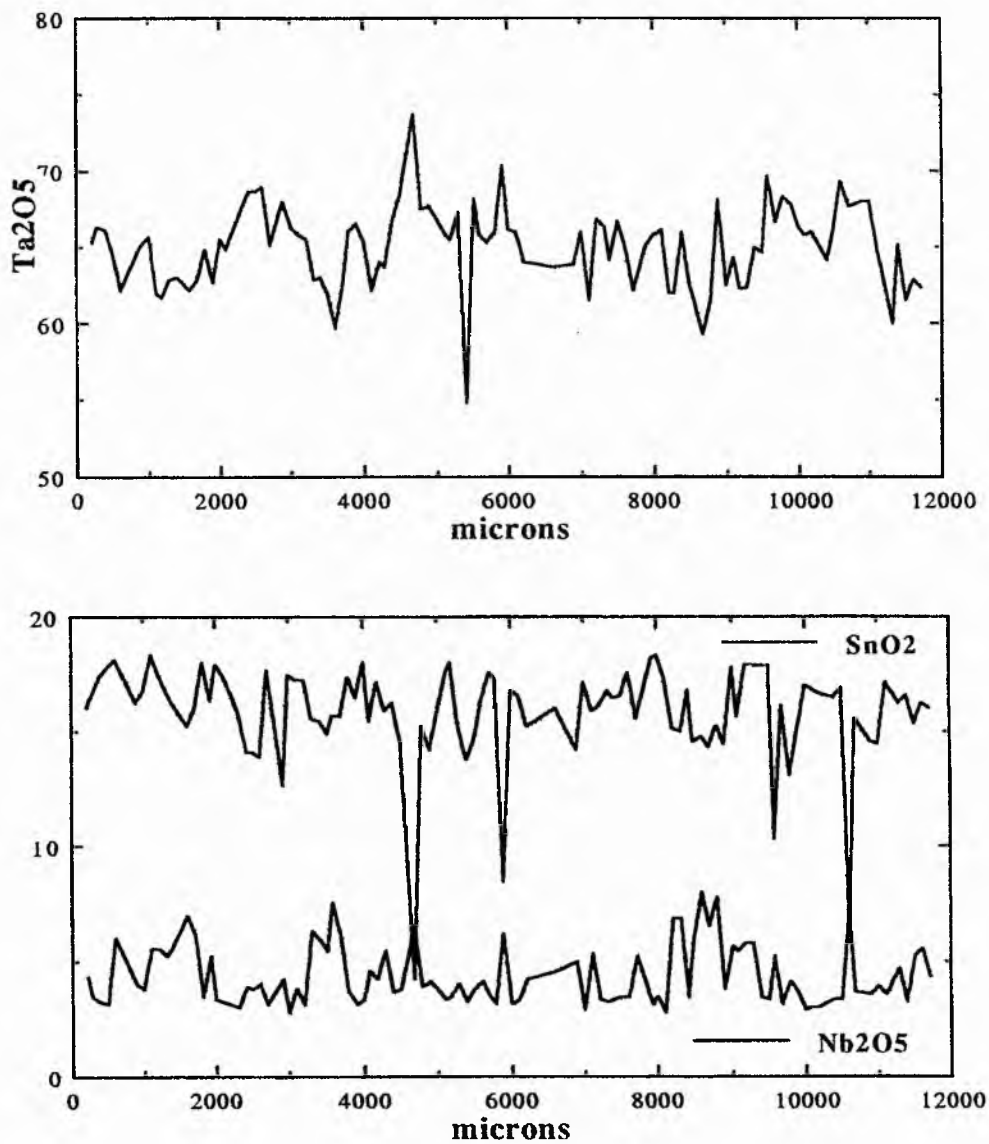


Fig. 4.8. Variation in the SnO_2 content in comparison with the contents Nb_2O_5 and Ta_2O_5 along a traverse across a crystal of wodginite, Okatjimukuju pegmatite, Karibib, Namibia. Sample 79 (ii)

TABLE 4.17b. Manganotantalite

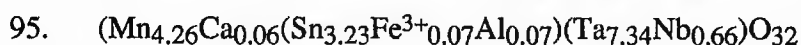
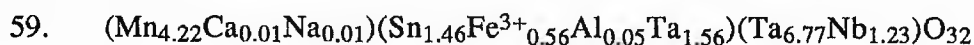
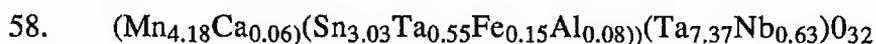
Crystal C, sample 79(i)				Light areas		
Dark areas (back-scatter image,Plate 4.13a)						
	79/17	79/19	79/21	79/18	79/20	79/22
Ta ₂ O ₅	69.24	69.40	69.11	70.48	70.03	70.18
Nb ₂ O ₅	15.09	14.75	14.99	14.31	14.33	13.60
TiO ₂	0.18	0.25	0.22	0.25	0.25	0.24
SnO ₂	0.17	0.11	0.14	0.22	0.17	0.16
WO ₃	0.00	0.08	0.10	0.07	0.12	0.07
FeO	1.80	1.78	1.74	1.77	1.64	1.68
MnO	13.44	13.47	13.56	13.46	13.47	13.56
Total	99.92	99.84	99.86	100.56	100.01	99.49
No. of ions on the basis O=6						
Ta	1.459	1.465	1.457	1.482	1.480	1.496
Nb	0.529	0.518	0.525	0.500	0.503	0.482
Ti	0.010	0.015	0.013	0.014	0.015	0.014
Sn	0.005	0.003	0.004	0.007	0.005	0.005
W	0.000	0.002	0.002	0.001	0.002	0.001
Fe	0.117	0.116	0.113	0.115	0.107	0.110
Mn	0.882	0.886	0.890	0.882	0.887	0.900
Total	3.002	3.002	3.004	3.001	2.999	3.008

occur in cleavelandite and Li-mica (see Plate 4.12) in the replacement zone of the M3 pegmatite. An automatic traverse was completed at 100 micron intervals across a crystal of approximately 12 mm (107 analyses), owing to the rarity of these minerals to establish possible relationships with other Ta-minerals. However, with this particular crystal, zoning is apparent but no intergrowth with other Ta-minerals was observed. The data have been used to show negative and positive correlations in wt. % oxides, and correlation coefficients, between the different elements. Consistent with columbite-tantalite and tapiolite, Ta-Nb shows a negative correlation, along with Fe-Mn (Fig.4.7a), with Mn and Ta giving a positive correlation (see Fig. 4.7). The correlation coefficient between MnO and FeO (calculating all the Fe as FeO) is high (0.89) however, between Ta₂O₅ and Nb₂O₅ the correlation is low (0.153, Fig.4.7b) in comparison with Mn-tantalite (0.876). However, Sn-substitution for Nb or Ta may account for part of the low correlation.

SnO_2 and Ta_2O_5 give a negative correlation (correlation coefficient: 0.239), however, there is low correlation between Sn and Nb. However, along the traverse of wodginite in sample 79 (ii) SnO_2 varies from 4-18%, Ta_2O_5 from 55-75% and Nb_2O_5 from 3-8% (see Fig. 4.8). Selected examples with the maximum and minimum SnO_2 contents are given in Table 4.19; a comparison between analyses 58 and 59 show Sn^{4+} substitution for both Ta^{5+} and Nb^{5+} or vice versa. An excess + charge at the B-site with Sn^{4+} substitution for Ta^{5+} is balanced by incorporating vacancies at the B-site into the A-site and possibly the C-site.

In general, the wodginite composition is close to the ideal formula $\text{MnSnTa}_2\text{O}_8$. Analysis 95 with 18.37% SnO_2 is among the most Sn-rich compositions found in wodginites. Cerny et al. (1985) quote 2 analyses with 18.3 and 19.2% from the Peerless pegmatite South Dakota. Site assignments were made according to Cerny et al. (1985). Mn^{2+} was assigned to the A-site, all Nb and Ta = (8-Nb) to the B-site and Ti, Sn and excess Ta from the B-site were assigned to the C-site. $\text{Fe}^{2+} : \text{Fe}^{3+}$ were calculated from the total iron of the analysis assuming that Fe^{2+} is assigned to the A-site and Fe^{3+} to the C-site. Minor amounts of Al were assigned to the C-site and Ca and Na to the A-site. Von Knorring (1969) reported ferroan wodginite from Nyanga, Uganda by wet chemical methods and determined the iron as 6.7% FeO (Table 4.19 anal.ovk2). (Where the A-site is over subscribed, the remaining vacancies were assumed to be located at the C-site).

Following this procedure the analysed wodginites in Table 4.19 (selected from Appendix Table 4.18) are given the following formulae: -



These formulae compare favourably with the formulae for wodginite from von Knorring et al. (1981) and Cerny et al. (1985) which have been recalculated in Table 4.19 this study.

The Ta/(Ta+Nb) versus Mn/(Mn+Fe) ratios for wodginite have been plotted in Figure 4.9a which shows the range in composition of wodginites (data from Tables this study). Figure 4.9b shows the wodginite data from African pegmatites in general in comparison with the data from M3 this study. The data from this study will cover the range of wodginite data given in Table 4.7.

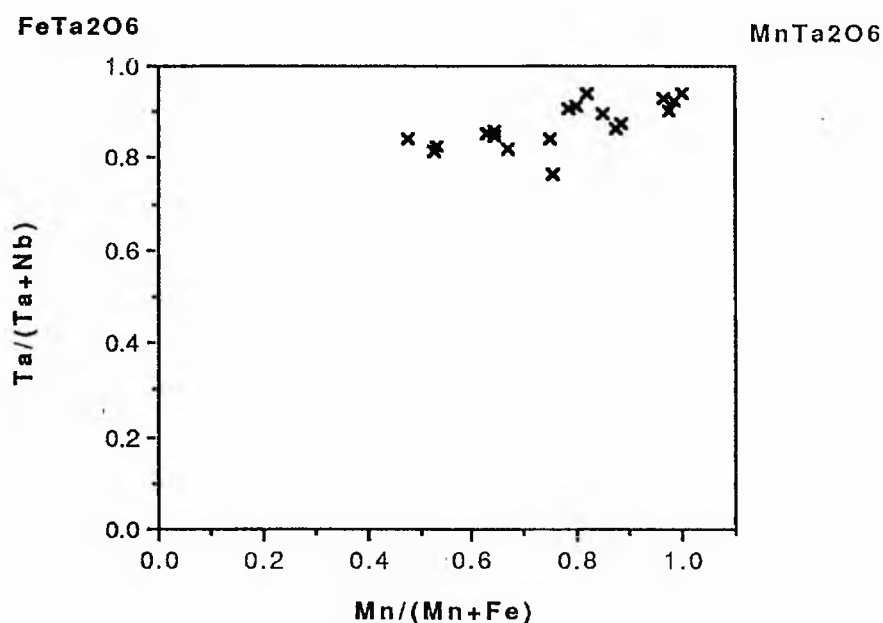


Fig. 4.9a. The Ta/(Ta+Nb) versus Mn/(Mn+Fe) (atomic) plot for wodginite, M3 pegmatite, Okatjimukuju, Karibib and east Africa. Data from Tables 4.14, 4.16, 4.19.

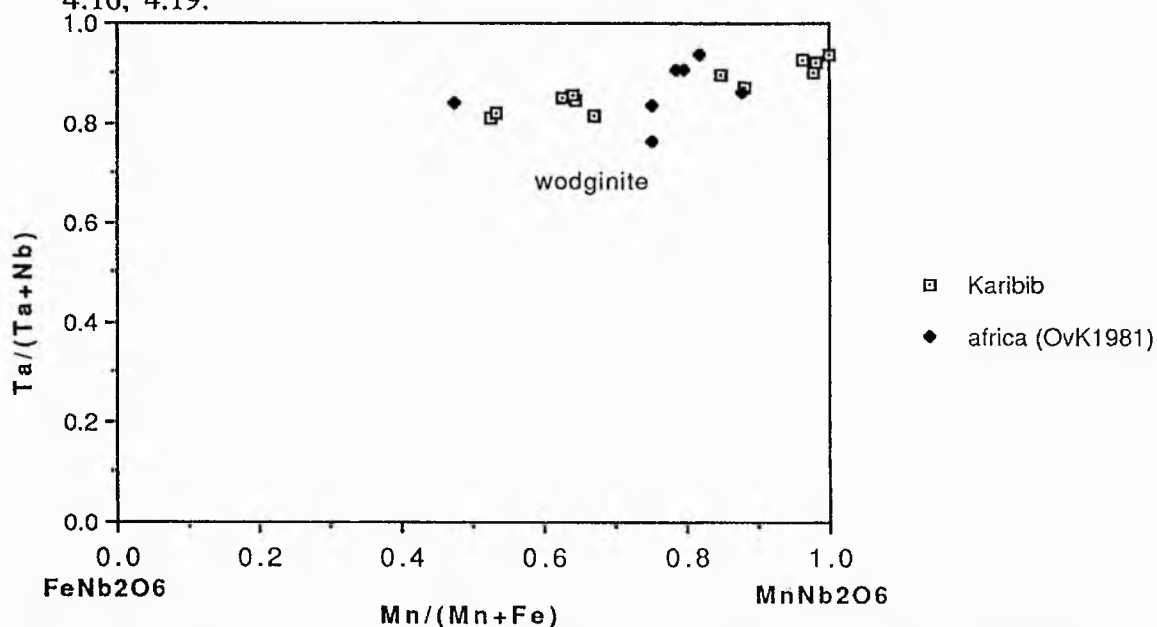


Fig. 4.9b. The wodginite data from this study (M3 pegmatite, Okatjimukuju) plotted with the data from von Knorring and Fadipi, 1981.

TABLE 4.19. Compositions of wodginite from Okatjimukuju, Karibib

79(ii)	58.	59.	95.	Ovk1.	PC	ovk2(i)	ovk2(ii)
Ta ₂ O ₅	66.03	70.31	64.74	74.00	64.9	67.66	
Nb ₂ O ₅	3.14	6.24	3.30	3.00	4.2	4.76	
TiO ₂	0.00	0.00	0.00	0.00	0.2	0.00	
SnO ₂	17.24	8.41	8.37	13.00	19.2	15.52	
Al ₂ O ₃	0.16	0.09	0.14	0.00			
Fe ₂ O ₃	0.46	1.72	0.22	tr	0.3		0.89
FeO						1.78	1.20
CaO	0.13	0.10	0.12				
MnO	11.19	11.45	11.14	10.00	10.9	9.95	
Na ₂ O	0.00	0.01	0.00	0.00			
Total	98.35	98.33	98.30	100.00	99.5	99.68	

No of ions based on 32 (O)

79(ii)	58.	59.	95.	Ovk1	PC	Ovk2	Ovk3
Ta	7.917	8.330	7.754	8.880	7.629	7.994	7.96
Nb	0.626	1.229	0.657	0.598	0.821	0.935	0.93
							B-site
Ti	0.000	0.000	0.000		0.065	0.00	0.00
Sn	3.030	1.460	3.225	2.287	3.308	2.688	2.68
Al	0.083	0.047	0.073				
Fe ^{III}	0.153	0.563	0.073		0.098		0.29
							C-site
Fe ^{II}						0.650	0.36
Ca	0.061	0.049	0.057				
Mn	4.178	4.223	4.256	3.737	3.990	3.661	3.64
Na	0.000	0.007	0.00				
							A-site
Total	16.048	15.908	16.095	15.502	15.917		

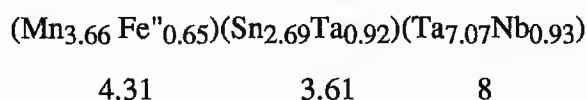
58,59,95. Points on automatic traverse across crystal (Edinburgh microprobe, this study)
 Ovk1. Von Knorring and Fadipe (1981), Okatjimukuju, Karibib
 PC. Cerny, Roberts, Ercit and Chapman (1985)
 Ovk2(i) Von Knorring (1970) Fe determined as FeO. Analyst: J.R. Baldwin (gravimetric).
 Ovk2 (ii) Ovk3 recalculated with Fe^{II} and Fe^{III} Okatjimukuju, Karibib

* Ercit et al. (1992) have reversed the B- and C-sites nomenclature

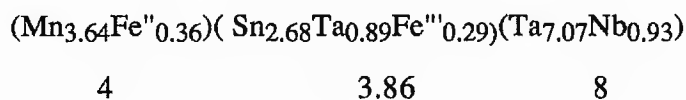
(see Table 4.16 for ionic distribution)

4.4.3 Discussion - geochemical considerations

Heating experiments by Gouder de Beauregard et al. (1967) suggest that wodginites and at least some ixiolites originate under fO_2 conditions distinctly higher than those characteristic for the stability of columbite-tantalite and tapiolite. They converted natural columbite into wodginite through heating in air and concluded that the transformation of orthorhombic columbite into monoclinic wodginite is due to the oxidation of iron; and therefore Fe_2O_3 is present in wodginite. The wodginite from Okatjimukuju has been originally analysed by gravimetric methods and Fe was determined as FeO 1.79% (see Table 4.19, ovk2). The formula for this analysis may be written as:



The A-site is oversubscribed and the analysis has been recalculated with Fe_2O_3 as 0.89% and FeO as 1.0% which is more consistent with the formula as follows : although the C-site is low:



Although the above formula is in support of the presence of both Fe^{2+} and Fe^{3+} in wodginite, there is a possibility, in sample preparation for gravimetric analysis, of contamination with tantalite even though the samples were handpicked for purity under the stereobinocular microscope. Tantalite could account for the Fe^{2+} and perhaps a lower Sn^{4+} content in the analysis. For example manganotantalite (sample 79{i}) is edged with wodginite, however, conversely a systematic electron probe traverse across sample 79 (ii) did not reveal the presence of any other tantalite mineral in addition to wodginite. The presence of Fe^{2+} and Fe^{3+} is in agreement with Cerny and Ercit (1989) who point out that

structural refinement has led to the definition of the three cation sites $A_4C_4B_8O_{32}$ with Fe^{2+} in the A-site and Fe^{3+} in the C-site.

Ercit et al. (1992b) have defined a procedure for the calculation of formulae of electron microprobe data, which permits calculation of Li-contents and the $Fe^{2+}:Fe^{3+}$ ratio. They point out that most wodginite-group minerals are very fine-grained and it is doubtful that adequate $Fe^{2+}:Fe^{3+}$ and Li determinations could be made with great accuracy. However, the wodginite 79(ii) sample, in this study, along which an analytical traverse was completed, appears quite homogeneous with only one point in 43 analyses with 4% SnO_2 and 73.7% Ta_2O_5 which may differ considerably from the bulk of the data (see Fig. 4.9, and Appendix Table 4.18). This sample will be investigated further.

Wodginite is considered to be a primary mineral and rarely undergoes replacement by later Ta-bearing phases such as manganotantalite and microlite (Cerny, 1989). However, wodginite from the Peerless pegmatite South Dakota is associated with cassiterite containing exsolved tantalite, tapiolite and microlite (Cerny et al. 1985). The wodginite from Okatjimukuju, this study, is associated with manganotantalite and further investigation of the relationship with manganotantalite in the sample from Okatjimukuju should be undertaken. Wodginite may be considered late in the fractionation sequence of Nb-Ta phases; it occurs at the edges of manganotantalite in Plate 4.13b. This is in agreement with the work of Gouder de Beauregard et al, (1967) and Cerny et al., (1985) who found similar ratios in their investigation. In this study manganotantalite fractionation progresses from 0.711 to 0.796 in $Ta/(Ta+Nb)$ and from 0.54 to 0.84 in $Mn/(Mn+Fe)$. In wodginite, fractionation progresses from 0.828 to 0.937 in $Ta/(Ta+Nb)$ and from 0.525 to 1 in $Mn/(Mn+Fe)$ in the sample without Fe (von Knorring, 1967) through the crystallization sequence manganotantalite -----> wodginite. The sample without Fe with the highest Ta content is the most highly fractionated sample. The manganotantalite sample 79(i) has probably crystallized wodginite at the periphery of crystal C (Fig 4.13a).

The precipitation of wodginite in late cleavelandite zones at Okatjimukuju suggests an oversaturation of tin. The yellowish muscovite associated with cleavelandite is fine-grained and altered and small cavities are filled with quartz crystals and montmorillonite. The altered nature of the muscovite and the numerous cavities suggest penetration by late fluids containing Sn which seem responsible for the late formation of wodginite, a Sn-bearing tantalite, rather than and in addition to manganotantalite: the two minerals have closely related structures, the unit cell of wodginite is $4/3$ times that of columbite-tantalite (Sturdivant, 1930).

4.5

TAPIOLITE

The aim of this section is to describe occurrences of tapiolite in the Karibib lithium pegmatites of Namibia with a comparison from pegmatite carrying tapiolite from Warmbad, Namibia which does not contain lithium; and to describe the paragenesis of the mineral with reference to the tapiolite-tantalite gap.

The tetragonal mineral tapiolite has a tri-rutile structure and is a comparatively rare Ta mineral. In colour it is pure black, sometimes superficially brownish-black. In transmitted light, it is light yellowish to reddish brown and very strongly pleochroic. As this mineral is generally found in pegmatites poor in lithium (von Knorring and Fadipe, 1981) tapiolite does not generally occur in the Li-rich pegmatites being studied and only a few occurrences in the Karibib area contain this mineral (von Knorring, 1985b). A tapiolite from a non-lithium pegmatite, Farm Schonau, Warmbad (see locality map 2.3) which has replacement of microlite has been included for these two reasons.

Tapiolite $(\text{Fe,Mn})(\text{Ta,Nb})_2\text{O}_6$ is essentially an oxide or tantalate of iron and tantalum, with Mn and Nb substituting for Fe and Ta respectively. It occurs in late albite or quartz muscovite replacement zones. It may be closely associated with columbite-tantalite, ixiolite, wodginite and is commonly altered to a secondary microlite, which may completely envelop the mineral (von Knorring, 1985b). However tapiolite may occur alone. In contrast to microlite, tapiolite contains few trace elements; the Ta and Fe contents are generally high and Nb and Mn generally low.

Tapiolite has been recovered from 3 localities in the Karibib area, Mon Repos, Navashab 55, E tiro 1 pegmatite E tiro 50 (see location map 2.9) and from Farm Schonau, near Warmbad, in the south of Namibia. Tapiolite may be frequently seen in varying stages of replacement by radioactive fibrous microlite for example at the Farm Schonau

pegmatite; the alteration proceeds along the margins and continues along fractures until most of the mineral is replaced (see Plate 4.14).

TABLE 4.21. Compositions of tapiolite in pegmatites from Namibia

Sample	FS	Etiro	MR	Mic
Ta ₂ O ₅	72.50	83.05	82.205 ±0.36	67.55
Nb ₂ O ₅	8.32	3.13	3.54 ±0.12	6.86
TiO ₂	1.78	0.16	0.20 ±0.02	1.84
SnO ₂	0.01	-	-	
ZnO ₂	-	-	0.03	
WO ₃	-	-	0.02	
FeO	14.01	11.54	12.09 ±0.25	0.93
MnO	0.01	2.48	1.87	0.31
CaO	0.01	-	-	17.15
Na ₂ O	0.04	-	-	0.78
UO ₂	-	-	0.00	pr
Total	96.67	100.36	98.92	95.42

No. of ions based on O=6

Ta	1.632	1.883	1.869
Nb	0.303	0.118	0.131
Ti	0.108	0.01	0.013
Sn	0.0003	0.00	0.00
Zr	-	-	0.002
W	-	-	0.004
Fe	0.944	0.804	0.844
Mn	0.001	0.175	0.132
Ca	-	-	0.000
Na	0.006	-	-
Total	2.9893	2.990	2.985

FS. Farm Schonau, west of Warmbad, Namibia (Analyst. J.R. Baldwin. Average 9 analyses).

Etiro Etiro 50, Karibib, Namibia (von Knorring, 1985).

MR. Mon Repos, Navashab 58, Karibib, Namibia (analyst. R.Davies and J.R. Baldwin).
(Y,La,Al: 0) (Johannesburg microprobe).

Mic Microlite, Farm Schonau, Warmbad, Namibia (H₂O & U present).

A traverse was completed across the crystal of tapiolite from Farm Schonau as indicated in Plate 4.14. The crystal appeared to be varying in composition from 71- 72.5% Ta₂O₅. (see Table 4.22). The pegmatite at Farm Schonau is not Li-rich. The Karibib tapiolites, with high tantalum are compatible with the high concentrations of tantalum in Ta-minerals in the Karibib-Usakos area.

The tapiolite from Mon Repos appears to be unzoned, the crystals are anhedral and black in colour, they were recovered from the eluvium. An analytical traverse was completed across the Mon Repos tapiolite of 10mm to observe the variation in composition. The crystal appeared very uniform in composition with an average of 82.4% Ta₂O₅ and a standard deviation of 0.36 (see Table 4.21). The mineral does not contain any trace elements.

The compositional difference between tetragonal ferrotapiolite FeTa₂O₆ and orthorhombic tantalite was recognized by Ford (1930). Cerny et al. (1989) have established a nomenclature for tapiolite, ferrotapiolite and manganotapiolite dependent on the amount of Fe and Mn present in the A-site. The existence of the tapiolite-tantalite gap was discovered rather later and has only been emphasized since the recent compilations of data by Zelt (1975), Sahama (1980), von Knorring and Fadipe (1981), Cerny and Ercit (1985) and Cerny et al. (1992). Cerny et al. (1989) have produced diagrams from the literature to demonstrate this gap (see Fig. 4.10a). Experiments from intergrown tapiolite and tantalite specimens from various localities have widened the boundaries of the original two phase field and compositions which cross the gap are considered to be metastable and likely to unmix under suitable conditions (Cerny et al., 1992). Boundaries of the two phase field are controlled by temperature, oxygen fugacity, increasing $f(\text{O}_2)$ which favours the orthorhombic mineral tantalite, structural state, impurities disturbing the stoichiometry and possibly pressure (Cerny et al. 1992).

Microlite (Table 4.21) is a late mineral in the crystallization sequence, after depletion of Fe and Mn, minerals containing Ca may form by Ca metasomatism (Fig.3.7). In the crystallization sequence at farm Schonau microlite has replaced tapiolite along the margins of the two minerals. The paragenesis of the tapiolite from the Etiro pegmatite is also not known; the pegmatite is lithium-rich in contrast to the Farm Schonau pegmatite. In the Karibib area, tapiolite is very rare and there are only three known occurrences of the

the mineral. Tapiolite has not been recovered from Tantalite Valley, Namaqualand (Steinkopf) or the Kenhardt area, South Africa.

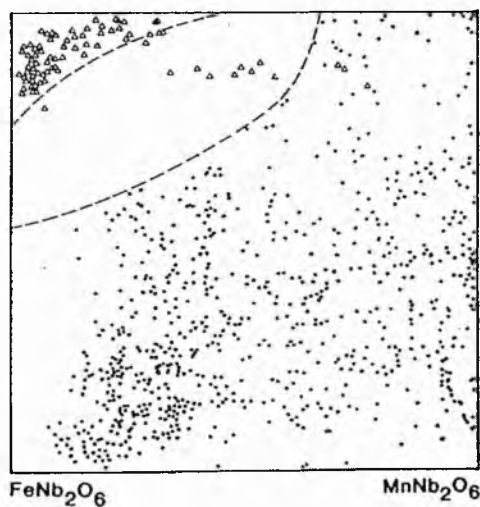


Fig. 4.10a. The columbite quadrilateral which demonstrates the tantalite-tapiolite gap (from Cerny et al. 1989).

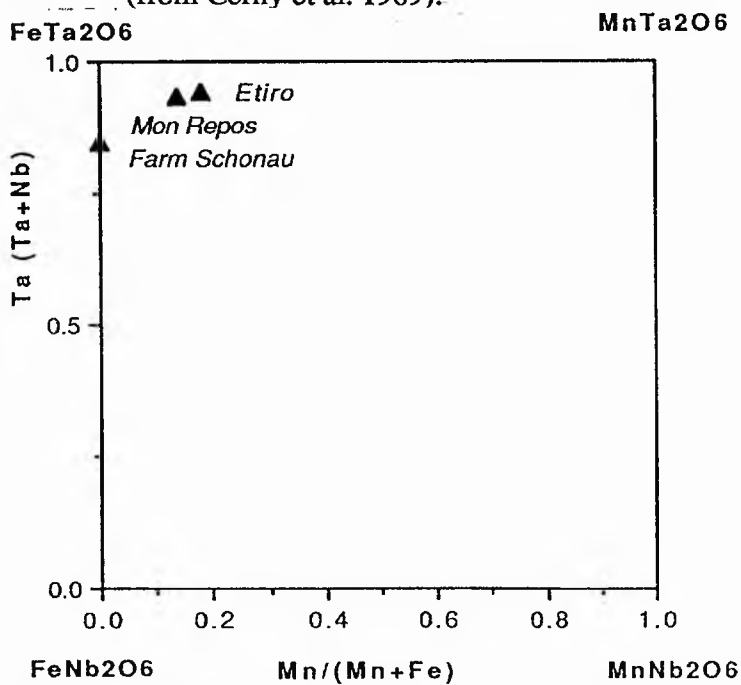


Fig. 4.10b. Tapiolite compositions from Namibia plotted on the same axes.

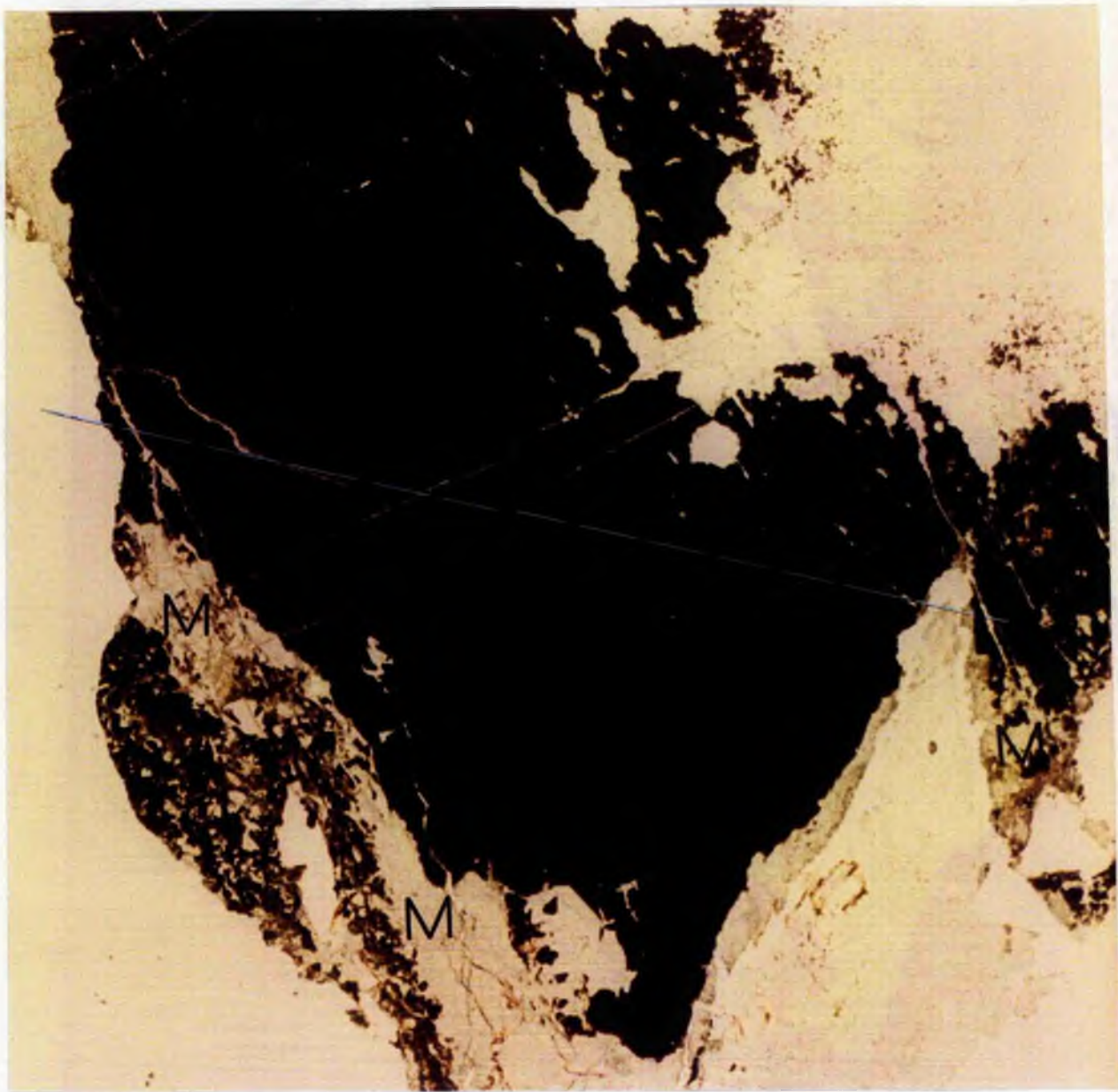


Plate 4.14. Photomicrograph showing crystal of tapiolite (black) (with line of analytical traverse) and microlite replacement at the margins, Farm Schonau pegmatite, Warmbad, Namibia. Length of section: 1 cm.

4.6.

DISCUSSION

COLUMBITE- TANTALITE, WODGINITE AND TAPIOLITE

The tantalum data for sample XX from Rubicon, Karibib (Tables 4.8-4.12) has been plotted on a Ta/(Ta+Nb) versus Mn/(Mn+Fe) diagram (see Fig. 4.11a). This clearly shows i) a division between manganotantalites, tantalites and ferrotantalites and ii) the range in composition in tantalum minerals in one pegmatite.

The columbite-tantalite data for the Okatjimukuju M1 and M3 pegmatites, Karibib, plotted on a similar Ta/(Ta+Nb) versus Mn/(Mn+Fe) diagram (see Fig. 4.11b) shows in addition to the type minerals shown in Figure 4.11a, the range in composition from manganotantalite to manganocolumbite and a division between the two fields (Fig.4.11b).

Columbite-tantalite data from the Karibib pegmatites in general (data from Table 4.2, 4.3, 4.5) plotted on a similar Ta/(Ta+Nb) versus Mn/(Mn+Fe) diagram with data from the Kenhardt area (Table 4.1) in the Northern Cape of South Africa (see Fig. 4.12a) shows the range in composition in the whole columbite-tantalite series: - columbite, ferrocolumbite, manganocolumbite, tantalite and manganotantalite, from pegmatites in general in the Karibib area, Namibia, and a limited range in compositions, columbite and ferrocolumbite in the Kenhardt area. The localities of the pegmatites are shown in Figure 4.12b, in particular to emphasize the tantalite from Ricksburg which plots within the tantalite-tapiolite gap. This mineral was not analysed by the electron microprobe and therefore may not be considered as a mixed phase analysis. Therefore data analysed by probe techniques are included if they fall within the tantalite tapiolite gap. Figure 6.10 shows, in addition, tantalum data plotted for the Steinkopf area, Namaqualand and Tantalite Valley, Namibia. A comparison of the four pegmatite

fields show that the pegmatites from Tantalite Valley carry manganotantalite very rich in Mn and Ta in comparison with the other three pegmatite fields.

Columbite is the most common member of the columbite-tantalite series in the Karibib pegmatites of Namibia as it is in other regions of Africa (von Knorring, 1985). Figure 4.12a emphasizes the range in composition of the columbite-tantalite series, i.e from ferrocolumbite to manganotantalite which occur in simple to complex differentiated pegmatites in Karibib. Figures 4.11a, 4.11b in comparison show the particular types of columbite-tantalite i.e. manganotantalite and manganocolumbite which are prevalent in the rare-element differentiated pegmatites of Karibib.

Nb is available for crystallization of solid phases in earlier stages of pegmatite evolution relative to the bulk of Ta as Ta-bearing complexes are stable to lower temperatures than Nb complexes (Wang et al. 1982). Consequently this leads to extensive ranges of columbite-tantalite compositions and likewise Nb/Ta ratios, even in one pegmatite body. This is demonstrated in the Rubicon and Okatjimukuju pegmatites, Karibib (Figs. 4.11a, 4.11b). Figure 4.13 shows the Ta versus Nb/Ta trends for columbite-tantalite, tapiolite and wodginite for the Karibib area (data this study and von Knorring, 1985). Figure 4.14 shows the same trends for African pegmatites (data from von Knorring and Fadipe, 1981 and from this study). The Ta versus Nb/Ta plots for the African pegmatites have a range in composition of Ta and Nb with 74.61% Nb₂O₅ and 2.78% Ta₂O₅ (Nb/Ta 23.8) in columbite from Lunyo, Uganda to 0.25% Nb₂O₅ and 85.51% Ta₂O₅ (Nb/Ta) in manganotantalite from the White City pegmatite, Tantalite Valley, Namibia (data this study).

The reasons for the Ta-enrichment during pegmatite evolution has been attributed to several causes. Firstly, Hildreth (1979, 1981) has pointed out that complexing of Nb and Ta and their response to liquid fractionation, including transport in a hydrous phase, can be expected to operate during the early differentiation of a leucogranitic

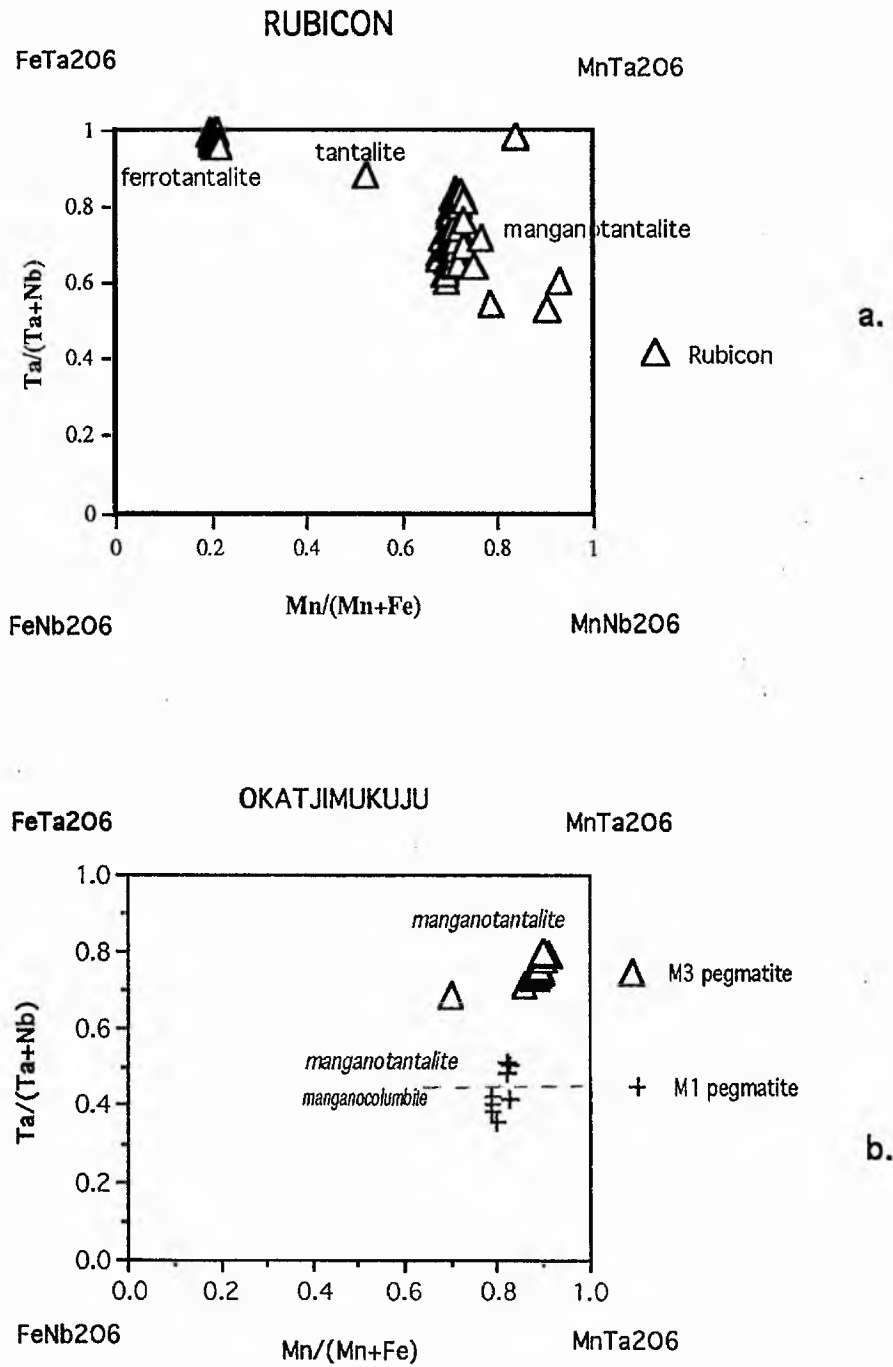
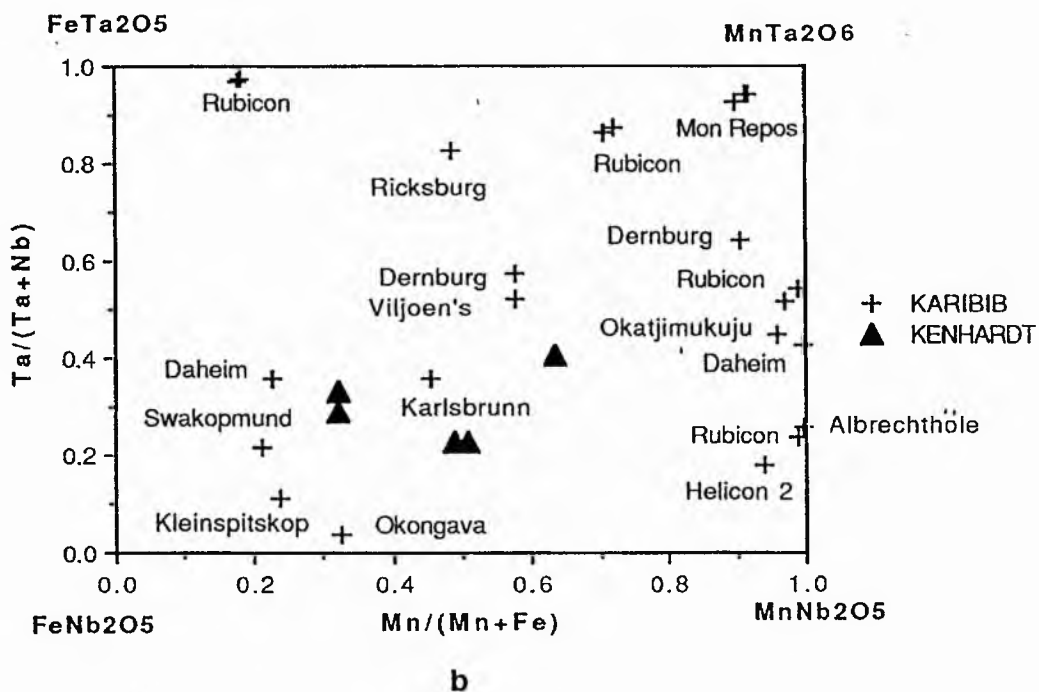
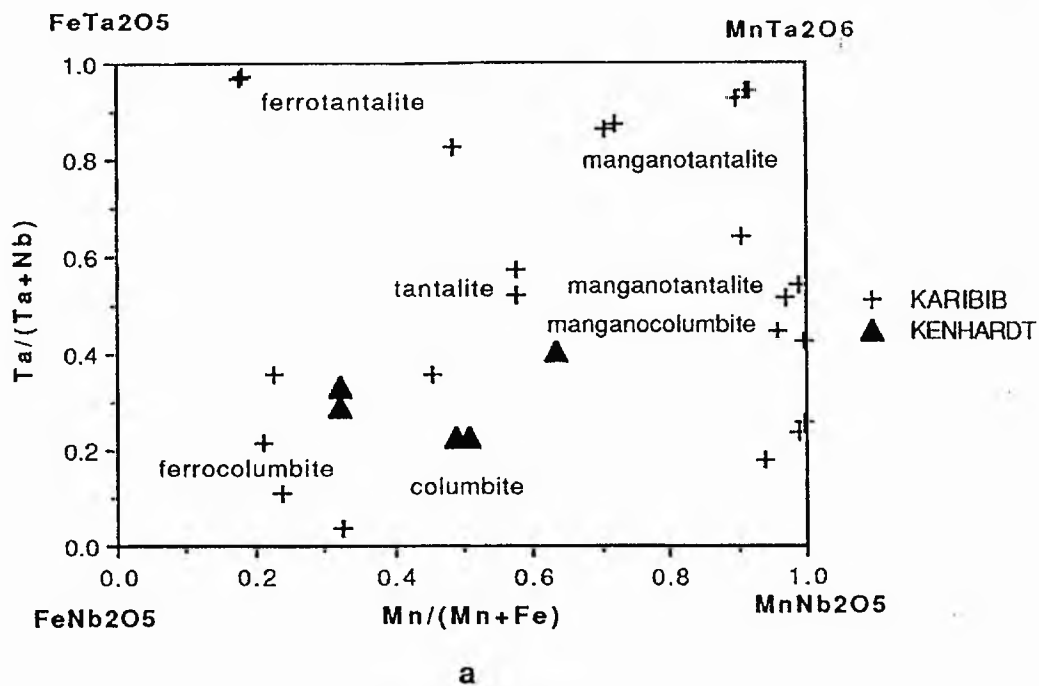


Fig. 4.11. Ta/(Ta+Nb) versus Mn/(Mn+Fe) plot for a) manganotantalite, tantalite and ferrotantalite from Rubicon, Karibib, and b) manganotantalite and manganocolumbite, Okatjimukuju, Karibib.



Figs. 4.12. a) Ta/(Ta+Nb) versus Mn/(Mn+Fe) plot to show the range in composition of the columbite-tantalite series and b) the localities of the minerals from Karibib.

magma, as in rhyolitic melts. Secondly, F-based Nb and Ta complexes have different thermal stabilities, the Ta-bearing complexes are stable to lower temperatures than Nb complexes (Wang et al., 1982) with the result that columbite is the most common phase in granite pegmatites and the only phase in early formed less complex pegmatites which do not contain lithium.

The increase in abundances of Nb and in particular the Ta-enrichment trend in rare-element pegmatites indicate a change in the Nb/Ta ratio during pegmatite evolution. The Nb/Ta ratio of the niobium-tantalum minerals reflects the level of fractionation attained by the parent melt or by the melts or fluids parental to the individual pegmatite units (Cerny et al. 1985). Columbite, tantalite, tapiolite and microlite found in most types of pegmatite have broad ranges of Nb/Ta substitution, therefore the distribution of individual tantalum minerals is partly governed by the ratio of Nb/Ta and reflects the level of fractionation of the parent melt.

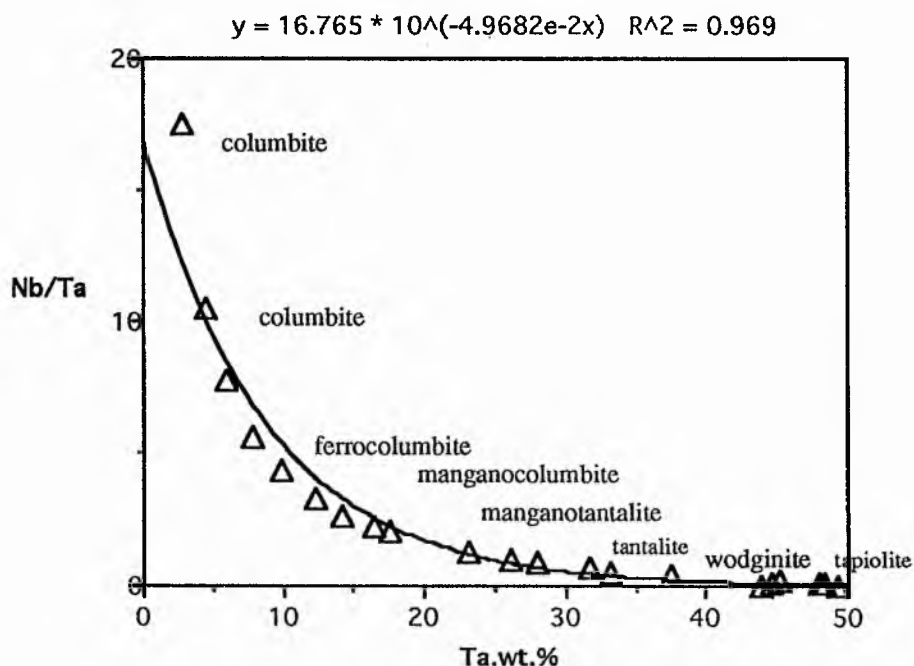


Fig. 4.13. Ta versus Nb/Ta trends for columbite - tantalite, tapiolite and wodginite for the Karibib area, Namibia (data from Table 4.2 and von Knorring, 1985).

CHAPTER 5.

MICROLITE

5.1. INTRODUCTION

This study presents new data on uranoan microlite, plumbomicrolite, plumbian uranmicrolite and uranmicrolite as defined by the IMA Pyrochlore Subcommittee (Hogarth, 1977). Changes in composition of these minerals and replacements of manganotantalite by various microlites have been studied in order to establish the composition of late stage magma and fluids from which these minerals crystallized.

Microlite $(Ca,Na,U)_2(Ta,Nb,Ti)_2(O,OH,F)_7$ is the tantalum end-member of the pyrochlore-microlite-betafite series. It is a comparatively rare accessory mineral of lithium pegmatites and is frequently associated with other tantalum minerals, often replacing them. Microlite is often difficult to detect since it may be completely camouflaged in the host mineral matrix, because of its unusually small size, irregular form, multiplicity of colours and its dispersed nature.

Hogarth (1977) in his report on the classification and nomenclature of the pyrochlore group, specified the microlite subgroup with $Nb+Ta$ greater than $2Ti$ with Ta greater than or equal to Nb . Within the subgroups, individual species are defined with respect to A-atoms (viz Na,Ca,K,Sn,Ba,REE,Pb,U) in the following manner :-

- a) Na-Ca members: Na or Ca, but no other A-atoms, shall exceed 20% of the total A-atoms present
- b) Other members : One or more A-atoms other than Na and Ca shall exceed 20% of the total A-atoms present.

The use of additional adjectival prefixes is optional and should normally be restricted to the A-atoms next in abundance after the principal constituent.

Microlite minerals of the pyrochlore-group have been analysed with the electron microprobe, initially because of their rare occurrence and unusual and varied composition, and also because of their association with, and replacement of, other tantalum minerals. On a preliminary investigation the microlites appeared to be inhomogeneous although all the microlite crystals are isotropic. Detailed traverses have been completed across several crystals to investigate zoning. This study presents new data on uranmicrolite, uranoan microlite and plumbomicrolite with detailed traverses on the later two. New data are also given on primary microlite; and replacement of manganotantalite by microlite (termed as secondary microlite by von Knorring and Fadipe, 1981), from differentiated lithium pegmatites in (1) Steinkopf, Namaqualand, South Africa, (2) Tantalite Valley, Namibia; and (3) the Karibib/Usakos area, Namibia. The microlites have been confirmed by X-ray diffraction photographs at the Natural History Museum and by O. von Knorring with the exception of the uranmicrolite from Okongava, Karibib, and the uranoan microlite from Tantalite Valley due to insufficient material.

Microlite most frequently is found in small amounts either associated with or replacing other tantalum minerals (see Plates 5.1-5.7). The mineral is mostly disseminated in "sugary albite", in cleavelandite and lithian mica (see Plate 3.2) or in more complex albite-spodumene-lithium mica units marginal to the quartz core. Only rarely are larger concentrations of the mineral found in specific zones of Li-pegmatites. Being a (F,OH)-bearing mineral, microlite is one of the last minerals to crystallize and is found in the latest micaceous replacement units. The microlite structure can accommodate many elements; the mineral is therefore invaluable as an indicator of the composition of trace and minor elements in the late stage fluid environment.

Von Knorring (1981) has divided microlites from Africa into 3 major groups : - a) primary or common microlite b) secondary microlites c) uraniferous microlites. The uraniferous microlites may also be secondary in origin, but in this study the individual species as defined by Hogarth (1977) will each be treated separately : - a) primary, common microlite with $Ca+Na > 20\%$ A atoms b) secondary, common microlite with $Ca+Na > 20\%$ A atoms, and c) separate species : - i) uranmicrolite, ii) plumbomicrolite. Typical abundances in uranoan microlite, from the Lepidolite pegmatite, Tantalite Valley are demonstrated in Figure 5.1a and the secondary microlites analysed in this study are plotted in Figure 5.1b, according to the Hogarth (1977) ternary diagram (Fig. 5.1c).

5.2. PRIMARY MICROLITE

This variety is commonly found disseminated in lithian mica and cleavelandite albite units. In addition to lithium, fluorine is a characteristic constituent of this association indicated by the presence of lithian mica and topaz. The major economic microlite deposits are to be located in this pegmatite type. This variety of microlite is generally high in Ta and Ca with varying amounts of Nb and Na ; the trace elements are usually low, generally reflecting the specific geochemistry of the pegmatites in question.

In this study, primary microlites are represented by reddish-brown microlite from the White City pegmatite in Tantalite Valley (see Fig. 2.8 for locality) and black and yellow microlite from Jooste's pegmatite, Karibib (Fig. 2.10). The mineral associations of both microlites are similar, each occurring in lithian mica or lepidolite with albite, but the types of occurrence differ. In the former the microlite crystals are sparsely distributed and up to 1 cm in size and are situated in fine-grained lithian mica intergrown with albite. In contrast, the microlite from Jooste's pegmatite is disseminated quite liberally in fine-grained purple lithian mica intergrown with albite. The lithian mica unit at Jooste's is extensive in

ABUNDANCES

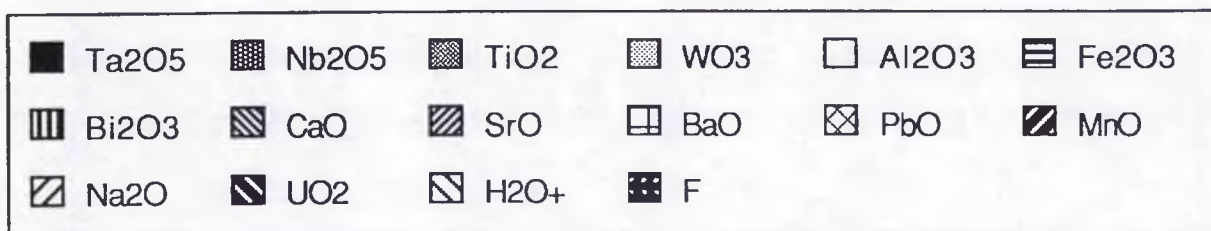
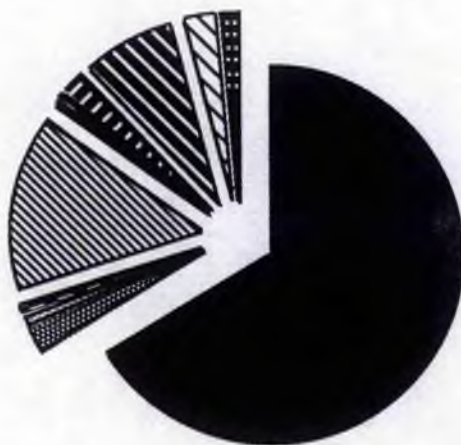


Fig.5.1a. A diagram to demonstrate the abundances of Ta₂O₅ 66.6%, CaO 15.3%, UO₂, 7.7%, Nb₂O₅ 2.3%, MnO 1.7%, F 1.6% and H₂O 2.5% (by difference) in uranoan microlite from the Lepidolite pegmatite, Tantalite Valley, Namibia (see Table 5.2, anal 3a, abundances less than 1% are not distinguishable).

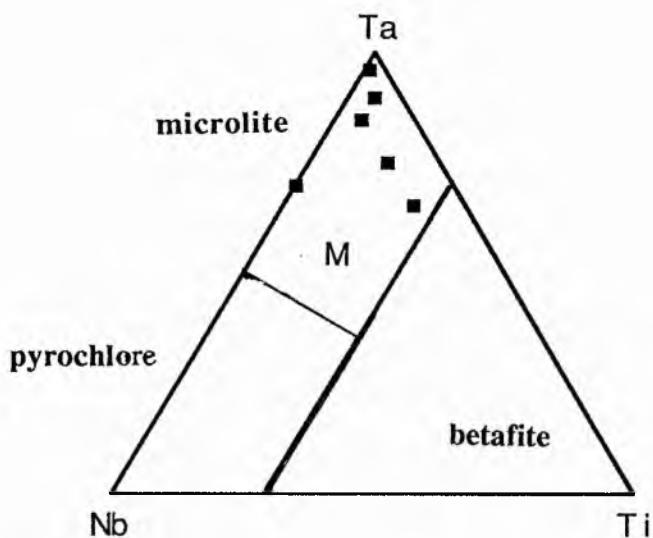


Fig. 5.1b. Data from Table 5.2 plotted on a Ta, Nb, Ti (+Fe^{III}+Al) ternary diagram. The data plot into the microlite field of the pyrochlore group of minerals, as specified by Hogarth (1977) see Fig 5.1c.

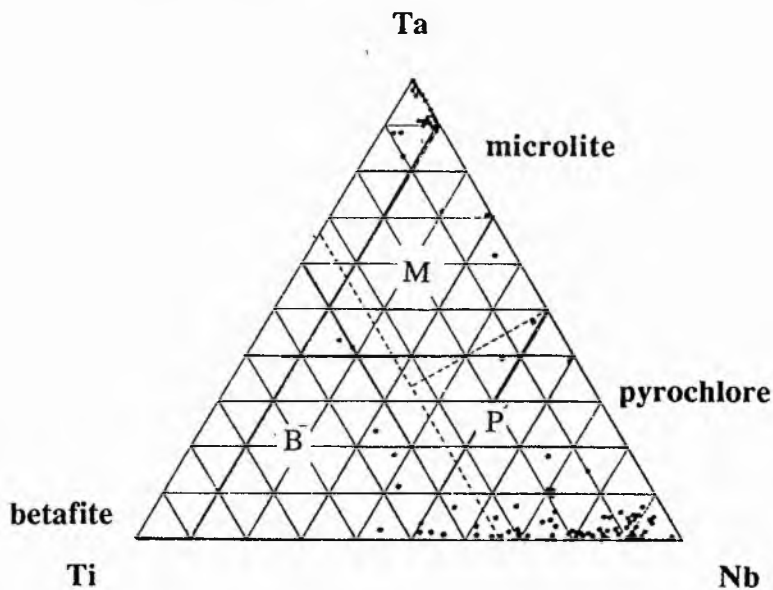


Fig.5.1c. The three subgroups of the pyrochlore group, from Hogarth (1977), M denotes microlite; P denotes pyrochlore and B betafite.

comparison with the irregular pods at the White City pegmatite and the microlite crystals are mostly between 1 and 2 mm in size.

TABLE 5.1. Compositions of primary microlite

Sample	Hs1.	JM2.	3.	4.	5.
Ta ₂ O ₅	77.90	71.85	73.97	72.03	72.71
Nb ₂ O ₅	2.52	9.29	8.17	8.40	10.26
TiO ₂	0.56	0.00	0.00	0.02	0.00
WO ₃	0.19	0.84	0.00	-	-
ZrO ₂	0.16	0.00	-	-	-
SnO ₂	0.30	-	0.00	0.12	0.00
Al ₂ O ₃	0.00	0.00	-	0.02	-
Fe ₂ O ₃	0.00	tr	0.26	0.08	0.03
CaO	11.98	9.96	10.14	11.38	10.44
SrO	-	0.00	-	-	-
BaO	0.00	0.00	-	0.03	-
PbO	0.00	0.56	-	0.01	-
MnO	tr	tr	-	0.03	0.03
Na ₂ O	5.78	6.45	6.78	5.40	6.75
H ₂ O+	nd	nd	nd	0.40	-
F	0.00	2.85	0.00	2.69	-
	99.39	101.90	99.32	100.61	100.31
-O=F		1.20	-	1.13	
	99.39	100.70	99.32	99.48	100.31

- Hs1. White City pegmatite, Tantalite Valley, Namibia; analyst: J.R. Baldwin
 JM2. Black microlite, Jooste's pegmatite, Karibib, Namibia (UO₂ = 0.10); analyst: J.R. Baldwin
 3. Okawayo pegmatite, Karibib, Namibia (von Knorring 1981) (XRF analysis).
 4. Ricksburg pegmatite, Karibib, Namibia (von Knorring, 1981) (ThO₂ 0.17; La₂O₃ 0.25; Ce₂O₃ 0.19; Cs₂O 0.03, XRF analysis).
 5. Yellow microlite, Jooste's pegmatite, Karibib, Namibia (unpublished analysis O. von Knorring) _ = not determined.

Primary microlites are represented by analyses 1 - 5 (Table 5.1). The content of Ta₂O₅ is high with 77.9% at White City and 71.8% at Jooste's and corresponding Nb₂O₅ values of 2.5% and 9.3% respectively. The Na₂O contents are high and the trace elements are low. These analyses of the microlite and their field occurrence are similar to those analysed by von Knorring and Fadipe (1981); in connection with primary microlite they showed that this variety occurs in lithian mica and cleavelandite units or as a late mineral in cavities of lithian pegmatites. The microlites are not associated with other tantalum minerals. Yellow microlite from Jooste's pegmatite contains no fluorine and more niobium in

comparison with black microlite from the same pegmatite, this however could be due to different methods of analysis.

5.3. SECONDARY MICROLITE

Secondary microlites are formed by various alteration processes of hydration or replacement of other tantalum minerals; and their chemistry frequently reflects the composition of the replaced minerals (von Knorring and Fadipe, 1981). Two examples of secondary microlites replacing manganotantalite have been investigated with the microprobe from (1) the Noumas pegmatite, Namaqualand, and (2) the Homestead pegmatite in Tantalite Valley.

Black tantalite from the Noumas pegmatite is partially replaced by brown microlite at certain edges of the crystal (Plate 5.1). The main mineral is manganotantalite which is opaque in transmitted light. Three specific areas of microlite (1,2,3, Plate 5.1) were analysed with the microprobe and an average analysis contains 73.48% Ta_2O_5 (range 72.99-75.92%) and 5.20% Nb_2O_5 (4.32-6.11%) with CaO 13.77% (12.88-15.15%) and Na_2O 2.4 (Table 5.2, anal.1, ave 8 analyses). A traverse across the manganotantalite showed the mineral to be variable in composition with Ta_2O_5 over the range 71.84-73.63% (ave. 72.34% in 5 analyses); Nb_2O_5 11.48-14.80%; MnO 13.46-14.14% and FeO 0.50-1.11%. The minor elements in both the microlite and manganotantalite are similar in value.

A backscattered electron image of the Mn-tantalite (white) with distinct grain boundaries, shown in Plate 5.2 clearly shows replacement by microlite (grey). The opaque Mn-tantalite crystal may be located in area 3 in the photomicrograph (Plate 5.1). Plate 5.3, a backscattered image enlargement of part of area 2 (Plate 5.1) shows the relationship of the three minerals, Mn-tantalite, microlite and cleavelandite more clearly: i) irregular

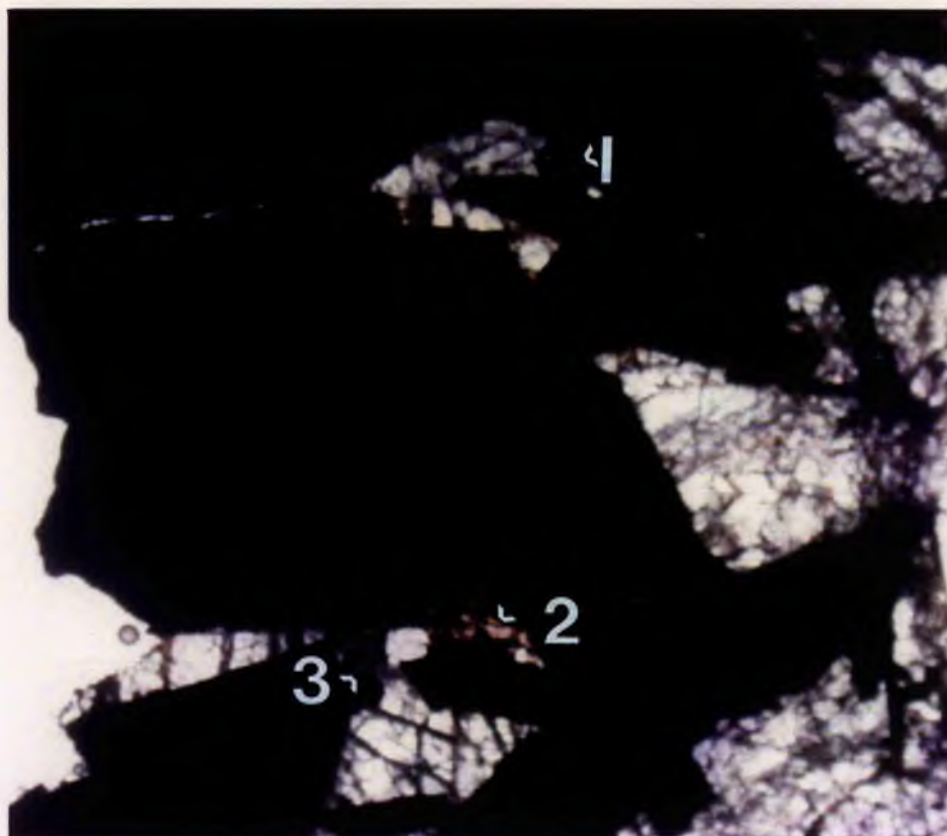


Plate 5.1. Photomicrograph of microlite (light grey, area 1,2,3) partly replacing Mn-tantalite (black) in cleavelandite (white), Noumas pegmatite, Steinkopf, Namaqualand, South Africa. Sample REP 2. Length of section: 14 mm.

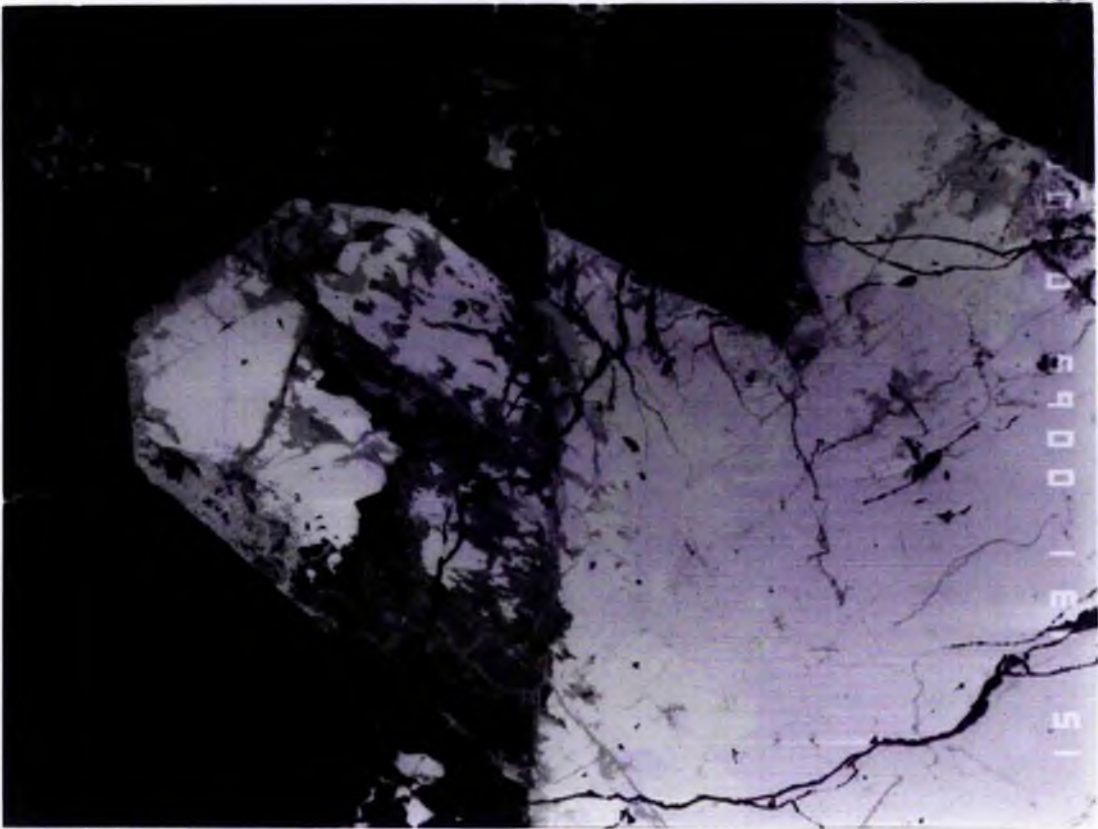


Plate 5.2. Backscattered image of area 3 indicated in Plate 5.1 showing tantalite (white) with irregular grey replacement of microlite. The tantalite crystal is reversed left to right from Plate 5.1 where it is opaque, Noumas pegmatite, Namaqualand. Scale bar: 100 microns.

Plate 5.3. Backscattered image of an enlargement of part of area 2 indicated in Plate 5.1, showing cleavelandite (black) being replaced by tantalite (white) with distinct grain boundaries, and irregular patches of microlite (grey). Scale bar: 100 microns.



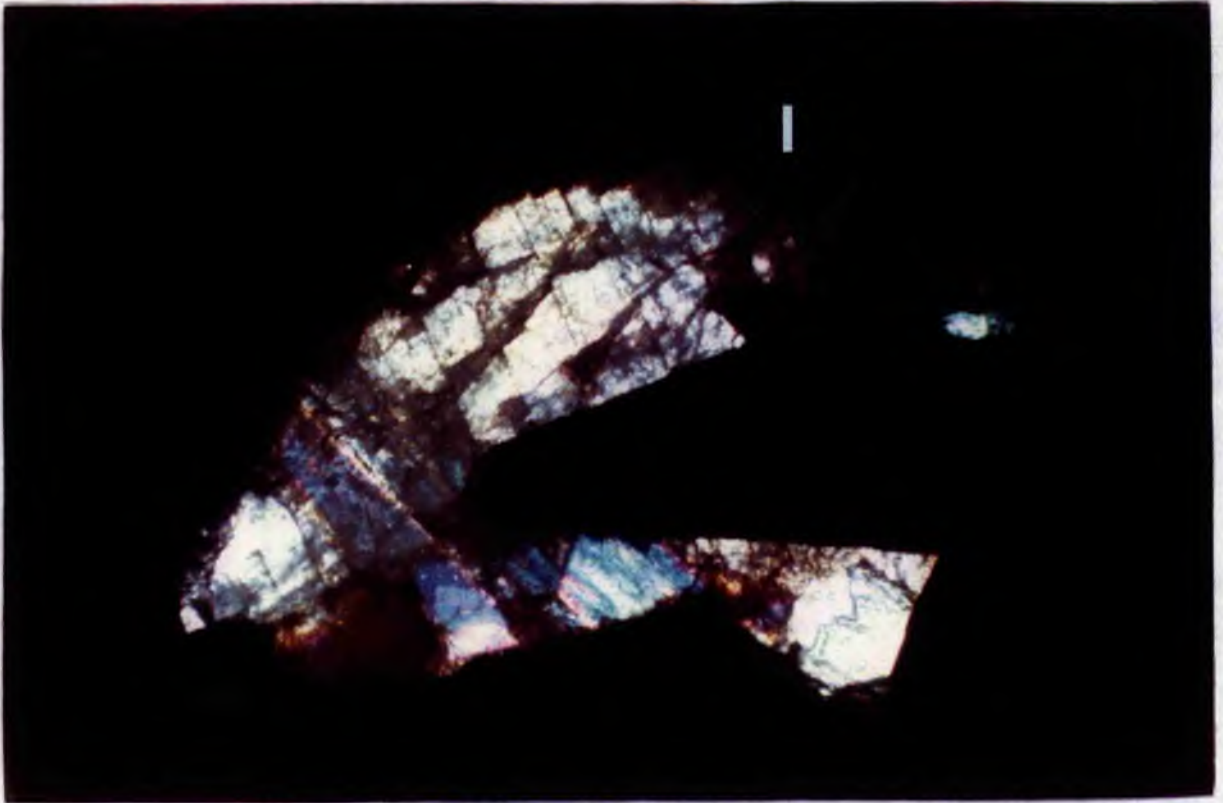


Plate 5.4. Photomicrograph of area 1 indicated in Plate 5.1 showing tantalite (opaque), cleavelandite (light), and microlite replacement (brown), Noumas pegmatite, Steinkopf, Namaqualand. Scale bar: 200 microns

Plate 5.5. Backscattered image of part of area 1 showing Mn-tantalite (white) with microlite replacement and intergrowth (grey) and irregular grain boundaries with cleavelandite (black). Scale bar: 100 microns.





Plate 5.6 Photomicrograph of microlite veins (grey) replacing Mn-tantalite (black), cleavelandite (white) Homestead pegmatite, Tantalite Valley, Namibia. Scale bar: ----- 2 mm.

Plate 5.7. Photomicrograph of fibrous microlite replacing tantalite (orange brown) with cleavelandite inclusions, (reversed left to right from Plate 5.6) Homestead pegmatite, Tantalite Valley, Namibia. Scale bar: ----- 1000 microns.



TABLE 5.2.

Secondary and uranoan microlites from South Africa and Namibia

	1.	2.	3a.	3b.	4a.	4b.	5.
Ta ₂ O ₅	73.48	82.57	66.64	73.74	57.14	67.26	56.12
Nb ₂ O ₅	5.20	1.24	2.29	2.63	5.56	5.43	13.18
TiO ₂	1.11	0.16	0.04	0.07	6.96	3.00	0.00
WO ₃	0.77	0.62	0.68	0.99	0.39	0.45	0.00
Al ₂ O ₃	tr.	0.00	0.24	0.24	0.12	0.41	0.00
Fe ₂ O ₃ *	0.26	tr.	0.64	0.97	0.13	0.17	0.58
UO ₂ **	0.56	0.23	7.71	8.41	4.03	0.77	14.35
Bi ₂ O ₃	-	-	-	-	4.27	1.67	-
CaO	13.77	10.60	15.29	4.61	16.21	14.62	6.87
SrO	0.13	0.00	0.26	1.13	0.00	0.00	0.54
BaO	0.00	0.00	0.21	0.37	0.00	0.00	0.00
PbO	tr.	0.00	0.40	0.53	0.53	0.15	1.03
MnO	0.47	tr.	1.66	1.38	0.85	0.81	0.59
Na ₂ O	2.44	5.23	0.43	0.25	0.91	1.90	0.86
F	2.17	1.20	1.62	0.33	1.78	2.27	0.47
Total	100.36	101.85	98.11	95.65	98.88	98.91	94.59
-O=F	0.91	0.50	0.68	0.14	0.75	0.95	0.19
	99.45	101.35	97.43	95.51	98.13	97.96	94.40

IONS per 2B

Ta	1.696	1.928	1.801	1.777	1.316	1.540	1.409
Nb	0.199	0.048	0.103	0.105	0.213	0.207	0.550
Ti	0.071	0.010	0.003	0.005	0.443	0.190	0.000
W	0.017	0.014	0.017	0.023	0.009	0.010	0.000
Al	0.000	0.000	0.028	0.025	0.012	0.041	0.000
Fe	0.017	0.000	0.048	0.064	0.008	0.011	0.041
Total B site	2.0	2.0	2.0	2.0	2.0	2.0	2.0
U	0.011	0.005	0.170	0.166	0.076	0.015	0.295
Bi	-	-	-	-	0.094	0.037	-
Ca	1.251	0.975	1.627	0.438	1.470	1.320	0.679
Sr	0.007	0.000	0.015	0.058	0.000	0.000	0.029
Ba	0.000	0.000	0.008	0.013	0.000	0.000	0.000
Pb	0.000	0.000	0.011	0.013	0.012	0.004	0.026
Mn	0.034	0.000	0.140	0.104	0.061	0.058	0.046
Na	0.401	0.870	0.083	0.043	0.150	0.310	0.154
Total A site	1.704	1.85	2.054	0.835	1.863	1.744	1.229
F	0.58	0.33	0.50	0.09	0.47	0.61	0.14

1. Secondary microlite, Noumas pegmatite, Namaqualand, South Africa (REP2)
 2. Secondary microlite, Homestead pegmatite, Tantalite Valley, Namibia (HO2)
 - 3a. Uranoan microlite (Ave. central area), Lepidolite pegmatite, Tantalite Valley, Namibia (M10)
 - 3b. Uranoan microlite (Ave. rim of crystal), Lepidolite pegmatite, Tantalite Valley, Namibia (M10)
 - 4a. Uranoan microlite (2) (central area), Kokerboomrand pegmatite, Namaqualand, South Africa (KB)
 - 4b. Uranoan microlite (2) (Ave. intermediate area), Kokerboomrand pegmatite, Namaqualand, South Africa (KB)
 5. Uranmicrolite, Okongava Ost, Karibib, Namibia (MR2)
- * Total iron as Fe₂O₃. ** Total U as UO₂. Analyst: J.R. Baldwin. REP2, HO2, M10, KB and MR2 represent section nos., courtesy of Dept. of Geology, University of Witwatersrand, Johannesburg.

replacement of microlite in tantalite, ii) zoning in the Mn-tantalite and iii) tantalite and microlite replacement of cleavelandite (black) which has irregular grain boundaries. Irregular grain boundaries at the contact between Mn-tantalite (white) and Mn-tantalite (black) are also apparent in the backscattered image (Plate 5.5) of area 1 (see Plate 5.4). The order of crystallization of the three minerals may be suggested as cleavelandite, and tantalite, followed by microlite.

Microlite forming pink veins in orange brown tantalite (Plates 5.6, 5.7) at the Homestead pegmatite, Tantalite Valley, is almost certainly a replacement feature. The replacement in this tantalite is more definite and complete than the previous example from Noumas. In certain areas the microlite is fibrous (Plate 5.7), in other areas the replacement of the tantalite is incomplete and the microlite is overlain by remnants of tantalite. A traverse across the tantalite showed this mineral to be manganotantalite with a relatively uniform composition containing 83.14% Ta_2O_5 (ave. 13 analyses, range 82.17- 84.13%), 1.4% Nb_2O_5 and 13.83% MnO (range 13.56-14.07). The microlite contained 82.57% Ta_2O_5 , 1.24% Nb_2O_5 and 0.23% UO_2 (Table 5.2, anal.2), Ta_2O_5 and minor element values are similar to those in the tantalite.

5.4. URANOAN MICROLITE AND URANMICROLITE

Two examples of uranoan microlite and one example of uranmicrolite as defined by the IMA Pyrochlore Subcommittee (Hogarth, 1977) have been analysed by the electron microprobe: (1) an isolated crystal of uranoan microlite, of maximum length 1.3 mm, occurring in lepidolite in the replacement unit of the Lepidolite pegmatite, Tantalite Valley, Namibia and (2) radioactive crystals of uranoan microlite occurring in green mica greisen in the Kokerboomrand pegmatite, Steinkopf, Namaqualand. The uranmicrolite occurs in the Li-mica replacement unit of Jooste's pegmatite, Okongava Ost, Karibib, Namibia.

The crystal from the Lepidolite pegmatite, Tantalite Valley showed two different compositions when initially analysed (Table 5.2, anal. 3a, 3b). Traverses were made across the crystal at right angles to examine the composition in detail.

The variation in composition is represented diagrammatically for each element in Fig. 5.2. The dashed line represents the traverse across the crystal from south to north (Y microns) and the unbroken line the traverse from east to west (X microns). Analyses (13) were made at 100 μm intervals across the first traverse Y and the results are presented in Table 5.3. Two essentially different compositions were obtained; a rim area approximately 130-200 μm wide (Fig. 5.2, points 1, 11-13) and a central area (points 2-10). The contact area was investigated in detail at 25 μm intervals and there is no transitional area between the two compositions: there is, however, some variation within each of the two different compositions (Table 5.3). At the edges of the crystal, Ta, Sr and W increase. Ta increases from an average value of 66.64% as Ta_2O_5 in the core to 72-78% in the outer zone. Pb, Ba and Fe, present in small amounts, also increase in the rim. Ca and F show a definite decrease in the rim: CaO decreasing from approximately 15% as in the centre to values between 3 and 8% in the rim. With the exception of analysis 13, F shows a definite decrease in the rim from 1.62% in the centre to 0.2-0.3%.

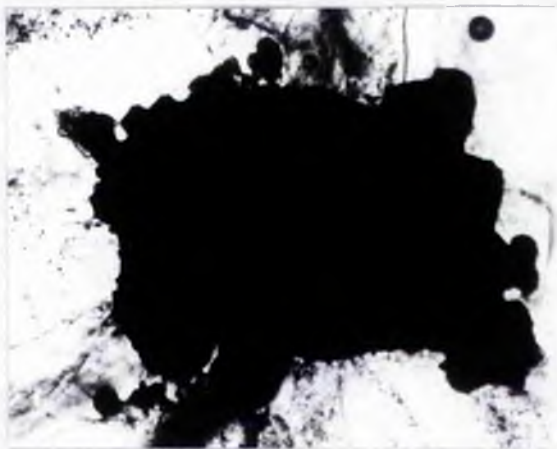


Plate 5.8. A crystal of microlite (1.3mm) enclosed in lepidolite, Lepidolite pegmatite, Tantalite Valley, Namibia. An analytical traverse was made across the crystal from east to west (X) and from south to north (Y)

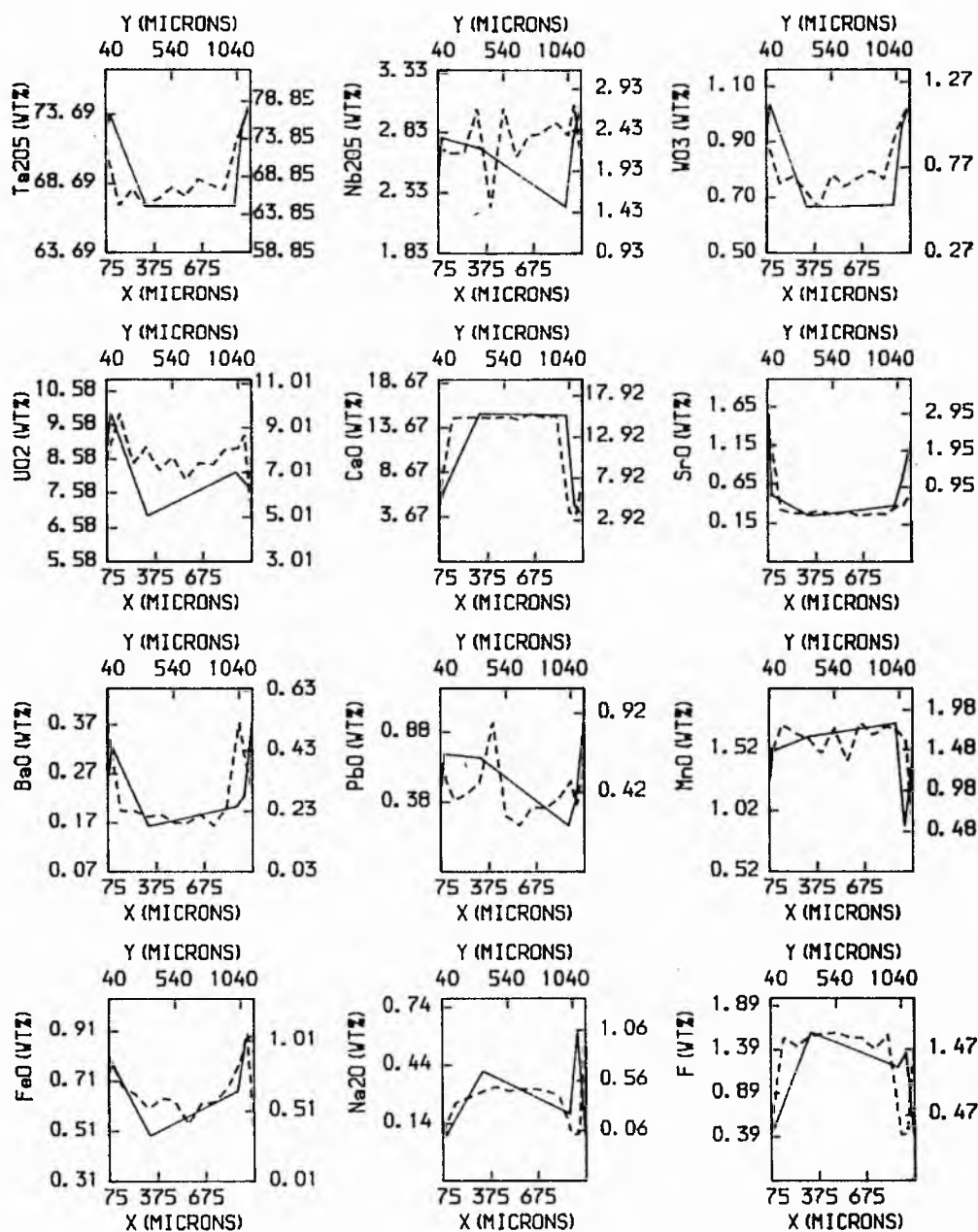


Fig. 5.2. Analyses along two traverses at right angles of uranoan microlite, Lepidolite pegmatite, Tantalite Valley, Namibia. Traverse x, 'continuous' and traverse y, 'dashed'; 75 microns represents the distance from the L.H. edge of the crystal along traverse x; values along Y and X are given in Tables 5.3 and 5.4. respectively.

TABLE 5.3. Traverse (Y) across uranoan microlite, Lepidolite Pegmatite, Namibia

Sample	M10/1.	M10/2.	M10/3.	M10/4.	M10/5.	M10/6.	M10/7.	M10/8.	M10/9.	M10/10.	M10/11.	M10/12.	M10/13.
Ta ₂ O ₅	72.56	65.05	67.19	64.85	66.04	67.38	66.19	68.42	67.61	67.04	73.68	76.07	78.34
Nb ₂ O ₅	2.22	2.14	2.17	2.69	1.49	2.70	2.10	2.37	2.40	2.53	2.37	2.74	2.07
TiO ₂	0.04	0.04	0.04	0.04	0.04	0.03	0.04	0.03	0.03	0.05	0.06	0.07	0.02
WO ₃	0.95	0.68	0.72	0.63	0.54	0.73	0.66	0.71	0.75	0.70	0.98	1.07	1.14
Al ₂ O ₃	1.59	0.15	0.40	0.19	0.11	0.10	0.40	0.28	0.42	0.11	0.27	0.18	0.08
Fe ₂ O ₃ *	0.99	0.76	0.69	0.58	0.67	0.63	0.46	0.62	0.63	0.74	0.96	1.18	0.37
UO ₂ **	7.61	9.64	7.42	8.13	7.08	7.70	6.65	7.41	7.33	8.01	8.10	8.67	5.05
CaO	5.32	15.12	15.31	15.25	15.10	15.42	14.98	15.69	15.28	15.43	3.81	3.39	7.99
SrO	2.95	0.33	0.24	0.28	0.32	0.19	0.30	0.18	0.25	0.23	0.45	0.49	0.87
BaO	0.51	0.23	0.23	0.21	0.22	0.19	0.19	0.22	0.18	0.24	0.52	0.39	0.30
PbO	0.60	0.37	0.41	0.49	0.86	0.27	0.21	0.33	0.32	0.38	0.49	0.34	0.60
MnO	1.33	1.79	1.68	1.61	1.43	1.75	1.33	1.81	1.66	1.77	1.69	1.60	0.54
Na ₂ O	0.04	0.33	0.39	0.44	0.49	0.45	0.47	0.47	0.45	0.39	0.01	0.02	1.03
F	0.29	1.64	1.50	1.67	1.70	1.72	1.64	1.63	1.46	1.68	0.16	0.18	1.45
Total	97.00	98.27	98.39	97.06	96.09	99.26	95.62	100.17	98.77	99.30	93.55	96.39	99.85
-O=F	0.12	0.68	0.63	0.70	0.71	0.72	0.69	0.68	0.61	0.71	0.07	0.08	0.61
	96.88	97.59	97.76	96.36	95.38	98.54	94.93	99.49	98.16	98.59	93.48	96.31	99.24

Anal. 1-10 were made at 100 micron intervals, anal.11-13 at 50 micron intervals. Anal. 1 was made at 40 microns from the edge and anal.13 at 35 microns from the opposite edge of crystal. * Total iron as Fe₂O₃. ** Total uranium as UO₂. Sample M10, courtesy of University of Witwatersrand, Johannesburg.

U shows random variation across the traverse, values varying from 9.9 to 5.05% as UO_2 . However on average there is an increase in UO_2 of 0.70% core to rim. Nb shows random and minimal variation. Na present in small amounts decreases in the rim (see Table 5.2, anal. M10/3a, 3b).

TABLE 5.4. Traverse (X) across uranoan microlite, Lepidolite pegmatite, Tantalite Valley, Namibia (Sample M10)

	M10/D	M10/E	M10/H	M10/L	M10/M	M10/N
Ta ₂ O ₅	72.60	73.59	<u>66.98</u>	<u>67.07</u>	72.91	74.38
Nb ₂ O ₅	2.46	2.79	2.71	2.21	2.78	3.06
TiO ₂	0.08	0.10	0.05	0.05	0.04	0.09
WO ₃	0.92	1.03	<u>0.66</u>	<u>0.67</u>	0.95	1.03
Al ₂ O ₃	0.38	0.19	0.28	0.80	0.11	0.30
Fe ₂ O ₃	0.83	0.86	0.54	0.74	0.97	1.00
UO ₂	8.98	9.91	6.91	8.18	7.93	7.66
CaO	4.87	6.34	<u>15.24</u>	<u>15.01</u>	4.87	3.77
SrO	1.56	0.50	0.24	0.38	0.75	1.20
BaO	0.26	0.32	0.16	0.20	0.22	0.37
PbO	0.49	0.72	0.69	0.21	0.40	0.95
MnO	1.26	1.50	1.62	1.73	0.89	1.39
Na ₂ O	0.13	0.08	0.41	0.19	0.61	0.08
F	0.45	0.51	1.58	1.18	1.35	0.41
*Total	95.31	98.50	98.11	98.66	94.79	95.70
-O=F	0.19	0.21	0.66	0.50	0.57	0.17
	95.12	98.29	97.45	98.16	94.22	95.53
From edge - 75 microns		100	325	875	975	(100 from opp. edge)

Anal. H and L, represent the central area; low total in outer area may contain a higher water content

* including SnO₂: 0.04, 0.06, 0.04, 0.04, 0.01, 0.01. opp. = opposite

The same general trend may be observed for the X traverse (unbroken line, Fig. 5.2). From the diagrams it may be clearly seen that, at the edges of the crystal, Ta, W, Sr, Ba and Fe increase in content and Ca, F, Mn and Na decrease.

Uranoan microlite is commonly formed by the replacement of other niobium-tantalum minerals and therefore may be grouped with the secondary microlites (von Knorring and

Fadipe, 1981). However uranoan microlite ("djalmaitite") from a Siberian pegmatite has also been reported as being first generation (Kornetova and Kazakova, 1964).

A back-scattered electron image of one section of the uranoan microlite from Tantalite Valley shows that the crystal has a fissured structure and is broken into subspheroidal areas, in some cases resembling octahedra (Plate 5.9). Alteration, possibly initiated by lattice damage from radiation appears to have developed along the very fine fissures and has proceeded to divide the crystal into areas, giving the effect of radiating septa. A similar fabric has been observed in barium pyrochlore ("pandaite") from Mrima Hill, Kenya, by Harris (1966). A detailed examination (Plate 5.10) shows that the subspheroidal areas are zoned, the lighter coloured central areas representing elements with a high atomic number such as Ta (73) and U (91) contrasting with Nb (41) and Ca (20), thus accounting for the range in composition of these elements throughout the traverse of the centre of the crystal. For example Ta varies from 64.85 to 68.42% Ta_2O_5 and U from 6.65 to 9.64% UO_2 (see Table 5.3, anal. M10/2-10). The edges of the crystal, from their lighter colour, are thought to contain more higher atomic-number elements than the centre of the crystal. This observation is consistent with the higher Ta content of approximately 10% Ta_2O_5 in the rim of the crystal (see Table 5.2, anal. 3b).

The second example of uranoan microlites is from the Kokerboomrand pegmatite, Namaqualand. The radioactive crystals range from one to eight mm in diameter; they occur in greenish mica greisen as brownish-black octahedra intergrown with muscovite, and are in various stages of development, some skeletal in outline, less commonly anhedral. Electron probe examination shows the crystals to be zoned. A traverse was studied and analyses were made at 100 μm intervals across two separate crystals. Crystal 1, a comparatively well-formed crystal, approximately 2 mm in diameter was chosen for analysis. Only four faces are partly developed, the other sides being incomplete. Complex zonation may be seen in the well-formed lower edge (Plate 5.11) and there is

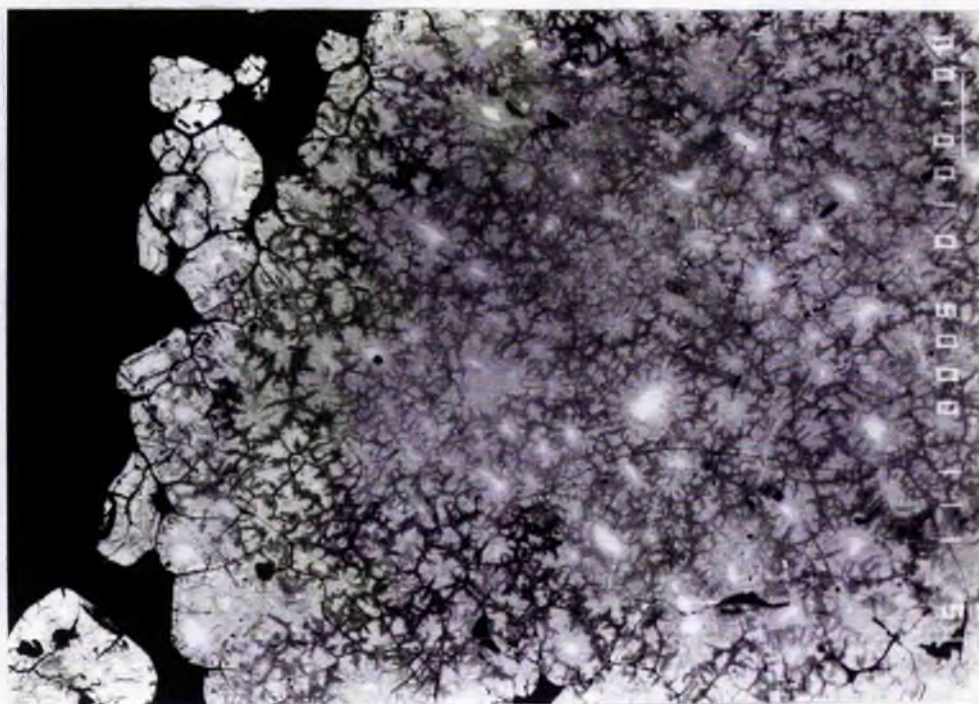
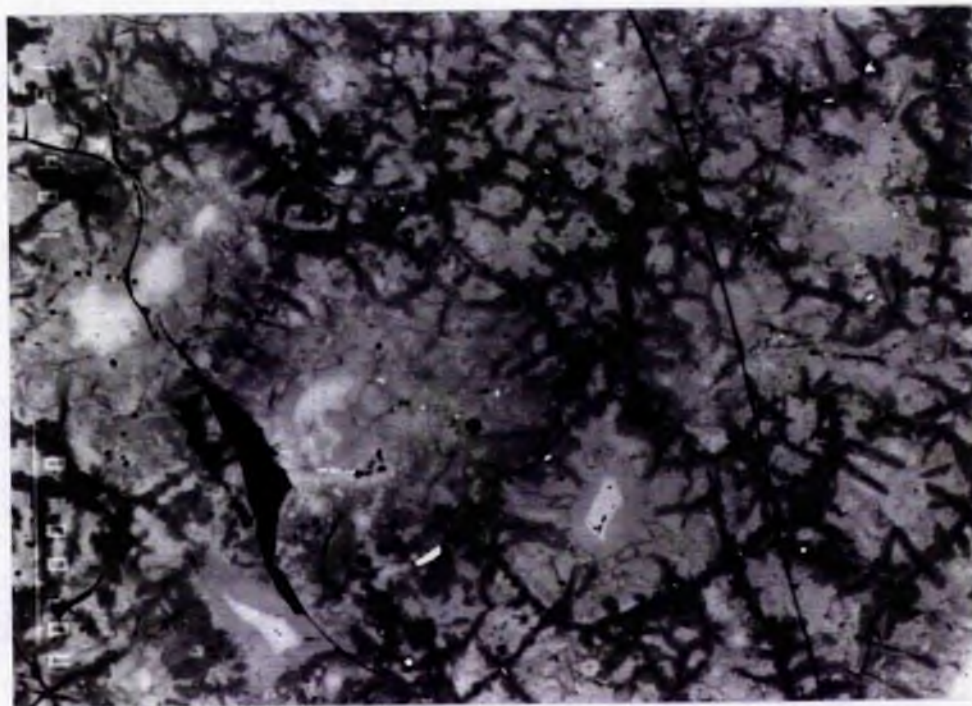


Plate 5.9. Backscattered electron image of uranoan microlite, Lepidolite pegmatite, Tantalite Valley, Namibia. Scale bar : 100 microns

Plate 5.10. Enlargement of lower section of Plate 5.9, showing lattice damage due to radiation in uranoan microlite, Lepidolite pegmatite, Tantalite Valley, Namibia. Scale bar: 100 microns.



an area of different composition in the centre (Plates 5.12), possibly containing relics of a previous Ta mineral. Von Knorring and Fadipe (1981) state that corroded fragments of the original mineral may commonly be located in the matrix of the replaced microlite, indicating the composition of the primary mineral.

The profiles of the traverse across crystal 1 for each element are shown in Figure 5.3. On average Ta, Na, W and F seem to increase towards the centre while Nb, Ti, U and Bi decrease, with Ca, Mn and Fe showing no definite trend. Pb, with the exception of one point (6) (see Fig. 5.3) at 550 μm appears to be constant. The very bright areas in the centre of the crystal (Plates 5.11 and 5.12) contain a bismuth phase, in part bismuth metal, suggesting that a former phase may have been composed of bismutotantalite. Von Knorring and Fadipe (1981) suggest that microlite can replace tapiolite, bismuto- and stibiotantalite.

The results of the traverse across crystal 2, of diameter 1 mm, are illustrated in Figure 5.4. which shows the crystal to have distinct changes from the intermediate areas to the core; Ta, W, Na, Mn and F decrease in the centre; whereas Bi, Ti, U, Ca, Pb and Fe increase. The element which is affected to a major extent is Ta which, decreases in the centre to 57% as Ta_2O_5 from 67.86% in the intermediate areas (Table 5.2, analys. 4a, 4b). There is more U, Bi and Ti in crystal 2 than in crystal 1. A back-scattered electron image (Plates 5.13 and 5.14) shows the crystal to have at least two distinct zones with primary growth zoning in the outer rim. In addition, the tiny bright areas resemble the areas containing a bismuth phase in the centre of crystal 1.

The uranmicrolite from Jooste's pegmatite, Okongava Ost, Karibib (Table 5.2, anal. 5) is rather sparsely distributed in lepidolite. It is very similar to the crystal from the Lepidolite pegmatite, with very fine cracks and the development of subspheroidal areas. These areas, however, have no inner zoning. An average of 8 analyses contained 14.35% UO_2 (range

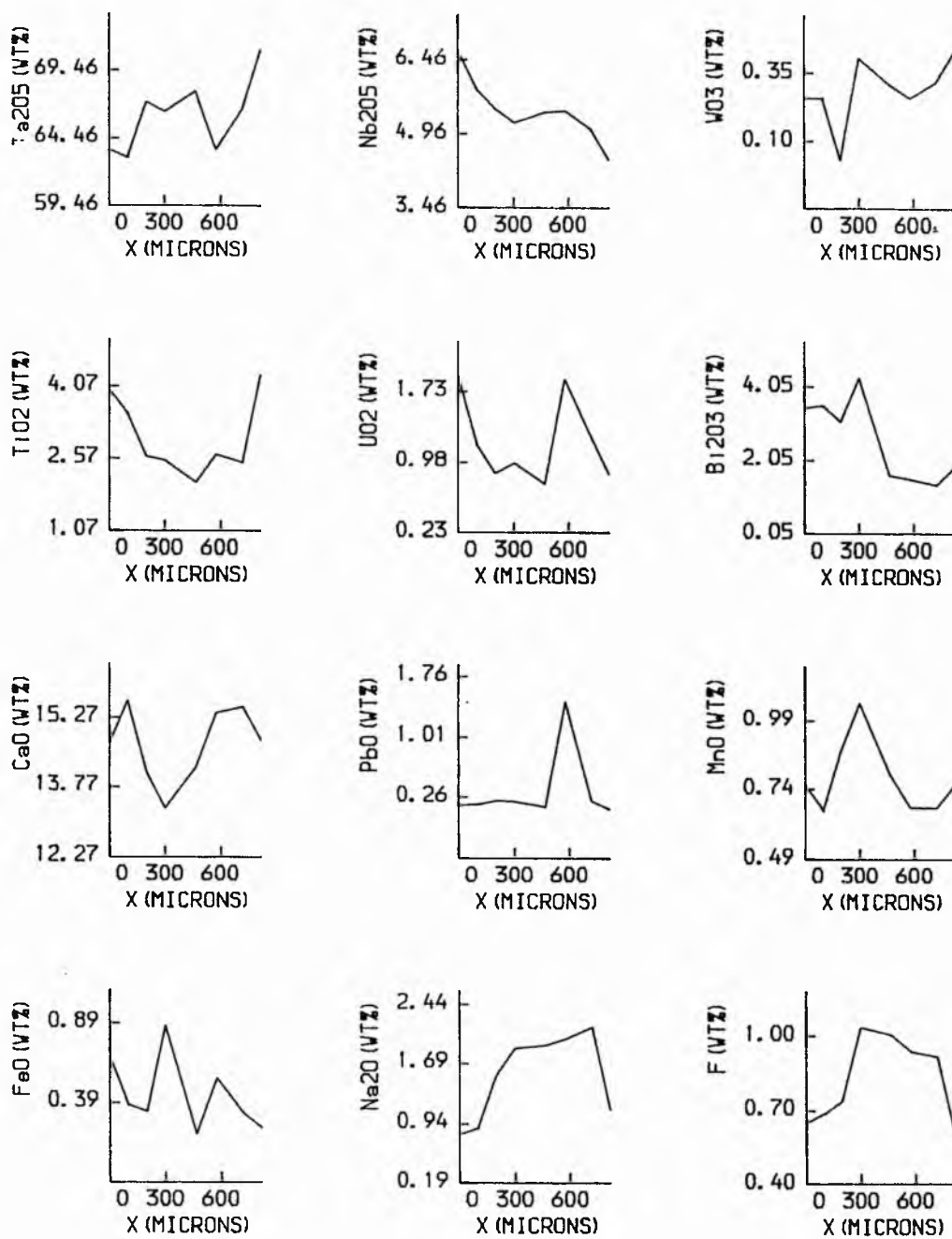


Fig. 5.3. Analytical traverse across uranoan microlite crystal 1, Kokerboomrand pegmatite, Steinkopf, Namaqualand, South Africa.

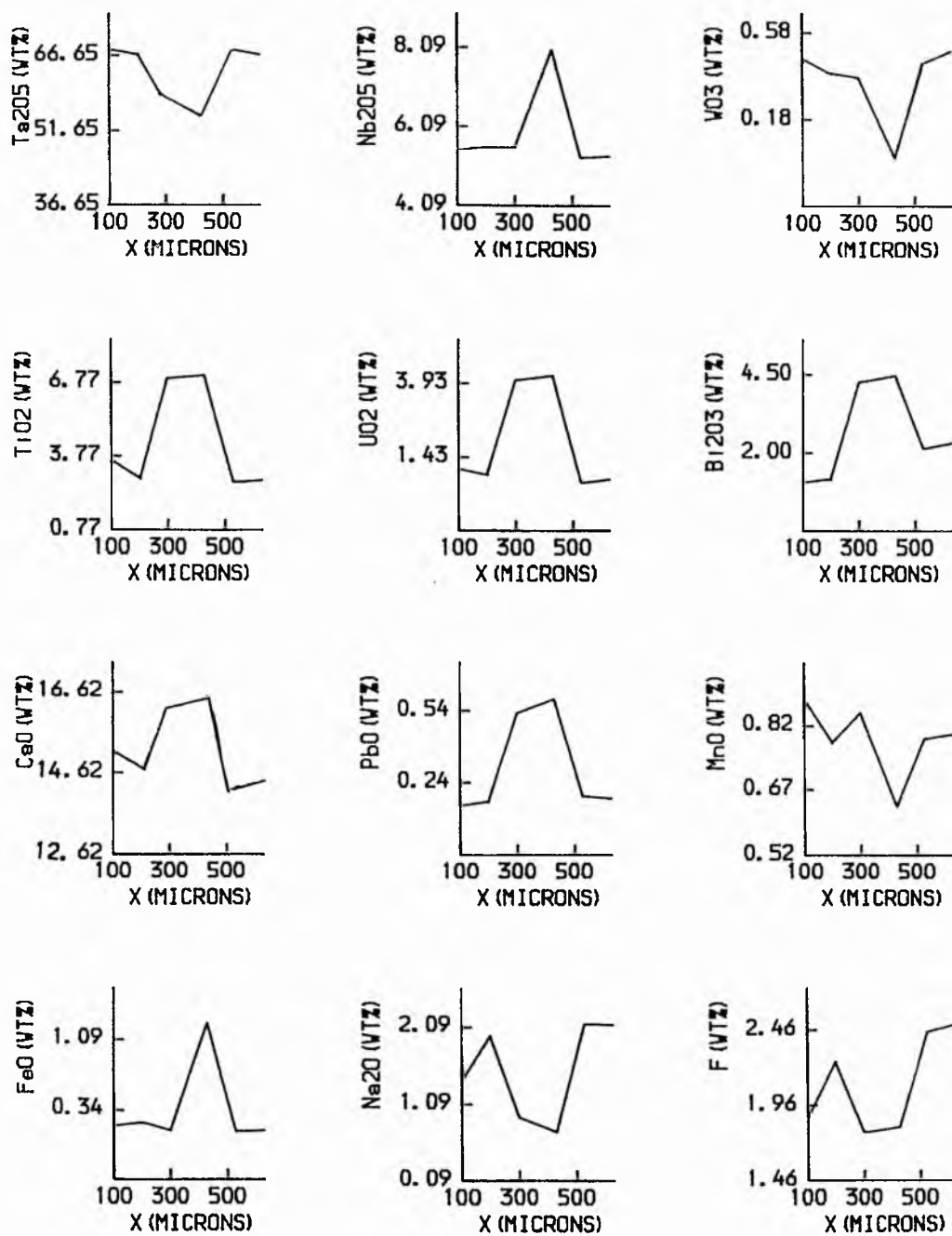


Fig. 5.4 . Analytical traverse across uranoan microlite crystal 2, Kokerboomrand pegmatite, Steinkopf, Namaqualand, South Africa



Plate 5.11. Backscattered electron image of uranoan microlite (crystal 1), Kokerboomrand pegmatite, Steinkopf, Namaqualand. Scale bar: 1000 microns.

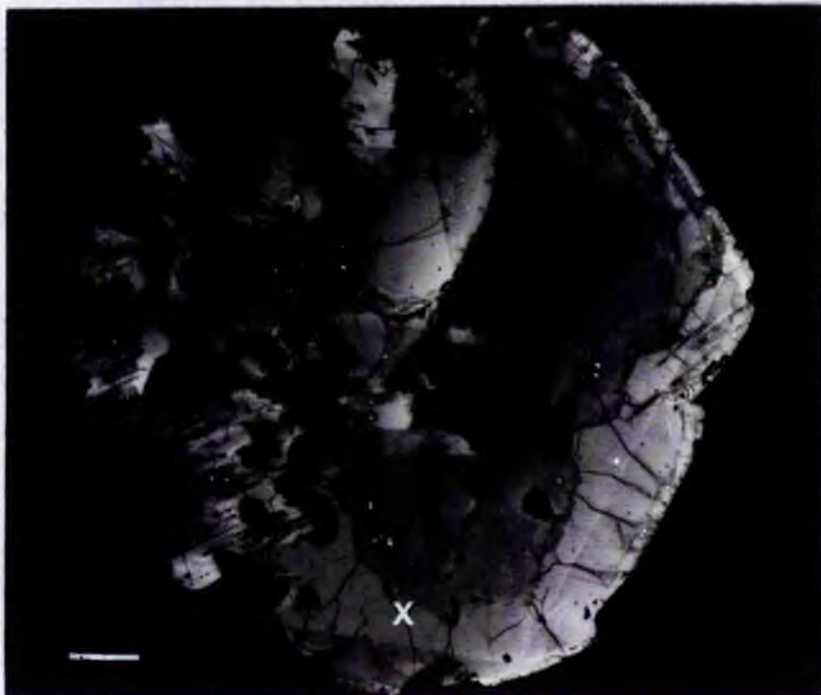
Plate 5.12. Enlargement of central area in Plate 5.11 of uranoan microlite, Kokerboomrand pegmatite, Steinkopf, Namaqualand, showing a bismuth phase (white). Scale bar: 100 microns.





Plate 5.13. Backscattered electron image of uranoan microlite (crystal 2), Kokerboomrand pegmatite, Steinkopf, Namaqualand showing zoning in outer rim and secondary alteration in the centre. Scale bar: 100 microns.

Plate 5.14. Backscattered electron image of altered uranoan microlite crystal 2, Kokerboomrand pegmatite, Steinkopf, Namaqualand. X marks the beginning of an analytical traverse (south to north) across the crystal ; data illustrated in Fig. 5.4. Scale bar: 100 microns.



11.31-15.77%); 56.12% Ta₂O₅ (52.8-59.79%); 13.18 % Nb₂O₅ (10.97-13.9%) and CaO 6.87% (6.2-7.67%). The chemical content of this uranmicrolite varies across the crystal but, unlike the uranoan microlite from Tantalite Valley, is without any concentric pattern in the rim. A composition of this type has been referred to as "djalmaitite" in the literature (Guimaraes, 1939).

5.5. DISCUSSION

The composition of an ideal mineral of the pyrochlore group may be represented by the general formula A₂B₂X₇ (Machatschki 1932, Borodin and Nazarenko 1957, Von Gaertner 1930, Brandenberger 1931, Hogarth 1961, Ginzburg and Gorzhevskaya 1960, Van der Veen 1963 and Hogarth 1977).

In the uranoan microlites containing larger amounts of water and uranium there is a considerable deficiency of cations in the "A" site. This deficiency has been explained by Borodin and Nazarenko (1957) as follows: in pyrochlore, because the substitution in both the "A" and "B" sites is heterovalent rather than isovalent, in the "A" site Na⁺ is replaced by the higher valence cation U⁴⁺ and to a lesser degree by Ca²⁺. This may be compensated for by Ti⁴⁺ replacement of Nb⁵⁺ in the "B" site, and before hydration there is no deficiency in the "A" site. The univalent cation is mainly leached from the less hydrated varieties of pyrochlore; as the hydration process continues, Ca²⁺ is also leached out. The same principles apply to microlite except that Ti⁴⁺ is replaced by Ta⁵⁺.

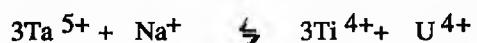
This may be illustrated in microlite by the crystal from the Lepidolite pegmatite. From analyses 3a and 3b (see Table 5.2), if the deficiency in wt.% totals may be considered as water, it can be inferred that a high water content (anal. 3b) is compatible with a low Ca content (4.61% CaO) and a less hydrated centre (anal. 3a) with a high Ca content (15.29% CaO). The rim of the microlite has a total of 0.8 cations in the "A" site, whereas the

water, it can be inferred that a high water content (anal. 3b) is compatible with a low Ca content (4.61% CaO) and a less hydrated centre (anal. 3a) with a high Ca content (15.29% CaO). The rim of the microlite has a total of 0.8 cations in the "A" site, whereas the centre has a total of 2.05 cations (see Table 5.2). Consequently, there is a deficiency in the "A" site cations in the rim with its high water and low Ca content. Eid (1976) observed that the deficiency of "A", cations is usually greater in altered microlite, which contains high water and low F. High water, low F and low Ca characterize the periphery of the microlite from the Lepidolite pegmatite (Table 5.2, anal. 3b).

The change in composition in the crystal from the Lepidolite pegmatite (Fig. 5.2) is quite distinct with no intermediate phases. This is in agreement with Harris (1966) who found compositional changes in pyrochlore to be similarly distinct. However, this contrasts with microlite reported by Mihalik (1967) who found alteration from a deep brown to a clear green variety and a gradual change in composition. Mihalik found that the alteration was effected by the removal of Ca and Mn ions, hydration, and the introduction of Cu and Si; Ta, Nb and U remain unaffected.

The rim area of the microlite from the Lepidolite pegmatite and the uranmicrolite from Okongava (Table 5.2, anal. 5) have some similarities. Ca is low in both; however U is low in the former (averaging 8% as UO_2) and high in the latter (14.35%). This difference is compensated by the combined Ta and Nb contents (Table 5.2, anals. 3b, 5) and corresponds to the suggestion (von Knorring and Fadipe, 1981) that high uranium in microlite is usually accompanied by low tantalum. Both of these microlites have low totals, suggesting high water, and both are deficient in "A" site cations (see Table 5.2, anals. 3b and 5).

Usually the lowest fluorine contents are found in the altered microlites and in Bi, Pb and U microlite (Eid, 1976). In the Kokerboomrand crystal (2) the lowest F content is found with the highest Bi-U-Pb values, in the centre of the crystal (Table 5.2, anals. 4a, 4b). In this crystal, compositional changes from the intermediate to the central area suggest major substitutions of the type:



The two crystals from the Kokerboomrand pegmatite show different characteristics in both fabric and composition. On average, crystal 1 has a low F content (0.8%, see Fig. 5.3) in comparison with crystal 2 containing 1.78-2.27% (Fig. 5.4 and Table 5.2, anals. 4a, 4b). Crystal 1 has also a higher water content (denoted by a low total). Does this denote a higher degree of alteration in crystal 1? It has been suggested (Eid, 1976) that the degree of alteration in microlite is characterized by the amount of hydration and the lowest F contents. Traverses across the two crystals show different trends (see Figs. 5.3. and 5.4) and this may be substantiated by comparisons of the back-scattered electron images of the two crystals (Plates 5.11-5.14). Crystal 1 is simple; as well as having zoning in the rim, there are at least two phases of mineralization. Crystal 2 is complex; it has at least three distinct compositional zones.

5.6. URANIUM PLUMBOMICROLITE

Since completing the paper on replacement phenomena in tantalum minerals (Baldwin, 1989), an opportunity to analyse a Pb-U-microlite materialized. The aim of this investigation is to select specific zoned areas, highlighted by the backscattered electron images, for point analyses rather than taking a general traverse across the crystal, in contrast to the analytical procedure with the microlite crystals from the Lepidolite and Kokerboomrand pegmatites.

Uranium plumbomicrolite is enclosed in an aggregate of manganotantalite at the Rubicon Mine, Okongava Ost, Karibib (Plate 5.15). The crystal aggregate of tantalite with broken grain boundaries, lying in lithian mica, is intergrown or possibly partially replaced by microlite. In contrast to the Kokerboomrand crystals, the microlite areas, although having distinct grain boundaries, are totally anhedral. The relationship between the crystal aggregate of manganotantalite and the microlite is shown in more detail in Plate 5.16. The tantalite and microlite are very intergrown.

Two specific inclusions of microlite which were used for detailed analysis, designated as Incl/1 and Incl/2 are indicated in Plate 5.15. The areas of analyses were selected in conjunction with the backscattered images which show the change in composition in the crystal; 15 analyses were taken on "inclusion 1" including 2 analyses of the matrix mineral manganotantalite and one specific area on Incl/2 for verification. The analysed areas are numbered in Plates 5.17 (Incl/1) and 5.18 (Incl/2) and the resulting analyses are given in Table 5.5.

The very bright areas seen on the backscattered image of Incl/1 (Plate 5.17) at the periphery of the microlite contain the highest concentrations of lead (Table 5.5. anal. R/5, R/6, R/12-14) from 11.37 to 21.98% PbO. Analyses in the inner areas contain

approximately 2% PbO. Analysis R/7 with 8.25% PbO is located in a darker zoned area just in from the periphery.

This particular texture in microlite is typical of metamict varieties of uranmicrolite. The UO_2 content varies from 12.89 to 16.81, the highest values of 16.71 and 16.81% correspond to the lighter zoned area near the centre, and analysis 16 with 15.91% UO_2 (Plate 5.18) corresponds also to a lighter, brighter zoned area, which verifies the previous result on Incl/1. The Ta_2O_5 content varies from 46 to 59%, it appears to correlate more with Pb than with U. Analyses R/5, R/6, R/12, R/13 with high lead contain 57, 59, 46, 52% Ta_2O_5 ; perhaps there is more correlation between Pb and combined water. There is less than 0.80% F in this microlite therefore H_2O can be expected and this may be suggested by the low totals.

Nb_2O_5 varies from 2 to 12%, however the sum of Nb and Ta is not constant throughout the crystal, the highest combined values being in the lighter zoned areas (anals R/ 3,4 and 16.) corresponding to the highest uranium. These areas also appear to contain the least water and this being the only real correlation that is apparent, apart from the fact that Pb is concentrated round the periphery of the crystal. Pb has a negative correlation with Nb, U, Mn, Na, Ca and F and a positive correlation with Ta however, the highest correlation coefficients are 0.54 with Ca and 0.56 with Nb.

The ions per 2B are presented in Table 5.5 (calculated according to Hogarth, 1989). This microlite is a uranmicrolite as it contains more than 20 % of U atoms in the 'A' site. Pb is the principal constituent in analyses R/ 5, R/12, and R/14, containing more than 20% of Pb atoms in the 'A' site, over and above the U atoms, therefore these are plumbomicrolite or uranium plumbomicrolite. In addition, analyses R/6, R/7 and R/13 are plumbian uranmicrolite (Hogarth, 1977). The B-site cations are plotted on the similar Ta, Nb, Ti (+Al+Fe+Sn) ternary diagram plotted from Table 5.2 (see Fig. 5.1b) and these are

shown in Figure 5.5. The new data plots into the microlite field as established by Hogarth (1977) (see Fig. 5.1c). The microlite is lying in manganotantalite with 53% Ta_2O_5 , 29% Nb_2O_5 , 16% MnO and 0.53% FeO (R/11). There are only traces of PbO (0.06%) and 0.32% UO_2 in this manganotantalite which is zoned (see Plate 5.16).

Plate 5.15 shows patchy intergrowths of uranmicrolite and manganotantalite. However, the outlines of the microlite intergrowths studied are distinct and a replacement origin for the microlite cannot be identified by the textural intergrowth. The manganotantalite aggregate on the otherhand has corroded edges perhaps implying that the manganotantalite was the primary phase, with Li-mica and possibly microlite as later phases.

The accumulation of Pb around the periphery of the crystal is an interesting feature. One explanation may be a zoning effect whereby late metasomatic fluids were enriched in Pb. The zoning in the crystal due to radioactive decay may suggest radiogenic lead. However, the actual decay process should not cause a migration of Pb or U and proportionally the relationship of Pb to U, if this is radiogenic Pb, should technically be the same throughout the crystal even though the decay rates of the three isotopes are different. Another process must be involved if Pb has migrated to the periphery of the microlite.

Other minerals containing lead occur in the Rubicon pegmatite, for example, pyromorphite $Pb_5(PO_4)_3Cl$ and mottramite $PbCu(VO_4)OH$ were located in a matrix of bismuth minerals and quartz. The analyses of the pyromorphite and mottramite are shown in Table 5.6. The presence of other Pb minerals at Rubicon supports an origin of late crystallization in the periphery of the microlite crystals from the same pegmatites.

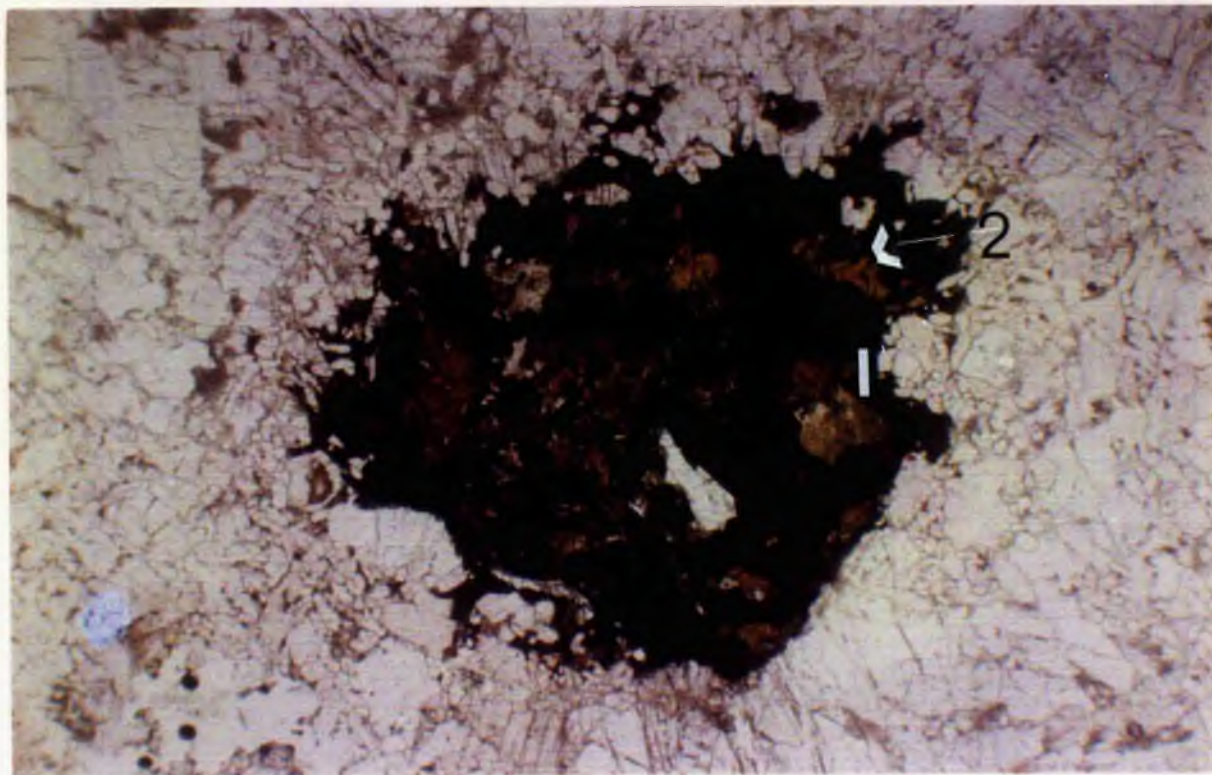
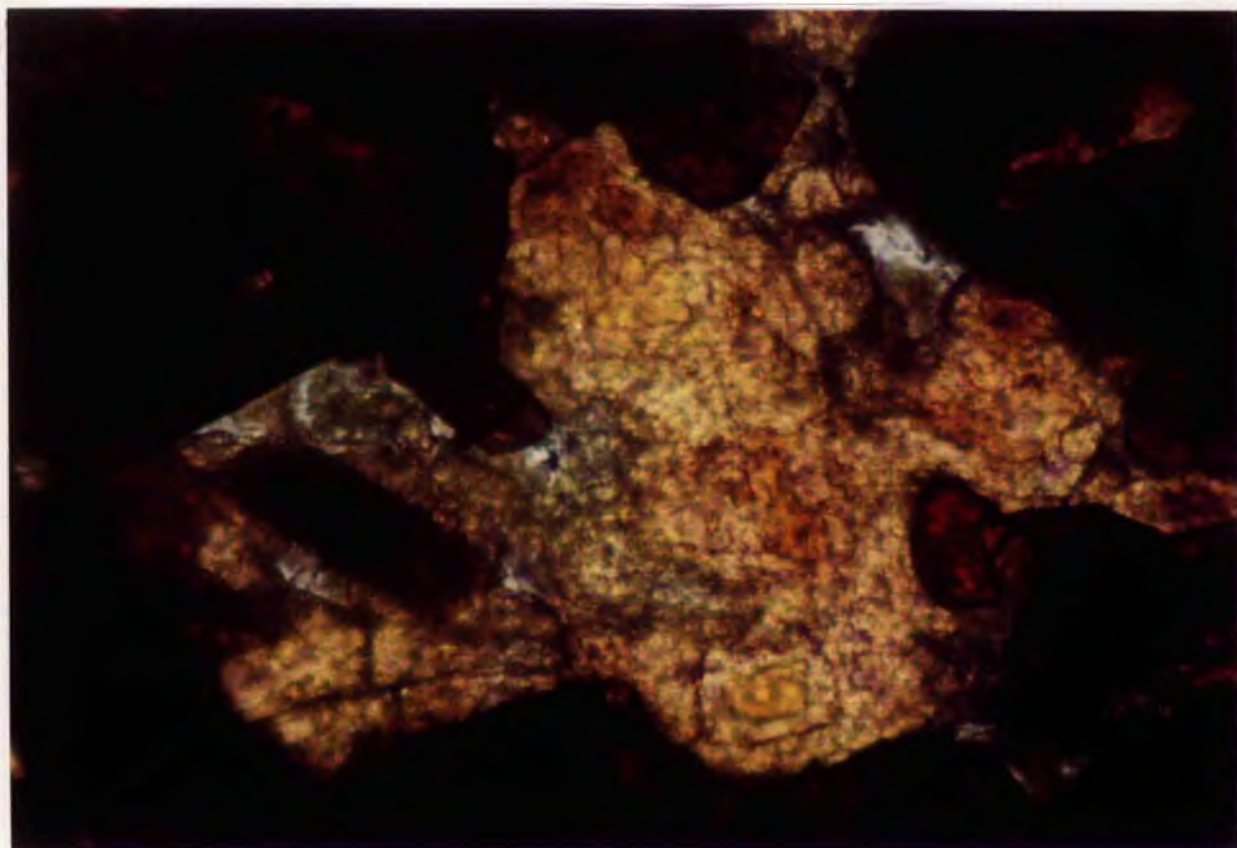


Plate 5.15. An aggregate of manganotantalite (black) containing inclusions of microlite (light brown) enclosed in purple Li-mica (colourless in this photomicrograph) Rubicon pegmatite, Karibib, Namibia. Manganotantalite aggregate 2 x 2 mm.

Plate 5.16. An enlargement of centre top area of Plate 5.16 showing intergrowths of zoned manganotantalite (red-brown) and microlite (yellow). Scale bar: _____ 200 microns



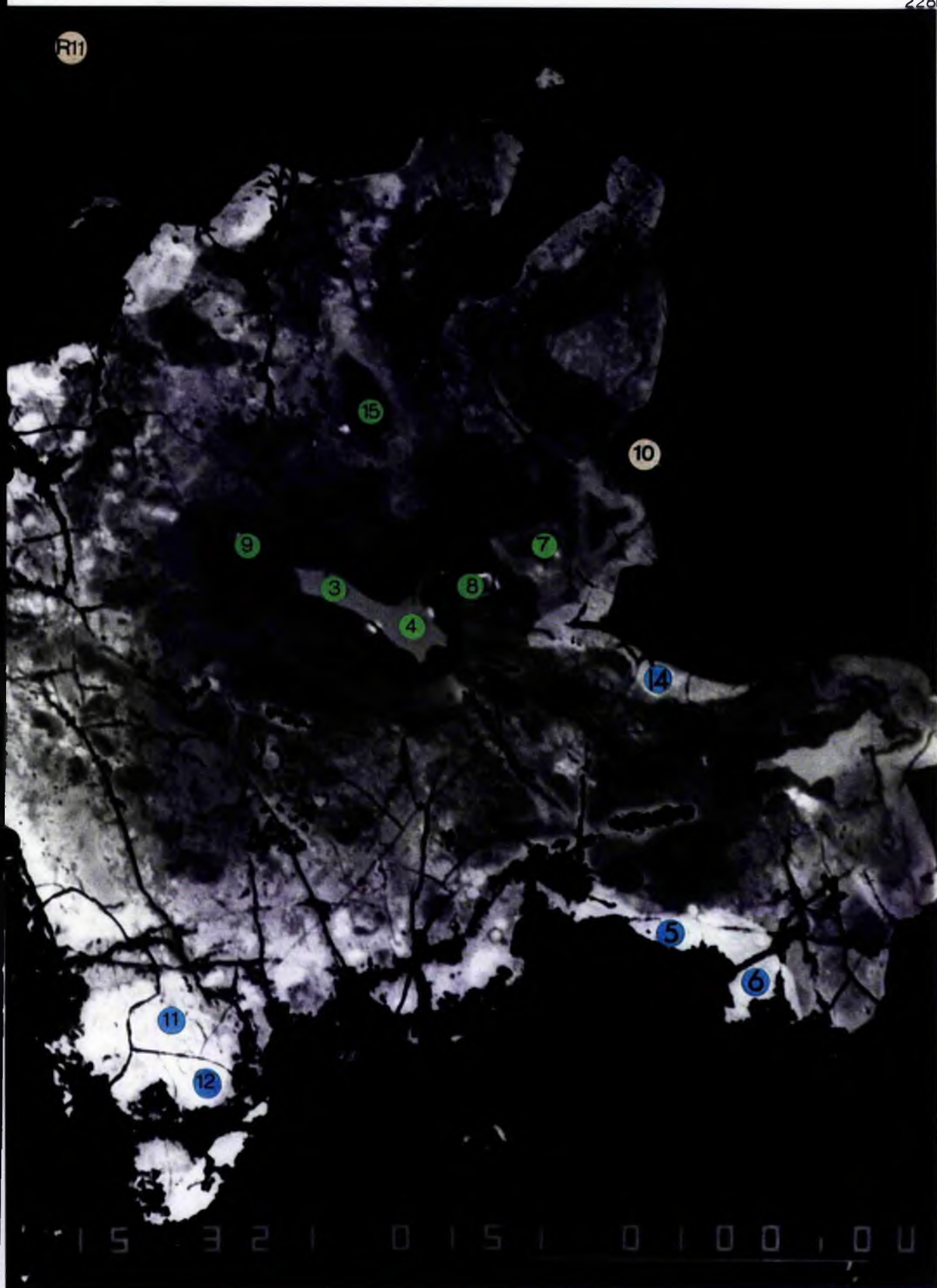


Plate 5.17. A BSE image of Pb-U-microlite (inclusion1) occurring in manganotantalite. The zoning is due to lattice damage caused by radiation; point analyses shown in Table 5.5 & 4.3
Scale bar: 100 microns

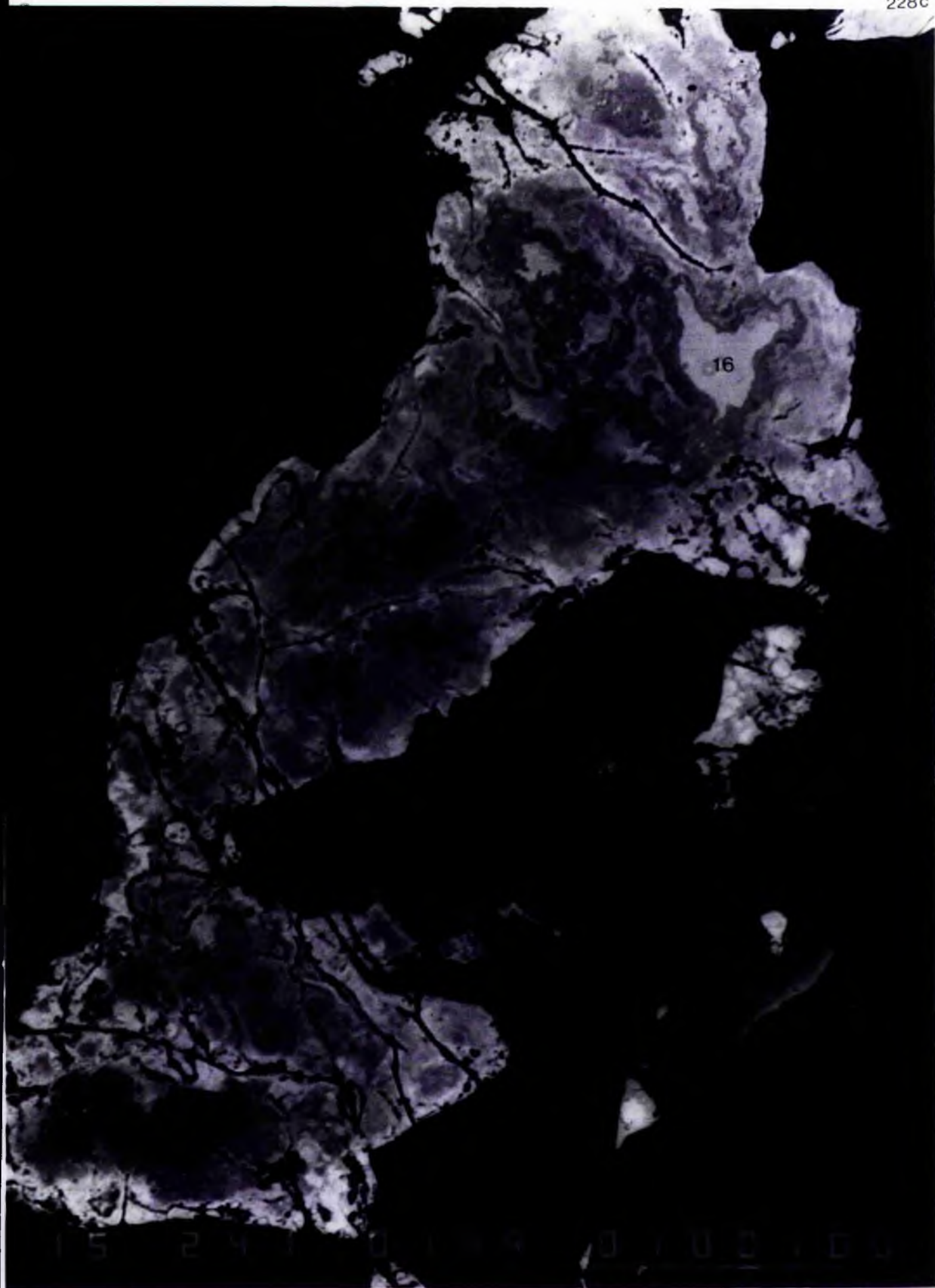


Plate 5.18. A BSE image of Pb-U-microlite (inclusion 2). The zoning is due to lattice damage caused by radiation. Point 16 represents a U-rich area (see Table 5.5) and the light area at the periphery a Pb-rich area. Scale bar: 100 microns.

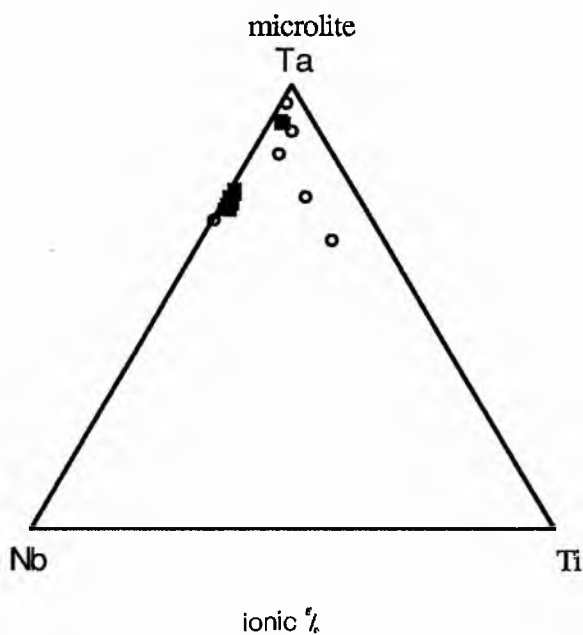


Fig. 5.5. Pb-U-microlite plotted on a Ta, Nb, Ti (+Sn+Al+Fe^{III}) ternary diagram (data from Table 5.5, denoted by black symbol). The diagram includes the data of secondary, uranoan and uranmicrolite from Table 5.2 (denoted by "o"). Ti includes minor amounts of Al, Fe, Sn.

TABLE 5.5. Plumbomicrocline, plumbian uranmicrocline, Rubicon pegmatite, Karibib (sample R)

R	R/3.	R/4.	R/5.	R/6.	R/7.	R/8.	R/9.	R/12.	R/13.	R/14.	R/15.	R/16.
Ta ₂ O ₅	58.31	57.85	57.06	59.86	51.92	53.38	54.51	46.24	52.33	58.33	52.39	58.01
Nb ₂ O ₅	11.42	11.76	2.23	2.20	10.71	11.37	12.00	8.09	9.63	2.16	11.46	10.45
SnO ₂	0.13	0.15	0.16	0.20	0.19	0.13	0.17	0.11	0.16	0.17	0.16	0.25
Al ₂ O ₃	0.07	0.07	0.08	0.07	0.08	0.06	0.07	0.06	0.06	0.07	0.07	0.06
UO ₂	16.71	16.81	13.11	14.06	15.67	16.20	16.22	12.89	14.91	13.74	16.15	15.91
Fe ₂ O ₃	0.01	0.04	0.29	0.43	0.26	0.05	0.08	0.12	0.16	0.21	0.28	0.00
Bi ₂ O ₃	0.00	0.00	0.08	0.00	0.00	0.00	0.00	0.00	0.00	0.07	0.00	0.00
CaO	3.41	3.37	0.99	0.95	2.63	4.26	2.96	1.00	1.76	0.70	7.41	4.27
PbO	2.25	2.09	15.44	11.37	7.70	2.89	1.57	21.98	12.19	15.59	1.58	1.90
MnO	2.14	1.86	0.94	0.54	1.07	1.11	1.64	1.38	0.81	1.26	1.94	2.19
Na ₂ O	2.16	2.41	0.08	0.08	0.05	0.02	0.06	0.03	0.19	0.43	0.62	3.49
F	0.05	0.24	0.00	0.00	0.07	0.32	0.21	0.00	0.00	0.00	0.79	0.00
	96.66	96.65	90.46	89.76	90.35	89.79	89.49	91.9	92.2	92.73	92.85	96.53

	IONS per 2B											
site B	2	2	2	2	2	2	2	2	2	2	2	2
Ta	1.499	1.483	1.836	1.833	1.461	1.465	1.449	1.530	1.511	1.850	1.440	1.527
Nb	0.488	0.501	0.119	0.112	0.501	0.519	0.530	0.445	0.462	0.114	0.524	0.457
Sn	0.005	0.006	0.008	0.009	0.008	0.005	0.007	0.005	0.007	0.008	0.006	0.010
Al	0.008	0.008	0.011	0.009	0.010	0.007	0.008	0.009	0.008	0.010	0.008	0.007
Fe ⁺⁺⁺	0.001	0.003	0.026	0.036	0.020	0.004	0.006	0.011	0.013	0.018	0.021	0.000
Total	2	2	2	2	2	2	2	2	2	2	2	2
site A	0	0	0.002	0	0	0	0	0	0	0.002	0	0
Bi	0.351	0.352	0.345	0.352	0.361	0.364	0.353	0.349	0.352	0.356	0.363	0.342
U*	0.345	0.340	0.126	0.115	0.292	0.461	0.31	0.130	0.200	0.088	0.802	0.443
Ca	0.057	0.053	0.492	0.345	0.214	0.079	0.041	0.720	0.348	0.489	0.043	0.050
Pb	0.171	0.149	0.094	0.052	0.094	0.095	0.136	0.142	0.073	0.125	0.166	0.180
Mn	0.396	0.440	0.018	0.018	0.01	0.04	0.011	0.007	0.039	0.097	0.122	0.655
Na	1.321	1.334	1.077	0.880	0.971	1.002	0.851	1.348	1.012	1.157	1.496	1.668
Total	0.003	0.013	0.0	0.0	0.004	0.017	0.011	0.0	0.0	0.0	0.042	0.0

5,12,14, plumbomicrocline or uranium-plumbomicrocline. 6,7,13, plumbian uranmicrocline. 3,4,8,9,15,16, uranmicrocline.

TABLE 5.6. PYROMORPHITE AND MOTTRAMITE

Section 5	<u>Pyromorphite</u> $Pb_5(PO_4)_3Cl$						
	5/1	5/2	5/3	5/4	5/5	5/6	5/7
P ₂ O ₅	18.23	17.42	16.41	18.46	17.05	17.11	17.97
Bi ₂ O ₃	0.23	0.51	0.47	0.00	0.11	0.25	1.00
SiO ₂	2.54	0.57	0.26	0.13	0.55	0.28	0.09
CaO	3.71	3.42	0.59	4.02	2.14	2.19	5.48
PbO	73.25	74.20	79.27	75.20	76.75	77.21	72.69
CuO	0.21	0.27	0.29	0.19	0.54	0.06	0.37
Cl	3.02	2.61	2.70	2.99	2.89	2.64	2.88
V ₂ O ₅	0.03	0.08	0.03	0.21	0.06	0.04	0.00
Total	101.2	99.1	100.0	101.2	100.1	99.8	100.5

No. of ions based on 13 oxygens

P	2.96	3.08	3.13	3.17	3.09	3.13	3.08
Cl	0.98	0.92	1.03	1.03	1.05	0.97	0.99
V	0.00	0.01	0.00	0.00	0.01	0.01	0.0
Pb	3.79	4.17	4.81	4.11	4.43	4.50	3.95
Si	0.49	0.12	0.06	0.03	0.12	0.06	0.02
Ca	0.76	0.77	0.14	0.87	0.49	0.51	1.19
Cu	0.03	0.04	0.05	0.03	0.09	0.01	0.06
Bi	0.01	0.03	0.03	0.00	0.01	0.01	0.05

9.0 9.1 9.2 9.2 9.3 9.2 9.3

Mottramite $PbCu(VO_4)OH$

	5/8	5/9	5/10	5/11	5/12	5/13	5/14	5/15	5/16	5/17
P ₂ O ₅	5.20	0.72	0.69	0.58	5.49	0.78	5.76	6.04	3.32	2.52
V ₂ O ₅	17.31	20.81	20.13	20.27	17.02	20.84	16.53	16.54	19.75	11.27
PbO	52.12	53.22	54.50	53.83	52.48	53.25	51.72	51.67	51.69	55.77
CuO	18.45	17.50	17.11	17.51	18.45	17.90	18.62	18.86	19.21	19.50
CaO	1.13	0.29	0.33	0.33	1.42	0.36	1.17	1.32	1.16	0.33
SiO ₂	0.07	1.03	0.79	0.71	0.20	0.94	0.28	0.11	0.16	0.49
Bi ₂ O ₃	0.39	0.44	0.45	0.43	0.31	0.10	0.39	0.16	0.30	8.20
Cl	0.10	0.29	0.04	0.01	0.14	0.11	0.00	0.15	0.04	0.04
Total	94.77	94.3	94.04	93.67	95.51	94.28	94.47	94.85	95.63	98.12
H ₂ O	2.30	2.20	2.15	2.14	2.33	2.21	2.31	2.33	2.32	1.94

No. of ions based on 10 oxygens

P	0.57	0.08	0.08	0.07	0.60	0.09	0.63	0.66	0.36	0.33
V	1.49	1.88	1.86	1.87	1.45	1.87	1.42	1.41	1.68	1.15
Pb	1.83	1.95	2.05	2.03	1.82	1.95	1.81	1.80	1.80	2.32
Cu	1.82	1.80	1.80	1.85	1.80	1.84	1.82	1.83	1.87	2.28
Ca	0.16	0.04	0.05	0.05	0.20	0.05	0.16	0.18	0.16	0.06
Si	0.01	0.14	0.11	0.10	0.03	0.13	0.04	0.01	0.02	0.08
Bi	0.01	0.01	0.02	0.02	0.01	0.00	0.01	0.01	0.01	0.33
Cl	0.00	0.07	0.01	0.00	0.03	0.02	0.00	0.03	0.01	0.01
OH	1.0	1.0	1.0	1.0	1.0	1.0	1.0	1.0	1.0	1.0

6.9 6.97 6.98 6.99 6.9 6.9 6.9 6.9 6.9 7.6

Analyst: P.Hill

5.7.

GENERAL DISCUSSION

A uranmicrolite from Okongava, Karibib, contains 14.35% UO_2 and 56.12% Ta_2O_5 . This appears to be the second occurrence of the species according to the IMA definition (pers. comm., Hogarth, 1989). In general, the major changes in composition in uranoan microlite in this study are characterized by a loss in Ca and F, hydration and a gain in Ta. In uranoan microlite, containing Bi, the major changes involve U, Bi, Ca and Ti on the one hand and Ta and Na on the other. The role of water is unclear.

A traverse across a 1.3 mm crystal of uranoan microlite revealed two essentially different compositions; a rim, 200 μm wide and a central area. The transition zone between the two compositions is very distinct. Electron probe examination does not reveal any zoning, only that the rim contains more Ta than the central area. Alteration appears to have developed along very fine fissures and has proceeded by dividing the original crystal into subspheroidal areas. Both the uranoan microlite from the Lepidolite pegmatite and the uranmicrolite from Okongava appear similar in internal structure. These textures characterize metamict varieties of the pyrochlore group.

The crystals from the Kokerboomrand pegmatite have completely different characteristics from the two previous crystals and are also different in replacement from each other. They are both distinctly zoned, showing both primary zoning and replacement features. Crystal 2 is complex; the outer zones show crystal face parallel zoning and wedge zoning and the internal area an unzoned encrustation, probably replacement, with specs (approximately one micron) of a bismuth phase. Crystal 1 is simpler, the outer zones are similar to crystal 2 with oscillatory and wedge zoning, probably primary in the outer rim, with patchy non-planar zoning in the centre. However, although the bismuth phase, (partially bismuth metal) characterized by the very bright areas in the centre of Figs 5.11 and 5.12 is more pronounced, the replaced area or area showing alteration which occurs

Table 5.7 shows a schematic diagram with the suggested alteration sequence of tantalite and tapiolite and the processes responsible for these changes.

Tantalite and microlite are associated with cleavelandite albite and Li-mica. Therefore Ta (Nb) are associated primarily with albitization and the formation of relatively coarse-grained cleavelandite units - the last stage of coarse-grained crystallization that preceded the fine-grained post magmatic pseudomorphism of the primary lithium minerals which are contemporaneous with the post magmatic alteration of microlite to secondary microlite.

It is suggested that microlite may form in two different ways, from a highly differentiated source magma rich in Na, Ta, Nb etc. contemporaneous with the formation of cleavelandite and tantalite and at a later metasomatic stage associated with Li-muscovite - perhaps forming simultaneously, which will account for the replacement and intergrowth of microlite crystals.

Li-mica intergrowths with microlite crystals is the rule rather than the exception and it is suggested that the anhedral or subhedral formation of microlite crystals is due to replacement possibly by post magmatic fluids where the octahedral crystals have been corroded at the edges. The crystals show compositional wedge and oscillatory primary zoning and are affected by internal alteration and replacement. It is suggested that these microlite crystals were formed from a highly differentiated late-stage magma rich in Ta, Nb, Bi and U containing acidic volatiles, specifically fluorine. The internal alteration may be attributed to 1) radiation due to U in which case the whole crystal texture has been altered to spheruloids or 2) post magmatic fluids, rich in bismuth etc. which have affected certain areas and corroded the crystal., the primary growth compositional zoning is still present in the centre and the bismuth phases are associated with the corroded areas. However, certain crystals have no bismuth phase and relatively large corroded areas in the centre. The muscovite matrix mineral is a fine-grained green greisen most probably

replacement in origin. The F composition of the crystals are different probably reflecting the F content of the fluids at the time of crystallization. Peripheral alteration of microlite grains is most probably due to post magmatic fluids effecting metasomatic alteration with OH being exchanged for F; the aqueous fluids, possibly rich in Ta, leaching Ca from the outer rims of the crystals.

It is suggested that in the presence of F and OH species and Ca and Na metasomatism (alkaline metasomatism) that tantalite may be replaced by microlite. In this case as there are no backscattered images it has not been ascertained whether this replacement microlite is compositionally zoned or not. In the two cases documented in this study, this microlite (and tantalite) are both occurring in cleavelandite.

TABLE 5.7.

Microlite occurrences

Locality	Compositional zoning	Matrix Mineral	Microlite Replacement.	Alteration
Jooste's, Karibib White City, Tantalite V	unzoned discontinuous	Li-mica + cleavelandite Li-mica + cleavelandite	— —	
Noumas, Namaqualand Homestead, Tant. Valley Rubicon, Karibib	dendritic replacement patchy zoning unzoned	Cleavelandite Ta-laths montebrasite	Tantalite Tantalite	
Rubicon, Karibib *Lepidolite, Tant. Valley	U and Pb(radiation) Lattice distortion due to U radiation	Li-mica Li-mica	Tantalite —	Y
*Kokerboomrand	Wedge and oscillatory	Green mica greisen	—	Y
Farm Schonau, Warmbad	Radioactive	albite	Tapiolite	
Okongava Ost, Karibib	Lattice distortion due to radiation	Li-mica	—	

* Secondary alteration of the microlite due to post magmatic fluids

It is suggested that the Ta laths in microlite are contemporaneous with the post magmatic fluid alteration of montebrasite to secondary montebrasite and apatite. The presence of Ca in late stage fluids could account for the presence of microlite; the leaching of Ca from microlite could account for the formation of apatite at the junction of the montebrasite and crosscutting the tantalite. It is suggested that the Mn-tantalite laths are intergrown with the microlite because of a lack of F due to the simultaneous crystallization of montebrasite. F and Ca released from microlite (+P) enabled apatite to form and cut across the microlite and Ta laths.

The usual occurrence of tantalite is in cleavelandite, suggesting that the "late stage differentiated magma" is rich in Ta and (Nb, U, Bi, W, Pb, Sn); when F-rich post magmatic fluids are available in conjunction with Ta, microlite is formed.

Tourmaline is usually associated with major cleavelandite and minor Li-mica. On the basis that cleavelandite is earlier than Li-mica, late differentiated magma still contains boron. Though black tourmaline, schorl, is prolific in the primary zones of pegmatite crystallization and boron is not necessarily available in the postmagmatic late stage fluids. This is due to the lack of availability of boron generally in the late stages as boron tends to crystallize in black tourmaline in the primary wall rock magmatic crystallization (London, 1992). Experimental evidence of tantalite and tapiolite crystallization temperatures are scarce, however, see wodginite for some details. Otherwise on the suggested temperature scale given by some authors tantalite and tapiolite crystallize at temperatures below 400°C (see Chapter 7).

CHAPTER 6.

EXTREME FRACTIONATION OF Rb, Cs, Ba, Ta AND Mn

6.1. INTRODUCTION: THE K/Rb AND K/Cs RATIOS

The aim of this chapter is to show different fractionation trends in Rb, Cs, Ba, Mn and Ta. This will highlight varying paths of differentiation in contrasting rare element pegmatites in Karibib and Tantalite Valley, Namibia, and the Steinkopf area, Namaqualand. As Rb and Cs partition into late crystallizates and are generally controlled by the lithian micas (and K-feldspar) these elements are useful indicators of evolving magmas and fluids.

The lithian micas may have substantial concentrations of Rb and Cs (Gordiyenko, 1971; Rinaldy et al., 1972, Baldwin, 1985). So far, no independent minerals of Rb are known, whereas caesium forms only one, pollucite. This mineral is a characteristic, though very rare, constituent of complex rare-element pegmatites which have reached the highest level of differentiation, either as a late member of primary crystallization or as a product of late-replacement and albitization (von Knorring, 1985; Cerny et al. 1985).

Several authors have investigated Rb, Cs and Li concentrations in Li-micas or microcline including Gordiyenko (1971), Rinaldy et al. (1972), Trueman and Cerny (1982), Cerny et al. (1985), Baldwin (1985) and von Knorring (1985). Gordiyenko (1971), who made a study of the distribution of Li, Rb and Cs in lepidolite specimens from various pegmatite fields, including the Karibib pegmatites, reports Cs values of 1.13%, Rb values of 1.43% and Li values of 2.05%. These results are in agreement with the present results from the Karibib pegmatites with regard to Cs, but higher Li and Rb values have been recorded from the pegmatites investigated in this study.

Von Knorring (1985) has determined Li_2O on Li-mica samples from Karibib rare-element

pegmatites and some of these samples have been additionally used to determine Rb and Cs in this study. Cerny et al. (1985) have reviewed the available data of Rb and Cs from various pegmatite fields and have presented their results diagrammatically as elemental abundances and various ratios. The results from this present study have been plotted to show the elemental concentrations and levels of fractionation of Rb and Cs in the three separate co-genetic pegmatite groups from Karibib and Tantalite Valley, Namibia, and the Steinkopf area, Namaqualand.

Rb behaves in a similar way to K geochemically. The radii of these two singly-charged cations are very close and consequently Rb^+ is able to substitute for K^+ freely, which accounts for their mutual fractionation in igneous processes. Cerny et al. (1985) have pointed out that additional factors may be their almost equal ionization potentials and electronegativities. Rb-enrichment occurs in high silica granitic melts. An even more marked concentration of Rb occurs in the transition from leucogranites and pegmatitic granites to highly fractionated pegmatites (Cerny et al. 1985). The mechanism of Rb-enrichment, however, is not entirely understood. Hildreth (1979, 1981) and Ludington (1981), advocate liquid fractionation, in particular thermogravitational convection-diffusion whereby Ta, Li, Rb, Cs along with volatiles such as F, P and B partition into the low density phase which accumulates in the apex of the solidifying granite. Volatile saturated alkali-rich granitic liquid is therefore concentrated in the roof zone of the granite. The lithophile affinity of Rb for H_2O and F, with the ability to form complexes, are favoured by some authors (Hildreth 1979; Burt et al., 1982) as a means of concentration. An appeal to marked changes in crystal/melt partition coefficients as the bulk-composition moves from lower to higher concentrations of SiO_2 have been made by other authors (see Cerny et al., 1985). Rb-enrichment reaches 4.98 wt.% in K-feldspar, 6.35% in muscovite and 4.72% in lepidolite with respective K/Rb ratios of 1.90, 1.15 and 1.37 (Cerny et al., 1985).

In contrast to Rb, the geochemical behaviour of Cs is less closely related to that of K, the governing factor being the large size of the ionic radii of Cs⁺ (1.67 Å) compared to K⁺ (1.33 Å). Therefore Cs⁺ is admitted into K⁺ minerals more selectively than Rb⁺ and consequently the dispersion of Cs⁺ in igneous processes is more marked than Rb (Ahrens, 1966). The main carriers of Cs in complex differentiated pegmatites in order of increasing concentration are K-feldspar, micas, beryl and pollucite. Cerny et al. (1985) have summarized Cs and Rb concentrations from the literature. In pollucite-bearing pegmatites K-feldspar attains 500-4000 ppm Cs in the Varutrask pegmatite, Sweden and in the Tanco pegmatites, Manitoba. The highest Cs concentration ever recorded seems to be 4240 ppm in a microcline from northeastern Manitoba, with K/Cs of 22.4. In lithian mica and lepidolite Cs reaches 1.79wt.% , with K/Cs close to 4.

Li, Rb and Cs were determined in lithian mica, muscovite, biotite, and in K-feldspar from differentiated pegmatites in 1) the Karibib/Usakos area, 2) Tantalite Valley, and 3) the Steinkopf area, Namaqualand. In addition, two pegmatites in Tantalite Valley, Witkop and Chickenfoot, were sampled more extensively to obtain representative samples of K-feldspar from each specific pegmatite zone. The Kenhardt area of the Northern Cape, South Africa contains only sporadic lithium minerals and few samples have been analysed from this area. Analyses were carried out by XRF and flame photometric techniques with a few additional determinations by the electron microprobe (see Appendix 2). These three methods verified the consistency of the results.

Unless otherwise stated, all the plotted data showing abundances of Rb and Cs and levels of fractionation, are given in weight % and ratios. The experimental error bars are smaller than the symbols in the following plots. For Cs by AA techniques the experimental error up to the 1% level is ± 5 ppm, for Rb by this method the error is up to the ± 50 ppm at the 3% level. The error for Rb by XRF by which method most Rb determinations were made is ± 200 ppm at the 2-3% level and ± 20 to ± 50 ppm. at levels of 1% . B has a higher

experimental error : at the 300 ppm level ± 40 ppm and at the 30 ppm level $\pm 10-15$ ppm. At the 10% K level the error is $\pm 0.05\%$.

6.2. RUBIDIUM AND CAESIUM IN LITHIAN MICAS

6.2.1 Rb,Cs and Li data from the Karibib/Usakos rare-element pegmatites, Namibia

The commonly used plot of Rb versus Cs in pegmatitic Li-mica shows a broadly scattered but essentially positive correlation for the Karibib rare-element pegmatites (Fig. 6.1).

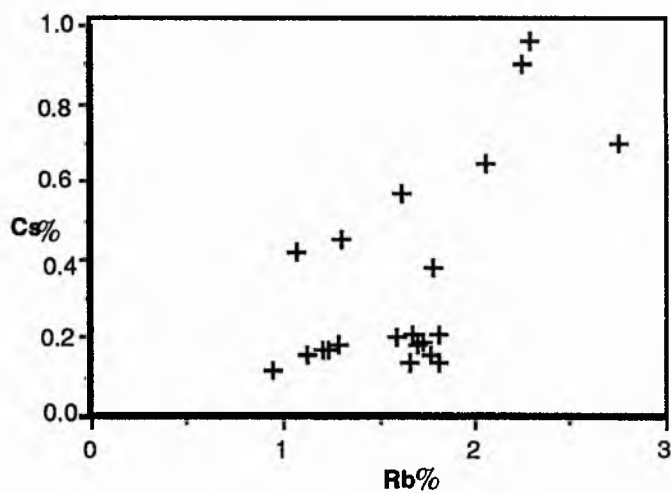


Fig. 6.1. Plot of Rb versus Cs wt.% in pegmatitic Li-micas for the Karibib area, Namibia, with a correlation coefficient of 0.429 (error for Rb ± 50 ppm, Cs ± 5 ppm, error bars are insignificant).

The data for Rb, Cs, K_2O and Li_2O and the K/Rb, K/Cs and Rb/Cs ratios for lithian micas from the Karibib area are shown in Table 6.1. Specimens were collected from eight pegmatites; five individual pegmatites, namely Daheim, Okongava (Jooste's), Okatjimukuju, Rubicon and E tiro have been sampled more extensively (see Figs. 2.9, 2.10 for localities).

The Daheim pegmatite contains the highest Rb in Li-micas with 2.76 wt.% followed by the

Okongava pegmatite with 2.25% Rb and the pegmatite Li-micas from Okatjimukuju and Rubicon with Rb contents as high as 1.81 and 1.73% respectively (see Table 6.1). The K/Rb ratios increase from 3.3 at Daheim to 5.1 at Rubicon. There is a variation within each pegmatite, for example the K/Rb ratio at Daheim varies from 3.3 to 3.9 and at Etiro from 7.1 to 9.3. Figure 6.2 shows the K/Rb versus Rb trends for Li-mica for the three series of rare-element pegmatites, Karibib, Tantalite Valley and Namaqualand. The trends are largely parallel, in fact identical for Tantalite Valley and Namaqualand, but the trend for Karibib shows a small but significant difference in the rate of Rb accumulation, Rb is more highly fractionated in the Karibib pegmatites, the K/Rb ratio is closer to 1, resulting in a less steep gradient.

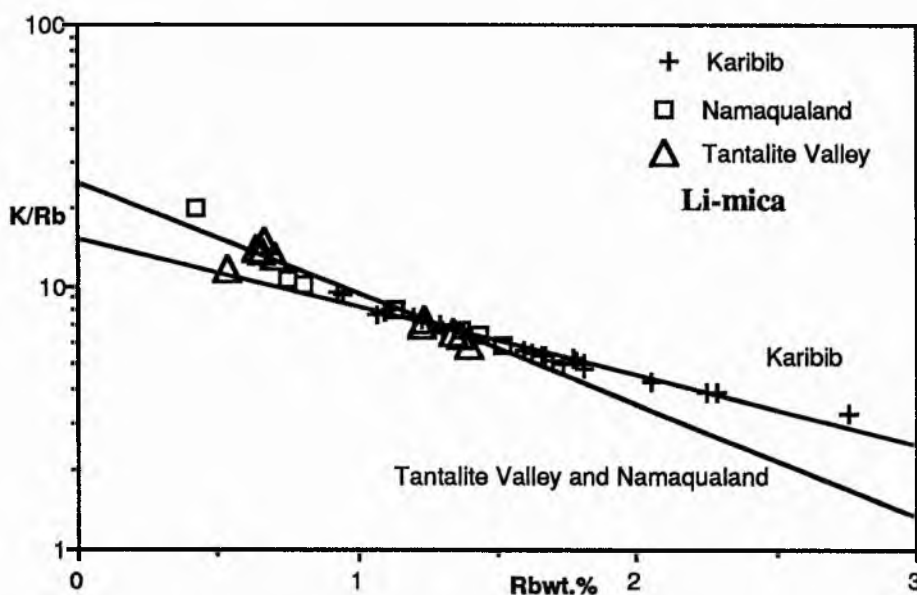


Fig. 6.2. The K/Rb versus Rb trends for Li-mica for the rare-element pegmatites from Karibib, Namaqualand and Tantalite Valley.

Figure 6.3 gives in addition to the data in Figure 6.2 the trend for biotite granite from the Lac du Bonnet batholith, southeastern Manitoba (Cerny, 1985). This shows in general, that the K/Rb ratios decrease with advancing crystallization, due to the rapid depletion of K and relative accumulation of Rb in the residual melt. The sharp Rb-enrichment continues through pegmatitic crystallization with extreme fractionation in rare-element pegmatites.

However, the K/Rb ratio appears to decrease less rapidly at the very extreme fractionation stage in the case of the Karibib, Tantalite Valley and Namaqualand rare-element pegmatites i.e. the steeper the gradient in Figure 6.3 the less fractionated are the granites and the pegmatites. Compare the very steep slopes for biotite granite (Cerny et al. 1985) with low Rb, with the flat gradients and high Rb in the rare-element pegmatites investigated in this study. The data from this study is plotted on a logarithmic scale in Figure 6.3 to compare with the data from biotite granite from Cerny et al. (1985).

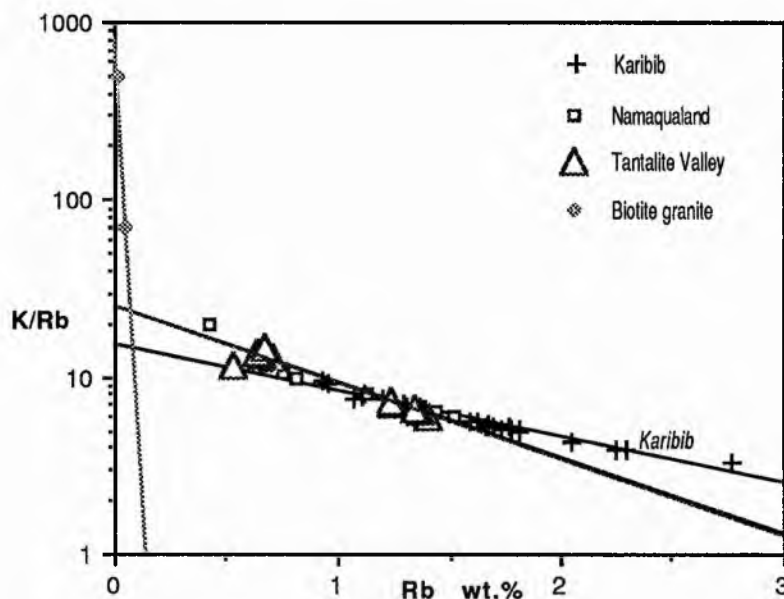


Fig. 6.3. The K/Rb versus Rb steep trend for biotite granite (data from Cerny et al. 1985) in comparison with the low gradient trends for Karibib, Tantalite Valley and Namaqualand rare-element pegmatites (data this study) (correlation co-efficients for Karibib, Namaqualand and Tantalite Valley, 0.972, 0.932, 0.929 respectively, see Fig. 6.2).

Cs contents reach 0.96% in Li-micas at Daheim and 0.90% at Okongava down to 0.12 wt.% at E tiro with the K/Cs ratios increasing from 9.3 at Daheim to 73.7 at E tiro. Although these levels are high and compare favourably with those given by Cerny et al. (1985) for pegmatite micas from highly fractionated spodumene pegmatites from the Cross Lake pegmatite field, Manitoba, with K/Cs ratios of 30 increasing to 500, they do not reach the highest level so far reported with 1.79% Cs in lithian mica and lepidolite (Cerny et al. 1985).

The K/Cs versus K/Rb plots for the Karibib Li-micas and those given by Cerny et al. (1985), Li-micas from the Cross Lake pegmatite field, Manitoba are shown in Figures 6.4 and 6.5 respectively. The differentiated petalite-rich pegmatites in the Karibib area, Namibia have reached a higher level of fractionation, especially with regard to Cs than the Southern Cross Lake spodumene pegmatites, this is reflected in Figure 6.4 (the Karibib micas) where K/Cs is closer to 1 in comparison with Figure 6.5 (the Southern Cross Lake muscovites). However the two areas have a considerable overlap.

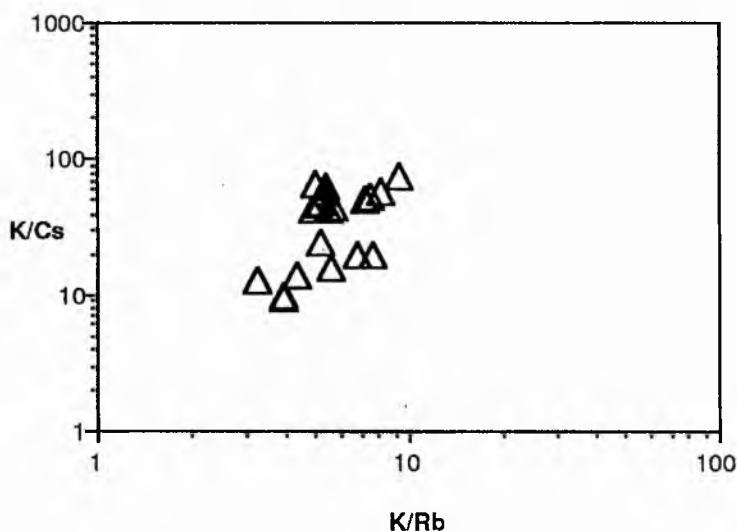


Fig. 6.4. The K/Cs versus K/Rb ratios for Li-mica from Karibib pegmatites, Namibia. Data from Table 6.1.

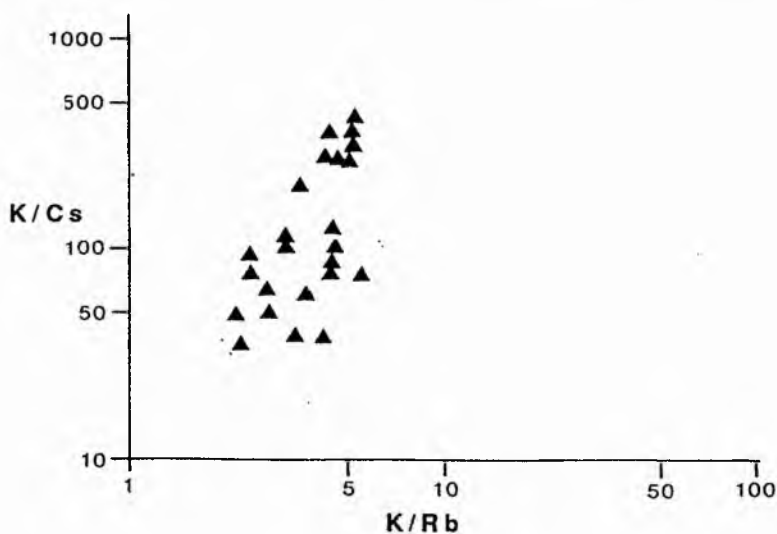


Fig. 6.5. The K/Cs versus K/Rb ratios for Li-mica from the Southern Cross Lake spodumene pegmatites, Manitoba. Data from Cerny et al. (1985).

6.2.2. Rb, Cs and Li data from rare-element pegmatites in Tantalite Valley, Namibia and the Steinkopf area, Namaqualand

The Rb, Cs and Li data for Li-mica, muscovite and biotite for Tantalite Valley and Namaqualand is shown in Table 6.2. In Tantalite Valley, Rb values reach 1.34 wt % in Li-mica at the Homestead pegmatite; the K/Rb corresponding ratio is 6.6. At the Lepidolite pegmatite, Rb reaches 1.4 wt % with a K/Rb ratio of 5.95. The corresponding Cs values are comparatively lower with 0.18 and 1.34 wt. %, K/Cs ratios of 49 and 76 respectively. The K/Cs versus K/Rb plots for both Tantalite Valley and Namaqualand are given in Fig. 6.6. The fractionation trends show firstly that the Steinkopf area Namaqualand pegmatites are more highly fractionated with regard to Cs than the Tantalite Valley pegmatites, in fact the K/Cs ratios in Tantalite Valley Li-micas are very high showing a lack of Cs in that area. In Figure 6.6 the very high ratios of K/Cs and K/Rb in muscovite in comparison with Li-micas shows that the muscovites in rare-element pegmatites in the Karibib, Namaqualand and Tantalite Valley area are not rich in Rb and Cs. Also as Rb is concentrated in Li-mica rather than muscovite this verifies the fact that Rb follows Li to some degree.

Figure 6.7 gives the K/Cs versus K/Rb plots for Li-micas for the three groups of pegmatites from Karibib, Namaqualand and Tantalite Valley. Although there is an overlap, essentially the pegmatites may be divided into three groups with the Karibib pegmatites showing the highest fractionation trends with regard to both Rb and Cs. With respect to the high concentration of Cs in the Karibib pegmatites, it may be significant that the Karibib pegmatites, notably Rubicon and Helicon contain large bodies of pollucite and other pegmatites, notably Daheim, Jooste's (Okongava) and Okatjimukuju reach rare-alkali concentrations suggestive of the presence of pollucite. In contrast, in Cs content, the Tantalite Valley pegmatites do not match the geochemical signature of pollucite-bearing pegmatites and pollucite has not been located in this pegmatite area. Pollucite has

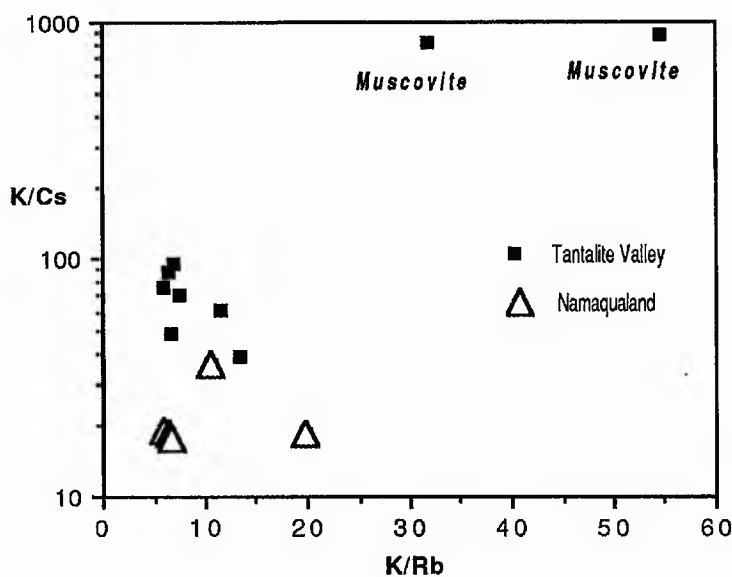


Fig. 6.6. The K/Cs versus K/Rb plot for Li-micas from Tantalite Valley and Namaqualand and for two muscovites from Tantalite Valley. The Figure essentially shows two groups based mainly on a difference in Cs content.

been noted at the Berger's pegmatite (see location map Fig. 2.10) in the Albrechtshöhe area in Karibib (pers. comm. von Knorring) however, owing to deficiency in material it has not been possible to determine rare-alkali concentrations in this pegmatite.

Of the Steinkopf pegmatites in Namaqualand (see Fig 2.4), Norrabees 1 contains pollucite, and the Cs content in Li-mica is 0.5 wt. %, with a K/Cs ratio of 18 (see Table 6.2). The Uranoop and Noumas pegmatites have similar K/Cs ratios in Li-mica; however pollucite has not been located at either of these pegmatites and the huge Noumas mine has been extensively excavated. Therefore low K/Cs ratios in Li-mica are not always an indication of pollucite mineralization.

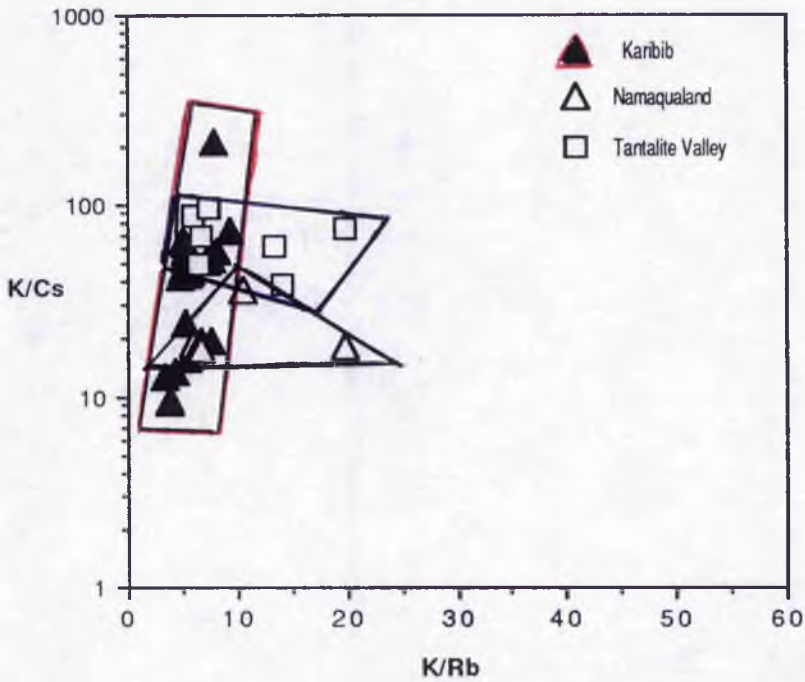
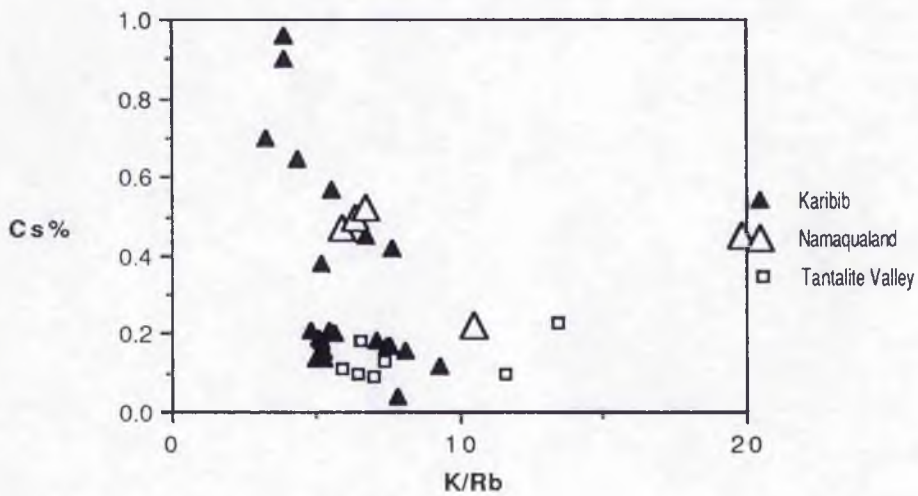


Fig. 6.7. The K/Cs versus K/Rb plots for lithian mica in the three pegmatite groups from Karibib and Tantalite Valley, Namibia; and Namaqualand, South Africa.

To emphasize the lack of correlation between Rb and Cs the K/Rb versus Cs trends in Li-mica for the three series of pegmatites are shown in Figs. 6.8. The trends are largely parallel but not necessarily sequential suggesting different sources or different styles of fractionation or both.



Figs. 6.8. The Cs versus K/Rb trends for pegmatites in Karibib and Tantalite Valley, Namibia and Namaqualand, South Africa

TABLE 6.1. Lithium, rubidium and caesium in lithian mica, Karibib-Usakos area, Namibia and associated mineralization

MINERAL and sample No.	Assoc. Mins	Rb%	Li ₂ O%	Cs%	K ₂ O%	K/Rb	K/Cs	Rb/Cs	Locality
Li-mica (5)	alb-rubellite	2.76	4.75	0.70	10.87	3.269	12.889	3.943	Daheim
Purple-grey Li-mica 85	cl + col-tant	2.29	-	0.96	10.80	3.914	9.338	2.385	Daheim
Li-mica 43	mic+albite	2.25	-	0.90	10.61	3.914	9.785	2.500	Okongava
Grey mica 84	cleavelandite	2.05	-	0.65	10.75	4.352	13.727	3.154	Daheim
Li-mica-globular (17)	col+cleavelandite	1.81	5.57	0.21	10.61	4.865	41.935	8.619	Okongava
Li-mica-grey (1)	Li-mica(pink)	1.81	3.97	0.14	10.95	5.021	64.918	12.929	Okatjimukuju(M1)
Li-mica-grey (3)	cass+topaz	1.78	5.34	0.38	11.09	5.171	24.223	4.684	Okatjimukuju(M4)
Li-mica-purple (2)	Li-mica(grey)	1.77	4.13	0.16	11.23	5.266	58.256	11.062	Okatjimukuju(M1)
Li-mica-purple 47	massive	1.73	-	0.19	10.60	5.086	46.305	9.105	Rubicon
Glob. Li-mica 74	cleavelandite	1.70	-	0.18	10.61	5.180	48.924	9.444	Okongava
Li-mica-grey(52)	col+albite +REE	1.67	3.22	0.21	10.96	5.447	43.318	7.952	Helicon 2
Purple fine-grained 48	massive	1.66	3.96	0.14	10.68	5.340	63.317	11.857	Rubicon
Li-mica (11)	cass+albite	1.62	4.33	0.57	10.86	5.564	15.814	2.842	Sandamap
Li-mica(fine-grained)(90)39	massive	1.59	4.09	0.20	10.90	5.690	45.235	7.950	Rubicon
Li-mica(fine-grained)66	alb+microlite	1.30	-	0.45	10.61	6.768	19.551	2.889	Okongava
Li-mica plates(24)	topaz	1.29	6.20	0.18	11.09	7.135	51.137	7.167	Eitiro
Li-mica (32)	topaz	1.23	5.98	0.17	11.04	7.450	53.901	7.235	Eitiro
Li-mica(satellite cryst.) (56)	on large books Li-mica	1.20	6.04	0.17	10.91	7.546	53.266	7.059	Eitiro
Purple mica plates 70	topaz	1.12	-	0.16	10.95	8.115	56.803	7.000	Eitiro
Li-mica-glob.grey plates(23)	not known	1.10	1.71	0.04	10.38	7.832	19.545	27.500	Rubicon
Grey mica (86)	tant+microlite	1.07	-	0.42	9.89	7.672	73.732	2.548	Okatjimukuju(M1)
Li-mica grey plates(20)	columbite	0.95	4.41	0.12	10.66	9.313	73.732	7.917	Eitiro
Globular muscovite 72	K-feldspar	0.93	-	-	10.70	9.549	-	-	Viljoen's
*Li-mica (Mor)	montebrasite+ap+indicolite	0.92	-	-	9.81	8.840	-	-	Mon Repos
*Green muscovite greisen(S)	cassiterite	0.41	-	-	10.25	20.750	-	-	Strathmore, Cape Cross

alb=albite; rubell=rubellite; mic=mica; cl=cleavelandite; col=columbite/tantalite; - = not determined; Assoc. Mins.= associated minerals

cass=cassiterite; tant=tantalite; micr=microlite; K.feld=K-feldspar; ap=apatite; cryst=crystals; glob=globular

Sample nos. given in Appendix

Li data from von Knorring, 1985, sample nos in brackets

Rb by XRF (St. Andrews); flame photometry (St. Andrews) and microprobe (Edinburgh)* sample name in brackets

Cs by flamephotometry, (St. Andrews and Leeds).Analysts: J.R. Baldwin, R.Batchelor, F.Buckley

TABLE 6.2. Lithium, rubidium and caesium in lithian mica, the Steinkopf Area, Namaqualand

MINERAL+Assoc. Mins Sample No.	LOCALITY	Zone	Rb%	Li ₂ O%	Cs%	K ₂ O%	K/Rb	K/Cs	Rb/Cs
Li-mica greisen(81(+cl))	Uranoop	R	1.52	3.56	0.47	10.85	5.925	19.16	3.234
Li-mica greisen(78)(+alb+qtz)	Norrabees	C	1.43	3.27	0.47	11.09	6.437	18.409	2.860
Li-mica greisen 92(+cl)	Uranoop	R	1.13	-	-	10.88	7.992	-	-
Purple Li-mica(79)(+micr)	Norrabees	R	1.37	3.05	0.52	11.20	6.785	17.877	2.635
Purple Li-mica plates87(+sp+r)	Norrabees	C	0.81	-	-	9.80	10.42	-	-
Green mica greisen42(+micr)	Kokerboomrand	R	0.75	-	0.22	9.49	10.50	35.803	3.409
Grey musc. plates95(+sp+alb)	Noumas	R	0.42	-	0.45	10.01	19.782	18.463	0.933
*Purple Li-mica(+cl+sp+poll)	Norrabees	R	1.45	-	-	9.83	5.76	-	-
*Purple Li-mica(+cl+sp+poll)	Norrabees	R	1.57	-	-	9.83	5.24	-	-
*Purple Li-mica(+cl+sp+poll)	Norrabees	R	1.80	-	-	9.83	4.53	-	-

alb=albite; r=rubellite; mic=mica; cl=cleavelandite; col=columbite/tantalite; sp=spodumene; poll=pollucite; qtz=quartz;
 cass=cassiterite; tant=tantalite; micr=microlite; cryst=crystals; - not determined; R=replacement; C=core; Assoc.Mins=associated minerals.

Sample nos. given in Appendix

Li data from von Knorring, 1985, sample nos in brackets

Rb by XRF (St. Andrews); flame photometry (St. Andrews) and microprobe * (Edinburgh)

Cs by flamephotometry, (St. Andrews and Leeds) Analysts: J.R. Baldwin, R.Batchelor, F.Buckley

TABLE 6.3.

Lithium, rubidium and caesium in lithian mica, muscovite and biotite from pegmatites in Tantalite Valley, Namibia

MINERAL and sample No.	Locality	zone	Rb%	Li ₂ O%	Cs%	K ₂ O%	K/Rb	K/Cs	Rb/Cs	Ba
Li-mica-dark purple greisen 49	Lepidolite		1.40	-	0.11	10.04	5.952	75.756	12.727	0
Li-mica-globular grey (26)	Lepidolite		1.37	2.58	0.10	10.77	6.525	89.391	13.70	
Li-mica-purple(+amblyg) (4)	Homestead		1.34	3.58	0.18	10.62	6.578	48.97	7.444	
Li-mica-purple compact(+lith) (7)	Homestead		1.24	2.15	0.13	10.99	7.356	70.167	9.538	
Green mica plates 68	White City		1.23	0.48	0.09	10.37	6.998	95.634	13.667	0
Li-mica-grey compact(+beryl) 50	Homestead		0.70	-	-	10.88	12.901			0
Li-mica (+garnet + sphal)(55)46	Homestead		0.67	-	-	11.92	14.767			0
Li-mica-purple compact(+micr)40	White City		0.64	-	-	10.80	14.006			1
Green mica compact 40	White City	R	0.66	-	0.23	10.70	13.456	38.613	2.87	289
Li-mica greisen-compact(+tant) 72	White City		0.53	-	0.10	7.39	11.573	61.337	5.30	
*Muscovite 33	Witkop		0.16	-	0.01	10.52	54.572	873.16	16.00	0
Muscovite 32	White City		0.26	-	0.01	9.99	31.891	829.17	26.00	0
Muscovite 94	White City		0.63	-	-					0
Muscovite 93	Homestead		0.28	-	-					0
Muscovite	White City			-	-	10.05				
Muscovite	White City		0.08	-	-	9.80				
*Biotite(+pink K-feldspar)71	Chickenfoot	Wall	0.18	-	-	8.70				237
*Biotite 69	Chickenfoot		0.10	-	-	4.67				195

sphal=sphalerite, amblyg=amblygonite, lith=lithiophilite; tant=tantalite; micr=microlite; R=replacement zone; - = not determined; * = non-Li pegmatite
 Sample nos. given in Appendix

Li data from von Knorring, 1985, sample nos in brackets

Rb by XRF (St. Andrews); flame photometry (St. Andrews) and microprobe (Edinburgh)

Cs by flamephotometry, (St. Andrews and Leeds).Analysts: J.R. Baldwin, R. Batchelor, F. Buckley

6.3. RUBIDIUM AND CAESIUM IN K-FELDSPAR

Table 6.4 shows data for Rb and Cs values in K-feldspar for the Karibib and Tantalite Valley pegmatites and Table 6.5 the data for the pegmatites from Steinkopf, Namaqualand. Full analyses of selected K-feldspar from each general locality are given in Appendix 3.3. Extreme enrichment in Rb and steep gradients in fractionation of K/Rb in K-feldspars are the rule in complex rare-element pegmatites containing lithium minerals (Cerny et al. 1985). Fractionated pegmatites devoid of Li-minerals also have steep gradients but the levels of Rb are generally lower in pegmatites with simple mineralization. This is demonstrated in the results from the Witkop and Chickenfoot pegmatites in Tantalite Valley (i.e. pegmatites with no Li-minerals) where the levels of Rb vary from 0.06 - 0.29 wt.%, in comparison with 0.86 wt.% Rb in the Homestead rare-element pegmatite; K/Rb ranges from 168 in the Witkop pegmatite to approximately 13 in the Homestead pegmatite (see Table 6.4). Steep gradients in fractionation of K/Rb in individual pegmatitic K-feldspars are apparent in the Witkop pegmatite where Rb in K-feldspar ranges from 623 ppm to 1771 ppm and from 168 to 55 K/Rb, from contact zone to the central K-feldspar-bearing zone (see Table 6.4). In the Chickenfoot pegmatite Rb ranges from 0.12 to 0.29% and from ratios of 86 to 35 in K/Rb, from the wall zone to the central core margin.

This phenomenon of steep gradients of K/Rb is also apparent in zoned individual mica crystals which show extreme K/Rb fractionation in Li-Rb-Cs-enriched complex pegmatites. In the Norrabees pegmatite, Steinkopf, Namaqualand, an individual crystal of Li-mica showed a variation in Rb₂O from 1.67 to 1.93%. The variation was not sequential from margin to core however, but there is generally less Rb in the centre of the crystal. Very fine-grained Li-mica at the Rubicon pegmatite, Karibib, varies in Rb from 1.21 to 1.75% and K/Rb ranges from 7 to 5. Brock (1974) revealed that the K/Rb ratio of approximately 10 in a single crystal with a lepidolite rim, is about 50% below the K/Rb ratio of approximately 22, observed in the muscovite core. Foord (1976) also reported extreme K/Rb fractionation in individual mica crystals.

In the Karibib rare-element pegmatites, Namibia, unfortunately no systematic sampling of K-feldspar was taken through the zones, due to lack of exposure. However, extreme levels of enrichment of Rb occur in these pegmatites as demonstrated by the levels in Li-mica. In the Daheim 3 pegmatite K-feldspar Rb reaches 1.84% with a K/Rb ratio of 6.21.

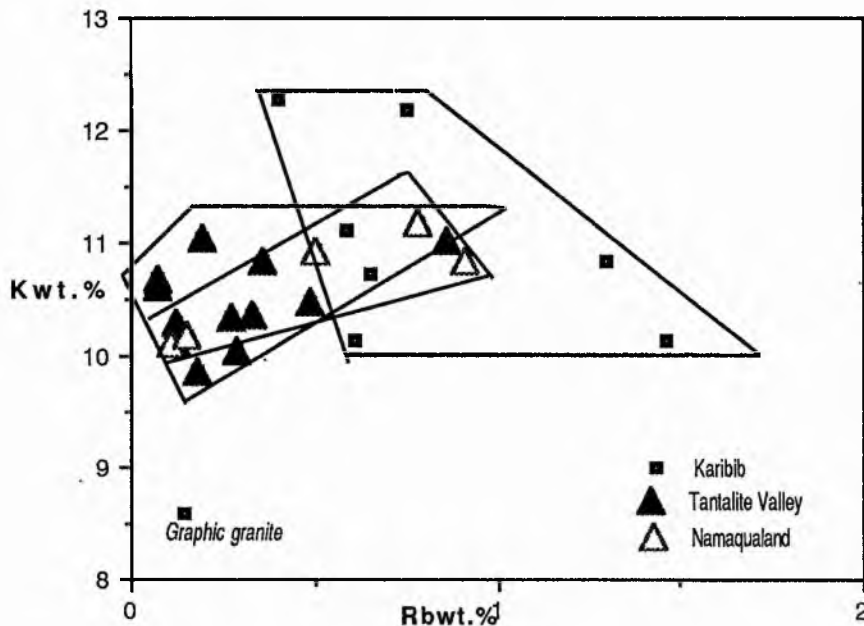


Fig. 6.9. Rb versus K plot for K-feldspars for pegmatites from Karibib, Tantalite Valley and Namaqualand. The graphic granite from Karibib represents an early portion of the granite magma from which the Karibib pegmatites derived.

Figure 6.9 a plot of Rb versus K in K-feldspar for each of the three pegmatite groups. Two groups show similar concentrations of Rb: the groups from Tantalite Valley and Steinkopf, Namaqualand. They differ from the Karibib rare-element pegmatites which have a greater spread. This does not entirely support the results obtained on the micas for the distribution of Rb, i.e. that Rb is a characteristic element in the Karibib area rare-element pegmatites, and it appears to be less abundant in the Namaqualand belt co-genetic group of pegmatites, and in Tantalite Valley in the pegmatites connected with the ultrabasic complex of the Namaqualand Pegmatite province. However, both the latter two groups fall in the Namaqualand Pegmatite Belt. In Table 6.2 two microclines from non-

lithium pegmatites in Namaqualand, the Quartzkop and Swartzburg pegmatites near Noumas, Steinkopf (see Fig. 2.5) contain the lowest amount of Rb. They emphasize the coherence of rubidium and lithium or that lower Rb contents in K-feldspar are found in pegmatites which do not contain lithium.

Cs does not correlate uniformly with Rb. Figure 6.10 shows the different rates of Rb and Cs accumulation in K-feldspar in the Karibib, Tantalite Valley and Namaqualand pegmatite groups. Note the position of the graphic granite, a less fractionated early portion of the granite magma from which the Karibib pegmatites are said to have derived (pers. comm. von Knorring). Unfortunately data for Cs in K-feldspar is incomplete owing to difficulties in the analytical procedure.

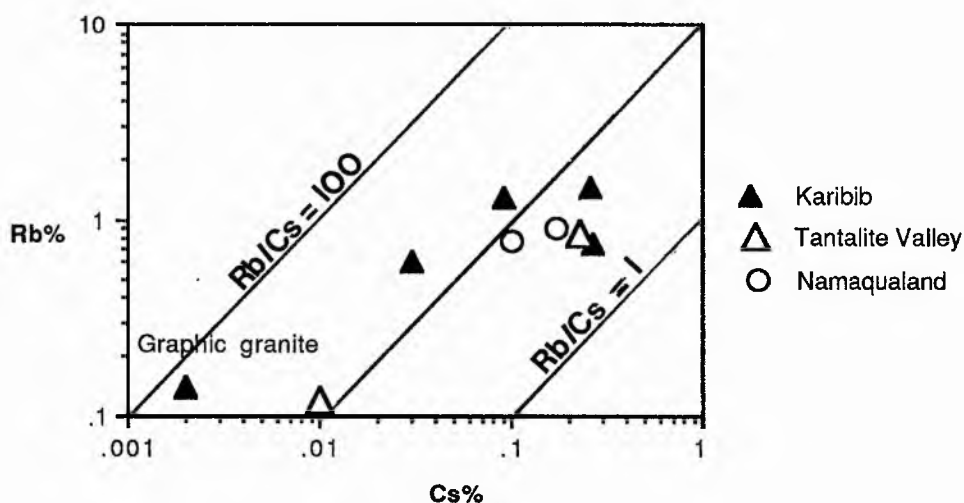


Fig. 6.10. The Rb versus Cs plots for K-feldspar from the Karibib, Tantalite Valley and Namaqualand pegmatites.

Cerny et al. (1985) used K/Rb versus Cs in blocky microcline for characterization of pegmatite groups and correlation of their alkali fractionation with different types of potentially economic mineralization. Cerny et al. (1985) noted that pollucite-rich, and potentially pollucite-rich pegmatites have K-feldspar distinctly less concentrated in Cs in

comparison with Rb, relative to other pegmatites in the group. They suggest that this fact invites speculation that in some pegmatites a complexing mechanism may operate that may hinder the incorporation of Cs into K-minerals, retaining it for late crystallization of pollucite, while Rb enters the K-phases unimpeded. Certainly in the case of Helicon and Rubicon with known large quantities of pollucite, the Cs content of Li-micas is low. However, Norrabees, in Namaqualand with admittedly smaller quantities of pollucite does not support this suggestion in the case of Li-micas.

Figure 6.11 shows the K/Rb versus Rb trend for K-feldspar for the three series of pegmatites (data from Tables 6.4, 6.5). The trends are largely parallel, however, the Karibib pegmatites reach a higher level of fractionation with higher Rb levels. However, the trends for the K-feldspar are not quite as definitive as the trends for the Li-mica if compared with Figure 6.2. This may be due to the lack of data for the K-feldspar in comparison with the Li-mica. In general, similar trends but different concentrations are apparent for the Li-micas and K-feldspars. The rate of Rb accumulation differs in the Karibib pegmatites. The different correlation of alkali fractionation for the Karibib series of pegmatites reflects the different type of mineralization and a different class of pegmatite type for example petalite type pegmatites, as opposed to spodumene type which occurs in the rare-element pegmatites of the Namaqualand Pegmatite Belt. The different correlation reflects a different source for the rare-alkalis, and, or a different fractionation path, the Karibib and Namaqualand pegmatites being from two different structural provinces, the Pan African and the Kibaran Structural Belts respectively.

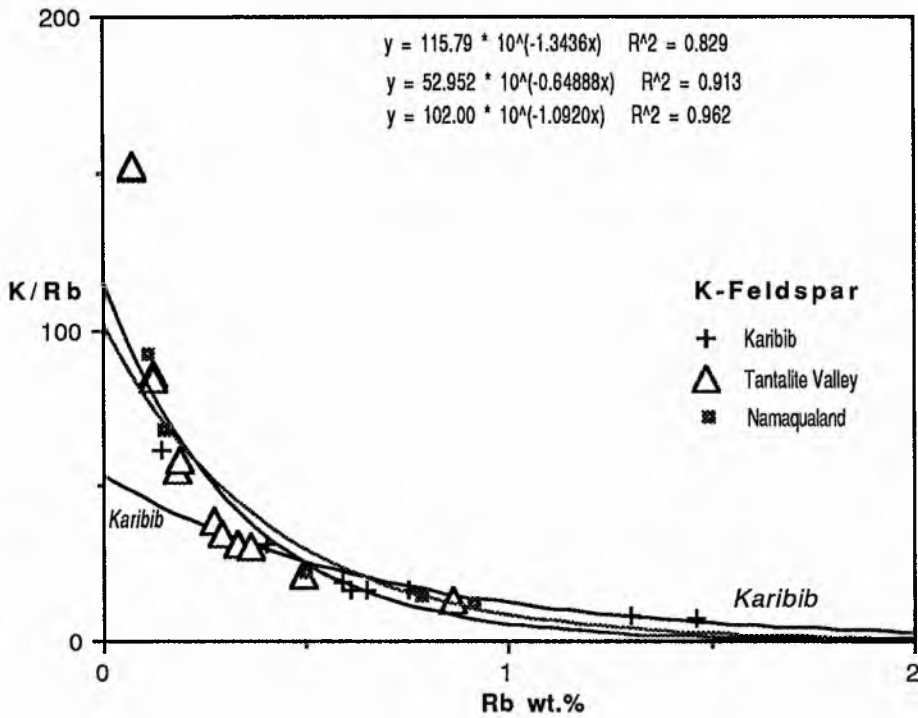


Fig. 6.11. The K/Rb versus Rb trends for K-feldspar from the Karibib, Tantalite Valley and Steinkopf, Namaqualand rare-element pegmatites with their respective regression lines with correlation co-efficients of 0.962, 0.913 and 0.829. The trends for the three areas are largely parallel.

TABLE 6.4, Rubidium, caesium, barium and strontium in K-feldspar from pegmatites in Karibib, and Tantalite Valley, Namibia

LOCALITY	ZONE	Rb%	Assoc. Minerals	Cs%	K ₂ O%	K%	K/Rb	K/Cs	ppmSr	ppmBa
KARIBIB-USAKOS										
**Daheim 3		1.84		-	13.77	11.29	6.21		nd	nd
Daheim3 (80)	Core	1.46	tantalite	0.26	12.21	10.13	6.94	38.98	134	0
Daheim (54)	Rep.	1.30	Li-mica, tantalite	0.09	13.07	10.85	8.34	120.53	21	66
Okatjimukuju (M1,77)	Core	0.75	columbite/tantalite	0.27	14.69	12.19	16.26	45.16	0	28
**Okatjimukuju M1		0.65		-	15.39	12.77	19.65		nd	nd
Sandamap (96)	O.Int.	0.65		-	2.93	10.73	16.51		0	0
Rubicon (88)	Core	0.61	quartz	0.03	12.20	10.13	16.60	337.53	0	0
Kohero (56)	Int.	0.59	cassiterite	-	13.40	11.12	18.85		37	0
Dernburg (64)	wall	0.40	apatite	-	14.80	12.28	30.71		?	347
**Mon Repos	Int	0.01	petalite,tourmaline	-					nd	nd
GRAPHIC GRANITE (97)	CR	0.14	mica	0.002	10.36	8.60	61.42		97	det
TANTALITE VALLEY										
Homestead (HM1)	Int.	0.86	albite & mica	0.23	13.29	11.03	12.83	47.96	49	106
White White City (WCM1)	Int.	0.49		-	12.61	10.47	21.36		13	0
White City(36)		0.47								
Lepidolite (44)	Int.	0.33	tourmaline	-	12.49	10.36	31.41			0
*CHICKENFOOT (5)	Core	0.29	quartz	-	12.10	10.04	34.63		5	0
Chickenfoot (7)	I.Int.	0.27		-	12.46	10.34	38.30		11	0
Chickenfoot (6)	O.Int.	0.19		-	13.30	1.04	58.10		16	0
Chickenfoot (8)	Wall	0.12		0.01	12.40	10.29	85.77		106	976
Top Chickenfoot (24)	Contact	0.36		-	13.07	10.85	30.13		32	99
*WITKOP	I.Int.	0.18		-	11.88	9.86	54.78		9	26
Witkop (22)	O.Int.	0.12		-	12.19	10.12	84.31		10	0
Witkop (W6)	Contact	0.07		-	12.80	10.62	151.77		147	795
Witkop (W7)pink	Contact	0.07		-	12.86	10.67	152.48		181	1225
Witkop (26)	R.bed C	0.06	graphic granite	-	12.59		168		150	1016

* = non-lithium pegmatites ** = analysis by electron microprobe, - and nd = not determined. CR = country rock, near Rubicon, Karibib Rep. = replacement zone, O.Int. = outer intermediate zone, I.Int. = inner intermediate zone, R.bed C = river bed contact.

TABLE 6.5. Rubidium, caesiums, barium, strontium in K-feldspar from pegmatites in the Steinkopf area, Namaqualand

LOCALITY	ZONE	Rb%	Associated Minerals	Cs%	K ₂ O%	K%	K/Rb	K/Cs	Sr	Ba
NAMAQUALAND										
**Norrabees	Rep.	1.13	pollucite, cleav. spod.	-	15.45	12.83	11.35	-	nd	nd
Noumas (76)	Rep.	0.91	Li mica	0.17	13.05	10.83	14.33	63.72	-	0
Noumas (98)	Rep.	0.78	Mn-tantalite, micr.	0.10	13.47	11.18	21.87	111.80	-	-
Noumas(pink)(45)	Rep.	0.50	Green spodumene	-	13.18	10.94	11.35	-	-	0
*Quartzkop (89)	Int.	0.15	major mineral	-	12.27	10.18	67.89	-	-	-
*Swartburg (51)	Int.	0.11	major mineral	-	12.19	10.12	91.98	-	-	0

Int.= intermediate; Rep.= replacement

Micr.= microlite* non-lithium pegmatite; Cleav.= cleavelandite; Spod.= spodumene

** = electron microprobe analysis; -- = not determined

Sr and Ba in ppm

6.4. BARIUM AND THE Ba/Rb RATIO

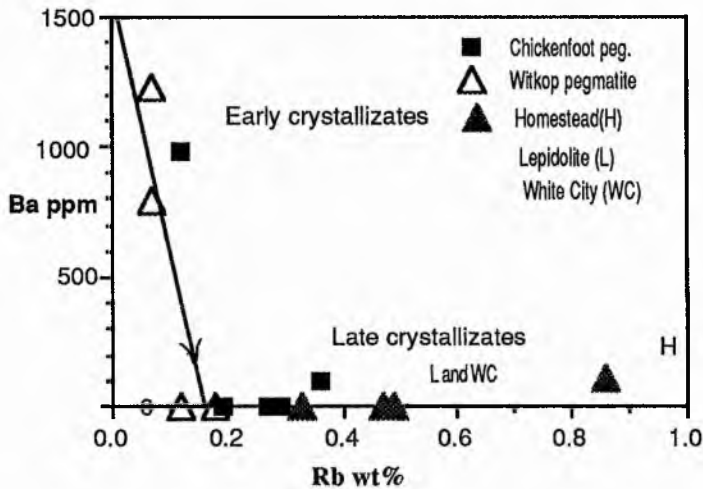
The size of the Ba^{2+} cation is almost the same as the K^+ cation. Ba^{2+} is partitioned into the K-feldspar structure rather than the structure of biotite. Therefore the K-feldspars control the distribution of Ba in differentiated pegmatites, however biotite does incorporate a certain amount of Ba^{2+} in its structure.

In rare-element pegmatites, steep gradients in Ba content within single zoned pegmatites are the rule. Ba is incorporated into the first crystallizing zones - the contact and wall zones, and the Ba - content in the crystallizing medium may be completely depleted in the inner and core zones. This is demonstrated in the K-feldspars at the Witkop pegmatite, Tantalite Valley in which Ba shows a decrease from 1225 ppm in the contact zone to undetectable levels in the outer intermediate zone (Fig. 6.12) with a decrease in the Ba/Rb ratio from 1.75 to 0 (Table 6.1). Similarly in the Chickenfoot pegmatite Ba decreases from 987 ppm in the wall zone to undetectable levels in the intermediate zones and the core. Fig. 6.12 shows the general distribution of Ba and Rb in K-feldspars from the Homestead, Lepidolite and White City pegmatites in Tantalite Valley. The pegmatites containing Li-minerals, Homestead and Lepidolite have high Rb contents in the inner zones which are depleted in Ba; the K-feldspar in the outer zones was not sampled.

Figure 6.13 shows the Ba versus Rb fields of K-feldspar for the three pegmatite groups, Karibib, Tantalite Valley and Namaqualand, and illustrates a wide scatter of Ba/Rb ratios, each group overlapping in spite of some paragenetic differences. In general, in these highly fractionated, rare-alkali-enriched pegmatites, extensive depletion of Ba occurs in the inner zones of all the pegmatites in each co-genetic group.

The data for the micas show extensive depletion in the Li-micas and also in the muscovites. However, data are available for biotite at the Chickenfoot pegmatites in

Tantalite Valley - a pegmatite type without Li-minerals but containing Rb. A wall zone "Chickenfoot biotite" (biotite occurring with pink feldspar and quartz) contains 237 ppm Ba, and in a similar "Chickenfoot biotite" with white feldspar Ba reaches 195 ppm. In the White City pegmatite, a fringe border zone mica contains 942 ppm Ba, the inner zone muscovite is completely depleted of Ba.



Figs. 6.12. a) Distribution of Ba and Rb in K-feldspar from different zones of the Chickenfoot and Witkop pegmatites, Tantalite Valley, Namibia and data for the inner zones of the Homestead, White City and Lepidolite pegmatites, Tantalite Valley (see Table 6.4 for data). The arrow indicates the trend from the early to the late crystallizates.

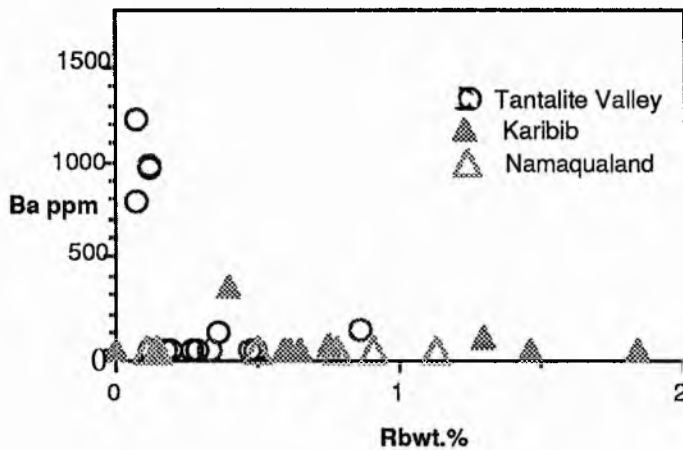


Fig. 6.13. The Rb versus Ba plots for K feldspar from Karibib, Tantalite Valley and Namaqualand pegmatites. (Data from Table 6.4 and 6.5).

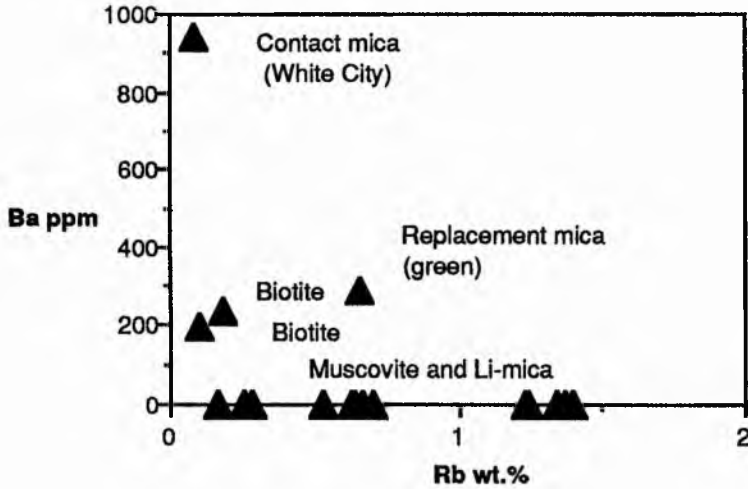


Fig. 6.14. Rb versus Ba for biotite, muscovite and Li-mica from pegmatites in Tantalite Valley, Namibia (data from Table 6.3). The muscovite and Li-mica are from the inner zones.

Fig. 6.14 demonstrates the Rb and Ba contents of micas from the Tantalite Valley pegmatites. Muscovite and Li-mica from the inner zones of the pegmatites are depleted in Ba whereas a contact zone muscovite has a high barium content. The green replacement muscovite may have inherited Ba from the replaced feldspar.

6.5. Fe/Mn VERSUS Nb/Ta FRACTIONATION TRENDS

The fractionation trends of Fe/Mn, Nb/Ta, Rb/Cs, Rb/Ba and Rb/Sr and accumulation of rare-elements, Be, Sn, U, Bi, (Zn, Pb), B, P and F proceed more or less simultaneously (Cerny et al. 1985) The fractionation of individual pairs proceed at different rates (von Knorring, 1974) and it has been pointed out that this is partly regional and possibly typical of diverse pegmatite types (Cerny et al. 1985).

In rare-element highly fractionated pegmatites manganotantalite, tapiolite and wodginite feature in the pegmatites of Karibib, Tantalite Valley, and Steinkopf, Namaqualand. With progressive fractionation the columbite-tantalite group of minerals show a tendency towards Mn and Ta enrichment but the mineral populations of individual pegmatites, pegmatite groups and fields rarely show a proportional increase in both elements. Conspicuous discrepancies in the fractionation rate of Nb/Ta and Fe/Mn occur during pegmatite evolution. Figure 4.11a shows Ta fractionation while Mn remains static in manganotantalite from the Rubicon pegmatite while in the Okatjimukuju pegmatite Figure 4.11b shows both Ta and Mn fractionation occurring simultaneously.

Geochemically primitive pegmatites i.e. less differentiated or fractionated pegmatites tend to carry columbite and ferrocolumbite, for example the Kenhardt pegmatite field. This is in contrast to the Karibib pegmatite field which shows a progression through ferrocolumbite, manganocolumbite to manganotantalite. Figure 6.15_a plots the $Ta/(Ta + Nb)$ versus $Mn/(Mn+Fe)$ ratios for four pegmatite fields, this study, the Kenhardt and Steinkopf fields, South Africa, and the Tantalite Valley and Karibib-Usakos fields, Namibia. The Steinkopf field shows a progression through columbite to manganotantalite while the Tantalite Valley field is extremely fractionated in Mn and Ta in manganotantalite (Fig. 6.15a); Figure 6.16_a in addition includes the data for tapiolite and wodginite; wodginite extends the manganotantalite field into the tantalite field.

Figure 6.15a compares well with Figure 6.15b from Cerny et al. (1985) who showed the different pegmatite progressions in pegmatites from North America and Asia. In comparison with Figure 6.15b (after Cerny et al. 1985) the Karibib field, this study, is most similar to the Southern Cross Lake Series of pegmatites, central Manitoba. The Southern Cross Lake Series show notable Mn-enrichment in Nb-rich pegmatites followed by Ta-enrichment in manganotantalite and wodginite in spodumene-bearing pegmatites (Cerny et al. 1985). This is analogous to the Karibib series of pegmatites which reach a certain Mn-enrichment in less evolved Nb-bearing pegmatites such as the Kleinspitskop and Okongava pegmatites (see Fig. 4.12b) followed by manganotantalite and wodginite enrichment in the M3 pegmatite, Okatjimukuju and manganotantalite enrichment in the Rubicon, Mon Repos and Dernburg pegmatites (see Plate 4.12b). However, in contrast to the Southern Cross Lake Series spodumene-rich pegmatites, the Karibib pegmatite field is characterized by petalite-rich pegmatites. The Karibib pegmatite field also corresponds to the Li-mica and Lepidolite type of pegmatite (Cerny and Ercit, 1985a), rich in fluorine (see Fig. 6.16b) where extreme fractionation of Mn is attained in the F-rich pegmatites in which F persists in the melt and fluid phase until the final phase of consolidation, similar to the Himalayan Dyke System, Mesa Grande, California (Foord, 1976) (see Figs. 6.16b and 6.17). Pegmatites in the Karibib field with extreme fractionation of Mn in manganocolumbite are represented by Helicon 2 which contains a sizeable unit of lepidolite, and Albrechthole, Daheim, Okatjimukuju and Rubicon (see Table 4.12b). The Rubicon pegmatite falls into both the Peerless and the Himalayan Dyke System progressions (see Figs. 6.16b and 6.17).

A manganocolumbite-manganotantalite progression characterizes the Mongolia Altai field (see Fig. 6.15b) which also characterizes the Okatjimukuju pegmatites, this study (Fig. 4.11). The Okatjimukuju pegmatites also show similar progressions as the Peerless pegmatite (see Fig. 6.17) which contains wodginite with a sizeable central unit of lithian muscovite (Cerny et al. 1985b), similar mineralogical units are seen in the Okatjimukuju

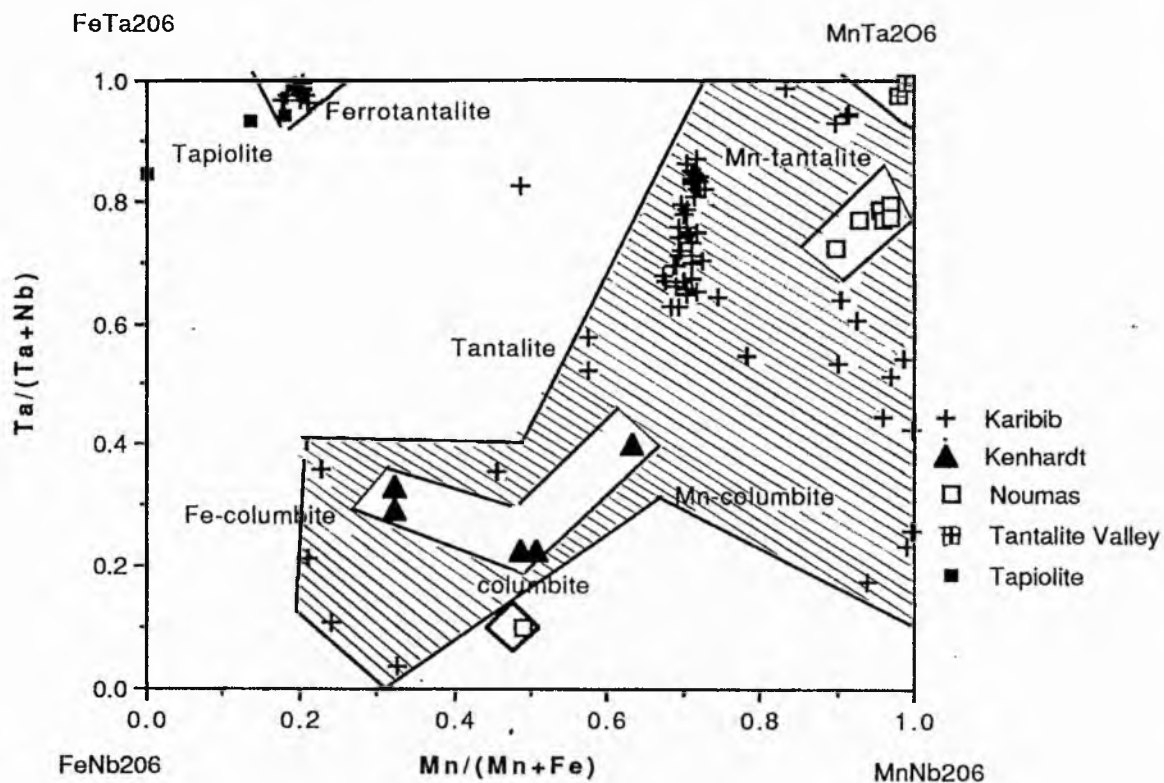


Fig 6.15a. The $Ta/(Ta+Nb)$ versus $Mn/(Mn+Fe)$ plot for columbite-tantalite and tapiolite for four individual pegmatite fields, Kenhardt and Steinkopf, South Africa and Tantalite Valley and Karibib, Namibia. Data from Tables 4.1-4.5 and 4.8-4.12. //// represents the Karibib field.

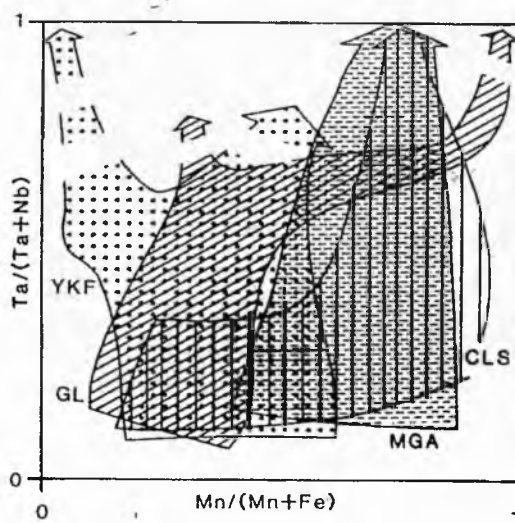


Fig. 6.15b. The $Ta/(Ta+Nb)$ versus $Mn/(Mn+Fe)$ plot for columbite-tantalite and related minerals (from Cerny et al. 1985) from four individual pegmatite fields in North America and Mongolia, YKF: Yellowknife, N.W.T, CLS: Cross Lake Southern Series, central Manitoba, MGA: Mongolian Altai and GL: Greer lake, southeastern Manitoba

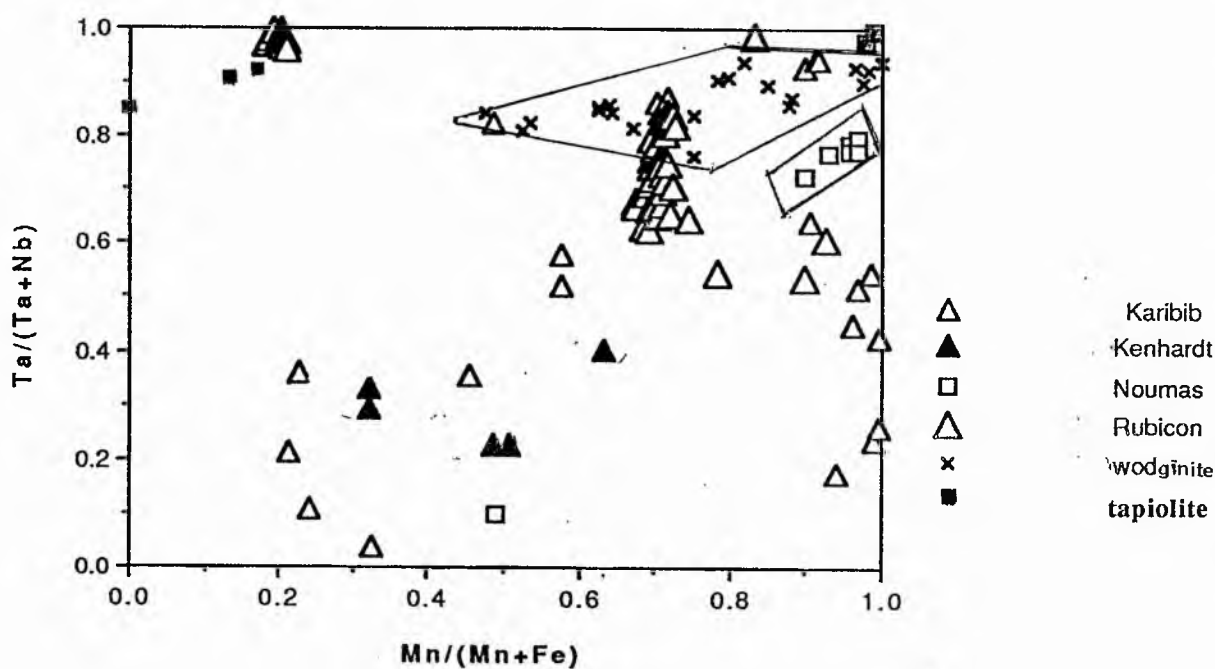


Fig. 6.16a. The Ta/(Ta+Nb) versus Mn/(Mn+Fe) plot (atomic) of columbite-tantalite, wodginite (+) and tapiolite from four individual pegmatite fields, i) the Kenhardt, Northern Cape and ii) Noumas, Steinkopf, Namaqualand, South Africa and iii) Tantalite Valley (TV) and iv) Karibib-Usakos, Namibia.

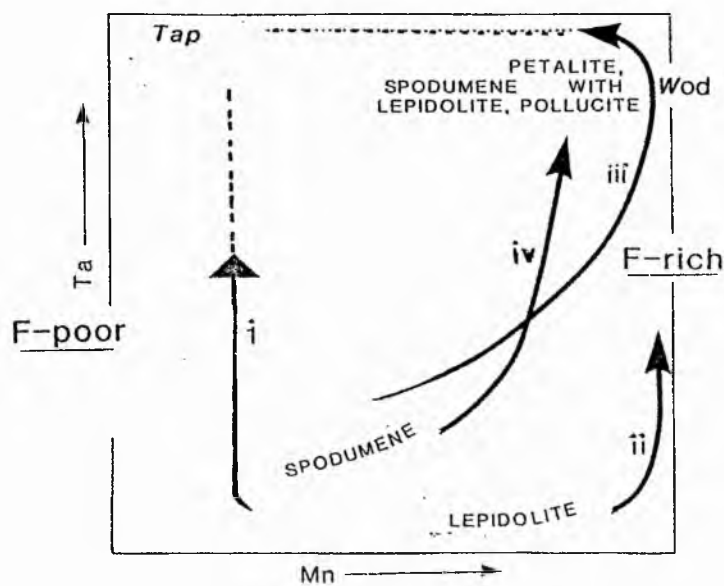


Fig. 6.16b. General fractionation trends of columbite-tantalite, tapiolite and wodginite plotted on the columbite quadrilateral (after Cerny, 1989). The arrows represent the fractionation trends in i) columbite, generally F-poor pegmatites, Angelienspan, Kenhardt and Karibib, ii) F-rich lepidolite pegmatites iii) spodumene (Tantalite Valley, Straussheim, Noumas) and iv) petalite with pollucite and lepidolite.

pegmatites, Karibib. The Kenhardt field is similar to the Huron Claim Deposit, a primitive Nb-rich pegmatite (Paul, 1984) (see Fig. 6.17).

However, the four fields in this study show different fractionation patterns, from each other, although there is an overlap between the Kenhardt and the Karibib fields with the Karibib field being more fractionated and more evolved from an original granite magma (Fig. 6.15a).

Figure 6.17 (after Cerny et al,1985) shows the Ta/(Ta+Nb) versus Mn/(Mn+Fe) plot (atomic) for columbite-tantalite and related types for individual pegmatites from the Huron Claim, Manitoba (Paul, 1984), the Peerless pegmatite, Pennington County, South Dakota (Cerny et al. 1985b) and the Himalayan Dyke System, Mesa Grande District, California (Foord, 1976) in comparison with the pegmatite progressions for the Rubicon pegmatite, Karibib, this study.

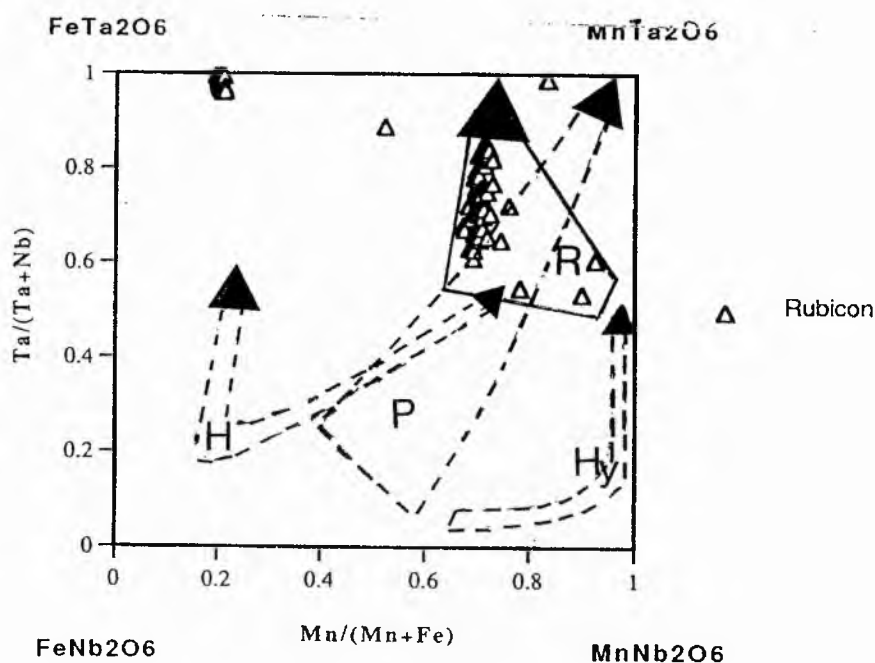


Fig. 6.17. The Ta/(Ta+Nb) versus Mn/(Mn+Fe) plots for individual pegmatites from North America (after Cerny et al. 1985) compared with the Rubicon pegmatite (R) from Karibib, Namibia; P: the Peerless pegmatite, (Cerny et al.1985b) Hy: the Himalayan Dyke System (Foord, 1976) and H: the Huron Claim, Manitoba (Paul, 1984).

The Okatjimukuju field (see Fig 4.11) in comparison with the Rubicon field is more fractionated, while the Rubicon field has a greater spread; the fractionation trends are different possibly implying separate injection of initial differentiated magma from a similar parental source. The trends in Fig. 6.17 from Cerny et al. (1985) represent different types of pegmatite from widely different areas.

The Ta dominant minerals which occur with progressive fractionation, indicate a high degree of Fe, then Mn depletion in late crystallization stages and as a result minerals containing Ca, Na and Sn are generated, and finally only Ta is available for crystallization of solid phases with very minor amounts of Nb, Mn and Fe. Microlite crystallizes in late replacement units with cleavelandite and lithian mica, possibly replacing late generations of manganotantalite. For example, in the White City pegmatite in Tantalite Valley a late generation of manganotantalite contains only 0.25% Nb₂O₅ with microlite from the same pegmatite containing 2.52% Nb₂O₅, and undetectable amounts of Fe and Mn (Table 5.1). Microlite replacing manganotantalite in the Homestead pegmatite in the same area contains a very low content of Nb₂O₅ (1.23%, Table 5.2).

In conclusion, the Karibib pegmatite field reaches maximum fractionation in petalite-lithian mica-bearing type pegmatites with subordinate amblygonite-montebrazite in the following manner. Ta-enrichment proceeds from columbite, ferrocolumbite, manganocolumbite, manganotantalite, along with wodginite and microlite. Pegmatite zones rich in Li, Rb, Cs and F assemblages-with abundant Li, F micas to the exclusion of K-feldspar contain manganotantalite and wodginite with extremely low Fe/Mn values i.e. high Mn/Mn+Fe ratios. The Tantalite Valley and Steinkopf, Namaqualand pegmatites have a similar though not quite as extensive field with regard to Ta and Mn as the Karibib field, they reach maximum fractionation in Li-mica, spodumene-rich pegmatites. The data presented adequately documents the diversity in the pattern of Nb-Ta and Fe-Mn fractionation, some typical of different types of pegmatite.

6.6. THE K/Rb VERSUS Nb/Ta RATIOS IN TANTALUM MINERALS AND K-FELDSPAR

In order to establish a relationship between tantalum and increasing fractionation of rare-alkalis in differentiated pegmatites, the K/Rb ratio in K-feldspar has been plotted against the Ta/(Ta+Nb) ratio in columbite-tantalite and related microlite from the three pegmatite groups from Karibib and Tantalite Valley, Namibia and the Steinkopf area Namaqualand (see Fig. 6.18). Unfortunately no K-feldspar was collected from the Kenhardt area.

The fractionation trend of Rb/K and Ta enrichment is noticeable though the data is rather limited. The data spread within some individual pegmatites is considerable for both Rb and Ta. However, whereas a data spread for microcline from two individual pegmatites is available from Tantalite Valley, Ta and Nb do not occur in these pegmatites, therefore sampling of K-feldspar from each zone should be undertaken from Ta-rich differentiated pegmatites in order to obtain the quantitative characterization of the relationship at the level of individual pegmatites within cogenetic groups.

The pegmatites show a broad trend in the series from Karibib, with less spread in Tantalite Valley and the Steinkopf region of Namaqualand. In most cases, however, advanced fractionation of Ta (i.e. Ta/(Ta+Nb) close to 1.0) is reached at a low K/Rb ratio (40 in comparison with 100) the most advanced fractionation being reached in the Tantalite Valley pegmatites and at Noumas, Namaqualand.

In general, this is in agreement with Ginsburg (1960), Beus et al. (1968) and Cerny et al. (1985) who linked enrichment in Ta with increasing fractionation of rare-alkalis, though the pegmatites in this study have reached a higher level of fractionation than the pegmatites in Manitoba (see Fig. 6.5).

The data in this study essentially represents advanced fractionation, because the data is mostly from rare-alkali-tantalum-rich pegmatites although some data from less fractionated pegmatites in the Karibib-Usakos-Cape Cross field has been included (see Table 4.2). Additional documentation is required to more exactly define different trends in the correlation of Nb/Ta with both K/Rb and K/Cs. In Figure 6.18 the different fractionation trends may be related to the two different pegmatitic types ; i) the petalite-Li-mica-amblygonite type from Karibib and ii) the spodumene-Li-mica + amblygonite type from Tantalite Valley and Steinkopf, Namibia which probably represent different parental sources.

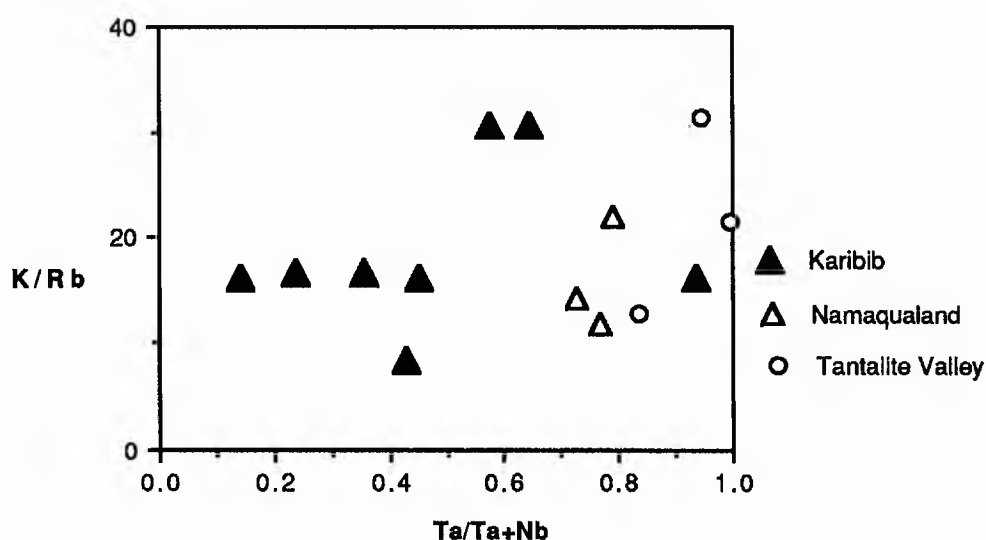


Fig. 6.18. The K/Rb ratio (wt.%) of core-margin K-feldspar versus Ta/(Ta+Nb) (atomic) plot of columbite-tantalite and microlite from three individual cogenetic groups from Karibib and Tantalite Valley, Namibia and Steinkopf, Namaqualand.

PART IV

DISCUSSION AND CONCLUSIONS

Chapters 7 and 8

CHAPTER 7

PETROGENESIS OF LITHIUM PEGMATITES

7.1. Classification of rare-element pegmatites

The rare-element pegmatites mainly studied in this thesis may be termed as "Lithium Pegmatites" von Knorring (1970, 1981, 1985). It is only in Li-pegmatites that Ta predominates over Nb, to such an extent that in the most evolved rare-element pegmatites the Ta/(Ta+Nb) ratio is practically 1 (see Fig. 6.16). The pegmatites in three out of the four field areas studies: i) Steinkopf, Namaqualand, ii) Tantalite Valley, Namibia and iii) Karibib, Namibia have been classified according to Cerny (1990) as follows:

Lithium, columbite-tantalite pegmatites derived from peraluminous leucogranites that concentrate Li, Rb, Cs, Be, Sn, and Ta > than Nb in the presence of B, P, F

The "Li-columbite-tantalite pegmatites with Ta>Nb" (lithium pegmatites containing ferrotantalite and manganotantalite) may be further extended into less evolved types:

"Li-pegmatite with Ta= Nb" (containing mainly tantalite)

"Li-pegmatite with Nb>Ta" (containing mainly columbite)

The Angelienspan -Kenhardt pegmatites may be classified as a less evolved type i.e. with Nb>Ta", producing largely Be and Nb dominant minerals. They have lower concentrations of Li, Rb and Cs and are less fractionated than the more evolved complex rare-element pegmatite type which is characterized by substantial concentrations of Li, Rb and Cs and the greatest variety of mineralization. These rare-element lithium

pegmatites are characterized by accumulation of Li, Rb, Cs, Be, Sn, Ta > Nb (B, P, F) in their more complex fractionated members.

The pegmatite areas investigated in this study, Karibib, Tantalite Valley and Namaqualand may be described as belonging to this latter, highly fractionated more evolved type of lithium pegmatite. Of the three field areas, the Tantalite Valley pegmatites (largely lithium-bearing in the form of spodumene, amblygonite and Li-mica) are the most highly Ta-fractionated (see Fig. 6.16) i.e. the Li-mica - spodumene - amblygonite group of which the pegmatites, Homestead, White City and Lepidolite and in addition the lesser fractionated Witkop pegmatite are encompassed. There are less evolved pegmatites in the area of which Chickenfoot "Be-bearing with Nb > Ta", may be included. Chickenfoot contains green beryl which tends to signify less fractionation and little concentration of Li, Rb, Cs (see Chapter 6).

The "Li-type" pegmatites may be subdivided into:

- Li-spodumene
- Li-petalite
- Li-amblygonite
- Li-lepidolite or Li-mica type

No substantial differences in the initial or main mineralization were observed amongst the high-P spodumene "lithium-type" (i.e. Steinkopf, Namaqualand and Tantalite Valley, Namibia), the low-P petalite "lithium-type" (i.e. Karibib) and the amblygonite - high PFO₂ "lithium-type" (i.e. Rubicon, Karibib). However, divergence in K/Rb and K/Cs fractionation has been observed, with the Karibib pegmatites, the low-P petalite type and the Li-mica-type (generated from fluids containing high Li, F and K) being the most fractionated (Fig. 6.7).

of spodumene replacement are abundant in the Steinkopf area, Namaqualand. Spodumene has been replaced by albite, pollucite and Li-mica at Norrabees and at Noumas by Li-mica and albite, in addition to pockets of entirely kaolinized spodumene crystals up to 1 foot in length occurring with fresh pink K-feldspar crystals of 4 inches i.e. late K-feldspar. Examples of amblygonite replacement also occur in the pegmatites at Karibib. In the Daheim pegmatites montebrasite is altered to apatite, Cs-mica and natromontebrasite; in the pegmatites at Okatjimukuju to brazilianite, apatite, and at Rubicon and Mon Repos to apatite. Tantalite minerals occur in the cleavelandite and Li-mica units.

7.2. GENERAL PETROGENESIS OF LITHIUM PEGMATITES

7.2.1. Pegmatite zonation - a framework

Introduction- lithium minerals

In the initial stages of pegmatite evolution, the "magma" may initially crystallize only quartz, feldspar and muscovite forming the spodumene-free units observed in the outermost parts of spodumene pegmatites but when the Li concentration reaches that of the thermal minimum in the system albite-quartz-spodumene-H₂O, a lithium mineral will begin to crystallize. This lithium mineral will be spodumene which normally crystallizes from the melt at moderate T and high P. Under lower P ($P_{H_2O} < 2\text{kb}$) the liquidus does not reach the low temperature of spodumene crystallization and the higher temperature mineral petalite, crystallizes from the melt, analogous to the Karibib pegmatites. Commonly as the solidified pegmatite becomes cooler the petalite changes to spodumene plus quartz, unlike the Karibib pegmatites where spodumene is very rare.

Spodumene-petalite interactions have not been observed in the Karibib "Petalite pegmatites" and have also not been observed in either Tantalite Valley or Steinkopf

Namaqualand. The fact that the Karibib pegmatites are petalite-rich and the Tantalite Valley and Steinkopf pegmatites are spodumene-rich places limits on the P-T regime of the Karibib pegmatites on the one hand and the Tantalite Valley and Namaqualand pegmatites on the other hand.

The suggested initial temperature of pegmatite formation is 750 to 800°C (Zakharchenko, 1964) analogous to the temperatures of the beginning of melting of solid phases in inclusions. Processes of differentiation and crystallization continue as long as the fluids remain active, the active fluids are available from the initial stages of pegmatitization (800-700°C) as volatile compounds of the petrogenetic elements, but later as aqueous solutions of halides and other soluble compounds (Jahns and Burham, 1969; Jahns, 1982).

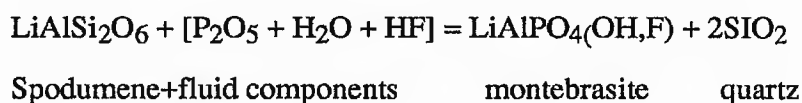
The pegmatites are enriched in the alkalis, first K and then Na and they are enriched also in rare-elements that are concentrated mostly in the feldspathic zone, and in volatiles (F, P and B) The process of accumulation of volatiles, differentiation, crystallization, segregation and deposition of material continues throughout the pegmatite crystallization in an essentially closed system.

London (1984, 1990) (see Fig 3.1a) produced a qualitative P-T phase diagram in the system LiAlSiO_4 - SiO_2 illustrating the fundamental aspects of natural lithium aluminosilicate stability relations. The Figure indicates that spodumene is stable at relatively high P and moderate T, petalite is stable at moderate P and high T, and eucryptite + quartz is stable at relatively low P and T. London (1984) investigated this diagram experimentally for quartz saturated bulk compositions. The Figure shows that at 2 kbar, petalite is apparently stable with respect to spodumene + quartz down to at least 440°C. The invariant point (Bsp) lies in the vicinity of 300 - 350°C at 1200-1700 bars. Therefore the spodumene + petalite field prevails over a narrow range of moderate to high P and T.

7.2.2. Crystallization of primary lithium minerals and lepidolite

Petalite is the first primary lithium mineral to crystallize in the pegmatites in the Karibib region, Namibia. Petalite is considered by some authors (Stewart, 1978) to be last primary lithium mineral to have crystallized from a magma. Primary lithium phosphates appear to have crystallized after petalite implying that successive fluid-saturated magmas in the district became increasingly rich in phosphorus, and phosphates, rather than silicates, were the last primary minerals to crystallize with quartz. Thus amblygonite-montebbrasite (and lithiophilite) apparently succeeded petalite as the stable primary lithium phases in the pegmatites of the Karibib area. The sequence implies that the activities of the acidic volatiles, P and to a lesser extent F increased as crystallization proceeded and that petalite eventually became unstable with respect to montebbrasite + quartz. The composition of amblygonite-primary montebbrasite indicates that the pegmatites were F-rich, which is emphasized by the fact that lepidolite and Li-mica are abundant and in several pegmatites topaz has formed in addition to Li-mica.

In the pegmatites in Tantalite Valley primary lithium phosphates appear to have crystallized after spodumene and primary feldspars, again implying that successive fluid-saturated magmas in the Tantalite Valley area also became increasingly rich in phosphorus, with the same result that phosphates, rather than silicates, were the last primary minerals to crystallize with quartz.



The composition of primary montebbrasite indicates that the pegmatites in Tantalite Valley were F-rich, similar to the Karibib pegmatites; lepidolite is also abundant, however, in contrast to the Karibib pegmatites topaz has not been observed.

The processes responsible for the formation and destruction of lithium aluminosilicates in these differentiated pegmatites may be responsible for the dramatic concentration of rare-ores of tantalum, niobium, tin, caesium, rubidium, bismuth and beryllium in zones composed of cleavelandite and lepidolite which may have formed at the expense of spodumene-bearing pegmatite. The abundance of minerals Li, Be, Mn, Nb, Ta and Bi in the pegmatites in Karibib; Steinkopf, Namaqualand; and Tantalite Valley imply that they originated from a highly differentiated parental source magma (Hildreth, 1979, 1981).

Relatively coarse-grained cleavelandite units, which contain the same rare-element mineralization found in the three field localities investigated in this study, have been reported from localities throughout the world (Cameron et al., 1954; Beus 1960; Vlasov, 1961; Hornung and von Knorring, 1962; Lowenstein 1969; von Knorring, 1970, Jahns and Ewing, 1976). The origin of the cleavelandite units is still open to speculation. London and Burt (1982) feel that textural features in the White Picacho pegmatites, Arizona, indicate that at least some parts of cleavelandite or cleavelandite-lepidolite complexes replaced quartz-spodumene pegmatite either by reaction with residual magma or aqueous fluids. However, in the pegmatites in Karibib and Tantalite Valley, Namibia, the formation of these cleavelandite assemblages seem to represent the last stage of coarse-grained crystallization, that preceded the fine-grained postmagmatic pseudomorphism of the primary lithium minerals and these cleavelandite units appear to be the basis for tantalum, niobium and bismuth mineralization, which obviously originated from a highly differentiated source parental magma which continued to differentiate and fractionate Ta-Nb-Bi-Rb-Cs as the pegmatite developed (see Chapters 4 and 6). In addition, tantalite laths which are in contact with montebrasite (Plates 3.22, 3.23) are cut by hydroxyapatite which occurs at the contact of the two minerals; therefore this suggests that the tantalite laths in a microlite matrix preceded the

postmagmatic alteration of montebrasite to hydroxyapatite and hence the fine-grained pseudomorphism of primary lithium minerals.

The lithiumaluminosilicates alter to muscovite and lepidolite and theoretically topaz in the presence of acidic fluids (K+H) which have a high capacity to react and hydrolyse solid phases (Burt and London, 1982). In Karibib there is evidence that petalite alters to albite (see Plates 3.8, 3.9) and amblygonite is replaced by lithian mica (see Plates 3.11, 3.12). At the M4 pegmatite, Okatjimukuju, Karibib, (Plate 3.19) topaz, it is clear and unaffected, could possibly have been the last to crystallize, and the amblygonite is highly altered (see Plate 3.20), amblygonite is therefore presumably one of the first to have formed and this is compatible with the schematic diagrams (Figs. 3.1b, 3.4) produced by Burt and London (1982). After the formation of albite, postmagmatic (K+H)-rich fluids, in the presence of amblygonite have formed topaz along with lepidolite at localities in the Karibib area (M4, Jooste's), due to the local simultaneous crystallization of micas causing a deficiency of potassium, and an excess of fluorine.

In Tantalite Valley, topaz has not been located, Li-mica is prevalent, at the Homestead and Lepidolite pegmatites (see Plate 2.8 and Table 3.22); postmagmatic fluids were highly (K+H)-rich. In Namaqualand, Li-mica is present only in minor amounts and postmagmatic fluids were not K-rich. Amblygonite-montebrasite is present in Tantalite Valley in at least one pegmatite, Homestead (see Table 3.8) and locally there is a possibility of an influx of F- and P-rich fluids.

Generally, in an environment with K-rich postmagmatic fluids the lithium aluminosilicates are replaced by F-rich micas, i.e., lepidolite rather than topaz and these conditions are reflected in the rare-element pegmatites of Karibib, and in Tantalite Valley, Namibia.

In Namaqualand Li-mica is present in minor quantities and there is no amblygonite, and spodumene is the predominant lithium mineral. Therefore fluids were not significantly P and F-rich to enhance the formation of amblygonite-montebrazite and late micas but in some pegmatites minor phosphates are present in the form of lithiophilite. The formation of lithiophilite and Mn-apatite reflects the high Mn/(Mn+Fe) ratio in these pegmatites (Table 3.19) which favoured the formation of Li, Mn phosphates rather than amblygonite. However, the high Mn/(Mn+Fe) ratio in lithiophilite (see section 3.5) and manganotantalite (see Fig. 6.15a and 6.16) reflects the highly fractionated and differentiated nature of the pegmatites in Namaqualand, compatible with the high Mn/(Mn+Fe) ratios in lithiophilite and manganotantalite in Tantalite Valley (Fig. 6.16) and in Karibib, Namibia.

7.2.3. The melt and supercritical fluid and the process of accumulation of volatiles: Jahns and Burnham model

The following pages (277-282) concern the Jahns and Burnham' model (1969) for pegmatite crystallization from a hydrous silicate melt. As the interpretation of the pegmatite paragenesis in this study has been mostly considered in the light of the Jahns and Burnham model a few major points have been summarized below. However, since writing the present study London (1992) put forward another concept in favour of disequilibrium fractional crystallization through liquidus undercooling which would account for the coarse-grained textures displayed in pegmatites.

Jahns and Burham (1969) Jahns (1982) in considering an initial crystallization from a hydrous silicate melt recognize three major fundamental changes in the process from a hydrous melt containing as little as 0.1% water to final hydrothermal replacements of pre-existing minerals.

- i) Crystallization from a hydrous silicate melt
- ii) Crystallization from both a hydrous silicate melt and a coexisting supercritical aqueous fluid of considerably lower viscosity (yielding both giant sized textures along with finer grained, even aplitic, mineral aggregates).
- iii) Crystallization, in the absence of silicate melt, from a supercritical aqueous fluid yielding a wide variety of late stage products. and mineral aggregates formed through exchanges of material among aqueous fluids [+F+ P (halides)]. This stage in the crystallization sequence produces evidence for vigorous corrosion and replacement of quartz, K-feldspar and other minerals simultaneously with crystallization of the same minerals at other points within the same pegmatite bodies.

The appearance of an exsolved supercritical aqueous fluid derived from the crystallizing melt is regarded as the decisive event which is followed by fundamental changes in distribution and texture of the solid phases being formed.

The derivative magma is a confined silicate liquid with a water content which may range from 0.1%. If the liquid is not already saturated with water, its water content increases as crystallization proceeds in response to falling temperature, with development wholly or principally of anhydrous solid phases and the (restite) rest liquid. Continuation of the crystallization process, with or without reaction between solid phases and silicate melt, can lead to saturation of the rest liquid with water and hence to the phenomenon generally termed alternately as second boiling, resurgent boiling, or retrograde boiling. If the P is reduced (by fracturing of containing rocks) boiling or saturation may be induced earlier. A water-saturated magma, however formed, is the key condition for pegmatite formation of Jahns and Burnham' model. They suggest that the appearance of a supercritical fluid is correlated with the first appearance of giant crystals within regular zoned units. The supercritical fluid is synonymous with the beginning of large scale replacements that are not readily attributable to simple reaction between crystals and silicate liquid.

Under all conditions of pegmatitic crystallization the aqueous fluid is likely to be supercritical in terms of both the critical temperature and the critical pressure of pure water. The properties of a fluid at supercritical temperatures undergo continuous change with increasing pressure, above the critical pressure the normal distinction between liquid and gas loses most of its significance.

The term "gas" may be used for the aqueous fluid (supercritical fluid) i.e. at supercritical pressures. This term is also the proper designation for the fluid at supercritical temperatures and supercritical pressures in the few pegmatite systems that appear to have existed at very shallow depths in the earth's crust (Low P). In the ranges of P-T to which

the formation of igneous pegmatites normally corresponds, the aqueous phase is more liquid than gas-like in terms of its density, viscosity, solvent characteristics and other properties.

Owing to its co-existence with silicate melt which clearly can be designated as a liquid, the supercritical fluid also has been referred to as a vapour by some geologists even though the compositions of the silicate melt and aqueous phase are quite different. From the point of view of semantics, Jahns and Burnham (1969) feel it is appropriate to employ the more general terms: supercritical fluid, aqueous phase, aqueous fluid as an alternative among gas, liquid, and vapour.

The aqueous fluid initially separates on a sub-microscopic scale and then progressively assumes the role of an interstitial fluid within the silicate melt (magma). Under favourable conditions, time being an important factor, the aqueous fluid also can migrate upwards through the denser liquid and become concentrated in structurally high parts of the consolidating pegmatite body.

In general, crystallization within the two-fluid system yields relatively coarse-grained products from the aqueous phase and much finer-grained products from the melt. Inevitably, considerable reaction between solid and fluid phases is to be expected especially where the less viscous aqueous fluid is involved.

The solid phases formed from the silicate melt and aqueous fluid (stage ii) together with those formed earlier from magma alone (stage i) before any separation are thought to constitute the great bulk of the material found in most bodies of pegmatite.

A reduction in confining pressure, caused for example by the loss of combined water in the system (a magma of granitic composition), is reduced fairly rapidly through fracture

fillings at any time when quenching of the silicate liquid occurs. In effect loss of considerable dissolved water suddenly moves the liquid into the subsolidus region and quick consolidation follows. A typical product is an aplite. i.e. boiling is induced earlier.

7.2.4. Late stage fluid phases (hydrothermal stage of pegmatite formation)

After the disappearance of silicate melt, deposition and reaction would involve crystals and supercritical aqueous fluid, or at considerably lower T and P various combinations of crystals, aqueous liquid and aqueous vapour.

Some reaction between crystals and silicate rest liquid is to be expected throughout the consolidation process, but reactions involving the much less viscous fluid or fluids should be considerably more effective in converting one solid phase into another within a pegmatitic body. Most of the widespread results of corrosion and mineral replacement that have been observed in pegmatites are attributed to reactions of this kind.

If interpreted from the Jahns and Burham model (1969) cleavelandite units could be attributed to a supercritical fluid. Therefore cleavelandite replacement units probably involve crystals, silicate melt and supercritical fluid at the critical temperature and the critical pressure.

Finally, the actions of aqueous liquid and vapour are responsible for alterations of some minerals and development of others at relatively low temperatures i.e., in the hydrothermal stage or low temperature stage as designated by most investigators. pseudomorphic replacements are attributed to this low temperature aqueous liquid and vapour stage. Pseudomorphic replacements - so called "hydrothermal" - do not involve a

silicate melt, it has been used up, they involve aqueous fluid and vapour below the critical temperature and crystals, i.e., at relatively lower temperatures.

At these temperatures reactions would involve crystals and a (supercritical) fluid which under low confining pressures would have condensed at its critical temperature to permit reactions involving aqueous liquid plus vapour. Such conditions of condensation within the system would form a liquid with highly corrosive properties with respect to earlier crystalline phases (Bowen 1933). Resulting mineral replacement is responsible for features such as partial and complete crystal pseudomorphs.

Jahns and Burnham (1969) emphasize however that crystallization and replacement described in this later stage could be attributed to an earlier stage when some silicate liquid was still present.

Jahns and Burnham (1969), Jahns (1982) state that the coarseness of many rocks formed from water-bearing magmas in the absence of a free aqueous phase could be reasonably attributed to very slow crystallization. London (1992) advocates a process of supersaturation due to undercooling and limited nucleation points which he believes is responsible for the formation of coarse textures in pegmatites.

Alternatively, the coarseness might reflect rapid transfer of nourishing materials to centres of crystallization in highly fluid magmas. However, although water, F and other volatiles lower the isothermal viscosity of granitic melts the addition of volatiles at the same time lowers the solidus-liquidus region for such melts, thereby tending to increase their viscosity in the range of consolidation. The presence of water thus imposes opposite effects, one thermal and one compositional on the viscosity of a crystallizing magma.

Munoz (1971) showed that lepidolite is stable at low temperatures in pegmatite mineral assemblages and that it can form by subsolidus reaction of spodumene and K-feldspar by F-rich aqueous fluids in outer intermediate zones.

Norton (1973) pointed out that textural and structural relations of lepidolite, spodumene and microcline at many localities indicate that lepidolite does form by replacement at lower temperatures. However, although lepidolite assemblages may have a very disordered texture with abundant and very coarse-grained features on the whole they lack evidence of any pre-existing lithium minerals when they occur in the inner zones of pegmatites.

Lepidolite may have crystallized directly from a siliceous "gas" (Stewart 1963) if lepidolite is occurring with quartz. However, Norton (1973) pointed out that in some pegmatites lepidolite is associated with cleavelandite albite and its origin from a "gaseous medium" becomes questionable. However, volcanological studies on Mount Etna (Tazieff, 1970) have shown that volcanic gases can precipitate alkali-feldspar. If lepidolite can form at low T by subsolidus reaction as a replacement mineral in an 'outer zone' - spodumene zone for example, then it should crystallize as a dual precipitate of whatever residual fluid remains at these temperatures trapped in the centre of the pegmatites.

The mechanism of replacement may be interpreted in terms of a supercritical fluid. The evolution of a supercritical fluid is a typical stage of evolution in volatile-rich granitic magmas (Jahns and Burnham, 1969; Jahns, 1982). Rare-element pegmatites consolidate largely from a silicate melt co-existing with an exsolved supercritical fluid which subsequently reacts extensively with solid phases after the melt is exhausted (Jahns, 1982).

7.2.5. The pegmatite P-T regime

Most intrusive granite magmas containing 1% H₂O could be expected to begin to crystallize in the region of 1000-900° C with increasing H₂O the range would decrease progressively downwards into a minimum region below 700°C in confining P and not saturated with water - therefore a minimum temperature between 900-650°C in the absence of a supercritical fluid i.e., not saturated with water (Jahns and Burnham, 1969)

Jahns and Burnham (1969) point out that a value for the critical temperature is difficult to derive from that of pure water because of the lack of data on the type and effect of dissolved "volatiles". Some suggestions are as follows :-

Fersman (1931)	400°C
Vogt (1926)	400-425°C (upper limit)
Gillingham (1948)	500°C (below)

It can be inferred through experimental studies of Jahns and Burnham (1969) on the beginning of melting of pegmatites in the presence of water that the silicate melt phase could have persisted to temperatures in the range 600-500°C, especially those with a high percentage of Li, F present which lowers the liquidus T.

The lower limit for the hydrothermal stage is set at 100°C (see Jahns and Burnham, 1969) therefore the hydrothermal stage may range between 400-100°C and is characterized by crystals, aqueous liquid and vapour at temperatures too low for a 'supercritical fluid'.

At T between 600-400°C (when the silicate melt has been used up) and the system is characterized by crystals and supercritical fluid (referred to as pneumatolitic by Fersman, (1931), Quensel (1956) and Schneiderhohn (1961).

Jahns and Burnham (1969) prefer to consider each stage by the development of a new phase; there P-T regime is shown below.

T From above 800° ----> 600° SILICATE Melt + crystals

T From above 600° -----> 500° SILICATE MELT + CRYSTALS +
SUPERCRITICAL FLUID

650-100° CRYSTAL+ FLUID

500-100° Crystals + liquid + vapour
(condensation of supercritical fluid)

7.2.6 Evidence of hydrothermal activity : and the effect of postmagmatic fluids.

Subsolidus metasomatic alteration of spodumene and montebrasite in this study was pseudomorphic in nature and produced a large number of fine-grained secondary phases and replacement assemblages. Examples of spodumene pseudomorphic replacements are given from the Norrabees, and Noumas pegmatites, Namaqualand and the SW Witkop pegmatite in Tantalite Valley (see Plates 3.2-3.6). Examples of montebrasite replacement by secondary minerals such as natromontebrasite, crandallite and brazilianite are shown in Plates 3.17-3.20 and section 3.4.5) respectively as well as by secondary montebrasite (see Chapter 3).

Figs. 3.7. shows the alteration sequences for amblygonite-montebrasite in the Karibib area, Namibia and the alteration sequence for spodumene in the Steinkopf area

pegmatites, Namaqualand and Tantalite Valley, Warmbad, Namibia and the inferred chemical processes that give rise to the observed alteration sequences.

The alteration of these primary minerals (spodumene and amblygonite) involved cation exchange with a fluid rich in Na and Ca relative to Li. During the alteration, lithium was removed from the primary Li-minerals and incorporated in fine-grained secondary micas with the addition of K + H-rich fluids and Rb and Cs which were highly fractionated elements in the postmagmatic fluid effecting the pseudomorphic alteration.

In addition, at higher temperatures during albitization, cleavelandite units were formed and these were later converted in part also to fine-grained micas (see Plates 3.28-3.30). Spodumene albitization may have been produced as Na-rich fluids escaped along fractures from cleavelandite zones into overlying quartz-spodumene pegmatite.

The widespread formation of secondary mica in spodumene, montebrasite, tourmaline and feldspar signifies a gradual change from alkaline to relatively acid postmagmatic fluids, as (K+H)-metasomatism produced alteration characteristic of sericitization.

Late-stage fluids were F-rich, as evidenced by the formation of Li-mica with a high F content and topaz. Topaz was formed during the later part of acid metasomatism after the conversion of late stage micas, and due perhaps to a deficiency in K after the formation of the micas.

Fluid composition probably varied with location and time in the pegmatites accounting for the sporadic distribution and variations in observed alteration assemblages. Throughout the sharply zoned pegmatites much of the pseudomorphic alteration may have been produced by upward migrating fluids along fractures, (see Plates 3.5 and 3.6) attempting to equilibrate with different solid phase assemblages from zone to zone.

The initial subsolidus metasomatism of lithium minerals in the pegmatites in the Karibib area took place in an alkaline environment as evidenced by the Na-for-Li exchange in petalite and Ca-for-Li exchange in amblygonite -montebrasite. This observation implies that the fluid chemistry changed significantly from the later primary stage when acidic P- and F-rich fluids promoted the formation of montebrasite + quartz, to subsolidus conditions sufficiently alkaline to stabilize eucryptite + albite.

London and Burt (1982) consider the postmagmatic stage to be equivalent to the "supercritical fluid" (with depletion of silicate liquid) as interpreted by the Jahns and Burnham model (1969); Jahns (1982). Within the higher temperature region of the supercritical fluid, cleavelandite and lithian mica were formed, before the "hydrothermal stage" which Jahns and Burnham consider to be at a lower temperature with the condensation of the supercritical fluid into an aqueous liquid and vapour stage. It is suggested by London and Burt (1982) that cleavelandite units were formed during albitization due to metasomatic reaction with spodumene, for example the term albitization appears to be used for both cleavelandite replacement and crystallization of massive coarse-grained zones, and also for minor pseudomorphic replacements. Perhaps albitization could apply to the formation of cleavelandite zones, initially, but with decreasing temperature and a depleted and diluted fluid, low temperature pseudomorphic replacements may occur, similar to those found in the pegmatites at Norrabees, Noumas and SW Witkop in spodumene.

However, from data on fluid inclusions, London (1990,1992) considers cleavelandite also to be a primary mineral. He points out that there is a sharp change in fluid inclusion composition between 410 and 475° C and over this narrow P-T interval, the silicate components of the late-stage melt crystallize as rare-element albite-mica units.

Primary montebrasite forms in F-poor conditions at the expense of amblygonite; while natramblygonite- fremontite forms with the addition of fluids rich in Na. In acid P- and F- rich fluids, all the LiAl silicates become unstable relative to amblygonite or montebrasite + quartz or amblygonite + albite with additional Na-rich fluids. LiAl-silicates (petalite) alter to albite and amblygonite alters to mica .

7.3. PARAGENETIC SEQUENCE OF THE RARE-ELEMENT PEGMATITES

7.3.1. Pegmatites in the Karibib-Usakos area

The general paragenetic sequence of the Karibib rare-element pegmatites is shown in Figure 7.1.

The Rubicon pegmatite is believed to have primary crystallized from a silicate melt of granite bulk composition which generated at depth during the peak of regional metamorphism (Smith, 1961) about 530 Ma ago . Similar ages for Li-rich rare-metal pegmatites in the Cape Cross-Uis pegmatite field have been obtained (Diehl and Schneider , 1990). Rare-alkali fractionation which is pollucite-bearing, combined with "late-stage" Na-Li metasomatism in many phases, they feel strongly emphasizes the complexity of melt-vapour reaction which continued in the subsolidus.

Petalite reflects P-T conditions of 1.8-2kb at 560-480OC during the crystallization of petalite from a silicate-rich aqueous fluid. Stewart (1978) considered that the petalite zone was the last to crystallize from a melt. Rubicon is thought to belong to Ginsburg's "Intermediate level" pegmatites (H-T and Low-P). Cleavelandite, lithian mica and

petalite are intergrown at Rubicon and field relations of several cross-cutting lithian mica veins suggest a sequence of albite and lepidolite after petalite, though albite and lepidolite are dominantly parallel to the zonation in other areas. However, some of the contacts of petalite and lepidolite are corrosive (Roering, 1961).

The sequence of crystallization and replacement units in the Rubicon and Karibib pegmatites may be specified, according to Roering (1961) and Diehl and Schneider, (1990) as follows: -

- 1) Primary crystallization from the margin to the core,
- 2) Due to changes in chemical equilibrium conditions, either caused by melt-fluid-ion-exchange processes- or more likely by re-opening and the new influx of a melt-vapour phase, Na-Be-Li metasomatic fluids led to the replacement of the primary zones from the core to the margin, cross-cutting the zonation of the body.
- 3) The primary granitic composition of the melt is reflected in the composition of the outer intermediate zone which lacks Li-mineralization.
- 4) Crystallization of petalite began when remaining supercritical fluid was enriched in Na, Li and volatile fluid phases.

This is an interpretation based partly on the Jahns and Burnham's model (1969) of a corrosive, supercritical reactive fluid, though Diehl and Schneider (1990) favour a partially open system, in contrast to Jahns and Burnham.

7.3.2. Paragenetic sequence of mineral assemblages in the Tantalite Valley, Namibia and Steinkopf area, Namaqualand pegmatites

A schematic diagram showing the sequence of mineral assemblages for Steinkopf, Namaqualand the Tantalite Valley pegmatites is shown in Figures 7.2 and 7.3 respectively. In the rare-element fractionated pegmatites, of Tantalite Valley the outer zones generally are composed of muscovite, albite and quartz. The intermediate zone incorporates the lithium minerals, spodumene and lepidolite generally associated with cleavelandite and K-feldspar, while the core is composed of quartz and microcline.

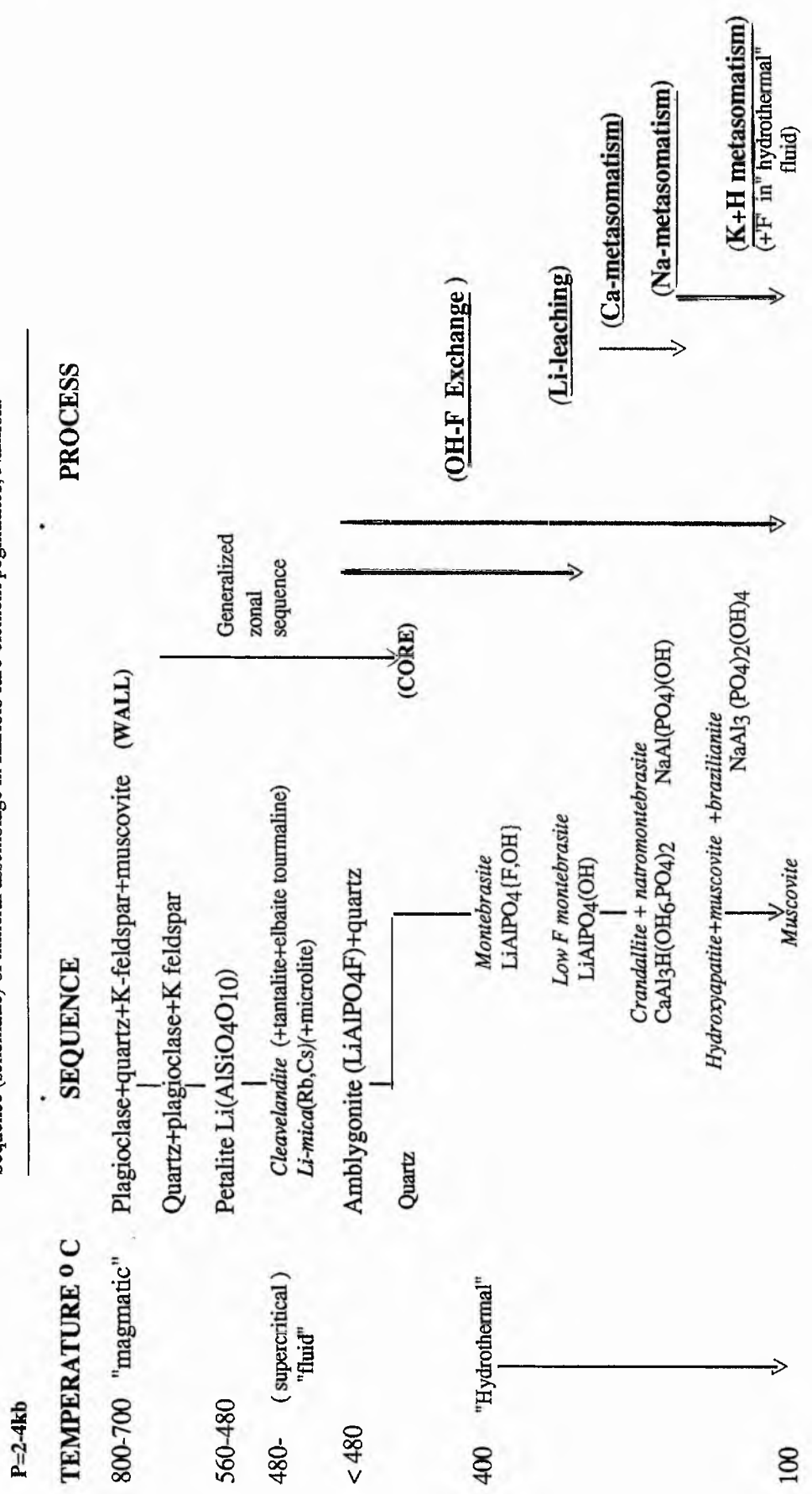
The available data on the homogenization temperatures (i.e. minimum filling temperatures) of multiphase fluid inclusions suggest that spodumene or spodumene-bearing pegmatite crystallizes in the range of 300 - 650° C (Sheshulin, 1963; Bazarov and Motorina, 1969; Taylor et al. 1979). Sheshulin (1963) identified two generations of spodumene in pegmatites from the Soviet Union; homogenization temperatures were 500-650° C for first generation spodumene and 290-390° C for second generation spodumene. Estimates of filling pressure for saline or CO₂-rich inclusions indicate pegmatite crystallization pressures in the range of 1.5-2.5 kbar (Bazarov and Motorina, 1969; Taylor et al. 1979). The results of these studies imply that spodumene (+quartz) is stable to pressures at least as low as 2 kbar and at low to moderate temperatures.

Lithium-rich pegmatites crystallize in the range 1.5-2.5 kbar (Bazarov and Motorina, 1969). Spodumene + quartz assemblages probably are restricted to temperatures below 350-475 °C over this pressure range 1.5-2.5 kbar (London and Burt, 1982c, Fig. 3). This is compatible with Cook's (1979) results: - a temperature near 425° ± 50°C at 2.0-2.5 kbar for primary spodumene + quartz at the Harding Pegmatite, New Mexico.

Spodumene assemblages in Tantalite Valley and Steinkopf, Namaqualand have been placed at 480°C (see Fig 3.1a) within the pressure range of 1.5-2.5 kbar. Spodumene hydrothermal replacement (see Plates 3.5-3.6) are placed in the temperature range 400-100°C (see Jahns and Burnham, 1969, this study pages 277-284).

Cleavelandite crystallization generally, either primary or replacement, is placed at temperatures between the spodumene crystallization temperature and the hydrothermal maximum. Large lepidolite units are placed at the hydrothermal maximum as lepidolite replacements of cleavelandite are in evidence (see Plates 3.28-3.29, and page 132, this study). Crystallization of the cleavelandite zone probably involving both a late-stage Na-rich residual melt and a supercritical Na-rich fluid as evidenced from fluid inclusions which are alkaline and sodic in bulk composition (London, 1990) at temperatures near the solidus (London, 1992). Excess Na-rich fluids may then sequentially be the source of fluids which form replacement lepidolite complexes by reacting with spodumene units and creating an excess of K by ion exchange (London, 1990). The cleavelandite complexes host beryl (see Appendix 1, the Angelienspan pegmatites) and columbite-tantalite (see Plate 4.2) and cleavelandite-lepidolite intergrowths host both manganotantalite, wodginite and microlite (see Plates 4.12, 3.28) (P-T data is not available for columbite-tantalite). In addition columbite-tantalite, in contrast to manganotantalite, occurs in both mica and K-feldspar (Plates 4.7, 4.10, 4.11), so in this case either the columbite-tantalite formed earlier in the crystallization sequence or the pegmatite is less evolved. (see Chapter 6).

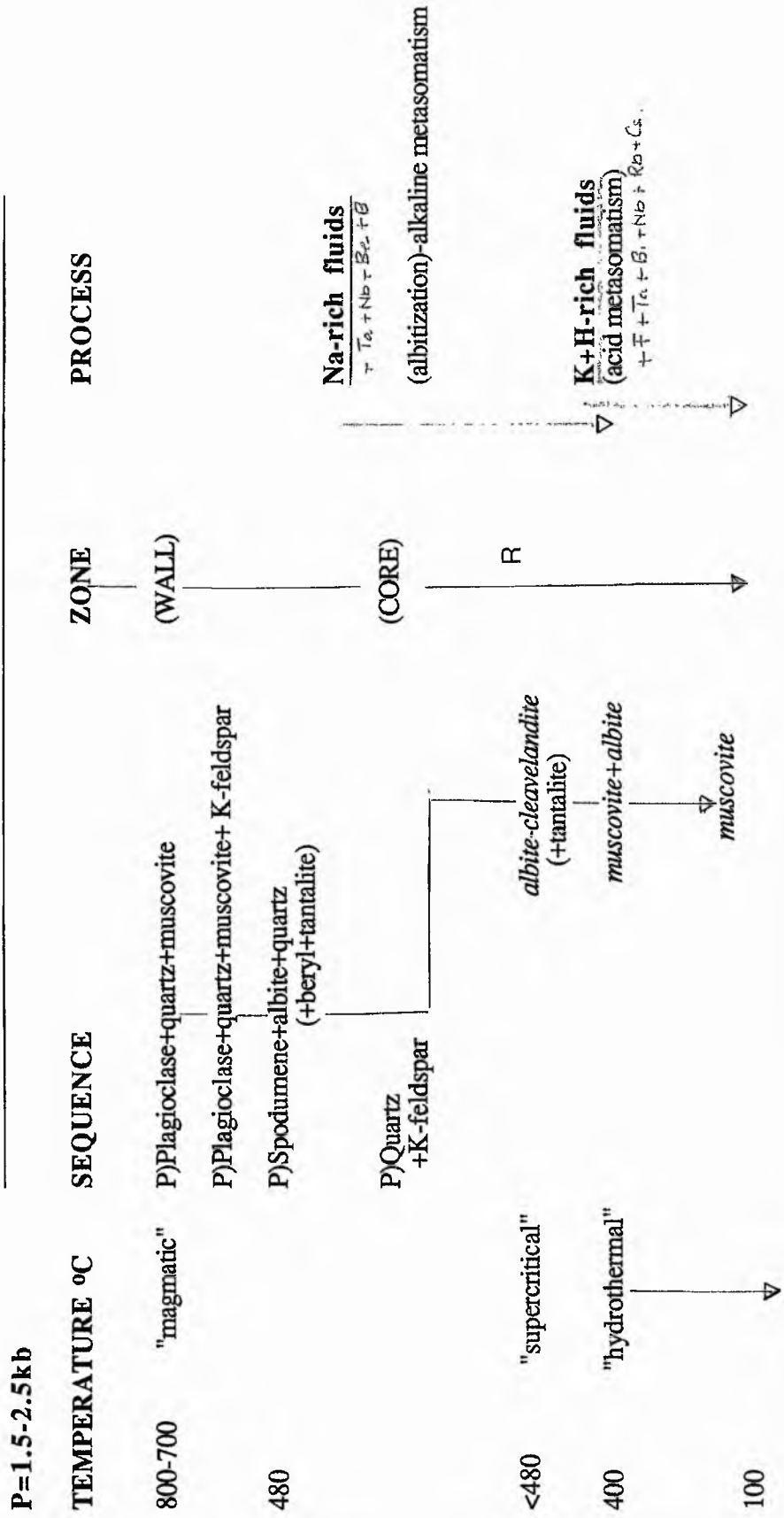
FIGURE 7.1
Sequence (schematic) of mineral assemblage in Karibib rare-element pegmatites, Namibia



Zonal and Secondary Replacement minerals in italics

FIGURE 7.2.

Sequence of mineral assemblage in the rare-element pegmatites from Steinkopf, Namaqualand

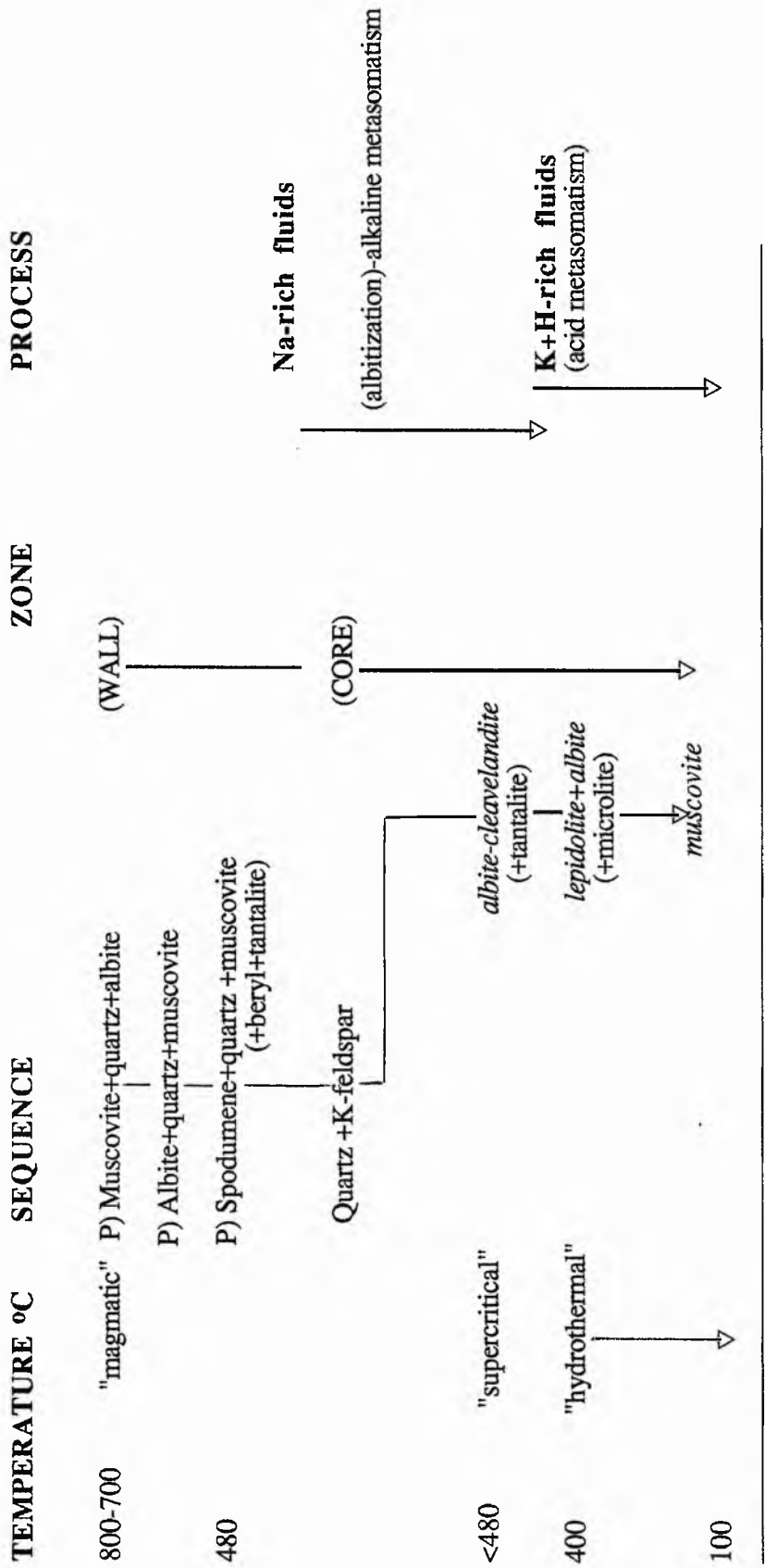


P=primary minerals; R= replacement
 Oblique arrows are diagrammatic
 Minerals in italics are replacement

FIGURE 7.3

Sequence of mineral assemblage in the rare-element pegmatites from Tantalite Valley, Namibia

P = 1.5-2.5 kb



P= Magmatic primary minerals;

Minerals in italics are replacement (see Fig. 7.1)

7.3.3. Thermogravitational diffusion

Thermogravitational diffusion as described by Hildreth (1979) provides a mechanism for the concentration of rare-elements, to be available for injection, from the roof zones of zoned silicic granitic bodies from which strongly differentiated capping magmas commonly erupt.

Hypotheses concerning the metal concentrations in rare-metal plutons by Kovalenko (1978) and Kovalenko et al. (1970, 1984) consider that concentrations of rare-metals in the upper zones of apogranitic plutons occurs during crystallization in the presence of an aqueous-rich fluid phase. The textural features of many rare-metal granites and the distribution of rock types are consistent with crystallization in the presence of an aqueous-rich fluid phase, and suggest concentrations of volatiles in the upper portion of the magma chamber from a very early stage. Disseminated rare-metal mineralization is localized within the upper contact zones of small steep-sided plutons, or within irregularities on the upper surface of larger plutons. Within these areas the granites exhibit important textural and mineralogical variations which can usually be rationalized into a vertical zonation scheme. Hildreth (1979) points out that compositional and thermal gradients existed in the liquid in the magma chamber prior to phenocryst precipitation and developed largely independently of crystal liquid equilibria. Within water- and halogen-enriched high-silica roof zones of large magma chambers, chemical separations take place through the combined effects of convective circulation, internal diffusion, complexation, and wall-rock exchange to develop compositional gradients, which are linked to gradients in the structure of the melt and are controlled by the thermal and gravitational fields of the magma chamber itself (Hildreth, 1979).

The Bishop Tuff of eastern California provides evidence for the origin of compositional zonation in silicic magma chambers (Hildreth, 1979). W, Mo, Nb, Sb, Ta and U were enriched greatly upward in the magma chamber, while Ba for example was depleted in

the roof (Ba is depleted in early crystallizing phases (see Chapter 6). Dykes or stocks and pegmatites injected above a magma chamber undergoing thermogravitational diffusion will be either barren of, or enriched in, rare-elements susceptible to subsequent (hydrothermal) concentration, dependent upon the timing and emplacement relative to cycles of enrichment and eruption. Hildreth (1979) points out that crystal-liquid equilibrium probably predominated during initial generation of the dominant magma volume as during its ultimate plutonic consolidation.

On the basis of geothermometry, geobarometry, isotope and fluid inclusion studies, pegmatite crystallization is considered as an extension of plutonic granite consolidation, to lower temperatures and pressures, in the presence of increasing concentrations of fluxing components and volatiles (London 1986, Shearer et al. 1987). Li (Rb, Cs), Be, B, P, F and H₂O depress the liquidus and solidus of the pegmatite melt and reduce its viscosity. The most fluid and thermally stable melts can migrate farthest away from plutonic sources (Cerny, 1989).

Progressive evolution of fertile granites into rare-element pegmatites has been confirmed by numerous studies of trace-element fractionation (Goad and Cerny 1981; Cerny et al. 1985; Shearer et al. 1987). Progressive fractionation of leucogranitic melt into compositions close to highly evolved rare-element pegmatites has been documented on the example of Macusani glass and enclosing tuff (Pichavant et al. 1987).
scheme.

In addition to lowering the liquidus and solidus T, fluorine causes a reorganization of melt structure (Manning 1981) promoting depolymerization and the creation of new complex species in the melt. In this process the number of structurally favourable sites for the incorporation of lithophile elements increases, resulting in enhanced transport of these elements. F also promotes an increase in melt diffusivities (Dingwell, 1985) and

experiments in Soret diffusion indicate a concentration of Na and F in the cooler end of the cell. These data provide support for a model whereby chemical gradients are established in the pluton at an early age, partly as a result of diffusion-controlled processes, with the accumulation of F, Na and ore-forming elements towards the roof of the pluton.

The degree of enrichment within differentiated tops of a given magma chamber probably reflects the repose time between eruptions, the volatile flux, and the rate of energy transfer from the mantle more than it does the bulk composition of the unerupted dominant volume.

Rare-element pegmatites may represent injections from an enriched roof-zone of one of these magma chambers with less evolved pegmatites perhaps representing either i) tapping of the magma chamber at a lower differentiated or less enriched layer or ii) perhaps representing a time lapse between eruptions insufficient to have developed a highly evolved and enriched roof zone in the magma chamber. Therefore it is suggested that each rare-element pegmatite involves a separate emplacement or injection from the magma chamber in time. The less evolved pegmatites occurring on the same time scale and the more evolved fractionated pegmatites occurring subsequently but on a different time scale.

7.3.4 Derivation of the rare-element pegmatites

Derivation of fertile peraluminous granites from which complex rare-element lithium pegmatites have originated are due to partial melting of upper crustal rocks undergoing their first anatectic event (Cerny , 1989). Peraluminous rare-element lithium-type pegmatites were traditionally regarded as orogenic, either late-tectonic or post-tectonic. For example, the Precambrian Damara Sequence of Namibia is known for its numerous granite pegmatites which Smith (1962) considered to be related to the Damaran Orogeny, the economic highly fractionated pegmatites have intruded tightly folded mica schists, marbles and quartzites. They are predominantly concordant with the host rocks, are unmetamorphosed and therefore post-tectonic; their relationship with the granite is not clear.

The rare-element pegmatites of the 'Namaqualand Pegmatite Belt' in the Northern Cape of South Africa and Namibia , which includes the Kenhardt area in the west, the Tantalite Valley area in the centre and the Steinkopf area in the west, are connected with Precambrian granites and granite gneisses and are intrusive into Archean rocks. In the Tantalite Valley area in the central region of the Belt Moore (1975) considered the distribution of rare-element pegmatites to be related to several periods of deformation and to an ultrabasic complex known as the "Tantalite Valley Complex".

7.3.5 Disequilibrium versus equilibrium fractional crystallization

Jahns (1953) favoured disequilibrium crystallization as a means of explaining the textures and crystallization features in granite pegmatites. He attributed the zonal features and progressive coarsening of pegmatite minerals to "fractional crystallization and incomplete reaction between successive crops of crystals and rest liquid from a silicate melt of low viscosity with masses of pegmatite crystallizing inward from the

walls of an original magma chamber in a restricted system". He considered nearly all giant crystals were formed during what has been designated by most investigators as the primary or magmatic stage of pegmatite development with giant crystals forming rapidly under restricted-system conditions involving rather delicate temperature and chemical balance, with T below 600 C and the confining pressure sufficiently great to prevent major escape of volatile constituents.

With the advent of their experimental studies Jahns and Burnham (1969), next favoured equilibrium crystallization in place of disequilibrium fractional crystallization. (this was the favoured hypothesis at the time) in spite of the fact that they also recognized that the compositions of granitic pegmatites approach those of the haplogranite eutectic at moderate pressures of H₂O. They favoured equilibrium crystallization with simultaneous crystallization of giant crystals and fine-grained textures, with widespread replacement activity acting at the same time throughout the pegmatite system via a separate exsolved supercritical fluid which acted independently, and in addition to, the silicate melt. The constraints of a model for equilibrium crystallization of a eutectic composition faced Jahns with several problems, particularly the simultaneous rather than sequential development of segregated and texturally distinct zones which equilibrium crystallization obviously implied. Jahns recognized (1979, pers. comm. to London) that the textural and zonal features of pegmatites were inconsistent with equilibrium crystallization at the eutectic of haplogranitic melts. This required another agent, an aqueous phase or exsolved supercritical fluid, to accomplish what magmatic crystallization apparently could not do.

London (1992) presented an experimentally and theoretically based model in favour of disequilibrium fractional crystallization through liquidus undercooling for pegmatite systems which reaffirmed the original hypothesis presented by Jahns (1953). London (1992) by his model, more adequately explains the textures and zonation in pegmatites

and points out that the degree of liquidus undercooling and the concentrations of quartz-feldspar-incompatible components in the silicate melt, in particular H₂O, B, P and F govern the textural development of granitic magmas by controlling the rate and number of crystal nuclei formed.

The presence or not of a saturated aqueous phase during the early stages of crystallization in most pegmatites is still open to conjecture (London, 1992) although there is good evidence from petrological and fluid inclusion data that pegmatites do not attain saturation in an aqueous phase until they are practically consolidated (until they approach their solidi). This evidence requires that granite systems are also undersaturated at the time of withdrawal of the pegmatite forming magma ; granites themselves are the products of H₂O under-saturated crystallization.

London (1992) from recent studies (London et al. 1988, 1989) has demonstrated that there is no unique simple relationship between an aqueous phase and the textural transition from granitic to pegmatitic texture in experiments, in fact saturation in an aqueous phase may actually impede the formation of pegmatites.

The genetic link between granites and pegmatites is still poorly understood (London 1992). Granite-pegmatite relations have been studied by chemical trends (Goad and Cerny, 1982 ; Cerny et al. 1985; Cerny, 1991) but not in terms of process. The characteristics of most pegmatite groups suggest a single main pulse of magma injection from the domes of parental granites, followed by sporadic closure of dyke conduits and subsequent internal differentiation of restricted bodies of pegmatite (London 1990). London (1992) points out that if pegmatite-forming magmas are produced from a differentiated silicate liquid which has originally fractionated crystals in a large source magma chamber, they must originate by very efficient separation of silicate liquid from crystals. The field relations in pegmatites imply that much of the chemical differentiation

within a pegmatite has already taken place at the time of emplacement (London 1992) and is inherited in the liquid state from the source body (Cerny 1982). The parental source, by hypothesis, is a vertically zoned magma chamber with a thermal gradient which has been produced by thermogravitational convection diffusion (Hildreth, 1981).

7.3.6. Derivation of the fertile granites

Studies of trace-element fractionation have documented the progressive evolution of fertile granites into rare-element pegmatites with extreme enrichment of trace components (Goad and Cerny, 1981; Cerny et al., 1985 and Shearer et al., 1987). The fractionation trends ultimately begin with concentrations of trace elements in metamorphic protoliths from which the pegmatitic-generating granites are derived (Cerny, 1985). Partial melting and the degree of volatile saturation is requisite in producing the type of rare-element concentrations in the initial magma (Hildreth, 1979, 81). Internal evolution of magma bodies produces highly silicic melts greatly enriched in rare-elements and volatiles through crystal-melt fractionation, liquid fractionation and transport in a hydrous phase, through either diffusion or exsolution. These melts eventually solidify as late intrusive masses of fertile, pegmatite-generating leucogranites. Pegmatitic crystallization is an extension of plutonic granite consolidation to lower temperatures and pressures in the presence of increasing fluxing components and volatiles such as Li (Rb,Cs), Be, B, P, F and H₂O which depress the liquidus and solidus of pegmatite melt and reduce its viscosity (London 1986b, 1992). Extreme crystal-melt partition co-efficients of Li, Rb, Cs, Ba and Sr and complexing are important contributory factors in the accumulation of tantalum and lithium (+Cs) in rare-element pegmatites.

CHAPTER 8

CONCLUSIONS

The petrogenesis of Li-pegmatites depends on 3 major processes:

1. A highly differentiated source magma with extreme fractionation of elements such as Ta, Rb and Cs which accompany Li. At the stage of initial lithium crystallization, the differentiated source magma is in the state of crystals, which make up the primary magmatic zones, silicate melt and possible aqueous fluid.

The order of crystallization of Li-minerals follows this general sequence:

**spodumene,
petalite
amblygonite**

Spodumene and petalite form large primary crystals in the zoned lithium pegmatites (primary refers to minerals or assemblages of minerals which crystallize from a magma [\pm an aqueous fluid]). Petalite may be the last of these mineral to crystallize from a magma.

2. Replacement minerals such as cleavelandite and Li-mica (forming in some cases huge zones) which occur in the subsolidus and form from replacement of previous minerals by reactions with the supercritical fluid and perhaps from the residual magma.

These two major replacement minerals host the Ta-minerals which includes:

**columbite
tantalite
tapiolite
wodginite
microlite**

Amblygonite is contemporaneous with tantalite and therefore may be contemporaneous with cleavelandite in the crystallization sequence.

Lithian mica (lepidolite) is the last mineral to crystallize in the lithium sequence and it "extremely" fractionates Rb and Cs in the Karibib, Steinkopf and Tantalite Valley pegmatites. Similarly, manganotantalite "extremely" fractionates tantalum (and manganese). Therefore the minerals lithian mica (lepidolite) and manganotantalite reflect extreme differentiation and fractionation of an original silicate magma by enrichment in Rb, Cs and Ta in rare-element pegmatites which have inherited their geochemical signature from pre-enriched rare-element parental granites.

3. "Hydrothermal" replacement or late stage replacement of Li and Ta-minerals by "post-magmatic fluids" rich in OH, F and P volatiles. The aqueous phase is no longer in the state of the supercritical fluid but rather that of an aqueous vapour and liquid at relatively low temperatures.

This process encompasses the formation of:

Li-mica (replacing spodumene)
montebrasite (replacing amblygonite)(±crandallite,
±natromontebrasite± brazilianite)
microlite (replacing tantalite)

REFERENCES

- AHRENS, L.H. (1966): Notes on the Rb-Cs dispersion relationship, with particular reference to pegmatitic microclines from the Sayen Mountains, U.S.S.R. *geochim. Cosmochim. Acta* 30, 105-107.
- BALDWIN, J. R. (1979): Manganese garnet and associated minerals in pegmatites. M.Sc. thesis. Univ. St. Andrews.
- BALDWIN, J. R. (1985): Some geochemical aspects of rare-element pegmatites from southern Africa *Abstr. CIFEG. 13th Coll. afr. Geol. St. Andrews*, 340-341.
- BALDWIN, J. R. (1989): Replacement phenomena in tantalum minerals from rare-metal pegmatites, South Africa and Namibia. *Mineralog. Mag.* 53, 571-581.
- BAZAROV, L.S. & I.V. MOTORINA. (1969): Physicochemical conditions during formation of rare-metal pegmatites of the sodium-lithium type. *Doklady Akademii Nauk USSR*, 188, 194-97. (Trans, *Doklady of the Acad. Sci. USSR Earth Sci. Sect.* 188, 124-126).
- BERGGREN, T. (1940): Minerals of the Varutrask pegmatite, XV. Analyses of the mica minerals and their interpretation. *Geol. For. Forh. Stockholm*, 62, 182.
- BEUS, A.A. (1960): *Geochemistry of Beryllium and Genetic Types of Beryllium Deposits.* Acad. Sci. USSR., Moscow; English trans (1966): Freeman & Co., San Francisco.
- BEUS, A.A. & A.A.SITNIN (1968): Geochemical features of the distribution of tantalum in granitoids. *Geochem Int.* 5, 490-495.
- BORODIN, L.S. & I.I. NAZARENKO (1957): Chemical composition of pyrochlore and diadochic substitutions in the $A_2B_2X_7$ molecule. *Geochem.* 4, 330-349.
- BOWEN, N. L. (1933): The broader story of magmatic differentiation, briefly told, in ore deposits of the Western States: *Amer. Inst. Min. & Met. Eng.* 106-128. New York.
- BRANDENBERGER, E. (1931): Die Kristallstruktur von Koppit. *Kristallogr.* 76, 322-334.
- BROCK, K.J. (1974): Zoned lithium-aluminium mica crystals from the Pala pegmatite district. *Am. Mineral.*, 59, 1242-1248.
- BURT, D.M., LONDON, D & M.R. SMITH (1977): Eucryptite from Arizona and the lithium aluminosilicate phase diagram. (abstr.) *Geol. Soc. SAM Er., Abstr. Progr.* 9 (7), 917.
- BURT, D.M. & LONDON, D (1982): Subsolidus equilibria. *MAC. Short Course Handbook* 8, 329-346.

- BURT, D.M., SHERIDAN, M.F., BIKUN, J.V. & E.H. CHRISTIANSEN (1982):
Topaz rhyolites-distribution, origin and significance for exploration.
Econ. Geol. 77, 1818-1836.
- CAMERON, F.N., JAHNS, R.H., McNAIR, A.H. & L.R. PAGE (1949): Internal structure
of Granite Pegmatites. *Econ Geol. Mon.* 2.
- CAMERON, F.N. (1955): Concepts of the internal structure of granitic pegmatites and
their applications to certain pegmatites of South West Africa. *Trans.*
geol. Soc.S. Afr., 58, 45-70.
- CERNA, I; P.CERNY & R.B. FERGUSON (1972): Some physical properties of the
amblygonite-montebbrasite minerals. *Am. Mineral.* 58, 291-301.
- CERNY, P. (1975): Granitic pegmatites and their minerals, selected examples of recent
progress. Anatomy and classification of granitic pegmatites. *Fortschr.*
Miner. 52, 225-250.
- CERNY, P. (1982): Anatomy and classification of granitic pegmatites. In granitic
pegmatites in Science and Industry. (Ed. P. Cerny) MAC. Short Course, 8
1-39.
- CERNY, P. (1989): Characteristics of pegmatite deposits of tantalum. In : Lanthanides,
Tantalum and Niobium. P.Moller, P.Cerny and F. Saupe (Eds.) . Springer
Verlag . Berlin . Heidelberg. 195-239.
- CERNY, P. & T.S. ERCIT (1985): Some recent advances in the mineralogy and
geochemistry of Nb and Ta in rare-element granitic pegmatites. *Bull.*
Mineral. 108; 499-532.
- CERNY, P & T.S. ERCIT (1989): Mineralogy of Niobium and Tantalum: Crystal chemical
Relationships, Paragenetic Aspects and their Economic Implications. In
Lanthanides, Tantalum and Niobium, Springer-Verlag Berlin-Heidelberg.
Eds. Moller, P, Cerny, P and F Saupe.
- CERNY, P; ERCIT T.S. and M.A. WISE (1992): The tantalite tapiolite gap: natural
assemblages versus experimental data. *Can. Mineral.* 30.
- CERNY, P. and R.B. FERGUSON (1972a): Niobium-tantalum minerals from granitic
pegmatites at Greer Lake, southeastern Manitoba. *Can. Min.* 10, 755-772.
- CERNY, P & R.B. FERGUSON (1972b): Petalite, spodumene relations. *Can. Mineral.* 11,
660-675.
- CERNY, P ; GOAD, B.E., HAWTHORNE, F.C., & R.CHAPMAN (1986): Fractionation
of the Nb-and-Ta-bearing oxide minerals in the Greer Lake pegmatite
granite and its pegmatite aureole, southeastern Manitoba, *Am.Mineral.* 71,
501-517.
- CERNY, P., MEINTZER, R.E. & A.J. ANDERSON (1985): Extreme fractionation in
rare-element granitic pegmatites: selected examples of data and
mechanisms. *Can. Mineral* 35; 381-421.

- CERNY, P., ROBERTS, W.L., ERCIT, T.S. & R. CHAPMAN (1985b): Wodginite and associated minerals from the Peerless pegmatite, Pennington County, South Dakota. *Am. Mineral.* 70, 501-517.
- CERNY, P. & A.C. TURNOCK (1971): Niobium-tantalum minerals from granitic pegmatites at Greer Lake, southeastern Manitoba. *Can. Mineral.* 10, 755-772.
- CHAKOUMAKOS, B.C. (1978): Replacement features in the Harding Pegmatite, Taos County, New Mexico. (abstr.). *New Mexico Acad. Sci. Bull.* 18, 22.
- CHAROY, B., LHOE, F., DUSAUSOY, Y. & F. NORONHA (1992): The crystal chemistry of spodumene in some granitic aplite-pegmatite bodies. *Can. Mineral.* 30, part 3, 639-652.
- CHAUDHRY, M.N. & R.A. HOWIE (1973): Lithium aluminium mica from the Meldon Aplite, Devonshire, England. *Mineral. Mag.* 39, 289-296.
- CLIFFORD, T.N. (1966): Tectono-metallogenic units and metallogenic provinces of Africa. *Earth Planetary Sci. Lett.*, 1, 421.
- COOK, C.W. (1979): Fluid inclusions and petrogenesis of the Harding pegmatite, Taos County, New Mexico. M.Sc. thesis, Univ. New Mexico, Albuquerque, New Mexico.
- CROUSE, R.A., CERNY, P., TRUEMAN, D.L. and BURT, R.O. (1979): The Tanco pegmatite, southeastern Manitoba. *Can. Inst. Mining Metall. Bull.* 2, 1-10.
- DEER, W.A., HOWIE, R.A. & J. ZUSSMAN (1978): Rock forming minerals. Vol. 2A Wiley, New York.
- DEER, W.A., HOWIE, R.A. & J. ZUSSMAN (1962): Rock forming minerals. Wiley, New York.
- DIEHL, M. & G. SCHNEIDER (1990): The geology of the Rubicon pegmatite, Karibib, Namibia.
- DINGWELL, D.B. (1985): The structure and properties of fluorine-rich silicate melts: implications for granite petrogenesis. In: Taylor R.P., Strong, D.F. (eds). *Granite-related mineral deposits: geology, petrogenesis and tectonic setting* (ext abs). *CIM. Halifax* 72-79.
- DUBOIS, J., J. MARCHANT and P. BOURGUIGNON (1973): Donnees mineralogique sur la serie amblygonite-montebrazite. *Annales Soc. Geol. Belgique*, 95, 285-310.
- EKEBERG, A.G. (1803): *Gilbert's Ann.* 14, 246.
- EID, A.S. (1976): The geochemistry of microlite. M.Sc. Thesis. Univ. Leeds.
- ERCIT, T.S., CERNY, P. and F. C. HAWTHORNE (1992): The wodginite gap. III Classification and new species. 30, part 3, 633-638.

- FERGUSON, R.B, HAWTHORNE, F.C. and J. D.GRICE (1976): The crystal structure of tantalite, ixiolite and wodginite from Bernic Lake, Manitoba. II. Wodginite. *Can. Min.*14, 550-560.
- FERSMAN, A.E. (1933-1939): *Geokhimiya (Geochemistry)*. Nos. 1-4, Leningrad, Goskhimtekhnizdat.
- FLEISHER, M. (1987): *Glossary of Mineral Species*. 5th edition. Min. Rec. Tucson.
- FOORD, E.E. (1976): *Mineralogy and Petrogenesis of layered pegmatite-aplite dykes in the Mesa Grande District, San Diego County, California*. Ph.D thesis, Stanford Univ., Stanford, California.
- _____ (1982): Minerals of tin, titanium, niobium and tantalum in granitic pegmatites. *MAC Short Course*, 8. *Can. Mineral.* 187-238.
- FORD, (1930): *Dana's Textbook of Mineralogy (4th edit)*: Wiley and Sons, New York.
- FOSTER, M.D. (1960): Interpretation of the composition of lithium-micas. U.S. *Geol. Surv. Prof. Paper* 354-E, 115-146.
- FROMMURZE, H.F.; GEVERS, T.W. & P.J. ROSSOUW (1942): The geology and mineral deposits of the Karibib area, South West Africa. *Expl.Sht S.W.A (Karibib) geol.Surv.S.Afr.*
- GEOLOGICAL MAP OF SOUTH WEST AFRICA/NAMIBIA. (1980): *Geol. Surv. S.Afr. Government Printer, Pretoria.*
- GEVERS, T.W. and H.F. FROMMURSE (1929): The tin -bearing pegmatites of the Erongo Area, South west Africa. *Trans. Geol. Soc. S.A.* 111-149.
- GEVERS, T.W., PARTRIDGE, F.C. & G. K. JOUBERT (1937): The pegmatite area south of the Orange River in Namaqualand. *Mem. geol. Surv. S.Afr.* 31, 172.
- GEVERS, T.W. (1937): Phases of mineralization in Namaqualand pegmatites. *Trans. Geol. Soc. S. Africa.* 39, 331-375.
- GILLINGHAM, T.E. (1948): The solubility and transfer of silica and other non-volatiles in steam. *Econ. Geol.*, 43, 242-272.
- GINSBURG, A.I. (1955): Mineralogical-geochemical characteristics of lithium pegmatites. *Trudy Mineralogicheskogo Muzeya Akademii Nauk SSSR*, 7, 12-55.
- _____ (1960): Specific geochemical features of the pegmatite process. *Int. Geol. Congress (Norway)* 17, 111-121.
- _____ & S.A. GORZHEVSKAYA (1960): Characteristics of titano-tantaloniobates. *Geol. Mest. Redk. Elem., Vses Nauchn Issled.* 10, 5-10.
- _____ TIMOFEYEV, I.N. & L.G. FELDMAN (1979): Principles of geology of the granite pegmatites. *Nedra, Moscow* 296p.
- GOAD, B.E. & P. CERNY (1981): Peraluminous pegmatitic granites and their pegmatitic aureoles in the Winnipeg River district, southeastern Manitoba. *Can. Mineral.* 19; 177-194.
- GORDIYENKO, V.V. & G.E. KALENCHUK (1966): The chemical nature of spodumene. *Zap. Vses. Min. Obshch.*, 95, 169-180.

- GORDIYENKO, V.V. (1971): Concentration of Li, Rb and Cs in potash feldspar and muscovite as criteria for assessing the rare-metal mineralization in granite pegmatites. *Intern. Geol. Review.* 13, 134-142.
- GOUDER DE BEAUREGARD, C., DUBOIS, J. ET P. BOURGUIGNON (1967): Comportement thermique des columbotantalites: *Ann. Soc. Geol. Belg.*, T. 90, 501.
- GRICE, J.D.; FERGUSON, R.B. & F.C. HAWTHORNE (1976): I. Tantalite and ioxiolite, *Can. Mineral.* 14, 540-549.
- GUIMARAES, C.P. (1939): *Annaes. Acad. Brasil. Ciencias.* 11, 347-350.
- HAAK, U. & E. GOHN (1989): Rb-Sr data on some pegmatites in the Damara Orogen (Namibia). *Communs geol. Soc. S.W. Africa/Namibia*, 4, 13-17.
- HAAPALA, I. (1966): On the granitic pegmatites of the Paraseinajoki-Alvus area, South Pohjanmaa, Finland. *Bull. Comm. geol. Finlande.* 224, 1-98.
- HATCHETT, C. (1802): *Nicholson's journal* 1,32; *Phil.trans.*92.49
- HARRIS, P.M. (1966): Pandaite from the Mrima Hill deposit (Kenya). *Mineral. Mag.* 35, 277-290.
- HAWTHORNE, F.C. & P. CERNY (1982): The Mica Group. In , *Granitic pegmatites in Science and Industry.* (p.Cerny, ed). *Mineral Assoc. Can., Short Course Handbook* 8.
- HENSEN, B.J. (1967): Mineralogy and petrology of some tin, lithium and beryllium-albite pegmatites near Doade, Galicia, Spain . *Leidse Geol. Med.* 39, 249-259.
- HEINRICH, E.W. (1962): Radioactive columbite. *Am. Mineral.* 47, 1363-1379.
- _____ (1975): Economic geology and mineralogy of petalite and spodumene pegmatites. *Indian Journ. Earth Sci.*2, 18-29.
- HILDRETH, W. (1979): The Bishop Tuff: evidence for the origin of compositional zoning in silicic magma chambers. *Geol. Soc. Amer., Spec. Pap.* 180, 43-75.
- _____ (1981): Gradients in silicic magma chambers: implications for lithospheric magmatism. *J. Geophys. Res.* 86, 10153-10192.
- HOGARTH, D. D. (1961): A study of pyrochlore and betafite. *Can. Mineral.* 6, 610-633.
- _____ (1977): Classification and nomenclature of the pyrochlore group. *Am. Mineral.* 62, 403-410.
- _____ (1989): Non metamict uranium pyrochlore and uran pyrochlore from tuff near Ndale, Fort Portal area, Uganda. *Min. Mag* 53, 257-262.
- HORNUNG, G. & O. VON KNORRING,(1962): The pegmatites of the North Mtoko Region, Southern Rhodesia .*Trans. geol. Soc. South Afr.* 65, 153-180.
- HUGO, P.J. (1969): The pegmatites of the Kenhardt and Gordonia district, Cape Province. *Mem. geol. Surv. S.Afr.* 58.

- JAHNS, R.H. (1953): The genesis of pegmatites, I. Occurrence and origin of giant crystals. *Amer. Mineral* 38, 563-598.
- JAHNS, R.H. (1982): Internal evolution of granitic pegmatites In: *Granitic Pegmatites in Science and Industry* (P. Cerny ed.) MAC. Short Course Handbook 8, 293-346.
- JAHNS, R.H. & C. W. BURNHAM (1969): Experimental studies of pegmatite genesis: I. a model for the derivation and crystallization of granite and pegmatites. *Econ. Geol.* 64, 843-864.
- JAHNS, R.H. & R.C. EWING (1976): The Harding Mine, Taos County, New Mexico. *New Mexico Geol. Soc. Guidebook*, 27th Field Conference, Vermejo Park, 263-276.
- KALLIO, P. (1978): A new X-ray method for the estimation of fluorine content in montebrasite. *Amer. Mineral.* 63, 1249-1251
- KELLER, P & O. von KNORRING(1989): Pegmatites at the Okatjimukju farm, Karibib, Namibia. Part I; Phosphate mineral associations of the Clementine II pegmatite. *Eur. J. Mineral.* 567-593.
- KELLER, P. (1991): The occurrence of Li-Fe-Mn phosphate minerals in granitic pegmatite of Namibia. *Communs geol.Surv.Namibia*.7, 21-34.
- KORNETOVA, V.A. & M.E. KAZAKOVA (1964): Uranium-bearing microlite-djalmaite, in a Siberian pegmatite deposit. *Tr. Mineral. Muz., Akad. Naut. SSSR.* 15, 219-222.
- KORZHINSKII, D.S. (1957): Physicochemical basis of the analyses of the paragenesis of minerals. *Izvestiya Akademii Nauk SSSR, Moscow* (transl. Consult. Bureau, New York 1959).
- KOVALENKO, V.I. (1978): The genesis of rare-metal granitoids and related ore deposits. In: Stempok, M, Burnol, L. Tischendorf, G (eds). *Metallization associated with acidic magmatism. Geol. Surv. (Prague)* 3:235:258.
- KOVALENKO, V.I. & N.I.KOVALENKO (1984): Problems of the origin, ore-bearing and evolution of rare-metal granitoids. *Phys. Earth Planet. Int.* 35, 51-62.
- KOVALENKO, V.I. ; KUZ MIN M.I. & F.A. LETNIKOV(1970): Magmatic origin of lithium- and fluorine-bearing rare-metal granite. *Dokl.Ac. Sci. USSR Earth Sci. Sect.* 190, 189-192.
- LLOYD, G.E (1987): Atomic number and crystallographic contrast images with the SEM: a review of backscattered electron techniques. *Mineral. Mag.* 51,3-19.
- LEVINSON, A.A. (1953): Studies in the mica group: relationship between polymorphism and composition in the muscovite-lepidolite system. *Am. Mineral.* 38, 88-107.
- LONDON, D & D.M.BURT (1982a): Lithium aluminosilicate occurrences in pegmatites and the lithium aluminosilicate phase diagram. *Am. Min.* 67, 483-493.

- LONDON, D & D.M. BURT (1982b): Lithium minerals in pegmatites. In: *Granitic Pegmatites in Science and Industry*. P.Cerny (Ed.). Mineral Assoc. Can., Short Course Handbook 8, 99-113.
- LONDON, D & D.M.BURT (1982c): Alteration of spodumene, montebrasite and lithiophilite in pegmatites of the White Picacho district, Arizona. *Am. Mineral.* 67, 97-113.
- LONDON, D (1984a): Experimental phase equilibria in the system $\text{LiAlSiO}_4\text{-SiO}_2\text{-H}_2\text{O}$: a petrosensitive grid for lithium-rich pegmatite. *Am. Mineral*, 69, 995-1004.
- LONDON, D. (1984b): The role of lithium and boron in fluid evolution and ore deposition in rare-metal pegmatites. *Geol. Soc. Amer. Abstr. Programs* 16, 578.
- LONDON, D. (1986a): Magmatic-hydrothermal transition in the Tanco rare-element pegmatite: evidence from fluid inclusions and phase-equilibrium experiments. *Am. Mineral.* 71, 376-395.
- LONDON, D. (1986b): Formation of tourmaline-rich gem pockets in miarolitic pegmatites. *Am. Mineral* 71; 396-405.
- LONDON, D. (1987): Internal differentiation of rare-element pegmatites: effects on boron, phosphorus and fluorine. *Geochim Cosmochim Acta* 51; 403-420.
- LONDON, D. (1989): Qualitative information on the kinetics of crystal growth. *Can. Abstr.*
- LONDON, D. (1990): Internal differentiation of rare-element pegmatites, a synthesis of recent research. *Geol.Soc. Am. Special Paper* 246.
- LONDON, D. (1992): The application of experimental petrology to the genesis and crystallization of granitic pegmatites. *Can. Mineral.* 30, part 3, 499-540.
- LOWENSTEIN, P. (1969): The geology and geochemistry of tin and beryllium mineralization in southwest Ankole, Uganda. Univ. Leeds Ph.D. thesis.
- LUDINGTON, S. (1981): The Redskin granite: evidence for thermogravitational diffusion in a Precambrian granite batholith. *J. Geophys. Res.* 86, 10423-10430.
- MACHATSCHKI, F. (1932): *Chem. Erde*, 7, 56-76) *Min Abst.*5, 185.
- MANNING, D.A.C. (1981): The effect of fluorine on liquidus phase relationships in the system Qz-Ab-Or with excess water at 1kb. *Contr. Min. Pet.* 76, 206-215.
- MIHALIK, P.G.V.(1967): A chemical and mineralogical study of microlite from the Noumas pegmatite. Msc. Thesis. Univ. Witwatersrand. Johannesburg. S.Africa.
- MILLER, R.M. (1968-69): The geology of the Etiro pegmatite, Karibib district. S.W.A. *Annals. Geol. Surv. S.Afr.* vol 7, 125-130.
- MOLLER, P. (1989): REE(Y), Nb and Ta enrichment in pegmatites and carbonatite-alkalic rock complexes. In *Lanthanides, Tantalum and Niobium*. P. Moller, P.Cerny and F. Saupe (Eds.) Springer-Verlag. Berlin . Heidelberg.

- MOORE, A.C. (1975): The petrography and the regional setting of the Tantalite Valley Complex, South West Africa. *Trans. Geol.Soc. S. Afr.*, 8, 235-249.
- MROSE, M.E. (1971): Lacroixite: its redefinition and new occurrences. (abstr.) 20th Clay Minerals Conference, 8th Ann.Meeting Clay Min.Soc. with Min. Soc, Amer., Abstr. Prog. 10.
- MUNOZ, J. L. (1971): Hydrothermal stability relations of synthetic lepidolite. *Am. Mineral.* 56, 2069-2087.
- MUNOZ, J. L. and H.P. EUGSTER (1969): Experimental control of fluorine reactions in hydrothermal systems. *American Mineralogist*, 54, 943-959.
- NEL, H.J. (1946): Petalite and amblygonite from Karibib, Southwest Africa. *Am. Mineral.* 32, 51-57.
- NICKEL, E.H., ROWLAND, J.F. & R.C. McADAM,(1963): Wodginite - a new tin manganese tantalite from Wodgina, Australia and Bernic Lake: Manitoba. *Can. Mineral.*, 7, 390.
- NORTON, J.J., PAGE, L.R. AND D.A. BROBST (1962): Geology of the Hugo pegmatite, Keystone, South Dakota. *U.S. Geol. Surv. Prof. Paper*, 297-B, 49-127.
- NORTON, J.J. (1973): Lithium, cesium and rubidium- the rare-alkali metals, *U.S. Geol. Surv. Prof. Paper* 820, 365-378.
- NORTON J. J. (1983): Sequence of mineral assemblages in differentiated granitic pegmatites. *Econ. Geol.* 78, 854-874.
- PARDEE, J. T.,GLASS, J.J. & R.E.STEVENS (1937): Massive low-fluorine topaz from Brewer mine, South Carolina. *Am. Mineral.* Vol. 22, 1058
- PAUL, B.J. (1984): Mineralogy and geochemistry of the Huron Claim Pegmatite, Southeastern Manitoba, M.Sc. thesis, Univ. Manitoba, Winnipeg, Man.
- PECORA & FAYEY, (1949): *Am. Min.*, 34, 83.
- PICHAVANT, M. (1981): An experimental study of the effect of boron on a water saturated haplogranite at 1 kbar vapour pressure. *Contrib. Mineral. Petrol.* 76; 430-439.
- PICHAVANT, M (1983): Melt-fluid interaction deduced from studies of silicate - B₂O₃-H₂O systems at 1 kbar. *Bull. Mineral* 106: 201-211.
- PICHAVANT, M, HERRERAJ.V., BOULMIER,S.,BRIQUEU L; JORON J-L; JUTEAU M; MARIN,L., MICHARD,A., SHEPPARD,S.M.F., TREUIL,M., AND VERVET (1987): The Macusani glasses, S.E .Peru: evidence of chemical fractionation in peraluminous magmas. In: *Magmatic processes: physicochemical principles.* *Geochem Soc. Spec. Publ.*1, 359-373.
- POLLARD, P.J. (1989): Geochemistry of granites associated with tantalum and niobium mineralization. In *Lanthanides, Tantalum and Niobium.* P. Moller, P.Cerny and F. Saupe (Eds.) Springer-Verlag. Berlin. Heidelberg
- QUENSEL, P. (1937): *Geol. For. Forh.*, Vol.59, 257.

- QUENSEL, P. (1938): Minerals of the Varutrask pegmatite. X. Spodumene and its alteration products. *Geol. For. Forh. Stockholm* 60, 201-215.
- QUENSEL, P. (1946): Minerals of the Varutrask Pegmatite. XXXVII. A spodumene-quartz symplectite. *Geol. Foren. i Stockholm Forh.* 68, 47-50.
- (1956): The paragenesis of the Varutrask pegmatite: *Arkiv for Mineral; Och Geol.*, 2, 9-125.
- RINALDY, R., CERNY, P & R.B. FERGUSON (1972): The Tanco pegmatite at Bernic Lake Manitoba. IV. lithium-rubidium-caesium micas. *Can. Mineral.* 11, 690-707.
- ROCKHOLD et al., (1987): *Geochim, Cosmochim Acta* 51; 487-496.
- ROERING, C. (1961): The mode and emplacement of certain Li-and Be-bearing pegmatites in the Karibib district. S.W.Africa. *Econ Geol.Res.Un Joburg. S.Africa. Inf. Circular* 4. June 1961.
- ROERING, C. and T.W. GEVERS (1962): Lithium- and beryllium-bearing pegmatites in the Karibib district, South West Africa. *Econ. Geol. Res. Un., Joburg. S.Africa Inf. Circular* 9. Oct.1962.
- ROERING, C. (1966): Aspects of the genesis and crystallization sequence of the Karibib pegmatites. *Econ Geol.* 61, 1064-1089.
- ROSE, H. (1844): *Pogg. Ann* 63, 317.
- SAHAMA, T. G., O.von KNORRING M. LEHTINEN (1968): Cookeite from the Muiane pegmatite, Zambezia, Mozambique. *Lithos* 1, 12-19.
- SAHAMA, T.G. (1980): Minerals of the tantalite-niobite series from Mozambique. *Bull. Mineral.* 103, 190-197.
- SARTORI, F. (1976): The crystal structure of a IM lepidolite. *Tscher. Min. Petrol. Mitt.* 23, 65-75.
- SEBASTIAN, A & M. LAGACHE (1991): An experimental study of lithium-rich granite pegmatites; Part 1. Petalite and albite and quartz equilibrium. *Am Mineral.* 76, 205-210.
- SCHALLER, W.T. (1911) Natramblygonite, a new mineral. *Amer. J. Sci.* 181, 48-50.
- SCHALLER, W.T. (1950): An interpretation of the composition of high-silica sericites. *Min.Mag.*, 29, 403.
- SHAW, H.R., SMITH, R.L. & W.HILDRETH(1976): Thermogravitational mechanism for chemical variations in zoned magma chambers. *Geol. Soc. Am. Abst. Progr.* 8; p 1102.
- SHEARER, C.K., PAPIKE, J.J. & J.C. LAUL (1987): Mineral and chemical evolution of a rare-element granite-pegmatite system: Harney Peak Granite, Black Hills, South Dakota. *Geochim Cosmochim Acta* 51; p 473-486.
- SHESHULIN, G.I. (1961): Composition of gas-liquid inclusions in the minerals of spodumene pegmatites. In *New data on Rare Element Mineralogy* Ginsburg (ed). New York (Consultants Bureau), 47-55.

- SIMMONDS, W.B., HEINRICH, E.W. (1980): Rare earth pegmatites of the South Platte District, Colorado. Col. Geol. Surv. Denver. Resource Ser. 11; 131p
- SMITH, D.A.M. (1961): The geology of the area around the Khan and Swakop rivers in South West Africa. unpublished Ph.D. thesis. University of the Witwatersrand.S. Africa.
- SMITH, D.A.M. (1965): The geology of the area around the Khan and Swakop rivers. in South West Africa . Mem.geol. Surv. South Africa, 113p
- SMITH, D.A.M. (1966): Geological Map of Khan and Swakop Rivers, South West Africa. 1: 125,000. Govt. Printer, Pretoria.
- SCHNEIDERHOHN, H (1961): Die erzlagerstätten der Erde, Vol.II. Die pegmatite. Stuttgart Fischer Verlag, 543-636.
- STEWART, D.B. (1963): Petrogenesis and mineral assemblages of lithium-rich pegmatites. Geol. Soc. Amer. Spec. Pap. 76, 159.
- STEWART, D.B. (1978): Petrogenesis of lithium-rich pegmatites. Am. Mineral 63; p 970-980.
- STURDIVANT, J.H. (1930): The crystal structure of columbite. Zeits. Krist. 75, 88-108.
- SWANSON, T.H. & S.W. BAILEY (1981): Redetermination of the lepidolite -2M₁ structure. Clay and Clay Minerals 29, 81-90.
- SWARTZ, G.M. and R.J. LEONARD (1926): Alteration of spodumene in the Etta mine, Black Hills, S.D. 303-317.
- SWEATMAN, T. and LONG, J. V.P. (1969): Quantitative electron-probe micro-analysis of rock forming minerals. J. Petrol. 10, 332-379.
- TAYLOR, B.E.; FOORD, E.E. & H.FREIDRICHSEN (1979): Stable isotope and fluid inclusion study of gem-bearing granite pegmatite - aplite dyke. San Diego County, California. Contr. Min. Pet. 68, 187-205.
- TAZIEFF, H. (1970): New investigations on eruptive gases: Bull. Volc., 34, 1-18.
- Van der VEEN, A.H. (1963): A study of pyrochlore. Nederlands Geol. Mijnbouwkg. Gen. Verh., Geol. Ser. 22, 188 p.
- VESASALO, A. (1959): On the petalite occurrence of Tammela , S.W. Finland. Bull Comm. geol. de Finlande. 184, 59-75.
- VLASOV, K.A. (1966): Geochemistry and mineralogy of rare-elements and genetic types and their deposits . 1. Geochemistry of rare elements. 1st Progr. Sci. Transl, Jerusalem, 688 p.
- VOGT, J.H.L. (1926): Magmas and igneous ore deposits. Econ. Geol., 21, 207-332.
- Von BACKSTRÖM J.W. & J. de VILLIERS (1972): The geology of the Orange River Valley between Onseepkans and Ricktersveld. Expl. Sheet Geol. Surv. S. Afr.

- Von BACKSTRÖM, J.W. (1976): The geology and mineral deposits of Tantalite Valley, Warmbad district, South West Africa. Geol. Div. Atomic Energy Board, S.Afr.
- Von GAERTNER, H.R. (1930): Neues Jahrb Mineral. 61, 1-30.
- Von KNORRING, O. (1964): Report on mineralogical research. Pegmatite minerals from Uganda and Somalia. 8th ann. rep.res.Inst.afr. Geol., Univ.Leeds , 11-13.
- Von KNORRING, O. (1965): Niobium-tantalum minerals. 9th ann. rep.res.Inst.afr. Geol., Univ. Leeds, 42-43.
- Von KNORRING, O.(1966): Pegmatite Investigations: Uganda, Rwanda, Rhodesia and South West Africa. 10th ann. rep.res.Inst.afr. Geol., Univ. Leeds, 32-33.
- Von KNORRING, O. (1967): Pegmatite Investigations: Niobium-tantalum minerals. 11th 11th ann. rep.res.Inst.afr. Geol., Univ. Leeds , 36-37.
- Von KNORRING, O. (1968): On the geochemistry of some niobium-tantalum minerals. 12th ann. rep.res.Inst.afr. Geol., Univ.Leeds , 50-53.
- Von KNORRING, O. (1970): Mineralogical and Geochemical Aspects of Pegmatites from Orogenic Belts of Equatorial and Southern Africa. In Clifford, T.N. and Gass, I.G. (eds.). African Magmatism and Tectonics 157-184. Oliver and Boyd, Edinburgh.
- Von KNORRING, O. (1971): Geochemical and mineralogical aspects of columbite-cassiterite-bearing alkali-granitic rocks. 15th ann. rep. res. Inst. afr. Geol., Univ. Leeds , 18-22.
- Von KNORRING, O (1972): On the occurrence of bismuth minerals in some African pegmatites. 16th ann. rep. res. Inst. afr. Geol., Univ. Leeds , 63.
- Von KNORRING, O. (1974): On tantalum mineralization in some pegmatites from equatorial and southern Africa. 20th ann. rep.res. Inst.afr. Geol., Univ. Leeds, 34-38.
- Von KNORRING, O.(1976): Mineralogical note from Southern Africa. 22nd ann. rep. res. Inst. afr. Geol. Univ. Leeds 53-55.
- Von KNORRING, O.(1985): Some mineralogical, geochemical and economic aspects of lithium pegmatites from the Karibib Cape Cross egmatite field in South West Africa/ Namibia. Communs Geol. Surv. SW. Africa/Namibia, 1,79-84.
- Von KNORRING, O.(1985b): Niobium and tantalum minerals. Comm. geol. Surv. S.W. Africa/ Namibia. 1, 85-88.
- Von KNORRING, O.(1987): Mineralized pegmatites in Africa. Geol. Journ. 22, 253-270.
- Von KNORRING, O. & A. FADIPE (1981): On the mineralogy and geochemistry of niobium and tantalum in some granite pegmatites and alkali granites of Africa. Bull. Mineral 104, 496-507.

- Von KNORRING, O. & E. CONDLIFFE: (1984): On the occurrence of niobium and tantalum and other rare-element minerals in Meldon Aplite, Devonshire. *Min. Mag.* 48, 443-448.
- Von KNORRING, O., SAHAMA, TH.G. & M. LEHTINEN (1969): Wodginite from Karibib, South West Africa. *Ind Mineral.*, 10, 105-108.
- WANG, Y., LI, J., LU, J. & FAN WENLING (1982): Geochemical mechanism of Nb, Ta-mineralization during the late stage of granite crystallization. *Geochemistry Beijing* 1, 175-185.
- WEITZEL, H. (1976): Kristallstrukturverfeinerung von Wolframiten und Columbiten. *Zeits. für Krist.* 144, 238-258.
- WINKLER, H.G.F. (1976): *Petrogenesis of Metamorphic Rocks*. 4th Edition, Springer-Verlag, New York.
- ZAKHARCHENKO, A.L. (1964): Physicochemical conditions and processes of formation of granite pegmatites. *Geochem Int.* 1057-1067.
- ZELT, G.A.D. (1975): Data from some African columbite-tantalite specimens. *Bull. Geol. Soc. Finland* 47, 117-125.

PART V

APPENDICES

APPENDIX 1	THE MINERALIZED PEGMATITES	Page
A1.1.	KENHARDT AREA, NORTHERN CAPE, SOUTH AFRICA	A1
A1.2.	STEINKOPF AREA, NAMAQUALAND, SOUTH AFRICA	A4
A1.3.	TANTALITE VALLEY, WARMBAD, NAMIBIA	A7
A1.4.	KARIBIB-USAKOS-CAPE CROSS, NAMIBIA	A11
APPENDIX 2	ANALYSES AND METHODS	
A2.1.	ANALYSES	A12
A2.2.	ANALYTICAL METHODS	A21
APPENDIX 3	SAMPLE NUMBERS	A24

APPENDIX 1 THE MINERALIZED PEGMATITES

The following descriptions are a compilation of descriptions given in the literature and observations made in the field between 1980 and 1984 in the four areas under study in this thesis.

A.1.1. The KENHARDT AREA, NORTHERN CAPE, SOUTH AFRICA

In the eastern Kenhardt district four mines were visited at Angelierspan, 2 mines Jack 1 and Jack 3 and the Welgevonden pegmatite at Ellandsgate Farm.

The Angelierspan pegmatites lie 88 km southeast of Kenhardt

Angelierspan 1 pegmatite is situated 2 miles northeast of the homestead and is a complex beryl-bearing pegmatite, striking north-south. Hugo (1969) has given the following description of zones.

1. A core consisting of large subhedral crystals of white to pink perthite and milky quartz which becomes markedly smokey towards the contact.
2. An intermediate zone of coarse-grained albite-oligoclase, quartz and muscovite with accessory beryl, between 1-2 m thick.
3. A wall zone consisting essentially of perthitic graphic granite with subordinate plagioclase and muscovite, varying in thickness from 3 cm-1m.

The excavation in 1980 was approximately 70 m in length and about 10 m in depth. An idiomorphic beryl crystal, 6ft by 11ft occurred in quartz on the edge of the core and intermediate zone. The intermediate zone consists here of a 10 m depth exposure of herringbone mica in Na-feldspar. On the edge of the intermediate zone smaller beryl crystals were embedded in both quartz and feldspar. During the period 1950-53 about 135 tons of beryl were produced from this pegmatite, and Angelierspan No.1 became known for a single tabular mass of beryl weighing 63 tons, which was found near the surface forming a hood over the core.

Angelierspan 2 is an excavation about 55m in length lying east-northwest and in 1980 was being mined for K-feldspar for the ceramic industry. Large veins, 1-3 m of green muscovite and globular grey muscovite occur in massive feldspar. Glassy-green beryl also occurs in feldspar.

Angelierspan 3 differs from No.1 and No.2 in that there is in addition to beryl, lepidolite and spodumene. The pegmatite has been classified by Hugo (1969) as a beryl-columbite-tantalite pegmatite with Li-mica and spodumene. The pegmatite strikes N-S and is smaller in length than No.1. Although no columbite was located in 1980, cassiterite was found associated with lepidolite. Hugo 1969 recognizes 3 zones in an excavation 5 by 7 m and 4 m deep, made along the strike of the body.

1. A core zone consisting of milky quartz with large euhedral perthite crystals occupying the western half of the excavation.
2. A replacement zone consisting of lithian mica, minor cleavelandite and columbite -tantalite.
3. An intermediate zone consisting of quartz and spodumene with accessory beryl.

In 1980 this pegmatite had obviously been excavated further than 1969 and had been mined for feldspar in the intermediate zone; pure K-feldspar is necessary for the ceramics industry. In the core and replacement zones, muscovite mica surrounds pods of quartz and is intergrown with cleavelandite. A wall zone of graphic granite was visible.

Angelierspan 4 is a smaller excavation consisting of an intermediate zone consisting essentially of glassy K-feldspar with some veins of muscovite. Small areas of quartz are visible.

The Welgevonden pegmatite has not been described in the literature. It is located just north of the Homestead on Angelierspan. It is a zoned pegmatite striking northwest-southeast and has been excavated along strike for about 70 m. It may be classified as a beryllium pegmatite and has been mined for both beryllium and feldspar. The pegmatite consists essentially of feldspar with secondary muscovite and a quartz core. Euhedral beryl crystals up to 2 ft. in length occur in both quartz and feldspar in the inner intermediate zone.

Jack 1: The name denotes a group of pegmatites lying parallel to each other in a more or less echelon arrangement (Hugo 1969). The pegmatites lie about 9.5 km due south of the homestead of Crieff. They have been classified by Hugo (1969) as essentially beryl-bearing pegmatites, they are well zoned and strike nearly north-west. Hugo (1969) recognizes three zones.

1. A wall zone consisting of perthite, albite-oligoclase and quartz with accessory muscovite. Perthite is graphically intergrown with quartz.
2. The intermediate zone consists essentially of quartz, albite and muscovite with accessory beryl, apatite and lithian mica. Large embedded crystals of quartz are confined to the contact with the core (yellowish-green).

3. The core consists of quartz and perthite. cleavelandite with associated masses of apatite and lithian mica, occurs near the core.

Jack 1 pegmatite was visited in 1980. It was a small excavation about 10 m square. Lepidolite in some quantities had been stockpiled because of the low price. Pink and blue lepidolite with intergrown pale blue apatite, garnet intergrown with apatite and pink beryl with quartz were collected.

Jack 3 pegmatite lies 6.5 km due south of the Mottels River near the eastern boundary of the Kombaers Breand. It forms one of a few prominent pegmatite ridges which relieve the otherwise featureless topography. The pegmatite strikes N-S and is visible over a distance of 233 metres. Only the northern part has been mined for beryl - about 50 tons of which was mined 1964-65. the pegmatite is zoned and 4 units were recognized by Hugo (1969).

1. A quartz perthite core.
2. A thin intermediate zone consisting of cleavelandite, muscovite and quartz with accessory beryl. Probably partly a replacement zone, a second intermediate zone of plagioclase, quartz and muscovite with accessory beryl, apatite and tourmaline. Masses of beryl occur in other intermediate areas close to the core.
3. A border zone of a fine-grained mixture of quartz, plagioclase, perthite and muscovite.

A large crystal 10 X 4 cm of black tourmaline was collected(1980)

Straussheim 1 pegmatite occurs about 35 km north of Kenhardt, (see Fig. 2.6) on the portion of N'Rougas Noord, known as Straussheim. there are several very prominent pegmatites and No.1 forms a hill known locally as Micakop. Mining since 1952 has produced several hundred tons of beryl from the three main pegmatites in the area. Beryl production ceased when Straussheim mine started producing cassiterite. Since 1965 the monthly mica production of the mine exceeds on average, 100 tons.

The Straussheim 1 pegmatite outcrops over a distance of 400 m and dips at a rather steep angle; it strikes approximately northwest, and varies in width from 15 to 100 m. Excavations, 50 by 17 m and a smaller one along strike are confined to the footwall side of the core. Hugo (1969) and von Backström (1976) have recognized several distinct zones.

1. A core of quartz and perthite
2. An intermediate zone of beryl and accessory apatite, triplite, spodumene and black tourmaline. Spodumene idiomorphic crystals occur close to the core whereas apatite, beryl and triplite are concentrated in the outer part of the zone. The beryl forms small yellowish-green idiomorphic crystals

3. An outer intermediate zone in width from several cm to several m composed essentially of sugary albite and cleavelandite, with accessory fine-grained garnet, apatite, muscovite and quartz throughout which occur disseminated crystals of cassiterite and black tourmaline.
4. A wall zone medium to coarse-grained, more than 10 m wide composed of plagioclase, quartz, perthite, tourmaline and mica.
5. A border zone of width 1-8 cm consisting of quartz, plagioclase and muscovite with accessory tourmaline, fine-grained in texture.

In 1980 a small cavity of approximately 3 m wide showed a small concentration of phosphate mineralization occurring with quartz and mica on the edge of a feldspar zone. Samples were collected on which identification will be carried out.

A1.2 STEINKOPF AREA, NAMAQUALAND

Namaqualand is incorporated in a belt of pegmatites which occupy the rugged mountain tract south of the Orange River between Onseepkans and Richtersveld. It is about 200 m long and has been described by von Backstrom and de Villiers (1972) and von Backstrom (1976).

Since 1929 the pegmatites of Namaqualand have been the source of most of the beryl produced in South Africa. In Namaqualand a multitude of homogeneous and heterogeneous pegmatites occur within a well defined belt which extends westwards from the farms Ramans Drift and Hom, east of Goodhouse to Groendoorn. Most of the pegmatites of economic importance lie within this zone in metamorphosed rocks of the Kheis System and in Archean granite and gneiss. In the rugged scenery of this region the numerous pegmatites are conspicuously exposed on mountain slopes and on the sides of deep gorges. The pegmatites are characterised by irregularity in shape, size and continuity along strike and they form either steeply dipping dykes or massive bodies of low inclination - the former usually with more definite outlines than the latter. The most important base metal minerals found in these pegmatites generally are beryl, the lithium minerals, spodumene and lepidolite, tantalite, columbite, native bismutite and the tungsten-bearing mineral scheelite. Minor amounts of lithiophilite, triphylite, molybdenite and uranium ochre have been reported but they are of little economic value.

Spodumene, lepidolite, lithiophilite and triphylite are widely distributed in the Namaqualand pegmatites but it is only spodumene which is present in economically important quantities. Nowhere has lepidolite been seen to occur in large masses comparable to those in South West Africa.

The **Noumas 1** pegmatite was the largest and most economically viable pegmatite of the area visited. At the present time it is being mined for mica, feldspar, and tantalite-columbite. The pegmatite lies about half way between Steinkopf and Vioolsdrif, approximately 10 km west of the main road. The pegmatite is elongated and dyke-like and is discordantly emplaced in granodioritic grey gneiss. The pegmatite length is 1,100 m and the width varies between 10 and 45 m and it

is exposed to a length of 160 m. The pegmatite has been described by De Jeger (1968). It is well-zoned pegmatite with five recognizable units :- border, wall, intermediate, core and replacement.

1. A border zone between 1 and 15 cm consisting of plagioclase, quartz and muscovite with accessory garnet.
2. A wall zone varying between 1 and 10 m consisting of muscovite, quartz, plagioclase and microcline perthite, with accessory beryl, bismuth minerals, apatite, triplite and garnet. Mica which averages 100 tons per month comes from this zone.
3. An intermediate zone between 1 and 8 m wide consisting of spodumene, albite and quartz with accessory beryl and tantalite columbite. This zone has been mined for spodumene, beryl and tantalite-columbite.
4. The core consists of large subhedral microcline-perthite and quartz. The feldspar is mined for the ceramic industry.
5. Replacement bodies with diameters 1-10 m composed of lithian mica, cleavelandite with accessory tantalite-columbite, microlite, thorite, orangite and gummite.

In a separate core a new phosphate mineral has been found in association with a concentration of primary lithiophilite $[\text{Li}(\text{Mn})^{2+}\text{P}_0_4]$.

The **Norrabees** pegmatite 1 is situated on the Steinkopf Reserve about 8 km southeast of Jackalswater and about 3 km east of the Uranoop River. The pegmatite is on the southern slope of a hill and is exposed over a total distance of more than 100 m; it varies in width between 7 and 25 m. An excavation 60 by 25 m and extending down to about 28 m has revealed a well-zoned pegmatite with the following units:-

1. A wall zone consisting of quartz, plagioclase, biotite and muscovite with accessory beryl; width between 2 and 8 m.
2. An intermediate zone consisting of cleavelandite, spodumene and quartz, with accessory beryl and bismuth minerals. Spodumene and quartz predominate in places, elsewhere spodumene and cleavelandite are more prevalent.
3. A core consisting of microcline-perthite and quartz.
4. Replacement bodies consisting of lithian mica greisen, tourmaline, cleavelandite and pollucite.

BLUE FELDSPAR REEF

A series of small pegmatites are being mined principally for K feldspar, west of the pegmatite **Swartzberg** which is situated on the eastern side of the entrance to the Henkries Valley. This is left of the main Violsdrif-Steinkopf road north of the Noumas turnoff. The microcline which is very pure and albite are mined for the ceramic industry. In addition the pegmatites are also mined for small

quantities of tantalite-columbite but at a price of 150,000 Rand a ton, (1980) this is economically viable.

The pegmatites are zoned and consist of microcline-perthite, quartz, albite, muscovite with accessory beryl, black tourmaline, columbite-tantalite and garnet. The wall zone is composed essentially of graphic granite, with small amounts of mica.

East of the pegmatite Swartzberg are another similar series of small pegmatites which are similar in structure and mineral content to the Swartzberg west series. In addition these pegmatites contain accessory amounts of monazite and uranium minerals in association with quartz.

Spodumene Kop No. 1 is about 7 km east of the Norra-bees No. 1 pegmatite. It forms the top of a hill, it is approximately 70 m long by 12 m wide and dips at a steep angle to the south. Its excellent zonal structure is revealed in a huge prospecting trench.

Spodumene Kop No. 2 lies about 3 km to the east of the Violsdrif-Steinkopf main road, approximately 7 km north of the turnoff to Noumas. On the western side of the Henkies Valley appreciable quantities of spodumene are contained in certain beryl-bearing pegmatites which form part of a swarm of pegmatites occurring around Spodumene Kop. Some of the pegmatites were mined for beryl, columbite and bismuth minerals. These spodumene pegmatites also contained lepidolite and lithiophilite.

The **Kokerboomrand No. 1** pegmatite lies in flat terrain about 1.6 km east of the main road from Violsdrif to Springbok, opposite the turnoff to Noumas. The pegmatite has been described by von Backstrom (1976). It strikes southwards, plunges to the north and dips about 70° to the west. It has been exposed over a length of 50 m, varies in width between 8 and 12 m and has been mined to a depth of 12 m. The following zones have been recognised:

1. A wall zone consisting of quartz, plagioclase and muscovite with accessory microcline perthite, beryl, spodumene and garnet.
2. An intermediate zone consisting of quartz, cleavelandite, spodumene and accessory beryl, muscovite and columbite-tantalite.
3. A core of massive milky-white quartz and subsidiary microcline perthite.
4. Replacement bodies at the contact between the intermediate zone and core consisting of lithian mica greissen.

In April 1982, green mica greissen containing microlite was located adjacent to core quartz. Samples of microlite, green mica greissen, lepidolite and (spodumene) are to be analysed.

A1.3 TANTALITE VALLEY, WARMBAD, NAMIBIA

Pegmatites in South Africa and Namibia occur mainly as small sporadic deposits that are connected with intrusions of Precambrian granites (von Backstrom, 1976). However, there are some pegmatites in gneiss, schist and other ultrametamorphosed rocks which have no visible connection with granite intrusives and may be the result of partial melting.

In the Warmbad district south of Karasburg, Namibia, an area about 50 km square known as Tantalite Valley is situated about 10 km north of the Orange River and about 40 km due south of Warmbad (see Fig. 2.3). The Namaqualand rocks in Tantalite Valley are considered to be part of the Namaqualand Gneiss Complex and have undergone several periods of deformation. The distribution of economic, mineralized pegmatites in the Valley is related to the "Tantalite Valley Complex during deformation in a shear zone" (Moore, 1975). The Tantalite Valley Complex is composed of peridotite-gabbro with minor Cu and Ni sulphide mineralization.

The pegmatites in Tantalite Valley outcrop along steep sides of high mountains, which facilitates exploitation by means of adits driven into the mountain side. The pegmatites are typically zoned, up to 400 m along strike, transgressive and most commonly have shallow angles of dip. However, variable forms are apparent; they occur as thin lenses and dykes and as sheet-like bodies and there is thought to be more than one generation of pegmatite in the area (Moore, 1975). The most recent and largest have been dated as 988 ± 50 my (Nicolaysen, 1962).

Four large pegmatites, Witkop, White City, Homestead and Lepidolite and three small pegmatites, Chickenfoot, Signaalberg (see Fig. 2.8) and the T pegmatite have been investigated. In the adjacent northern Valley, lying east-west several small pegmatites were visited, the main pegmatite being SW Witkop.

Homestead is the largest of four pegmatites lying west of the Tantalite Valley homestead. The pegmatite is emplaced in amphibolite and the contact is both folded and sheared. The pegmatite has an almost horizontal disposition and is no more than 10 m thick. It outcrops over a length of 450 m and a width of 45-180 m. Four zones have been recognized:

1. A contact zone about 5 cm wide composed of fine-grained mica and quartz
2. A wall zone consisting of herringbone mica.
3. An intermediate zone consisting essentially of albite and cleavelandite, with radiating globular mica and blocky microcline; accessory columbite-tantalite occurs in association with albite. Spodumene, pale pink and blue beryl occur together with mica near the quartz core.
4. A quartz core.

Lepidolite greisen containing microlite and occasional inclusions of phosphate were found in the dumps.

The **White City** pegmatite forms an elongate body 180 m long and between 10-30 m wide, which bulges on the northern side. It terminates abruptly and reappears a little further along strike and continues as a much narrower body for another 70 m. The pegmatite strikes approximately N-S and is emplaced in gabbro and hornfels rock. Four zones have been recognized:

1. An intermittently developed contact zone 2-5 m thick consisting of a fine-grained greisen of muscovite flakes lying parallel to the contact and intergrown with some quartz.
2. A wall zone from 15-50 cm wide consisting predominantly of large muscovite sheets at right angles to the contact zone mica intergrown with quartz and feldspar.
3. An intermediate zone varying from 1-3 m in thickness which has produced quality beryl, tantalite-columbite and microlite. This zone consists essentially of cleavelandite and quartz and associated blocky microcline.
4. A core zone consisting of huge blocks and irregular masses of quartz and microcline.

Phosphate nodules occur on the edge of the quartz core. Lithiophilite containing 37.56% MnO and 6.81% FeO is associated with triplite, also Mn-rich containing 47.65% MnO with an FeO content of 11.59%.

Green muscovite greisen containing tantalite were found, not in situ, also green and purple altered spodumene, pollucite and possibly eucryptite associated with quartz and small amounts of lepidolite. Specs of yellow bismuth occur in quartz in connection with mica and kaolinized albite. The microlite is of varying colour and is usually associated with pink mica.

Pink lithiophilite also occurs in purplish mica, albite and quartz. Garnet occurs in the south end of the pegmatite in albite.

The **Lepidolite** pegmatite is exposed in the walls of a deep ravine near the boundary between farms Umeis and Kinderzitt. It is a tabular body striking N 42° W, dips 27° SW and is intrusive into a mafic-ultramafic plug being enclosed in amphibolite, diorite and biotite. It is more than 330 m in length and is a strikingly zoned body (see Plate 2.7) as follows:

1. A contact zone consisting of phlogopitic mica contaminated with lithium from lepidolite; approximately 2 cm in thickness. Followed by a garnetiferous band consisting of albite, approximately 28 cm wide.
2. A wall zone consisting of feldspar with radiating mica and quartz.
3. An intermediate zone, which could in part be replacement, of lepidolite with accessory red tourmaline and microlite, albite, cleavelandite and some quartz.
4. A discontinuous quartz core with large microcline perthite crystals

The lepidolite in this pegmatite, although extensively developed is not as rich in microlite as the Homestead granular lepidolite. However, one zoned crystal of microlite has been found with a varying U content ranging from 6.08% at the rim to 9% in the centre.

The **Witkop pegmatite** forms a prominent ridge, over 1000 m long and 120 m wide and it is situated on the south side of the Tantalite Valley Complex. It is emplaced in pink gneiss and straddles a small stream. The pegmatite has been described by von Backström (1976) who recognized four major zones:

1. A wall zone consisting essentially of medium to coarse-grained quartz feldspar rocks of quartz in a feldspar matrix with accessory green muscovite and garnet or a quartz and feldspar graphic intergrowth. This zone well developed in the eastern side of the pegmatite reaches a width of 70 m in the river bed.
2. An outer intermediate zone developed in the central area of the pegmatite up to a width of 10 m consisting of a fine-grained quartz-feldspar-muscovite rock with accessory columbite-tantalite, beryl and bismuth. These economic minerals are mostly concentrated in the close vicinity of the quartz core.
3. An inner intermediate zone less consistent than the outer zone, developed essentially south of the river and consisting of almost pure feldspar.
4. A quartz core of milky fine-grained quartz and rose quartz. In the northern most portion (north of the river bed it attains a length of 220 m and a width of 17 m. Southeast of the river bed, the quartz core has an approximate length of 170 m and a maximum width of 35 m.

In 1980 the northern section of this pegmatite was examined and a section through the pegmatite exposed at the river bed revealed the graphic granite which is composed of albite and quartz, followed by an albite and mica zone, next an albite zone and finally in the centre quartz and blocky microcline. Albite graphic granite is only developed on the eastern flank; the mylonite contact on the western flank is in contact with with albite and muscovite. Bismuthinite occurs in rose quartz with its alteration product of greenish yellow bismutite. Garnet occurs in wavy bands in a feldspar, mica matrix.

The **T" pegmatite** strikes approximately north-south; it owes its name to the fact that it has been excavated in the shape of a "T", and is situated just west of the Homestead pegmatite at a slightly higher elevation on the same side of the road. Five zones were recognized in 1980:

1. A wall zone of "chickenfoot" (biotite with microcline feldspar) 5 m wide. The biotite formation is in the shape of a chicken's foot. This intergrowth also contains radiating intergrowths of mica and quartz.
2. A zone of graphic granite approximately 5 m wide.

3. An intermediate zone, 1-2 m long, of sugary albite, mica and blocky microcline containing beryl crystals, yellow-green in colour, idiomorphic crystals lie in the albite and cleavelandite with associated garnet crystals and 1 cm aggregates of columbite-tantalite. This zone contains intergrowths of beryl, garnet and tantalite.
4. A quartz core containing blocky microcline.

The **Chickenfoot pegmatite** is situated close to the "T" pegmatite and takes its name from the biotite-microcline feldspar intergrowth. The biotite is emplaced in the cream coloured feldspar in a branching pattern resembling a chicken's foot - a most striking wall zone, 9 m wide. The pegmatite is emplaced in amphibolite. Three zones were recognized in 1983:

1. A wall zone of "chickenfoot".
2. An intermediate zone of albite with accessory garnet and pink beryl.
3. A small quartz core with some rose quartz.

A1.4. Details in text.

APPENDIX 2

A2.1. Analyses

Data used in Figures, not required immediately by the reader have been transferred to the Appendix as follows. Ordinarily the tables will be referred according to their context in the text but will be prefixed by the letter "A" and are compiled in the following order.

A 3.4.

Table A 3.5. (i)

A 4.6. (ii)

A 4.7. (i)

A 4.8. (i)

A 4.12.(ii)

A 4.18.(i)

APPENDIX 2 TABLE A 3.4. Traverse across Noumas sample (see Plate 3.4), Steinkopf, Namaqualand

	20	21	22	23	24	25	26	27	28.	29.	30.	31.	32	33
SiO ₂	48.73	48.83	48.81	48.58	46.61	46.64	46.03	68.89	69.33	46.73	45.64	68.84	68.94	48.61
TiO ₂	0.01	0.03	0.01	0.02	0.02	0.02	0.01	0.00	0.01	0.03	0.02	0.02	0.01	0.04
Al ₂ O ₃	31.10	31.23	30.72	31.21	36.20	37.14	37.21	19.86	20.07	38.45	38.60	20.00	20.06	35.42
FeO	0.61	0.63	0.65	0.62	0.88	0.41	0.41	0.01	0.00	0.31	0.31	0.00	0.00	0.65
MnO	0.18	0.16	0.19	0.15	0.25	0.22	0.21	0.01	0.01	0.29	0.26	0.00	0.02	0.14
CaO	0.01	0.00	0.00	0.00	0.01	0.01	0.00	0.07	0.08	0.01	0.01	0.14	0.17	0.03
MgO	2.94	3.09	3.19	2.94	0.63	0.46	0.33	0.02	0.01	0.04	0.01	0.02	0.02	0.05
Na ₂ O	0.17	0.17	0.17	0.21	0.29	0.25	0.28	11.83	11.94	0.38	0.41	12.00	11.89	1.30
K ₂ O	10.93	10.92	10.82	10.90	10.72	10.61	10.74	0.13	0.12	10.35	10.56	0.07	0.08	8.80
P ₂ O ₅	0.0	0.0	0.01	0.02	0.02	0.00	0.01	0.00	0.00	0.00	0.01	0.01	0.00	0.03
F	0.39	0.51	0.55	0.31	0.08	0.07	0.01	0.00	0.01	0.01	0.01	0.01	0.00	0.00
Total	95.07	95.57	95.12	94.96	95.71	96.46	95.24	100.82	101.58	96.6	95.84	101.11	101.17	95.07
-O=F	0.16	0.21	0.23	0.13	0.03	0.29	-	-	-	-	-	-	-	-
Total	94.91	95.36	94.89	94.83	95.68	96.17	95.24	100.82	101.58	96.6	95.84	101.11	101.17	95.07
Distance	316	309	314	323	327	329	331	337	338		342			

	34.	35.	36.	37.	38.	39.	40.	41.	42.	43.	44.	45.	46.
SiO ₂	69.02	69.03	68.81	68.81	44.83	45.22	44.82	44.94	44.74	45.05	44.93	44.60	45.31
TiO ₂	0.01	0.01	0.00	0.01	0.56	0.56	0.73	0.82	0.76	0.70	0.58	0.65	0.56
Al ₂ O ₃	19.93	20.10	20.20	20.12	30.83	30.74	29.81	29.41	29.19	30.04	29.76	30.17	29.18
FeO	0.03	0.01	0.00	0.01	4.49	4.76	4.93	5.25	5.22	4.67	5.04	4.71	4.92
MnO	0.02	0.01	0.01	0.03	0.32	0.36	0.41	0.41	0.46	0.32	0.39	0.37	0.38
CaO	0.09	0.17	0.13	0.21	0.00	0.00	0.00	0.01	0.00	0.00	0.00	0.01	0.00
MgO	0.01	0.00	0.03	0.01	1.47	1.49	1.65	1.68	1.76	1.52	1.57	1.58	1.49
Na ₂ O	11.95	11.94	12.17	11.86	0.45	0.45	0.46	0.41	0.39	0.37	0.34	0.41	0.35
K ₂ O	0.07	0.04	0.08	0.11	10.22	10.05	9.95	10.07	10.08	10.03	10.16	10.06	10.08
F	0.00	0.00	0.00	0.00	0.86	0.79	0.87	0.86	1.00	0.58	0.89	0.94	1.48
Total	101.13	101.31	101.43	101.17	94.03	94.42	93.63	93.86	93.6	93.08	93.66	93.50	93.75
-O=F	-	-	-	-	0.36	0.33	0.37	0.36	0.42	0.24	0.37	0.39	0.62
Total	101.13	101.31	101.43	101.17	93.67	94.09	93.26	93.50	93.18	92.84	93.29	93.11	93.13

20-26,29,30,33 Mica after spodumene (24-25, clear area on specimen).
 27,28,31,32,34-37 Albite ; 38-46 Mica plates (muscovite);

TABLE A3.5. Spodumene, mica and albite replacing spodumene, and cleavelandite, on traverse in Plate 8.
SW. Witkop pegmatite, Tantalite Valley, Namibia

	<u>Spodumene</u>										
	49.	50.	51.	52.	53.	54.	56.	61.	69.	70.	71.
SiO ₂	65.23	66.42	66.46	66.61	66.39	66.38	66.71	66.57	66.75	66.64	66.36
TiO ₂	-	0.02	-	-	-	-	-	-	0.02	-	0.02
Al ₂ O ₃	27.55	28.44	28.45	28.40	28.26	28.51	28.54	28.32	28.57	28.17	28.42
*FeO	-	0.06	0.04	0.09	0.06	0.06	0.18	0.05	0.04	0.06	0.05
MnO	0.01	0.06	0.11	0.10	0.08	0.08	0.08	0.05	0.05	0.10	0.07
CaO	0.05	-	-	-	0.01	0.02	0.02	-	-	0.11	0.07
MgO	0.01	0.01	-	-	-	0.02	-	-	-	-	0.11
Na ₂ O	1.04	0.13	0.13	0.14	0.14	0.15	0.11	0.10	0.10	0.09	0.07
K ₂ O	0.04	0.01	-	-	-	-	-	-	-	-	-
Li ₂ O**	7.71	7.71	7.71	7.71	7.71	7.71	7.71	7.71	7.71	7.71	7.71
P ₂ O ₅	-	-	-	-	-	-	-	-	-	-	-
Total	101.66	102.87	102.90	103.05	102.65	102.91	103.29	102.80	102.34	102.96	102.93

* total iron as FeO, ** Lithium by flame photometer

Mica replacing spodumene: K-feldspar(62)

	55.	57.	60.	62.	63.
SiO ₂	47.81	45.10	44.87	64.12	45.38
TiO ₂	0.29	0.14	0.19	0.02	0.12
Al ₂ O ₃	32.56	38.35	36.62	18.69	39.02
FeO	0.29	0.14	0.19	0.02	0.12
MnO	0.85	0.20	0.41	0.02	0.20
CaO	0.00	0.00	0.02	0.06	0.10
MgO	0.04	0.01	0.05	0.01	0.02
Na ₂ O	0.28	0.33	0.28	0.24	0.35
K ₂ O	10.16	10.51	10.56	15.77	10.56
F	1.77	0.21	0.52	0.03	0.12
Total	93.78	94.94	93.71	99.01	95.99
-O=F	0.74	0.08	0.22	0.01	0.05
Total	93.04	94.91	93.49	99.00	95.94

Albite and cleavelandite.

	58.	59.	64.	65.	66.	67.	68.
SiO ₂	68.56	68.58	70.58	68.73	68.34	68.53	68.55
TiO ₂	0.00	0.12	0.01	0.00	0.01	0.04	0.02
Al ₂ O ₃	20.25	20.36	20.49	20.27	20.42	20.43	20.27
FeO	0.01	0.00	0.01	0.02	0.02	0.01	0.01
MnO	0.03	0.02	0.02	0.00	0.01	0.00	0.01
CaO	0.12	0.19	0.07	0.19	0.22	0.16	0.10
MgO	0.01	0.01	0.02	0.01	0.00	0.00	0.01
Na ₂ O	11.90	11.99	8.04	11.89	11.87	11.99	12.11
K ₂ O	0.06	0.07	0.04	0.06	0.08	0.08	0.04
P ₂ O ₅	0.14	0.14	0.15	0.15	0.17	0.21	0.20
Total	101.08	101.48	99.43	101.32	101.14	101.45	101.32

APPENDIX 2 ANALYSES

TABLE 4.6. MICROLITE (Sample XX) Rubicon, Namibia

Sample XX	T1/1.	T1/2.	T1/3.	T1/4.	T1/5.	T1/6.	T1/7.	T1/8.	T1/9.	T1/10.	T1/11.	T1/12.	T1/13.	T1/14.
Ta ₂ O ₅	80.00	79.49	79.73	79.84	80.00	79.69	79.96	79.90	79.08	79.12	79.71	79.71	80.09	79.55
Nb ₂ O ₅	0.85	0.90	0.86	0.79	0.72	0.69	0.66	0.74	0.80	0.69	0.60	0.65	0.73	0.84
UO ₂	0.04	0.02	0.00	0.42	0.40	0.13	0.02	0.00	0.00	0.00	0.00	0.00	0.00	0.00
Bi ₂ O ₃	0.02	0.03	0.03	0.00	0.03	0.00	0.00	0.08	0.02	0.03	0.00	0.00	0.14	0.03
CaO	10.74	10.74	10.61	10.82	10.75	10.79	10.60	10.58	10.66	10.66	10.59	10.51	10.66	10.67
MnO	0.02	0.04	0.07	0.01	0.02	0.07	0.07	0.03	0.07	0.07	0.04	0.03	0.07	0.01
Na ₂ O	7.01	7.15	7.02	7.10	6.96	7.15	7.07	7.04	6.97	7.06	7.06	7.04	6.95	7.05
F	4.10	3.91	3.85	3.96	4.11	3.99	3.86	3.98	3.97	3.82	4.21	3.78	3.48	3.86
	102.78	102.28	102.17	102.94	102.99	102.51	102.24	102.35	101.57	101.45	102.21	101.72	102.12	102.01
-O=F	1.72	1.64	1.62	1.66	1.73	1.68	1.62	1.67	1.67	1.60	1.77	1.59	1.46	1.62
	101.06	100.64	100.56	101.28	101.26	100.83	100.62	100.68	99.90	99.85	100.44	100.13	100.66	100.39
	T1/15.	T1/16.	T1/17.	T1/18.	T1/19.	T1/20.	T1/21.	T1/22.	T1/23.	T1/24.	T1/25.	T1/26.	T1/27.	T1/28.
Ta ₂ O ₅	79.64	80.01	79.61	78.96	79.84	79.86	79.89	79.79	79.37	78.87	79.28	78.77	78.12	78.74
Nb ₂ O ₅	0.79	0.74	0.80	0.67	0.90	0.86	0.72	0.60	0.82	1.11	1.32	0.86	1.97	1.61
TiO ₂	0.00	0.42	0.06	0.02	0.03	0.02	0.04	0.05	0.05	0.02	0.06	0.05	0.04	0.06
UO ₂	0.00	0.00	0.07	0.00	0.05	0.02	0.05	0.04	0.05	0.00	0.01	0.06	0.00	0.00
Bi ₂ O ₃	0.00	0.39	0.00	0.01	0.04	0.01	0.05	0.04	0.00	0.00	0.00	0.01	0.02	0.00
CaO	10.59	10.54	10.64	10.36	10.65	10.61	10.53	10.61	10.62	10.72	10.69	10.50	10.70	10.65
MnO	0.07	0.02	0.05	0.10	0.02	0.04	0.05	0.03	0.05	0.02	0.08	0.16	0.05	0.05
Na ₂ O	7.08	7.02	7.03	6.85	7.02	7.06	7.05	6.90	7.11	7.06	6.97	7.01	7.17	7.03
F	1.79	4.22	4.11	3.54	4.04	3.99	4.01	3.88	4.21	4.14	3.82	4.08	4.12	3.81
	99.96	103.36	102.37	100.51	102.59	102.47	102.39	101.94	102.28	101.94	102.23	101.5	102.19	101.95
-O=F	0.75	1.77	1.73	1.49	1.70	1.68	1.68	1.63	1.77	1.74	1.60	1.71	1.73	1.60
Total	99.21	101.59	100.64	99.02	100.89	100.79	100.71	100.31	100.51	100.20	100.63	99.79	100.46	100.35

Sample XX	T1/29	T1/30	T1/31	T1/32	T1/33	T1/34	T1/35	T1/36	T1/37	T1/38	T1/39	T1/40	T1/41	T1/42
Ta ₂ O ₅	80.04	79.49	79.84	79.82	79.73	80.11	79.40	78.89	79.63	79.52	79.85	79.33	78.78	79.43
Nb ₂ O ₅	0.58	0.77	0.91	0.65	0.68	0.79	0.66	1.51	0.74	0.80	0.89	0.68	1.60	1.17
TiO ₂	0.06	0.05	0.05	0.06	0.00	0.02	0.04	0.09	0.00	0.05	0.05	0.17	0.02	0.06
Bi ₂ O ₃	0.03	0.03	0.00	0.00	0.00	0.04	0.00	0.00	0.00	0.01	0.00	0.00	0.04	0.06
CaO	10.58	10.65	10.62	10.72	10.59	10.55	10.62	9.67	10.67	10.68	10.74	10.55	10.60	10.58
MnO	0.05	0.04	0.05	0.05	0.00	0.03	0.13	0.90	0.09	0.50	0.05	0.22	0.05	0.03
Na ₂ O	6.88	6.86	7.03	5.01	6.97	7.06	6.99	7.06	6.26	7.01	7.02	6.94	7.03	6.96
F	3.75	3.86	3.91	3.91	3.90	3.92	3.71	3.43	4.11	3.83	3.93	3.74	4.03	3.73
Total	101.97	101.75	102.41	101.22	101.87	102.52	101.55	101.46	101.5	102.4	102.53	101.63	102.15	102.02
-O=F	1.58	1.62	1.64	1.64	1.64	1.65	1.56	1.44	1.73	1.61	1.65	1.57	1.69	1.57
Total	100.39	100.13	100.77	99.58	100.23	100.87	99.99	100.11	99.77	100.79	100.88	100.06	100.46	100.45

Traverse across microlite enclosed in MnFe tantalite lathes. Analyses made at 50 um intervals. U=trace

APPENDIX 2

TABLE 4.7 (SAMPLE XX) Rubicon, Karibib

Manganotantalite								
SampleXX	T1/43	T1/44	T1/45	T1/46	T1/47	T1/48	T1/49	T1/50
Ta ₂ O ₅	75.17	67.22	73.70	65.79	76.45	63.91	67.31	66.20
Nb ₂ O ₅	9.08	17.04	11.06	19.06	0.60	20.02	17.28	17.34
TiO ₂	0.03	0.05	0.06	0.05	0.00	0.03	0.05	0.03
SnO ₂	0.04	0.02	0.00	0.05	6.56	0.03	0.02	0.03
FeO	4.20	4.22	4.30	4.29	2.53	4.03	4.19	4.64
MnO	10.40	10.76	10.05	9.61	10.05	11.29	10.49	10.62
Tot:	98.9	99.31	99.17	98.85	96.	99.31	99.34	98.86

SampleXX	T1/51	T1/52	T1/53	T1/54	T1/55	T1/56	T1/57	T1/58	T1/59
Ta ₂ O ₅	65.27	64.40	64.43	71.34	65.73	67.43	79.29	82.58	70.10
Nb ₂ O ₅	18.73	19.70	20.09	13.30	17.72	17.40	11.65	1.57	14.33
TiO ₂	0.06	0.03	0.04	0.03	0.01	0.03	0.04	0.03	0.05
SnO ₂	0.11	0.01	0.02	0.00	0.04	0.07	0.00	0.14	0.05
FeO	4.50	4.56	4.47	3.83	4.73	4.44	3.70	1.76	4.31
MnO	10.49	10.31	10.95	11.05	10.57	9.83	11.11	11.03	10.54
	99.16	99.01	100.0	99.55	98.80	99.20	97.79	97.11	99.38

Ferrotantalite						
Sample XX	T1/61	T1/62	T1/63	T1/64	T1/65	T1/66
Ta ₂ O ₅	84.39	82.86	82.92	84.71	83.73	84.62
Nb ₂ O ₅	0.24	1.74	1.95	1.13	0.82	0.67
TiO ₂	0.04	0.04	0.02	0.06	0.05	0.05
SnO ₂	0.02	0.15	0.05	0.11	0.04	0.05
FeO	11.07	11.16	9.86	11.16	11.33	11.09
MnO	2.87	2.88	4.40	2.89	2.93	2.85
/	98.63	98.83	99.20	100.06	98.90	99.33

Automatic traverse (Edinburgh microprobe unit). Analyses not in the order of traverse. Traverse across lamellae, manganotantalite & ferrotantalite (totals include traces of other elements) associated with microlite and bismuth minerals.

TABLE 4.8. APPENDIX TABLE

Composition of manganotantalite and microlite Rubicon Mine, Karibib

TABLE 4.8a. Microlite, Rubicon, Karibib

Sample XX	XX/40	XX/41	XX/42	XX/43	XX/44
Ta ₂ O ₅	75.38	75.67	74.51	75.21	74.99
Nb ₂ O ₅	4.53	4.63	4.19	4.60	4.53
CaO	10.02	10.00	9.84	10.13	10.13
Na ₂ O	5.43	5.48	5.72	5.24	5.14
F	2.99	3.25	2.78	2.66	2.92
	98.35	99.03	97.04	97.84	97.71
-O=F	1.26	1.36	1.17	1.12	1.23
Total	98.09	97.67	95.87	96.72	96.48

H₂O⁺ not determined.

TABLE 4.8b Manganotantalite laths and between laths

Sample XX	XX/45	XX/46	XX/47	XX/48	XX/49	XX/50	XX/51	XX/52
Ta ₂ O ₅	62.43	51.94	79.51	75.51	74.05	73.84	75.66	75.80
Nb ₂ O ₅	21.25	31.41	4.69	8.19	9.91	10.16	8.60	8.68
MnO	11.60	10.38	11.01	11.22	11.43	11.51	11.37	11.47
FeO	0.05	0.05	tr	tr	tr	tr	tr	tr
Na ₂ O	0.01	0.08	tr	tr	tr	tr	tr	tr
	99.26	99.51	98.38	98.47	98.59	98.79	99.89	99.11

XX45,XX46. Manganotantalite laths

XX47-52. Manganotantalite between laths

TABLE 4. 12. Tantalites on traverse across XX sample, Rubicon, Karibib

	4.	5.	6.	7.	9.	32.	33.	34.	37.	38.
Ta ₂ O ₅	67.748	63.700	63.280	61.076	70.178	64.528	68.080	66.886	68.578	68.444
Nb ₂ O ₅	16.244	20.153	21.417	23.600	14.769	19.679	15.888	17.099	15.197	15.998
TiO ₂	0.052	0.065	0.048	0.048	0.032	0.018	0.047	0.058	0.053	0.028
SnO ₂	0.041	0.018	0.089	0.083	0.063	0.046	0.022	0.062	0.011	0.074
FeO	4.393	4.478	4.369	4.483	4.299	4.381	4.501	4.267	4.527	3.498
MnO	10.258	10.340	9.640	9.981	9.966	10.150	9.571	9.831	10.577	10.933
CaO	0.045	0.008	0.014	0.008	0.041	0.021	0.036	0.042	0.041	0.021
Na ₂ O	0.075	0.046	0.089	0.070	0.054	0.066	0.066	0.050	0.031	0.070
Total	98.855	98.809	98.946	99.350	99.402	98.889	98.211	98.296	98.959	98.999

	No. of ions on the basis O=6										
Ta	1.435	1.320	1.302	1.236	1.494	1.341	1.456	1.419	1.457	1.450	
Nb	0.572	0.694	0.733	0.794	0.523	0.68	0.565	0.603	0.537	0.564	
Ti	0.003	0.004	0.003	0.003	0.002	0.001	0.003	0.003	0.003	0.002	
Sn	0.001	0.001	0.003	0.002	0.002	0.001	0.001	0.002	0.000	0.002	
Fe	0.286	0.285	0.276	0.279	0.281	0.280	0.296	0.278	0.296	0.228	
Mn	0.677	0.667	0.618	0.629	0.661	0.657	0.637	0.649	0.700	0.722	
Ca	0.004	0.001	0.001	0.001	0.003	0.002	0.003	0.004	0.003	0.002	
Na	0.011	0.007	0.013	0.010	0.008	0.010	0.010	0.008	0.020	0.011	
Total	2.990	2.978	2.949	2.954	2.975	2.971	2.970	2.966	3.016	2.980	

	39.	45.	46.	47.	48.	49.	50.	51.	52.	53.
Ta ₂ O ₅	78.100	74.911	74.332	82.912	82.757	82.038	83.231	80.592	82.292	82.495
Nb ₂ O ₅	5.970	9.277	9.726	1.486	1.538	2.113	1.701	1.714	1.900	2.016
TiO ₂	0.063	0.043	0.042	0.033	0.050	0.045	0.0409	0.000	0.025	0.045
SnO ₂	0.056	0.019	0.024	0.071	0.091	0.137	0.090	2.888	0.081	0.080
FeO	7.005	4.406	4.561	11.283	11.487	11.499	11.485	11.050	11.355	11.249
MnO	7.563	10.227	10.236	2.861	2.848	2.941	2.921	2.856	2.907	3.001
CaO	0.018	0.007	0.022	0.000	0.022	0.017	0.045	0.049	0.015	0.024
Na ₂ O	0.067	0.069	0.057	0.106	0.069	0.074	0.050	0.075	0.078	0.090
Total	98.754	98.959	98.999	98.754	98.863	98.864	99.562	99.225	98.653	98.999
Ta	1.762	1.654	1.635	1.929	1.922	1.898	1.918	1.857	1.911	1.908
Nb	0.224	0.340	0.356	0.057	0.059	0.081	0.065	0.066	0.073	0.077
Ti	0.004	0.043	0.042	0.033	0.050	0.045	0.040	0.000	0.025	0.003
Sn	0.002	0.001	0.001	0.002	0.003	0.005	0.003	0.008	0.003	0.003
Fe	0.486	0.299	0.309	0.807	0.820	0.818	0.814	0.783	0.811	0.800
Mn	0.531	0.703	0.701	0.207	0.206	0.212	0.210	0.205	0.210	0.216
Ca	0.002	0.001	0.002	0.000	0.002	0.002	0.004	0.004	0.001	0.002
Na	0.011	0.011	0.009	0.018	0.011	0.012	0.008	0.012	0.013	0.015
Total	3.021	3.011	3.015	3.024	3.027	3.030	3.024	3.025	3.025	3.024
54.	55.	57.	58.	59.	60.	66.	68.	69.	74.	
Ta ₂ O ₅	82.579	83.921	83.102	83.181	83.059	82.719	66.692	70.349	65.505	65.568
Nb ₂ O ₅	1.488	0.309	1.037	1.076	0.950	1.275	16.624	12.786	19.819	18.079
TiO ₂	0.04	0.038	0.037	0.060	0.042	0.032	0.040	0.035	0.042	0.070
SnO ₂	0.050	0.061	0.077	0.000	0.133	0.009	0.043	0.020	0.008	0.000
FeO	11.271	11.142	11.369	11.340	11.304	11.122	4.545	0.271	0.289	0.281
MnO	2.974	2.925	2.834	2.894	2.859	2.877	10.552	10.753	10.351	10.269
CaO	0.015	0.053	0.022	0.020	0.027	0.004	0.049	0.035	0.034	0.148
Na ₂ O	0.077	0.106	0.086	0.088	0.061	0.078	0.088	0.015	0.007	0.013
Total	98.493	98.556	98.665	98.658	98.434	98.116	98.633	98.123	98.311	98.570
Ta	1.926	1.971	1.943	1.942	1.945	1.940	1.411	1.531	1.324	1.377
Nb	0.058	0.012	0.040	0.042	0.037	0.050	0.585	0.463	0.487	0.631
Ti	0.003	0.002	0.002	0.004	0.003	0.002	0.002	0.002	0.002	0.004
Sn	0.002	0.002	0.003	0.000	0.005	0.000	0.001	0.001	0.000	0.000
Fe	0.808	0.805	0.816	0.814	0.814	0.802	0.296	0.271	0.289	0.281
Mn	0.216	0.214	0.206	0.210	0.209	0.210	0.695	0.729	0.672	0.672
Ca	0.001	0.005	0.002	0.002	0.002	0.000	0.004	0.003	0.003	0.012
Na	0.009	0.018	0.011	0.012	0.008	0.012	0.013	0.015	0.007	0.013
Total	3.026	3.029	3.027	3.028	3.024	3.019	3.008	3.014	2.984	2.990

TABLE 4.18 Wodginite, M3, Karibib

	SnO ₂	microns	Ta ₂ O ₅	FeO	Nb ₂ O ₅	MnO
1	15.980	100.000	65.370	1.330	4.380	10.510
2	16.550	200.000	66.390	0.820	3.440	10.790
3	17.280	300.000	66.160	0.390	3.170	11.080
4	17.810	400.000	64.490	0.710	3.070	10.340
5	18.110	500.000	62.110	2.660	6.020	9.220
6	16.210	600.000	65.100	4.840	4.020	7.540
7	16.740	700.000	65.640	4.090	3.780	7.890
8	18.320	800.000	61.980	2.670	5.610	9.260
9	17.400	900.000	61.710	2.790	5.530	8.980
10	16.680	1000.000	62.900	3.640	5.220	8.610
11	16.230	1100.000	63.050	4.830	5.610	7.450
12	15.230	1200.000	62.130	5.420	6.990	7.100
13	15.980	1300.000	62.790	5.040	6.100	7.500
14	18.050	1400.000	64.860	2.530	3.460	9.150
15	16.380	1500.000	62.610	3.870	5.200	8.240
16	17.920	1600.000	65.550	0.220	3.280	11.040
17	17.400	1700.000	64.820	1.760	3.210	9.620
18						
19	15.730	1900.000	67.430	0.190	3.040	10.780
20	14.130	2000.000	68.620	0.050	3.870	10.680
21	14.070	2100.000	68.690	0.070	3.730	10.640
22	13.880	2200.000	68.940	0.070	4.040	10.790
23	17.700	2300.000	65.200	0.160	3.130	11.050
24						
25	12.620	2500.000	67.940	0.810	4.220	11.260
26	17.390	2600.000	66.260	1.140	2.750	10.210
27	17.230	2700.000	65.830	0.220	3.730	11.120
28	17.180	2800.000	65.580	0.920	3.090	10.530
29	15.550	2900.000	62.850	5.570	6.310	6.830
30	15.420	3000.000	63.000	5.570	5.930	6.890
31	14.920	3100.000	61.950	4.790	5.470	7.470
32	15.680	3200.000	59.680	5.440	7.560	6.860
33	15.720	3300.000	62.500	5.590	6.090	6.790
34	17.280	3400.000	65.960	0.400	3.630	11.010
35	16.390	3500.000	66.460	0.370	3.100	10.920
36	17.950	3600.000	65.370	0.130	3.370	11.230
37	15.440	3700.000	62.220	4.070	4.560	7.760
38	17.120	3800.000	63.920	3.810	4.200	8.040
39	15.840	3900.000	63.690	4.100	5.440	7.990
40	16.210	4000.000	66.710	0.100	3.630	10.970
41	14.450	4100.000	68.580	0.090	3.740	10.700
42	4.187	4200.000	73.739	1.180	6.477	12.540
43	15.210	4300.000	67.510	0.340	3.850	10.650
44	14.260	4400.000	67.750	0.180	4.090	10.780

APPENDIX 2 .2

A2.2 ANALYTICAL METHODS

Most of the data in this thesis (unless otherwise specified) were determined by electron microprobe. Standardization was by the electron microprobe units and unless otherwise stated, the analyses were done by the author.

Electron microprobe analysis

The microanalysers used :

1) A CAMBRIDGE INSTRUMENT MICROSCAN 5 (EDINBURGH) with an accelerating potential of 20 kV: and a beam current measured by a Faraday cage of 30nA for crystal spectrometry. A full ZAF correction procedure as described by Sweatman and Long (1969) was used to calculate final concentrations.

For the tantalum minerals the standards used were tantalum metal (Ta), niobium metal (Nb), uranium metal (U), rutile (Ti), galena (Pb), celestite (Sr), jadeite (Na), wollastonite (Ca), manganese metal (Mn), iron metal (Fe), tungsten metal (W), bismuth metal (Bi), baryte (Ba) and magnesium fluoride (F). In WDS techniques the 95% confidence limit for Ta and Nb up to the 75% level is ± 0.46 wt.%; for Ca, Fe, Mn and U at the 15% level ± 0.08 , ± 0.09 ; ± 0.10 and $\pm 0.27\%$ repectively ; with similar values for the minor elements.

2) Backscattered electron imaging by the JCXA - 733 SUPERPROBE (St Andrews) with an accelerating voltage = 15 kV: Beam current 20 nA

3) CAMIBAX MICROPROBE (Edinburgh)

4) ARL MICROPROBE (Johannesburg)

Backscattered electron imagery

Textural features in minerals, due to variations in composition are well displayed by backscattered electron imagery. It is shown by this technique that compositional zonation patterns occur in cassiterite, tantalite, wodginite and microlite and in the case of the lithium minerals the technique also highlights very rare accessory minerals associated, in particular, with amblygonite .

The number of backscattering events increases with increasing atomic number (Z), or in the case of compounds the mean atomic number (z). (z) is defined by the following equation (Lloyd,1987):

$$z = \sum (NAZ) / \sum (NA)$$

Where N is the number of atoms of each element of atomic weight A and atomic number Z. By rastering the primary beam a number of different images are obtained, that give quantitative information about a target specimen . One of these type of images, (Z contrast images)displays the difference in backscattering events in shades of grey from white to black , i.e. variations in z of the specimen, either a rock with a number of different phases or a zoned mineral. Therefore variations in composition are normally displayed as different grey-levels, the brighter areas having high values of z. This is the type of image that has been used in this study . It must however be pointed out, that as the contrast levels may be enhanced artificially, grey-levels of the same mineral may not be compared from one backscatter image to another, especially if other different minerals are involved.

Other methods of analysis.

Wet Chemical Gravimetric Methods (St.Andrews and Leeds)

Classical gravimetric for spodumene and tantalites

Li analyses by Flame photometric analysis (Leeds and St. Andrews)

Rb and Cs by Flame Transmission (St. Andrews and Leeds)

Rb and Ba was determined by XRF (St. Andrews). The precision is given in Chapter 6.

Li, Rb and Cs were determined by wet chemical means. The precision for Rb and Cs is given in Chapter 6.

Whole rock XRF analysis

Major elements were determined using fused glass beads prepared from 0.5 gms of rock powder, 2.5 gms of spectroflux 105 and ammonium nitrate as an oxidant. Analyses were performed on a Philips PW 14 50 the method essentially Norrish and Hutton (1969).

Rb, Ba and Cs were determined using pressed powder discs prepared with moviol as a binder.

All samples were prepared by crushing, washing and hand picking in the binocular microscope to remove impurities.

APPENDIX 3

TABLE A1 Sample Nos(used for XRFand probe*)

Mineral	Pegmatite	Locality
26. Microcline	graphic granite, river bed, Witkop	Tantalite Valley
31. Albite	graphic granite, top elevation, Witkop	Tantalite Valley
32. Muscovite	contact, White City	Tantalite Valley
33. Muscovite	top elevation, White City	Tantalite Valley
34.	Lower Chickenfoot pegmatite 1	Tantalite Valley
35.	Lower Chickenfoot pegmatite 2	Tantalite Valley
36. Microcline	White City	Tantalite Valley
37. Feldspathic gneiss (W2)	White City	Tantalite Valley
38. Feldspathic gneiss (W1)	White City	Tantalite Valley
39. Purple Li-mica	Rubicon	Okongava Ost, Karibib Namibia
40. Green mica greisen(compact)	White City	Tantalite Valley
41. Purple Li-mica greisen(compact)	White City	Tantalite Valley
42. Green-grey mica greisen (compact)	Kokerboomrand	Steinkopf, Namaqualand
43. Li-mica, small dark plates	Jooste's	Okongava Ost, Karibib, Namibia
44. Microcline(+rubellite)	Lepidolite	Tantalite Valley
45. Pink microcline(+spodumene)	Noumas 1	Steinkopf, Namaqualand
46. Compact grey mica(+garnet & sphalerite)	Homestead	Tantalite Valley
47. Li-mica	Rubicon	Okongava Ost, Karibib, Namibia
48. Li-mica	Rubicon	Okongava Ost, Karibib, Namibia
49. Dark Li-mica	Lepidolite	Tantalite Valley
50. Grey mica(+pink beryl)	Homestead	Tantalite Valley
51. Microcline	Swartzberg	Steinkopf, Namaqualand
52. Li-mica+quartz+albite+microcline	Lepidolite	Tantalite Valley
53. Albite (+green beryl)	pegmatite vein,	Windhoek area, Namibia
54. Microcline	Daheim 1	Daheim 106, Namibia

APPENDIX 3

TABLE A2

Sample No. (used for XRF and Probe*)

Mineral(s)	Pegmatite	Locality
55. Grey Li-mica	Homestead	Tantalite Valley
56. Microcline	Kohero	Karibib, Namibia
57. Albite(black tourmaline)	Myer's Kamp (M1)	Okatjimakuju 55, Karibib, Namibia
58. Albite(+1mm garnets)	Border zone, Lepidolite	Tantalite Valley
59. Microcline	Top Chickenfoot	Tantalite Valley
60. Albite	White City (contact zone)	Tantalite Valley
61. Albite	"T" pegmatite,	Tantalite Valley
62. Microcline(+mica)	White City (contact zone),	Tantalite Valley
63. Biotite mica(+feldspar)	White City (contact zone)	Tantalite Valley
64. Pink microcline(+apatite + albite?)	Dernberg	Karibib 54, Karibib, Namibia
65. Microcline	Swartzburg 3	Steinkopf, Namaqualand
66. Li-mica(+black microlite)	Jooste's	Okongava Ost, Karibib, Namibia
67. Albite	Chichenfoot	Tantalite Valley
68. Green mica greisen plates(+tantalite)	White City,	Tantalite Valley
69. Biotite(+albite 67)	Chickenfoot	Tantalite Valley
70. Li-mica plates	Etiro	Etiro 50 Karibib, Namibia
71. Biotite	Lower Chickenfoot	Tantalite Valley
72. Globular grey Li-mica	Viljoen's	Okongava Ost, Karibib, Namibia
73. Pink albite(+globular mica72)	Viljoen's	Okongava Ost, Karibib, Namibia
74. Globular Li-mica(+cleavelandite)	Jooste's	Okongava Ost, Karibib, Namibia
75. Li-mica(amblygonite)	Homestead	Tantalite Valley
76. Microcline + Li-mica greisen	Noumas 1	Steinkopf, Namaqualand
*77. Microcline+manganotantalite+mica	Myer's Kamp (M1)	Okatjimakuju 55, Karibib, Namibia
*78. Tantalite+cassiterite+mica+ montebrasite+fremontite	Daheim 3	Daheim 106, Karibib, Namibia
*79. Cleavelandite+ mica + wodginite +manganotantalite	Myer's Kamp (M3)	Okatjimakuju 55, Karibib, Namibia
*80. Yellow tourmaline+microcline+ amblygonite+petalite	Daheim 3	Daheim 106, Karibib, Namibia

APPENDIX 3

TABLE A3

Sample No.(used for XRF and probe)

Mineral(s)	Pegmatite	Locality
81. albite	Etiro	Etiro 50 Karibib, Namibia
82. Green muscovite(+feldspar 81)	Etiro	Etiro 50 Karibib, Namibia
83. Blue cleavelandite	Daheim 1	Daheim 106 Karibib, Namibia
84. Grey mica	Daheim 1	Daheim 106 Karibib, Namibia
*85. Purple-grey Li-mica + tantalite	Daheim 1	Daheim 106 Karibib, Namibia
86. Grey Li-mica(from77)	Myer's 1 (M1)	Okatjimikuju 55 Karibib, Namibia
87. Purple Li-mica plates	Etiro	Etiro 50 Karibib, Namibia
88. Microcline	Rubicon	Ogongava Ost Karibib, Namibia
89. Microcline	Quartzkop	Steinkopf, Namaqualand
90. Dark purple Li-mica	Uranoop	Steinkopf, Namaqualand
91. Muscovite(+feldspar)	Straussheim	Creif Farm, Kenhardt Area,Northern Cape,S.A.
92. Li-mica	Uranoop	Steinkopf, Namaqualand
93. Muscovite(+feldspar+quartz)	Homestead	Tantalite Valley
94. Muscovite	White City	Tantalite Valley
*95. Muscovite+spodumene(pseudo)+ Cleavelandite +quartz	Noumas 1	Steinkopf, Namaqualand
96. Microcline	Sandamap	Sandamap 64, Damaraland, Namibia
97. Graphic granite-microcline+mica		Karibib area, Namibia
*98. Microcline+Mn-tantalite+microcline	Noumas 1	Steinkopf, Namaqualand
*99. White petalite(+albite 100)	Helicon 2	Okongava Ost, Karibib, Namibia
*100. Blue albite(+petalite 99)	Helicon 2	Okongava Ost, Karibib, Namibia
101. Green mica(+cassiterite)	Petalite	Strathmore, Cape Cross, Namibia

APPENDIX 3

TABLE 2. Minerals analysed from pegmatites in the Karibib-Usakos area

Pegmatite & locality	Mineralization	Ref. SampleNos.
Rubicon, Okongava Ost 72	tantalite,tapiolite,microcline,montebrasite apatite,petalite,Li-mica, pyromorphite,mottramite,microcline,pink beryl,lithiophilite	XX,R,5,6,Mor, 54 J-39,47,48 90 (23)
Helicon 1, Okongava Ost 72	lepidolite, albite, tantalite+quartz, pollucite, beryl	J-99,100,52
Helicon 2, Okongava Ost 72	pollucite + quartz, lepidolite,petalite, montebrasite, blue cleavelandite	OK J-43,74,66
Jooste's, Okongava Ost 72	Li-mica, black & yellow microcline, cleavelandite, Mn-apatite	MR,2M,3M,MB,M J-72,73
Mon Repos, Okongava Ost 72	manganotantalite+quartz,tapiolite,indicolite,rubellite,microcline,montebrasite	(20,24,32,56)70J
Viljoen's, Okongava Ost 72	tantalite+green mica+pink albite,beryl	77J (1,2) 86J
Eitro 50	topaz,pink beryl+muscovite,Li-mica, apatite,columbite	J-57,79
(M1), Okatjimakuju 55	Li-mica, tantalite+microcline,microcline,lithiophilite	M4 (3)
(M3), Okatjimakuju 55	wodgite+cleavelandite+mica,Mn-tantalite,Mn-apatite+quartz +cleavelandite+tourmaline	B
(M4), Okatjimakuju 55	grey topaz+montebrasite+crandallite,pink beryl,cleavelandite + Li-mica + cassiterite brazilianite	D4 J-83,84,85(5)
Daheim 1, Daheim 106	tantalite,montebrasite,cookeite,apatite,Cs-mica, Li-mica	J-78,80
Daheim P, Daheim 106	grey petalite	J64
Daheim 3, Daheim 106	pink petalite,montebrasite+fremontite, tourmaline+petalite,cassiterite +mica	J96,(11)
Dernburg, Karibib 54	manganotantalite+quartz,purple apatite+pink microcline,cleavelandite,montebrasite	101J
Sandamap 64, Damaraland	Li-mica,cassiterite,petalite,tantalite	
Ricksburg, Okakoara 43	tantalite,microcline,Li-mica+blue topaz	
Strathmore, Cape Cross	ferrocolumbite,petalite,cassiterite,green mica +felspar	
Uis	Li-mica,cassiterite,spodumene,eucryptite	

Numbers in brackets: Li-mica samples, Ovk